



analytical chemistry

Volume 46, No. 2
February 1974

ANCHAM 46(2) 85A-264A/185-328 (1974)
ISSN 0003-2700

Contents

Our cover, in honor of the Silver Anniversary of the Pittsburgh Conference on Analytical Chemistry and Applied Spectroscopy, presents a reproduction of an oil painting of the Golden Triangle of Pittsburgh, Pa., in the early 1950's. The artist is Adriaan van Hoften, a native of Rotterdam, Holland, who came to the United States in 1947. He studied at the Academy of Science and Fine Arts at Rotterdam and the Royal Academy in London and especially enjoys painting portraits and landscapes. Adriaan van Hoften has been exhibits manager for Varian Associates for the past 11 years. This painting of Pittsburgh was commissioned by the Pittsburgh Conference officials to celebrate their 25th year and is used on our cover with their kind permission.

The Golden Triangle, which is symbolized also in the Pittsburgh Conference official seal, denotes the coming together of the Allegheny and Monongahela Rivers to form the Ohio River. The bridges portrayed are no longer in existence but have been replaced by new structures. The remains of Fort Pitt, important in Revolutionary days, are located in the area. Features of a modern view of the Golden Triangle area would include a park and the vastness of Three Rivers Stadium.

The Pittsburgh Conference took place in Pittsburgh until 1968 when it moved to Cleveland to take advantage of the improved facilities offered by the Cleveland Convention Center. Many of us still speak of going to Pittsburgh when we really mean going to Cleveland for the Pittsburgh Conference, and the light hearted speak of "Cleveland." The name of the Conference remains the same, and the original analytical and spectroscopy groups from Pittsburgh still plan and carry out the Conference in Cleveland.

REPORT

Rudolf Seitz and Michael Neary discuss chemiluminescence and bioluminescence in chemical analysis. Although limited by the number of available reactions, BL and CL methods are quite successful because of unique advantages **188 A**

INSTRUMENTATION

L. B. Kreuzer of DIAX Corp. discusses laser optoacoustic spectroscopy, a new technique of gas analysis, with particular promise for application in gaseous air pollution detection **235 A**

PITTSBURGH CONFERENCE

The 25th Pittsburgh Conference on Analytical Chemistry and Applied Spectroscopy will be held March 4 to 8, 1974, in Cleveland, Ohio. The complete technical program is given **119 A**

PITTSBURGH CONFERENCE: EXPOSITION

The latest instrumentation, equipment, and laboratory services and chemicals will be shown at the Exposition. Exhibitors and their products are listed **165 A**

NEWS AND VIEWS

Stanley Crouch, Harold McNair, and David Seligson, M.D., are appointed to ANALYTICAL CHEMISTRY's Instrumentation Advisory Panel. Toxic substance regulations and sensing of environmental pollutants are given attention by Federal officials and others at meetings **203 A**

BOOKS

Books on mass spectrometry of inorganic and organometallic compounds, programmed introduction to GLC, absorption of light and ultraviolet radiation, and instrumental and separation analysis are reviewed by William P. Weber, J. J. DeStefano, Raymond F. Chen, and Jonathan W. Amy **223 A**

EDITORS' COLUMN

A recent study among the Indians in the Amazon jungles shows that blood serum mercury levels are unusually high and lead levels unusually low. No apparent reasons for these phenomena are known **233 A**

EDITORIAL

Factors involved in the recent renaissance of analytical chemistry suggest that the renewed interest may continue **185**

Author Index **92 A**

Briefs **101 A**

Future Articles **264 A**

Call for Papers **210 A**

Meetings **210 A**

Short Courses **210 A**

New Products **251 A**

Chemicals **256 A**

Manufacturers' Literature **259 A**

Articles

Determination of Lead in Atmospheric Air and in Aluminum by Helium-3-Induced Nuclear Reactions. *Bahman Parsa and S. S. Markowitz* **186**

Quantitative Analysis of Light Elements (Nitrogen, Carbon, and Oxygen) in Sputtered Tantalum Films by Auger Electron Spectroscopy and Secondary Ion Mass Spectrometry (SIMS). *J. M. Morabito* **189**

X-Ray Photoelectron Spectroscopic Studies of Palladium Oxides and the Palladium-Oxygen Electrode. *K. S. Kim, A. F. Gossman, and Nicholas Winograd* **197**

Correction of Inner Filter Effects in Fluorescence Spectrometry. *V. A. Mode and D. H. Sisson* **200**

Nondispersive Soft X-Ray Fluorescence Spectrometer for Quantitative Determination of the Major Elements in Rocks and Minerals. *A. J. Hebert and Kenneth Street, Jr.* **203**

Contents

Automatic Correction System for Light Scatter in Atomic Fluorescence Spectrometry. <i>T. C. Rains, M. S. Epstein, and Oscar Menis</i>	207	Determination of the Noble Metals in Geological Materials by Neutron Activation Analysis. <i>R. A. Nadkarni and G. H. Morrison</i>	232	Determination of Antimony Using Forced-Flow Liquid Chromatography with a Coulometric Detector. <i>L. R. Taylor and D. C. Johnson</i>	262
Inductively Coupled Plasma-Optical Emission Analytical Spectroscopy. Tantalum Filament Vaporization of Microliter Samples. <i>D. E. Nixon, V. A. Fassel, and R. N. Kniseley</i>	210	Instrumental Neutron Activation Analysis for Mercury in Dogs Administered Methylmercury Chloride: Use of a Low Energy Photon Detector. <i>M. H. Friedman, Eugene Miller, and J. T. Tanner</i>	236	Characterization of Heavy Residual Fuel Oils and Asphalts by Infrared Spectrophotometry Using Statistical Discriminant Function Analysis. <i>F. K. Kawahara, J. F. Santner, and E. C. Julian</i>	266
Mode-Locked Laser Raman Spectroscopy—A New Technique for the Rejection of Interfering Background Luminescence Signals. <i>R. P. Van Duyne, D. L. Jeanmaire, and D. F. Shriver</i>	213	Determination of Trace Elements in Coal, Fly Ash, Fuel Oil, and Gasoline—A Preliminary Comparison of Selected Analytical Techniques. <i>D. J. von Lehmden, R. H. Jungers, and R. E. Lee, Jr.</i>	239	Molecular Interactions of Asphalt: An Infrared Study of the Hydrogen-Bonding Basicity of Asphalt. <i>R. V. Barbour and J. C. Petersen</i>	273
Information Content of Mass Spectra as Determined by Pattern Recognition Methods. <i>J. B. Justice and T. L. Isehour</i>	223	Ion Electrode Based Enzymatic Analysis of Creatinine. <i>Huvin Thompson and G. A. Rechnitz</i>	246	Determination of Total Mercury in Air by Charcoal Adsorption and Ultraviolet Spectrophotometry. <i>F. P. Scaringelli, J. C. Puzak, B. I. Bennett, and R. L. Denny</i>	278
Analysis of the Polychlorinated Biphenyl Problem. Application of Gas Chromatography-Mass Spectrometry with Computer Controlled Repetitive Data Acquisition from Selected Specific Ions. <i>J. W. Eichelberger, L. E. Harris, and W. L. Budde</i>	227	Serum Protein Monitoring and Analysis with Ion-Selective Electrodes. <i>P. W. Alexander and G. A. Rechnitz</i>	250	Informing Power of a Chromatographic Method and Its Use as a Quality Criterion. <i>D. L. Massart and R. Smits</i>	283
		Glass Electrode Responses Interpreted by the Solid State Homogeneous- and Heterogeneous-Site Membrane Potential Theory. <i>R. P. Buck, J. H. Boles, R. D. Porter, and J. A. Margolis</i>	255		

Notes

Informing Power of a Chromatographic Method and Its Use as a Quality Criterion. *D. L. Massart and R. Smits* **283**

© Copyright 1974
by the American Chemical Society



MANUSCRIPT REQUIREMENTS published in December 1973 issue, page 2451, outlines scope and copy requirements to be observed in preparing manuscripts for consideration. Manuscript (4 copies) should be submitted to ANALYTICAL CHEMISTRY, 1155 Sixteenth St., N.W., Washington, D.C. 20036.

The American Chemical Society assumes no responsibility for the statements and opinions advanced by contributors to its publications. Views expressed in the editorials are those of the editors and do not necessarily represent the official position of the American Chemical Society.

1974 Subscription Rates

	1 yr.	2 yr.	3 yr.
Members, domestic and foreign	\$ 5.00	\$ 9.00	\$12.00
Nonmembers, domestic and Canada	7.00	12.00	16.00
Nonmembers, foreign except Canada	15.00	27.50	40.00

Postage: Canada and Pan-American Union, \$4.00; foreign, \$5.00. Air freight rate available on request. Single copies: current, \$2.00 except Annual Reviews, \$3.00 each. Rates for back issues and volumes are available from Special Issues Sales Dept., 1155 Sixteenth St., N.W., Washington, D.C. Send all new and renewal subscriptions with payment to: Office of the Controller, 1155 Sixteenth Street, N.W., Washington, D.C. 20036. All correspondence and telephone calls regarding changes of address, claims for missing issues, subscription service, the status of

records, and accounts should be directed to: Manager, Membership and Subscription Services, American Chemical Society, P.O. Box 3337, Columbus, Ohio 43210. Telephone (614) 421-7230.

On changes of address, include both old and new addresses with ZIP code numbers, accompanied by mailing label from a recent issue. Allow four weeks for change to become effective.

Subscriptions should be renewed promptly to avoid a break in your series.

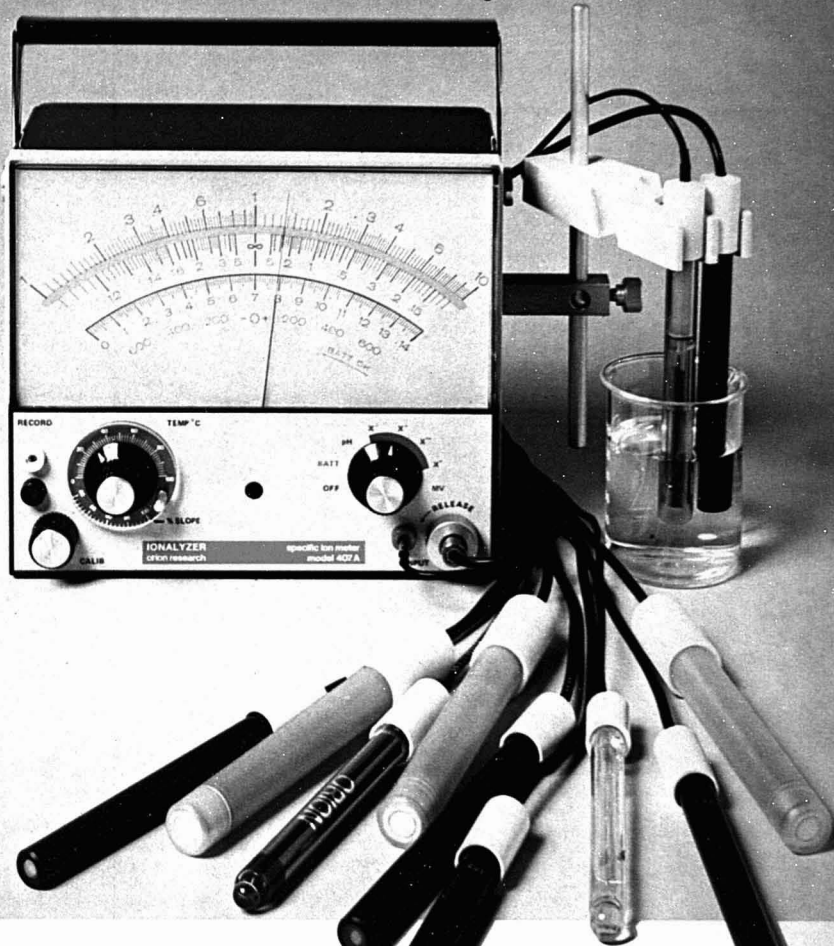
Claims for missing numbers will not be allowed (1) if received more than sixty days from date of issue plus time normally required for postal delivery of journal and claim, (2) if loss was due to failure of notice of change in address to be received before the date specified in (1), or (3) if the reason for the claim is "issue missing from files."

Those interested in joining the American Chemical Society should write to Admissions Department at the Washington Office.

Published monthly with Review issue added in April and a Laboratory Guide in August by the American Chemical Society, from 20th and Northampton Sts., Easton, Pa. 18042; Executive Offices and Editorial Headquarters, 1155 Sixteenth St., N.W., Washington, D.C. 20036; Advertising Office, 142 East Ave., Norwalk, Conn. 06851. ANALYTICAL CHEMISTRY and other ACS periodicals are available on microfilm. For information write to: MICROFILM, Special Issues Sales Dept., American Chemical Society, 1155 Sixteenth St., N.W., Washington, D.C. 20036. Second class postage paid at Washington, D.C. and at additional mailing offices.

Electroordinary!

Here is the extraordinarily versatile electrode instrument from Orion Research, the Model 407A Specific Ion Meter. Choose any electrode — specific ion, gas sensing, redox or pH. Name your method — special scales for pH measurements, titrations, direct reading of ion concentrations and analyses by known addition and subtraction methods. Use it anywhere — the 407A operates on line power and rechargeable batteries.



name _____
title _____ dept. _____
company _____
address _____
city _____ state _____ zip _____

Send me information on:

- 407A specific ion meter
 ORION chemical sensing electrodes

ORION RESEARCH

380 Putnam Avenue, Cambridge, Mass. 02139

FLOW
CONTROLLED

ELKAY
"Solvent
Flexible"
**MANIFOLD
PUMP
TUBING**

**OVER ONE YEAR IN RESEARCH
AND DEVELOPMENT AND MONTHS
OF FIELD EVALUATION.**

Solvent flexible (yellow) auto analysis pump tubing. Manufactured to Elkay specifications and formulation. This tubing is specially formulated to yield longer pumping life when solvents are being used. This solvent flexible tubing is continuously monitored in our own quality control laboratory to assure consistent flow, performance and time of efficiency. The tubing is cut to 16 inch lengths with color coded wishbone bridges affixed to yield a 6 inch center pumping section.

Each lot manufactured is carefully controlled under stringent I.D., O.D., and wall thickness specifications.

IMMEDIATE DELIVERY

ELKAY PRODUCTS, INC.

95 Grand St. Worcester, Mass. 01610
Tel: (617) 757-4435

Thin Layer Chromatographic-Spectrofluorometric Analysis of Amphetamine and Amphetamine Analogs after Reaction with 4-Chloro-7-Nitrobenzo-2,1,3-Oxadiazole.
François Van Hooft and Aubin Heyndrickx 286

Rapid, Sensitive Gas-Liquid Chromatographic Screening Procedure for Cocaine. *J. W. Blake, R. S. Ray, J. S. Noonan, and P. W. Murdick* 288

Dual-Load Porous-Layer Open Tubular Gas Chromatography Columns. *J. G. Nikely* 290

Cryostat for Optical Spectroscopy. *J. Szoke and I. Szilagyi* 292

Multiclass Linear Classifier for Spectral Interpretation (Pattern Recognition). *C. F. Bender and B. R. Kowalski* 294

Identification of Heroin and Its Diluents by Chemical Ionization Mass Spectroscopy. *Jew-Ming Chao, Richard Saferstein, and John Manura* 296

Spectrometric Assay of Aldehydes as 6-Mercapto 3-substituted-s-triazolo(4,3-b)-s-tetrazines. *N. W. Jacobsen and R. G. Dickinson* 298

Liquid-Liquid Extraction of Zinc with Aliquat 336-S-1 from Aqueous Iodine Solutions. *C. W. McDonald and Thornton Rhodes* 300

Rapid Determination of the Nitrogen Content of Cellulose Nitrate and Other Nitrate Esters by Means of a Modified Devarda Method. *J. G. M. M. Smeenk* 302

Consecutive Titration of Calcium and Magnesium in Ethanol-Water Mixture. *Bo Wallen* 304

Solvent Extraction Studies of Chromium(III) with Tri-n-octylamine. *B. E. McClellan, M. K. Meredith, Ray Parmelee, and J. P. Beck* 306

Selective Separation and Concentration of Silver via Precipitation Chromatography. *W. P. Zeronza, Gregory Dabkowski, and Sidney Siggia* 309

Contents

Determination of Total Cyanide in the Presence of Palladium. *G. W. Latimer, Jr., L. R. Payne, and Marguerite Smith* 311

Sampling Variance in Analysis for Trace Components in Solids. Preparation of Reference Samples. *W. E. Harris and Byron Kratochvil* 313

New Method for Calibration of Permeation Wafer and Diffusion Devices. *R. N. Dietz, E. A. Cote, and J. D. Smith* 315

Correspondence

Self-Reversal in a Copper Pulsed Hollow Cathode Lamp. *G. J. DeJong and E. H. Piepmeier* 318

Aids for Analytical Chemists

Relay Circuit for Integrating a Gas-Liquid Chromatography Temperature Programmer with an Automatic Sample Injector. *H. A. McLeod, Ronald Bolohan, and Maarten Van Dyk* 320

Simple Method for Continuous Monitoring of Electrode Rotation Rate. *I. B. Goldberg, R. S. Carpenter II, and W. F. Goepfinger* 321

Device for the Accurate Electronic Measurement of Microliter Sample Volumes. *L. R. Layman and G. M. Hietlje* 322

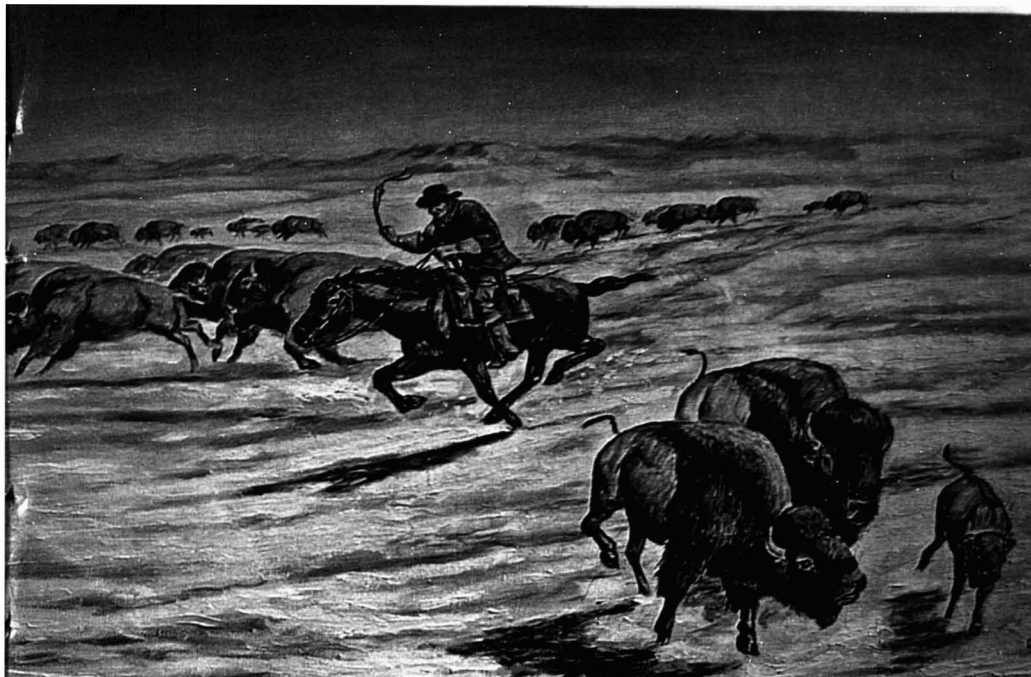
Analysis of Background Copper Concentration in Sea Water by Electron Spin Resonance. *Y. P. Virmani and E. J. Zeller* 324

Device to Seal Ends of Gas Chromatography Columns with a Filter Disk. *Francis W. Karasek* 325

Teflon Apparatus for Vapor Phase Destruction of Silicate Materials. *J. W. Mitchell and D. L. Nash* 326

Correction. Annual Subject Index. 289

Correction. Potentiometric Determination of Cyanide with an Ion Selective Electrode. 328



The Pony Express we ain't. But we do deliver locally.

Compared to today's delivery problems, the old Pony Express rider had a picnic. As a national distributor of laboratory equipment, supplies and scientific instruments, we have to make 130,000 items available to you as fast, or faster than our competition. Or die. So we developed what we call our "S/P national local delivery service."

We established 23 strategically located sales and distribution centers throughout the country. We manned them with 400 local Sales Representatives. Then we installed a special communication system between our sales and distribution centers so your order can be filled from the nearest source.

Once you place an order with your local S/P Representative, he makes a single phone call and all 130,000 items are available to you. In most cases, your items are picked, packed and shipped the same day. Most of our deliveries are made locally by our own fleet of trucks. When it comes to delivery, we really ride herd on your order.



To take advantage of our "national local delivery service," call your S/P Representative or write Scientific Products, Division of American Hospital Supply Corporation, 1430 Waukegan Road, McGaw Park, Illinois 60085.

S/P... a single source for laboratory equipment, supplies and scientific instruments.

CIRCLE 217 ON READER SERVICE CARD

Arsenic in old lace*

(*and blood, urine, air
and other things too!)

It's no longer a mystery! Finally, there is a rapid, direct method for arsenic determinations down to the nanogram levels which can be performed in your laboratory on a routine basis, without any awkward-to-use accessories — just our standard anodic stripping voltammeters.

If arsenic determination, linear over a concentration range of from 20 to 400 ppb, is of interest, please call or write ESA for further information, or visit us in Booths 702 and 704 at the Pittsburgh Conference.

*METHODOLOGIES FOR THE ANALYSIS OF TRACE METALS e.g. Pb, Cd, Cu, Zn, Hg, etc., IN A WIDE VARIETY OF MATRICES AVAILABLE UPON REQUEST.



ENVIRONMENTAL SCIENCES ASSOCIATES, INC.

175 BEDFORD STREET, BURLINGTON, MASSACHUSETTS 01803
TELEPHONE 617-272-1200

Author Index

Alexander, P. W.	250	Markowitz, S. S.	186
Barbour, R. V.	273	Massart, D. L.	283
Beck, J. P.	306	Menis, O.	207
Bender, C. F.	294	Meredith, M. K.	306
Bennett, B. I.	278	Miller, E.	236
Blake, J. W.	288	Mitchell, J. W.	326
Boles, J. H.	255	Mode, V. A.	200
Bolohan, R.	320	Morabito, J. M.	189
Buck, R. P.	255	Morrison, G. H.	232
Budde, W. L.	227	Murdick, P. W.	288
		Nadkarni, R. A.	232
Carpenter, R. S., II	321	Nash, D. L.	326
Chao, J.-M.	296	Nikelly, J. G.	290
Cote, E. A.	315	Nixon, D. E.	210
		Noonan, J. S.	288
Dabkowski, G.	309	Parmalee, R.	306
DeJong, G. J.	318	Parsa, B.	186
Denny, R. L.	278	Payne, L. R.	311
Dickinson, R. G.	298	Petersen, J. C.	273
Dietz, R. N.	315	Piepmeyer, E. H.	318
		Porter, R. D.	255
Eichelberger, J. W.	227	Puzak, J. C.	278
Epstein, M. S.	207		
		Rains, T. C.	207
Fassel, V. A.	210	Ray, R. S.	288
Friedman, M. H.	236	Rechnitz, G. A.	246, 250
		Rhodes, T.	300
Goeppinger, W. F.	321	Saferstein, R.	296
Goldberg, I. B.	321	Santner, J. F.	266
Gossmann, A. F.	197	Scaringelli, F. P.	278
		Shriver, D. F.	213
Harris, L. E.	227	Siggia, S.	309
Harris, W. E.	313	Sisson, D. H.	200
Hebert, A. J.	203	Smecen, J. G. M. M.	302
Heyndrickx, A.	286	Smith, J. D.	315
Hieftje, G. M.	322	Smith, M.	311
		Smits, R.	283
Ishenhour, T. L.	223	Street, K., Jr.	203
		Szilágyi, I.	292
Jacobsen, N. W.	298	Szöke, J.	292
Jeanmaire, D. L.	213	Tanner, J. T.	236
Johnson, D. C.	262	Taylor, L. R.	262
Julian E. C.	266	Thompson, H.	246
Jungers, R. H.	239		
Justice, J. B.	223	Van Duyn, R. P.	213
		Van Dyk, M.	320
Karasek, F. W.	325	Van Hoof, F.	286
Kawahara, F. K.	266	Virmani, Y. P.	324
Kim, K. S.	197	Von Lehmden, D. J.	239
Kniseley, R. N.	210		
Kowalski, B. R.	294	Wallén, B.	304
Kratochvil, B.	313	Winograd, N.	197
Latimer, G. W., Jr.	311	Zeller, E. J.	324
Layman, L. R.	322	Zeronsa, W. P.	309
Lee, R. E., Jr.	239		
McClellan, B. E.	306		
McDonald, C. W.	300		
McLeod, H. A.	320		
Manura, J.	296		
Margolis, J. A.	255		

Determination of Lead in Atmospheric Air and in Aluminum by Helium-3-Induced Nuclear Reactions

A new method using ^3He activation analysis is developed to determine trace concentrations of lead. The limits of detection extend to about 0.5 ppb.

Bahman Parsa and Samuel S. Markowitz, Department of Chemistry and Lawrence Berkeley Laboratory, University of California, Berkeley, Calif. 94720 *Anal. Chem.*, 46, 186 (1974)

Quantitative Analysis of Light Elements (Nitrogen, Carbon, Oxygen) in Sputtered Tantalum Films by Auger Electron Spectroscopy and Secondary Ion Mass Spectrometry (SIMS)

SIMS detection limits for O and C are in the ppm range and for N in the 0.1 at. % range. Auger detection limits are in the 0.3-0.4 at. % range.

J. M. Morabito, Bell Telephone Laboratories, Inc., Allentown, Pa. 18103 *Anal. Chem.*, 46, 189 (1974)

X-Ray Photoelectron Spectroscopic Studies of Palladium Oxides and the Palladium-Oxygen Electrode

ESCA studies of oxidized palladium metal surfaces reveal the presence of chemisorbed oxygen atoms and PdO. This approach verifies the presence of PdO and PdO₂ on electrochemically oxidized palladium electrodes.

K. S. Kim, A. F. Gossmann, and Nicholas Winograd, Department of Chemistry, Purdue University, West Lafayette, Ind. 47906 *Anal. Chem.*, 46, 197 (1974)

Correction of Inner Filter Effects in Fluorescence Spectrometry

An analytic expression for correcting data from front-surface spectrofluorometry is obtained.

V. Alan Mode and D. H. Sisson, Lawrence Livermore Laboratory, University of California, Livermore, Calif. 94550 *Anal. Chem.*, 46, 200 (1974)

Nondispersive Soft X-Ray Fluorescence Spectrometer for Quantitative Determination of the Major Elements in Rocks and Minerals

An instrument is described which provides determinations of the elements from O to Fe with 1-2% reproducibility and accuracy for elements present at the 1% level.

A. J. Hebert and Kenneth Street, Jr., Lawrence Berkeley Laboratory, University of California, Berkeley, Calif. 94720 *Anal. Chem.*, 46, 203 (1974)

Automatic Correction System for Light Scatter in Atomic Fluorescence Spectrometry

The method described is applied to the determination of 0.11 and 0.26 $\mu\text{g Cd/gram}$ in SRM's Orchard Leaves and Liver, respectively, without any prior separation or pre-concentration.

T. C. Rains, M. S. Epstein, and Oscar Menis, Analytical Chemistry Division, National Bureau of Standards, Washington, D.C. 20234 *Anal. Chem.*, 46, 207 (1974)

Inductively Coupled Plasma-Optical Emission Analytical Spectroscopy. Tantalum Filament Vaporization of Microliter Samples

One set of operating conditions suffices for the determination of many elements at the ng/ml level in 100- μl samples.

David E. Nixon, Velmor A. Faisel, and Richard N. Kniseley, Ames Laboratory—USAEC and Department of Chemistry, Iowa State University, Ames, Iowa 50010 *Anal. Chem.*, 46, 210 (1974)

Mode-Locked Laser Raman Spectroscopy—A New Technique for the Rejection of Interfering Background Luminescence Signals

A technique for rejection of background using a mode-locked Ar ion laser and single photon timing detection is described. Experimental signal-to-noise ratio is compared with theoretical predictions.

Richard P. Van Duyne, David L. Jeanmaire, and D. F. Shriver, Department of Chemistry, Northwestern University, Evanston, Ill. 60201 *Anal. Chem.*, 46, 213 (1974)

Information Content of Mass Spectra as Determined by Pattern Recognition Methods

Predictive ability increases in the order Sum Spectra < Binary Spectra < Normalized Sum Spectra < Nonlinear Transform = Learning Machine < Nearest Neighbor.

J. B. Justice and T. L. Isenhour, Department of Chemistry, University of North Carolina, Chapel Hill, N.C. 27514 *Anal. Chem.*, 46, 223 (1974)

Analysis of the Polychlorinated Biphenyl Problem. Application of Gas Chromatography-Mass Spectrometry with Computer Controlled Repetitive Data Acquisition from Selected Specific Ions

Data acquisition from subsets of the ions used in conventional mass spectrometric scans makes increased sensitivity possible without loss of the qualitative information contained in the complete mass system.

James W. Eichelberger, Lawrence E. Harris, and W. L. Budde, Environmental Protection Agency, National Environmental Research Center, Analytical Quality Control Laboratory, Cincinnati, Ohio 45268 *Anal. Chem.*, 46, 227 (1974)

Determination of the Noble Metals in Geological Materials by Neutron Activation Analysis

Au, Ru, Pd, Os, Ir, and Pt are determined using thermal neutron irradiation, selective adsorption of the noble metal group on ion exchange resin, and high resolution gamma spectrometry.

R. A. Nadkarni and G. H. Morrison, Department of Chemistry, Cornell University, Ithaca, N.Y. 14850 *Anal. Chem.*, 46, 232 (1974)

Instrumental Neutron Activation Analysis for Mercury in Dogs Administered Methylmercury Chloride: Use of a Low Energy Photon Detector

Instrumental Hg analysis based on ^{197}Hg in central nervous system tissues achieves greater sensitivity and specificity with a thin Ge(Li) low energy photon detector than with a conventional large volume Ge(Li) detector.

Melvin H. Friedman, Eugene Miller, and James T. Tanner, Bureau of Foods, Food and Drug Administration, Washington, D.C. 20204 *Anal. Chem.*, 46, 236 (1974)

\$395

Model 5112-1 single pen recorder with 1, 2, 5, 10 in./min. chart speeds and 10 mv fixed input spans.



\$445

Model 5110-2 single pen recorder with 2, 2.5, 5, 10, 20 cm/min. chart speeds and 5 input spans of 10 mv up.



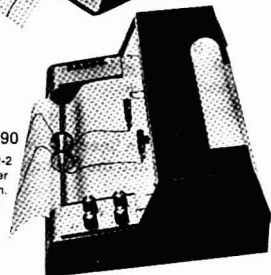
\$595

Model 5212-1 two pen recorder with 1, 2, 5, 10 in./min. chart speeds and 10 mv fixed input spans.



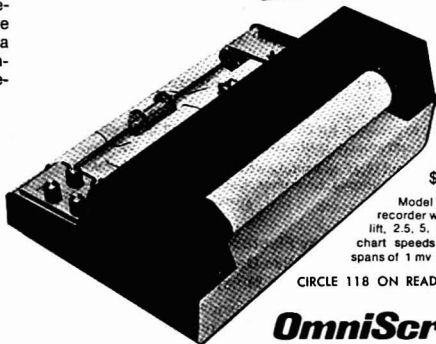
\$690

Model 5212-2 two pen recorder with 1, 2, 5, 10 in./min. chart speeds and 5 input spans of 10 mv up.



\$990

Model 5220-5 two pen recorder with electric pen lift, 2.5, 5, 10, 20 cm/min. chart speeds and 5 input spans of 1 mv up.



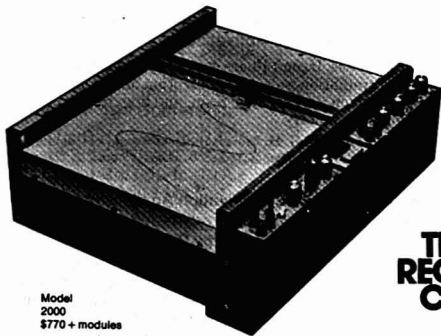
CIRCLE 118 ON READER SERVICE CARD

Here's how you draw the right conclusions:

Omnigraphic[®] *x-y and strip chart recorders*

If you want one pen or two . . . for GC or spectrometry . . . for thermo-couple or strain gauge . . . the Omnigraphic recorder with options will give you a full range of inputs combined with operational conveniences. Consider switching to Omnigraphic recorders . . . built by The Recorder Company.

27-plug-in modules for virtually every laboratory function make this the most versatile recorder



Model 2000 \$770 + modules

OEM DISCOUNTS CIRCLE 119 ON READER SERVICE CARD

OmniScribe[™] *strip chart recorders*

Here's the newest low cost strip chart recorder from The Recorder Company. And when you compare the costs with the performance you'll understand why it pays to buy from a company whose entire resources are devoted to building and servicing the finest laboratory recorders in the world. Mail for your copy of the OmniScribe brochure today.

**THE
RECORDER
COMPANY**

**houston
instrument**

4950 TERMINAL AVENUE, BELLAIRE, TEXAS 77401
(713) 667-7403 CABLE HOINCO TWX 910-881-5782

European Office Rochesterlaan 6 8240 Gistel Belgium
Telephone 059-27445 Telex BAUSCH 19399B

Briefs

Determination of Trace Elements in Coal, Fly Ash, Fuel Oil, and Gasoline—A Preliminary Comparison of Selected Analytical Techniques

The wide range in interlaboratory comparisons for trace elements points out the need for standard reference materials for use in analytical methods evaluation and quality control.

Darryl J. von Lehmden, Robert H. Jungers, and Robert E. Lee, Jr., Quality Assurance and Environmental Monitoring Laboratory, National Environmental Research Center, Research Triangle Park, N.C. 27711 *Anal. Chem.*, 46, 239 (1974)

Ion Electrode Based Enzymatic Analysis of Creatinine

An analytical method for creatinine, based on the use of the enzyme creatinase and an ammonia membrane electrode, is tested.

Huvin Thompson and G. A. Rechnitz, Department of Chemistry, State University of New York, Buffalo, N.Y. 14214 *Anal. Chem.*, 46, 246 (1974)

Serum Protein Monitoring and Analysis with Ion-Selective Electrodes

Potentiometric methods are proposed for the characterization and determination of serum proteins based on the use of a silver sulfide membrane electrode to measure protein-silver ion interactions.

P. W. Alexander and G. A. Rechnitz, Department of Chemistry, State University of New York, Buffalo, N.Y. 14214 *Anal. Chem.*, 46, 250 (1974)

Glass Electrode Responses Interpreted by the Solid State Homogeneous- and Heterogeneous-Site Membrane Potential Theory

The new solid state theory is used to fit experimental sodium, lithium, and hydrogen ion responses of five pH glasses and a sodium-selective glass at temperatures from 6 to 55°C.

Richard P. Buck, John H. Boles, Robin D. Porter, and Jeffrey A. Margolis, The William Rand Kenan, Jr., Laboratories of Chemistry, University of North Carolina, Chapel Hill, N.C. 27514 *Anal. Chem.*, 46, 255 (1974)

Determination of Antimony Using Forced-Flow Liquid Chromatography with a Coulometric Detector

The electrocatalyzed oxidation of Sb(III) is used for the determination in the effluent of a liquid chromatograph. The detection limit for the separation and determination is approximately 1 nanogram.

Larry R. Taylor and Dennis C. Johnson, Department of Chemistry, Iowa State University, Ames, Iowa 50010 *Anal. Chem.*, 46, 262 (1974)

Characterization of Heavy Residual Fuel Oils and Asphalts by Infrared Spectrophotometry Using Statistical Discriminant Function Analysis

Discriminate function analysis of transformed IR measurements yields a more precise method for the characterization of heavy residual products of petroleum and shows excellent promise for their identification.

F. K. Kawahara, J. F. Santner, and E. C. Julian, U.S. Environmental Protection Agency, National Environmental Research Center, Analytical Quality Control Laboratory, Cincinnati, Ohio 45268 *Anal. Chem.*, 46, 266 (1974)

Molecular Interactions of Asphalt: An Infrared Study of the Hydrogen-Bonding Basicity of Asphalt

Asphalts exhibit a strong hydrogen-bonding basicity toward phenol which increases upon air oxidation. Evidence suggests the occurrence of molecular aggregation within asphalt via hydrogen-bonding.

R. V. Barbour and J. C. Petersen, Laramie Energy Research Center, Bureau of Mines, U.S. Department of the Interior, Laramie, Wyo. 82070 *Anal. Chem.*, 46, 273 (1974)

Determination of Total Mercury in Air by Charcoal Adsorption and Ultraviolet Spectrophotometry

Total mercury in air is collected effectively on charcoal, pyrolyzed, purified by amalgamation, and detected by UV absorption. Precision and accuracy is greater than 95% at concentrations of 0.15 to 1.5 $\mu\text{g}/\text{m}^3$.

Frank P. Scaringelli, John C. Puzak, Berne I. Bennett, and Robert L. Denny, Quality Control Branch, Quality Assurance and Environmental Monitoring Laboratory, National Environmental Research Center, Environmental Protection Agency, Research Triangle Park, N.C. 27711 *Anal. Chem.*, 46, 278 (1974)

Notes

Informing Power of a Chromatographic Method and Its Use as a Quality Criterion

Informing power is a more fundamental quantity than resolution and is not limited to two-peak separations.

D. L. Massart and R. Smits, Pharmaceutical Institute, Vrije Universiteit Brussel, 67, Paardenstraat, B-1640 Sint Genesius Rode, Belgium *Anal. Chem.*, 46, 283 (1974)

Thin Layer Chromatographic-Spectrophotofluorometric Analysis of Amphetamine and Amphetamine Analogs after Reaction with 4-Chloro-7-Nitrobenzo-2,1,3-Oxadiazole

Amphetamine is assayed at concentrations of 0.1 $\mu\text{g}/\text{ml}$ blood and 1 $\mu\text{g}/\text{ml}$ urine as a NBD derivative with a precision of about 6% relative standard deviation.

Francois Van Hoof and Aubin Heyndrickx, Department of Toxicology, State University of Ghent, Ghent, Belgium *Anal. Chem.*, 46, 286 (1974)

Rapid, Sensitive Gas-Liquid Chromatographic Screening Procedure for Cocaine

This test employs an acylated derivative and can determine cocaine concurrently with amphetamine and methamphetamine using GLC and an electron capture detector. Sensitivity is 20 ng/ml.

J. W. Blake, R. S. Ray, J. S. Noonan, and P. W. Murdick, Equine Research Center, Ohio State University, Columbus, Ohio 43210 *Anal. Chem.*, 46, 288 (1974)

Dual-Load Porous-Layer Open Tubular Gas Chromatography Columns

Under suitable conditions, dual-load porous-layer tubular columns perform up to 30% better than equivalent single-load columns.

J. G. Nikelly, Department of Chemistry, Philadelphia College of Pharmacy and Science, Philadelphia, Pa. 19104 *Anal. Chem.*, 46, 290 (1974)

Dual wavelength single- and dual-channel capability

Altex means UV detection for liquid chromatography

If you believe you must compromise when choosing a UV detector for liquid chromatography, then let us demonstrate the new Altex Model 151 or 152. These instruments have the sensitivity, features and cell geometry to fit your applications.

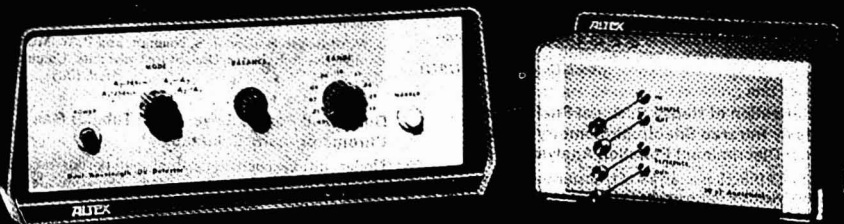
You get dual wavelength capability at 254 nm and 280 nm. Both wavelengths are present at all times in the flow cell and the effluent can be monitored at each wavelength individually or simultaneously. Both detectors feature 0.005 O.D. sensitivity and double beam optics. Analytical, preparative and biochemical flow cells are interchangeable for maximum flexibility. In addition, cell inlets and outlets are made with quick-connect zero dead volume Altex fittings to minimize leaks and bubble formation.

We'll make it easy for you to compare these instruments with any UV detectors on the market. Just contact us for a demonstration in your lab.

ALTEx

SCIENTIFIC INC.

1450 Sixth Street/Berkeley, California 94710/(415) 525-5500



CIRCLE 1 ON READER SERVICE CARD

Briefs

Cryostat for Optical Spectroscopy

Comparison of spectra measured with two different cooling techniques showed that the desired temperature is rapidly and reliably attained only with the gas-flow type device.

J. Szöke and I. Szilágyi, Physical Optics Department, Central Research Institute for Physics, Budapest, Hungary
Anal. Chem., 46, 292 (1974)

Multiclass Linear Classifier for Spectral Interpretation (Pattern Recognition)

A novel approach for using linear classifiers is presented and applied to low resolution mass spectral data. A voting technique is used to interpret the results of a number of binary decisions.

C. F. Bender, Lawrence Livermore Laboratory, University of California, Livermore, Calif. 94550, and B. R. Kowalski, Department of Chemistry, University of Washington, Seattle, Wash. 98195
Anal. Chem., 46, 294 (1974)

Identification of Heroin and Its Diluents by Chemical Ionization Mass Spectroscopy

This procedure requires no sample preparation or prior chromatographic treatment, and its sensitivity permits a direct, rapid identification of microgram quantities of illicit heroin preparations.

Jew-Ming Chao, Richard Saferstein, and John Manura, New Jersey State Police Forensic Science Bureau, West Trenton, N.J. 08625
Anal. Chem., 46, 296 (1974)

Spectrometric Assay of Aldehydes as 6-Mercapto-3-substituted-5-triazolo(4,3-b)-5-tetrazines

A new spectrometric analytical procedure for the assay of low concentrations of formaldehyde (adaptable for use with other aldehydes) in industrial products is described.

N. W. Jacobsen and R. G. Dickinson, Department of Chemistry, University of Queensland, St. Lucia, 4067, Queensland, Australia
Anal. Chem., 46, 298 (1974)

Liquid-Liquid Extraction of Zinc with Aliquat 336-S-I from Aqueous Iodide Solutions

A rapid quantitative method for extracting zinc ions from iodide solutions is described. An extraction method for separating Cd and Zn is also presented.

Curtis W. McDonald and Thornton Rhodes, Department of Chemistry, Southern University, Baton Rouge, La. 70813
Anal. Chem., 46, 300 (1974)

Rapid Determination of the Nitrogen Content of Cellulose Nitrate and Other Nitrate Esters by Means of a Modified Devarda Method

Use of the modified Devarda method described reduces analysis time compared to the classical method. Absolute standard deviation is 0.03%.

J. G. M. M. Smeenk, Technological Laboratory, The Netherlands Organization for Applied Scientific Research TNO, Rijswijk (Z.H.), The Netherlands
Anal. Chem., 46, 302 (1974)

Consecutive Titration of Calcium and Magnesium in Ethanol-Water Mixture

A titrimetric method for the determination of Ca and Mg with EGTA in 80% ethanolic solution is described. In the range 0.2-2 mg, the error does not exceed 1% in Ca and 2.5% in Mg.

Bo Wallén, Department of Analytical Chemistry, University of Uppsala, S-751 21 Uppsala 1, Sweden
Anal. Chem., 46, 304 (1974)

Solvent Extraction Studies of Chromium(III) with Tri-*n*-octylamine

Separation of other transition metal ions from Cr(III) is achieved based upon the slow rate of formation of the Cr(III) complex.

B. E. McClellan, M. K. Meredith, Ray Parmalee, and J. P. Beck, Department of Chemistry, Murray State University, Murray, Ky. 42071
Anal. Chem., 46, 306 (1974)

Selective Separation and Concentration of Silver via Precipitation Chromatography

At the ppb level, silver ions are selectively separated and concentrated by coating a support with a long chain acetylenic phase. Recoveries are good and sample handling is minimal.

William P. Zeronsa, Gregory Dabkowski, and Sidney Siggia, Department of Chemistry, University of Massachusetts, Amherst, Mass. 01002
Anal. Chem., 46, 309 (1974)

Determination of Total Cyanide in the Presence of Palladium

Cyanide in Pd-containing solutions and Pd(CN)₂ is determined by complexing the Pd with mercaptoacetic acid, distilling, and determining the cyanide iodometrically. The procedure appears applicable to other acid-stable cyanides.

George W. Latimer, Jr., L. Ruth Payne, and Marguerite Smith, PPG Industries, P.O. Box 4026, Corpus Christi, Texas 78408
Anal. Chem., 46, 311 (1974)

Sampling Variance in Analysis for Trace Components in Solids. Preparation of Reference Samples

The relation between sampling error and amount of sought-for substance, particle size, and particle composition is treated statistically for particulate solids.

W. E. Harris and Byron Kratochvil, Department of Chemistry, University of Alberta, Edmonton, Alberta, Canada
Anal. Chem., 46, 313 (1974)

New Method for Calibration of Permeation Wafer and Diffusion Devices

A permeation wafer device, capable of being calibrated by a pressure technique in 1 day at permeation rates as low as 5 ng/min is designed for noncondensable and condensable gases.

Russell N. Dietz, Edgar A. Cote, and James D. Smith, Department of Applied Science, Brookhaven National Laboratory, Associated Universities, Inc., Upton, N.Y. 11973
Anal. Chem., 46, 315 (1974)

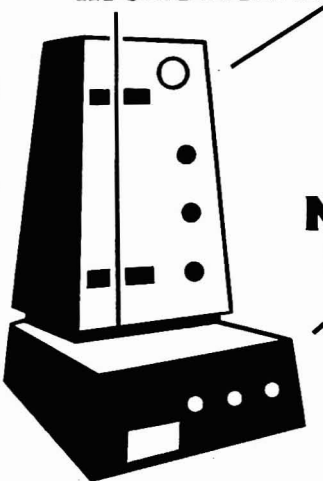
The first \$4500 dual-purpose LC

**Analytical/preparative
in one instrument**

**Research
performance**

Low cost

**Modular
design**



The DuPont 841.

The new Du Pont 841 Liquid Chromatograph fills the need for a research instrument, capable of performing both analytical and preparative work, without sacrificing performance for price.

An extremely versatile performer, the 841 LC features a high-pressure pumping system with a wide range of flow rates, allowing both analytical and preparative work with the same instrument. Yet this kind of dual-purpose versatility costs only \$4500.

The 841 LC is the ideal instrument for people just getting into liquid chromatography, for quality control applications,

and for university labs where it can handle basic research and instructional works. And modular design allows for add-on capabilities.

Before you buy a liquid chromatograph, at any price, check into all that the Du Pont 841 LC has to offer. For complete information, write Du Pont Company, Room 23885, Wilmington, DE 19898.

Offices in major U.S. cities and Frankfurt, (Friedberg), London, (Hitchin), Toronto, Paris, Milan, Mexico City, Caracas and São Paulo.

DU PONT Instruments
REG. U.S. PAT. OFF.

Visit DuPont Instrument Booth (122-131)
at the Pittsburgh Conference

CIRCLE 60 ON READER SERVICE CARD

Briefs

Correspondence

Self-Reversal in a Copper Pulsed Hollow Cathode Lamp

G. J. DeJong and E. H. Piepmeier, Department of Chemistry, Oregon State University, Corvallis, Ore. 97330
Anal. Chem., 46, 318 (1974)

Aids for Analytical Chemists

Relay Circuit for Integrating a Gas-Liquid Chromatography Temperature Programmer with an Automatic Sample Injector

H. A. McLeod, Ronald Bolohan, and Maarten Van Dyk, Food Research Laboratories, Health Protection Branch, Department of National Health and Welfare, Ottawa, Ontario
Anal. Chem., 46, 320 (1974)

Simple Method for Continuous Monitoring of Electrode Rotation Rate

Ira B. Goldberg, Richard S. Carpenter II, and W. F. Goepfinger, Science Center, Rockwell International, Thousand Oaks, Calif. 91360
Anal. Chem., 46, 321 (1974)

Device for the Accurate Electronic Measurement of Microliter Sample Volumes

L. R. Layman and G. M. Hieftje, Department of Chemistry, Indiana University, Bloomington, Ind. 47401
Anal. Chem., 46, 322 (1974)

Analysis of Background Copper Concentration in Sea Water by Electron Spin Resonance

Y. P. Virmani and E. J. Zeller, Radiation Physics Laboratory, Space Technology Center, University of Kansas, Lawrence, Kansas 66044
Anal. Chem., 46, 324 (1974)

Device to Seal Ends of Gas Chromatography Columns with a Filter Disk

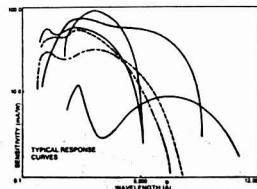
Francis W. Karasek, Department of Chemistry, University of Waterloo, Waterloo, Ontario, Canada
Anal. Chem., 46, 325 (1974)

Teflon Apparatus for Vapor Phase Destruction of Silicate Materials

J. W. Mitchell and D. L. Nash, Bell Laboratories, Murray Hill, N.J. 07974
Anal. Chem., 46, 326 (1974)



Hamamatsu produces photomultiplier tubes so you don't have to make mechanical or electrical changes when you want to change window material or spectral responses. Side-on tubes with standard 11-pin bases are available in the spectral responses shown. Windows are available in UV glass, fused silica or borosilicate. Cathode materials include bialkali, multialkali and GaAs as well as solar blind and S-1. The same is true for end window detectors. For new design requirements, replacement or upgrading, Hamamatsu tubes show they are different where it counts—on the inside. **Call or write for free catalog on our complete line.**



Only Hamamatsu makes a full line of interchangeable detectors.

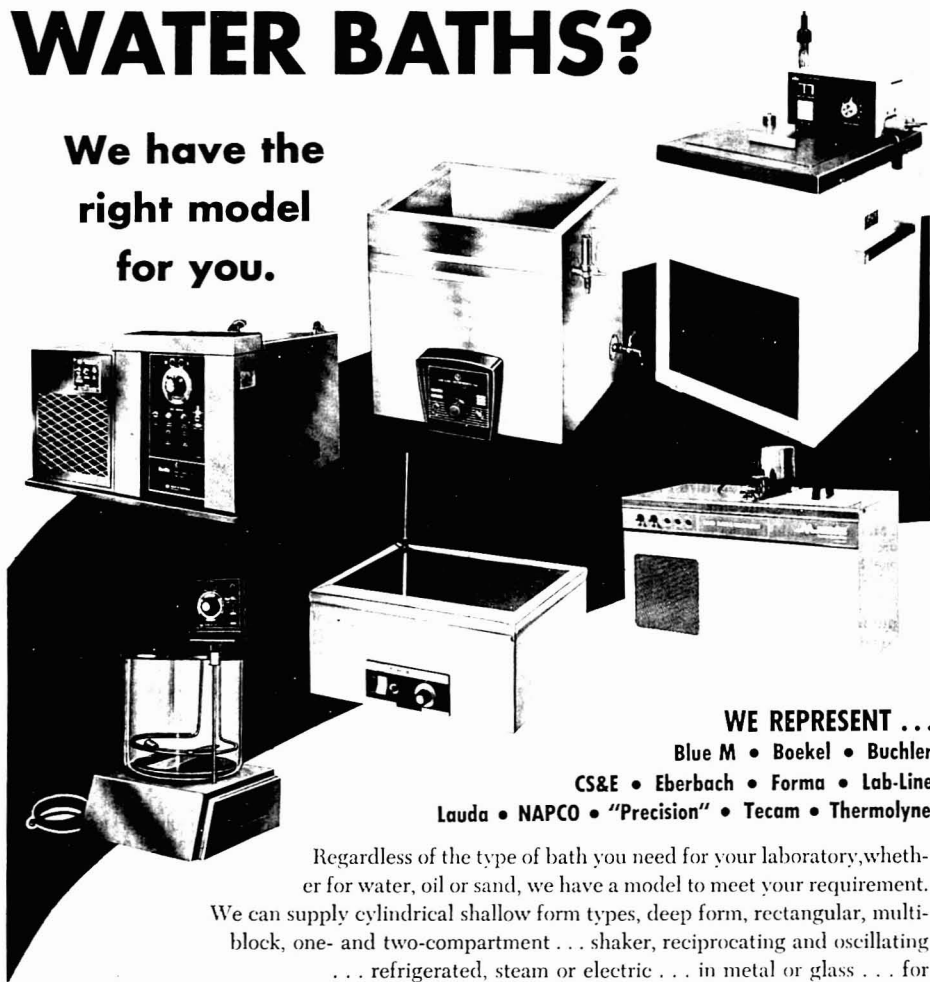
HAMAMATSU CORPORATION

120 Wood Avenue
Middlesex, New Jersey 08846
(201) 469-6640

CIRCLE 115 ON READER SERVICE CARD

WATER BATHS?

We have the
right model
for you.



WE REPRESENT . . .

Blue M • Boekel • Buchler
CS&E • Eberbach • Forma • Lab-Line
Lauda • NAPCO • "Precision" • Tecam • Thermolyne

Regardless of the type of bath you need for your laboratory, whether for water, oil or sand, we have a model to meet your requirement. We can supply cylindrical shallow form types, deep form, rectangular, multi-block, one- and two-compartment . . . shaker, reciprocating and oscillating . . . refrigerated, steam or electric . . . in metal or glass . . . for such tests as controlled temperature incubations, stability, aging, serological, paraffin tissue section, etc. We also have a variety of circulating systems for converting suitable containers into efficient, closely controlled water baths. In addition to water baths and circulating systems, we stock over 30,000 other items. So whether you are in the market for a simple little test tube or a sophisticated laboratory instrument, we can meet your requirement. *Ask us for literature.*

SGA
SCIENTIFIC
BLOOMFIELD, N. J. 07003



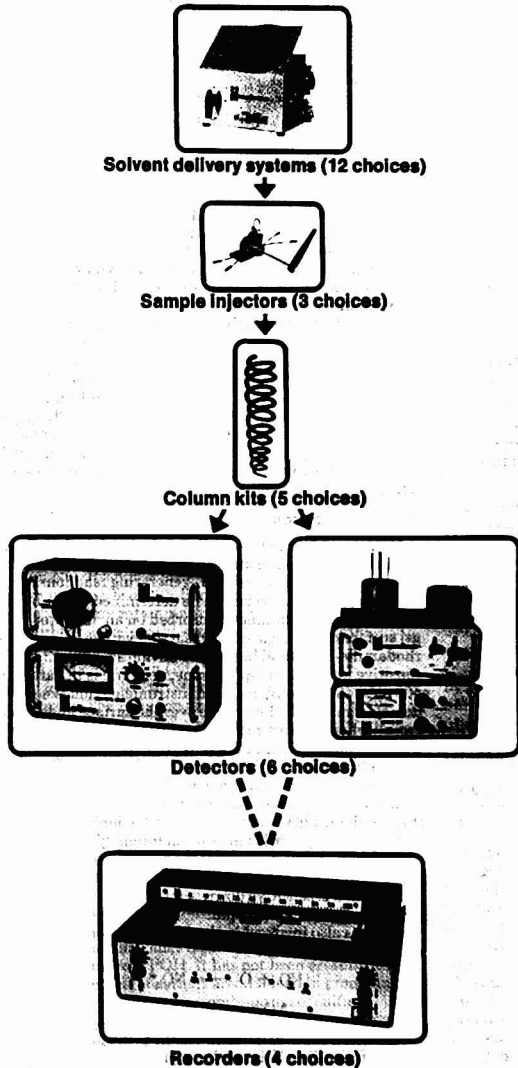
LABORATORY . . .
♦ APPARATUS
♦ INSTRUMENTS
♦ CHEMICALS
♦ GLASSWARE

Branches: Boston Mass. • New Haven Conn. • Elk Grove Village Ill. • Fullerton Calif. • Philadelphia Penna. • Silver Spring Md. • Syracuse N. Y.

CIRCLE 218 ON READER SERVICE CARD

LDC doesn't build the best LC —but LDC's customers do.

LDC "building blocks" for liquid chromatographers*



*Space permits us to show only a few of the LDC modular LC components now available. Why not find out about all of them?

They do it with Laboratory Data Control's *modular components*.

No single liquid chromatograph can fill all the many different needs of the many different liquid chromatographers. But with the LDC modular "building block" approach to high-speed, high-pressure LC, you can select the components that exactly fit your requirements today and still permit expansion of capabilities next year.

Only LDC gives you a choice of 12 solvent delivery systems (pressures up to 3,000 psi). And 3 sample injectors. And 5 column kits. And 6 LC detectors based upon four different principles (uv absorption, differential refractive index, electrolytic conductivity, fluorescence). And 4 strip chart recorders (both single and dual pen models).

Result: 4,320 possible LC combinations. Or select individual LC modules. Either way, you get exactly what you need. You don't waste money on equipment you won't use. And you don't lose time hunting for the right parts.

Any LDC module is compatible with most other manufacturers' LC equipment. Installation's simple—three Swagelok fittings at most. We can demonstrate performance on the same day you receive the components. It's easy to add or remove LDC modules in a "building block" LC. Since they're separately removable, maintenance does not require a field service engineer.

An LDC specialist will be glad to discuss your LC instrument needs with you. No obligation. Call or write us now. You'll see how little it costs to have customized LC—and how much it pays.



**LABORATORY
DATA CONTROL**
P.O. Box 10235, Interstate
Industrial Park, Riviera Beach,
Florida 33404. (305) 844-5241

A Division of Milton Roy Company

CIRCLE 158 ON READER SERVICE CARD

Chemiluminescence and Bioluminescence

W. Rudolf Seltz and Michael P. Neary

Department of Chemistry, University of Georgia,
Athens, Ga. 30602

Light accompanying a chemical reaction is known as chemiluminescence (CL). CL that occurs in a living system or is derived from one is known as bioluminescence (BL). Three conditions are required for CL to occur: The chemical reaction must release sufficient energy to populate an excited energy state; the reaction pathway must favor the formation of excited state product; and the excited state product must be capable of emitting a photon itself or transferring its energy to another molecule that can emit.

The efficiency of CL, ϕ_{CL} , can be defined:

$$\phi_{CL} = \frac{\text{number (or rate) of photons emitted}}{\text{number (or rate) of molecules reacting}}$$

It is equal to the efficiency of excited state production (number molecules going to excited state/number molecules reacting) times the efficiency of emission (number of photons emitted/number of molecules in excited state). The highest efficiencies are observed for BL. The firefly reaction has an efficiency close to unity. For nonbiological CL, ϕ_{CL} rarely exceeds 0.01 even for the brightest reactions.

CL reactions can be used for chemical analysis by adjusting concentrations so that the CL intensity, I_{CL} , is related to the concentration of the reactant to be determined. At any time, t , I_{CL} is given by the expression:

$$I_{CL}(t) \left(\frac{\text{photons}}{\text{sec}} \right) = \phi_{CL} \left(\frac{\text{photons}}{\text{molecule reacting}} \right) \frac{dc(t)}{dt} \left(\frac{\text{molecules reacting}}{\text{sec}} \right)$$

where $dc(t)/dt$ is the reaction rate for the starting material forming an electronically excited state. I_{CL} can be measured as a function of time (kinetic analysis), or it can be integrated for a known time period. For chemical analysis, a convenient means of performing the integration is to carry out the reaction in a flow system observing steady-state CL intensity.

CL and BL offer three important advantages for chemical analysis:

CL and BL methods are extremely sensitive because it is easy to measure low levels of light emission. It is possible to calculate theoretical detection limits for CL and BL methods from ϕ_{CL} and the capability of modern instrumentation to measure low light levels. In practice, however, sensitivity is usually limited by reagent purity, rather than by light-measuring capability.

The only apparatus required for CL analyses is a light detector, a system to mix the reactants, and in some cases a filter to resolve the CL of interest from other sources of light. Because of the high intrinsic sensitivity of CL methods, the light detector often does not need to be particularly sensitive.

For many of the available CL and BL reactions, response is linearly proportional to reactant concentration over several orders of magnitude.

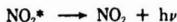
The first section of this article describes some CL reactions that have been applied analytically, and the second section deals with BL methods. The number of CL and BL methods is small because of a lack of available reactions. However, those methods that have been developed are quite successful because of the unique advantages of CL.

Chemiluminescence

Ozone and Nitric Oxide. Recently developed methods for atmospheric ozone and nitric oxide provide a good example of the advantages of CL-generating reactions for chemical analysis. Ozone can be determined either by its reaction with rhodamine-B adsorbed on an activated silica gel surface or by its gas-phase reaction with ethylene. The rhodamine-B method has all the advantages of CL: it is sensitive to less than 1-ppb ozone, response is linear up to 400 ppb, and the only required instrumentation is a gas flow system to pull the sample over the surface and a photomultiplier to measure CL intensity. The only problem with this method is that the sensitivity of the CL surface changes with time as rhodamine-B is consumed in the reaction, thus necessitating frequent recalibration.

Analysis based on the ozone-ethylene reaction avoids this problem. This reaction produces CL emissions in the 300-600-nm region with maximum intensity close to 435 nm. Like the rhodamine-B reaction, this reaction is specific for ozone so that no optical resolution is required. The method is sensitive down to 0.003-ppm ozone, and response is linear up to 30 ppm.

Ozone is also involved in the determination of NO by use of the CL reaction:



CL emission is a continuum from 0.6 to 3.0 μ . In the presence of excess O_3 , CL intensity is proportional to NO concentration. Greatest sensitivity is obtained at reduced pressure because of quenching effects at higher pressures. Nevertheless, ambient NO concentrations can be measured at atmospheric pressure. At reduced pressure with a

in Chemical Analysis

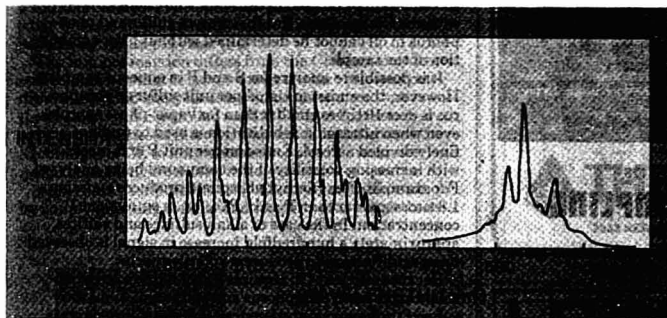


Figure 1. Chemiluminescence spectra for S_2 (left) and POH (right) recorded while aspirating aqueous SO_2 and phosphoric acid, respectively, in hydrogen-nitrogen diffusion flame

cooled photomultiplier tube, this method can detect 0.001-ppm NO. Response is linear up to 10,000 ppm, a linear dynamic range of 10^7 . Because ozone reacts with other atmospheric contaminants to generate CL, a cutoff filter absorbing wavelengths shorter than 600 nm is included in NO monitors.

Total oxides of nitrogen ($NO + NO_2$) can be determined by reducing NO_2 to NO with carbon before reacting with ozone. The NO_2 concentration is equal to the difference between total oxides of nitrogen and NO concentration.

The instrumentation used for CL in air pollution monitors is described in detail in the April 1973 Instrumentation feature of *Analytical Chemistry*.

Sulfur and Phosphorus. Gas-phase CL can also result from the recombination of species generated in a flame. The most important analytical applications of flame CL have been to determine sulfur and phosphorus by observing the molecular emission that occurs when sulfur and phosphorus compounds are burned in a hydrogen-rich flame.

The sulfur emission comes from S_2 molecules, whereas phosphorus comes from POH. It has not been established exactly what chemical reactions are involved in producing CL. For sulfur, it may be the recombination of sulfur atoms, whereas for phosphorus, CL may come from the reaction between hydrogen atoms and PO.

Figure 1 shows the CL spectra for both S_2 and POH. For analytical applications the peak emission bands at 394 nm for sulfur and 526 nm for phosphorus can be resolved by use of interference filters. Sulfur and phosphorus can be detected simultaneously with two detection channels,

each with the appropriate filter. Because two sulfur atoms are required to produce one excited molecule, CL intensity is proportional to the sulfur concentration squared.

The potential advantages of CL are not all realized when a flame is required to generate the reactants. Emission from the flame itself produces a background signal that limits sensitivity. This background can be reduced by shielding the flame. When the shield separates the burned gases above the flame from the outside air, CL from the recombination reactions is observed well above the flame itself. Thus, the CL can be viewed by the detector without looking directly at the flame.

Maximum efficiency for S_2 and POH CL is observed at temperatures below 400°C. This limits the temperature of the flame used to generate the reactive species. A hydrogen-oxygen flame is too hot and must be diluted with nitrogen to reduce the temperature. Hydrogen-air flames are satisfactory. Shielding of the flame helps to reduce the temperature of the burned gases and permits the use of hotter flames. Flame temperatures up to 1400°C have been achieved while maintaining efficient CL.

Flame CL analysis for phosphorus and sulfur works best with vapor-phase samples. Commercial detectors are available that use flame CL to selectively detect sulfur- and phosphorus-containing compounds as they elute from a gas chromatograph. They are sensitive down to minimum detectable levels of 0.04 ng of P and 0.2 ng of S. Response is linear up to 300 ng of P, and the square root of response is linear up to 100 ng of S. This application is discussed in more detail in the December 1973 Report in *Analytical Chemistry*.

With liquid-phase samples introduced as aerosols to the

EXTEND SEPTUM LIFE...

AND PREVENT
BENT NEEDLES

SEPTUM NEEDLE GUIDE

Precision Sampling's needle guide has proven effective in lengthening septum life. Provides a single pierced hole for injection rather than multiple torn jagged openings. Repetitive use (50 injections) of a single pierced hole has withstood leakage tests to 100 psi. Plus.....

- [] Effectively guides needle to prevent bending
- [] "Cool" needle entrance, eliminating premature flashing
- [] Spacer for repetitive needle penetration depth
- [] Assists in pushing out old septum, convenient holder of hot septum caps.

Easily mounts on any conventional chromatograph inlet. Save time...effort...money...with our Septum Needle Guide today.

Catalog Number 450050 \$7.50

PS

Telephone (504) 927-1128

PRECISION SAMPLING CORPORATION

P. O. BOX 15119 BATON ROUGE, LOUISIANA 70815
CIRCLE 201 ON READER SERVICE CARD



Accuracy...Precision... and Low Cost...

This Microsyringe Has It All!

Our new Series C-160 Pressure-Lok micro-syringe was designed with one goal in mind - to deliver excellent reproducibility and long life at minimum cost. It's every bit as precise as our more expensive syringes, and its design is clean and basic, to save you money. The C-160 has the following special features:

1. Teflon Plunger Tip - leak-free to 250 psi.
2. No Plunger Freeze-Up - the Teflon tip is self-lubricating and inert. It can't stick, it stays leak-tight, and there's never a gummy build-up around the plunger.
3. Fixed needle, 26 ga. x 2", with hollow-ground point, for longer septum life.
4. Four Popular Sizes - *1 T M D. P. 201*
 - No. 160022 (10.0 ul)
 - No. 160023 (25.0 ul)
 - No. 160024 (50.0 ul)
 - No. 160025 (100.0 ul)

ONE LOW PRICE - \$12.00

PS

PRECISION SAMPLING CORPORATION

P. O. BOX 15119 BATON ROUGE, LOUISIANA 70815
PHONE 504-927-1128
CIRCLE 202 ON READER SERVICE CARD

Table I. Analytical Applications of Sulfur and Phosphorus Flame Chemiluminescence

Analysis	Performance
Sulfur- and phosphorus-containing gas chromatography effluents	Detection limits: 0.2 ng sulfur; 0.04 ng phosphorus
Sulfur-containing air pollutants	Detection limit: 5 ppb; H ₂ S, CH ₃ SH, and SO ₂ can be resolved by gas chromatography
Sulfur in petroleum products	Detection limit: 0.5 ppm; requires combustion of sample
Phosphorus in detergents	Detection limit: 1.2 ppm; greater accuracy with prior ashing
Phosphorus in water	Detection limit: 0.003 ppm; measures dissolved phosphorus only

hydrogen-rich flame, there are several problems. Organic solvents cannot be used because they interfere directly with the CL reactions. For this reason, sulfur and phosphorus in oil cannot be determined without prior combustion of the sample.

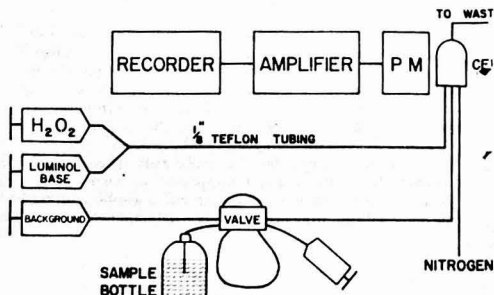
It is possible to analyze for S and P in aqueous samples. However, the emission signal per unit sulfur or phosphorus is over 10 times smaller than for vapor-phase samples, even when ultrasonic nebulization is used to produce a finely divided aerosol. Emission per unit P or S increases with increasing volatility of the compound being analyzed. For example, P as triethyl phosphate produces emission 1.8 times greater than P as H₃PO₄ for an equivalent P concentration. In the case of alkali sulfides and sulfites, approximately a hundredfold increase in signal is observed upon acidification to produce a volatile species.

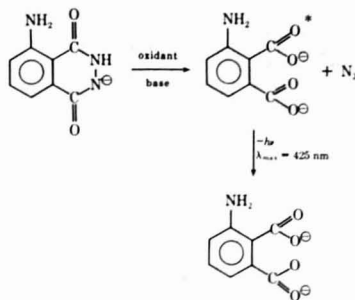
Because efficient CL requires a cool flame even when shielding is used, phosphorus and sulfur emissions are subject to chemical interferences. All metal ions depress emission intensity to a greater or lesser extent because the flame does not possess sufficient energy to break up the salt particles that form in the flame as the aerosol dries. Prior to an analysis, metal ions need to be removed by treatment with an ion-exchange resin.

Table I lists some applications of flame CL analysis for P and S. Gas-phase analysis of P- and S-containing GC effluents and sulfur-containing air pollutants has been much more widely applied than analysis of aqueous samples. However, improvements in sensitivity by using ultrasonic nebulization of aqueous samples may increase use of flame CL for solution analysis.

Luminol. The oxidation of luminol (5-amino-2,3-dihydrophthalazine-1,4-dione) in basic solution is one of the best known and most efficient CL reactions. The CL spectrum matches the fluorescence of the amino-phthalate oxidation product:

Figure 2. Diagram of flow system for making steady-state chemiluminescence measurements





The most frequently used oxidant is hydrogen peroxide in the presence of a catalyst such as $\text{Fe}(\text{CN})_6^{-3}$, $\text{Cu}(\text{II})$, and $\text{Co}(\text{II})$. Other CL-generating oxidants include hypochlorite, iodine, permanganate, and oxygen in the presence of a suitable catalyst. The optimum pH for CL varies somewhat with catalyst and oxidant. Most oxidizing systems have an optimum pH close to 11.

The luminal reaction differs from the CL reactions discussed above in that it occurs under a wide variety of conditions. Specific analysis using luminal requires that the chemistry be controlled so that CL is proportional only to the species of interest. This extends the unique advantages of CL to a wide variety of possible analyses rather than being restricted to only a couple of species.

Apparatus. It is possible to do CL analysis with luminal by simply injecting sample and reagents into a sealed con-



Figure 3. Typical data using flow system for chemiluminescence measurements. Peaks are for slugs of $\text{Cr}(\text{III})$ passing through cell
 Conditions: $10^{-3} \text{ M H}_2\text{O}_2$; 10^{-3} M luminal; $10^{-4} \text{ M KOH-H}_2\text{BO}_3$ buffer; pH 10.5; peak 2 = $2.0 \times 10^{-4} \text{ M}$ $\text{Cr}(\text{III})$; peak 4 = $4.0 \times 10^{-4} \text{ M}$ $\text{Cr}(\text{III})$; peak 6 = $6.0 \times 10^{-4} \text{ M}$ $\text{Cr}(\text{III})$

QUALITY LABORATORY APPARATUS muffle furnace



- FAST HEAT-UP
- SAFE DOOR DESIGN
- LARGE, EASY TO READ PYROMETER
- PLUG-IN PORTABILITY

TYPE 1400
PRICE \$170.00

$3\frac{1}{2}$ " dual-scaled indicating pyrometer . . . positive control of working temperatures up to 1900°F (1038°C) . . . reaches 1600°F in 40 minutes . . . safe and cool latch mechanism glides door to the open position forming a handy work shelf . . . compact . . . only 26 lbs. . . . plugs in anywhere . . . quality built for trouble-free service life. For details write to:



THERMOLYNE

SYBRON CORPORATION

2555 KERPER BOULEVARD, DUBUQUE, IOWA 52001

CIRCLE 227 ON READER SERVICE CARD

LOW FLOW INSTRUMENT PRESSURE REGULATORS

IR400 SERIES-20LPM

IR500 SERIES-5LPM

FEATURES:

- Corrosive or non-corrosive high purity service
- 316 stainless steel or brass construction
- Teflon lined 301 stainless steel diaphragm and Kel-F seat
- Max. inlet pressure: 3000 psig
- Adjustable outlet ranges: 0-30, 0-100, 0-300, 0-500 psig



VERIFLO
CORPORATION

VERIFLO CORPORATION
INSTRUMENT DIVISION

250 Canal Blvd., Richmond, CA 94804
(415) 235-9590

CIRCLE 244 ON READER SERVICE CARD

Jarrell-Ash does it again!

Spectroscopic versatility unequaled in Direct Readers.

137,000 12-bit words of Random Access memory provides:

- 300 working curves and 75 matrices on one disk and many more with 3-second disk interchange
- Individual preburn and exposure times for each channel
- Interelement corrections
- Automatic spectrum line changes for hi-lo concentrations
- Single and double point standardization
- System tells you what standards to use for every matrix
- Automatic white light test with COV's calculated, plus diagnostic tests on system modules
- Power failure safeguard

Computer control of system provides:

- Dynamic range up to 400,000 counts in 10-second exposure
- Greater reliability and fewer electronic components
- The user with remarkable ease of operation

Versatile-Reliable-Simple...

... Our 90-750 Atom Comp[®] with random access disk is also very reasonably priced.



Jarrell-Ash Division
590 Lincoln Street
Waltham, Mass. 02154

A division of Fisher Scientific Company



25th consecutive Pittsburgh Conference Exhibitor

CIRCLE 141 ON READER SERVICE CARD

Table II. Analytical Characteristics of Some Metal Ions That Catalyze Luminol Chemiluminescence*

Cat- alysts	Approx detection limit, M	Linear range, M	Remarks
Co(II)	10 ⁻¹¹	10 ⁻¹¹ –10 ⁻⁷
Cu(II)	10 ⁻⁹	Nonlinear
Ni(II)	10 ⁻⁸	10 ⁻⁸ –10 ⁻⁶
Cr(III)	10 ⁻⁹	10 ⁻⁹ –10 ⁻⁶
Fe(II)	10 ⁻¹⁰	10 ⁻¹⁰ –5 × 10 ⁻⁷	Catalyst with oxygen
Mn(II)	10 ⁻⁸	Requires amines to be a catalyst

* The data for Fe(II) were obtained by use of oxygen to stir the CL cell. All the other catalysts are effective only with H₂O₂. The conditions were 10⁻⁴M H₂O₂, 10⁻⁴M luminol, 10⁻³M KOH–H₃BO₃ buffer and cell pH between 10 and 11.

Table III. Analytical Characteristics of Some Oxidants That React with Luminol to Produce Chemiluminescence

Oxidant	Approx detection limit, M	Linear range, M	Remarks
OCl ⁻	10 ⁻⁹	Requires O ₂
I ₂	10 ⁻⁹	10 ⁻⁹ –3 × 10 ⁻⁷	Second- and third-order response also observed
MnO ₄ ⁻	10 ⁻¹⁰	10 ⁻¹⁰ –10 ⁻⁷	No O ₂ needed
H ₂ O ₂	10 ⁻⁹	Excess Cu(II) catalyst

tainer surrounded by photographic film and measuring film exposure as a function of concentration. Alternatively, a stopped-flow spectrophotometer can be used to measure CL vs. time-after-mixing. However, for chemical analysis there are several advantages to performing the reaction in a flow system like that diagrammed in Figure 2. "Background" solution, usually the solvent of the analyte, is mixed with reagents in a cell positioned in front of a photomultiplier which measures CL intensity. This provides a reference level of light emission characteristic of the background solution. Slugs of samples are inserted into the background flow line with a sampling valve. As a slug of sample (catalyst or oxidant) passes through the cell, steady-state CL is observed with intensity proportional to sample concentration. Typical data are shown in Figure 3. The advantages of this system are: Background light emission from reagents provides a continuous reference level of CL rather than having to be subtracted out as a blank; the data come out in the form of peaks; a flow system can be readily adapted to continuous analysis, or if necessary it can be used as a detector for a chromatographic column; and the sample can be maintained at any pH in any electrolyte until it enters the cell as long as it does not conflict with the requirement of a basic pH for luminol CL.

Either overhead stirring or gas bubbling can be used to mix the reactants in the cell. Gas bubbling makes it possible to use a gas as a reactant and has been successfully used for luminol oxidizing systems involving oxygen. However, overhead stirring reduces the noise level observed on steady state CL.

Analytical Performance. Table II lists some catalysts of luminol oxidation along with their analytical characteristics. The advantages of CL are apparent. Response is sensitive and linear over several orders of magnitude for most metals tested. The detection limits in Table II are imposed by background CL that is over two orders of magni-

tude greater than the PM dark current. Reagent purification should lead to even lower levels of detection.

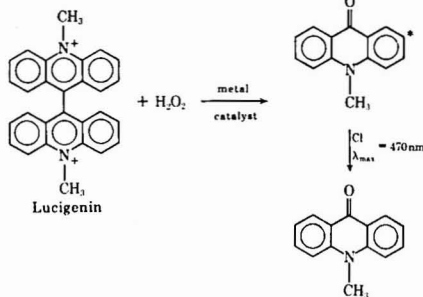
Table III lists oxidants that can be determined by use of the luminol reaction along with their analytical characteristics. In the absence of peroxide, background CL is about 100 times less. Therefore, CL intensities are about 100 times less than for the catalyst systems in Table II for equivalent detection limits.

Indirect analysis based on luminol CL is also possible. For example, CL can be used to determine complexing agents by measuring the extent to which they solubilize metal ions from insoluble metal salts. Since several of the oxidants in Table III are commonly used as titrants, luminol CL can be used to follow oxidant concentration as a function of the quantity of oxidant added to a sample. This extends CL analysis to species that do not directly interact with luminol. Table IV lists analytical applications of luminol CL. Some of these applications have already been demonstrated, whereas others are feasible on the basis of present data. The chemical basis for obtaining selectivity for a particular species is included in the table.

Other CL Reactions. The CL reactions discussed above all have demonstrated analytical application. Several other CL reactions appear to have potential analytical applications but require further developmental work.

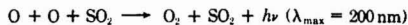
Ozone Reactions. Ozone reacts with a variety of compounds in the gas, liquid, and solid phases to generate CL. For example, the rhodamine-B method for ozone could be turned around to measure rhodamine-B concentration, and the ethylene-ozone reaction could be used to measure ethylene and other olefins. Since CL spectra are a function of olefin structure, it might be possible to use CL to characterize types of olefins.

Lucigenin. Lucigenin is similar to luminol in that it chemiluminesces upon oxidation by peroxide in basic solution in the presence of metal ion catalysts.



However, it has been reported in the Russian literature that lucigenin CL is catalyzed by Pb(II), Bi(III), Tl(III), and Hg(II), none of which catalyze luminol CL. If this is correct, then the lucigenin reaction could provide the basis for analytical applications not possible with luminol.

O Atom Reactions. Oxygen atoms undergo several gas-phase CL reactions that could be applied to trace air pollutant analysis. For example:



is sensitive down to 0.001 ppm SO₂.



QUALITY LABORATORY APPARATUS

maxi-mix



**SUPERIOR
VORTEX
MIXING
ACTION**

MODEL NO. M 16715
UNIT PRICE \$75.00

The new Maxi-Mix is the most efficient means yet devised for fast, thorough vortex mixing. Four or more test tubes can be mixed simultaneously. Top-mounted pushbutton on-and-off switch is operated by light touch of finger or test tube; variable mixing action is inherent in the resiliency of the replaceable foam rubber top.

Write for new Bio-Medical Apparatus Catalog #100



THERMOLYNE
SYBROK CORPORATION

2555 Kerper Blvd., Dubuque, Iowa 52001

CIRCLE 228 ON READER SERVICE CARD

MICROBALANCES

Fully automatic.

MICROBALANCES

Easy operation.

MICROBALANCES

Digital readout.

MICROBALANCES

**Instrument Division,
Perkin-Elmer Corp.,
Main Avenue,
Norwalk, Conn. 06856.**

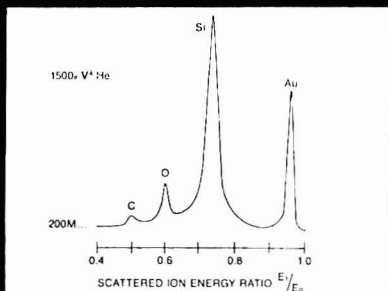
PERKIN-ELMER

CIRCLE 195 ON READER SERVICE CARD

3M BRAND ION SCATTERING SPECTROMETER



for an in-depth look
into your
SURFACE PROBLEMS



ISS surface spectrum from a partial film of Au on a Si wafer. Note the carbon and oxygen contaminants.

EXCLUSIVE ISS FEATURES INCLUDE—

- First atomic layer sensitivity
- Detection of all elements above helium
- Intrinsic composition depth-profile analyses
- Direct examination of insulating surfaces (without disturbing surface charging)
- Semi-quantitative output

The 3M Brand ION SCATTERING SPECTROMETER has been successfully applied to a large number of surface problems . . . quite possibly a problem similar to yours. For an immediate answer or for more information, call or write:

Ion Scattering Spectrometry
3M Company
3M Center, Bldg. 209-BS
St. Paul, Minnesota 55101
(612) 733-6596

See us at the Pittsburgh Conference, Booth 1236-38
CIRCLE 173 ON READER SERVICE CARD

Table IV. Some Analytical Applications of Luminol Chemiluminescence

Type of analytes	Application	Basis for selectivity
Single catalyst	Fe(II) in water	Different oxidation potential from other catalysts of luminol oxidation by oxygen
	Cr(III) in water	EDTA used to quench other catalysts; Cr(III)-EDTA is kinetically slow to form
Multiple catalyst	Cu, Ni, Co, etc.	CL detection combined with ion-exchange separation
Organic analysis by measuring catalyst solubilization	Complexing agents in natural waters	Ion-exchange separation
Oxidant	Chlorine in waste water	Only CL-generating species present
	Protein-bound iodine	Different oxidation potential from other oxidants
Titrations	H ₂ O ₂ generated by oxidase enzymes	Only CL-generating species present
	SO ₂ in air titrated with I ₂	Selective collection of SO ₂
	Arsenic titrated with I ₂	Distillation of AsCl ₃

Table V. Luciferin-Luciferase Sources

Firefly	<i>Photinus</i>
	<i>Photuris</i>
	<i>Luciola</i>
Ostracod crustacea	<i>Cypridine</i>
	<i>Pyrocypria</i>
Bacteria	<i>Achromobacter fischerii</i>
	<i>Photobacterium fischerii</i>
Protozoa (dino flagellate)	<i>Gonyaulax polyedra</i>
Sea pansy	<i>Renilla reniformis</i>
Jellyfish	<i>Aequorea</i>

is an alternate method for NO which would have the advantage of producing emission partly in the visible, therefore requiring a less expensive photomultiplier tube. The problem in developing these and other methods is the lack of a suitably stable source of O atoms.

Flame CL. When NO or NO₂ is introduced into a hydrogen-rich oxy-hydrogen flame, CL from HNO is observed with a maximum at 690 nm. This reaction could be used to monitor NO and NO₂ emissions from gasoline engines. Conceivably, it could be adapted to develop a nitrogen-specific gas chromatography detector.

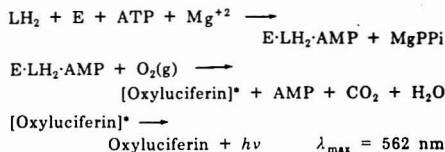
Riboflavin-H₂O₂. Riboflavin reacts with H₂O₂ to generate CL. CL is initiated either by adding a reducing agent or by irradiating with visible light ("photoinduced CL"). Because CL intensity is significantly enhanced by the presence of copper and is not greatly affected by other metal ions, this system can be used for copper analysis.

Bioluminescence

Background. Around 1885 Raphael Dubois, using the luminescing photogenic organ of the West Indian elaterid beetle, *Pyroporus*, discovered that when it was immersed in hot water until its light emission ceased, a heat-stable compound was extracted. He also observed that when the

cells of the photogenic organ were triturated in water at room temperature until the light emission ceased, a heat-labile compound was extracted. When the two oxygen-saturated extracts were mixed, light emission was immediately observed. The former extract was named Luciferin (LH₂) (*Lucifer* means light bearing in French) and is referred to as the substrate; the latter extract was named Luciferase (E) and is known to be an enzyme. It was at first thought that LH₂ was a protein; this is, in general, not true with the exception of the *Aequorea* bioluminescing system in which LH₂ is tightly bound to a protein matrix. There are many different sources for as many different luciferins and luciferases. Table V gives a few representative sources. The choice of a source for LH₂ and E is primarily governed by the chemistry involved, as will be discussed later; however, availability, stability, and cost are other important factors. Owing in part to these factors, certain BL systems have been favored for study. The firefly and bacterial systems have been extensively studied during the past 75 years: *Cypridina*, *Aequorea*, and *Renilla reniformis* are BL systems studied more recently.

Firefly Bioluminescence System. Of all the bioluminescing systems, that of the firefly is the most studied. The following scheme summarizes the firefly mechanism as presently understood.



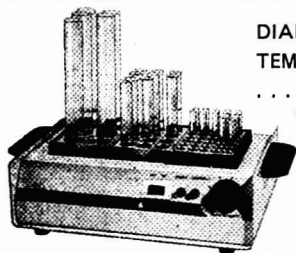
where ATP = adenosine triphosphate, AMP = adenosine monophosphate, and PPi = inorganic pyrophosphate. A BL efficiency of one is routinely observed for this reaction.

When this reaction is carried out so that the analyte is ATP, 0.1 to 1.0 picomole is claimed for a minimum detection limit with linearity of response extending five orders of magnitude. Such a detection limit and linear range is obtainable from a so-called "crude" extract of ATP. Some investigators, after taking extreme care with their ATP extraction as well as with pH control and reactant purity, have been able to detect the ATP in a single bacterium, i.e., 2.0×10^{-9} to 1.0×10^{-2} picomoles. An accompanying increase in the linear range is also observed. The difference in the two minimum detection limits arises from contamination of the reactants with ATP or the presence of the interferent AMP in the ATP extract.

Specificity of the firefly LH₂ is high for ATP; however, studies have shown that both cytidine-5'-triphosphate (CTP) and inosine-5'-triphosphate (ITP) stimulate light production to the same extent as ATP. However, the contribution by these contaminants to the total light emission is small in a normal ATP-containing sample, since in natural systems the concentration of ATP is much greater than that of CTP and ITP. Other contaminants have been shown to act as inhibitors to the emission of light in the following order of activity Ca > K > Na > Rb > Li. Hg(II) at 2 ppm inhibits the emission of light, owing to its influence on E.

A typical ATP analysis utilizes firefly LH₂ (1.0 mg/ml), E (1.0 mg/ml) in 0.05M THAM buffer (pH 7.4), and 0.01M Mg(II). The mixture may be lyophilized and stored at -65°C. This is a convenient form for the reactants since they can be stored in this way indefinitely without losing their activity, and a simple addition of deionized water reconstitutes them for immediate use. For an analysis, no less than 0.5% dissolved O₂ must be present in the reaction solution. ATP is determined by adding it to excess

QUALITY LABORATORY APPARATUS modular dri-bath



DIAL YOUR
TEMPERATURE
... AMBIENT
TO 110° C

MODEL NO. DB-1625
UNIT PRICE \$150.00

The Modular Dri-Bath has been designed for the flexibility and accuracy required to perform a variety of lab procedures. Seven interchangeable heating blocks allow heating and intermixing of different size test tubes. Positive temperature control to $\pm 1^\circ \text{C}$. Wide temperature range ... ambient to 110° C.

Write for new Bio-Medical Apparatus Catalog #100



THERMOLYNE
SYBRON CORPORATION

2555 Kerper Blvd., Dubuque, Iowa 52001

CIRCLE 230 ON READER SERVICE CARD

Gas-Dry FILTER TRAP

for drying and filtering
carrier gas Remove moisture, oil
and dust from carrier gas before it flows
into your instrument. Get improved base-
line stability; more accurate data.

FEATURES:

- Clear acrylic tube allows visual monitoring
- No wrench needed to change cartridge contents
- "O" ring seal allows pressure to 100 psi
- Two sizes: 120 and 400 cc



New! BASE PLATE

Allows mounting Gas-Dry
Filter Trap on bench top for
continuous observation

Gas-Dry Filter Traps and hundreds
of other helpful G. C. tools
are described in Catalog 600.
Send for your FREE copy.



Send me a copy of Catalog 600.

Name/Title _____
Company/Institution _____
Address _____
City _____ State & Zip _____



Chemical Research Services, Inc.
852 Westgate Drive • Addison, Illinois 60101 AC-2

CIRCLE 43 ON READER SERVICE CARD

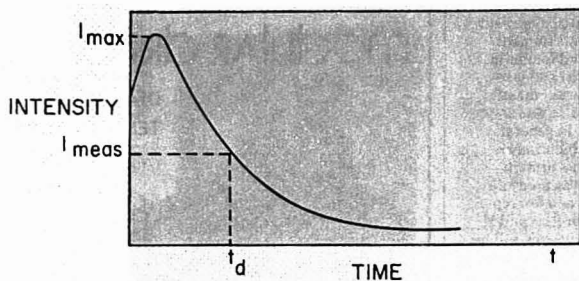


Figure 4. Typical bioluminescence vs. time-after-mixing curve observed for ATP analysis

I_{max} = maximum observed intensity
 I_{meas} = intensity after fixed time interval, t_d

reactants and measuring the light intensity vs. time. A typical response curve is shown in Figure 4. Calibration curves are generated from measurements of either I_{max} or I_{meas} or the total integrated intensity as a function of ATP concentration.

ATP is present in *all* living cells regardless of whether the cell is photosynthetic or heterotrophic. ATP's phosphate bonds serve as an energy reservoir for the cell; thus, ATP becomes involved in many important metabolic reactions and is analytically important.

It was previously mentioned that it was possible to measure the ATP content in a single bacterium; with such knowledge, ATP analysis of a bacteria-containing sample would give information regarding their number. In practice, however, the ATP per bacterium is not determined on the basis of a single bacterium but rather on some large number of them. From various studies it is concluded that in any analysis of a particular bacterium for the concentration of ATP per bacterium, the investigator should compare the firefly-ATP analysis with plating of the same bacteria. The advantages of doing bacterial counting by ATP assay instead of plating include speed, accuracy, and expense. Moreover, certain filamentous microorganisms cannot be counted by conventional techniques and may best be counted by the ATP method. To illustrate these advantages, consider the study in which bacterial counts were made of samples of food, water, and urine. As few as 1000 bacterial cells could be measured in less than 5 min per sample. For such a measurement, log (ATP) vs. log (number of cells) exhibited a 0.93 positive linear correlation coefficient.

A typical extraction of ATP from the cell is accomplished by treating the triturated cells with five volumes of boiling ethanol for 1 min. After air drying, the extract is stored at -20°C to be reconstituted later at the time of analysis. Table VI lists some applications of the BL assay for ATP. This reaction is so widely used that it has given rise to commercially available instruments specifically for this assay, such as Aminco's Chem-Glow photometer and Du Pont's biometer. Table VII lists some of the other species determinable by the firefly reaction along with their importance.

Bacterial Bioluminescence System. The bacterial system follows the firefly system in popularity for study. The following reactions schematically represent the bacterial system.

Table VI. Applications of Bioluminescence Assay for ATP

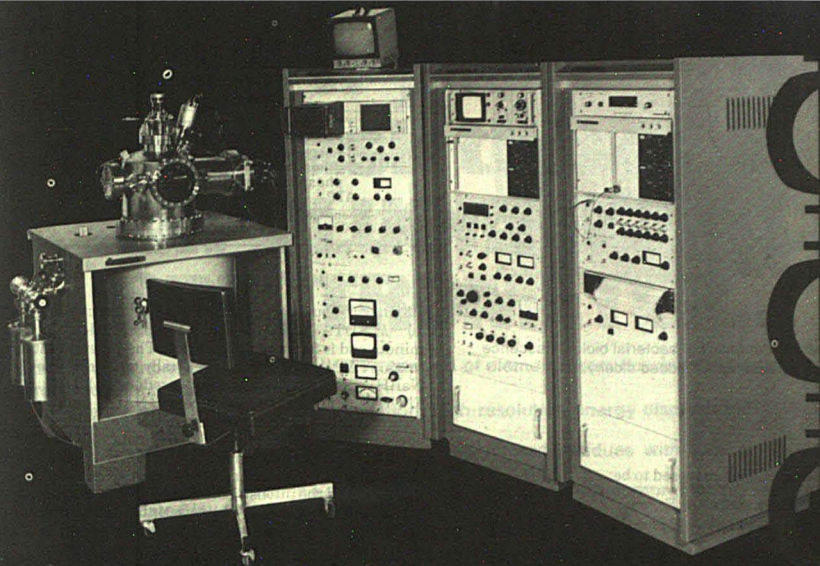
Application	Area of application
Monitoring of fermentation rates	Process control in food, beverage, and drug industries
Detection of bacterial contamination	Quality control in food, beverage, drug, and cosmetic industries
Measuring biomass in water	Control of activated sludge waste water treatment processes
Detecting presence of life	Fundamental studies in limnology and oceanography
Determining viability of red blood cells	Extraterrestrial investigations
Measuring infection-causing bacteria	Medical

Table VII. Applications of Firefly Reaction to Species Other Than ATP

Species analyzed	Importance
Creatine phosphate	Energy reservoir for muscle activity
Cyclic AMP	Mediator of hormone activity
Dissolved oxygen	Measure of water quality
Inorganic pyrophosphate	Medical
	Starting material for several biological compounds

Table VIII. Sensitivity of Analytical Methods for FMN

Method	Min detectable concn, $\mu\text{g}/100 \mu\text{l}$
Paper chromatography	10^1
Cytochromic reductase	10^2
Lactic oxidase	1
Fluorometry	10^{-4}
Bacterial BL	10^{-7}



HAVE YOU SEEN SAM?

Probably not, because SAM is the all new SCANNING AUGER MICROPROBE just announced by PHI[®]. However, if you're concerned with materials analysis problems involving surfaces and thin layers, you'll probably want to learn all you can about it. It's the latest advancement in surface and thin film analysis.

It'll perform a nondestructive determination of surface composition with atom-layer depth resolution and micron lateral resolution.

It'll perform a selected-area determination of thin film composition as a function of depth.

Its detectability limits are measured in fractions of a monolayer, and light elements are detected and identified as easily as heavy elements.

It'll analyze insulators, conductors, or semiconductors.

On top of all that, it's easy to operate, the data is simple, and it has the same built-in, proven reliability of previous PHI equipment.

You say you'd like to know more about SAM . . . ?

Call PHI.[®]

See SAM at the Pittsburgh Conference, Booth 317

PHYSICAL ELECTRONICS INDUSTRIES, INC.

Main Office:
7317 South Washington Avenue
Edina, Minnesota 55435
(612) 941-5540, TLX 29-0407

Eastern Regional Office:
960 South Springfield Ave.
Springfield, New Jersey 07081
(201) 376-3850

Western Regional Office:
Suite 408, 1922 The Alameda
San Jose, California 95126
(408) 247-7767

In Japan:
Ulvac Corporation
1-1 Kyobashi, Chuo-Ku
Tokyo 104, Japan
03-635-6381

In Europe:
Balzers AG
FL-9496 Balzers
Principality of Liechtenstein
075/4 11 22

In Canada:
Vp. Scientific Limited
312 Dolomite Drive
Downsview, Ontario
(416) 638-7373

CIRCLE 200 ON READER SERVICE CARD



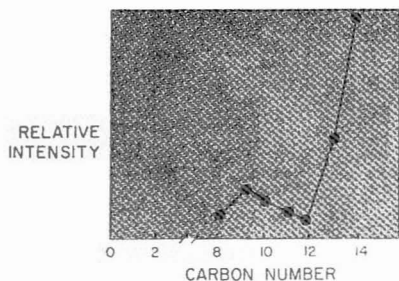
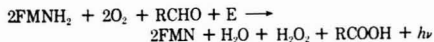


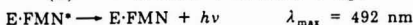
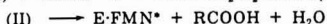
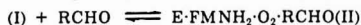
Figure 5. Relative intensity of bacterial bioluminescence as function of chainlength of added aldehyde

The overall reaction is proposed to be:



which is thought to be the sum of reaction series A and B.

Series A:



FMN = Flavin mononucleotide

Series B:



The BL efficiency for this reaction is about 0.05.

The oxidation of FMNH₂ proceeds with or without the aldehyde in the presence of O₂ to give 27 kcal/mol free energy, but emission from an excited FMN molecule of 492 nm would require 54.9 kcal/Einstein. The additional energy is provided by the oxidation of the long chain aldehyde to a carboxylic acid. The total free energy thus provided is approximately 95 kcal/mol. The intensity of the emission from this reaction depends on the chainlength of the aldehyde as shown in Figure 5.

Data in Table VIII show that the bacterial BL system exhibits a minimum level of detection for the analysis of FMN which is superior to other popular methods. It also shows that fluorometry might compete for the analysis of FMN; however, its lack of specificity vitiates its use. Compounds commonly found in samples of biosystems interfere with the fluorometric analysis of FMN.

Bacterial BL has high specificity for FMN. Some substituted FMN's and flavin adenine dinucleotide (FAD) react with the bacterial (E) to produce light; however, the level of emission is low enough so that it is of little analytical concern. The relationship between light output and FMNH₂ concentration is linear from 1.0 × 10⁻⁴ to 1.0 μg/ml.

The two most popular sources of the bacterial luciferase (E) are the bacteria *Photobacterium fischerii* and *Achromobacter fischerii*. The luciferin, FMN, may be obtained from virtually any living system. The luciferase is generally used at a concentration of 1.0 μg/ml in 0.05M THAM buffer (pH 7.4). Dodecylaldehyde complexed with bisulfite is widely used as the required aldehyde. The FMN may be extracted from the sample by treating it with a boiling so-

Table IX. Nucleotide Activators of *Renilla Reniformis* Bioluminescence

Activator	Rel activity, %
3'-Dephosphoadenosine	100
2'-Dephosphoadenosine	1
Coenzyme A	7
3'-Phosphoadenosine-5'-phosphosulfate (PAPS)	15-98*
ATP	0

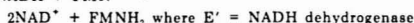
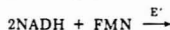
* Depends on extent of acid hydrolysis.

lution of 6% butanol in 0.01M THAM buffer containing 10⁻³M EDTA. The extraction is complete in less than a minute and is followed by filtration. The supernatant containing FMN and FMNH₂ is generally treated with either NaBH₄ with PdCl₂ as a catalyst to reduce FMN to FMNH₂, or FMN may be reduced by NADH (reduced form of nicotinamide adenine dinucleotide) in the presence of H⁺. Following the above treatment, the extracted, reduced FMN is mixed with the enzyme (E) and the long chain aldehyde-bisulfite complex before a light sensitive detector, and the intensity of the emission is compared with a calibration curve. The noise or background in this analytical scheme is primarily endogenous light from the reactants and is eliminated by the calibration procedure since the background is generally constant for a given experiment.

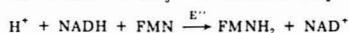
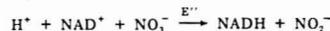
The BL assay for FMN is applicable to many of the same systems as the ATP method. It has been used to monitor infectious bacteria and has been extensively investigated as a possible detector of extra terrestrial life.

Another type of application involves exposing the bacteria to organic vapors and observing the decrease in luminescence. This can be used to study the effect of anesthetic vapors or to detect the presence of various compounds such as alcohols, aldehydes, and ketones.

The dependence of the bacterial BL on FMNH₂ and FMN's participation in the following reaction leads to the possibility of analyses which do not depend directly on FMN but on some substrate being oxidized by NADH or reduced by NAD⁺.



For example, a method for NO₃⁻ could be based on the following reactions:



E''' = nitrate reductase

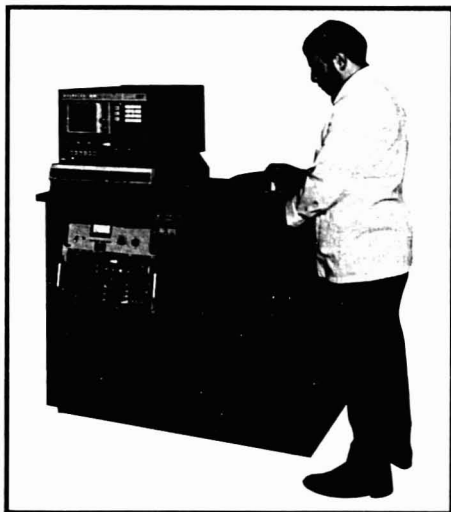
The concentration of the resulting FMNH₂ is proportional to the initial concentration of nitrate.

Other BL Systems. *Aequorea*. The BL system of the hydromedusa, *Aequorea*, is unusual among BL systems in that it seems not to rely on either the typical LH₂ and E or O₂. The luminescence involves only the photoprotein aequorin in the presence of Ca(II) ions. It is thought that the protein provides a matrix for the LH₂, E and O₂ thus forming a complex which, when triggered by Ca(II), bioluminesces.

Early research proposed that the *Aequorea* system was specific for Ca(II); however, later research has shown that the photoprotein aequorin can be stimulated to bioluminescence by over a dozen other cations, such as Co(II), Pb(II), and Yb(III). However, since these cations are not normally present in significant amounts in biologi-

if you would ask this of an X-RAY FLUORESCENCE SPECTROMETER...

- simultaneous nondestructive quantitative analysis of elements from fluorine to uranium
- direct element readout on CRT display
- a complete system with x-ray tube excitation, high-resolution energy dispersive detection and high speed automatic data processing
- analysis of solids, solutions, powders, slurries and filtered residues with little or no sample preparation
- push button operation for routine work, computer operation with comprehensive software for more sophisticated investigations
- tape cassettes for loading programs and recording spectra
- pulsed x-ray generator to provide unsurpassed stability and enhanced data acquisition rates
- analysis of concentrations from parts-per-million
- switch selection of sample atmospheres—air, vacuum or helium
- automated 4- or 18-sample changer



...ask about our **MODEL 500**



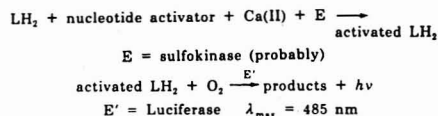
Box 641 • Princeton, New Jersey 08540 • Telephone (609) 924-7310

CIRCLE 197 ON READER SERVICE CARD

ANALYTICAL CHEMISTRY, VOL. 46, NO. 2, FEBRUARY 1974 • 199 A

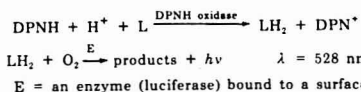
cally derived samples, the aequorin reaction may still serve as a means of Ca(II) trace analysis in samples of biological origin.

Renilla Reniformis. *Renilla reniformis*, commonly referred to as the sea pansy, produces blue-green bioluminescence in concentric waves across its surface. The emission wavelength maximum is 485 nm and follows the reaction scheme:



The feature of this BL system which is of analytical significance is the required nucleotide activator. Table IX shows some activators and their relative activity in the reaction. PAPS is of some interest in the study of brain metabolism.

Fungal. The fungal BL systems are pyridine-nucleotide linked and are thought to follow the path shown in producing light.



The pyridine-nucleotide linkage of this system makes it potentially important analytically, owing to the broad range of reactions involving the pyridine-nucleotide.

References

General

- M. J. Cormier, D. M. Hercules, and J. Lee, Eds., "Chemiluminescence and Bioluminescence," Plenum Press, New York, N.Y., 1973.
- K. D. Gundermann, "Chemilumineszenz Organischer Verbindungen," Springer-Verlag, New York, N.Y., 1969.
- W. D. McElroy and B. Glass, Eds., "Light and Life," Johns Hopkins Press, Baltimore, Md., 1961.
- F. H. Johnston and Y. Haneda, Eds., "Bioluminescence in Progress," Princeton University Press, Princeton, N.J., 1966.
- E. N. Harvey, "Bioluminescence," Academic Press, New York, N.Y., 1952.
- A. C. Gese, "Photophysiology," Vols II, IV, V, Academic Press, New York, N.Y., 1970.
- E. White and H. H. Seliger, "Bioluminescence," *Sci. Amer.*, **207** (12), 76-89 (1962).
- B. L. Strehler, "Bioluminescence Assay: Principles and Practice" in "Methods of Biochemical Analysis," D. Glick, Ed., **16**, 99-179 (1968).

Air Pollutants

- A. Fontijn, P. Golomb, and J. A. Hodgson, "A Review of Experimental Measurement Methods Based on Gas-Phase Chemiluminescence," in "Chemiluminescence and Bioluminescence," M. J. Cormier, D. M. Hercules, and J. Lee, Eds., pp 393-426, Plenum Press, New York, N.Y., 1973.
- R. K. Stevens and J. A. Hodgson, "Applications of Chemiluminescent Reactions to the Measurement of Air Pollutants," *Anal. Chem.*, **45**, 443A (1973).
- J. A. Hodgson, K. J. Krost, A. E. O'Keefe, and R. K. Stevens, "Chemiluminescent Measurement of Atmospheric Ozone," *Anal. Chem.*, **42**, 1795 (1970).
- G. J. Warren and G. Babcock, "Portable Ethylene Chemiluminescence Ozone Monitor," *Rev. Sci. Instrum.*, **41**, 280 (1970).
- V. H. Regener, "Measurement of Atmospheric Ozone with the Chemiluminescent Method," *J. Geophys. Res.*, **69**, 3795 (1964).
- G. W. Nederbragt, A. van der Horst, and J. van Duijn, "Rapid Ozone Determination Near an Accelerator," *Nature*, **206**, 87 (1965).
- A. Fontijn, A. J. Sabadell, and R. J. Ronco, "Homogeneous Chemiluminescent Measurement of Nitric Oxide with Ozone," *Anal. Chem.*, **42**, 575 (1970).
- P. N. Clough and B. A. Thrush, "Mechanism of Chemiluminescent Reaction Between Nitric Oxide and Ozone," *Trans. Faraday Soc.*, **63**, 915 (1967).

Sulfur and Phosphorus

- A. Fontijn, D. Golomb, and J. A. Hodgson, "A Review of Experimental Measurement Methods Based on Gas-Phase Chemiluminescence," in "Chemiluminescence and Bioluminescence," M. J. Cormier, D. M. Hercules, and J. Lee, Eds., pp 393-426, Plenum Press, New York, N.Y., 1973.
- R. K. Stevens and J. A. Hodgson, "Applications of Chemiluminescent Reactions to the Measurement of Air Pollutants," *Anal. Chem.*, **42**, 1795 (1970).
- H. W. Grice, M. L. Yates, and D. J. David, "Response Characteristics of the Melpar Flame Photometric Detector," *J. Chromatogr. Sci.*, **8**, 90 (1970).
- R. M. Dagnall, K. C. Thompson, and T. S. West, "Molecular-Emission Spectroscopy in Cool Flames. Part I. The Behavior of Sulphur Species in a Hydrogen-Nitrogen Diffusion Flame and in a Shielded Air-Hydrogen Flame," *Analyst*, **92**, 506 (1967).
- R. M. Dagnall, K. C. Thompson, and T. S. West, "Molecular-Emission Spectroscopy in Cool Flames. Part II. The Behavior of Phosphorus Containing Compounds," *Analyst*, **93**, 72 (1968).
- K. M. Aldous, R. M. Dagnall, and T. S. West, "The Flame-spectroscopic Determination of Sulfur and Phosphorus in Organic and Aqueous Matrices by Using a Simple, Filter Photometer," *Analyst*, **95**, 417 (1970).
- A. Sity, "Determination of Phosphorus in Detergents by Flame Emission Spectrometry," *Anal. Lett.*, **4**, 531 (1971).
- M. J. Prager and W. R. Seitz, "A Flame Emission Photometer for Determining Phosphorus in Natural Waters," submitted to *Anal. Chem.*

Luminol

- W. R. Seitz and D. M. Hercules, "Chemiluminescence Analysis for Trace Elements," in "Chemiluminescence and Bioluminescence," M. J. Cormier, D. M. Hercules, and J. Lee, Eds., pp 427-49, Plenum Press, New York, N.Y., 1973.
- W. R. Seitz and D. M. Hercules, "Determination of Trace Amounts of Iron(II) Using Chemiluminescence Analysis," *Anal. Chem.*, **44**, 2143 (1972).
- W. R. Seitz, W. W. Suydam, and D. M. Hercules, "Determination of Trace Amounts of Chromium(III) Using Chemiluminescence Analysis," *Anal. Chem.*, **44**, 957 (1972).
- In addition, there are many papers in Russian journals authored or coauthored by A. K. Babko that describe various luminol systems.

Other Reactions

- R. L. Bowman and N. Alexander, "Ozone-Induced Chemiluminescence of Organic Compounds," *Science*, **154**, 1454 (1966).
- B. J. Finlayson, J. N. Pitts, Jr., and H. Akimoto, "Production of Vibrationally Excited OH in Chemiluminescent Ozone-Olefin Reactions," *Chem. Phys. Lett.*, **12**, 495 (1972).
- L. I. Dubovenko and E. Ya. Khotinets, "Catalytic Effect of Bi(III) on the Chemiluminescent Reaction of Lucigenin with Hydrogen Peroxide," *Ukr. Khim. Zh.*, **37**, 1154 (1971).
- K. J. Krost, J. A. Hodgson, and R. K. Stevens, "Flame Chemiluminescence Detection of Nitrogen Compounds," *Anal. Chem.*, **45**, 1800 (1973).
- E. L. Wehry and A. W. Varnes, "Selective Determination of Copper(II) in Aqueous Media by Enhancement of Flash-Photolytically Initiated Riboflavin Chemiluminescence," *Anal. Chem.*, **45**, 348 (1973).
- M. O. Stone and R. H. Steele, "Studies on the Chemiluminescence from an O₂ and/or H₂O₂ Adduct Derived from the Riboflavin-Copper(I) Chelate," *Biochem.*, **9**, 4343 (1970).

Firefly System

- L. Dufresne and H. J. Gitelman, "A Semiautomated Procedure for Determination of ATP," *Anal. Biochem.*, **37**, 402-08 (1970).
- E. Beutler and M. C. Baluda, "Simplified Determination of Blood ATP Using the Firefly System," *Blood*, **23** (5), 688-96 (1964).
- N. Suzuki and T. Goto, "Studies of Firefly Bioluminescence II," *Tetrahedron*, **28** (15), 4075-82 (1972).
- R. A. Johnson, J. G. Hardman, A. E. Broadus, and E. W. Sutherland, "Analysis of Adenosine 3',5'-monophosphate with Luciferase Luminescence," *Anal. Biochem.*, **35**, 91-97 (1970).
- J. B. St. John, "Determination of ATP in Chlorella with the Luciferin-Luciferase Enzyme System," *Anal. Biochem.*, **37**, 409-16 (1970).
- E. W. Chappelle and G. V. Levin, "Use of the Firefly Bioluminescent Reaction for Rapid Detection and Counting of Bacteria," *Biochem. Med.*, **2**, 41-52 (1968).
- P. E. Stanley and S. G. Williams, "Use of the Liquid Scintillation Spectrometer for Determining ATP by the Luciferase Enzyme," *Anal. Biochem.*, **29**, 381-92 (1969).

Price is not the best reason to buy a System Industries GC/MS data processor.

But it's a good place to start...

System Industries, 535 Del Rey Avenue, Sunnyvale, California 94086, (408) 732-4650

QUOTATION

SUBMITTED TO:

REFERENCE #	DELIVERY DATE	BY F.O.B.	TERMS	DATE	QUOTE #
90 days ARO	Sunnyvale, CA		Net 30 days	9/18/73	17324

ITEM	QUANTITY	DESCRIPTION	UNIT PRICE	TOTAL PRICE
1	1	Model 150 GC/MS Data System Capable of acquiring and processing gas chromatography/mass spectral data from quadrupole or time-of-flight GC/MS instruments. Prices include installation, demonstration and a one-year warranty. Basic unit includes: Digital Equipment Corporation PDP-8 Central Processor with 8192 words of core memory, 1.7 million word (24 million bit) disk memory with removable cartridge (3 cartridges are supplied with the unit), 12 bit analog-to-digital converter, 16 bit digital-to-analog converter, GC/MS interface with associated electronics. Software includes: resident monitor and executive programs, data acquisition programs with real time GC sensitivity and saturated peak detection facility. Special data output features include background subtraction identification, single spectrum output, RGC print, and limited range RGC, mass chromatogram, special calibration diagnostic program, utility and maintenance programs, automatic signal-to-noise control program (IPSS), and automatic processing (QUEUE). Graphic software for use with digital plotter or CRT display.		\$30,900
2	1	ASR 33 Teletype with 8/m interface and data output software	\$ 1,000	
3	1	CRT display, keyboard, modem capability, and data output software	\$ 7,000	
4	1	Digital plotter with interface and associated software	\$ 4,850	

QUOTATION FIRM: SYSTEM INDUSTRIES

DATE: 9/18/73

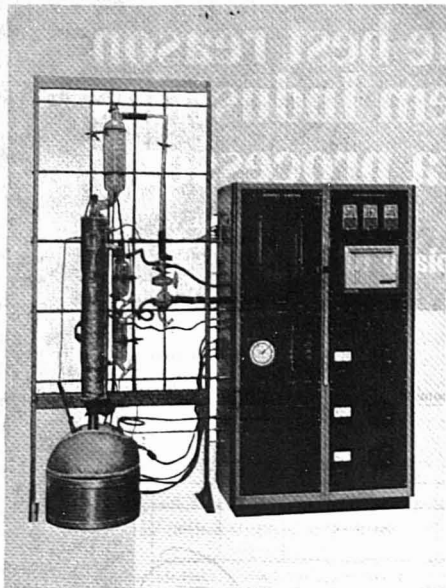
Signature: Neville Crook
Manager, Instrumentation

The System Industries data processor is appropriate for Quadrupole or Time of Flight GC/MS instruments, including those manufactured by Bendix, Extranuclear, Finnigan, and Hewlett-Packard. There are more System Industries GC/MS data processors installed than all others combined. Contact us to find out why the lowest price is just one of many reasons more chemists rely on the System 150.

System Industries

535 Del Rey Avenue, Sunnyvale, California 94086, (408) 732-1650, Telex 346-459

CIRCLE 216 ON READER SERVICE CARD



Sarnia Mark II: A crude fractionator that's highly sophisticated.

Our Sarnia Fractionator is the most efficient, advanced, packaged distillation unit available for precision batch fractionation.

The Sarnia Mark II, as listed in ASTM 2892-70T (15/5), is ideal for crude assay work—but it can be adapted for high efficiency separations where pure compounds are to be removed in quantity from mixtures.

We have also designed the Sarnia for continuous distillation, to allow the engineering of a field scale unit to be pretested for process performance at a fraction of the costs of conventional methods.

These unique fractionators are shipped complete with self-contained controls, plumbing, and circuitry for all major functions. Or, the glass system is available separately.

Kettle sizes (charge capacity) range from 1 liter to 2 barrels; column I.D.'s from 11 mm. to 140 mm. Other column sizes or special construction features are available.

For complete information, worldwide references, and recommendations for your requirements, write or call: (312) 475-0707.

KONTES/MARTIN

1916 Greenleaf Street, Evanston, Illinois 60204

CIRCLE 146 ON READER SERVICE CARD



- J. W. Patterson, P. L. Brezonik, and H. D. Putnam, "Measurement and Significance of ATP in Activated Sludge," *Environ. Sci. Technol.*, 4 (7), 569-75 (1970).
- O. Holm-Hansen and C. R. Booth, "The Measurement of ATP in the Ocean and Its Ecological Significance," *Limnol. Oceanogr.*, 11, 510-19 (1966).
- O. Holm-Hansen, "Determination of Microbial Biomass in Ocean Profiles," *Limnol. Oceanogr.*, 14, 740-47 (1969).

Bacterial System

- E. W. Chappelle, G. L. Piccolo, and R. H. Altland, "A Sensitive Assay for FMN Using Bacterial Bioluminescence Reaction," *Biochem. Med.*, 1, 252-60 (1967).
- P. E. Stanley, "Determination of Subpicomole Levels of NADH and FMN Using Bacterial Luciferase and Liquid Scintillation Spectrometer," *Anal. Biochem.*, 39, 441-53 (1971).
- D. E. White and C. R. Dundas, "Effect of Anaesthetics on Emission of Light by Luminous Bacteria," *Nature*, 226, 456-58 (1970).
- J. Lee, "Bacterial Bioluminescence," *Biochem.*, 11, 3350 (1972).

Other Systems

- O. Shimomura, F. H. Johnson, and Y. Saiga, "Microdetermination of Calcium by Aequorin Luminescence," *Science*, 140, 1339 (1963).
- E. B. Ridgway and C. C. Ashley, "Calcium Transients in Single Muscle Fibers," *Biochem. Biophys. Res. Commun.*, 29 (2), 229-34 (1967).
- J. P. Hamman and H. H. Seliger, "The Mechanical Triggering of Bioluminescence in Marine Dinoflagellates: Chemical Basis," *J. Cell. Physiol.*, 80 (3), 397-408 (1972).
- K. T. Izutsu, S. P. Felton, I. A. Siegel, W. T. Yoda, and A. C. N. Chen, "Aequorin: Its Ionic Specificity," *Biochem. Biophys. Res. Commun.*, 9 (4), 1034-39 (1972).



W. Rudolf Seitz received an AB in chemistry from Princeton University in 1965 and a PhD from MIT in 1970 where he studied with D. N. Hume. Dr. Seitz recently joined the faculty at the University of Georgia after working for three years at the Southeast Environmental Research Laboratory in Athens, Ga. His principal research interest is applying chemiluminescence to chemical analysis. Dr. Seitz was a coordinator of the symposium on Recent Advances in the Analytical Chemistry of Pollutants held in Athens in May 1973.

Michael P. Neary is a graduate student of Professor Hercules at the University of Georgia where he is carrying out research in analytical applications of chemiluminescence. Mr. Neary earned a BA degree in chemistry from the University of Colorado in Boulder and subsequently worked for five years with the atmospheric chemistry group at the National Center for Atmospheric Research in Boulder and five years with Beckman Instruments, Inc., in Fullerton, Calif.

ANALYTICAL CHEMISTRY Appoints Three Members to Its Instrumentation Advisory Panel

ANALYTICAL CHEMISTRY has appointed three new members to its Instrumentation Advisory Panel. They are Stanley R. Crouch of Michigan State University, Harold M. McNair of Virginia Polytechnic Institute and State University, and David Seligson, M.D., of Yale University School of Medicine. Members who are leaving the board after serving three-year terms are Charles E. Klopfenstein, University of Oregon; Harry L. Pardue, Purdue University; and Ralph E. Thiers, BioScience Laboratories. Members who will continue to serve on the nine-member board are Jonathan W. Amy, Purdue University; Richard A. Durst, Copenhagen (on leave from the National Bureau of Standards); J. Jack Kirkland, E. I. du Pont de Nemours & Co.; Ronald H. Laessig, University of Wisconsin Medical School; Marvin Margoshes, Technicon Corp.; and Howard J. Sloane, Beckman Instruments.

The Advisory Panel members lend their expertise to the continued development of interesting and provocative editorial coverage of the interdisciplinary field of instrumentation. They aid both in the selection of subject matter and possible authors and in the development of the scope and aims of the feature itself. Panel members also review material for the feature and sometimes contribute directly as authors or coauthors.

The goal of the feature is to help broaden and deepen the reader's knowledge in related disciplines so that cross-fertilization of ideas might provoke original and useful thinking in the area of instrumentation for solving analytical problems. Coverage does not concern itself only with design but also deals with specific applications, such as in biomedical instrumentation, pollution measurement devices, and computer applications. Experts in other disciplines such as physicists, instrument designers, and solid-state specialists are often invited to contribute to the col-

umn. Readers are invited to suggest potentially interesting topics or authors or to submit a manuscript in their own field if they feel it might be appropriate to the goals of the feature.

Brief biographical sketches of our new panel members appear below.



Stanley R. Crouch



Harold M. McNair



David Seligson

Stanley R. Crouch is associate professor of chemistry at Michigan State University. He received his MS degree from Stanford University in 1963 and his PhD degree from the University of Illinois in 1967. He is currently an Alfred P. Sloan Foundation Fellow (1973-75). Professor Crouch's research interests are in the areas of kinetics of analytical reactions, reaction-rate methods of analysis, atomic emission, absorption and fluorescence spectrometry in flames, nonflame atomization in atomic spectrometry, molecular absorption and luminescence spectrometry, signal-to-noise ratio theory in spectrometry, mini-computers in chemistry, and chemical instrumentation. He is the author or coauthor of about 25 publications in these areas and the coauthor of four modules and one book, "Electronic Measurements for Scientists" in the "Instrumentation for Scientists Series" edited by H. V. Malmstadt and C. G. Enke.

Harold M. McNair, professor of analytical chemistry at Virginia Polytechnic Institute and State University, received his BS from the University of Arizona in 1955 and his MS and PhD degrees in 1957 and 1959 from Purdue University. He held a Fulbright Fellowship in 1960 in Eindhoven, Holland. His eight years of industrial experience include work at Esso Research, F&M Div. of Hewlett-Packard, and Varian Aerograph. Gas and liquid chromatography are his principle research interests, and he has been professor in charge of four ACS short courses on these topics. Dr. McNair is the author of 20 research papers, three books, five technical movies, and eight slide/tape programs. He is an adjunct professor for the National University at Mexico City, Mexico, and a consultant for Bendix Corp., NASA, and the Air Pollution Control Office of EPA. He also serves on the editorial boards of *J. Chromatography* and *Chromatographia*.

News and Views

David Seligson is chairman and a professor in the Department of Laboratory Medicine at Yale University School of Medicine and Director of Clinical Laboratories at Yale-New Haven Hospital. He earned his BS in 1940 at the University of Maryland in Baltimore, his ScD at Johns Hopkins University in 1942, and his MD in 1946 from the University of Utah in Salt Lake City. He also holds an honorary MA from Yale University. Dr. Seligson has won the John G. Reinhold Award of the Philadelphia Section of the American Association of Clinical Chemists (AACC), the Donald D. Van Slyke Award of the New York Metropolitan Section of AACC, and the 1971 AACC Ames Award. Before joining the Yale University School of Medicine and Yale-New Haven Hospital, he held positions at the University of Pennsylvania.

Sensing of Environmental Pollutants

The 2nd Joint Conference on Sensing of Environmental Pollutants was held December 10-12, 1973, at the Sheraton Park Hotel in Washington, D.C. From the time of its planning to the actual meeting, the energy crisis struck. There are obviously energy



Stanley M. Greenfield

as well as money costs in cleaning the environment. Russell Train, administrator of the Environmental Protection Agency (EPA), has suggested that increased energy costs may be between 1 and 2%. Another source at EPA suggests that this figure might well be 3 or 4%. It appears that in light of the energy problems, cleaning the environment will be delayed somewhat. One thing is certain: to make the hard decisions needed, really good environmental data are required, and much research is needed to improve the quality of the data.

The conference on sensing pollutants is a joint enterprise involving nine organizations: five scientific associations, including the American Chemical Society, and four governmental entities. William O. Davis, general chairman of this meeting who is with the National Oceanic & Atmospheric Administration, one of the government sponsoring bodies, opened the meeting. He stressed the need for physical, chemical, and biological information and the role of the joint conference in information exchange in the sensing field, particularly in an interdisciplinary sense.

Nearly half the technical papers at the conference dealt with remote sensing which, according to Stanley M. Greenfield, assistant administrator for Research and Development at EPA and conference keynote speaker, is required to get an adequate picture of pollution problems. Sessions were devoted to remote sensing for both air and water pollutants and ranged from an airborne television system for oil-spill detection to optical correlation systems for measurements of air pollutants. Visibility in air and turbidity in water were the subjects of other technical presentations.

In his keynote address Dr. Greenfield emphasized the need for high-quality data for decision-making purposes: "It is becoming clear that to perform the Nation's environmental monitoring task adequately, a combination of contact along with remote instrumentation is absolutely necessary. Remote monitoring as an adjunct to contact monitoring provides a cost effective method to survey large geographical areas. Remote instrumentation mounted on flying platforms provides valuable information in support of contact monitoring, such as surveys for monitoring networks, data for model verification, and 'quick looks' at environmental quality violations."

The instrumentation and methodology needed for environmental appraisal derived from various research and development programs are vital needs in developing realistic and enforceable environmental standards.

Dr. Greenfield predicts that the monitoring of the future will go beyond wet chemistry and in situ sensors and will capitalize on remote sensing R&D and experience from other agencies, not just EPA. However, the need for more research is overwhelming, and the need to apply the broadest perspectives to take into account all the implications so that what is done does not cause other, more serious problems is also great.

One of the papers presented at the conference dealt with the laser optoacoustic spectroscopic technique for measuring gaseous air pollutants. L. B. Kreuzer, who presented this paper, is the author of our Instrumentation feature this month, page 235 A, on this system.

Toxic Substances

As the Federal government moves more and more into areas concerned with the safety of the consumer public, more and better analytical systems will be needed. Analytical chemists and those charged with the safety of industrial workers are well aware that the time is coming when they will need data to show that chemicals used or released into the environment are not liable to cause damage. It is now incumbent on industry to routinely test new chemicals for their impact on health and the environment before they are released into the commercial marketplace. The consumer public wants assurances that they will not be poisoned by their air, water, food, or otherwise.

Thus, Russell Train, administrator of the Environmental Protection Agency, addressed the Manufacturing Chemists Association (MCA) in mid-November to give his views on the likely impact of the Toxic Substances Act, then in a Senate-House Conference Committee. As this is written in mid-December, the bill is still in Conference, so the exact provisions have yet to be defined. In any case, it is likely that chemical makers will need to supply data on identification, volume, etc., on chemical production so that EPA can have an opportunity to assess in advance the risks that could be posed by the distribution of hazardous chemicals. It is expected that the bill will direct EPA to require manufacturers, distributors, processors, and importers to test selected chemicals in accordance with protocols set by EPA. The Act is also likely to permit citizens to bring suits to enjoin violations of the Act.

Although this sounds quite stringent, Mr. Train compared its impact

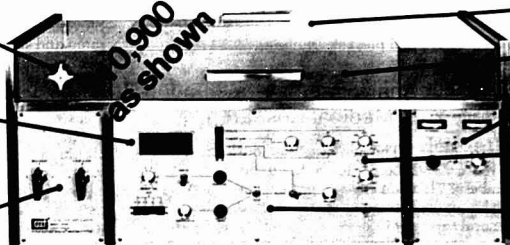
NEW Model 7000 Liquid Chromatograph

...with more features than other Chromatographs—for less money!

HIGH PRESSURE SEPTUMLESS INJECTOR VALVE. INJECTS 1, 2, 4, OR 8 MICROLITERS OF SAMPLE.

DIGITAL PANEL METER READS OUT PRESSURE, FLOWRATE, TEMPERATURE, AND % STRONG SOLVENT.

SOLVENT SELECT VALVES — ALLOWS SELECTION OF ANY 2 OF 5 SOLVENTS



SOLVENT COMPARTMENT FOR FIVE 1-LITER RESERVOIRS

COLUMN OVEN COMPARTMENT

HIGH PRESSURE-HIGH SENSITIVITY ULTRAVIOLET DETECTOR.

UPPER & LOWER PRESSURE LIMIT CONTROLS

GRADIENT ELUTION WITH LINEAR, CONCAVE AND CONVEX PROGRAMMING

FEATURING THE ONLY HYDRAULIC PUMP THAT ...

HAS CONSTANT FLOW REGARDLESS OF BACK PRESSURE CAN OPERATE FROM AN UNLIMITED RESERVOIR DELIVERS PULSELESS FLOW WITHOUT A PULSE DAMPER REQUIRES ONLY ONE PUMP FOR SOLVENT PROGRAMMING OPERATES IN CONSTANT FLOW OR CONSTANT PRESSURE MODE

Booth 101-106
1974 Pittsburgh Conference



FOR DETAILED INFORMATION ON THE MODEL 7000, CALL OR WRITE—DONALD W. DAWSON, LIQUID CHROMATOGRAPHY PRODUCTS SALES MANAGER, 5680 CUSHEN SPRINGS ROAD, NORCROSS, GEORGIA 30071 404-448-8282

CIRCLE 175 ON READER SERVICE CARD

HARRICK

INNOVATORS
in
OPTICAL INSTRUMENTATION



DOUBLE BEAM
GONIOMETER
SPECTROMETER

(circle 135)

RAPID or SLOW SCANNING
SPECTROMETER

up to 1000 spectra/sec
in UV-VIS-NIR

(circle 134)



STOCK AND CUSTOM
UV-VIS-IR ACCESSORIES

(circle 136)

and

OPTICAL FABRICATION

(circle 137)

... and more from



HARRICK SCIENTIFIC CORPORATION

Circle Dept. 103, Box 907, Ossining, N.Y. 10562 • 914-762-0021

Exhibits at Pittsburgh Conference, Booth 534; APS-OSA, Booth 78

MINIPULS
PERISTALTIC PUMPS
miniature pumps with superior performance



- Continuous flow adjustment 1-1300 ml/hr.
- Digital speed control
- Tubing can be replaced while motor is running
- Very low pulsation

Available in 1-, 4-, 8- and 16-channel models

CALL OR WRITE

Gilson Medical Electronics, Inc.
P.O. BOX 27, MIDDLETON, WIS. 53561 • PHONE 414-763-1100

CIRCLE 95 ON READER SERVICE CARD

News and Views

with the consequences of the 1972 amendments to the Federal pesticides law. These amendments recognize that even highly toxic compounds can, under carefully monitored conditions, be used in such a way that human health and environmental values will not be harmed. Also recognized is the value of testing and efficacy data for the pesticide developer. Use can be classified as general or restricted, and regulations are tuned carefully to control use of these materials with safety. Therefore, it is expected that the Toxic Substances Act would permit flexibility throughout the whole range of chemical compounds and that this flexibility would help ensure the technological viability of the chemical industry.

Mr. Train expressed the hope that the Act will not blunt the R&D thrust of industry and welcomed the MCA standing committee, with C. B. Shaffer of American Cyanamid as chairman, to provide suggestions on the implementation of toxic substances legislation.

Mr. Train expressed listeners that EPA can safeguard proprietary information and that they will develop streamlined procedures to prevent delays in marketing of new products. Industry itself should take the lead in identifying and remedying hazards, as would be expected of responsible commercial firms in any case. The agency cannot possibly regulate more than a fraction of the total commercial chemical compounds of concern. Mr. Train predicted that the chemical industry would not only survive the Act but would thrive under it, and he stated, "Technical progress based on chemistry will continue to be a major force in our society, an active and useful instrument for reaching our common objective of a higher quality of life for ourselves and future generations."

What is the analytical chemist's role in these matters? It seems that more will be asked of analytical chemists as the Federal government moves to establish testing protocols and sets limits on accuracy and precision. Professional analytical chemists should play a key part in the decision-making processes and not leave the choices and analytical problems for others to deal with. They should be generously represented on committees and task forces set up to in-

vestigate and recommend procedures. These procedures, once enacted, will have the force of law behind them and therefore should be carefully considered from their inception. With their unique training and experience, analytical chemists are in a position to contribute usefully to the varied demands made to ensure the safety and health of humans.

Analytical Instrumentation in Medical Research

The Schering Foundation of Bloomfield, N.J., has given impetus to an ongoing project of cooperation between researchers at the New Jersey College of Medicine and Dentistry at Newark (NJCMD) and Stevens Institute of Technology by granting \$66,000 for the acquisition, maintenance, and operation of a chemical ionization mass spectrometer at the Stevens campus in Hoboken. The program will be directed by Ajay K. Bose, professor of chemistry at Stevens, and John Bauman, associate professor of physiology at NJCMD, and will involve faculty members and doctoral degree candidates at Stevens and medical staff and faculty from NJCMD. It is hoped that this program will give medical students a better understanding of the new tools and methods of science and engineering available to meet research problems in medicine.

Several areas of research will involve the use of chemical ionization mass spectrometry and stable isotope labeling of biologically important molecules. The stable isotope technique makes it possible to study the metabolic course of drugs in humans directly, rather than relying on extrapolation from animal experiments with radioactive isotopes. The planned research will bring together trained organic chemists, spectroscopists, and medical doctors and spur transfer of technology from science and engineering to the medical clinic. Research projects proposed include studies of biochemical changes in pancreatitis, variations in membrane lipids, steroids associated with the placenta, and bile acid changes in cancer of the liver.

Undergraduates from Stevens have been working with members of the medical staffs of several metropolitan New York medical schools in Undergraduate Projects in Technology and Medicine (UPTAM) since 1972. Projects carried out at NJCMD as part of UPTAM have resulted in a new portable artificial respirator, development of a technique for the determination of diffusion through red blood cells, and a convenient mass spectral

analysis for bile acids. The success of these undergraduate programs led to interest in a similar program involving faculty and graduate students at Stevens. With leadership from Kenneth C. Rogers, president of Stevens, and Erich Hirschberg, associate dean of research at NJCMD, researchers at Stevens and NJCMD have collaborated and shared facilities of the nuclear magnetic resonance and mass spectroscopy labs at Stevens. Research is underway in several medical areas.

This multidisciplinary approach is absolutely necessary if medical research is to take advantage of the marvelous tools that physical scientists have developed. Using these tools should aid greatly in developing an understanding of complex biological systems and disease processes. And this understanding should hasten the time when clinical medicine can offer better answers to man's ills.

Symposium on Teaching Analysis

Dawson College in Montreal, Canada, is sponsoring a symposium on "Teaching Analytical Chemistry and Instrumentation Analysis," to be held May 16-17, 1974. Scheduled speakers include W. Blaedel of the University of Wisconsin; J. Dick, Sir George Williams University; W. Harris, University of Alberta; F. Karasek, University of Waterloo; H. McNair, Virginia Polytechnic Institute and State University; R. Skogerboe, Colorado State University; and S. Siggia and R. Barnes, University of Massachusetts.

The fee of \$75 includes lunches and a cocktail party and dinner. Registration forms and checks are due by March 31, 1974.

For further information or registration forms, contact A. David Adley, Dawson College, 350 Selby St., Montreal, P.Q., Canada. 514-931-8731, ext. 332

Standards for Environmental Improvement

The American National Standards Institute, with the American Society for Testing and Materials, the American Society of Mechanical Engineers, and other standards developing organizations, is sponsoring a conference on environmental standards, February 20-21, at the Marriott Twin Bridges Motel, Washington, D.C. This conference is designed to call attention to the strengths of the private

NOW YOU CAN AUTOMATE CLASSICAL CHEMISTRIES.



THE DISCRETE WAY.

The Beckman AMA 40 Automated Materials Analyzer is, technologically, as up-to-date as tomorrow. But its procedures are classical.

Here is the instrument that knows your methodology... that analyzes discrete samples much the same as you would manually. So that you're not locked into a manufacturer's machine-dictated technique. With AMA 40's full modularity, you enjoy the greatest possible versatility in automated assay methods.

Setup is fast. You can trim hours off test changeover time. AMA 40 doesn't gulp reagents, either. It consumes as little as 1/100th the amounts of reagents needed with other instruments. And, because of discrete rather than continuous analysis, you have minimal carry-over and a constant, correct baseline.

Those are just a few benefits. There are dozens more. If you're involved in wet-chemistry batch analysis, learn more about the advanced AMA 40—the instrument that does chemistry your way.

Write for Data File #2055, Scientific Instruments Division, 2500 Harbor Boulevard, Fullerton, California 92634, or contact your local Beckman representative.

See the AMA 40 running different analyses each day at the Pittsburgh Conference, Cleveland, Mar. 4-8.

Beckman

INSTRUMENTS, INC.

CIRCLE 24 ON READER SERVICE CARD



News and Views

sector in developing standards for environmental improvement. The present policy chosen by EPA is to develop its own standards, largely through contract research and development organizations. Conference planners maintain that the standards thus developed pose major compliance problems for industry and do not meet the objectives of the environmental protection acts. Participants from government, industry, and standards developing organizations will attend. The program will explore the need for sound standards, examine standards in existing law, and consider other aspects of standards development. Registration information may be obtained from ANSI, 1430 Broadway, New York, N.Y. 10018.

Call for Papers

8th Great Lakes Regional ACS Meeting

Purdue University, West Lafayette, Ind. June 3-5. Abstracts on standard ACS forms by March 1 to J. Wolinsky, Chemistry Dept., Purdue University, West Lafayette, Ind. 47907.

Meetings

Meetings previously scheduled for 1974 are listed in the January issue, beginning on page 36 A. The following meetings are newly listed in ANALYTICAL CHEMISTRY

- **NMR in 1974 and Beyond.** "Nuclei of Low Sensitivity." Feb. 27-Mar. 1. University of Western Ontario, London, Canada. Contact: Peter Macintyre, Varian Assoc. of Canada Ltd., 45 River Dr., Georgetown, Ont., L7G 2J4, Canada
- **Spring Meeting Optical Society of America.** Apr. 22-25. Shoreham Americana and Sheraton Park Hotels, Washington, D.C. Includes sessions on high-power lasers, ultraviolet and X-ray lasers, very long base line interferometry, submillimeter waves and their applications, etc. Contact: J. W. Quinn, Optical Society of America, 2100 Pennsylvania Ave., N.W., Washington, D.C. 20037. 202-293-1420
- **Journées de Calorimétrie et d'Analyse Thermique.** May 9-10. University of Rennes, France. Contact: Secretariat des Journées de

Calorimétrie et d'Analyse Thermique, Laboratoire de Cristallographie, U.E.R. "S.P.M.," Université de Rennes I, Avenue du Général Leclerc, 35031 Rennes Cedex, France

- **American Industrial Hygiene Conference.** May 12-17. Fontainebleau Hotel, Miami Beach, Fla. Of particular interest to those concerned with the Federal Occupational Safety and Health Act. Contact: William E. McCormick, Managing Director, American Industrial Hygiene Assoc., 66 S. Miller Rd., Akron, Ohio 44313
- **Meeting on Analytical Chemistry.** June 10-12. Lindau (Lake Constance). Contact: Gesellschaft Deutscher Chemiker, D-6000 Frankfurt (M), Federal Republic of Germany, Postfach 90 04 40, Germany
- **Surface Properties of Materials.** June 24-27. University of Missouri-Rolla. Contact: Leonard L. Levenson, Graduate Center for Materials Research, University of Missouri-Rolla, Rolla, Mo. 65401
- **6th ACS Northeast Regional Meeting.** Aug. 18-21. Lake Champlain, Burlington, Vt. Contact: Robert C. Woodworth, University of Vermont, Burlington, Vt. 05401
- **Fourth International Conference on Raman Spectroscopy.** Aug. 26-30. Bowdoin College, Brunswick, Me. Contact: J. E. Griffiths, Bell Laboratories, Murray Hill, N.J. 07974
- **Colloquium on Applications of Particle Size Analysis to Environmental Pollution.** Sept. 18-19. Nottingham, England. Contact: M. W. G. Burt, Bldg. B9C5, Atomic Weapons Research Establishment, Aldermaston, Berkshire, RG7 4PR, England

Short Courses

ACS Courses. For more information, contact: Department of Educational Activities, American Chemical Society, 1155 16th St., N.W., Washington, D.C. 20036. 202-872-4508

Intermediate NMR Spectroscopy
Chicago, Ill. Feb. 21-22. Joseph B. Lambert. \$125

Intermediate Gas Chromatography
Hollenden House, Cleveland, Ohio. Mar. 2-3. H. McNair, R. Juvet, Jr., S. Cram. \$135

Intermediate Chromatographic Systems: Maintenance and Troubleshooting
Hollenden House, Cleveland, Ohio.

Mar. 8-9. J. Q. Walker, M. T. Jackson, Jr., M. P. T. Bradley. \$135

Modern Liquid Chromatography
Atlantic City, N.J. Apr. 6-7. L. Snyder, J. Kirkland. \$140

Interpretation of Infrared Spectra
New York City. Apr. 19-20. Norman Colthup. \$125

Principles of Color Technology
Boston, Mass. May 15-17. Fred Billmeyer, Jr. \$150

UV/VIS Spectrophotometry
Los Angeles, Feb. 2; Washington, D.C., Feb. 25; Philadelphia, Feb. 27. Free. Contact: Varian, Instrument Div., 611 Hansen Way, Palo Alto, Calif. 94303. 415-493-8100

Atomic Absorption Spectroscopy
Denver, Feb. 5; Salt Lake City, Feb. 7; Atlanta, Feb. 12; Houston, Feb. 14; Los Angeles, Feb. 19; San Francisco, Feb. 21. Free. Contact: Varian, Instrument Div., 611 Hansen Way, Palo Alto, Calif. 94303. 415-493-8100

Recent Developments in Gel Permeation Chromatography
Washington University, Feb. 5-6. Contact: Washington University, Box 1048, St. Louis, Mo. 63130. 314-863-0100, ext. 4778

Differential Thermal Analysis of Organic Materials
Washington University, Feb. 7-8. Contact: Washington University, Box 1048, St. Louis, Mo. 63130. 314-863-0100

Drug Analysis
Central, N.J. Feb. 25-27. \$275. Contact: Center for Professional Advancement, 29 Division St., Somerville, N.J. 08876

Four One-Day Programs: Competitive Protein Binding Assays and Related Techniques; Radioimmunoassay in the Clinical Lab; Improving Clinical Enzyme Analysis; Aspects of Agarose Electrophoresis

Washington, D.C., Mar. 4-7; New York City, Mar. 18-21; Boston, Mass., Mar. 25-28; Los Angeles, Calif., Apr. 8-11; San Francisco, Calif., Apr. 15-18. Contact: Beckman Technical Education Center, 2500 Harbor Blvd., Fullerton, Calif. 92634. 714-521-3700

Photomicrography
Chicago, Ill. Mar. 4-8. \$350. Contact: McCrone Research Institute, 2820 South Michigan Ave., Chicago, Ill. 60616. 312-842-7105

Boosted efficiency, boosted versatility in X-ray Spectrochemical Analysis..... from Rigaku, of course

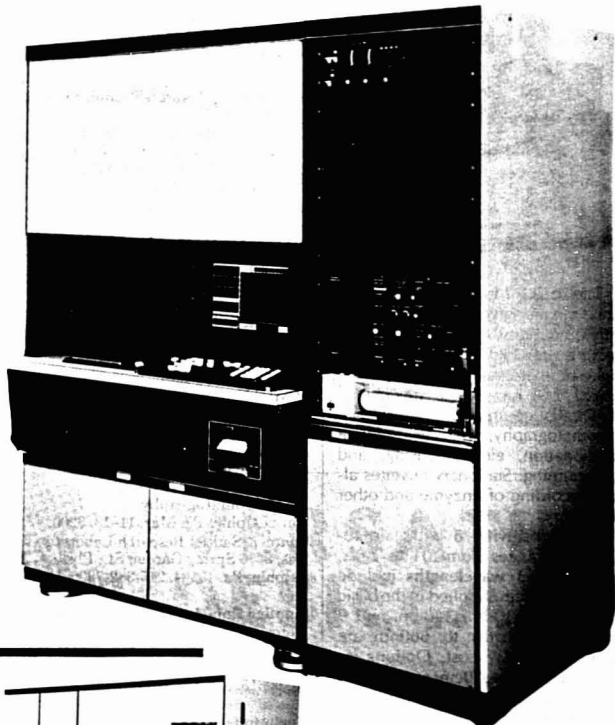
Geigerflex

sequential X-ray spectrometer

With Rigaku's "Geigerflex" SX3064M2 sequential X-ray fluorescent analyser, labs are assured quality analysis, operator safety and convenience, and room to expand.

The 3064M2 analyses 6 samples using up to 8 analytical crystals. The 3KW rhodium X-ray target tube eliminates the need for tube changes when both heavy and light elements are being measured. A wire cleaner, one of the maintenance-reducing components, cleans the flow proportional counter during operation without breaking vacuum.

To utilize the full potential of the practical options available from Rigaku, the best in up-to-date technology has been included. A built-in minicomputer which memorizes the analytical conditions of up to 80 elements and 200 channels. Digital goniometer drive control. Total IC design. It's automated, of course, so there is no need to increase staff.



The "Simultix" system utilizes fixed-element optics and provides simultaneous analysis of up to twenty four elements and is available either as a laboratory tool or in a configuration suitable for use in a process control environment. The addition of devices which permit automatic sample preparation and introduction into the "Simultix" makes this an attractive unit for process control in ferrous and non-ferrous rock industries.



Simultix

simultaneous X-ray spectrometer

See this and other Rigaku equipment on display at the '74 Pittsburgh Conference on Analytical Chemistry and Applied Spectroscopy. Or write—we'll be glad to send you full details.

For further information, contact our local distributors or write to:

Rigaku

Rigaku Denki Co., Ltd.

SEGAWA BLDG 2-8, Kanda Surugadai, Chiyoda-ku, Tokyo JAPAN

Cable RIGAKUDENKI TOKYO

Telex J24931 RDXRAY. Phone Tokyo 295-3311

Rigaku USA

Lakeside Office Park Door 18, 607 North Avenue,

Wakfield, Massachusetts 01880, U.S.A.

Telex 7103486710. Phone 617-245-6014

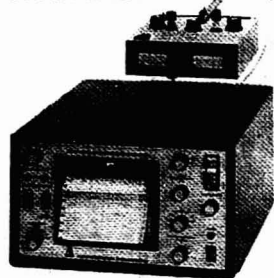
Distributors in U.K., France, West Germany, D.D.R., The Netherlands, Switzerland, Austria, Italy, Czechoslovakia, Canada, Mexico, Chile, Argentina, Brazil, Australia, India, Pakistan.

CIRCLE 208 ON READER SERVICE CARD

ANALYTICAL CHEMISTRY, VOL. 46, NO. 2, FEBRUARY 1974 • 211 A

HIGH
PERFORMANCE

absorbance monitor



The ISCO Model UA-5 absorbance monitor gives you the high sensitivity, stability, and response speed required for high speed, high pressure chromatography—plus the wide absorbance ranges and specialized flow cells required for conventional chromatography, density gradient fractionation, electrofocusing, and gel scanning. Stationary cuvettes allow recording of enzyme and other reactions.

High sensitivity. 8 full scale absorbance ranges from .01 to 2.0A, plus %T. **13 wavelengths** include 254 and 280nm supplied in the basic instrument; 310nm, 340nm, and 9 other wavelengths to 660nm are available at low cost. Options include a **built-in 10cm recorder**, a **Peak Separator** to automatically deposit different absorbance peaks into different tubes, and a **multiplexer-expander** which allows monitoring of two separate columns or one column at any two wavelengths. Automatic 4X scale expansion prevents oversized peaks from going off scale.

The current ISCO catalog describes the Model UA-5 as well as ISCO fraction collectors, metering and gradient pumps, and additional instruments for chromatography and other scientific research. Your copy is waiting.



BOX 5347 LINCOLN, NEBRASKA 68505
PHONE (402) 464-0231 TELEX 48-6453

CIRCLE 131 ON READER SERVICE CARD

News and Views

Introductory Infrared Techniques Clinic

Cleveland, Ohio. Mar. 6. \$30 (Includes lunch). *Contact:* R. W. Hannah, The Coblenz Society, Perkin-Elmer Corp., 761 Main Ave., Norwalk, Conn. 06852

Introductory Raman Techniques Clinic

Cleveland, Ohio. Mar. 6. \$30 (Includes lunch). *Contact:* R. W. Hannah, The Coblenz Society, Perkin-Elmer Corp., 761 Main Ave., Norwalk, Conn. 06852

Advanced Infrared Techniques Clinic

Cleveland, Ohio. Mar. 8. \$50 (Includes lunch). *Contact:* R. W. Hannah, The Coblenz Society, Perkin-Elmer Corp., 761 Main Ave., Norwalk, Conn. 06852

Pesticide Analysis

Central, N.J. Mar. 11-13. \$250. *Contact:* Center for Professional Advancement, 29 Division St., Somerville, N.J. 08876

Gas Chromatography

Philadelphia, Pa. Mar. 11-13. \$200. *Contact:* Sadtler Research Laboratories, 3316 Spring Garden St., Philadelphia, Pa. 19104. 215-382-7800

Applied Polarized Light Microscopy

Chicago, Ill. Mar. 11-15. \$325. *Contact:* McCrone Research Institute, 2820 South Michigan Ave., Chicago, Ill. 60616. 312-842-7105

Techniques of Infrared

Philadelphia, Pa. Mar. 11-15. \$275. *Contact:* Sadtler Research Laboratories, 3316 Spring Garden St., Philadelphia, Pa. 19104. 215-382-7800

New Techniques in Analytical Solution Chemistry

Central, N.J. Mar. 13-15. \$260. *Contact:* Center for Professional Advancement, 29 Division St., Somerville, N.J. 08876

Gas Chromatography

Los Angeles, Calif. Mar. 18-20. \$150. *Contact:* R. L. Amey, Dept. of Chemistry, Occidental College, Los Angeles, Calif. 90041. 213-255-5151

Identification of Small Particles

Chicago, Ill. Mar. 18-22. *Contact:* McCrone Research Institute, 2820 South Michigan Ave., Chicago, Ill. 60616. 312-842-7105

INSTRUMENTATION IN ANALYTICAL CHEMISTRY

An ACS Reprint Collection comprising 43 articles from Volumes 41-44 of *Analytical Chemistry*.

Collected by Alan J. Senzel, Associate Editor of *Analytical Chemistry*.

This up-to-date collection of articles provides an extensive and authoritative account of the latest advances in the various fields of instrumentation.

Over forty articles deal with four broad areas of analytical chemistry—spectrometry, chromatography, electrochemistry, and combination and other techniques. Specific topics focus upon instrument design, biomedical instrumentation, pollution measurement devices, and computer applications.

These papers will prove valuable as both a research and teaching aid. Each article is complete with a list of references, and important concepts are summarized at the end of each paper. A short commentary is also provided for most articles.

428 pages with index. Hardback \$7.95, Paper \$4.50; 20% discount on paperback edition for 5 or more copies. Postpaid in U.S. and Canada, plus 40 cents elsewhere.

Order from:
Special Issues Sales
American Chemical Society
1155 16th Street, N.W.
Washington, D.C. 20036

Whatever you can do with present xray fluorescence analysis techniques, you'll do it faster, cheaper, and more accurately with the EDAX®/EXAM® System.

The EDAX/EXAM System is the latest state of the art technique in xray analysis. Its energy dispersive (EDAX) operating principle gives you simultaneous analysis and display of all elements from Sodium through Uranium. Qualitative analysis in seconds, quantitative in minutes. Detailed brochures available from EDAX International, Inc., P.O. Box 135, Prairie View, Ill. 60069.

EDAX

Pittsburgh Conferees

Come see us at Booth Nos. 1605-1607



CIRCLE 70 ON READER SERVICE CARD

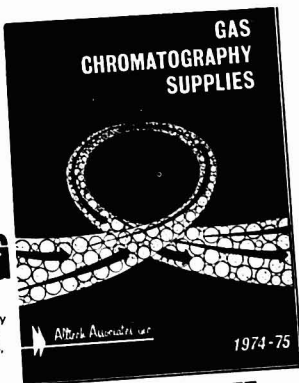
NOT OFF THE PRESS...

NEW...

FREE

CATALOG

of gas chromatography supplies & accessories complete with photos, description & prices.



* 77 pages

Attek Associates

202 Campus Drive, Arlington Heights, Ill. 60004
(312) 392-2670

See us at the Pittsburgh Conference, Booth 832
CIRCLE 5 ON READER SERVICE CARD

VERSATILE DESICCANT

DRIERITE is a low-cost, all-purpose anhydrous calcium sulfate used in desiccators, U-tubes, drying columns, drying tubes and large drying cabinets to dry air and gases. DRIERITE is also ideal for drying organic liquids in either the liquid or vapor phase.

The moisture remaining in a gas after drying with DRIERITE amounts to only 0.005 mg per liter.

DRIERITE is available in two forms—Regular or Indicating—from all leading Laboratory Supply Dealers.

REGULAR DRIERITE is constant in volume, inert except toward water, insoluble in organic liquids and refrigerants, non-disintegrating, non-wetting, non-poisonous, non-corrosive, repeatedly regenerative, and non-channeling.

INDICATING DRIERITE has all of the properties of Regular DRIERITE, but is impregnated with C.P. cobalt chloride and, hence, makes a clearly visible change from blue when dry to pink when exhausted.



W. A. HAMMOND
DRIERITE CO.
Xenia, Ohio 45385



CIRCLE 130 ON READER SERVICE CARD

News and Views

Laboratory Computers

Central, N.J. Mar. 25-27. \$275. Contact: Center for Professional Advancement, 29 Division St., Somerville, N.J. 08876

Analytical Separation/Purification

Central, N.J. Mar. 25-27. \$260. Contact: Center for Professional Advancement, 29 Division St., Somerville, N.J. 08876

Biomedical Instrumentation

Madison, Wis. May 13-17. \$300. Contact: University of Wisconsin Extension, 432 North Lake St., Madison, Wis. 53706

Minicomputers in Instrumentation and Control

Madison, Wis. May 20-24. \$350. Contact: University of Wisconsin Extension, 432 North Lake St., Madison, Wis. 53706

Applying Multivariate Statistics to Foods, Flavors, and Cosmetics

Chicago, Ill. Apr. 15-16. \$235 (Includes materials and lunches). Contact: SRF, 3810 Stratford Lane, Louisville, Ky. 40207. 502-895-4995

For Your Information

The Chemical Data Center, 3620 North High St., Columbus, Ohio 43214, 614-261-7101, offers computer searching of chemical literature via a phone call. The user states his request and while on the line receives the needed information. The cost is \$2.50/min with the average search taking 12 min. Available data bases include the Chemical Abstracts Condensate file, National Technical Information Services file, and TOX-LINE file. The complete service is also available to those with data terminals at \$1.00/min. Parameters that can be searched to find a product include chemical and physical properties, health and environmental data, end uses, functions, structure, substructure, fragments, functional groups, availability, and source of supply. A chemist can first search for information on a process and then go to the product file, if desired.

The London Co., U.S. representative for Radiometer A/S, Copenhagen, Denmark, manufacturer of electrochemical instruments for analytical research, has opened a regional office at 2313A McKelvey Rd., Maryland Heights, Mo.

CVC Products, Inc., is a new company formed by five key executives from **Bendix** who purchased the facilities and product line of Bendix Scientific Instrument and Equipment. Product lines include high vacuum distillation equipment, mass spectrometers, high vacuum pumping equipment, and others. Included in the purchase are eight domestic operations and three European subsidiaries in England, France, and Germany. Headquarters of the company is at 1775 Mt. Read Blvd., Rochester, N.Y. 14603. 716-458-2550

Pope Scientific, Inc., of Menomonee Falls, Wis., has acquired the complete facilities for the manufacture of the entire line of vacuum vessels for laboratory use formerly marketed by the Thermos Div. of **King-Seeley Thermos Co.**

Comstock & Wescott Inc., 765 Concord Ave., Cambridge, Mass. 02138, 617-547-2580, offers a new laboratory testing service for optical component testing and instrument calibration for ultraviolet and visible spectrometers. Typical tests include grating efficiency, minor reflectance measurements, filter transmission measurements, source studies, and detector response.

From General Electric . . .
A low volume-low pressure on-site hydrogen generator that helps you meet OSHA requirements.

- Reliable long life inherent in solid polymer electrolyte.
- No caustic solutions — add only distilled water.
- Compact — less than a cubic ft.
- Eliminate high pressure storage cylinders.
- Maintain gas purity without palladium diffuser.
- Accurate output pressure control — 0.5% — 150 or 225 cc/min STP Units.
- Operates from either 115 or 230 VAC — 50 or 60 Hz.
- Low pressure — low volume-on-demand generation.



This compact, lightweight hydrogen generator is designed for users of gas chromatographs, flame ionization detectors and related equipment who require an on-site, on-demand source of high purity hydrogen.

FOR MORE INFORMATION WRITE:

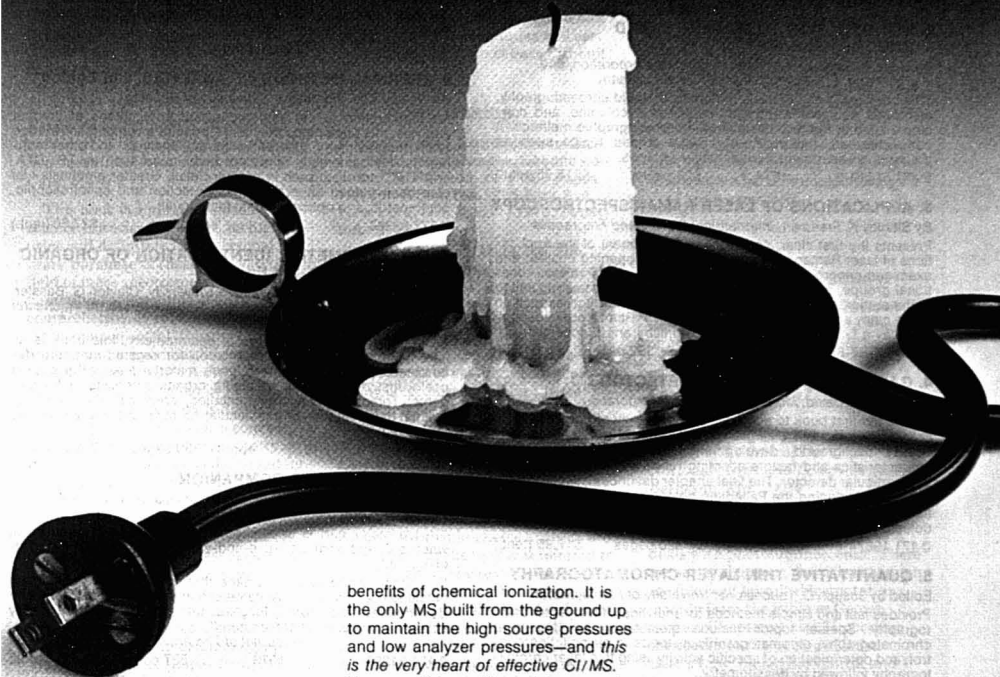
General Electric Company, Aircraft Equipment Division, Direct Energy Conversion Programs, 930 Western Avenue, Lynn, Massachusetts 01910.

AIRCRAFT EQUIPMENT DIVISION

GENERAL ELECTRIC
183-03

CIRCLE 97 ON READER SERVICE CARD

Sometimes, a new idea calls for a whole new design.



A technological advance can turn yesterday's bright idea into today's antiquated thinking.

That's exactly what has happened in the field of mass spectrometry. At one time, electron impact ionization was the method of choice to ionize samples for analysis. Now, a brighter idea has come along—chemical ionization. As a result, electron impact mass spectrometry alone, is not adequate.

Today most manufacturers are merely modifying their existing EI/MS equipment to operate as a CI/MS system. Only one company has come up with a wholly new design that makes the new idea work best. The company is Scientific Research Instruments. The result is Biospect.

Biospect is the only instrument on the market that gives you the full

benefits of chemical ionization. It is the only MS built from the ground up to maintain the high source pressures and low analyzer pressures—and *this is the very heart of effective CI/MS*. However, if you still need to generate EI spectra, Biospect can operate equally well in an EI mode.

With Biospect, you get almost complete control of sample ionization, greater sensitivity, finer selectivity, and spectra which are much easier to interpret.

Biospect also gives you a whole new approach in the field of CI/MS accessories. You can name your own brand of gas chromatograph and/or computer hardware, the one that's best for your job—then we'll put the system together for you and take systems responsibility.

Biospect . . . *The Chemical Ionization Mass Spectrometer.*

If you want to know more about CI/MS, Biospect, and the comparative features CI/MS vs EI/MS, ask for our brochure B101.



SEARLE

Scientific Research Instruments

Subsidiary of G. D. Searle & Co.
6707 Whitestone Road
Baltimore, Maryland 21207
(301) 944-4020

CIRCLE 219 ON READER SERVICE CARD

Books of a kind with the Chemist in mind

1. DETERMINATION OF pH: Theory and Practice

By Roger C. Bates, *University of Florida*

A complete, authoritative description of the theory of pH and of acidity and basicity in aqueous and nonaqueous media. Tells the scientist exactly what pH is, how it can be interpreted usefully, and what its limitations are. It describes precisely internationally accepted standard practice, sets forth the state of the art, and extends the pH concept to nonaqueous solutions. For the technician, it tells how to prepare standard solutions, how to care for electrodes, how to avoid temperature errors, and how to detect malfunctions of his equipment.

0 471 05647-2 1973 479 pages \$19.95

2. INTRODUCTION TO MODERN LIQUID CHROMATOGRAPHY

By Lloyd R. Snyder, *Technicon Instrument Corporation*, and J. J. Kirkland, *E. I. DuPont de Nemours & Company*

This book explains the basic principles of liquid chromatography, discusses equipment and chromatographic columns, and considers each of the four basic liquid chromatographic methods. It concludes with treatments of several related topics such as preparative separations or quantitative analysis.

0 471 81019-3 1974 528 pages \$16.95 (tent.)

3. APPLICATIONS OF LASER RAMAN SPECTROSCOPY

By Stanley K. Freeman, *International Flavors and Fragrances*

Presents the first clear, comprehensive treatment of the applications of laser Raman spectroscopy. After an opening chapter that examines general considerations, the book treats various functional groups, providing previously unpublished data originating in the author's laboratory. It also presents a thorough exposition of the many and diverse areas in which laser Raman spectroscopy can play a critical role in polymer chemistry and biochemistry.

0 471 27788-6 1974 approx. 352 pages \$17.50

4. GAS CHROMATOGRAPHIC DETECTORS

By Donald J. David, *Monsanto Research Corporation*

This is the first book to compile the technology of gas chromatographic detectors in a single volume. Each of ten chapters discusses background, development, current design, response characteristics and factors affecting response, and performance of a particular detector. The final chapter describes miscellaneous detectors, including the Palladium detector, discharge detectors, flame emission detectors, and the semiconductive thin-film detector.

0 471 19674-6 1974 approx. 320 pages \$17.95 (tent.)

5. QUANTITATIVE THIN LAYER CHROMATOGRAPHY

Edited by Joseph C. Touchstone, *University of Pennsylvania*

Provides fast and simple methods for analytical thin layer chromatography. Special topics include quantitation by thin layer chromatography; chromatographic methods in air pollution control; and determination of specific activity using thin layer chromatography followed by densitometry.

0 471 88040-X 1973 330 pages \$14.95

6. TECHNIQUES OF COMBINED GAS CHROMATOGRAPHY/MASS SPECTROMETRY: Applications in Organic Analysis

By W. H. McFadden, *University of California, Berkeley*

Provides the organic chemist with the necessary background for understanding and using the combined technique, GCMS. The author discusses mass spectrometry, gas chromatography, vacuum technology, and computer methods as they interrelate in GCMS applications. A novel feature is a chapter covering various applications of GCMS which includes approximately 15 mini-papers prepared by research workers in such fields as flavors and fragrances, geochemistry, biochemistry, clinical and forensic chemistry, and ecology.

0 471 58388-X 1973 463 pages \$18.95

7. WINE AND MUST ANALYSIS

By M. A. Amerine and C. S. Ough, both of the *University of California, Davis*

Wine and Must Analysis is a compilation of the most up-to-date methods used throughout the world for wine analysis. With the help of details described in this book, the reader should be able to analyze wines (and other fermented beverages) for most of their pertinent constituents. The book is designed to furnish the chemist with enough information so that he can carry out his

functions, and it is detailed enough that students can use the book as a text for wine analysis courses.

0 471 02545-3 1974 144 pages In Press

8. NUCLEAR MAGNETIC RESONANCE SPECTROSCOPY OF NUCLEI OTHER THAN PROTONS

Edited by Theodore Axenrod, *City University of New York*, and Graham Webb, *University of Surrey*

This book provides a comprehensive account of the progress being made in many laboratories on the NMR spectra of nuclei other than protons. Covering both the experimental and theoretical aspects of the subject, the book gives special emphasis to paramagnetic NMR, F-T spectroscopy, and the theoretical treatment of NMR parameters.

0 471 03847-4 1974 approx. 416 pages 18.95 (tent.)

9. THERMAL METHODS OF ANALYSIS, 2nd Edition

By Wesley Wm. Wendlandt, *University of Houston*

An introduction to the techniques and applications of thermal analysis, this book helps the novice acquire a working knowledge of thermogravimetry, differential thermal analysis, and other techniques. Fundamentally important techniques such as TG, DTA, and DSC are discussed in greater detail. Greater emphasis has also been placed on evolved gas detection and spectroscopic, photometric, and optical thermal techniques.

0 471 93366-X 1974 560 pages \$27.50 (tent.)

10. SPECTROMETRIC IDENTIFICATION OF ORGANIC COMPOUNDS, 3rd Edition

By Robert M. Silverstein, *Syracuse University*, Clayton G. Bassler, *Hills Brothers Coffee Company*, and Terence C. Morrill, *Rochester Institute of Technology*

Assuming no prior knowledge of spectrometry, this book is an introduction to spectral interpretation for organic structure determination. Considerable reference material makes the book a useful first resource for practicing organic chemists or for students. Topics such as fragmentation, chemical shift, shift reagents, determination of a molecular formula, and many more are discussed.

0 471 79177-6 1974 approx. 350 pages \$12.95 (tent.)

11. THE CHEMIST'S COMPANION

By Arnold J. Gordon, *Pfizer Pharmaceuticals*, and Richard A. Ford, *Montgomery College*

"... a major part is composed of questions on 'how-to-do-it, what-is-it, and what-do-I-use-and-when, and where-do-I-find-it-or-buy-it.'

"... it is hard to open to a page that does not have something outstandingly useful... At its reasonable price, 'Companion' can be recommended strongly for personal purchase (the library copy is likely to be out most of the time)."

—*Journal of The American Chemical Society*

0 471 31590-7 1973 537 pages \$14.95

WILEY-INTERSCIENCE

a division of **John Wiley & Sons, Inc.**
605 Third Avenue, New York, N.Y. 10016
In Canada: 22 Worcester Road, Rexdale, Ontario

Prices subject to change without notice.

092-A4435-WI



WILEY-INTERSCIENCE, Dept. 926

605 Third Avenue, New York, N.Y. 10016

Please send me the book(s) whose number(s) I have circled below:

(1-05647-2) (1-81019-3) (1-27788-6) (1-19674-6)

(1-88040-X) (1-58388-X) (1-02545-3) (1-03847-4)

(1-93366-X) (1-79177-6) (1-31590-7)

My check (money order) for \$_____ is enclosed.

Please bill me. (Restricted to the continental United States.)

Name _____

Address _____

City/State/Zip _____

Please add state and local taxes where applicable.

Prices subject to change without notice.

092-A4435-WI

CIRCLE 253 ON READER SERVICE CARD

Comprehensive Survey of Mass Spectral Literature

Mass Spectrometry of Inorganic and Organometallic Compounds. M. R. Litzow and T. R. Spalding. xv + 620 pages. American Elsevier Publishing Co., Inc., 52 Vanderbilt Ave., New York, N.Y. 10017. 1973. \$51.50

Reviewed by William P. Weber, Department of Chemistry, University of Southern California, Los Angeles, Calif. 90007

This book is a must for purchase by science libraries. However, its high price will definitely limit personal library purchase to those active in the field of mass spectrometry of organometallic compounds. The book comprehensively reviews all aspects of the mass spectral literature on inorganic and organometallic compounds through 1970. A few references to work published in 1971 are also included. The book is divided into two parts. The first is a concise introduction to mass spectrometry. Basic instrumentation is discussed in Chapter 1. In Chapter 2, mass spectra, types of ions observed, resolution, metastable peaks, and fragmentation are reviewed. Chapter 3 covers information obtainable by mass spectrometry: molecular weight, isotopic abundance, ionization potentials, etc. It seems unfortunate to me that 77 pages are spent on such elementary material in an advanced monograph.

The second part (pages 79-617) is the heart of the book. Compounds of the nontransition elements are divided into chapters (4-10, pages 87-469) according to their periodic group. The chapters on the main group compounds III, IV, and V were particularly good. The compounds of the transition metals are considered in a single chapter (11, pages 471-610). It is organized by considering the types of ligands present (carbonyl, nitrosyl, cyclopentadienyl, etc). The final chapter considers the rare gases. Each chapter is provided with tabulations of data—for the natural abundance of isotopes, bond dissociation energies, appearance potential data, as well as considerable discussion of fragmentation pathways observed for various types of compounds. The diagrams, formulas, and tables are quite clear. However, the book does not include an author index, and the

subject index is only three and a half pages long. This brief index will certainly make location of data difficult.

GLC: How to Learn the Basics

A Programmed Introduction to Gas-Liquid Chromatography. Second edition. J. B. Pattison. xv + 303 pages. Heyden & Son, Inc., 225 Park Ave., New York, N.Y. 10017. 1973. Paperbound. \$8

Reviewed by J. J. DeStefano, Biochemicals Department, Experimental Station, E. I. du Pont de Nemours & Co., Wilmington, Del. 19898

This relatively painless programmed instruction into the theory and practice of gas-liquid chromatography is recommended for the training of new assistants and for use by novice chromatographers. In general, this soft-cover instruction booklet is easy to use. Short discussions are immediately followed by a question designed to test the reader's comprehension of the points which have been covered. Multiple-choice answers are provided, and the reader is referred to a given page of the text depending on his choice of answer. On that page, the reader is told whether the chosen answer is correct or not, and if it is not correct, additional information is provided which should enable him to go back and choose the correct answer.

Starting with a basic discussion of characteristics of organic compounds such as boiling points, vapor pressure, hydrogen-bonding, and partition coefficients, the text leads the reader to the use of these characteristics for predicting the retention and tailing behavior of these compounds in a gas chromatographic system. Various strategies are presented for the elimination of peak asymmetry and the achievement of peak resolution. The techniques of preparation of column packings, the packing of columns, sample introduction, and qualitative and quantitative analyses are adequately explained, and the components of a simple GC instrument are described. Basic gas chromatographic terms, such as theoretical plates, effective plates, and peak resolution,

are defined, and examples are given to explain their use. Appendices are included which refer the student to additional readings, introduce the Kovats retention index, and describe available solid supports. Overall, the knowledge gained from reading through this programmed text should provide most beginning chromatographers with a better understanding of gas chromatography.

Inorganic and Organic Luminescence

Absorption of Light and Ultraviolet Radiation: Fluorescence and Phosphorescence Emission. George H. Schenk. xii + 312 pages. Allyn & Bacon, Inc., College Order Dept., Rockleigh, N.J. 07647. 1973. Paperbound. \$6.50

Reviewed by Raymond F. Chen, Laboratory of Technical Development, National Heart and Lung Institute, Bethesda, Md. 20014

This book is useful either as a monograph or a classroom text and deals with photoluminescence. There are seven chapters, the titles of which are followed by suitable quotations, usually from the Bible or George Stokes. Chapters 1 and 2 introduce the reader to the nature of light, Beer's Law, molecular orbital and crystal field explanations of electronic transitions, and Jablonski diagrams. Chapter 3 introduces fluorescence and surveys its applications. Chapter 4 continues with luminescence, including the kinetics of emission, quenching, and phosphorescence. Chapter 5 concerns the triplet states of solids and liquids. Chapter 6 surveys the luminescence of inorganic ions and their chelates. Chapter 7 is a brief description of commercially available instrumentation for measurement of luminescence. About two dozen problems are given after each chapter and are instructive in themselves since they are based on actual data from the literature. A section containing laboratory experiments also follows each chapter. There are several appendices, solutions to selected problems, and, finally, an adequate index.

3 good reasons laboratories rely on Buchler for Polyacrylamide Gel Electrophoresis

1. POLY-PREP® for Concentration or Fractionation with Continuous Elution.

A temperature regulated preparative instrument for proteins, polynucleotides and heat sensitive materials, such as enzymes. Provides shorter electrophoresis times, flexibility in design of separation system and continuous elution.

2. POLYANALYST for Electrophoresis on an Analytical Scale.

Lower buffer chamber is temperature regulated and interchangeable to accommodate 18 tubes up to 250 mm in length. Ideal for analytical scale electrophoresis or for determining operating parameters of the Poly-Prep.

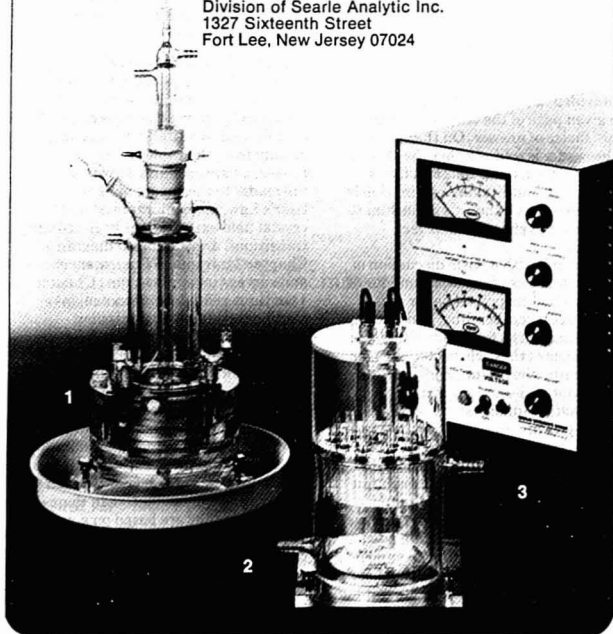
3. POWER SUPPLY-Constant Current or Constant Voltage.

Provides long-term stability. Setting maintained within $\pm 0.05\%$ for as long as it takes to complete separations. Full burnout protection and easy to read, separate voltmeter and milliammeter.

SEARLE

Buchler Instruments

Division of Searle Analytic Inc.
1327 Sixteenth Street
Fort Lee, New Jersey 07024



CIRCLE 26 ON READER SERVICE CARD

Books

There is an underlying feeling of enthusiasm for the subject throughout this book, and one suspects that the author is an effective teacher. As pointed out in the preface, there is a lacuna in the usual chemical curriculum which graduate students are left to bridge on their own if they are to work with luminescence. The author strikes a good balance between inorganic and organic luminescence. The book is enjoyable to read and can profitably be used in short courses dealing with luminescence spectroscopy.

Although some explanations are oversimplifications, they are never grossly erroneous. It can be argued that the most important goal of such a text is to maintain and develop the student's enthusiasm for an intrinsically interesting subject. Too often, the anxiety and negative reinforcement of formal course work ruin the subject for a student. To counteract the basically depressing nature of academia, the author includes titillating experiments (e.g., determining the quinine content of drinks), practical applications (e.g., use of luminescence to read chromatograms and identify solids), and illustrations from everyday life (criminology and pollution; make-up of TV phosphors and postage stamp coatings).

There are a number of minor criticisms one could level. A fair number of obvious misprints occur, including the emission maximum of tryptophan listed (page 140) as 438 nm rather than 348 nm. On page 275, a photomultiplier is described as a solid-state device. In the same section, a distinction is made between a phototube and a photomultiplier, although many use the two terms interchangeably. Some commercial instruments are described in greater detail than others, possibly because those are the ones used in the author's classes. In a subject as large as luminescence, a small book such as this inevitably will omit many aspects of the field. Still, one would have expected some mention of polarization and more discussion of the fluorescence lifetime. The author's research area seems to deal with inorganic photoluminescence, especially for analytical applications. This fact may explain the lack of attention given to fluorescence spectroscopy used in biophysical chemistry to study ligand binding by macromolecules, to study conformational changes, and to prove microenvironments. Energy transfer by the Forster mechanism is inadequately treated.

(continued on page 226 A)

Dispense and dilute any reagent with 0.1% precision... many models... 50% lifetime guarantee.

1.

Now L/I's REPIPET® dispenser comes with a convenient, extra wide-mouth low-profile two-opening bottle. Take your choice: pour reagent into the extra wide mouth. Or, leave your dispenser permanently in place on one opening, use the other opening to refill with reagent. Holds 1000 ml. Dispenses any analytical reagent except HF with 1% accuracy, 0.1% reproducibility. Stocked in 1, 5, 10, 20 and 50 ml sizes. Prices start at \$59.50.

Circle No. 152



REPIPET Dispensers with 2-opening container.

2.

Universal REPIPET dispenser fits any container up to 5-gallon carboys and dispenses any analytical reagent. Simply cut the tubing to fit into the lower extremity of your container and you'll get every bit of reagent out. Stocked in 1, 5, 10, 20 and 50 ml sizes. Prices start at \$75.00.

Circle No. 153

3.

The REPIPET Dilutor is the best on the market for under \$125. Why? Because it's precise and simple to operate. Accuracy is 1%, reproducibility 0.1%. Only glass and Teflon® contact reagent, so you can safely use any reagent except HF. All L/I Dilutors are self-cleaning, minimizing chances for cross-contamination. Square bottle provides firm base. A wide variety of tips is supplied at no charge. Many models to choose from 1 to 50 ml. Prices start at \$109.50.

Circle No. 154



UNIVERSAL REPIPET Dispenser.



REPIPET Dilutor.

4.

AUTO-REPIPET® Dispenser and Dilutor. Many times, two hands aren't enough when you are dispensing reagents into capped containers—or when you need the use of your hands to position equipment. The AUTO-REPIPET Dispenser or Dilutor uses your foot as a third hand, dispensing any reagent except HF with 0.1% reproducibility and 1% accuracy. Simply step on the air-activated foot pedal and the instrument dispenses automatically, leaving both of your hands free for other purposes. The safest way ever for dispensing corrosive reagents. Available from stock in 1, 5, and 10 ml sizes for dispensing or diluting. Prices start at \$160 each complete.

Circle No. 155



AUTO-REPIPET® Dispensers and Dilutors.

5.

Latest L/I catalogs give you complete details. Free for the asking.

Circle No. 156

Order from Labindustries or your distributor.

LABINDUSTRIES

1802 Second Street/Berkeley, CA 94710/Phone (415) 843-0220/Cable LABIND



CIRCLE 157 ON READER SERVICE CARD

New Bethlehem Hg VACUPICK



- simplifies retrieval of spilled mercury droplets from any surface
- lightweight, portable
- vacuum pump capable of 20" Hg
- salvages spilled mercury which would otherwise be lost
- complies with OSHA requirements

safe, efficient pickup of spilled mercury droplets

The Hg VACUPICK—the latest development from Bethlehem Apparatus—offers a convenient, simplified way to retrieve spilled mercury droplets as well as larger pools of mercury.

Modern, efficient operation

The Bethlehem Hg VACUPICK operates by means of an oilless vacuum pump which creates a vacuum of 20" Hg. A 40" soft plastic tube with a stainless steel pick retrieves the spilled mercury, which is conveyed into a plastic receiving bottle. A rubber ball shutoff valve prevents the mercury from being sucked into the pump. No detectable mercury vapor from pump exhaust.

Reduces losses

With the Bethlehem Hg VACUPICK it is now possible to salvage a much higher percentage of spilled mercury both in laboratories and production facilities.

WRITE FOR BULLETIN Hg 73



BETHLEHEM APPARATUS COMPANY, INC.

Hellertown, Pa. 18055 / (215) 838-7034

CIRCLE 31 ON READER SERVICE CARD

QUANTITATIVE ANALYSIS 3rd Ed. 1974

R. A. Day, Jr. and A. L. Underwood, both at Emory University

New from Prentice-Hall! This comprehensive new edition provides a complete and balanced mixture of the traditional and the modern in analytical chemistry—for the novice and more advanced chemistry student.

The authors stress basic concepts and offer discussions of such topics as elementary statistics and data, and all facets of gas-liquid and liquid chromatography. Other new chapters explore flame emission, atomic absorption, spectroscopy, fluorescence, and analog and digital electronics and automation in analytical chemistry.

Includes figures, illustrations, and challenging problems. A handy *Teacher's Manual* provides answers to the text's analytical problems. March 1974, 576 pp., \$13.95

For more information, write: Robert Jordan, Dept. J-854, College Division, PRENTICE-HALL, Englewood Cliffs, New Jersey 07632

CIRCLE 188 ON READER SERVICE CARD

Books

In spite of these criticisms, the book is a good one and deserves to be read and utilized in the classroom.

For Those with No Chemical Background

Instrumental and Separation Analysis. C. T. Kenner. xii + 338 pages. Charles E. Merrill Publishing Co., 1300 Alum Creek Dr., Columbus, Ohio 43216. 1973. \$11.95

Reviewed by Jonathan W. Amy, Department of Chemistry, Purdue University, Lafayette, Ind. 47907

This book is written as a text for a second semester of analytical chemistry taught from a viewpoint that students have no background in physical chemistry or calculus. Because many such students study disciplines of biological or medical sciences, emphasis is placed upon those methods commonly used in these branches of science. Thus, techniques such as radioactivity and electrophoresis are covered in more detail than in conventional texts on instrumental analysis. No laboratory procedures are presented. Short problem sets are included at the end of each chapter.

The text consists of 15 chapters and is organized into four sections. One third of the material concerns optical methods, and one sixth is devoted to electrochemical techniques. The subject of separations is covered in two chapters containing 20% of the text, and the remainder is devoted to a variety of miscellaneous methods such as NMR, MS, radioactivity, and even a short section of solid-state electronics. No references are given in the text; the appendix contains a section on the literature of analytical chemistry. General reference books are listed by chapter headings.

The style of writing is clear and concise. Chapter format starts with an introduction to and the physical principles of the method followed by a section on instrumentation. This is usually quite elementary with simple diagrams and photographs of some commercial equipment. Some discussion of errors and method limitations is included, and the chapters conclude with short applications sections.

A student spending a semester with this text will gain a vocabulary and should recognize common instrumental terms as he encounters them. The student's ability to appreciate the power or limitations of these techniques in solving practical problems will depend upon the skill of the in-

Eastman Organic Chemicals News

For your consideration . . . select products from a family grouping of specialties. One may just spark an application you're researching or developing. We'd like to help. Detailed product information is as close as the coupon below.

New additions

N-Methyl-(7-dimethylcarbamoyl)quinolinium Iodide (EASTMAN 11864). Fluorescent probe for acetylcholinesterase, sensitive to concentrations in the nanomolar range. Active sites of the enzyme can be titrated, since the first-order carbamoylation reaction rate is much higher than the concentration-independent decarbamoylation reaction. The number of active sites per molecule can be calculated from the turnover number and the enzyme normality. [*Biochemistry*, 10, 4114 (1971).]

Phenazine Methosulfate (EASTMAN 11509).

The combination of phenazine methosulfate and nitro BT (EASTMAN 11350) forms an activity stain for enzymes. Has been used for the *in situ* identification after acrylamide gel electrophoresis of threonine deaminase [*Science*, 170, 1414 (1970)] and of bovine LDH [*Biochemistry*, 9, 4372 (1970).]

pH Indicators

If you use pH indicators in your work, our wall chart, *pH Ranges and Color Changes of EASTMAN Indicators*, should be a useful addition to your laboratory. In addition to directions for preparing 67 indicator solutions, its four-color format illustrates the color changes over the active pH range of the indicators. Use the coupon below to request your copy of Kodak Publication No. JJ-13. CIRCLE 71 ON READER SERVICE CARD

For TLC

The KODAK Laboratory Sprayer (Catalog No. 13173), with dip tube and orifice designed for spraying TLC visualization reagents and other liquids of low viscosity. The slim aerosol unit is easy to hold and easy to clean after use.

Prepare your visualization reagents in advance. When you're ready to spray, simply screw the aerosol unit directly onto the bottle . . . no separate spray heads to buy or replace. Only 3 ounces of propellant, but a propellant-to-reagent spray ratio of 1:5, so you can spray approximately a pint of solution. More economical to use than many larger units having higher propellant-to-reagent ratios. Sold singly at a list price of \$4.00 each and in convenient four-packs at \$12.50. For more information, request a copy of Kodak Publication No. JJ-36.



CIRCLE 72 ON READER SERVICE CARD

List prices shown are suggested prices only and are subject to change without notice.

For electrophoresis

Eastman Kodak Company offers a large number of reagents for acrylamide gel electrophoresis . . . some with very special properties for special applications.

For instance, **N,N'-Diallyltartardiamide (EASTMAN 11444)** is a cross-linking agent which forms solubilizable gels. By substituting N,N'-diallyltartardiamide mole for mole in place of methylenebisacrylamide, gels are formed which are soluble in 2% periodic acid. These gels dissolve in 20 to 30 minutes at room temperature or in about 10 minutes at 37 C.

Quantitation by liquid scintillation counting is possible after this treatment, since periodic acid does not contribute to the quenching expected for the amount of water present in the system. [*FEBS Letters*, 7, No. 3, 293 (1970).]

For more information on the initiators, stains, buffer components, and specially purified monomers offered by Eastman Organic Chemicals, request a copy of Kodak Publication No. JJ-11, *Reagents for Acrylamide Gel Electrophoresis*.

CIRCLE 73 ON READER SERVICE CARD



Eastman Kodak Company
Organic Chemicals Markets
Dept. 412-L
Rochester, N.Y. 14650

2-40

Please send the following:
 Publication No. JJ-11, Reagents for Acrylamide Gel Electrophoresis Publication No. JJ-36, Data on KODAK Laboratory Sprayer for TLC use Publication No. JJ-13, pH Ranges and Color Changes of EASTMAN Indicators

Name _____

Company _____

Address _____

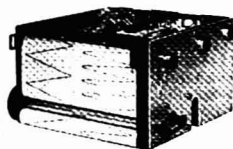
City _____

State _____

Zip _____

WIDE CHART RECORDERS

up to three
100 mm channels with
50 millisecond full scale
response



MFE's OEM, 19" rack mount or portable wide chart recorders are ten times as fast as potentiometric types. The inkless heated stylus on our patented galvanometric moving iron pen motor travels 100 mm in less than 50 milliseconds.

Ideal for high response systems such as electrophoresis densitometers, autoanalyzers and spectrometers that may now be recorder limited.

1, 2 or 3 channels with 1, 2 or 3 events available. 1, 2, 3, 4 or 7 speeds ranging from mm/hr to mm/sec.

Options include paper take-up, timers, digital edge printer, attenuators, internal calibration.

Write for complete specifications and prices.

MFE

MFE CORPORATION

Keewaydin Drive, Salem, N.H. 03079
Tel 603 893-1921 • TWX 710 366-1887
TELEX 94 7477

See us at the Pittsburgh Conference,
Booth 714

CIRCLE 164 ON READER SERVICE CARD

Books

structor and the development of a laboratory course to be used with the text.

New Books

Third International Congress of Atomic Absorption and Atomic Fluorescence Spectrometry: Vols 1 and 2. M. Pinta, Ed. 924 pages. Halstead Press, 605 Third Ave., New York, N.Y. 10016. 1973. \$35 (for both)

Included in these two volumes are most of the papers presented at the 3rd ICAFAS held in Paris in September 1971. Presumably, the poor quality of the text reproduction is not due to the process used (photolithography), but to the poor quality of the original copy used for reproduction. Nonexcusable are crossed-out words and handwritten insertions.

Catalysis: Vols 1 and 2. Joe W. Hightower, Ed. 1483 pages. American Elsevier Publishing Co., Inc., 52 Vanderbilt Ave., New York, N.Y. 10017. 1973. \$79 (for both)

This two-volume set contains the complete transactions (text and discussion) of 107 submitted papers and six invited lectures presented at the Fifth International Congress on Catalysis, Miami Beach, Fla., August 20-26, 1972.

Energy Transfer Parameters of Aromatic Compounds. Isadore B. Berlman, ix + 379 pages. Academic Press, Inc., 111 Fifth Ave., New York, N.Y. 10003. 1973. \$20

Presented in this book are tables of values for Forster's standard reference parameters as well as for an overlap integral using paired combinations of over 200 aromatic compounds in liquid solutions. Also included are an elementary discussion of spectroscopic concepts, a survey of inter- and intramolecular electronic energy transfer, and a look at ESR and laser techniques. This volume should serve as a companion to the author's second edition of "Handbook of Fluorescence Spectra of Aromatic Molecules."

Activation and Decay Tables of Radioisotopes. E. Bujdosó, I. Fehér, and G. Kardos. 575 pages. American Elsevier Publishing Co., Inc., 52 Vanderbilt Ave., New York, N.Y. 10017. 1973. \$36

Activation and decay data are presented in this volume. The data include half-lives, gamma-ray energies, and intensities of 249 radioisotopes formed by (n, γ) reactions on 173 stable isotopes of 80 elements.

Company Manuals

Clinical Chemistry Procedures Using Gas Chromatography. Part No. 990-9853. Perkin-Elmer Corp., Instrument Division, Main Ave., Norwalk, Conn. 06856. 1973. \$10

This handbook contains methods for the determination of many clinically important biological compounds. Individual determinations included are pregnanediol, pregnanetriol, estriol, cholesterol, vanillylmandelic acid, and homovanillic acid in urine, and restricted drugs in serum and urine. Perkin-Elmer scientists plan to continually augment the text with additional determinations and other useful information.

Elementary Theory of Gas Chromatography with Bibliography and Experiments. 42 pages. GOW-MAC Instrument Co., 100 Kings Road, Madison, N.J. 07940. 1973. Paperbound. \$5.00 (educational discounts available on multiple orders)

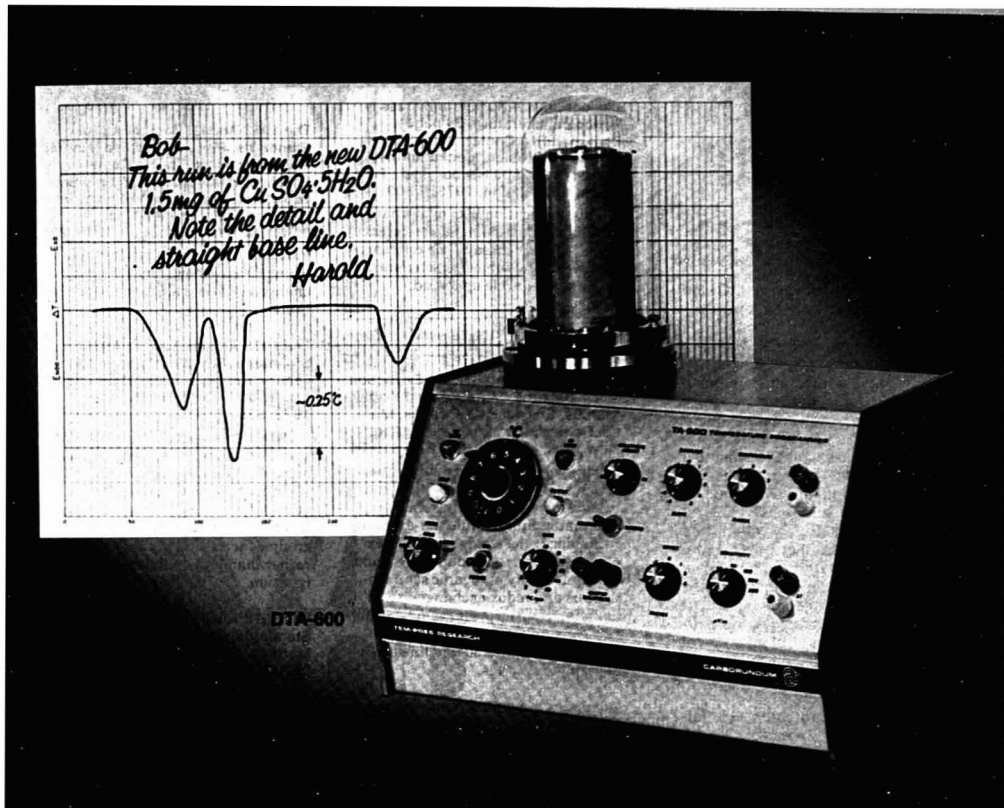
The first part of this booklet contains the basic theory of GC, including condensed but comprehensive operating instructions for a gas chromatograph. Part two is a selected bibliography, and part three is a collection of 13 experiments. New experiments will be available after they have been tested.

The Practice of Gas Chromatography. Part No. 5950-8225. Fred W. Rowland. 117 pages. Hewlett-Packard Co., Avondale Division, Route 41, Avondale, Pa. 19311. 1973. Paperbound. \$10

The author is attempting to bridge the gap between the hardware-oriented instrument manuals and the theoretical treatments found in many of the existing books and to put into perspective the many variables of equipment selection and operating procedures so that the user can make the proper choices for the solution of his particular problem. There is little theory, but a good deal of the tricks of the trade that come with experience, included. The book is available through any Hewlett-Packard sales office.

Liquid Crystal Bibliography. No. JJ-193. 26 microfiche cards. Eastman Kodak Co., Department 454, Rochester, N.Y. 14650. 1973. \$25

This microfilm bibliography contains 3281 references from the time period September 1888 to May 1973. Author and subject indexes are included, together with a numerical sequence file and a reference-frequency file.



Introducing the DTA-600 for Quality Control by Tem-Pres

Tem-Pres presents the New DTA-600. An economical Differential Thermal Analysis System designed to satisfy on-line and laboratory requirements for quality control.

The DTA-600 is a highly sensitive instrument with rapid heating and cooling rates for the maximum number of QC tests per day; simplified fixed position controls for ease in operation by technicians; a broad selection of sample cup materials and

volumes; and inexpensive thermo-couple assemblies easily replaceable in your laboratory.

Exclusive Tem-Pres Automatic Baseline Compensation is included for those flat reproducible baselines that are so important in calorimetric measurements.

Resolve your Quality Control Requirements with the DTA-600 at \$4950. For complete details and specifications, please contact: Mr.

Gerry Zimmerman, Tem-Pres Division, The Carborundum Company, 1401 South Atherton Street, State College, Pennsylvania 16801. Phone 814 237-7631



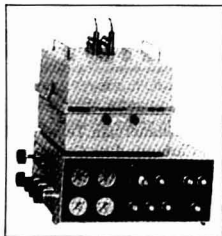
CARBORUNDUM

Updating your GC lab?

You've been in GC long enough now to know what you *really* need. You're working with a 1970-level budget. This time around, buy dedicated equipment. Specify the high-performance parameters you require — we'll specify the low-cost, off-the-shelf system to fit your needs. For instance, a typical Aminco/Shimadzu Dual F.I.D.* Isothermal GLC System, costing less than \$2000, features: large column oven, on-column injection system, unique injection port design, quartz jet detector, dual-glass columns, pressure flow control and no transfer lines. A lot for the money.

Updating your GC lab? Aminco/Shimadzu GC systems are available for every application, whether it be quality control (GC-4B Series), versatile research (GC-5A Series), or drug-screening (GC-3B Series). Send for literature describing Aminco/Shimadzu Gas Chromatography Systems.

* Flame Ionization Detector



AMINCO®

Shimadzu

AMERICAN INSTRUMENT CO.
DIVISION OF TRAVENOL LABORATORIES, INC.
8030 Georgia Avenue
Silver Spring, Maryland 20910

CIRCLE 7 ON READER SERVICE CARD

Books

Bibliography of Radioimmunoassay Periodical Literature. 34 pages. Beckman RIA Center, Scientific Instruments Division, Beckman Instruments, Inc., 2500 Harbor Blvd., Fullerton, Calif. 92634. 1973. \$3.00

This publication lists more than 950 clinical and biomedical references to radioimmunoassay. The references are indexed by subject matter and the date the article appeared.

Continuing Series

Ion Exchange and Solvent Extraction: Vol 4. Jacob A. Marinsky and Yizhak Marcus, Eds. xii + 265 pages. Marcel Dekker, Inc., 95 Madison Ave., New York, N.Y. 10016. 1973. \$19.75

This volume contains discussions on ion exchange in nonaqueous and mixed solvents; ligand-exchange chromatography; liquid ion-exchange technology; electronic and ionic-exchange properties, conductivity, and permselectivity of organic semiconductors and redox exchangers; and equations for the evaluation of formation constants of complexed ion species in crosslinked and linear poly-electrolyte systems.

Advances in Electrochemistry and Electrochemical Engineering, Vol 9: Optical Techniques in Electrochemistry. Rolf H. Muller, Ed. 542 pages. John Wiley & Sons, Inc., 605 Third Ave., New York, N.Y. 10016. 1973. \$29.95

This new volume contains articles on internal reflectance spectroscopy in electrochemistry, specular reflection spectroscopy of the electrode-solution interface, principles of ellipsometry, application of ellipsometry to electrochemistry, double-beam interferometry for electrochemical studies, holography and holographic interferometry in electrochemistry, and optical microscopy in electrochemistry. Included are subject and cumulative indexes for Vols 1-9.

The following are available from American Society for Testing and Materials, 1916 Race St., Philadelphia, Pa. 19103. For countries other than USA, Canada, and Mexico, add 5% shipping charges.

The 1973-1974 List of ASTM Publications. 30 pages. 1973. (A single copy of this publication, requested on company letterhead, will be sent free of charge.)

This booklet lists more than 600 ASTM publications dealing with the standardization of methods of test

and specifications for materials, the knowledge of materials, and materials evaluation.

The 1973 Annual Book of ASTM Standards, Part 22: Sorptive Mineral Materials; Soap; Engine Coolants; Polishes; Halogenated Organic Solvents; Activated Carbon; Industrial Chemicals. Publication Code No. 01-022073-15. 882 pages. 1973. \$29

Part 22 contains 177 standards of which 19% are new, revised, or changed in status since the 1972 edition.

The 1973 Annual Book of ASTM Standards, Part 23: Water and Atmospheric Analysis. Publication Code No. 01-023073-16. 1136 pages. 1973. \$35.75

Part 23 contains all of the ASTM standards on water and atmospheric analysis. Thirty percent of the 151 standards are new, revised, or changed in status. For the first time, all of the standards on water are grouped according to subject matter rather than alphanumerically by designation.

The 1973 Annual Book of ASTM Standards, Part 30: General Testing Methods. Publication Code No. 01-030073-41. 1658 pages. 1973. \$54

Of the 194 standards contained in part 30, 48 are new, revised, or changed in status.

The 1973 Annual Book of ASTM Standards, Part 31: Physical and Mechanical Testing of Metals. Publication Code No. 01-031073-23. 1272 pages. 1973. \$39

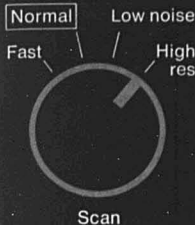
This book contains 126 standards of which 22 are new, revised, or changed in status.

The 1973 Annual Book of ASTM Standards, Part 33: Index to ASTM Standards. Publication Code No. 01-033073-42. 260 pages. 1973. \$4.25

This book lists all of the more than 4800 standards alphabetically by subject matter, indicates the numerical designation of each standard, and refers to the 33-part annual book in which each standard is published. The standards are also listed by numerical designation.

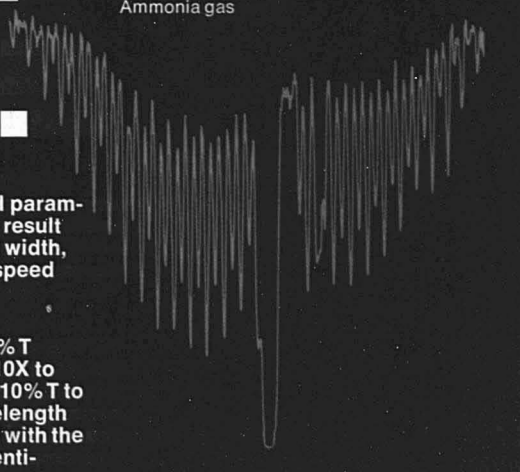
Miscellaneous ASTM Standards for Petroleum Products. Eleventh edition. Publication Code No. 03-402073-12. 1054 pages. 1973. Paperbound. \$27.50

This book is a supplement to Parts 17 and 18 of the 1973 Annual Book of ASTM Standards. Forty-six percent of the 235 standards are new, revised, or changed in status since the last edition (1971).



What you set is what you get.

High resolution
Wavenumber expansion 5X
Ammonia gas



On the new SP1100 IR one control optimizes all parameters. Select the desired result and the correct gain, slit width, time constant and scan speed are automatically set.

On the new SP1100 you also get *continuous* % T expansion from 0.8X to 10X to permit expansion of any 10% T to full scale . . . and 5X wavelength expansion synchronized with the chart for unequivocal identification of band positions . . . repetitive scan . . . fast scan (6 minutes is normal).

Call Frank Hamm, Manager Spectrophotometry and Chromatography at 914-664-4500. Ask him about the price. It is about \$1000 lower than you might think.

**PHILIPS
ELECTRONIC
INSTRUMENTS**

750 South Fulton Ave.
Mount Vernon, NY 10550
A North American Philips Co.

CIRCLE 198 ON READER SERVICE CARD

Send for your copy of this 44 page book. It spells out why FLORISIL® and FLORISIL TLC are widely used for column and thin layer chromatography. Gives you chemical composition, physical properties, adsorptivity data and a bibliography designed to show you how FLORISIL may be used to solve difficult separation problems in these twelve areas: general;

vitamins; alkaloids — nitrogen compounds — drugs; steroids — hormones; pesticide residues; antibiotics; petroleum and shale oil; enzymes; terpenes; lipids; carcinogens and miscellaneous studies.

Write for your free copy. Contact Floridin Company, Dept. A-16, Three Penn Center, Pittsburgh, Pa. 15235. Phone 412-243-7500.

New, Improved -and Free.

Bibliography of studies and applications of FLORISIL as an adsorbent for chromatography.



CIRCLE 77 ON READER SERVICE CARD

PG-208

Editors' Column

Trace Metals, Indians, and Urban Man

A recent National Science Foundation report tells that scientists, studying primitive tribes in remote areas of South America, have determined that chromosome damage and mercury levels in blood serum in some isolated Indian tribes exceed those normally found in urban man.

This discovery came about from a study started eight years ago. Working with the Indians in the Amazon jungles, the scientists were seeking to distinguish tribal genetic structures and gather biomedical data to serve as base line measurements to permit them to gauge the nature and tempo of modern man's evolution. They wanted to learn more about the biological adaptations of man as he progressed from a primitive hunter to an urban worker. The findings are surprising because chromosome damage and mercury levels are considered the price man pays for becoming civilized.

The study also found, besides the unusually high mercury levels, unusually low levels of cadmium and lead. Dr. Lawrence Hecker of the University of Michigan's School of Public Health, who headed the research portion of the study that was concerned with mercury and other trace metals said, "Mercury has been present in low levels in our environment for years with no apparent ill effect. At high levels in some areas, mercury is known to have ill effects on man. Some of the Yanomama (a tribe in Venezuela and northern Brazil) villages have much higher levels than people in cities in the United States, but it's having no apparent adverse effect on them. Fish, a common source of mercury, is not a major part of the Yanomama diet." "The mercury levels were expected to be much lower among these tribes because mines and factories that contribute to mercury in the environment do not exist in the area inhabited by the Indians. The low lead levels, among the lowest ever recorded in the world, could not be accounted for by just the absence of gasoline burning vehicles which may contribute to higher levels in the civilized world.

According to Dr. James Neel from

the University of Michigan's School of Medicine and the project's head, "These data imply two possibilities—modern man is not as badly off as he sometimes supposes, and genetic and biological damage has been with him a long time, probably through all stages of his development." Although the group of scientists were able to hypothesize that the chromosome damage may have been caused by a natural agent such as a virus, they could not explain the high incidence of mercury or the low levels of cadmium and lead encountered.

Unfortunately, Dr. Neel's comment that "modern man is not as badly off as he sometimes supposes," if taken out of context, could lend credence to the arguments of some that pollution is not as great a problem as was recently thought. This becomes especially important in this time of energy crisis when second thoughts are being had about emission controls on automobiles and the burning of sulfur-containing coal. His conclusion is based on an incomplete study, although to be fair, one must remember that the mercury, cadmium, and lead data were actually by-products of a different study. The reasons why the mercury levels are so high and the cadmium and lead levels so low must first be ascertained before one can conclude that modern man may be all right with regard to these trace metals.

The detection limits for these trace metals are constantly being lowered, and the determination of these metals is now being done in more and varied samples. Perhaps the time has come to emphasize the correlation of levels detected in environmental samples or in man with specific problems encountered by man because of these metals. How many times should we be told that a certain element can be determined in a specific sample by a specific analytical technique down to what may be an insignificant level? Shouldn't it be time to emphasize finding out if a certain level is significant or not and why—possibly starting with the Indians and working up to urban man?

A. A. Husovsky

KEITHLEY'S NEW CURRENT AMPLIFIER MAKES SMALL CURRENTS INTO GIANTS



...faster than anything

Whether used in mass spectroscopy, fast semiconductor production tests, photomultiplier outputs, or whatever, the Model 427 Current Amplifier opens new dimensions in low level current measurements. It can perform optimally for dynamic range or response time, according to user's wishes. It features sensitivity to 10^{-14} ampere, switch-selected rise times to 15 microsecond and over 80 dB dynamic range. Built-in zero suppression and overload protection add to operating convenience.

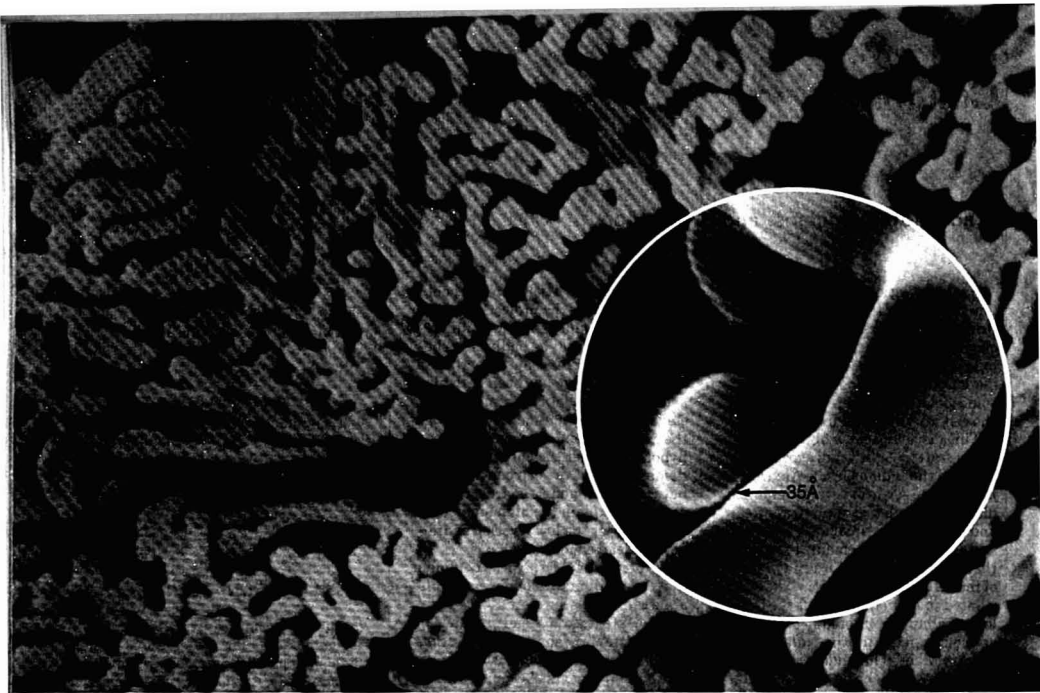
RANGE 10^{-14} to 10^{-3} A
RISE TIME 15 μ S to 0.3 sec.
DYNAMIC RANGE	. 40 to 80 dB
STABILITY 500 μ V/ $^{\circ}$ C
SUPPRESSION	... 10^{-3} to 10^{-10} A
PRICE \$895 U.S.A.

SEND FOR TECHNICAL LITERATURE TODAY



KEITHLEY
INSTRUMENTS

U.S.A. 28775 AURORA ROAD, CLEVELAND, OHIO 44139
EUROPE 14, AVENUE VILLARDIN, 1009 PULLY, SUISSE
CIRCLE 148 ON READER SERVICE CARD



Specimen: Aluminum-lungsten dendrite structures. 24,000X magnification (insert 100,000X). 14KV accelerating voltage. Resolution standard proposed by Dr. S. Ballard, National Bureau of Standards.

We Here Highly Resolve

Things are getting brighter all the time. Take these two remarkable photomicrographs, for instance. They happen to be 1000 times brighter than those images created from thermionic sources.

What's the secret?

Simple. We introduced the world's first commercial Field Emission Scanning Electron Microscope. And we're still in the business of bringing the seekers and searchers the brightest, high-resolution images in microscopy today.

A major difference lies in our revolutionary field emission electron gun. It really delivers. Fast scanning and dynamic viewing of even the finest microstructures. Coated or uncoated. And then there's our totally new system design that lets you scan specimens free from worry about damage, contamination, charging, or other elements that mess up your micrographs.

Each SEM in our growing family features reliable, all-solid-state electronics. Just plug one in, and start examining your own specimen. The same way more and more laboratory researchers throughout the world are doing day-after-day. Let Coates & Welter brighten up your life.

Write us for a current brochure: Coates & Welter Instrument Corporation, 757 North Pastoria Avenue, Sunnyvale, CA 94086, (408) 732-8200. A subsidiary of American Optical Corporation.



COATES \equiv WELTER

leading the resolution revolution

CIRCLE 38 ON READER SERVICE CARD

Laser Optoacoustic Spectroscopy— A New Technique of Gas Analysis

L. B. Kreuzer

DIAX Corp.
250 Sobrante Way
Sunnyvale, Calif. 94086

Laser Optoacoustic Spectroscopy gas analysis offers a single system which can automatically analyze a mixture of gases with high rejection ratios and sensitivity. One particularly promising field of application is gaseous air pollution detection, where a single LOS System can replace the collection of single gas analyzers which is currently required to provide a complete analysis of ambient air

The availability of laser sources of infrared light has greatly increased the range of analytical problems which can be solved by infrared spectroscopy. The optoacoustic effect has proved an effective method, in combination with a laser infrared source, for detecting weak IR absorptions in gases (1, 2). With the combination of a laser source and an optoacoustic method of detecting IR absorption, a new technique of gas analysis called Laser Optoacoustic Spectroscopy (LOS) has been developed. A prototype gas analyzer using LOS built by the author is able to detect gas concentrations as small as 1 part per billion (ppb). It is able to analyze automatically mixtures of gases and differentiate between gases with overlapping infrared absorption spectra.

The purpose of this paper is to describe the new technique of LOS gas analysis to potential users. Since many potential users may not have knowledge of laser infrared sources, a

discussion of lasers and the properties of the light they generate is presented in the next section. This is followed by sections which describe LOS gas analysis, present experimental results, describe the DIAX Model 100 LOS gas analyzer, and discuss applications.

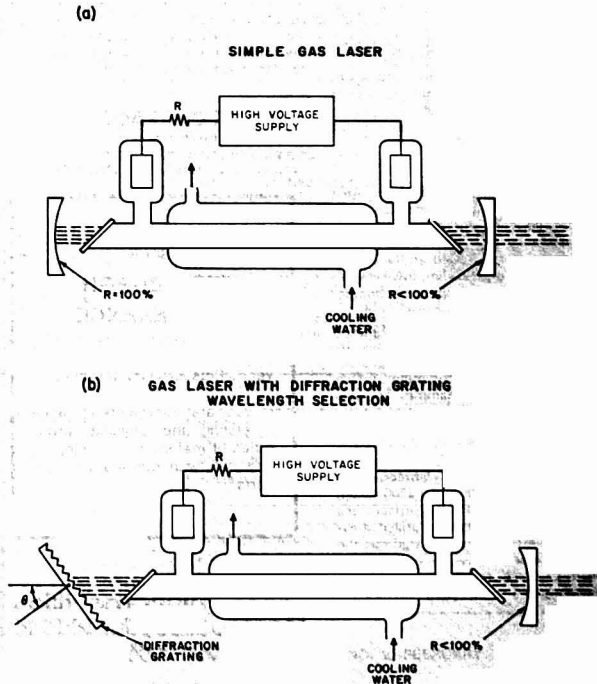
Laser Source of Infrared

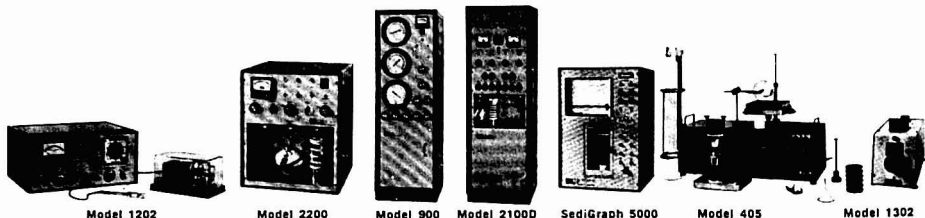
Laser action was first demonstrated at 6943 Å in ruby by Maiman in 1960. Since that time, the types of lasers

and the number of observed emission wavelengths have increased rapidly. Today, it takes 200 pages of the "Handbook of Lasers" (3) to list and describe the more common lasers and their emission wavelengths. Emission wavelengths are now available from the ultraviolet to the far infrared. The current state of laser development suggests that lasers will become increasingly more common as light sources in spectroscopy.

(continued on page 240 A)

Figure 1. Gas laser system. Laser tube is excited by high-voltage discharge between electrodes represented as bulbs at each end
(a) When optical cavity consists of two mirrors, laser emission occurs only at lines of high gain
(b) Discretely tunable laser results when one mirror is replaced by properly ruled and biased diffraction grating. This configuration generates a single wavelength at a time. Rotation of grating causes laser to emit both lines of high and low gain





micromeritics®

We Offer Industry's ONLY Complete Line Of Material And Particle Characterization Instruments

GAS 'SORPTION

DigiSorb 2500 Automatic Multi-Gas Surface Area and Pore Volume Analyzer—Totally automated instrument for gas adsorption-desorption measurement, pore volume, pore size, chemisorption and surface area analysis. EVERYTHING except sample weighing is automatic. Can analyze up to 5 samples without reloading. Can operate up to 4 days UNATTENDED. Specific surface areas greater than 0.001 m²/g can be determined using Krypton and Nitrogen as the adsorbates.

Model 2100D Orr Surface-Area Pore-Volume Analyzer—The most versatile, accurate manual surface area and pore volume analyzer on the market today. Features a live auto-ranging digital display of system pressure from 0.0001 to 1000.0 mm Hg. Measures surface areas from 0.001 m²/g up; performs pore size and volume analyses and chemisorption studies. Uses any non-corrosive gas as adsorbate. No calibration required. Utilizes classical low-temperature gas adsorption (BET) technique.

SURFACE AREA

Model 2200 High-Speed Surface Area Analyzer—A low cost, semi-automatic instrument designed for process control, quality assurance and many development applications requiring speed and accuracy. Utilizes the static equilibrium, low-temperature, gas adsorption (BET) technique. Measures specific surface areas from 1.0 to 1,500 m²/g using Nitrogen as adsorbate. Surface areas indicated automatically by direct digital readout; no calculations required. Can perform 3 complete surface area analyses per hour. Samples are also outgassed on instrument.

Model 2205 High-Speed Surface Area Analyzer—Similar to the model 2200 except specifically designed for low surface area materials. Measures specific surface areas from 0.2 to 100.0 m²/g using Argon as the adsorbate. Surface areas are indicated to the nearest 0.01 sq. meter by direct digital readout. Two to 3 surface area analyses per hour.

PARTICLE SIZE

SediGraph 5000 Particle Size Analyzer—This particle size analyzer provides rapid, automatic determination and direct recording of particle sizes from 100 microns to 0.1 micron diameter. At its very best in submicron to submicron ranges; handles larger sizes with ease. Analyses based on Stokes' Law of sedimentation for aqueous or organic systems. Operates unattended and yields results in minutes.

POROSIMETRY

Model 900 910 Mercury Penetration Porosimeters—Eighteen models in all. Range from 354 down to 0.0035 micron pore diameter, in powders or rigid shapes. Measures pore volumes up to 4.0 cc's. Determines pore volume, size, shape, distribution and porosity. Analyzes 1, 2 or 4 samples simultaneously. 10,000, 30,000 or 50,000 psi range. Series 910 models can measure porosity, pore volume, pore size and pore shape of large sample pieces up to 1-inch diameter by 1-inch high.

POWDER CHARACTERIZATION

Model 405 Powder Characteristics Tester—Gives you consistent, accurate powder property evaluation using ONLY ONE in-

strument. Measurement capabilities include characteristic angles, cohesion, uniformity coefficient, dispersibility, aerated and packed bulk densities, compressibility, distribution of sizes, flowability and floodability. This instrument is a significant advance over traditional, less sophisticated manual methods.

DENSITY

Model 1302 Helium Pycnometer—Determines absolute volume of powdered or porous materials and solid objects from which density can be calculated. Handles inert solids, reactive chemicals, or hygroscopic compounds. Is fast, accurate and easy to operate. Precision of plus or minus 0.03 cc absolute volume. Allows porosity determination when measured object has a definite shape or bulk volume is known.

ZETA POTENTIAL

Model 1202 Electrophoretic Mass-Transport Analyzer—For measuring the electrophoretic mobility of dispersions, including concentrated slurries from which zeta potential may be calculated. Analyzes a wide range of dispersions and suspensions up to 50% by volume without dilution. Handles particles from very small to approx. 1,000 microns diameter; conductivities to 100,000 microhmhos. For flotation, dispersion, flocculation coagulation particle interaction and electrokinetic phenomena studies.

POROSITY

Model 305 Gas Comparison Porometer—Precision instrument for non-destructively determining the bulk and pore volume, porosity and absolute density of porous solids. Uses a gas expansion technique instead of inferior conventional methods like boiling water. Measurements can be made on organic objects or reactive materials. Largest samples usable is 35mm diameter by 76 mm long with one smooth flat end.

MATERIALS ANALYSIS LAB

Micromeritics' complete laboratory services provide coordinated evaluation and characterization of the physical properties of your material samples. Our laboratory is fully equipped and is staffed with full-time particle technology experts.

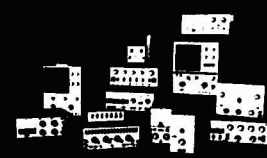
1974
**PITTSBURGH
CONFERENCE**

Our instruments will be on display in booth 101-106 at this year's Pittsburgh conference.

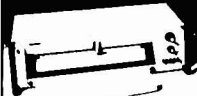
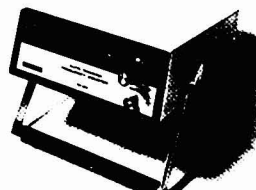
If you are interested in characterizing the physical properties of materials . . . stop by and talk with our team of experts.


micromeritics
 instrument corporation
5590 quaker terrace, houston, tx 77057 • phone 409/444-1500
CIRCLE 174 ON READER SERVICE CARD

New HEATH/SCHLUMBERGER INSTRUMENTS CATALOG FREE



Test Instruments
New \$335,
10mV-10V, 10 Speed
Chart Recorder
New \$325, auto-ranging
110MHz Counter

from Heath/
Schlumberger

Schlumberger
Copyright from Company 1972
Catalog 91-78

The latest issue... includes complete details and specifications on dozens of high performance, low cost instruments for design, R&D and teaching applications. Here are just a few examples:

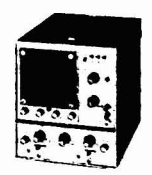
New 10 mV to 10 V Strip Chart Recorder... only \$335*. Four calibrated, hi-Z input ranges... full 10" chart... ten digitally-derived chart speeds from 10 to 0.01 inches or cm/minute... switchable input filtering... complete remote programming capability... easy conversion to metric work... pushbutton chart advance... rack mount design.



600 MHz Frequency Counter... just \$795*. 1 Hz to 600 MHz guaranteed range... input sensitivity: 10 mV @ 35 MHz, 15 mV @ 200 MHz, 50 mV @ 600 MHz... .50 and 1 megohm inputs... high stability TCXO time base... complete remote programming capability for all inputs, outputs & functions, plus BCD output... FCC type-approved for AM & FM broadcast.



Dual Trace 15 MHz scope... only \$595*. 15 MHz vertical bandwidth with 24 ns risetime... 50 mV/cm sensitivity... 1 megohm/35 pf input impedance... 9 position attenuator... 18 calibrated sweep rates from 0.2 us/cm to 100 ms/cm... Chop, Alternate, Ch. 1, Ch. 2 and X-Y modes... Internal/External, AC/DC, +/- triggering... external trigger input, sweep gate output. Standard camera mount bezel.



For your FREE copy, use postcard or coupon NOW!

HEATH	
Schlumberger	
Heath/Schlumberger Instruments	
Dept. 531-013	
Benton Harbor, Michigan 49022	
Please send electronic instruments catalog.	
Name _____	
Title _____	
Company/Institution _____	
Address _____	
City _____	State _____ Zip _____
*Mail order prices; FOB factory.	
EK-415	

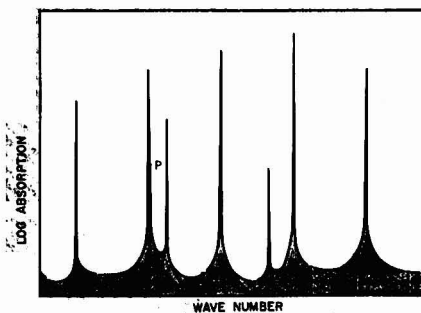
CIRCLE 121 ON READER SERVICE CARD

Gas lasers are particularly well suited as sources for LOS gas analysis. Lasers such as the CO and CO₂ molecular gas lasers provide practical discretely tunable sources. To understand how these lasers are used as effective light sources for LOS, it is not necessary to understand in detail how they operate. It is, however, important to understand those features of laser operation and the characteristics of laser light produced by these lasers which make them good LOS sources.

Gas lasers are often regarded as emitting one wavelength which depends on the composition of the laser gas. The CO₂ laser is commonly said to be a 10.6- μ m laser. This is because the laser configuration most commonly used, consisting of a laser discharge tube and two highly reflecting mirrors (Figure 1a), generates radiation at 10.6 μ m. If one of the highly reflecting mirrors is replaced with a properly ruled and blazed diffraction grating, then the laser can be tuned to emit other wavelengths in addition to 10.6 μ m by rotating the grating (Figure 1b). The wavelengths that such a laser can be tuned to emit correspond to transitions between energy levels of the CO₂ laser gas. A properly adjusted laser of this type will emit a single wavelength for a particular grating orientation. As the grating is rotated from this orientation, the wavelength will remain fixed until the grating has rotated a finite amount, at which point the emission wavelength will jump discontinuously to a new value. This discontinuous tuning property of the CO₂ laser is common to many other gas lasers such as the CO and the HeNe laser.

At first glance, the tuning characteristics of gas lasers may seem undesirable for spectroscopic applications. Their discontinuous tuning characteristics do not allow them to be used as light sources to record spectra in the usual manner that IR spectroscopists employ. This discontinuous tuning is a distinct advantage, however, when these sources are used to measure gas absorption in a LOS gas analysis system. This advantage comes from the great degree of frequency stability and reproducibility that this type of laser possesses. The exact wavelength emitted by a gas laser of this type depends on the energy levels of the laser gas and not on the exact grating orientation. The grating orientation need only be set exactly enough to select the proper laser emission line. This means that it is possible to build sources that will emit a sequence of exactly reproducible and known wavelengths. The value of such a source will become clear in the following sections which describe LOS and how it is used for gas analysis.

Figure 2. Sampling of gas absorption at CO₂ laser emission wavelengths



Solid curve, representing absorption spectrum of hypothetical gas, is made up of superposition of a number of collision broadened lines. Tails of these lines are represented by interrupted lines. Vertical lines represent narrow CO₂ laser emission wavelengths, and their height represents the absorption measured at each wavelength. Near coincidence between laser emission wavelength and gas absorption wavelength is indicated at point P.

Laser Optoacoustic Spectrometer

Infrared absorption properties of gases can be measured with discretely tunable gas lasers as sources by taking advantage of the many near coincidences that exist between laser emission wavelengths and gas absorption wavelengths (4-6). The infrared absorption lines which constitute the IR absorption spectrum of a gas are not infinitely narrow. Doppler and collisional effects broaden them to a finite width. The ability to measure gas absorption with a discretely tunable laser source depends on the existence of these broadening mecha-

nisms. The light beam generated by a discretely tunable laser has an extremely narrow spectral spread or line width and may be regarded from a practical point of view as possessing an infinitely narrow line width.

Since such a laser tunes discontinuously, it cannot be tuned so that its emission wavelength coincides with the center of an absorption line. Fortunately, however, since the absorption spectrum of a pure gas has many lines, which will be collisionally broadened at sufficient pressure, laser emission wavelengths are found that fall inside the line width of broadened absorption lines (Figure 2). The abili-

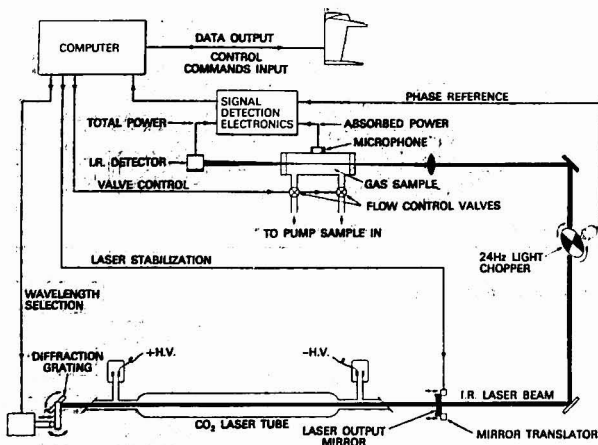


Figure 3. Prototype Laser Optoacoustic Spectrometer (LOS) gas analysis system

ty to use a particular type of laser, for example, a CO₂ laser, to measure a selected gas such as ethylene depends on the existence of CO₂ laser emission wavelengths which are absorbed by ethylene. The 10.5321- μ m line of the CO₂ laser is one example of a line which fits this situation.

Figure 3 depicts the prototype LOS system built by the author. The infrared source is a CO₂ laser which can be tuned to any of 50 wavelengths between 9.2 and 10.8 μ m. The laser beam, with a power of about 100 mW, is chopped at 24 Hz before it passes through the sample cell. Energy absorbed from the beam results in gas molecules making transitions from lower to higher rotation-vibration energy levels. These excited molecules decay through nonradiative processes, and the energy absorbed from the laser beam by the gas results in heating of the gas. Since the laser beam is interrupted by the light chopper at 24

Hz, this heating of the gas will have a 24-Hz modulation. This periodic temperature variation results in a periodic pressure variation.

Infrared absorption is detected in a LOS system by placing a pressure transducer or microphone in the absorption chamber to measure this periodic pressure variation. This effect is called the "optoacoustic effect" and was discovered by Bell (7), Tyndall (8), and Röntgen (9) in 1881. It has been used for many years in nondispersive-type IR gas analyzers (10). An optoacoustic effect detector consisting of an absorption chamber and a microphone is an extremely sensitive way to detect weak absorptions. It is possible to build a microphone and preamplifier combination which has a low noise level by using modern "state-of-the-art" components. In such a system, the main noise source is the Brownian motion of the microphone diaphragm. This

Brownian motion sets the lower limit of pressure variation that the microphone can detect.

The power of the laser beam after it has passed through the absorption cell is measured by an infrared detector. Signals from the microphone in the cell and the IR detector are detected with standard "lock-in amplifier" techniques. These signals are then fed into a small minicomputer via a multiplexer and an analog-to-digital converter. The laser is tuned from one emission wavelength to another by a stepping motor which rotates the diffraction grating. This motor is controlled by the computer. The gas sample is changed by opening a set of valves and drawing in a new sample with a suction pump. These valves are also controlled by the computer.

Experimental Results

The prototype LOS gas analyzer system described in the last section was built to evaluate the performance of such a system. Particular attention was directed toward high sensitivity, the ability to analyze mixtures of gases, and automatic operations. This section describes the results achieved in these areas and presents a description of how the apparatus functioned.

The prototype LOS system was used to measure the absorption of the 50 wavelengths which could be obtained from its CO₂ laser in a variety of gases and vapors. A sample of the gas or vapor under study was drawn into the sample chamber, and the laser was tuned through each of its emission wavelengths, and the measured absorption recorded. Figure 4 shows the absorption properties measured for five gases. These data were collected with the gas samples diluted to a concentration of about 100 ppm (parts per million) in an artificial mixture of nitrogen and oxygen mixed to simulate clean air.

The absorption properties of other gases have been measured. In each case, strong absorptions existed at some CO₂ laser emission wavelengths if the gas had an absorption band which was overlapped by the range of emission wavelengths of the CO₂ laser. The absorption spectra measured for gases of this type showed significant absorption at several different emission wavelengths. Each gas or vapor tested showed a spectrum significantly different from the others tested. These results indicate that LOS spectra of different gases often overlap, but that the spectra of different gases are unique and provide a good basis for the identification of components of a gas mixture.

The ability of the system to detect small concentrations of gases was

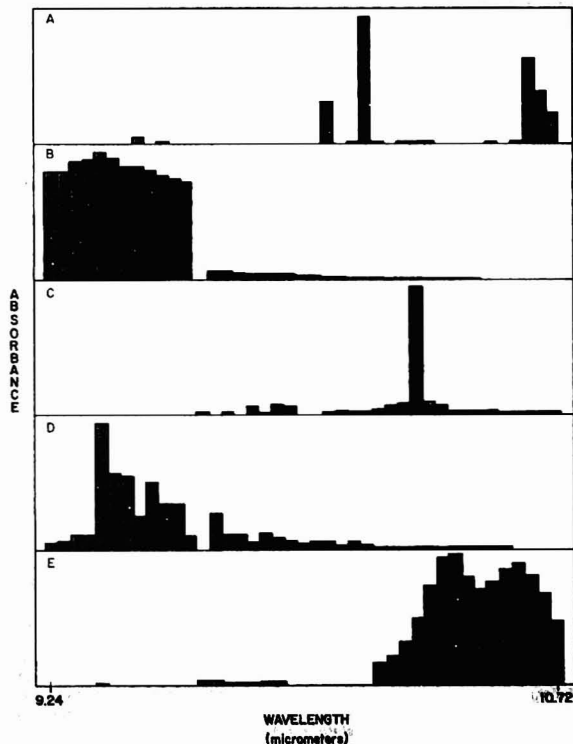


Figure 4. Laser optoacoustic absorption spectra taken with prototype LOS system at CO₂ laser emission wavelengths

A, ammonia; B, ethanol; C, ethylene; D, methanol; E, trichloroethylene

Springer-Verlag
New York
Heidelberg
Berlin

Topics in Current Chemistry for the Analytical Chemist

Volume 14/1

Inorganic and Analytical Chemistry

1970. 126p. 60 illus.
paper \$15.60

Volume 17

Laser Spectroscopy

By W. Demtröder

2nd ed.
1973. iv, 106p. 16 illus. 3 tables
cloth \$13.40

Volume 26

Inorganic and Analytical Chemistry

1972. iii, 112p. 6 illus.
paper \$14.80

Volume 29

Automation in Analytical Chemistry

1972. iii, 103p. 32 illus.
paper \$11.50

Volume 35

Inorganic Chemistry

1973. iii, 129p. 15 illus.
paper \$14.80

Volume 39

Computers in Chemistry

1973. iii, 195p. 13 illus.
cloth \$25.20

Write for your copy of the
brochure Analytical Chemistry to



Springer-Verlag
New York Inc.

175 Fifth Avenue
New York, NY 10010

CIRCLE 211 ON READER SERVICE CARD

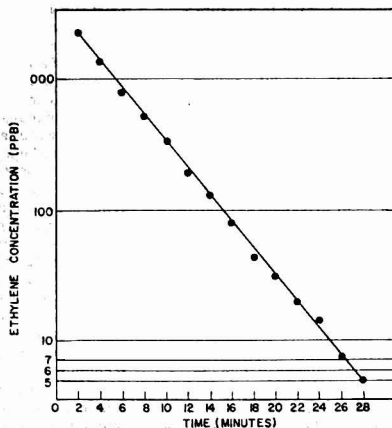


Figure 5. Measurement of ethylene concentration in air samples by use of single CO_2 emission wavelength

eventually. By comparing the strongest absorption in a gas LOS spectrum to the system noise level, it is possible to calculate gas concentrations which would give a unity signal-to-noise ratio. Calculated sensitivities range from 3 to 0.1 ppb. The sensitivity depends on the absorption strength of the gas. Gases tested include ammonia, benzene, 1,3-butadiene, 1-butene, 1,2-dichloroethylene, ethanol, ethylene, ethyl ether, methanol, nitric oxide, nitrogen dioxide, propylene, and trichloroethylene. This sensitivity range applies to the detection of any infrared absorbing gas by a LOS system of this type if the range of laser emission wavelengths overlaps a gas absorption band.

The ability of the system to detect a small concentration of ethylene in air was tested experimentally. The CO_2 laser was tuned to emit at $10.5321 \mu\text{m}$. This wavelength is strongly absorbed by ethylene. This line corresponds to the ethylene absorption maximum in Figure 3. A small quantity of ethylene gas was released into the air of the laboratory room. Air samples were drawn into the sample cell at 2-min intervals, and the sample absorption was measured. The ethylene concentration in the room air decreased exponentially with time because of the forced ventilation of the room by an air conditioning system and air exhausted by a chemical hood. The ethylene concentration of each air sample was calculated from the measured infrared ab-

sorption. These data are recorded in Figure 5. The straight line fit of the data points on a semilog plot indicates that the room air was well mixed by ventilation and that the LOS system has a linear response. The good fit of the data points at the low concentration readings demonstrates the practical achievement of high sensitivity.

Mixtures of gases can be analyzed by the LOS prototype system by taking advantage of the dependence of the microphone signal on gas absorbance. Suppose that the sample container contains a mixture of gases which has an absorbance A_i at laser emission wavelength λ_i . Then, according to Beer's law, the signal S_i , measured by the microphone in the sample container which is proportional to the power absorbed by the sample, is given by Equation 1:

$$S_i = P_i(1 - e^{-A_i}) \quad (1)$$

In Equation 1, P_i is the laser beam power at wavelength i . The beam power T_i , which is transmitted through the sample container, is measured by the IR detector placed behind the sample cell (Figure 3). This is given by Equation 2:

$$T_i = P_i e^{-A_i} \quad (2)$$

Equations 1 and 2 can be combined to solve for sample absorbance:

$$A_i = \log \left(\frac{S_i}{T_i} + 1 \right) \quad (3)$$

If the sample contains N component gases, then, according to Beer's law,

the absorbance A_i may be replaced by the sum of the absorbances of each of the components. In Equation 4 the absorbance:

$$A_i = b \sum_{x=1}^N a_{ix} C_x \quad (4)$$

of the g th component is given as the product of the path length b in the sample chamber, the absorptivity a_{ig} at wavelength i , and the concentration C_x . Substitution of Equation 4 into 3 gives Equation 5:

$$\sum_{x=1}^N a_{ix} C_x = \frac{1}{b} \log \left(\frac{S_i}{T_i} + 1 \right) \quad (5)$$

This equation is the key to using a LOS system to analyze a gas mixture. It shows that the gas concentrations C_x can be calculated from the measured quantities S_i and T_i by solving a set of simultaneous linear equations. The formal solution of Equation 5 is given by Equation 6. This equation

$$C_x = \frac{1}{b} \sum_{i=1}^N a_{ix}^{-1} \log \left(\frac{S_i}{T_i} + 1 \right) \quad (6)$$

shows that the gas concentrations C_x can be calculated from the measured quantities S_i and T_i with the aid of the inverse of the matrix a_{ig} . The matrix a_{ig} is composed of the absorption properties of each of the N components of the mixture.

Determining the composition of a mixture by solving a set of simultaneous equations is a technique that has been used for many years in multicomponent analysis. The effectiveness with which Equation 6 can be applied to solve practical problems and analyze gas mixtures depends on the properties of the inverse matrix a_{ig}^{-1} and on the precision with which S_i and T_i can be measured. If a_{ig}^{-1} is "badly behaved," then small measurement errors in S_i and T_i may lead to a large uncertainty in the calculated gas concentrations. It is important to select the measurement wavelengths so that a_{ig}^{-1} is as "diagonal as possible." Each measurement wavelength should be selected to be characteristic of one component and as free as possible from interference from other components.

The prototype LOS system analyzes gas mixtures by measuring S_i and T_i at selected wavelengths and then calculating the gas concentrations. The minicomputer memory stores the matrix a_{ig} and the programs necessary to solve Equation 6 and calculate gas concentrations. An important characteristic of this prototype system is the ability to detect a small quantity of one gas in the presence of a large concentration of another gas. This ability is described quantitatively by the *rejection ratio* between pairs of gases.

Table I. Rejection Ratios

COMPONENT BEING MEASURED	INTERFERING COMPONENT			
	Ethanol	Methanol	Ammonia	Trichloroethylene
Ethanol	...	270	3200	16000
Methanol	760	...	1900	300
Ammonia	1080	430	...	1080
Trichloroethylene	200	200	1000	...

The rejection ratio between a pair of gases is the concentration of the first (interfering) gas which will give a signal equal to that produced by a unit concentration of the second gas (gas being measured). For example, 1 ppm of ethanol can just be detected in the presence of 3200 ppm of ammonia. Rejection ratios have been calculated by using measured absorption properties and assuming that the LOS system can measure S_i to an accuracy of 1%. The calculated rejection ratios range from 200 to 10^4 , depending on the degree of spectral overlap. The prototype LOS system was used to analyze mixtures of gases to evaluate how well this system was able to achieve the calculated rejection ratios. These tests were conducted with mixtures of ethanol, methanol, ammonia, and trichloroethylene vapor. The selected measurement wavelengths were 9.25, 10.16, 10.33, and 10.57 μm , respectively. The measured rejection ratios are presented in Table I. These values are in good agreement with the calculated values.

DIAX Model 100 Gas Analyzer

The DIAX Model 100 gas analyzer (Figure 6) will be available after July 1974. It utilizes the LOS technique of gas analysis tested in the prototype system described above. Unlike the prototype system, which could only detect gases that absorb in the 9.2 to 10.8- μm region, the Model 100 will be able to detect all infrared absorbing gases. This results from the improved laser system in the Model 100 which produces over 200 different wavelengths over the range of 2-11 μm . The wavelengths are spread uniformly enough over this region to detect all IR absorbing gases.

Like the prototype system, this system will have two modes of operation. The first, the *absorption measurement mode*, automatically measures and records a sample's absorption strength at each of the laser system wavelengths. This mode is used to record the absorption properties of a gas sample containing a single chemical compound. It produces the absorption reference data needed for the second mode of operation which analyzes mixtures of gases. To analyze a mixture of gases, the system user must first store the



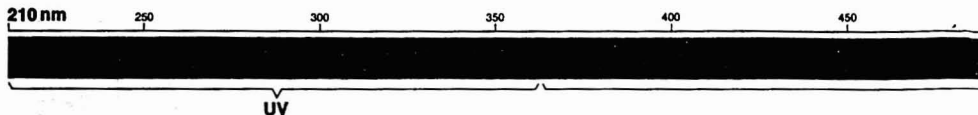
Figure 6. DIAX Model 100 gas analyzer

absorption properties of each component of the mixture in the minicomputer memory. This can be done either by measuring these properties in the absorption measurement mode or by using previously measured LOS spectra. A library of LOS spectra is being built up by DIAX Corp.

To analyze a mixture of gases, the system is operated in the second or *analysis mode*. Once the absorption properties of the components of the mixture are stored in the computer memory, the system can start automatic mixture analysis. More wavelengths than the number of gases present in the sample are selected. A sample is automatically drawn into the sample chamber, and the flow valves are closed. The laser source is then tuned in sequence to each of the selected wavelengths. The tuning pauses at each wavelength to allow sample absorption and laser power to be measured. At the end of the wavelength scan, the minicomputer

Variscan™ that lets you see

Variscan permits you to detect and analyze compounds that



Variscan detector, front center, can be used with liquid chromatograph models 4000, 4100 and 4200 (shown here).

Compared to Variscan, other LC detectors are almost blind. They operate at only one or a few wavelengths.

Variscan operates over the entire UV-Vis spectral region, from 210 to 780 nm, with no sacrifice in efficiency. At the turn of a dial you can set Variscan at the maximum absorption wavelength of virtually any compound.

And whenever you wish, you can quickly stop flow, push a button and obtain absorption spectra of individual peaks in your chromatogram.

Variscan can be used with gradient elution and is compatible with a wide range of chromatographically useful solvents.

Minimum detectable quantities are nanogram amounts. Cell volume is small, only 8 microliters, so that peak spreading is minimized; and the cell path is long, 1 centimeter, so that response to low concentrations is increased.

The Variscan LC detector is basically a unique Varian UV-Vis spectrophotometer. The spectrophotometer flow cells are a matched pair.

calculates the concentration of the gases present in the sample. This calculation, which is described above, requires a number of wavelengths equal to the number of different component gases present in the sample.

The system checks the consistency of the calculated gas concentrations by using measurements at the extra wavelengths also to calculate concentrations. Agreement between these different calculations indicates that the calculations accurately represent the mixture composition. This automatic consistency checking essentially eliminates the possibility that absorption produced by an unsuspected component of the mixture may cause measurement error. The results of the concentration and consistency calculations are typed out on the teletype unit. This information is also available at the digital output connector for recording on magnetic tape or transmission to a remote recording location. This system has been designed to analyze mixtures of 10 gases with a sensitivity of 1 ppb and a cycle time for a complete analysis of 5 min. The rejection ratio between gases with similar absorption spectra is greater than 200; the rejection ratio between gases with different spectra runs as high as 10⁶.

Applications of LOS

The technique of LOS gas analysis is expected to find a variety of applications. It offers a single system which can automatically analyze a mixture of gases with high rejection ratios and sensitivity. One particularly promising field of application is gaseous air pollution detection. A single LOS system can replace the collection of single gas analyzers which is currently required to provide a complete analysis of ambient air. The LOS system should become a useful research tool. It can be adapted to many specialized research uses by changing the computer software. It can be interfaced to a gas chromatograph (GC) by feeding the effluent gas from the chromatographic column into the LOS system. The small sample volume that can be used for LOS gas analysis makes this possible. It is possible to detect 1 ppb of analyte in 1 cc of inactive carrier gas. This means that picogram sensitivity is possible in a combined GC-LOS system.

A combined GC-LOS system has some of the same properties as a GC-MS (mass spectrometer) combination. However, it may offer advantages of simplicity, sensitivity, and cost. Since most GC carrier gases do not absorb infrared, there is no need as there is in a MS, to remove the

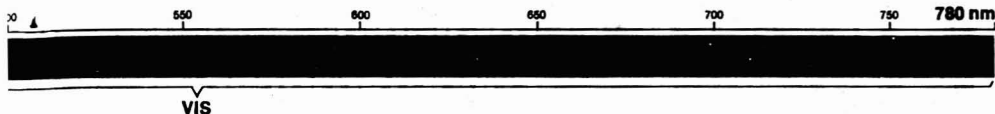
carrier gas. The spectrum recorded in a MS depends on the mass fragmentation pattern of the molecule, and the relative intensity of different peaks is not reproducible from one system to another. The LOS spectrum depends on laser wavelengths and IR absorption properties and is highly reproducible. It provides an accurate method for identifying GC peaks. Industrial process control is another field of application. The LOS system provides real time data in a digital format that can easily be interfaced to a process control computer.

References

- (1) Edwin Kerr and John Atwood, *Appl. Opt.*, 7, 915 (1968).
- (2) L. B. Kreuzer, *J. Appl. Phys.*, 42, 2934 (1971).
- (3) "Handbook of Lasers," R. J. Pressley, Ed., Chemical Rubber Publ., Cleveland, Ohio, 1971.
- (4) L. B. Kreuzer, N. D. Kenyon, and C. K. N. Patel, *Science*, 177, 347 (1972).
- (5) P. L. Hanst, *Appl. Spectrosc.*, 24, 161 (1970).
- (6) R. T. Menzies, N. George, and M. K. Bhaumik, *IEEE J. Quantum Electron.*, QE-6 (December 1970).
- (7) A. G. Bell, *Phil. Mag.*, 11, 510 (1881).
- (8) J. Tyndall, *Proc. Roy. Soc. (London)*, 31, 307 (1881).
- (9) W. C. Röntgen, *Phil. Mag.*, 11, 308 (1881).
- (10) "Infra-Red Physics," J. T. Houghton and S. D. Smith, pp 276-78, Oxford, England, 1966.

the LC detector one hell of a lot more

absorb at any UV-Vis wavelength from 210 nm to 780 nm.



Water-jacketed, they maintain stable temperature equilibrium between the cell and the solvent, even with flow programming. The carefully matched optical paths of the spectrophotometer also minimize noise and drift.

Overall system noise is $\leq 5 \times 10^{-4}$ absorbance unit from 210 to 780 nm; drift is lower than 10^{-2} absorbance unit/hour—performance specifications which ensure that you will see more with Variscan than with any other LC detector. LC is no longer detector-limited.

Now it is possible to detect and analyze a much broader range of compounds. Pardon our French, but you really can see one hell of a lot more with Variscan.

For complete details see your Varian representative or write: Varian Instrument Division, 611 Hansen Way, Box D-070, Palo Alto, California 94303.

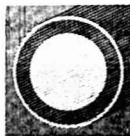
varian instruments 

Brand names: ANASPECT™ • CARY® • MAT • VARIAN®
VARIAN AEROGRAPH® • VARIAN TECHTRON

CIRCLE 243 ON READER SERVICE CARD

Photochemical Smog and Ozone Reactions

ADVANCES
IN CHEMISTRY
SERIES No. 113



Two symposia sponsored by the Division of Physical Chemistry and the Division of Industrial and Engineering Chemistry and by the Division of Water, Air, and Waste Chemistry of the American Chemical Society with Bernard Weinstock and Lyman A. Ripperton, Cochairmen.

Five papers in the symposium on "Photochemical Smog" cover the following aspects of photochemical air pollution:

- mechanisms of smog reactions
- simulation of air pollution
- models and abatement strategy

Seven papers comprising the symposium on "Ozone Reactions in the Atmosphere" present current research into the chemical behavior of ozone. Topics include:

- reactions of ozone with ammonia, olefins, organic sulfides, and with selected hydrocarbons to form aerosols
- formation and destruction of ozone
- role of carbon monoxide and hydrogen peroxide in the atmosphere
- photooxidation of propylene in the presence of NO_2 and O_2

285 pages with index. Cloth (1972) \$14.95 Postpaid in U.S. and Canada, plus 40 cents elsewhere.

Order from:
Special Issues Sales
American Chemical Society
1155 Sixteenth St., N.W.
Washington, D.C. 20036

Water baths At these prices why buy an ordinary bath?

Why indeed! Techne baths offer a remarkable performance for an extraordinary low cost. High quality stainless steel tanks using solid drawn construction. Available in five standard sizes. Using thermistor temperature sensor and all solid state switching. Control $\pm 0.05^\circ\text{C}$. Range 0 to 100°C or 200°C . These are stirred baths, available with optional pump for circulation to external apparatus.

A shaking water bath and a complete range of accessories are also available.

Prices start as low as \$215.00.

For free 16 page constant temperature bath catalog write to Techne Incorporated, 661 Brunswick Pike, Princeton, New Jersey 08540 or call (609) 452-9275.

Techne

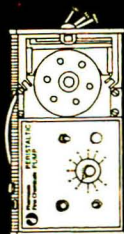
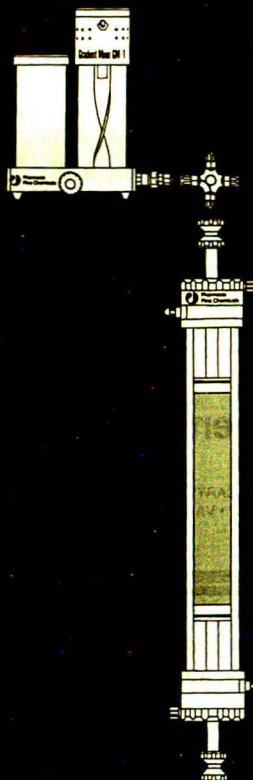
... leaders in
constant temperature
baths.



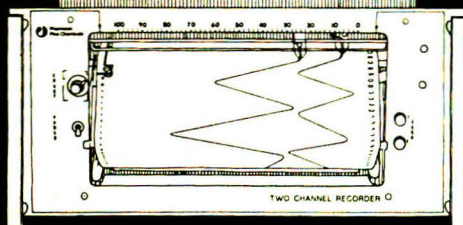
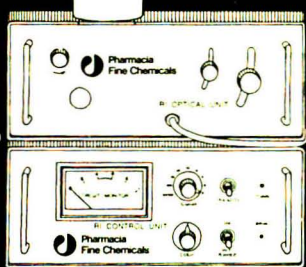
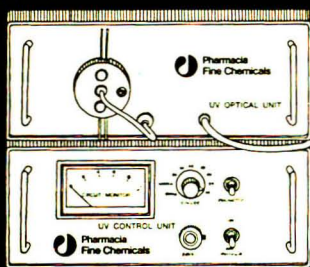
AVAILABLE THROUGH MAJOR LABORATORY SUPPLY HOUSES.

CIRCLE 229 ON READER SERVICE CARD

Modular components for liquid chromatography systems



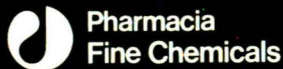
- Gradient Mixer GM-1
- Valve LV-3
- Reservoir R-9
- Flow Adaptor A-26
- Column K-26
- Peristaltic Pump P-3
- UV Monitor
- RI Monitor
- Two Channel Recorder



Monitors and Recorders available only in U.S.A. and Canada.

Pharmacia Fine Chemicals Inc.
800 Centennial Avenue
PISCATAWAY
New Jersey 08854
Phone (201) 469-1222

Pharmacia (Canada) Ltd
2044 St. Regis Boulevard
Dorval, Quebec, Canada
(514) 684-8881



For additional information write or call PHARMACIA FINE CHEMICALS INC., Piscataway, New Jersey

CIRCLE 185 ON READER SERVICE CARD

February 1974, Vol. 46, No. 2

Editor: HERBERT A. LAITINEN

EDITORIAL HEADQUARTERS
1155 Sixteenth St., N.W.
Washington, D.C. 20036
Phone: 202-872-4800 Teletype: 710-8220151

Managing Editor: Virginia E. Stewart

Associate Editors:
Josephine M. Petrucci
Alan J. Benzal

Assistant Editor:
Andrew A. Husovsky

PRODUCTION STAFF

Art Director: Norman W. Favin

Associate Production Managers:
Leroy L. Corcoran
Charlotte C. Burns

Editorial Assistant: Nancy J. Oddicino

EDITORIAL PROCESSING DEPARTMENT,
EASTON, PA.

Assistant Editor: Elizabeth R. Hufe

ADVISORY BOARD: Allen J. Bard, Fred Baumann, David F. Boltz, E. G. Brame, Jr., Warren B. Crummett, M. A. Evenson, Henry M. Fales, A. F. Findeis, Kenneth W. Gardiner, Jack M. Gill, Jeanette G. Grasselli, R. S. Juvet, Jr., Theodore Kuwana, Oscar Menis, Harold F. Walton

INSTRUMENTATION ADVISORY PANEL:
Jonathan W. Amy, Stanley R. Crouch,
Richard A. Durst, J. J. Kirkland, Ronald
H. Laessig, Marvin Mazgashis, Harold M.
McNair, David Seligson, Howard J. Sloane

Contributing Editor: Claude A. Lucchesi

Published by the
AMERICAN CHEMICAL SOCIETY
1155 16th Street, N.W.
Washington, D.C. 20036

Books and Journals Division

John K. Crum Director

Ruth Reynard Assistant to the Director

Charles R. Bertach Head, Editorial
Processing Department

D. H. Michael Bowen Head, Journals
Department

Becil Guiley Head, Graphics and
Production Department

Seldon W. Tarrant Head, Research and
Development Department

Advertising Management

CENTCOM, LTD.

(for Branch Offices, see page 258 A)

For submission of manuscripts, see
page 88 A

The Latter-Day Renaissance of Analytical Chemistry

Several factors seem to be responsible for a resurgence of analytical chemistry during the recent past. It is easy to point to a greater problem orientation in research support, both in industry and in governmental granting agencies. To be sure, this trend is real, and it works to the benefit of analytical chemistry in areas such as environmental science and clinical science. Deeper and more fundamental factors, however, appear to be involved.

The gradual shift in the boundaries of analytical chemistry, to encompass a deeper understanding of the phenomena involved in analytical measurements, is still continuing. As a result, instrumental analysis has progressed far beyond its most primitive form, in which an empirical calibration is made under carefully controlled conditions to yield a working curve using a matrix as similar as possible to an unknown, which is then analyzed under the same conditions. Instead, an understanding of the underlying phenomena is sought, to enable an optimization of conditions and design of appropriate instrumentation for the desired measurement. The greater intellectual challenge of the modern approach has attracted increasing numbers of highly motivated and talented students to become teachers, who in turn are producing students with a more basic outlook.

It is true, of course, that all branches of chemistry are becoming more oriented toward fundamentals. Analytical chemistry, however, stands out in stressing versatility and problem orientation. The fact that today's analytical graduate student often works on interdisciplinary and mission-oriented projects makes him exceptionally attractive to the industrial recruiter. Students, of course, are perceptive to the relatively favorable job situation, so it is a common phenomenon in graduate schools to find analytical enrollments increasing in the face of declines in chemistry as a whole.

How long this trend continues remains to be seen, but if this analysis of the underlying causes is correct, there is no reason to expect a reversal in the foreseeable future.



Determination of Lead in Atmospheric Air and in Aluminum by Helium-3-Induced Nuclear Reactions

Bahman Parsa¹ and Samuel S. Markowitz

Department of Chemistry and Lawrence Berkeley Laboratory, University of California, Berkeley, Calif. 94720

Helium-3 activation analysis has been applied to develop a very sensitive means of trace lead analysis. The procedure involves the bombardment of samples with ³He particles to induce a $Pb + {}^3He \rightarrow {}^{207}Po$ reaction on lead isotopes. The 992-keV γ -ray of 5.84-hr ²⁰⁷Po is used as the "signal" for lead determination. Only milligram amounts of sample are required. The excitation function for the production of ²⁰⁷Po from the reaction of ³He with lead of natural isotopic composition is presented. If necessary, destructive analysis may be carried out, and a radiochemical separation procedure to plate polonium onto a silver foil is discussed. The accuracy of the measurement is about 3 to 5% for comparative analyses. For absolute determinations, the error is estimated to be 9–12%. Under reasonable irradiation and counting conditions, the detection limit is approximately 50 pg/cm², corresponding to 0.5 ppb in a matrix 100 mg/cm² thick.

Sensitive lead assay by thermal neutron activation techniques is somewhat difficult, because the only long-lived (n, γ) product practical for analysis is 3.3-hr ²⁰⁹Pb, which has a very low formation cross section, and which decays purely by beta emission. Recent studies utilizing a reactor pulsing technique have enabled the detection of up to 0.4 μ g of Pb *via* production and analysis of 0.8-sec ^{207m}Pb (1, 2). Further activation analysis investigations have been carried out to measure lead concentration, with various degrees of success, by fast neutrons (3), photons (4), alpha-particles (5), protons, and deuterons (6). Moreover, lead analysis has been performed by atomic absorption spectroscopy (7) and X-ray fluorescence (8). Helium-3 induced nuclear reactions may provide an alternatively fruitful method for the determination of lead. Helium-3 activation analysis has been successfully performed in a number of matrices and its great potential for trace analysis study, especially for light elements, has been observed (9–12).

In the present work, we have investigated the application of the reaction $Pb + {}^3He \rightarrow {}^{207}Po$ to the analysis of

lead. Recently, the decay scheme of ²⁰⁷Po has been studied very accurately (13, 14). Using the result of the decay scheme work, the absolute excitation function for production of ²⁰⁷Po from the reaction of ³He with lead of natural isotopic composition has been determined. A number of analyses using the 992-keV γ -ray of ²⁰⁷Po as a "signal" for lead measurement were carried out.

EXPERIMENTAL

Target Preparation. The polonium samples used for measurement were produced by irradiating natural lead with ³He ions. The standard targets were made by evaporation of analytical grade lead metal in vacuum onto 1-inch diameter and 1/4-mil thick high purity aluminum disks (Republic Foil, Danbury, Conn.). The thickness of the lead deposit was about 2 mg/cm² for excitation function determinations. For sample analyses with unknown Pb content, targets were made into 1-inch diameter foils from the sample sheet. Comparative standards of lead were used for these experiments having a thickness of about 100 μ g/cm².

Irradiations. Irradiations were performed at the LBL 88-inch cyclotron with ³He ions. For the absolute excitation function measurements, the target foils were irradiated simultaneously at different energies by using the stacked-foil technique with the lead film facing the beam. Energy degradation was achieved by using aluminum degrader foils. Ranges in aluminum and lead were determined by means of the known range-energy tables (15, 16). In sample analysis experiments, the samples were irradiated together with the comparative standards. Routinely, two or three high purity Al disks, each of 1.58 mg/cm² thickness, separated the sample from the standard. The length of bombardment varied between 30 minutes to 1 hour, and the average beam current was about 1 μ A of ³He. Recoiling ²⁰⁷Po nuclei were caught in the Al backing and in the "upstream" Al cover foil. The beam-energy resolution is about 0.3% and as our lowest energy is 22 MeV, the particle energy is well-defined by the range-energy relations.

Sample Dissolution. After irradiation, the standard lead targets could be counted nondestructively. However, a radiochemical separation procedure was performed for samples with trace concentrations of Pb and relatively high concentrations of other γ -ray emitters. In this case, the metallic target, along with its "upstream" Al catcher foil, was dissolved in a boiling solution of 6N HCl containing a few drops of concentrated HNO₃. The paper targets along with their front and back Al catcher foils were dissolved in HClO₄ or HClO₄-HNO₃ mixture by a wet ashing technique. First the sample was placed in the beaker, acid solution introduced, and the sample heated until well decomposed. At this point, the evolution of brown fumes of oxides of nitrogen ceased and copious white fumes of HClO₄ were emitted. Then the solvent was decomposed by repeatedly adding concentrated HCl and evaporating to a small volume.

Radiochemical Separation. After sample dissolution, a polonium separation with standard plating techniques was carried out (17). This was done by adding several drops of a saturated solution of hydrazine dihydrochloride along with a few drops of Methyl Red-Bromthymol Blue-alcohol indicator (18). Then the solution was neutralized with NaOH pellets to a greenish color. Immedi-

¹ Visiting Fulbright-Hays Grantee. Permanent address, Tehran University Nuclear Center, Tehran, Iran.

- (1) H. R. Lukens, *J. Radioanal. Chem.*, **1**, 349 (1968).
- (2) M. Wiernik and S. Amiel, *J. Radioanal. Chem.*, **3**, 393 (1969).
- (3) P. Meyers, "Proceedings of the 2nd Conference on Practical Aspects of Activation Analysis with Charged Particles, Liege, 1967," Vol. 1, Euratom, Brussels, 1968, p. 195.
- (4) E. A. Schwelkert and Ph. Alberi, "Radiochemical Methods of Analysis," Vol. 1, IAEA ed. 1965, p. 323.
- (5) J. C. Cobb, *J. Geophys. Res.*, **69**, 1895 (1964).
- (6) E. A. Schwelkert, *Trans. Amer. Nucl. Soc.*, **13**, 58 (1970).
- (7) B. V. Lvov, "Atomic Absorption Spectrochemical Analysis," American Elsevier Publishing Co., New York, N.Y., 1970.
- (8) H. R. Bowman, E. K. Hyde, S. G. Thompson, and R. C. Jared, *Science*, **151**, 582 (1966).
- (9) S. S. Markowitz and J. D. Mahony, *Anal. Chem.*, **34**, 329 (1962).
- (10) E. Ricci and R. L. Hahn, *Anal. Chem.*, **39**, 794 (1967).
- (11) D. M. Lee, J. F. Lamb, and S. S. Markowitz, *Anal. Chem.*, **43**, 542 (1971).
- (12) D. M. Lee and S. S. Markowitz, *J. Radioanal. Chem.*, in press, LBL-682, June 1972.

- (13) G. Astner and M. Alpsten, *Nucl. Phys. A*, **140**, 643 (1970).
- (14) V. A. Shilin and V. R. Burmistrov, *Izv. Akad. Nauk SSSR, Ser. Fiz.*, **35**, 1653 (1971).
- (15) J. F. Lamb, Lawrence Radiation Laboratory Rept UCRL-18981, Ph.D. Thesis, 1969.
- (16) C. F. Williamson, J. Boujot, and J. Picard, Rapport CEA-R3042 (1966).
- (17) P. E. Figgins, "The Radiochemistry of Polonium," *NAS-N5 3039* (January 1961).
- (18) W. L. Minto, National Nuclear Energy Series, Div. VI, Vol. 3, R. M. Fink, Ed., McGraw-Hill, New York, N.Y., 1950, p. 15.

ately after the neutralization process, 5 ml of concentrated HCl was added, and then the sample was diluted with distilled water to a volume of 150 ml to make the resulting solution 0.4N in HCl. The polonium solution was contained in a 250-ml tall-form beaker which was suspended in a boiling water bath. A 1-inch diameter and 5-mil thick Ag disk was degreased in trichloroethylene, rinsed in H₂O, and introduced to the polonium solution. The heated solution was constantly stirred. To minimize any loss of Po, the sides of the beaker and the stirrer were washed down, and the volume of the solution was maintained constant at 150 ml every ½ hr during the plating period (19). After the Ag disk was exposed for 1½ hr, it was removed from the hot solution and rinsed with distilled water. Then the foil was air-dried. Finally, it was mounted on an Al sample card for counting.

The average chemical yield was determined with tracer techniques with a stock ²¹⁰Po standard solution followed by a gross α count. Furthermore, the pre- and post-chemistry variations of the 992-keV photopeak of ²⁰⁷Po produced from lead standards were also used for the chemical yield evaluation. Consequently, on the average, a chemical yield of 98.4 ± 1.4% for the metallic targets and a value of 91.3 ± 2.5% for the paper specimens were obtained.

Data Acquisition. The sources were analyzed by γ-ray spectroscopy with two Ge(Li) detectors, each having an active volume of 30 cm³. A Northern 1024- and a Victoreen 400-channel pulse-height analyzer were used to register the γ-ray spectra. The overall resolution (FWHM) of the system was about 3 keV for the 1.33-MeV γ-ray of ⁶⁰Co. The γ-ray energy calibrations and photopeak efficiency determinations were performed with a set of standard sources supplied by the International Atomic Energy Agency (IAEA), Vienna. In each experiment, the activity was followed by measuring the 992-keV photopeak, which is the most intense γ-ray of ²⁰⁷Po (13, 14).

RESULTS AND DISCUSSION

Excitation Function. The total cross section for the production of ²⁰⁷Po via Pb + ³He reactions was calculated from the 992-keV photopeak intensities. These values were corrected for the detection efficiency and appropriate decay time involved from the end of irradiation. A new ²⁰⁷Po half-life of 350.3 ± 4.1 min, as reported by Parsa and Markowitz (20), was adopted for these calculations. The absolute intensity of the 992-keV γ-ray of ²⁰⁷Po was calculated to be 0.59 ± 0.04, based on Astner and Alpsten's decay scheme and their table of transition intensities (13). A summary of experimental cross sections is presented in Table I. Each value in this table represents an average value of at least two replicates. The energy loss of the ³He beam within the lead target was about 0.2 MeV. The absolute cross section error is estimated to be 9–12%, depending on whether the source was chemically separated or nondestructively measured. The error is mainly due to the 7% quoted decay scheme uncertainty from Astner and Alpsten's work (13). Aside from statistical fluctuations in the γ-ray spectra, other factors contributing to the error include uncertainties in target uniformity, beam current measurements, range-energy relations, and γ-ray detection efficiency.

Figure 1 shows the excitation function for the production of ²⁰⁷Po from the reaction of ³He with lead of natural isotopic composition. The cross section for this reaction remains fairly constant at an average value of 385 mbarns within the ³He energy range of 34 to 38 MeV; the cross section remains above 300 mbarns from 31 to 40 MeV. This unique characteristic was utilized for the sample analyses so that the samples and the standards could both be irradiated at maximum cross sections for ²⁰⁷Po production.

Sample Analyses. To establish the feasibility of the measurement of lead concentration by this new technique, several analyses were undertaken. In each case, a compar-

Table I. Cross Sections for ²⁰⁷Po Production from ³He-Induced Reactions on Lead

Av ³ He energy, MeV	Cross section, mbarns	Av ³ He energy, MeV	Cross section, mbarns
22.3	32.5	35.8	384
23.2	47.7	36.0	370
24.1	54.2	36.3	417
25.0	65.4	36.7	400
25.1	70.7	36.8	373
26.0	91.1	37.2	375
26.9	114	37.4	375
27.8	143	37.7	405
28.7	184	38.0	383
29.6	216	38.1	378
30.9	293	38.3	368
31.8	336	38.8	374
32.7	349	39.1	354
33.0	346	39.6	341
33.6	392	39.8	298
33.8	361	40.7	256
34.2	386	41.6	181
34.5	394	42.6	142
35.3	380	43.7	124
35.4	380	44.7	109

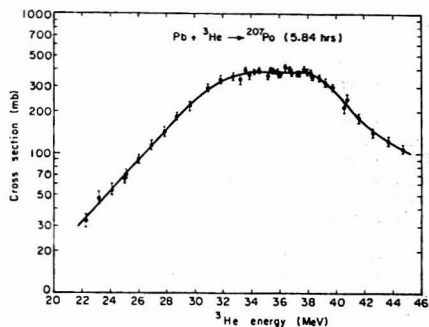


Figure 1. Excitation function for ²⁰⁷Po production from ³He-induced nuclear reactions with natural lead

ative lead standard was placed in the same stack with the "unknown" sample. Subsequently, the same pre- and post-irradiation treatments were applied to them. Then they were counted under identical conditions. In this manner errors in beam current, length of irradiation, decay scheme, and detection efficiency were eliminated. Subsequently, the overall experimental errors were 3 and 5%. The amount of lead present in the unknown was calculated by comparing the ratio of the 992-keV photopeak areas of the sample to the appropriate lead standard, corrected for radioactive decay. No correction for the production cross section was necessary since both the unknown and the standard were irradiated at the constant "plateau" part of the excitation function.

Atmospheric Lead Measurements. During the past decade, a series of filter papers was collected weekly from a sampling station in downtown Berkeley by the Safety Service Department of the Lawrence Berkeley Laboratory as part of an environmental survey system (21). The air was filtered through HV 70 filter paper at an average flow rate of 4 ± 0.5 cubic feet per minute, and the aerosols were collected on an open area of about 196 cm² of paper. The

(19) I. Feldman and M. Frisch, *Anal. Chem.*, **28**, 2024 (1956).

(20) B. Parsa and S. S. Markowitz, LBL-1902, *J. Inorg. Nucl. Chem.*, in press (June 1973).

(21) H. P. Cantelow, J. S. Peck, A. E. Salo, and P. W. Howe, UCRL-10255 (May 1962).

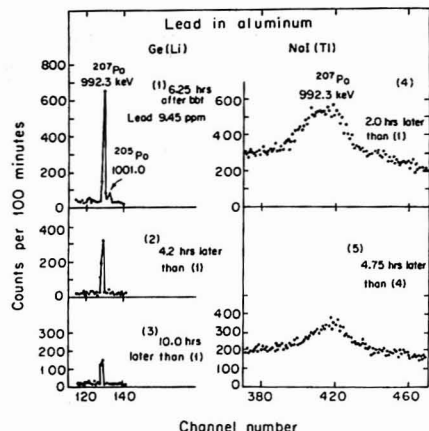


Figure 2. Comparison of the 992-keV γ -ray spectra of chemically separated Po taken with Ge(Li) and NaI(Tl) detectors at various times. The source was produced by irradiating the $\frac{1}{4}$ -mil thick Al foil with ^3He ions

collected filter papers have been routinely analyzed for lead and bromine content using the X-ray fluorescence technique (22, 23). Replicate samples from several filter papers collected at various times during 1971 were nondestructively analyzed for lead via ^3He activation analysis. Table II shows the average lead concentration in the downtown Berkeley atmosphere during those periods. For comparison, the results obtained for the same filter papers by X-ray fluorescence are also tabulated (24). The agreement is good.

Measurement of Lead in Aluminum Foils and Filter Papers. The measurement of lead concentration was further extended to the $\frac{1}{4}$ -mil (1.58 mg/cm² thick) Al backing foils used in this study. These particular Al sheets were of Type 1145-H18 (Republic Foil, Danbury, Conn.). A few experiments were carried out and because the lead content was found to be at trace levels, there was an attempt to measure the γ -ray spectrum with a 3×3 -inch NaI(Tl) crystal to increase the detection efficiency. Figure 2 presents a typical 992-keV γ -ray spectra of the chemically separated polonium portion; it was obtained by irradiating the $\frac{1}{4}$ -mil thick Al foil for 1.5 hr with ^3He particles of about 35 MeV at an average beam current of 3.8 μA . For comparison, the γ -ray spectra were taken with Ge(Li) and NaI(Tl) detectors at similar counting geometries. Although, as expected, the 992-keV peak area in the NaI(Tl) γ -ray spectrum is 10 times larger than its respective Ge(Li) spectrum, the peak-to-background ratio is only 2:1 in the NaI(Tl) case in comparison to 30:1 for the Ge(Li) detector. Consequently, it is concluded that for this study Ge(Li) γ -ray spectroscopy is far more advantageous, mainly because of its superior resolution. The results of lead analyses in Al foils together with the analyses of "blank" Whatman No. 41 and HV 70 filter papers are summarized in Table III. For filter papers, the irradiations were limited to a duration of $\frac{1}{2}$ hr and an average

(22) H. R. Bowman, J. G. Conway, and F. Asaro, *Environ. Sci. Technol.*, **6**, 558 (1972).

(23) L. Y. Goda, J. G. Conway, and H. R. Bowman, LBL-1235 (August, 1972).

(24) J. G. Conway, Lawrence Berkeley Laboratory, Berkeley, Calif. 94720, private communication, 1973.

Table II. Average Atmospheric Lead Concentration in Downtown Berkeley at Various Times during the Year 1971

Sample collection dates	Lead concn ($\mu\text{g}/\text{m}^3$)	
	This work	X-Ray fluorescence work ^a
Feb. 5 to Feb. 12	6.4 ± 1.0	^b
May 14 to May 21	1.5 ± 0.2	1.6
Oct. 22 to Oct. 29	2.1 ± 0.2	1.8

^a Reference 23. The standard deviation in this work is about 10% of the mean value. ^b X-ray fluorescence analysis was not performed on this sample, but qualitatively it was observed to have comparatively high lead content (24).

Table III. Lead Analysis of Various Samples

Sample	Lead content, ppm
$\frac{1}{4}$ -Mil thick Al (type 1145-H18)	9.5 ± 0.5
Whatman No. 41 filter paper	2.1 ± 0.4
HV 70 filter paper	6.5 ± 0.4

Table IV. Cross Section for the $^{207}\text{Bi}(^3\text{He}, 5n + p)^{207}\text{Po}$ Reaction

Average ^3He energy, MeV	Cross section, mbarns
29.6	16
34.9	38
39.7	303

beam current of 1 μA over 1 cm². Exceeding these values results in severe burning of the filter paper.

Interferences. By using ^{207}Po activity, lead analysis via ^3He activation is basically free from interferences produced by any other element. The only element which could possibly interfere in this technique is Bi. Bismuth, if present, could produce ^{207}Po via $^{209}\text{Bi}(^3\text{He}, p)^{207}\text{Po}$ and $^{209}\text{Bi}(^3\text{He}, 5n)^{207}\text{At}$ (1.81 h) \rightarrow ^{207}Po reactions. The threshold energies for these reactions are 25.8 MeV and 30.8 MeV, respectively. To estimate the magnitude of this potential interference, a series of bombardments at different ^3He energies was carried out; foils of 4 mg/cm² thick metallic Bi evaporated onto thin Al backings were irradiated for 1.5 hr at an average beam intensity of $\approx 1 \mu\text{A}$. A summary of experimental cross-section data is presented in Table IV. The experimental errors are about 10%. The cross section for ^{207}Po production from Bi + ^3He reaction at about 35 MeV, the energy region of optimum ^{207}Po production from the Pb + ^3He reaction, is 10 times lower than that for Pb + ^3He reaction. Therefore, at an equal concentration of lead and bismuth impurities in a given matrix, at that energy region, only 10% of the ^{207}Po activity will have been caused by an interfering Bi. However, because the radiochemical procedure in this work does not provide a separation of polonium from astatine, which is also deposited to a large extent on silver foil (25, 26), the presence of Bi can be determined unambiguously by the detection of astatine radioisotopes produced via Bi-

(25) W. Garrison, J. Gile, R. Maxwell, and J. Hamilton, *Anal. Chem.*, **23**, 204 (1951).

(26) E. H. Appelman, "The Radiochemistry of Astatine," NAS-NS 3012 (March 1960).

($^3\text{He},\text{xn}$) reactions. For example, our Bi + ^3He reaction studies revealed that 685- and 660-keV photopeak intensities of ^{208}At produced by the $^{209}\text{Bi}(^3\text{He},4n)^{208}\text{At}$ reaction are ≈ 10 times higher than the 992-keV peak intensity. In other words, bismuth—if indeed present—can clearly be determined via the ^{208}At gamma rays. No other element can produce this nuclide. Alternatively, if the analysis is made on a matrix with a high Bi/Pb concentration ratio, the Bi interference can be completely eliminated by bombardments near 25 MeV, which is lower than the threshold energy for production of ^{207}Po via Bi + ^3He reactions.

Estimate of Detection Limit. Under the following conditions: beam current 3.8 μA , length of bombardment 1.5 hr, overall detection efficiency 0.5%, we were able to detect Pb concentrations of 45 ng/cm 2 in an Al matrix (Figure 2). The background constituted only about $\frac{1}{2}$ of the total 992-keV peak area; at equal signal to background levels, under our easy conditions, we could detect 4.5 ng/cm 2 lead. Because the beam intensity can be increased by a factor of 10 (or greater, depending on the target matrix),

detection coefficients can be easily doubled, and the length of bombardment can be increased to at least one ^{207}Po half-life, the detection limit can be lowered to about 50 pg/cm 2 lead. If the matrix in which lead is imbedded is 10 to 100 mg/cm 2 thick, the concentration limit of detection would therefore be 5 ppb to 0.5 ppb, respectively.

It should be pointed out that for the analysis of paper, the detection limit is held down to only 1 ppm, under our present target-cooling system.

ACKNOWLEDGMENT

The authors wish to thank Diana M. Lee for her assistance during this work.

Received for review June 25, 1973. Accepted August 20, 1973. One of us (BP) would like to express his gratitude for a Senior Fulbright-Hays grant provided to him throughout this study. This research was performed under the auspices of the U.S. Atomic Energy Commission.

Quantitative Analysis of Light Elements (Nitrogen, Carbon, and Oxygen) in Sputtered Tantalum Films by Auger Electron Spectroscopy and Secondary Ion Mass Spectrometry (SIMS)

J. M. Morabito

Bell Telephone Laboratories, Inc., Allentown, Pa. 18103

The quantitative analysis of light elements (N, C, O) in sputtered tantalum films by Auger electron spectroscopy and secondary ion mass spectrometry (SIMS) via calibration with standards and electron microprobe analysis is described. The calibration standards were prepared by reactive sputtering, and the homogeneous distribution of the dopants (N, C, O) in these standards was established by SIMS and Auger in-depth profiling measurements. Although the electron microprobe could reproducibly detect the presence of low levels (<5 at.%) of N, C, and O, the accuracy of quantitative electron microprobe measurements for these light elements in tantalum below ~ 5 at.% was questionable due to the lack of sufficiently accurate X-ray absorption coefficients. The accuracy of electron microprobe quantitative results above ~ 5 at.%, however, was estimated to be within $\pm 10\%$. The analysis of nitrogen, carbon, and oxygen below ~ 5 at.% was accomplished by an extrapolation of the normalized Auger and SIMS data. SIMS detection limits for oxygen and carbon were in the ppm range and for nitrogen in the 0.1 at.% range depending on instrument background and amount of sample consumed. The Auger detection limits for N, C, and O were in the 0.3–0.4 at.% range.

The effects of varying oxygen (1, 2), nitrogen (2), and carbon (2, 3) contents on the structural and electrical properties of sputtered tantalum thin films have been discussed in the literature. Both structural and electrical properties have been found to be a function of the N, C,

and O concentration and of sputtering parameters (voltage, current, and substrate temperature). In general, transitions from a β -Ta (4) structure to a mixture of β -Ta and bcc-Ta, and finally to a single phase bcc (bulk) region followed by oxide, nitride, or carbide formation have been observed. These structural transformations have been studied by X-ray diffraction techniques (1, 2, 5). Quantitative information on the amount of these light elements in tantalum, assuming a homogeneous distribution, has been provided by electron microprobe analysis (1). Since the electron microprobe suffers from a lack of sufficient depth resolution to perform a localized analysis of the composition at the surface, bulk, and film-substrate interface, the quantitative analysis (1) provided by the electron microprobe represented an averaged or integrated concentration over a specific depth (e.g. 600 Å) of the film. The development, however, of ion sputtering-Auger (6, 7) and secondary ion mass spectrometry (SIMS) (8) has made localized analysis possible. Both techniques have unique features for localized thin film analysis, can be calibrated (9) for quantitative analysis, and are capa-

- (1) L. G. Feinstein and D. Gerstenberg, *Thin Solid Films*, **10**, 79 (1972).
- (2) D. Gerstenberg, *J. Electrochem. Soc.*, **113**, No. 6 (1966).
- (3) D. Gerstenberg and J. Klierer, *Proc. Electron. Components Conf.*, **1967**, 77.
- (4) M. H. Read and C. Altman, *Appl. Phys. Lett.*, **7**, 51 (1965).
- (5) R. D. Burbank, *J. Appl. Crystallogr.*, in press.
- (6) J. M. Morabito, Tenth National Meeting of the Society for Applied Spectroscopy, St. Louis, Mo., Oct. 18–22, 1971.
- (7) P. W. Palmberg, Fifth International Vacuum Congress, Boston, Mass., Oct. 1971.
- (8) R. Castaing and G. Slodzian, *J. Microsc. (Paris)*, **1**, 395 (1962).
- (9) J. M. Morabito, 19th National Vacuum Symposium, Chicago, Ill., Oct. 2–5, 1972, p. 278.

ble of in-depth profiling measurements with better than 100-Å resolution over a depth of 1000 Å for optically flat samples.

The analytical method and principles of operation of the electron microprobe, secondary ion mass spectrometry, and ion sputtering-Auger spectroscopy are discussed with particular emphasis on quantitative analysis. The calibration procedures developed for the quantitative analysis of N, C, O in tantalum by ion sputtering-Auger and SIMS measurements are based on the use of electron microprobe quantitative analysis of homogeneous standards prepared by reactive sputtering, and the measurement of parameters such as Auger peak heights and secondary ion currents of the dopants (N, C, O) and of the matrix (Ta). The homogeneous distribution of the dopants in the reactively sputtered films was established by the in-depth profiles obtained by a controlled and gradual *in situ* ion sputtering of the films in combination with simultaneous secondary ion or Auger electron detection. Homogeneous dopant distribution was necessary for accurate quantitative analysis with the electron microprobe.

EXPERIMENTAL

Electron Microprobe. The electron microprobe is a well established analytical technique based on the emission and analysis of characteristic X-rays produced by a focused electron beam. All elements can be detected with the exception of He, Li, and H. The escape depth for the emitted X-rays is dependent upon primary electron energy (E_p) and the density of the target. For tantalum (density of ~ 15 grams/cm³), the penetration depth can be calculated to be ~ 400 Å at a primary energy of 4 keV (10). X-Ray yields are a function of factors such as X-ray ionization cross sections, primary energy, target density, and other factors discussed by Reuter (11). X-Ray and electron images can also be obtained which provide information on the lateral distribution of elements within the area analyzed.

Quantitative analysis by the electron microprobe is based on the use of pure homogeneous standards and a model of the X-ray emission process first proposed by Castaing (12). Castaing's quantitative model has been refined, but remains essentially unchanged with regard to its basic concepts and procedure. For accurate quantitative information, the X-ray intensities must be corrected for the effects of fluorescence (i.e., secondary X-ray emission), X-ray absorption, and atomic number. Fluorescence, X-ray absorption, and atomic number corrections have been discussed in detail by Philibert (13).

The particular difficulties associated with light element ($Z < 10$) quantitative analysis have been discussed by Baird (14) and Ong (15). Both Baird (14) and Henke (16) have emphasized that accurate X-ray absorption correction factors are of extreme importance for the quantitative analysis of light elements. For light elements such as N, C, and O, however, the mass absorption coefficients (μ) are quite high and are not known with sufficient precision (17) for accurate (± 5 -10%) quantitative analysis of light elements below ~ 5 at. %. Borovskii (18) has, in fact, found that the available absorption correction formulas are not accurate when the primary energy (E_p) used is considerably greater than the ionization energy (E_k) of the excited level (< 1 keV for elements below atomic number 10). Yakowitz and Heinrich (19) have also emphasized the possibility of serious error in the absorption correction factor for the case of light element analysis. In addition to these complications, only those X-rays emitted in the outermost surface layers can emerge from the sample when the

absorption coefficients are high. Surface conditions [particularly carbon contamination (15)] can then have a pronounced effect on the X-ray intensities observed. It is for these reasons that low primary energies (19) (< 6 keV) should be used for the analysis of N, C, and O in tantalum and all samples subjected to either oxygen plasma or argon plasma cleaning prior to electron microprobe analysis. Under these conditions and with the use of extremely thin detector windows (16, 20) and appropriate diffracting crystals, accurate quantitative analysis of light elements at higher concentrations ($> \sim 5$ at. %) is possible and has been demonstrated (10, 21).

Secondary Ion Emission. The technique of secondary ion emission is based on the emission and subsequent analysis by mass spectrometry of secondary ions (positive or negative) produced by high energy ion bombardment in the range of 5-15 keV. Ion bombardment at low current densities ($\sim 10^{-7}$ A/cm²), under suitable vacuum conditions, allows for single monolayer (surface) analysis. Bulk analysis requires higher primary ion current densities. All elements, including isotopes, can be analyzed with a sensitivity for many elements in the ppm range and for some in the ppb range (22). Primary oxygen bombardment ($^{16}O_2^+$) is most commonly used, since in most cases it enhances secondary ion yields (K). Argon primary ions ($^{40}Ar^+$) are used when it is necessary to detect oxygen (e.g., O₂ in Ta) or eliminate mass interference from oxide molecular species.

Since only a small fraction (10^{-2} to 10^{-5} for argon bombardment) of the emitted neutral particles are ionized, a finite sample volume (22) must be volatilized or sputtered to detect a secondary ion current. This sample volume will depend on the concentration (C) of the element, secondary ion yield of the element (K), instrument transmission (η), atom density, and the required precision on the measurement. The yield (K) of the secondary ions from the target has been found to be a function of parameters such as primary ion energy (23), temperature of target (24), partial pressure of reactive gases surrounding the target (25), and the chemistry of the target (26). The processes resulting in sputtered atom ionization are not yet completely understood, but several mechanisms have been proposed (27, 28).

A complete mass spectra (0 to 300 mass units) can be taken or a selected secondary ion(s) monitored while sputtering through the sample, i.e., in-depth profile analysis. The in-depth profiles can be obtained with good depth resolution (29). In addition, the emitted secondary ions can also be focused by an ion optical system to produce ion images with a lateral resolution of 1 μ m. The Cameca Ion Analyzer, Cameca Instruments, Elmsford, N.Y., was used for the secondary ion emission measurements discussed in this paper. A detailed description of this particular instrument can be found in reference 22.

Quantitative analysis by secondary ion emission based on a thermal equilibrium model of the ion emission process and on an internal standard (e.g., composition of the matrix) has been proposed by Andersen and Hinthorne (30). Limitations on such a model include chemical and matrix effects which are known to influence the yield of secondary ions (22).

Morabito and Lewis (22) have recently described a method of quantitative analysis based on the use of suitable standards and the measurement of parameters such as the secondary ion current of the impurity ($i(i_{rel})$) and the secondary ion yield of the impurity relative to the matrix (K_{rel}). The equation (22) which relates the concentration of the impurity in a given matrix to these parameters is,

$$C = \frac{i_{in} \left(\frac{100}{a_i} \right) C_m}{i_m K_{rel} \left(\frac{100}{a_m} \right)} \quad (1)$$

(10) J. W. Colby, *Advan. X-Ray Anal.*, **10**, 287-305 (1967).

(11) W. Reuter, *Surface Sci.*, **25**, 80 (1971).

(12) R. Castaing, *These de Doctorat*, Universite de Paris (1951); Publication Onera (1955).

(13) J. Philibert, "Modern Analytical Techniques for Metal and Alloys," Vol. III, Part 2, R. F. Bunshah, Ed., Interscience Publishers, New York, N.Y., 1970, pp 419-531.

(14) A. K. Baird, *Advan. X-Ray Anal.*, **13**, 26-48 (1969).

(15) P. S. Ong, *Advan. X-Ray Anal.*, **8**, 341-51 (1964).

(16) B. L. Henke, *Advan. X-Ray Anal.*, **8**, 269-84 (1964).

(17) B. L. Henke and R. L. Elgin, *Advan. X-Ray Anal.*, **13**, 634-65 (1969).

(18) I. B. Borovskii, Proceedings of the 7th National Conference on Electron Probe Analysis, San Francisco, Calif., July 17-21, 1972.

(19) H. Yakowitz and K. F. J. Heinrich, *Mikrochim. Acta*, **1968**, 182.

(20) D. R. Wonsider, unpublished Bell Telephone Laboratories data.

(21) C. A. Andersen, "The Electron Microprobe," T. D. McKinley, K. F. J. Heinrich, and D. B. Wittry, Ed. Wiley, New York, N.Y., 1966, p 58.

(22) J. M. Morabito and R. K. Lewis, *Anal. Chem.*, **45**, 869-80 (1973).

(23) R. C. Bradley, *J. Appl. Phys.*, **30**, 1 (1959).

(24) H. E. Stanton, *J. Appl. Phys.*, **31**, 678 (1960).

(25) H. Beske, International Conference on Ion Surface Interaction—Sputtering and Related Phenomena, Garching, Germany, Sept. 25-28, 1972.

(26) H. W. Werner, *Develop. Appl. Spectrosc.*, **7A**, 239 (1969).

(27) R. Castaing and J. F. Hennequin, *Advan. Mass Spectrom.*, **5**, 88 (1972).

(28) C. A. Andersen, *Int. J. Mass Spectrom. Ion Phys.*, **2**, 61 (1969).

(29) C. A. Evans, Jr., and J. P. Pemsler, *Anal. Chem.*, **42**, 1130 (1970).

(30) C. A. Andersen and J. R. Hinthorne, *Anal. Chem.*, **45**, 1421 (1973).

where, C = concentration of impurity, $i(a_i)$ = secondary ion current of impurity, a_i = isotopic abundance of impurity, a_m = isotopic abundance of matrix, K_{re} = secondary ion yield of impurity relative to the matrix, C_m = concentration of matrix, and i_m = secondary ion current of matrix.

Normalizing the secondary ion current ($i(a_i)$) of the impurity to the measured secondary ion current of the matrix (i_m) eliminates the untractable effects of changes in sputtering rate (λ), sputtering yield (S) and surface atom density (σ) during a measurement or series of measurements (22). Normalization is of paramount importance for in-depth analysis since profile shape is particularly affected by changes in the secondary ion yield of the impurity and matrix. The observed changes in ion yields are often due to the presence of reactive elements such as oxygen (26, 27) which enhances the yield of both the matrix and impurity. Figure 1 shows the profile of nitrogen in a nitrogen doped tantalum film. The measured profile shows an apparent increase of nitrogen at the surface and interface due to the presence of oxygen (22). The in-depth profile of the matrix (Ta) was also affected by the presence of oxygen as shown in the same figure. The true profile of nitrogen could be obtained only by normalizing the nitrogen profile to the tantalum (matrix) profile. All the secondary calibration data discussed in this paper have been normalized to the matrix.

Ion Sputtering-Auger Electron Spectroscopy. Auger electron spectroscopy is based on the emission and subsequent energy analysis of secondary electrons produced by high energy (3-5 keV) electron bombardment. The energy of a small fraction of the secondary electrons emitted from the sample can be related to the core levels of the target atom and these electrons, the Auger electrons, have escape depths in the 5- to 20-Å range. This low escape depth makes Auger electron spectroscopy ideal for surface analysis and for in-depth analysis when combined with *in situ* ion sputtering (6, 7). All elements with the exception of He and H can be detected. Selected area Auger analysis is also possible by scanning the primary electron beam to obtain an image of the sample (31) or by a recently developed (32) optical technique.

The number of Auger electrons emitted per incident primary electron, the Auger yield, is dependent on factors such as the primary electron energy (E_p), the angle of incidence (α), ionization cross sections (σ), the Auger transition probability (ψ), escape depths (d_e), and on back scattering correction factors (r). The dependence of the $M_3N_4N_4$ Auger peak height with primary energy for the tantalum atom is shown in Figure 2. For a cylindrical mirror analyzer (CMA), the Auger peak height divided by the energy of the Auger transition is a relative measure of Auger yield. For quantitative Auger analysis consider:

Empirical Equation. The detected Auger current (i_d), for a fixed angle of primary electron incidence (α), from a particular Auger transition (β) (e.g., $KL_{23}L_{23}$ nitrogen) can be expressed by the following empirical equation: (33)

$$i_d = i_p C \psi \phi r (E/d_e) R \quad (2)$$

where, i_p = primary current (μA), C = concentration (atoms/cm²), ψ = Auger transition probability, ϕ = ionization cross section (cm²/atom), r = back scattering correction (>1), $\eta(E)$ = instrument transmission corrected for CMA energy resolution, d_e = escape depth (Å), and R = surface roughness factor.

The parameters in this expression can be a function of variables such as primary electron energy, surface atom density and homogeneity, angle of incidence, etc., and are not independent of each other. If these parameters were known, or easily measured, one could then calculate the concentration (C) from an accurate measurement of the Auger current. Unfortunately, parameters such as escape depths, backscattering corrections etc., are usually not available nor conveniently measured. Therefore, calibration by the use of homogeneous standards whose concentration can be accurately ($\pm 10\%$) measured appears at present to be the best approach to quantitative information from the Auger data.

Calibration Method Based on Ion Sputtering-Auger Analysis. The calibration of Auger measurements for quantitative analysis of dopants homogeneously distributed throughout the escape depth region has become possible with the development of simultaneous *in situ* ion sputtering-Auger analysis (6, 7). Prior to this development, quantitative analysis by calibration methods had been restricted to sub-monolayer, uniformly distributed surface deposits prepared and analyzed under ideal vacuum conditions as

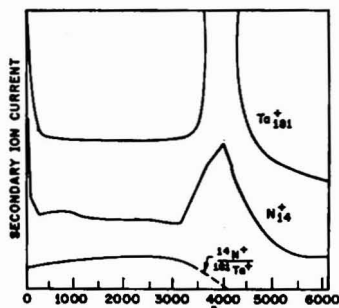


Figure 1. Nitrogen ($^{14}N^+$), tantalum ($^{181}Ta^+$), and normalized ($^{14}N^+/^{181}Ta^+$) profiles in a nitrogen doped tantalum film

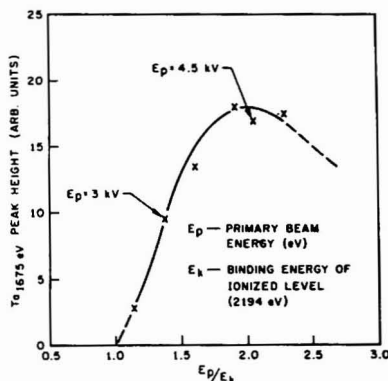


Figure 2. Tantalum $M_3N_4N_4$ Auger peak height vs. E_p/E_k

first described by Weber and Johnson (34). This work (34) established that the peak-to-peak Auger signal was a linear function of coverage below one monolayer, provided contaminants such as carbon and oxygen had not adsorbed on the deposited surface layers prior to the Auger measurements. A similar approach has recently been used by Gerlach and Ducharme (35) to determine the absolute and relative ionization cross sections for C, N, O adsorbed on a W(100) single crystal. The results obtained were in good agreement with the absolute and relative ionization cross section measurements of C, N, O in the gas phase previously reported by Glupe and Mehlhorn (36). The relative ionization cross sections for N, O, C were found to be the same (35, 36) within experimental error.

Figure 3 is a schematic of the arrangement used in this study to ion sputter and Auger analyze a sample simultaneously. Two ion guns and an electron gun were positioned above the sample. Primary ion energies of 1 keV A^+ or Xe^+ at current densities of 30 $\mu A/cm^2$ were used and a typical crater formed on the surface of the sample is shown in Figure 4. The electron beam ($d \sim 0.1$ mm) was placed in the center of this crater ($d > 1$ mm). The output from the lock-in amplifier was fed to a time base recorder or a multiplexer (32) interfaced into the Auger system (32) which allows for the monitoring of six selected Auger peaks simultaneously. The detection circuit of the multiplexer automatically measures the peak-to-peak amplitudes of the selected Auger signals. This information can then be displayed as a function of time via a point plotter.

(34) R. E. Weber and A. L. Johnson, *J. Appl. Phys.*, **40**, 314 (1969).

(35) R. L. Gerlach and A. R. Ducharme, *Surface Sci.*, **32**, 329 (1972).

(36) G. Glupe and W. Mehlhorn, *Phys. Lett.*, **25A**, 274 (1967).

(31) J. M. Morabito and D. F. Munro, *Appl. Phys. Lett.*, **21**, (12), 572 (1972).

(32) Physical Electronics, Inc., Instrument Brochure, Edina, Minn.

(33) H. E. Bishop and J. C. Riviere, *J. Appl. Phys.*, **40**, 1740 (1969).

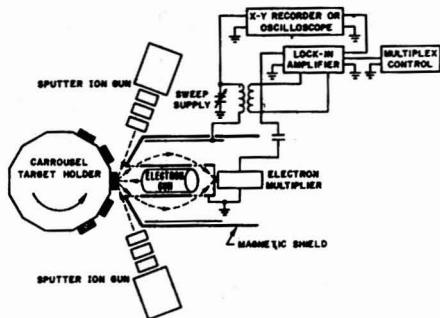


Figure 3. Experimental arrangement and electronic scheme used to ion sputter and Auger analyze a sample simultaneously



Figure 4. Crater formed on sample by 1-keV A^+ ions at a current density of $30 \mu A/cm^2$. The primary electron beam is placed in the center of this crater

Figure 5 shows the Auger spectrum of a Ta_2N film prior to and after *in situ* ion sputtering. Prior to sputtering, the tantalum (179 eV) and nitrogen (380 eV) Auger peak heights are attenuated by surface carbon (270 eV) and oxygen (512 eV). These surface contaminants must be removed to obtain a nitrogen to tantalum Auger peak height ratio which can be related to the known composition of this film (~33 at. % and ~67 at. % Ta). This contamination is most conveniently removed by *in situ* ion sputtering while monitoring the Auger spectra. For this film, the *in situ* ion sputtering completely removed the surface carbon and reduced the oxygen Auger peak height considerably. After sputtering, the oxygen peak height was indicative of the bulk oxygen concentration in the film, and the nitrogen to tantalum Auger ratio was increased and constant throughout the film.

In situ ion sputtering also prevents recontamination of the analyzed surface by contaminants such as water vapor and hydrocarbons. Under the conditions used to sputter the surface (5×10^{-5} Torr A^+ or Xe^+), the partial pressure of these contaminants is in the 10^{-9} Torr range. Calculations, based on the kinetic theory of gases and unit sticking probability, of the time necessary to form a monolayer of water vapor or hydrocarbon (i.e., C_4H_{10}) on tantalum as a function of the partial pressure of these contaminants in the vacuum chamber indicated that sputtering rates of 10 $\text{\AA}/\text{min}$ are more than adequate to prevent this contamination from depositing on the surface.

There is, however, a surface compositional change due to *in situ* ion sputtering. The magnitude of this compositional change for a binary system (AB) will be a function of the sputtering yield ratio (S_A/S_B), bulk concentration ratio (C_A/C_B) and of surface atom density. The region of this compositional change is small (~50 \AA) and steady state conditions should be established rather rapidly. Once steady state is reached, the magnitude of the Auger peak height ratio (e.g., N/Ta in Figure 5), monitored during ion sputtering, is a relative measure of the actual bulk composition of

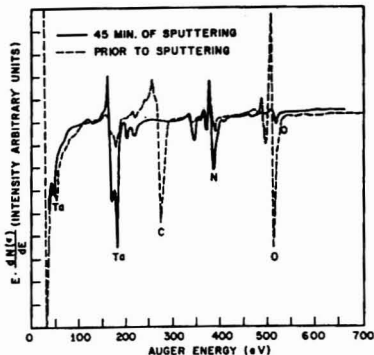


Figure 5. Auger spectrum of a Ta_2N film prior to and after *in situ* ion sputtering

the film. The actual steady state surface composition for a smooth, dense binary homogeneous film (e.g., Ta_2N) can be approximated (neglecting diffusion effects) by the product of the bulk concentration and sputtering yield ratio of the two major components (Ta, N). Unfortunately, the sputtering yields (S) for light elements such as N, C, O are not accurately known. P. Palmberg (37) has found that the surface composition of vacuum cleaved MgO (50 at. % Mg, 50 at. % O, bulk concentration) changed to 48 at. % O and 52 at. % Mg as a direct result of Xe ion sputtering. The sputtering efficiency ratio (S_{Mg}/S_N) in this case was 1.06.

PREPARATION OF HOMOGENEOUS STANDARDS BY REACTIVE SPUTTERING

Ion implantation has been found (38, 39) to be a useful means of preparing B, P, and As doped silicon samples for the quantitative calibration of Auger spectroscopy and SIMS. This method of sample preparation is less attractive for the controlled incorporation of light elements such as N, C, O in tantalum because of a lack of accurate range statistics (40) in tantalum. Reactive sputtering, however, is a very convenient means of incorporating dopants such as C, N, O, into tantalum or any metal, and is most usually accomplished by adding a varying, but well-controlled, partial pressure of a single reactant or reactant mixture (N_2 , O_2 , CH_4) to an inert gas such as argon during sputtering from a pure metal cathode. The sputtering parameters used for this study were 5 kV and 200 mA (single phase-unfiltered dc power supply) with a 9.5-cm cathode (35-cm diameter Ta) to anode spacing. The sputtered films were deposited on Corning 7059 glass substrates coated with a Ta_2O_5 etch stop layer (41). The films (~5000 \AA) were optically smooth and flat which minimized surface roughness effects on the Auger and secondary ion signal intensity. Methane + argon mixtures (3) were used to prepare the carbon doped films. The nitrogen and oxygen doped films were prepared by introducing small amounts of nitrogen or oxygen into the sputtering chamber (1, 2), and tantalum oxynitride films were prepared by introducing $N_2 + O_2$ mixtures (42).

(37) P. W. Palmberg, Auger Spectroscopy, 1972 Fall Workshop on Surface Analysis and Secondary Ion Mass Analysis, Nov. 2-3, 1972, Tarrytown, N.Y.

(38) J. M. Morabito and J. C. C. Tsai, *Surface Sci.*, **33**, 422 (1972).

(39) J. C. C. Tsai, J. M. Morabito, and R. K. Lewis, 3rd International Conference on Ion Implantation, IBM, New York (1972), to be published in the proceedings of this conference.

(40) J. Lindhard, M. Scharif, and H. Schliott, *Mat. Fys. Medd. Dan. Vid. Selsk.*, **33**, 1 (1963).

(41) R. D. Huttman, J. M. Morabito, and D. Gerstenberg, submitted to *IEEE J. Solid-State Circuits*.

(42) G. I. Parisi, *Proceedings of Electronic Components Conf.*, Washington, D.C., 1969.

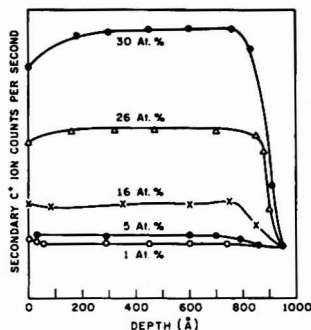


Figure 6. Secondary ion carbon profiles in tantalum thin films reactively sputtered in (A + CH₄) mixtures. ¹⁶O₂⁺ primary ions at 4.5 keV

In-depth profiles by Auger spectroscopy and SIMS measurements showed that the nitrogen and carbon were uniformly (homogeneously) distributed throughout the films over a wide concentration range. It was not possible, however, to prepare homogeneously distributed oxygen doped films below ~13 at. % with the sputtering conditions used (41). The homogeneous distribution of carbon in tantalum prepared by reactive sputtering in argon + CH₄ mixtures is shown in Figure 6 and that of the nitrogen to oxygen ratios in tantalum oxynitride films after surface oxide (~25 Å) has been removed in Figure 7. SIMS measurements prior to electron microprobe measurements indicated that these doped films also contained hydrogen and argon. Argon was also detected by Auger analysis. The amount of hydrogen is most probably <~7 at. % (5) since the temperature of the films during sputtering was as high as 400 °C. The argon content (20) by electron microprobe analyses was estimated to be ≤2 at. %.

The hydrogen and argon content did not change with increasing N, C, and O concentration in the films. Since the only variation in concentration for these doped films was that of the dopant (N, C, O) and the matrix (Ta), the films could be considered to be essentially binary systems.

RESULTS AND DISCUSSION

Quantitative Electron Microprobe Analysis of Homogeneous Standards Prepared by Reactive Sputtering. The electron microprobe analyses were performed at a primary energy of 5 keV. The X-ray emergence angle was 38.5° and the analyzed depth ~600 Å. The X-ray intensity ratios for the nitrogen, carbon, and oxygen measurements were obtained using Si₃N₄, graphite, and SiO₂, respectively, as reference standards. The data were corrected using MAGIC IV (43), and all samples were oxygen plasma cleaned prior to analysis. A nitrolicid (Biodynamics Research Corporation, Rockville, Md.) detector window was used for all the analyses. The diffracting crystal used for the nitrogen analyses was lead triacetonate. A lead stearate decanoate crystal was used for the carbon analysis and either chinchlore or rubidium acid phthalate for the oxygen analyses.

Since the prepared standards were essentially binary systems, the nitrogen, carbon, and oxygen compositional analysis could also be determined *indirectly* by difference (material balance). The *direct* (MAGIC IV and suitable X-ray detectors and diffracting crystals) and *indirect*

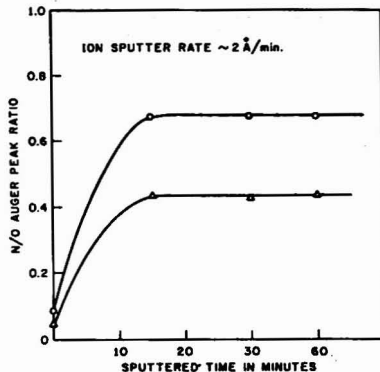


Figure 7. Ion sputtering-Auger in-depth profiles of N/O ratio for TaO_xN_y films

Table I. Comparative Data of Nitrogen Concentration Estimated by Indirect (Difference or Material Balance) and by Direct (Correction Model) Electron Microprobe Measurements

Specimen	Indirect, at. %	Direct, at. %
A. Si ₃ N ₄	59.06 ± 0.30*	58.35 ± 0.15*
B. Si ₃ N ₄	58.86 ± 0.32	58.17 ± 0.26
C. Ta-O-N	25.97 ± 0.39	26.72 ± 0.48
D. TaHfN	53.99 ± 0.38	54.19 ± 0.54

* Two sigma limits for 10 analyses.

methods are less accurate at low (<5 at. %) concentrations. However, analyses by the direct and indirect methods were in good agreement at higher concentrations (20), as shown for the case of nitrogen in Table I (20). The direct and indirect methods of analysis were also in good agreement for carbon and oxygen at higher concentrations.

A comparison of the quantitative analysis provided by the electron probe with that provided by nuclear microanalysis (44) is in progress, but not yet completed. The nuclear microanalysis technique is, in principle, capable of an absolute analysis of N, C, and O down to low concentrations (<1 at. %). Until this comparison is made, the accuracy of the quantitative analysis at low concentrations (<5 at. %) provided by the electron microprobe is speculative. However, an accuracy of a factor 2 at concentrations below ~5 at. % is perhaps reasonable. At higher concentrations, the relative error based on statistical deviation from the standards (two sigma limits) can be calculated to be within ±10%. The quantitative analyses provided by the electron microprobe were used to calibrate the SIMS and Auger data which are discussed in the next two sections.

Calibration of SIMS. The incorporation of light elements such as nitrogen, carbon, and oxygen into tantalum changes the crystallographic structure of the deposited films (1-3). These reactive gases can be accommodated into the sputtered tantalum lattice to form interstitial (random or ordered) solid solutions. Since the coordination number (i.e., number of nearest neighbors) will be

(43) J. W. Colby, Proc. 6th Natl. Conf. Electron. Probe Anal., Pittsburgh, paper 17 (1971).

(44) G. Amsel, J. P. Nadei, E. D'Artemar, D. David, E. Girard, and J. Moulin, Nucl. Instrum. Methods., 92, 481 (1971).

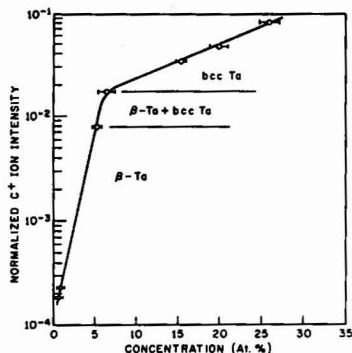


Figure 8. Normalized C^+ ion intensity vs. concentration of carbon (at. %) in tantalum thin films reactively sputtered in ($A + CH_4$) mixtures. $^{16}O_2^+$ primary ions at 4.5 keV

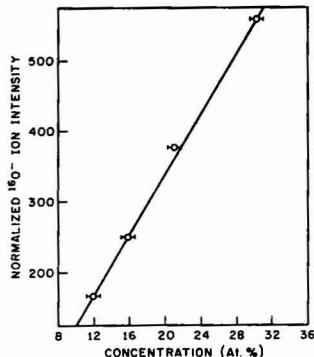


Figure 10. Normalized O^- ion intensity vs. concentration of oxygen (at. %) in tantalum thin films reactively sputtered in ($A + O_2$) mixtures. Primary A^+ ions at 14.5 keV

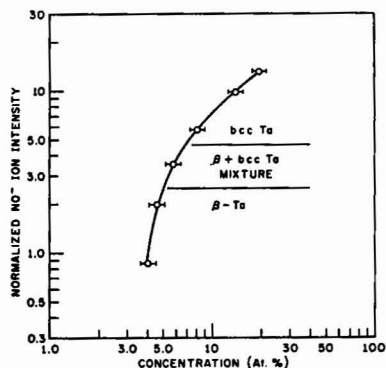


Figure 9. Normalized NO^- ion intensity vs. concentration of nitrogen (at. %) in tantalum thin films reactively sputtered in ($A + N_2$) mixtures. $^{16}O_2^+$ primary ions at 14.5 keV

different in a β -Ta (tetragonal) (4) and bcc structure, the relative secondary ion yield (K_{rel}) of these dopants in tantalum could be affected by structural changes. This was the case as shown in Figure 8 where the $^{12}C^+$ secondary ion current normalized to the $^{181}Ta^+$ secondary ion current as a function of carbon composition, determined by the electron microprobe, is shown along with structural information. The primary ions used for this analysis were $^{16}O_2^+$ at 4.5 keV. Although the yield of $^{12}C^-$ secondary ions was found to be higher than $^{12}C^+$, the secondary ion yield of $^{12}C^+$ was more than sufficient for calibration. Normalizing the $^{12}C^+$ secondary ion current to the major tantalum ($^{181}Ta^+$) secondary ion current eliminated the possible effects of changes in sputtering rate (\dot{z}), sputtering yield (S), and surface atom density (σ). The relative yield (K_{rel}) of carbon in tantalum is obviously different in the β -Ta and bcc-Ta phase regions. The normalized carbon secondary ion current was linear in these two phase regions, but nonlinear over the concentration range studied.

Similar results were obtained (Figure 9) for the normalized secondary $^{30}(NO)^-$ ion current. $^{30}(NO)^-$ was monitored since the secondary ion yield of $^{30}(NO)^-$ ions is

greater than the secondary ion yield of $^{14}N^+$. Oxygen primary ions ($^{16}O_2^+$) at 14.5 keV produced the most reproducible results and highest sensitivity for nitrogen in tantalum. $^{30}(NO)^-$ was normalized to $^{181}Ta^-$.

For the oxygen doped samples, $^{16}O^-$ secondary ions were monitored and normalized to $^{181}Ta^-$. The yield of $^{16}O^-$ was found to be higher than $^{16}O^+$. The resulting calibration curve is shown in Figure 10. It was not possible to obtain data below ~ 13 at. % due to a lack of homogeneous samples in this concentration range.

In all three cases (Figures 8, 9, and 10), the normalized data were a linear function of concentration above 13 at. %, and this linear dependence demonstrates that the secondary ion measurement is quantitative. The reproducibility of these results was better than 5%. Mass interference effects for $^{12}C^+$, $^{30}(NO)^-$, and $^{16}O^-$ in a tantalum matrix were not a problem. The nitrogen and carbon secondary ion calibration curves presented in this paper should be used only for quantitative estimates of nitrogen and carbon in films which are known to contain only small amounts of oxygen. The nitrogen secondary ion calibration curve should not, for example, be used to determine the concentration of nitrogen in a tantalum oxynitride film. The presence of oxygen would change the secondary ion yield of both the nitrogen and tantalum, and hence the normalized NO^- signal.

Although normalization corrects for variation in sputtering rate (\dot{z}) etc., it does not avoid the effect of surface roughness on the normalized ratio. Crosset (45) has found that boron to silicon ratios on optically polished surfaces were two times higher than those measured on rough surfaces. The effect of surface roughness on the secondary ion measurements discussed in this study was eliminated by the use of optically flat samples produced by sputtering on glass substrates.

Calibration of Auger Analyzer. The ion sputtering-Auger calibration curves generated for nitrogen, carbon, and oxygen are shown in Figure 11. The concentration of N, C, O in at. %, as determined by the electron microprobe, is plotted vs. the normalized Auger peak heights (N/Ta , C/Ta , O/Ta). Normalizing the data eliminates effects such as electron multiplier gain reduction with time, inadvertent changes in beam current over a series of measurements, etc. Since the nitrogen, carbon, and oxygen $KL_{23}L_{23}$ Auger transitions occur in the low energy (45) M. Crosset, International Meeting of Chemical Analysis by Charged Particle Bombardment, Namur, Belgium, Sept. 5-8, 1971.

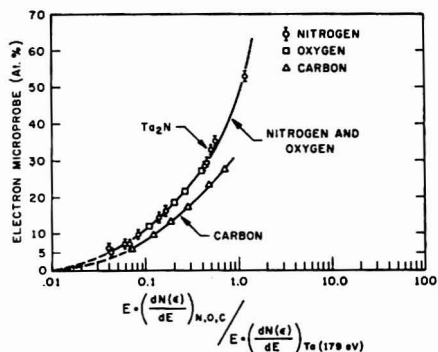


Figure 11. Ion-sputtering-Auger calibration curves for nitrogen, carbon, and oxygen, at. % N, C, and O vs. the normalized Auger peak heights (N/Ta, C/Ta, O/Ta)

(100 to 520 eV) portion of the Auger spectrum, these transitions were normalized to the low energy tantalum $N_5N_6N_6$ (179 eV) rather than the higher energy (>1000 eV) tantalum transitions. In the low energy region (≤ 1000 eV), the natural line widths of the Auger peaks are wider than the instrumental line width of the CMA. This makes the Auger peak height proportional to Auger electron energy since the CMA resolution is proportional to energy. The primary electron current (i_p) was 50 μA at a primary energy (E_p) of 3 keV. The peak-to-peak modulation was 2 volts with a 100-msec time constant on the lock-in amplifier. The sputtering ion current was 30 $\mu A/cm^2$ at a primary energy of 1 keV. This corresponds to a sputtering rate of approximately 10 $\text{\AA}/\text{min}$. These calibration curves are unique to the surface roughness and density of the standard, and to the *in situ* ion sputtering conditions (primary energy and current) used during the Auger measurements. The magnitude of the normalized Auger peak heights as a function of composition and hence the shape of the calibration curves was determined in part by the functional dependence of the selective sputtering process with sample composition and primary ion energy. Selective sputtering does occur during the ion sputtering-Auger analysis. In addition, parameters such as the backscattering correction factors (r) and the escape depth (d_e) could also be changing with film composition since the valence band structure and the crystallographic structure of the films are affected by the incorporation of these dopants. Because of these reasons, it is not surprising that the normalized Auger peak height ratios did not show a linear relationship with composition.

A plot of $\log C$ vs. the log of the normalized N, O, C Auger peak heights (X) is shown in Figure 12.

The resulting nitrogen calibration data could be expressed by the following mathematical Equation:

$$C_N = 48.6X^{0.55} \quad (3)$$

for concentrations above 5 at. % and up to 54 at. %. The oxygen data above 13 at. % could be expressed by the same equation and the carbon data above 5 at. % and up to 28 at. % by

$$C_C = 43.1X^{0.55} \quad (4)$$

where X is the normalized Auger peak heights. The reproducibility of the ion sputtering-Auger measurements was $\pm 2\%$ based on five measurements of the same sample. The above equations do not hold below 5 at. % because of the limitations of quantitative electron microprobe analy-

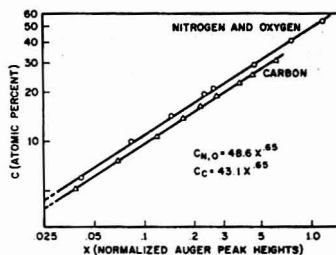


Figure 12. Log of concentration (C) vs. log of normalized N, O, C Auger peak heights (X)

Table II. Comparison of the O/N Ratio Determined by Electron Microprobe Analysis and the Oxygen to Nitrogen Ratio Determined by Auger Analysis

Sample	Electron microprobe	Auger
1	0.50	0.53
2	1.16	1.31
3	1.08	1.12
4	0.425	0.43
5	0.620	0.53
6	0.560	0.51

sis at low concentrations. Analysis below ~ 5 at. % was accomplished by extrapolating the Auger and SIMS data.

The ion sputtering-Auger analysis method of calibration is applicable to any homogeneous multicomponent system of known and accurate composition provided the sample is optically flat and the simultaneous sputtering does not selectively remove all or most of any one component. The situation of gross selective sputtering is not typical, but can occur. This calibration method would, perhaps, be more accurate if Auger currents (i_i) rather than Auger peak heights were measured. Convenient experimental techniques for accurate Auger current measurements are not yet available, however.

Table II is a comparison of the O/N ratio in Ta O_xN_y films determined by electron microprobe analysis and the oxygen to nitrogen ratio determined by taking the oxygen to nitrogen Auger peak height ratio. From this agreement, one can conclude that the relative Auger yield of oxygen and nitrogen in a tantalum matrix and the sputtering yields (S) of these elements in a tantalum matrix must be the same or very close in magnitude.

The fact that oxygen (510 eV) and nitrogen (380 eV) have similar relative Auger yields in tantalum is not unreasonable. Both are $KL_{23}L_{23}$ type transitions. In addition, the backscattering correction factors (r) for these light elements in a heavy matrix such as tantalum should also be quite similar. Since the escape depth is predominantly determined by the valence band structure of the sample, the escape depths (d_e) for nitrogen and oxygen from tantalum are not expected to be the same. The transmission of the CMA [$\eta(E)$] is not the same for the nitrogen and oxygen transitions because of their energy difference, and the absolute ionization cross sections (σ) for these two elements are also not the same (35, 36). However, the actual magnitudes of these parameters are apparently such that $(\psi\phi r)^O \eta(E_O) d_e^O \sim (\psi\phi r)^N \eta(E_N) d_e^N$.

Therefore, the oxygen to nitrogen concentration ratio (C_O/C_N) in a Ta O_xN_y can be determined by simply taking the oxygen to nitrogen Auger peak height ratio (I^O/I^N).

Table III. Comparison of S/N for N, C, O in Sputtered Tantalum Films by Ion Sputtering-Auger and Secondary Ion Detection

Element	Concn, at. %	S/N, Auger	S/N, SIMS
C	6.5	37/1	520/1
N	5.0	28/1	80/1
O	13	72/1	5200/1

SENSITIVITY COMPARISON OF ION SPUTTERING-AUGER AND SECONDARY ION DETECTION FOR N, C, AND O IN TANTALUM

It is very difficult to compare the ultimate sensitivities of ion sputtering-Auger and secondary ion emission analysis for the detection of N, C, and O in tantalum since the Auger signal is independent of the volume volatilized by sputtering, but the secondary ion signal is not. One should compare sensitivity for the same depth resolution and amount of sample consumed. However, accurate measurements of depth resolution are only possible for samples with known dopant distributions, e.g., ion implanted samples. For the case of ion implanted samples, Morabito and Tsai (38) have found that secondary ion detection is approximately two orders of magnitude more sensitive than ion sputtering-Auger analysis for P and As in silicon and could detect 10^{15} atoms/cm³ of boron in silicon compared to $\sim 5 \times 10^{19}$ atoms/cm³ with ion sputtering-Auger detection.

A comparison of the signal-to-noise (S/N) found with both techniques for typical operating conditions is summarized in Table III. From these measurements, it is clear that secondary ion detection is more sensitive than ion sputtering-Auger analyses, especially for the case of oxygen. By defining the detectability limit as the point where the signal to noise (S/N) ratio is 2/1 and assuming a linear dependence between signal and composition below 5 at. %, the detectability limit for N, C, and O in tantalum from the data presented in Table III is in the 0.3-0.4 at. % range. Under the same assumptions, the nitrogen detectability limits with the SIMS technique is in the 0.1 at. % range and in the ppm range for carbon and oxygen depending on the amount of sample consumed.

CONCLUSIONS

Secondary ion emission is, in general, a more sensitive analytical technique than ion sputtering-Auger spectroscopy, but data interpretation is complicated by chemical and matrix effects. This sensitivity advantage is necessary for the detection and profiling of the common dopants (38, 39, 46) (B, P, As) in silicon at the concentration levels (10^{18} - 10^{15} atoms/cm³) of interest for device fabrication. It is not necessary, however, for the detection and profiling of light elements (N, O, C) in tantalum at the concentration levels of most interest for the fabrication of tantalum based resistors and capacitors. Significant changes in

(46) M. Bonis, B. Blanchard, M. DeBrebisson, N. Hilleret, and J. Monnier, *Electrochem. Soc. Meeting, Abs. 226, Miami, Fla., 1972.*

resistivity, TCR, and stability of Ta₂N resistors due to the presence of carbon or oxygen occur at concentration levels which are within detection with ion sputtering-Auger analysis. The carbon contamination levels which affect the TCR and anodizability of TaO_xN_y resistor film are detectable with ion sputtering-Auger spectroscopy, and the oxygen to nitrogen ratio of TaO_xN_y resistor films is directly measurable from the Auger spectrum. The amount and distribution of these light elements in tantalum films and in the anodic oxide produced from these films for capacitor fabrication is also measurable by ion sputtering-Auger analysis (41).

Once escape depths, back-scattering correction factors, and Auger currents can be conveniently and accurately measured, the quantitative capabilities (47) of ion sputtering-Auger electron spectroscopy will approach that achieved by the electron microprobe provided gross selective sputtering of any one component does not occur.

NOMENCLATURE

- α = angle of incidence (degrees)
- a_i = isotopic abundance
- CMA = cylindrical mirror analyzer
- C = Concentration (ppm atomic or at. %)
- d_e = escape depth (Å)
- E_p = primary electron energy (keV)
- $i(a_i)$ = secondary ion current of impurity
- i_m = secondary ion current of matrix
- i_p = primary electron current (μ A)
- l = Auger peak height
- i_A = Auger Current
- K_{rel} = relative secondary ion yield
- η = instrument transmission
- r = backscattering correction factor
- R = surface roughness
- S = sputtering yield (atoms/incident ion) of matrix
- S/N = signal to noise ratio
- μ = mass absorption coefficient
- ψ = Auger transition probability
- ϕ = ionization cross section (cm²/atom)
- X = normalized Auger peak height
- σ = surface atom density (atoms/cm²/monolayer) of matrix
- \dot{z} = sputtering rate (Å/sec)

ACKNOWLEDGMENT

Special acknowledgment is made to D. R. Wonsider who established the optimum working variables for the operation of the electron microprobe in order to detect light elements and carried out all the measurements. It is also a pleasure to thank D. Gerstenberg who emphasized the importance of quantitative Auger analysis, R. K. Lewis of Cameca Instruments who performed the SIMS measurements, and R. Huttemann who prepared the films.

Received for review May 21, 1973. Accepted August 17, 1973.

(47) P. Palmberg, *Anal. Chem.*, **45**, 549A (1973).

X-Ray Photoelectron Spectroscopic Studies of Palladium Oxides and the Palladium-Oxygen Electrode

K. S. Kim, A. F. Gossmann, and Nicholas Winograd

Department of Chemistry, Purdue University, West Lafayette, Ind. 47906

The ESCA technique has been employed to characterize various palladium-oxygen species on the surface of oxidized palladium metal. Both oxygen-chemisorbed palladium atoms (PdO_{ads}) and PdO are observed on metal substrates exposed to air at 600 to 900 °C. These results have been applied to studying electrochemically oxidized palladium electrodes in 1N H_2SO_4 . Both PdO and PdO_2 are observed at potentials beginning at +0.90 V vs. N.H.E. In addition, since the mean escape depth of the photoelectron is on the order of 10 Å, estimates of oxide film thicknesses can be made. Electrodes oxidized at 0.9 V had a coating about 5 Å thick whereas at 1.7 V, the thickness increased to greater than 40 Å. By examining the peak areas of the Pd spectra and the oxygen spectra, the presence of excess oxygen as adsorbed and H_2O , hydrated PdO , PdO_2 , and $\text{Pd}(\text{OH})_2$ or $\text{Pd}(\text{OH})_4$ was clearly indicated.

The last decade has witnessed the emergence of several supplementary tools which aid the electrochemist in interpreting often-times hopelessly complicated current-voltage curves. Extensive development of optical spectroscopy, X-ray and electron diffraction, electron microscopy, field-ion microscopy, and radiotracer techniques substantiate this claim. Some approaches are valuable because they can be used *in situ*, that is, to monitor processes in the electrochemical cell while they are occurring. Others, particularly those involving X-ray or electron energy analysis, must be used as analytical tools after the electrochemical process is complete. These analyses are generally restricted to a chemical identification of species remaining in solution or to an elemental analysis of material remaining on the electrode.

The technique of X-ray Photoelectron Spectroscopy (XPES or ESCA) offers an ideal approach for the analysis of surface films remaining on electrodes after the electrochemical perturbation is complete. Although the technique cannot be applied *in situ*, information related to chemical structure and thickness of these films can be obtained in a straightforward manner. We first illustrated this approach to analysis by successfully identifying the two oxides of Pt (PtO and PtO_2) (1) on the surface of a platinum electrode oxidized in aqueous acidic solutions. The chemical identification of certain hydrates has also been confirmed for the Pb/PbO_2 electrode (2). In addition, Hulet and coworkers (3) have studied the passivation of some copper-nickel alloys and have confirmed the presence of NiO as the primary surface species.

The purpose of this paper is to describe the initial results we have obtained on the analysis of several palladium-oxygen species and to describe the application of

these results to the analysis of anodic oxide films formed on the palladium electrode, oxidized in sulfuric acid media. The ESCA data indicate the presence of both PdO and PdO_2 , as predicted by previous electrochemical investigations. The ESCA technique is also used for estimating the approximate thickness of these surface films since the mean escape depth for 1000-eV electrons is on the order of 10 Å (4, 5). The possible information obtained from ESCA and the value of this technique to electrochemists will also be discussed.

EXPERIMENTAL

Apparatus. Spectra were recorded on a Hewlett-Packard 5950 A ESCA spectrometer using monochromatic $\text{Al K}\alpha_{1,2}$ X-rays obtained from a quartz-crystal disperser. Binding energies were calibrated to the Au $4f_{7/2}$ level of evaporated Au at 84.0 eV or the C 1s level of graphite at 284.4 eV. The normal pressure in the spectrometer chamber was 5×10^{-9} Torr as read on the ion pump gauge. Electrochemical measurements were performed using a potentiostat of standard design built from operational amplifiers.

Reagents. Palladium foil (99.9%) was obtained from Alpha Inorganics and used without further purification.

Procedure. Electrochemical measurements were performed in 1N H_2SO_4 supporting electrolyte at 25 °C. Electrode potentials were measured with respect to the saturated calomel electrode but are reported with respect to the normal hydrogen electrode. Solutions were degassed with argon prior to the oxidations, although no attempt was made to sweep out any oxygen which may have formed during the experiment. After performing the oxidations, the electrodes were removed from the solution, rinsed carefully in distilled water, and immediately placed in the ESCA instrument.

Spectra were deconvoluted using a Dupont 310 curve resolver. The location and the full width at half maximum (FWHM) for a species was first determined using the spectrum of a pure sample. The location and FWHM of products which were not obtained as pure species were adjusted until the best fit was obtained. Symmetric gaussian shapes were used in all cases. Binding energies for identical samples were, in general, reproducible to within ± 0.1 eV.

RESULTS AND DISCUSSION

The ESCA spectrum of Pd foil abraded with SiC in air is shown in Figures 1a and 1b, and the binding energy values are summarized in Table I. The $3d_{5/2}$ and $3d_{3/2}$ peaks always show a slight skewness toward the high binding energy side. From previous investigations (1, 2, 6, 7), this behavior is normally attributed to chemisorbed oxygen, although for palladium this cannot be verified by the O 1s peak due to the presence of the Pd $3p_{3/2}$ line at 531.4 eV (Figure 1b). This value is very close to the value expected for the O 1s electron from chemisorbed oxygen atoms. Evaporation of Pd foil in the spectrometer cham-

(1) K. S. Kim, N. Winograd, and R. E. Davis, *J. Amer. Chem. Soc.*, **93**, 6296 (1971).

(2) K. S. Kim, T. J. O'Leary, and N. Winograd, *Anal. Chem.*, **45**, 2214 (1973).

(3) L. D. Hulet, A. L. Bacarella, L. LiDonnici, and J. C. Griess, *J. Electron Spectrosc.*, **1**, 169 (1972/73).

(4) T. A. Carlson and G. E. McGuire, *J. Electron Spectrosc.*, **1**, 161 (1972/73), and references cited therein.

(5) M. L. Traug and G. K. Wehner, *J. Appl. Phys.*, **44**, 1534 (1973).

(6) K. S. Kim and N. Winograd, *Chem. Phys. Lett.*, **19**, 209 (1973).

(7) K. S. Kim and R. E. Davis, *J. Electron Spectrosc.*, **1**, 251 (1972/73).

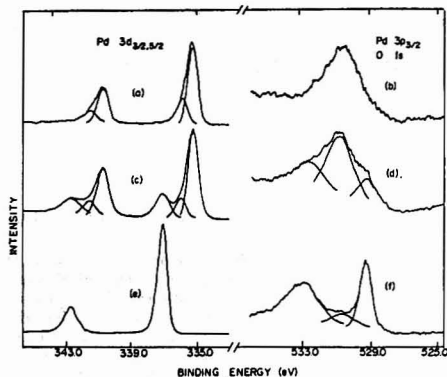


Figure 1. X-Ray photoelectron spectra of (a) Pd $3d_{5/2,3/2}$ and (b) O 1s and Pd $3p_{3/2}$ electrons for Pd foil cleaned by abrading with SiC. In (c) and (d), the foil was heated in air at 900 °C for several hours and in (e) and (f) the foil was heated in air at 600 °C for several hours. See Table I for binding energies corrected for charging. In (d) the highest binding energy peak consists of the $3p_{3/2}$ peak for both PdO and PdO_{ads}, since it is impossible to resolve it further.

ber at 10^{-6} Torr followed by bombardment with 400 eV Ar⁺ produced symmetric Pd 3d peaks. Various pretreatments of the Pd foil were tested. Washing with hot, concentrated H₂SO₄ yielded results essentially indistinguishable from those given in Figures 1a and b. Treatment with concentrated HNO₃, however, produced a surface layer of PdO. Electrochemical pretreatments resulting from cycling the potential in 1N H₂SO₄ also indicated that the surface was completely free of phase oxide but, as is shown in Figures 1a and b, it is partially covered with a chemisorbed oxygen type species which may be attributed either to oxygen atoms, water, or contamination from the supporting electrolyte. The origin of these species is as yet open to question, although surface studies on Pd evaporated in the spectrometer followed by argon ion surface cleaning and residual gas analysis are presently under way to further elucidate this point.

The spectrum of the $3d_{5/2,3/2}$ electrons for Pd foil heated in air to 900 °C is shown in Figure 1c. This treatment is known to produce PdO on the metal surface, however, since this temperature is near the evaporation temperature (8) of PdO (870 °C), a mixture of PdO, PdO_{ads}, and Pd metal can clearly be discerned. When heating at slightly lower temperatures, the surface is completely covered with PdO (Figures 1e and f) and the presence of PdO_{ads} and Pd metal is obscured. A small amount of surface charging is observed for PdO, and the actual binding energy value for the Pd $3d_{5/2}$ peak can vary from 336.3 to 336.9 eV depending on the thickness and morphology of the oxide layer. The oxide film in Figures 1c and d, for example, is equivalent to roughly a monolayer of material on the surface, as determined from an approximate escape depth of 1000 eV electrons through PdO of about 15 Å (4). The magnitude of the charging (~0.6 eV) plus the distinct appearance of PdO_{ads} strongly suggest that the oxide has clustered into small islands, leaving large sections of the Pd metal still exposed. The PdO films shown in Figures 1e and f are insoluble in 1N H₂SO₄ since this treat-

Table I. Binding Energies (eV) of Palladium $3d_{5/2}$, $3p_{3/2}$, and O 1s Electrons for Various Palladium-Oxygen Species^a

Species	Pd $3d_{5/2}$	Pd $3p_{3/2}$	O 1s
Pd	335.0	531.4	...
PdO _{ads}	335.6	N.R. ^b	N.R.
PdO	336.3	532.7	529.3
PdO ₂	337.9	534.3	N.R.

^a Binding energies are calibrated to the Au 4f_{7/2} electron peak at 84.0 eV.
^b Not resolvable.

Table II. Relative Peak Areas in the Palladium $3p_{3/2}$ and Oxygen 1s Binding Energy Region for Various Palladium-Oxygen Samples

Sample ^a	Area, % ^b			Ratio ^c
	$3p_{3/2}$ Pd (metal)	$3p_{3/2}$ Pd-oxygen	O 1s All oxygen-containing components	
Figure 1f	0	60	40	0.7
Figure 1d	53	27	20	0.7
Figure 2b	49	27	24	0.9
Figure 2d	17	28	54	1.9
Figure 3b	11	23	66	2.9
Figure 3d	0	26	74	2.8

^a Samples listed are those given in the designated Figure. Treatment conditions are given in the Figure caption. ^b See text for details of the deconvolution process. ^c Calculated by dividing the O 1s peak area for all oxygen species by the Pd_{3/2} peak area for all Pd-oxygen species. Values are approximate and are probably valid to ±20%.

ment does not change the $3d_{5/2}$ electron peak area ratio for PdO to Pd.

The Pd $3p_{3/2}$ and O 1s spectra for the above samples are shown in Figure 1, and the binding energy values for the known species are summarized in Table I. Not all peaks could be definitively assigned. For example, in Figure 1f, a peak appears at 530.5 eV which we do not associate with pure PdO. Speculatively, we guess that this peak arises from adsorbed water or oxygen chemisorbed on the PdO surface. In the other spectra (Figures 2 and 3), the lines are very broad and the number of peaks so numerous that it is possible to identify only the most obvious peaks. From Figure 1f, the coincidental interference of the Pd 3p and O 1s peak is clearly visible. Although this interference complicates a complete description of peaks observed in this energy region, it does provide a convenient approach to comparing the relative areas of the peaks arising from Pd and oxygen species. In Table II, we have compared the area ratio of total peak areas between the Pd $3p_{3/2}$ and O 1s peaks. For the spectrum in Figure 1f, for example, the relative areas for the Pd $3p_{3/2}$ peak and the O 1s peak of PdO are 60 and 40%, respectively. We have not included the 530.5-eV peak in this estimate since it probably arises from excess oxygen (chemisorbed oxygen and/or water) and therefore does not contribute to the Pd peaks. For the sample in Figure 1d, the areas are calculated by curve fitting the Pd $3p_{3/2}$ peaks in accord with the Pd 3d peaks and assuming any leftover area is attributed to the O 1s signal. The ratios for Figure 1d and Figure 1f are quite close, as expected for these samples. We shall use this ratio to detect the presence of excess oxygen species on the Pd-oxygen samples generated electrochemically.

The electrochemical behavior of the Pd-oxygen electrode has been studied by a number of workers by moni-

(8) J. C. Chaston, *Platinum Metals Rev.*, 9, 126 (1965).

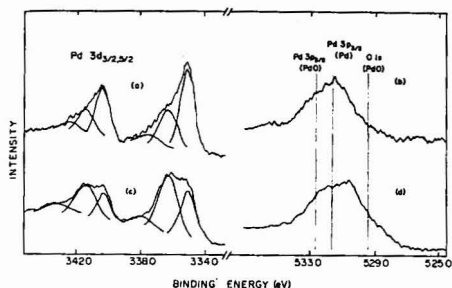
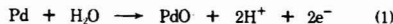
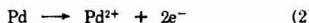


Figure 2. X-Ray photoelectron spectra of (a) Pd $3d_{5/2,3/2}$ and (b) O 1s and Pd $3p_{3/2}$ electrons for a Pd foil oxidized at +0.90 V for 1000 sec in 1N H_2SO_4 . In (c) and (d), a foil was oxidized at +1.28 V for 60 sec

toring the open-circuit potential of the palladium electrode after application of a controlled current and studying potential variations under various solution conditions (9-14). The rest potentials for the Pd/Pd and PdO_2 /Pd couples are generally considered to be about 870 and 1470 mV, respectively, in oxygen saturated 1N H_2SO_4 . Hoare (9) indicates that since the 870-mV potential depends on the oxygen pressure and does not depend on pH, the electrode reaction must be composed of a sequence of reactions. His scheme in the low potential region ($> \sim 800$ mV) consists of the formation of PdO at 870 mV



and the corrosion of the Pd electrode



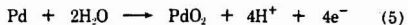
followed by the formation of PdO_2 on the electrode surface



The PdO species can then be formed through the slow decomposition of PdO_2



An equilibrating system of reactions then is set up yielding a few monolayers of PdO and a trace amount of PdO_2 on the electrode surface. The corrosion of the Pd electrode has recently been studied as a function of potential using radiotracer techniques (10) and the results are at least consistent with reaction 2. Hoare's proposed mechanism presents an interesting pathway for the production of PdO_2 at potentials far below its equilibrium electrochemical potential of 1470 mV. At the potential region above 1470 mV, in addition to Equations 1-4, Pd is oxidized directly to PdO_2



The ESCA spectra for all Pd electrodes oxidized below 800 mV were essentially identical to those given in Figures 1a and b, indicating a complete lack of any phase oxide

- (9) J. P. Hoare, *J. Electrochem. Soc.*, **111**, 610 (1964).
 (10) J. F. Llopis, J. M. Gamboa, and L. Victorri, *Electrochim. Acta*, **17**, 2225 (1972).
 (11) K. J. Vetter and D. Berndt, *Z. Elektrochem.*, **62**, 378 (1958).
 (12) A. Hickling and G. G. Vriosek, *Trans. Faraday Soc.*, **57**, 123 (1961).
 (13) J. A. V. Butler and G. Drever, *Trans. Faraday Soc.*, **32**, 427 (1936).
 (14) S. E. S. El Wakkad and A. M. Shams El Din, *J. Chem. Soc.*, **1954**, 3094.

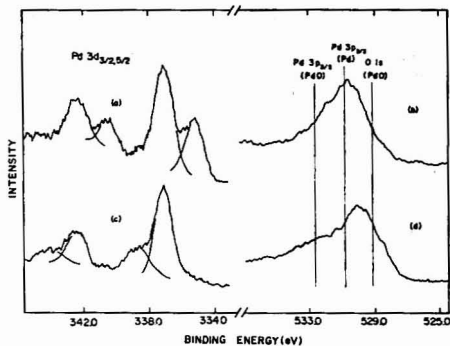


Figure 3. X-Ray photoelectron spectra of (a) Pd $3d_{5/2,3/2}$ and (b) O 1s and Pd $3p_{3/2}$ electrons for a Pd foil exposed to a potential increasing from +0.0 V to +1.71 V at 40 mV/sec. In (c) and (d), a foil was exposed to a constant potential of 1.71 V for 30 sec

formation. The major source of current flow in the cyclic voltammogram in this potential region is undoubtedly due to the direct corrosion of the electrode (reaction 2). This conclusion is consistent with the radiochemical observation that Pd corrodes before the onset of phase oxide at 870 mV (10).

The spectra for a Pd electrode which has been oxidized in 1N H_2SO_4 at 0.90 V for 1000 sec are shown in Figures 2a and b. The $3d_{5/2,3/2}$ peaks clearly indicate the existence of at least three forms of Pd: the pure metal at 335 eV, the phase oxide PdO at 336.3 eV, and another form occurring at still a higher binding energy of 337.9 eV. The chemical shift for the PdO species (+1.3 eV vs. Pd metal) corresponds to the value for the chemically produced PdO which shows no charging (336.3 eV). Since the area ratios for the $3d_{5/2}$ peak of PdO to Pd indicate a surface concentration of about 2 monolayer equivalents of PdO and since the charging effect is minimal, we suspect a rather smooth morphological distribution of the oxide about the surface.

It is most tempting to assign the high binding energy form to PdO_2 . We have unsuccessfully attempted to prepare PdO_2 chemically from the available literature preparations (15, 16) to confirm this assignment. The dioxide, however, is unstable in the anhydrous form (15) and apparently decomposes to the observed product, PdO, after exposure to the high vacuum conditions in the spectrometer. By comparing the magnitude of the observed binding energies for Pd, PdO, and the high binding energy form in Figure 2a (Table I) to those observed for Pt, PtO, and PtO_2 [71.1, 73.7, and 74.5 eV for $4f_{7/2}$ electrons (1)], the evidence for a PdO_2 type species on the electrode anodized at +0.90 V is very strong. It is interesting that this form of PdO_2 is quite stable in the ESCA instrument for several hours; this indicates that the environment of the Pd^{2+} is critical to its lifetime. Clearly, differences exist between the compounds we attempted to prepare chemically and those we prepared electrochemically but further investigation is needed to pin down these differences explicitly. These results strongly support the conclusions of Hoare (9) which were based on indirect electrochemical evidence.

The spectra of the Pd electrode oxidized at 1.28 V (Fig-

- (15) N. V. Sidgwick, "Chemical Elements and their Compounds," Oxford University Press, 1950, p 1575.
 (16) H. Remy, "Treatise on Inorganic Chemistry," Elsevier, Amsterdam, 1956, p 341.

ures 2c and d) for 60 sec also show three forms of Pd: Pd metal, PdO, and a small amount of the PdO₂ species. Again, the charging effect of PdO is minimal for this film estimated to be an equivalent of 4 or 5 layers thick, indicating the smooth rather than clumped nature of the film.

Oxidation at still higher potentials (Figures 3a-d) yields films of thicker oxide layers using shorter oxidation times. At 1.71 V, the ratio of PdO to PdO₂ always remains much larger than expected since the electrochemical data (reaction 5) predict that PdO₂ is the principal product in this potential region. This result could be due to either the decomposition of PdO₂ on the surface or to spontaneous reduction of PdO₂ as the electrode is removed from the solution. Note that in Figures 3c and d, the presence of Pd metal is completely obscured, indicating that the thickness of the oxide layer is at least 40 Å. In addition, the oxide film produced by sweeping the potential to 1.71 V rather than stepping to 1.71 V contains a much lower amount of PdO₂. This effect may be partially explained by the relatively shorter time the electrode is exposed to potentials above 1.47 V.

The O 1s spectra for all these Pd-oxygen electrode systems are difficult to quantitatively interpret because of the interference from the Pd 3p_{3/2} levels of Pd, PdO, and PdO₂. For all the electrochemically generated Pd-oxygen species, however, the area ratios between the Pd 3p_{3/2} and O 1s peaks exceeded those for the chemically formed PdO (Table II). These ratios were calculated by initially superimposing Pd 3p_{3/2} peaks, whose positions were determined using the corresponding Pd 3d peaks, on the composite Pd 3p_{3/2}-O 1s spectra to make a "best" fit. We did not attempt to deconvolute the O 1s peaks but rather estimated the peak area contribution for the sum of all the oxygen species as given by the difference between the Pd 3p_{3/2} assignments and the entire spectral curve. The fact that this ratio varies up to 4.2 times the chemically

formed PdO depending on the electrochemical potential is strong evidence for large quantities of excess oxygen in the form of adsorbed water, hydrated PdO or PdO₂, or the corresponding hydroxide Pd(OH)₂ or Pd(OH)₄.

CONCLUSIONS

The ESCA technique is a valuable aid in directly identifying the chemical nature of species produced at electrode surfaces. It is clear that many fundamental questions regarding electrode reactions can be quickly answered. For example, the spectrum in Figure 2a conclusively shows the presence of a phase oxide rather than chemisorbed oxygen atoms and also indicates the presence of PdO₂, lending strong support to Hoare's mechanism. We feel that, in addition to these direct assignments, future studies of the O 1s region using a variety of electrode materials will allow characterization of excess oxygen species such as OH⁻, adsorbed water, and bulk hydrates. The approach should also be valuable in identification of organic and inorganic films which often foil electrode behavior. Results of this kind can obviously be of great aid in proposing the electrochemical mechanism.

ACKNOWLEDGMENT

The invaluable assistance of Jon Amy and William Baitinger in spending countless hours keeping the instrument in excellent condition and the inspiration from their many helpful discussions are gratefully acknowledged.

Received for review July 5, 1973. Accepted August 22, 1973. The authors wish to thank the National Science Foundation (Grant No. GP-37017X) and the Air Force Office of Scientific Research (Grant No. AFOSR-72-2238) for financial support. The authors also appreciate the equipment grant from the National Science Foundation which allowed purchase of the ESCA instrument.

Correction of Inner Filter Effects in Fluorescence Spectrometry

V. Alan Mode and D. H. Sisson

Lawrence Livermore Laboratory, University of California, Livermore, Calif. 94550

Quantum efficiencies can be easily and rapidly determined by reference to a standard solution of known quantum yield using a quantum counter and front-surface, excitation-emission techniques. Because differences in the optical densities of the sample and reference solutions will result in the incident light exciting different volumes of solution, it is necessary to correct the data for the nonlinear losses of light out the sides and rear of the cell. It has been possible to derive an analytic expression to correct for these losses which provides consistent results for a wide range of optical densities.

The determination of photoluminescent quantum yields has not been a simple task. The techniques and problems associated with these measurements have recently been summarized in an extensive review article (1). In order to make these measurements of more practical use, several methods have been developed that employ "standard"

materials and comparison or ratio measurements. One of the most popular of these methods was developed by Bowen (2) and is based on the original Vavilov technique (3) for determining absolute fluorescent quantum efficiencies.

The fluorescent emission from the sample cell is caused to fall on a material which will absorb quanta over a broad spectral range, but which emits radiation with a fixed spectral distribution irrespective of the energy of absorbed quanta. This fluorescent screen when used with a phototube has been termed a *quantum counter* (2). This quantum counter effectively integrates the total fluorescent emission from the sample cell. The quantum counter's fluorescent emission is directly proportional to the total energy absorbed, independent of the spectral distribution of the exciting light. Because the photodetector views only the fixed spectral distribution of the quantum

- (1) J. N. Demas and G. A. Crosby, *J. Phys. Chem.*, **75**, 991 (1971).
- (2) E. J. Bowen, *Proc. Royal Soc., Ser. A*, **154a**, 349 (1936).
- (3) S. I. Vavilov, *Z. Phys.*, **22**, 266 (1924).

counter, the usual corrections for the wavelength dependence of the detector are eliminated.

Using a quantum counter, one can directly compare the total fluorescent emission of two materials having dramatically different spectral distributions. The only limitation is that the spectral range of the sample emission must be within the spectral range of the absorption band of the quantum counter.

If a material of known quantum efficiency is available (a standard), the quantum efficiency of an unknown can be determined by using a relatively simple comparison technique. While this technique is quite straightforward, some precautions must be observed.

In solutions which are optically dense, care must be taken to ensure that concentration-quenching and reabsorption-re-emission phenomena do not affect the fluorescent emission intensity. When using optically thin solutions, signal strengths may be so small as to require extensive data analysis or long measurement times.

Although there are advantages to using optically thin samples and standards, much of the ease and speed of the comparison method results from using solutions with relatively large optical densities. This has frequently resulted in workers employing samples and standards of dramatically different optical thicknesses. If the emitting volumes of the sample and standard are not equal because of differences in the penetration of the exciting light into the solutions, it is incorrect to assume that the quantum efficiency of the sample can be directly calculated from the fluorescent emissions from the front surface of the sample and standard cell.

Even for solutions that do not require correction for self-absorption of emission, it is necessary to correct all results obtained using the front-surface, quantum-counter comparison technique for the differences in the optical thicknesses of the sample and standard.

EXPERIMENTAL

The spectrophotofluorometer was an Aminco SPF which had been modified for automated data collection (4, 5). A front-surface attachment (Figure 1) was used for all fluorescent measurements. (The sample cell was originally described by Melhuish (6); the attachment used was a standard accessory obtained from the instrument manufacturer.) A 3-mm² microcell was centered in the block holding the exit slits and filters. The microcell was filled with rhodamine B (1.00 × 10⁻⁶M in absolute ethyl alcohol) and served as the fluorescent screen. The emission monochromator was set to observe the 600-nm emission peak of the rhodamine B. A Wratten 2B filter was placed between the sample cell and the quantum counter to remove excitation light reflected from the face of the sample cell. Slits were selected to give the maximum spectral resolution (~0.75 nm) consistent with maintaining at least a 15:1 signal:noise ratio. Standard techniques were used to obtain the spectral distribution of the excitation source (5, 6).

Quinine sulfate in sulfuric acid was used as the standard solution of known quantum efficiency. We used 5 × 10⁻³M quinine sulfate in 1.0N H₂SO₄ with a standard quantum efficiency of 0.508 (7). Measurement of the molar extinction coefficient (ϵ) of this standard solution, using a Cary Model 14 double-beam spectrophotometer, gave a value of (4.86 ± 0.27) × 10⁴ at λ_{max} = 346 nm (literature value 4.86 × 10⁴) (8). Solutions of lower optical density were prepared from the stock solution by accurate dilution with 1.0N H₂SO₄.

DISCUSSION

The rate of fluorescent emission (quanta/sec) from a small unit of volume (dV) is equal to the rate of light ab-

- (4) V. A. Mode and R. A. Thomas, *Rev. Sci. Instrum.*, **40**, 1241 (1969).
 (5) V. A. Mode, R. A. Thomas, and D. H. Sisson, *Rev. Sci. Instrum.*, **41**, 1714 (1970).
 (6) W. H. Melhuish, *J. Opt. Soc. Amer.*, **52**, 1256 (1962).
 (7) W. H. Melhuish, *J. Phys. Chem.*, **65**, 229 (1961).
 (8) S. S. Kanhere, R. S. Shah, and S. L. Bafna, *Indian J. Chem.*, **3**, 251 (1965).

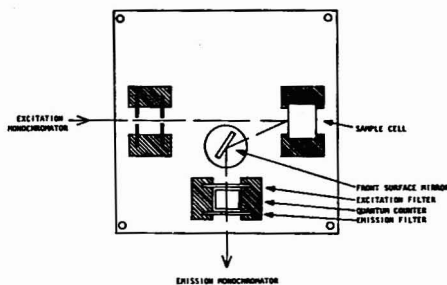


Figure 1. Front surface attachment for use in an Aminco SPF spectrophotofluorometer

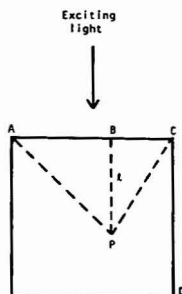


Figure 2. Geometry of light emission from within the sample cell. Only light passing through cell face AC will be observed

sorption (quanta/sec) multiplied by the quantum efficiency for fluorescence,

$$\frac{dQ}{dV} = \frac{dI_{\lambda}}{dV} \Phi \quad (1)$$

$$Q = \Phi \int_L \left(\frac{dI_{\lambda}}{dV} \right) dV \quad (2)$$

To integrate this expression, an appeal is usually made to Beer's law, and the form is reduced to

$$Q = I_0 \Phi (\epsilon c \ln 10) \int_0^L 10^{-\epsilon c l} dl \quad (3)$$

$$Q = I_0 \Phi (1 - 10^{-\epsilon c L}) \quad (4)$$

where ϵ is the molar extinction coefficient, c is the solute concentration in moles/liter, I_0 is the intensity of the incident light, and L is the total path length for adsorption. Equation 4 gives the commonly used relationship between fluorescent intensity and quantum efficiency assuming no self-absorption of the emission.

For front-surface excitation-emission, the depth of penetration of the incident light into the sample solution becomes important. The fraction of light emitted at a point P (Figure 2) which will pass through the cell surface, AC , will be

$$f = \frac{\text{Angle}(APC)}{2\pi} \quad (5)$$

and for the whole cell volume

$$f(V) = \frac{1}{2\pi} \int_0^V \left[\arctan\left(\frac{BC}{BP}\right) + \arctan\left(\frac{AB}{BP}\right) \right] dV \quad (6)$$

Table I. Numeric Integration of $\int_0^L 10^{-\epsilon l} f(l) dl$

Optical density	$L = 0.25$	$L = 0.50$	$L = 1.00$
1.0×10^{-4}	9.6236 $\times 10^{-1}$	1.6194 $\times 10^{-1}$	2.4998 $\times 10^{-1}$
2.0	9.6233	1.6193	2.4995
3.0	9.6231	1.6192	2.4993
4.0	9.6228	1.6191	2.4991
5.0	9.6226	1.6191	2.4989
6.0	9.6223	1.6190	2.4986
7.0	9.6221	1.6189	2.4984
8.0	9.6218	1.6188	2.4982
9.0	9.6215	1.6187	2.4979
1.0×10^{-1}	9.6213	1.6187	2.4977
2.0	9.6187	1.6178	2.4954
3.0	9.6162	1.6170	2.4931
4.0	9.6136	1.6162	2.4909
5.0	9.6111	1.6154	2.4886
6.0	9.6085	1.6146	2.4863
7.0	9.6060	1.6138	2.4840
8.0	9.6034	1.6130	2.4818
9.0	9.6009	1.6122	2.4795
1.0×10^{-1}	9.5983	1.6114	2.4772
2.0	9.5729	1.6033	2.4548
3.0	9.5476	1.5953	2.4326
4.0	9.5223	1.5874	2.4107
5.0	9.4972	1.5795	2.3892
6.0	9.4721	1.5717	2.3679
7.0	9.4471	1.5640	2.3469
8.0	9.4223	1.5563	2.3262
9.0	9.3975	1.5486	2.3058
1.0×10^{-1}	9.3728	1.5410	2.2857
2.0	9.1308	1.4680	2.0984
3.0	8.8975	1.3999	1.9342
4.0	8.6725	1.3363	1.7897
5.0	8.4555	1.2770	1.6620
6.0	8.2462	1.2216	1.5490
7.0	8.0442	1.1698	1.4484
8.0	7.8493	1.1213	1.3586
9.0	7.6611	1.0758	1.2783
1.0×10	7.4795	1.0332	1.2060
2.0	5.9684	7.2400 $\times 10^{-1}$	7.6139 $\times 10^{-1}$
3.0	4.8809	5.4620	5.5495
4.0	4.0813	4.3530	4.3747
5.0	3.4805	3.6102	3.6158
6.0	3.0197	3.0826	3.0841
7.0	2.6589	2.6899	2.6903
8.0	2.3710	2.3865	2.3866
9.0	2.1373	2.1451	2.1451
1.0×10^1	1.9444	1.9484	1.9484
2.0	1.0196	1.0196	1.0196
3.0	6.9172 $\times 10^{-1}$	6.9172 $\times 10^{-1}$	6.9172 $\times 10^{-1}$
4.0	5.2373	5.2373	5.2373
5.0	4.2151	4.2151	4.2151
6.0	3.5273	3.5273	3.5273
7.0	3.0328	3.0328	3.0328
8.0	2.6600	2.6600	2.6600
9.0	2.3689	2.3689	2.3689
1.0×10^1	2.1354	2.1354	2.1354
2.0	1.0757	1.0757	1.0757
3.0	7.1908 $\times 10^{-1}$	7.1908 $\times 10^{-1}$	7.1908 $\times 10^{-1}$
4.0	5.4009	5.4009	5.4009
5.0	4.3246	4.3246	4.3246
6.0	3.6061	3.6061	3.6061
7.0	3.0924	3.0924	3.0924
8.0	2.7067	2.7067	2.7067
9.0	2.4067	2.4067	2.4067

For a cell of unit width ($AC = 1$), the fraction of the total light emitted from the entire cell volume which will pass through the front face will be

Table II. Relative Quantum Efficiency of Dilute Quinine Sulfate Solutions^a

Optical density, ϵc	Measured quantum yield		Published quantum yield ^d
	Uncorrected ^b	Corrected ^c	
24.30	0.508	0.508 \pm 0.006	0.508
14.58	0.489	0.503 \pm 0.005	
4.86	0.441	0.504 \pm 0.004	
3.88	0.429	0.506 \pm 0.006	
2.43	0.394	0.509 \pm 0.007	

^a A $5 \times 10^{-3}M$ quinine sulfate solution in 1.0N sulfuric acid was used as the standard. This solution, excited at 366 nm, was assumed to have a quantum efficiency of 0.508. ^b Evaluated using Equation 10 without the geometric factors. ^c Evaluated using Equation 10. ^d See References 1 and 8.

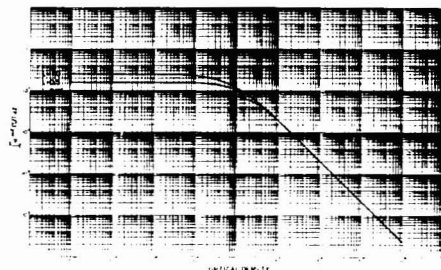


Figure 3. Inner filter correction factor as a function of optical density and total path length for absorption (L). L is expressed as a fraction of the cell width

$$f(l) = \frac{1}{\pi} \int_0^L \left[\arctan\left(\frac{1}{l}\right) - \frac{l}{2} \ln(l^2 + 1) + l \ln(l) \right] dl \quad (7)$$

where L is the total path length for absorption (CD in Figure 2) and $l = BP$.

It is possible to rewrite Equation 2 to include the geometric function, $f(l)$, given in Equation 7.

$$Q = \Phi \int_0^L \left(\frac{dI_A}{dV} \right) f(l) dl \quad (8)$$

$$Q = I_0 \Phi (\epsilon c \ln 10) \int_0^L 10^{-\epsilon l} f(l) dl \quad (9)$$

The use of Bowen's technique for the determination of quantum efficiencies by reference to a standard requires that Equation 9 be rewritten in the form

$$\Phi_u = \Phi_s \frac{A_u I_0(\lambda)_s (\epsilon c)_s \eta_s^2 \left[\int_0^L 10^{-\epsilon l} f(l) dl \right]_s}{A_s I_0(\lambda)_u (\epsilon c)_u \eta_u^2 \left[\int_0^L 10^{-\epsilon l} f(l) dl \right]_u} \quad (10)$$

where A is the integrated area under the corrected emission spectrum, $I_0(\lambda)$ is the intensity of the exciting light at wavelength λ , and η is the average refractive index of the solution to the luminescence. The subscripts s and u refer to the standard and unknown solutions, respectively. If a quantum counter is employed, the integrated areas of the sample and standard fluorescent emissions can be measured directly as the relative emission intensities of the quantum counter for the sample and standard solution.

In order to use the relationships given in Equations 9 or 10, it is necessary to calculate the value of the integral for each optical density of interest. We evaluated this func-

tion using a mathematical technique based on Simpson's rule for numerical integration. The Simpson's rule technique is described in a number of mathematics and computer science texts (9, 10). Our code was an adaptation for the CDC 7600 of an Algol algorithm given by McKeeman (11).

In the modified Simpson's rule used in this evaluation, the interval is integrated by one application of Simpson's rule and then by three applications of Simpson's rule on three equal subintervals. If the sum of the areas of the subintervals do not agree with the area of the interval within a specified limit, then the same procedure is used separately on each of the subintervals. When agreement of the calculated areas is obtained, the program proceeds to the next interval. A maximum of 11 levels of subdivisions is allowed. Thus, the function is evaluated a minimum of 7

or a maximum of $2 \times 3^{11} + 1$ times. The maximum percentage error between the calculated areas allowed in this work was 1×10^{-5} .

The results of the numerical integration are shown in Figure 3. A detailed tabulation of the results is given in Table I.

To demonstrate the error which can result from comparison of solutions with different optical thickness, dilute solutions of quinine sulfate were compared with a quinine standard of relatively large optical density. As shown in Table II, penetration of the exciting light into the cell volume results in a nonlinear loss of the fluorescent emission out the sides and rear of the cell. Analysis of the experimental data using Equation 10 results in an accurate evaluation of the quantum efficiencies of the dilute solutions.

Received for review May 29, 1973. Accepted September 4, 1973. Presented in part at the 24th Pittsburgh Conference on Analytical Chemistry and Applied Spectroscopy, Cleveland, Ohio, March 6, 1973. This work was performed under the auspices of the United States Atomic Energy Commission.

- (9) K. B. Wiberg, "Computer Programming for Chemists," W. A. Benjamin, New York, N.Y., 1965, p 35.
(10) R. H. Pennington, "Introductory Computer Methods and Numerical Analysis," Macmillan, New York, N.Y., 1965, p 193.
(11) M. W. McKeeman, *Commun. Ass. Computing Machinery*, 5, 604 (1962).

Nondispersive Soft X-Ray Fluorescence Spectrometer for Quantitative Analysis of the Major Elements in Rocks and Minerals

A. J. Hebert and Kenneth Street, Jr.

Lawrence Berkeley Laboratory, University of California, Berkeley, Calif. 94720

A lithium drifted silicon detector and a multichannel analyzer system have been combined with a multiple anode soft X-ray generator and a high vacuum sample handling system to provide an X-ray fluorescence unit for quantitative analyses of the elements from oxygen to iron. A relatively rapid, accurate, and reproducible sample preparation technique and a method for sample matrix absorption corrections are described.

The use of lithium drifted silicon detectors for the detection of X-rays was reported several years ago (1); however, inadequate resolution for photons of less than 10 keV made even qualitative soft X-ray analysis difficult. The production of better crystals and improvements in electronic detection techniques (2) have led to the present generator, a simple high vacuum sample transfer and ref. of detecting and resolving carbon, nitrogen, and oxygen X-rays (3, 4).

The spectrometer and techniques described here are the results of efforts to extend the use of these detectors to quantitative analysis of the elements from oxygen to iron

through the development of a multiple anode soft X-ray generator, a simple high vacuum sample transfer and referencing system, and a relatively rapid, accurate, and reproducible method of sample preparation.

In addition, a method of calculating sample matrix absorption effects is described which gives easily applied corrections for compositional differences between a calibration standard and an unknown sample. This, in turn, allows accurate analyses of widely varying types of samples by comparison with a single calibration standard.

EXPERIMENTAL

Apparatus. Multiple Anode Soft X-Ray Generator. A schematic sketch of the spectrometer is shown in Figure 1. The rotating anode mount accepts six hollow cylindrical anodes which are held in place by copper screws passing through the center of each anode. Each anode has two nickel plated copper partitions between it and its neighbors to eliminate cross contamination from line of sight sputtering. A summary of the anodes, filters, electron energies, and observed X-rays is given in Table I.

A cross sectional schematic diagram of the electron gun is shown in Figure 2. The interior of the nickel plated soft iron case is lined with tantalum foil. The back of the gun has a large opening which allows the outer tantalum surface, with its higher emissivity, to radiate to the chamber interior.

Thorium oxide coated iridium filaments readily provide adequate electron currents at a power input of roughly 4 watts and an estimated filament temperature of 1400 °C. The stable nature of the filament input power level indicates little, if any, appreciable filament deterioration during several months of operation.

For most analyses, 150 μ A of current to the anode is sufficient

- (1) H. R. Bowman, E. K. Hyde, S. G. Thompson, and R. C. Jared, *Science*, 151, 562 (1966).
(2) E. Elad, *Nucl. Instrum. Methods*, 37, 327 (1965).
(3) D. A. Landis, F. S. Goulding, R. H. Pehl, and J. T. Walton, *IEEE Trans. Nucl. Sci.*, 18 (1), 115, (1971).
(4) J. M. Jaklevic and F. S. Goulding, *IEEE Trans. Nucl. Sci.*, 18 (1), 187 (1971).

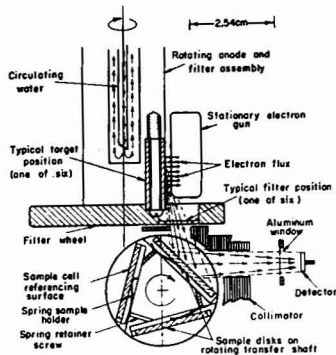


Figure 1. Schematic sketch of the spectrometer

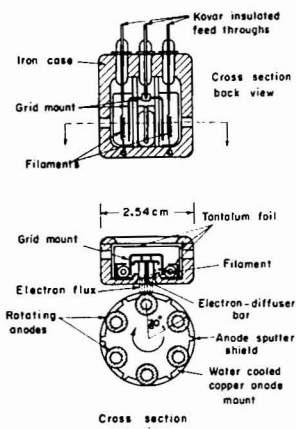


Figure 2. Cross sectional sketch of the electron gun and rotating anode mount

to generate several thousand detected events per second. Higher data acquisition rates are possible, but the present level of amplifier and analyzer dead time corrections make such rates undesirable when comparing quite different samples, such as a granite and a peridotite, where the counting rates may differ appreciably. Pulsed operation of the electron gun in a synchronous mode with the detector amplifiers may alleviate this restriction.

Experiments on X-ray flux reproducibility indicate variations on the order of 0.5% or less for each anode when rerun in place over a period of 1 hour. The reproducibility from day to day with anode rotation and sample changes is on the order of 1 to 2%.

Vacuum System. A cross sectional sketch of the spectrometer vacuum chamber is shown in Figure 3. The chamber walls are made of soft iron plate. The plate acts as an effective magnetic shield so that the electron gun and X-ray source geometry are constant even though conditions in the laboratory may vary. The chamber volume of roughly 2 liters is pumped with a 50-liter-per-second ion pump and a liquid nitrogen cold finger. The chamber interior is nickel plated to preserve a relatively noise-free background spectrum. The low fluorescent yield for nickel L X-rays (~ 0.005) is especially helpful in this respect. Under normal operating conditions, no noticeable Ni L X-rays or other unexpected background signals are observed.

All moving parts are provided with double or multiple O-ring seals which provide continuous differential pumping. The areas

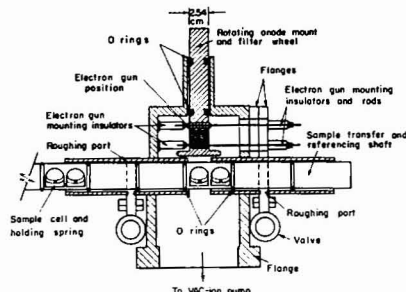


Figure 3. Cross sectional sketch of the spectrometer vacuum chamber

Table I. Anode and Filter Data

Anode	Filter element	Filter thickness, mm	Electron energy, keV	X-Ray energy, keV	Elements determined
Mg	Mg(K edge)	0.015	7	1.25	O, F, Na, and L X-rays of some heavier elements
Al	Al(K edge)	0.013	7	1.49	O, Na, Mg
Si	Si(K edge)	0.015	7	1.74	O, Na, Mg, Al
Ag	Ag(L edge)	0.001	7	2.98	Al, Si, P, S, Cl
Ti	Ti(K edge)	0.025	7	4.51	Si, Cl, K, Ca, Sc
Ni	Ni(K edge)	0.025	10	7.48	Cl, K, Ca, Sc, Ti, V, Cr, Mn, Fe

between the atmosphere and the spectrometer chamber are pumped with a cryo pump (5) that maintains a vacuum of 10^{-4} Torr or better. Movements of the rotating anode, the sample transfer shaft, or the detector window gate valve cause only minor fluctuations in the analysis chamber pressure, which usually holds at between 5×10^{-6} and 1×10^{-6} Torr.

When it is necessary to bring the spectrometer chamber up to air, a 0.13-mm thick beryllium window is moved in place of the $56 \mu\text{g}/\text{cm}^2$ aluminum window in order to maintain the detector at a high vacuum. The aluminum window between the detector and sample must be pinhole free to white light in order to provide an optical barrier to visible photons which generate interfering signals in the detector. The window also serves as a barrier to condensable molecules in the spectrometer chamber.

The sample transfer shaft has a series of seven O-rings surrounding two sets of six sample referencing cells. This allows insertion of a new set of six samples with maintenance of differential pumping while the set previously analyzed is being removed. Sample transfer is accomplished with the turn of a single crank, and roughing of the sample cells to 10^{-4} Torr or better occurs automatically as the transfer shaft moves the cells over roughing ports.

In cases of rock, mineral, alloy, or other low vapor pressure material analyses, the total time necessary to place six samples in their cells and transfer them to the analysis chamber, including a 4-minute stay in the roughing position, is 5 minutes. Analyses are usually performed at 8×10^{-7} Torr or less.

Detector. The lithium drifted silicon detector was built at Lawrence Berkeley Laboratory and is similar to those described previously (3, 4), with the exception that it uses a side mount detector arrangement with crystal cooling occurring via copper battery cable. The detector is of standard "top-hat" design with pulsed opto feedback circuitry. It has a resolution of 190 eV FWHM for iron $K\alpha$ X-rays, a Fano factor of 0.12, and electronic resolution of 108 eV. The observed FWHM for sodium X-rays at 1.04 keV is approximately 140 eV.

(5) R. Hintz and R. Parsons, UCRL-17299 (March 1967), distributed by National Technical Information Service, U.S. Department of Commerce, 5285 Port Royal Road, Springfield, Va. 22151.

Table II. Comparison of Present XRF Results and Preferred Values for Major Elements in USGS Standard Rocks as Per Cent Oxide*

Sample	Source	Na ₂ O	MgO	Al ₂ O ₃	SiO ₂	K ₂ O	CaO	TiO ₂	FeO
G-2	XRF	4.17(5)	0.77(2)	15.26(9)	69.2(2)	4.50(2)	1.98(2)	0.51(1)	2.40(1)
	Preferred values	4.15	0.77	15.31	69.29	4.51	2.00	0.48	2.38
	Difference	+0.5%	0	-0.3%	-0.1%	-0.2%	-1.0%	+6%	+0.8%
GSP-1	XRF	2.84(5)	0.99(2)	15.02(9)	67.1(2)	5.54(2)	2.08(2)	0.67(1)	3.81(1)
	Preferred values	2.86	0.95	14.92	67.32	5.52	2.06	0.66	3.82
	Difference	-0.7%	+3.9%	+0.6%	-0.4%	+0.3%	+1.1%	+2%	-0.1%
AGV-1	XRF	4.36(5)	1.51(2)	16.90(9)	59.6(2)	3.93(2)	4.97(2)	1.03(1)	6.03(1)
	Preferred values	4.32	1.53	16.92	59.10	2.92	4.98	1.05	6.04
	Difference	+0.9%	-1.5%	-0.1%	+0.8%	+0.3%	-0.3%	-2%	-0.2%
PCC-1	XRF	0.02(5)	43.42(8)	0.67(9)	41.2(2)	0.007(17)	0.54(2)	0.01(1)	7.42(1)
	Preferred values	0.0077	43.26	0.72	41.84	0.0031	0.54	0.01	7.34
	Difference	...	+0.4%	-6.7%	-1.5%	...	0	0	+1.1%
DTS-1	XRF	0.007(5)	49.68(8)	0.41(9)	40.2(2)	0.009(17)	0.12(2)	0.01(1)	7.73(1)
	Preferred values	0.0084	49.83	0.30	40.48	0.0015	0.03	0.01	7.79
	Difference	...	-0.3%	+37%	-0.5%	0	-0.8%
BCR-1	XRF	3.30(5)	3.52(2)	13.42(9)	55.0(2)	1.68(2)	7.02(2)	2.20(1)	12.06(1)
	Preferred values	3.32	3.46	13.44	54.22	1.70	7.00	2.22	12.08
	Difference	-0.7%	+1.9%	-0.2%	+1.5%	-1%	+0.2%	-1%	-0.2%

* Numbers in parentheses represent one standard deviation at the last digit for the observed counting statistics.

Procedure. Sample Preparation. Rocks and Materials Suitable for LiBO₂ Fusion: Sample powder with a particle size of the order of 0.1 mm or less is mixed with spectroscopic grade lithium metaborate (Southwestern Analytical Chemicals, Austin, Texas), LiBO₂, in a 10:1 ratio of LiBO₂ to sample. At present 200 mg of powdered sample is fused with 1.80 grams of LiBO₂. Each bottle of LiBO₂ is checked for weight loss on fusion and the correction, which is usually less than 2%, is applied to the ratio.

The fusion is performed over a Fisher burner with air and natural gas inlets. The weighed powders are carefully mixed in a gold plated platinum crucible. The mixture is then slowly brought to approximately 900 °C for 4 minutes. During this time, the crucible is swirled with tongs over the burner with a gloved hand. The liquid mass is also stirred with a 3-mm diameter vitreous carbon rod (Beckwith Carbon Corp., 16140 Raymer St., Van Nuys, Calif. 91406) which is rotated in a small battery powered stirrer. Following a final 5- or 10-second stir, the glass is poured into a nickel plated copper ring resting on a polished vitreous carbon disk (Beckwith Carbon Corp.) which is at 250 °C. A thick flat gold foil that is silver soldered to a copper block is then brought down on the molten glass to press it into the ring and against the carbon. The gold foil press is removed after 2 seconds and the glass pill is allowed to anneal at 250 °C for several minutes. The nickel plated copper rings which retain the glass preserve an analyzable surface in the event of cracking during the annealing process.

The polished vitreous carbon surface appears to be free of detectable major element contaminants, as judged from analysis in the spectrometer of pure LiBO₂ samples. The polished vitreous carbon surface is easily cleaned with distilled water and alcohol.

The time necessary to weigh and prepare a glass fusion sample is usually less than 10 minutes with a failure rate of less than 10%. Most failures in preparing a usable pill result from an incomplete transfer of molten glass from the gold plated platinum crucible. An improved crucible surface, which the molten glass does not adhere to, can usually be obtained by dipping the crucible for 2 seconds in a solution containing 3 parts of concentrated HCl, 1 part of concentrated HNO₃, and 4 parts of H₂O, and then quickly rinsing with distilled H₂O.

Fusions are carried out at temperatures less than 950 °C. At higher temperatures, both the sample and the vitreous carbon disk may be damaged by sticking and thermal shock chipping of the carbon. Vitreous carbon has a hardness close to that of silicon carbide, and damaged carbon disks may be reground and polished in the same manner as glass. In addition to sticking and thermal shock, we have observed significant losses of sodium and potassium from standard rock samples in cases where the fusion temperature has exceeded 1000 °C.

The glass sample pills are stored in a vacuum desiccator to minimize the effects of long term exposure to the laboratory atmosphere. Moisture pickup by the glass is less than 1 part in 10⁴ per day; however, surface changes have been observed for some samples after several months of laboratory exposure.

If less than 200 mg of sample is available, a ring or cup which requires less volume of glass may be used to scale down requirements, or the pill and standard may be made at a higher LiBO₂ to sample ratio.

Other Samples: Biological samples may be prepared by drying and powdering the solid or by freeze drying the liquid. The resultant powder is pressed into a 25-mm diameter by 0.75-mm thick pill. The pills are then held between thin aluminum washers for analysis.

For oxygen analyses on rocks or other minerals, powder is acted onto a Scotch brand (3M) tape surface with a sample ring acting as a frame.

Filter paper disks from air monitors or other filtration procedures may be analyzed by simply placing the disks between aluminum washers. The filter papers may be backed up with additional thicknesses of paper or with a pure nickel foil if the sample does not constitute an infinite thickness for some of the higher energy X-rays.

In cases where the samples have high moisture content or other volatiles present, they are stored in a vacuum desiccator prior to being placed in the spectrometer.

RESULTS AND DISCUSSION

Analyses of three separately prepared sets of six USGS standard rock powders indicate reproducibility and accuracy on the order of 1 to 2% for eight major elements when calibrated against published wet chemical results (6). A comparison of values is given in Table II. These results are not derived from our own calibrations, but were obtained for any one USGS standard sample by assuming that the listed preferred values are correct for the six standards and comparing the absorption corrected intensities. The reported values were obtained with a 5-minute average analysis time per element, or 40 minutes per sample. The deviations in the three sets are in agreement with the expected statistical uncertainties.

(6) I. S. E. Carmichael, J. Hampel, and R. N. Jack, *Chem. Geol.*, **3**, 59 (1968).

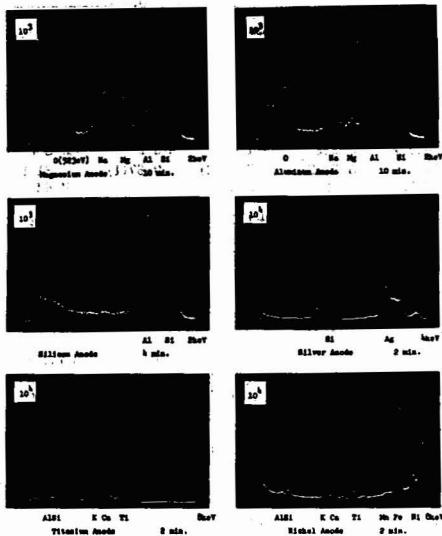


Figure 4. Spectra of 10:1 LiBO₂ to granite rock, (USGS G-2), fusion samples

Numbers in upper left-hand corners are counts full scale per channel, while the lower right-hand corners indicate energy full scale

Background, peak overlap, and interference corrections were determined with synthetic samples, such as pills containing only Na, Si, and Ti, or K₂Cr₂O₇ in the LiBO₂ matrix. Spectral peaks are integrated over roughly the full width of half maximum to obtain relative intensities. Overlap corrections for adjacent peaks amount to from 1 to 3%.

Examples of the spectra observed for granite G-2 with the six different anodes are shown in Figure 4. Aluminum in rocks is determined with the silicon anode, since the large amounts of silicon usually present in rocks tend to lead to large overlap corrections when the sample is fluoresced with silver L X-rays. A similar situation exists for the determination of sodium in the presence of large amounts of magnesium, and here sodium is determined with the magnesium anode. The observed magnesium peak is then mainly due to scattered radiations, with only a small fraction being excited in the sample by unfiltered bremsstrahlung.

Corrections for the absorption of X-rays due to the major elements in the sample were made in a manner similar to that used by Norrish and Chappell (7). Measured X-ray intensities are corrected to a "standard state" taken as an infinitely dilute LiBO₂ matrix, i.e., observed X-ray intensities were corrected to what they would be if the only absorber were LiBO₂. Using as an example the determination of potassium excited by titanium X-rays, the weight fraction, W_K , of K₂O in the original sample is given by

$$W_K = \frac{1}{f} B_{Ti}^{K} \{ 1 + f(Mg Y_{TiK}^{Mg} + Al Y_{TiK}^{Al} + \dots - L) \} I_K \quad (1)$$

where f = weight fraction of sample in LiBO₂ matrix

(7) K. Norrish and B. W. Chappell, "Physical Methods in Determinative Mineralogy," J. Zussman, Ed., Academic Press New York, N.Y., p. 196.

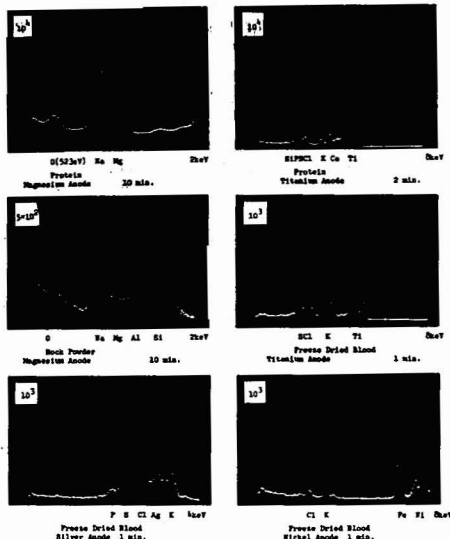


Figure 5. Spectra of pressed protein powder, pressed freeze-dried blood, and granite rock powder on tape

Numbers in upper left-hand corners are counts full scale per channel, while the lower right-hand corners indicate energy full scale.

(0.1016 in the analysis reported in Table II); B_{Ti}^{K} = a constant for given incoming X-rays (Ti in the example) and outgoing X-rays of potassium. It contains the geometrical and detection efficiency factors of the apparatus, the efficiency of production of potassium X-rays by Ti X-rays, and the absorption of an infinitely dilute LiBO₂ matrix. It is determined by a measurement using a sample with a known content of K₂O. I_K = the measured intensity of potassium X-rays per unit current.

The "absorption correction," A_{Ti}^{K} , is the factor in braces in the equation above.

$$A_{TiK} = 1 + f(Mg Y_{TiK}^{Mg} + Al Y_{TiK}^{Al} + \dots - L) \quad (2)$$

where Mg = weight fraction of MgO in the original sample. Al = weight fraction of Al₂O₃ in the original sample, etc. L = loss, i.e., weight fractions of volatiles lost in the fusion.

The Y 's are given by expressions like

$$Y_{TiK}^{Mg} = \frac{\phi(\mu_{Ti}^{Mg} - \mu_{Ti}^{LiB}) + (\mu_K^{Mg} - \mu_K^{LiB})}{\phi(\mu_{Ti}^{LiB} - \mu_K^{LiB})} \quad (3)$$

where Y_{TiK}^{Mg} corrects for the absorption due to MgO in the sample when the incoming X-rays are Ti X-rays and the outgoing X-rays are those of potassium. μ_{Ti}^{Mg} = mass absorption coefficient for Ti X-rays in MgO. μ_{Ti}^{LiB} = mass absorption coefficient for Ti X-rays in LiBO₂. μ_K^{Mg} = mass absorption coefficient for potassium X-rays in MgO. μ_K^{LiB} = mass absorption coefficient for potassium X-rays in LiBO₂. $\phi = \text{Sec } \alpha / \text{Sec } \beta$ where α is the angle of the incoming X-rays to the sample normal and β is the outgoing angle. In the present apparatus $\phi = 1.233$.

The mass absorption coefficients tabulated by McMaster *et al.* (8) were used in the work reported here.

(8) W. H. McMaster *et al.*, UCRL-50174 (May 1969), distributed by National Technical Information Service, U.S. Department of Commerce, 5285 Port Royal Road, Springfield, Va. 22151.

In the analysis of the USGS standard rocks, the largest absorption corrections occur in the determination of iron using nickel X-rays. The extreme values are $A_{Ni}^{Fe}(PCC-1) = 1.381$ and $A_{Ni}^{Fe}(BCR-1) = 1.592$. For the lighter elements, the absorption corrections are typically much smaller. For example, in analysis for magnesium using aluminum X-rays, the lowest and highest corrections are $A_{Al}^{Mg}(G-2) = 1.010$ and $A_{Al}^{Mg}(DTS-1) = 1.042$.

The consistency obtained in the analysis of the six USGS standards, which vary widely in composition, indicates that the calculated absorption corrections are adequate.

The sodium and magnesium analyses required 10 minutes each per sample. Under the same conditions, if 2 to 4% standard deviations are adequate for Na, Mg, and Ti at these levels, then 1% standard deviations can be obtained for the remaining elements that are present at or above the 1% level in a total analysis time of 10 minutes per sample.

Results obtained for manganese and chromium during these analyses have not been included in Table II because of uncertainties in absolute calibration. Once an accurate calibration is obtained, the spectrometer should yield 1% standard deviations for Mn or Cr analyses at the 1000-ppm level in less than 5 minutes, and at the same time provide analyses for the rest of the elements from potassium to iron.

The sensitivity corresponding to three standard deviations of the observed counting statistics for a 5-minute analysis at 10:1 dilution of rock in $LiBO_2$ varies from 0.09% for Na to 0.01% for Fe. The variation is due to differences in cross sections, absorption effects, and fluorescent yields.

The present sensitivity for biological samples such as pressed protein powder or freeze dried blood varies from

0.8% for oxygen to 0.001% for iron in a 5-minute analysis. Preliminary experiments indicate that 1 to 2% standard deviations for oxygen analyses may be obtained for rock or mineral powders in 10 minutes with the sample on tape procedure described above. Examples of observed spectra are shown in Figure 5.

In obtaining these results, we purposely operated the spectrometer below its design capabilities in order to guard against any changes in spectrometer efficiency or other uncertainties which arise from higher counting rates while analyzing the three standard rock sets. This also allowed an accurate check on our sample preparation technique.

The spectrometer is now being tested under more efficient operating conditions. The preliminary experiments indicate that it will perform reliably and provide analyses comparable to or better than those reported here in 15 minutes per unknown fused rock or mineral sample.

The present results are comparable to those obtained with conventional dispersive systems. One advantage that similar nondispersive systems may provide over dispersive ones is a significantly lower cost for the equipment. The present spectrometer was produced for a fraction of the cost of a conventional dispersive system.

ACKNOWLEDGMENT

We wish to thank Robert D. Giaque, H. R. Bowman, Frank Asaro, Joseph M. Jaklevic, and William L. Searles for many informative and useful discussions. We also thank Gardener G. Young for his expert advice and help in fabricating the spectrometer.

Received for review May 23, 1973. Accepted August 30, 1973. This work was performed under the auspices of the U.S. Atomic Energy Commission.

Automatic Correction System for Light Scatter in Atomic Fluorescence Spectrometry

T. C. Rains, M. S. Epstein, and Oscar Menis

Analytical Chemistry Division, National Bureau of Standards, Washington, D.C. 20234

Light scattering of incident radiation by solvent droplets and unvaporized solute particles in the flame is a major interference in atomic fluorescence spectrometry (AFS). A technique for the automatic correction of light scatter is described which increases the speed and accuracy of analysis. The light from an electrodeless discharge lamp and a 150-W xenon lamp is alternately passed through the flame. The resulting signal from the multiplier phototube is fed to a lock-in amplifier which corrects for the contribution of the light scattering to the fluorescence signal. The principles of the technique and apparatus for making the automatic correction are described. To accomplish this correction, scatter of the incident radiation from the electrodeless discharge and xenon lamps is balanced initially while aspirating a 1% lanthanum solution. The method has been applied to the determination of 0.11 and 0.26 $\mu\text{g Cd/gram}$ in SRM's Orchard Leaves and Liver, respectively, without any prior separation or preconcentration.

Atomic fluorescence spectrometry (AFS) has been shown to be a very sensitive analytical technique for the determination of many elements (1-5). However, the number of published applications of AFS for the determination of trace elements is limited (6). This can be attributed, in part, to a number of factors such as the unavailability of commercial instrumentation, the need for a high-intensity radiation source, and the effect of chemical and physical interferences. While commercial instruments for AFS are not available, flame photometers and atomic ab-

- (1) A. Syty, chapter in "Flame Emission and Atomic Absorption Spectrometry," Vol. 2, J. A. Dean and T. C. Rains, Ed., Marcel Dekker, New York, N.Y., 1971.
- (2) J. E. Willis, *Spectrosc. Lett.*, 2, 181 (1969).
- (3) R. L. Miller, L. M. Fraser, and J. D. Winefordner, *Appl. Spectrosc.*, 25, 477 (1971).
- (4) J. D. Winefordner, V. Svoboda, and L. J. Cline, *CRC Crit. Rev. Anal. Chem.*, p. 233 (August 1970).
- (5) G. F. Kirkbright, *Analyst*, (London), 96, 608 (1971).
- (6) J. D. Winefordner and T. J. Vickers, *Anal. Chem.*, 44, 150R (1972).

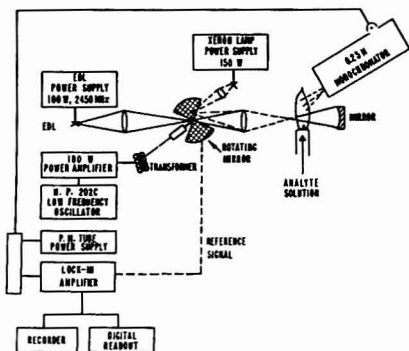


Figure 1. Schematic diagram of AFS instrumentation

sorption instruments can readily be modified for fluorescence work. Since a variety of excitation sources are available, the intensity and stability are the major criteria in selecting an excitation source. Electrodeless discharge lamps (EDL) are currently favored in AFS work (7-9). Frequently, these sources have been found to be unstable and nondependable for routine analytical work. Rains (10) and recently Browner *et al.* (11) have observed that by controlled heating of the air around the EDL, the sources can be stabilized and their intensity increased. A major problem in AFS is the physical interference from the scatter of the incident radiation by solvent droplets and unvaporized solute particles in the flame gases (1, 12-16).

The theoretical aspects associated with light scattering in flames have been delineated by Omenetto *et al.* (12). To correct for incident light scattering (17), a continuum source or a line source can be used. With a line source, a nonfluorescent line of equal or higher intensity is selected to correct for scattered radiation. The nonfluorescent line should be within 100 Å of the analyte line. Synthetic solutions, which simulate the unknown but without the analyte, are also used. Under proper conditions, these techniques will correct for light scatter, but they are time consuming. Polarizers (12) have been used to improve the ratio of the fluorescence-to-scattering signal by 3 to 16 times, depending upon the analyte. A significant reduction in sensitivity, however, was noted.

In the present investigation, a technique for automatic correction of light scatter is applied (18). The incident radiation from an EDL and a xenon lamp is alternately passed through the flame gases by a rotating sector mirror. The signals produced by the two sources, isolated by a $\frac{1}{4}$ -meter monochromator, are detected by a multiplier phototube and fed to a lock-in amplifier which is synchronized to the chopper frequency. In this arrangement, a

lock-in amplifier serves as a cross-correlator by providing an output dc signal which is the time average of the sum of the fluorescence signal plus noise with the reference. In our study, the reference is the electrical signal produced by phototube from scatter by the xenon source. The scatter signals from the reference and incident sources are balanced optically for the simultaneous correction and measurement of the fluorescence signal. By this design, the physical interference due to light scatter is automatically corrected without additional measurement at a non-fluorescent line. This technique increases the speed of analysis and improves the accuracy.

EXPERIMENTAL

Apparatus. A schematic diagram of the AFS instrumentation is given in Figure 1 and the instrumental operating parameters are given in Table I.

Preparation and Operation of Electrodeless Discharge Lamp. The cadmium EDL was prepared from the metal and a quartz ampule filled with neon to 1 Torr. The preparation of these lamps has been described previously (19). The lamps are excited in $\frac{1}{4}$ -wave (Everson type) or $\frac{3}{4}$ -wave cylindrical resonant cavities at 40 W. To increase the intensity and stability of the lamp, the air is preheated. With the $\frac{1}{4}$ -wave cavity, a miniature furnace is positioned just below the cavity to preheat the air before entering the cavity. In Table II are the data which show the effect of the radiant intensity of cadmium at 2288 Å as a function of air temperature. More important, however, is the increased stability of the lamp. For the $\frac{3}{4}$ -wave resonant cavity, the heating arrangement is that described by Ball (20). To improve the stability of the lamps, the side arm from the cavity to the coaxial line is water cooled. In this study, the lamp reached its maximum intensity and stabilized in 10-15 minutes.

Modulation Frequency. The method of modulating the sources is shown in Figure 1. To superimpose the two radiant sources on the same area in the flame, the conventional chopper was replaced with a rotating sector mirror. A dissected chopper on a synchronous motor which produced a chopping frequency of 60 Hz was initially installed. At this frequency, the output signal was limited because of the interference from the line voltage. To change the operating frequency of the chopper, a signal from a low-impedance audio oscillator was amplified and fed into the synchronous motor. By this arrangement, frequencies of 20 to 80 Hz were obtained. The lower limit is controlled by the operational amplifier while the upper frequency is limited by the potential danger of operating a glass chopper at high frequencies. As a safety precaution, the rotating mirror was placed in a metal case and blacked to reduce stray light.

Optics. The optics of the system were designed to superimpose the images of the two light sources within the solid angle of the monochromator, to assure that the light from each source would be scattered equally. The image of each source was defocused to a circular image of even intensity of about 5 mm in diameter at the burner head, and the backing mirror was adjusted to provide an image of about 30 mm in diameter, to flood the solid angle of the monochromator. The small movement of the lens necessary to focus and defocus the continuum source to maintain the system balance does not significantly change the size of the continuum image.

Detection System. In the initial studies, an R106 multiplier phototube was used as the detector, but difficulties with stray light in the monochromator developed with samples containing significant amounts of sodium (Cd:Na ratio of 1:10,000), which caused an enhancement of the fluorescence signal similar to the "sodium effect" described by Kahn (18). This interference was effectively reduced by the use of a solar blind multiplier phototube, to eliminate the sodium emission signal.

Instrument Operation. After the electrodeless discharge lamp is stabilized, the light from the continuum source is blocked and the wavelength of the monochromator is peaked at the Cd 2288-Å line. The instrumental parameters are then maximized while nebulizing a 1 µg/ml of Cd solution into the flame. To balance the continuum and excitation sources, a 1% lanthanum solution is nebulized into the flame and the two signals are balanced by opening or closing a diaphragm on the optics of the xenon source. An analytical curve is established by nebulizing a series of cad-

(7) J. D. Winefordner and R. A. Staab, *Anal. Chem.*, **36**, 1367 (1964).

(8) R. M. Dagnall and T. S. West, *Appl. Opt.*, **7**, 1287 (1968).

(9) D. Hingle, G. F. Kirkbright, and T. S. West, *Analyst (London)*, **93**, 522 (1968).

(10) T. C. Rains, *Nat. Bur. Stand. (U.S.) Tech. Note*, **504** (1969).

(11) R. F. Browner, M. E. Rietta, and J. D. Winefordner, Pittsburgh Conference on Analytical Chemistry and Applied Spectroscopy, Cleveland, Ohio, March 6-10, 1972, Paper No. 136.

(12) N. Omenetto, L. P. Hart, and J. D. Winefordner, *Appl. Spectrosc.*, **26**, 612 (1972).

(13) V. Sychra and J. Matoušek, *Anal. Chim. Acta*, **52**, 376 (1970).

(14) P. D. Warr, *Talanta*, **18**, 234 (1971).

(15) D. R. Demers and D. W. Ellis, *Anal. Chem.*, **40**, 860 (1968).

(16) M. S. Cressler and T. S. West, *Spectrochim. Acta, Part B*, **25**, 61 (1970).

(17) M. P. Bratzel, Jr., R. M. Dagnall, and J. D. Winefordner, *Anal. Chem.*, **41**, 713 (1969).

(18) H. L. Kahn, *At. Absorption Newsletter*, **7**, 40 (1968).

(19) O. Menis, Ed., *Nat. Bur. Stand. (U.S.) Note*, **454**, (1968).

(20) J. J. Ball, *Rev. Sci. Instrum.*, in press.

mium solutions, and then the intensity of the unknown solution is measured. If the light sources have been stabilized, the system will remain in balance; however, a frequent check is made using a 1% lanthanum solution. If any signal is observed, the radiant intensity from the continuum source is adjusted to rebalance the system. This adjustment does not affect the intensity of the fluorescence signal, or produce a change in the calibration curve.

Sample Preparation. A 3- to 5-gram test portion of SRM-1571 (Orchard Leaves) or SRM-1577 (Liver) is transferred to a Teflon beaker. The sample is digested for 1 hour in 25 ml of nitric acid. The beaker is cooled and the sides are rinsed with water. A mixture of 10 ml of HNO₃, 10 ml of HClO₄, and 5 ml of HF is added and the sample is heated to strong fumes of perchlorate. The sides of the beaker are frequently rinsed with water to assure that all the droplets have reacted with the acid mixture. After the sample is dissolved, the solution is transferred to a 100-ml volumetric flask and diluted to calibrated volume.

RESULTS AND DISCUSSION

Balancing the Optical System. The proposed technique is based on the requirement that the two sources be superimposed on the same area of the flame, and that the intensity of scattered light from each source passed by the monochromator be the same. In the initial study, several light sources such as a deuterium arc and Osram lamps were tested, but their radiant intensities were low and could not be balanced with the EDL. The radiant intensity of a 150-W xenon arc lamp, however, was found to be best suited for balancing the system. The fluorescence signal from the xenon arc continuum source was found to be more than 4 orders of magnitude smaller than that excited by the EDL, and did not interfere. By means of the optical arrangement and the lock-in amplifier, a balance was attained between scattered incident radiation from the EDL and the continuum source. The fluorescence signal and scattered radiation from the line source gives a positive signal while the scatter produced from the continuum source is negative. In this procedure, a solution containing relatively high solids was aspirated into the flame to create scattered radiation. The positions of the sources were adjusted until the scattered incident radiation from the two sources was equal as indicated by a zero reading on the lock-in amplifier. The EDL output was optimized to obtain the maximum fluorescence sensitivity, and only the continuum source was defocused to balance the system. As an aid in this adjustment, an iris diaphragm was placed in front of the lens of the xenon source. The solution used to obtain this balance must be free of the analyte. A 1% solution of high purity lanthanum was used in these measurements. It was found experimentally that this was sufficient for correcting scatter from the samples tested. The concentration is not critical, provided it can balance the maximum scatter encountered. However, for more intensely scattering solutions, a higher concentration would be required.

The compensation for scatter was measured at 2288 Å, the wavelength of interest. From Rayleigh's law, scatter is wavelength dependent, but the correction is valid provided the measurements are made at the same wavelength as the wavelength of interest. Also, a 1 to 2% solution of Na, Ca, Al, or Fe may be used, provided they are free of the analyte. However, the amount needed to assure an effective balance of our system was higher than required by lanthanum, and, therefore, did not offer any advantage.

Standard Reference Material. To determine whether this approach is effective in eliminating the light scatter encountered with a conventional optics system, the cadmium content of SRM-1571 (Orchard Leaves) was determined by both techniques. The values obtained by AFS, without scatter correction, were higher by a factor of 10, which indicates the magnitude of scatter.

The determination was repeated using the automatic

Table I. Instrumental Parameters

Monochromator	0.25-m Ebert; mount; f/3.6 aperture; dual gratings blazed at 3000 and 6000 Å; adjustable slits
Detector	HTV-R166, solar-blind multiplier phototube
Detector power supply	0 to 2100 V, 0-30 mA, 0.001% regulation
Amplifier	Phase sensitive lock-in amplifier with full-scale sensitivity ranges of 100 nV to 500 mV
Recorder	10-mV strip-chart recorder, 0.2 sec full scale response time
Readout system	Digital voltmeter, DCR-2B, with 4× averaging
Electrodeless discharge lamp power supply	RF generator from a medical-type diathermy unit which supplies 100 W at 2450 MHz with RF power meter
Resonant cavity	1/4-wave (Evenson) and 1/2-wave (cylindrical) cavities
Excitation source	Cadmium electrodeless discharge lamp
Chopping frequency	70 Hz
Scatter correction light source	Xenon lamp, 150 W
Burner	Premixed with cylindrical burner head
Oxidant-fuel	Argon (entrained air)-hydrogen flame

Table II. Effect of Air Temperature on Intensity of Cd-EDL

Air temperature, °C	Relative intensity
20	1
90	14
103	38
113	67
124	99
132	346
142	559
160	688
180	690
189	689
232	671

Table III. Comparison of Results of AFS and AAS Determination of Cd in SRM-1571 (Orchard Leaves)

Cd, µg/g		AAS	
AFS			
0.12	0.11	0.11	0.10
0.11	0.11	0.11	0.10
0.12	0.11	0.10	0.11
0.10	0.10	0.12	0.12
0.10	0.10	0.09	0.11
		0.10	
Average	= 0.10g		0.10g
Std dev	= 0.008		0.009
Rel std dev, %	= 7.3		8.7

scatter correction system without prior separation or pre-concentration (Table III). Values were also obtained by atomic absorption spectrometry which did require a preliminary separation with ammonium pyridine dithiocarbamate (APDC) in methyl isobutyl ketone.

The automatic scatter correction system was also applied to the determination of cadmium in SRM-1577 (Liver). A comparison of results obtained by AFS and

Table IV. Comparison of Results of AFS and AAS Determination of Cd in SRM-1577 (Bovine Liver)

AFS		AAS	
Cd, $\mu\text{g/g}$			
0.28	0.24	0.29	0.24
0.24	0.25	0.24	0.27
0.21	0.26	0.26	0.30
0.25	0.29	0.26	0.26
		0.27	
Average =	0.253		0.266
Std dev =	0.024		0.020
Rel std dev, % =	9.8		7.6

AAS is given in Table IV. Again, by AAS, a separation was required, while the AFS values were obtained without prior separations.

Interferences. The major constituents of SRM-1571 (Orchard Leaves) are Ca, 2.09%; K, 1.47%; Mg, 0.62%; and P, 0.21%. At these levels, they did not interfere with the AFS determination of cadmium. Standard solutions of cadmium, as well as the analyte, were prepared in 5% HClO_4 . In comparing the fluorescence intensity of cadmium in 5% HCl and HClO_4 , a slight enhancement was observed in a perchlorate medium.

The major constituents of SRM-1577 (Liver) are K, 0.97% and Na, 0.243%. Sodium produced a stray light interference as previously noted by Barnett and Kahn (21). In a 0.05 $\mu\text{g/ml}$ cadmium solution, sodium concentrations greater than 100 $\mu\text{g/ml}$ caused an enhancement. In the

(21) W. B. Barnett and H. L. Kahn, *Anal. Chem.*, 44, 935 (1972).

presence of 1000 $\mu\text{g/ml}$ of sodium, the apparent recovery of cadmium was greater than 170%; at the 5000 $\mu\text{g/ml}$ level, the apparent recovery was 370%.

To overcome stray light interference due to relative high concentrations of sodium, the (Hamamatsu) R-106 multiplier phototube was replaced with an R-166 solar blind multiplier phototube.

CONCLUSION

The results obtained by the automatic correction system indicate that scatter of incident radiation in AFS is readily subtracted. The speed of analysis is increased with improved accuracy. This technique eliminates the need for exact matrix matching or measurement at some non-fluorescent line to correct for scatter. The detection limit for cadmium is 0.05 ng/ml at 2σ above the mean obtained from a background or a matrix blank.

ACKNOWLEDGMENT

The authors are indebted to T. C. O'Haver for his helpful suggestion in changing the frequency of chopping, to K. D. Mielenz for his suggestions in optics, and to J. I. Shultz for his assistance in the preparation of this manuscript.

Received for review May 31, 1973. Accepted September 12, 1973. In order to adequately describe experimental procedures it is occasionally necessary to identify commercial products and equipment by the manufacturer's name or label. In no instances does such identification imply recommendation or endorsement by the National Bureau of Standards, nor does it imply that the particular product or equipment is necessarily the best available for that purpose.

Inductively Coupled Plasma-Optical Emission Analytical Spectroscopy

Tantalum Filament Vaporization of Microliter Samples

David E. Nixon, Velmer A. Fassel, and Richard N. Kniseley

Ames Laboratory—USAEC and Department of Chemistry, Iowa State University, Ames, Iowa 50010

The adaptation of a tantalum filament vaporization system as a sample introduction device for the inductively coupled plasma is described. The potential advantages of this analytical system for simultaneous multielement determinations of elements at the ng/ml level are discussed and a comparison of the plasma system with the filament techniques utilized in atomic absorption or fluorescence spectroscopy is presented. For one set of operating conditions, detection limits for 16 elements were in the ng/ml to fractional ng/ml range for 100- μl samples. Typical precision data and an analytical curve for the determination of Be in the range of 0.001 to 10 $\mu\text{g/ml}$ are included.

One of the most sensitive contemporary analytical techniques is based on the thermal atomization of microliter volumes of a sample in graphite furnaces (1-11) from graphite (12-20) or tantalum (21-24) filaments, and from platinum or tungsten wire loops (25), followed by the observation of the free atoms formed in either atomic absorption or fluorescence. Although exceptional relative and absolute powers of detection and acceptable reproducibility have been achieved by a multitude of variations of these atomization systems, this technique is subject to a rather extensive list of experimental constraints. The most important of these are: (a) for many of the systems, critical experimental parameters must be optimized for

each element (13, 16-18, 21, 23, 24); (b) reproducibility may be negatively affected by variations in the carbon filament or furnace tube porosity (1, 4, 6, 9, 14, 15, 20); (c) analytical curves may be nonlinear and limited in range of concentration (1, 6, 7, 10-16, 18, 20, 24); (d) background interferences may arise from nonspecific absorption and light scattering caused by incandescent particles produced in the furnace or above the filament (1, 4, 6-9, 11, 14, 15, 18, 24, 25); (e) the observed signals may be affected by interelement interferences which originate from the recombination and nucleation of the sample after atomization or from incomplete analyte vaporization and dissociation (6-11, 14-17, 19, 21, 23, 24); (f) simultaneous multielement determinations cannot be performed if the free atoms are observed by conventional atomic absorption or fluorescence techniques.

It has recently been demonstrated that inductively coupled plasmas are exceptionally sensitive excitation sources (26-34). The combination of either furnace or filament vaporization of samples followed by plasma excitation of the vapor therefore offers the attractive possibility of performing ultratrace determinations on a multielement basis on microliter or microgram sized samples. Moreover, the plasma system also offers promise of overcoming the other limitations discussed above. First, since the free atoms are actually generated in the plasma, a single set of parameters should suffice for the vaporization of many types of

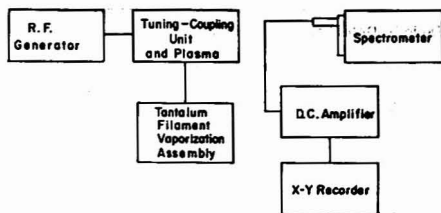


Figure 1. Block diagram of experimental facilities

Table I. Operating Conditions for the Tantalum Filament Vaporization Apparatus

Filament power supply:	General Electric transformer Model 9T51Y6172; 120-V primary; 12-V secondary; 80 °C temperature rise; 0.5 KVA. Transformer input controlled by a Standard Electrical Products Co. variable transformer type F1500BL; 115-V input; 0-115-V, 2 KVA, 15 A maximum output. 37 × 10 mm; 0.13 mm thick. Depressions formed with a die; maximum sample volume, 200 μl.
Tantalum strips:	Argon at 14.7 l./min proportioned through the coolant and plasma tubes to keep the plasma from melting the plasma tube. Argon at 1.2 l./min passes through the filament enclosure to the plasma. Hamilton 700 series; Model 710; 100-μl capacity with fixed standard needle. Teflon plunger substituted for the original plunger.
Gas flows:	Stock solutions were prepared by dissolving pure metals or reagent grade salts in dilute acid or conductivity water. Samples were conductivity water dilutions of the stock solutions; 100-μl samples were used throughout.
Syringe:	
Solutions and sample size:	

samples. Second, interelement interferences arising from recombination or nucleation of the vapor above the filament should be minimized because the plasma subsequently achieves atomization of the vapor cloud. Third, background interference from the filament or furnace tube does not exist. Fourth, analytical curves obtained from the toroidal shaped inductively-coupled plasma are commonly observed to be linear over a concentration range of 4 to 5 orders of magnitude (34).

In this communication, we present some preliminary results on the combination of the tantalum filament vaporization (TFV) of samples followed by the inductively-coupled plasma (ICP) excitation.

EXPERIMENTAL

Apparatus. A block diagram of the overall apparatus is shown in Figure 1. The plasma facility and the spectroscopic apparatus are described elsewhere (34). The operating conditions for the tantalum filament vaporization apparatus are described in Table I. A sketch of the filament vaporization device is shown in Figure

- B. V. L'vov, *Spectrochim. Acta*, **17**, 761 (1961).
- H. Massmann, *Spectrochim. Acta*, **23B**, 215 (1968).
- R. Woodriff, R. W. Stone, and A. M. Held, *Appl. Spectrosc.*, **22**, 408 (1968).
- B. V. L'vov, *Spectrochim. Acta*, **24B**, 53 (1969).
- B. V. L'vov, *Pure Appl. Chem.*, **23**, 11 (1970).
- D. C. Manning and F. Fernandez, *At. Absorption Newslett.*, **9** (3), 65 (1970).
- R. W. Marrow and R. J. McElhane, Paper presented at Sixteenth Conference on Analytical Chemistry in Nuclear Technology, Gatlinburg, Tenn., 1972.
- F. J. Fernandez and D. C. Manning, *At. Absorption Newslett.*, **10** (3), 65 (1971).
- H. L. Kahn, *Amer. Lab.*, August 1971, p 35.
- G. P. Sighinolfi, *At. Absorption Newslett.*, **11** (5), 96 (1972).
- G. Baudin, M. Chaput, and L. Feve, *Spectrochim. Acta*, **26B**, 425 (1971).
- T. S. West and X. K. Williams, *Anal. Chim. Acta*, **45**, 27 (1969).
- R. G. Anderson, I. S. Maines, and T. S. West, *Anal. Chim. Acta*, **51**, 355 (1970).
- M. D. Amos, P. A. Bennett, K. G. Brodie, P. W. Y. Lung, and J. P. Matousek, *Anal. Chem.*, **43**, 211 (1971).
- J. P. Matousek, *Amer. Lab.*, June 1971, p 45.
- J. Aggett and T. S. West, *Anal. Chim. Acta*, **55**, 349 (1971).
- D. Alger, R. G. Anderson, I. S. Maines, and T. S. West, *Anal. Chim. Acta*, **57**, 271 (1971).
- R. G. Anderson, H. N. Johnson, and T. S. West, *Anal. Chim. Acta*, **57**, 281 (1971).
- R. B. Baird, S. Pourian, and S. M. Gabrielson, *Anal. Chem.*, **44**, 1887 (1972).
- B. M. Patel, R. D. Reeves, R. F. Browner, C. J. Molnar, and J. D. Winefordner, *Appl. Spectrosc.*, **27**, 171 (1973).
- H. M. Donega and T. E. Burgess, *Anal. Chem.*, **42**, 1521 (1970).
- T. Y. Hwang, P. A. Ullucci, and S. B. Smith, Jr., *Amer. Lab.*, August 1971, p 41.
- J. Y. Hwang, C. J. Mokeler, and P. A. Ullucci, *Anal. Chem.*, **44**, 2019 (1972).
- T. Takeuchi, M. Yanagisawa, and M. Suzuki, *Talanta*, **19**, 465 (1972).
- M. P. Bratzel, Jr., R. M. Dagnall, and J. D. Winefordner, *Appl. Spectrosc.*, **24**, 518 (1970).
- S. Greenfield, P. B. Smith, A. E. Breeze, and N. M. D. Chilton, *Anal. Chim. Acta*, **41**, 385 (1968).
- S. Greenfield and P. B. Smith, *Anal. Chim. Acta*, **59**, 341 (1972).
- J. C. Soulliar and J. P. Robin, *Analusis*, **1**, 427 (1972).
- P. W. J. M. Boumans and F. J. de Boer, *Spectrochim. Acta*, **27B**, 391 (1972).
- R. H. Wendt and V. A. Fassel, *Anal. Chem.*, **37**, 920 (1965).
- V. A. Fassel and G. W. Dickinson, *Anal. Chem.*, **40**, 247 (1968).
- V. A. Fassel, "XVI Colloquium Spectroscopicum Internationale," Heidelberg, Germany, 1971.
- G. W. Dickinson and V. A. Fassel, *Anal. Chem.*, **41**, 1021 (1969).
- R. H. Scott, V. A. Fassel, R. N. Kniseley, and D. E. Nixon, *Anal. Chem.*, **46**, 75 (1974).

Table II. Detection Limits ($\mu\text{g}/\text{ml}$)

Element	TFV-ICP, 100- μl samples	Wavelength (\AA) ^a	AAS, 100- μl samples	AFS	Sample volume (μl), AFS
As	0.01	1936.96	0.003 (23)	0.25 (14)	2 ^b
Sb	0.001	2311.47	0.001 (2)	0.007 (2)	30
Se	0.006	1960.26	0.007 (23)
Te	0.007	2142.75	0.003 (23)
Hg	0.002	2536.52	0.002 (2)	0.01 (25)	2
Cd	0.006	2265.02	0.000003 (9)	0.000008 (2)	30
P	0.02	2136.18
Pb	0.003	4057.83	0.0001 (23)	0.001 (2)	30
Be	0.00002	2348.61	0.00002 (23)	0.015 (14)	2 ^b
Tl	0.003	5350.46	0.0001 (9)	0.04 (20)	1
Mn	0.00003	2576.10	0.00002 (9)
Sn	0.02	3175.05	0.025 (8)
Ag	0.0001	3280.68	0.000007 (9)	0.00005 (2)	30
B	0.0001	2497.73
Ba	0.0000003	4554.03	0.0001 (23)
Bi	0.002	3067.72	0.0004 (9)	0.01 (13)	1

^a Wavelengths used for TFV-ICP detection limits. ^b Exact volume not stated.

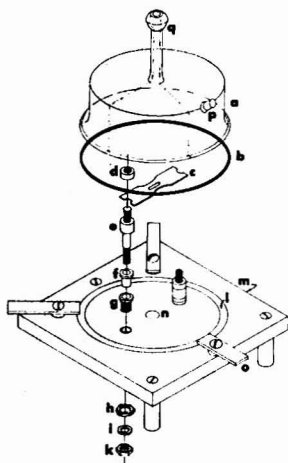


Figure 2. Tantalum filament vaporization apparatus. (a) quartz dome; (b) O-ring; (c) tantalum filament; (d-k) copper post assembly; (l) O-ring channel; (m) aluminum base; (n) argon gas inlet port; (o) aluminum tabs to seal the dome to the base; (p) sample injection port; (q) port from which argon flows to the torch sample introduction orifice

2. A 0.13-mm thick tantalum filament with dimensions of 37 mm by 10 mm (c) is positioned between two copper post assemblies (d-k) isolated from the aluminum base (m) by means of fired lava spacers (f). The copper posts and the argon gas inlet port (n) are covered with a quartz dome (a), 55-mm o.d. and 35 mm high. Three aluminum tabs (o) press the dome flange against the recessed O-ring (b) to provide a gas-tight seal.

The quartz dome is fitted with two ports (p and q) one of which allows the argon gas to flow from the inlet in the base (n) to the sample introduction orifice (q) of the plasma torch (34). The remaining port (p), fitted with a rubber septum, is positioned to allow the delivery of up to 200 μl of sample into a depression in the tantalum filament. The filament is heated by the flow of an electric current obtained from a low voltage, high current transformer controlled by a Variac.

Procedure. After the plasma has been generated and stabilized (34), the argon flowing through the filament chamber to the plasma is adjusted to a flow rate of 1.2 l./min and the spectrometer is set for the desired wavelength. A sample of 1 to 200 μl is deposit-

ed on the filament and a low current (from 10 to 17 A) is used to vaporize the water and to ash the deposit. At this point the Variac is adjusted to the vaporization setting (~ 100 A), and a toggle switch is used to rapidly and reproducibly deliver this current to the filament. The filament temperature quickly increases to approximately 1800 $^{\circ}\text{C}$ and the analyte together with the matrix elements are vaporized into the Ar carrier stream.

The photocurrent produced by the emission of the element of interest passing through the plasma is amplified and recorded on an X-Y recorder. Approximately 20 to 30 samples can be examined in one hour, and the filaments have an average lifetime of 200 to 300 samples.

RESULTS AND DISCUSSION

A summary of typical detection limits measured for some elements that are readily vaporized from the tantalum filament at the operating temperatures used in this study are shown in Table II, column 1. The reported values represent the concentration required to give a signal level that is three times greater than the standard deviation of the background noise level. The experimental parameters (height of observation in the plasma, filament currents, argon flow rates, and plasma power settings) for all elements were identical.

An overall comparison of the detection limits shows that, for a majority of the elements studied, the TFV-ICP technique provides relative powers of detection which overall are equivalent to the best values commonly reported for nonflame atomic absorption (AAS) or fluorescence (AFS) techniques. Absolute powers of detection were not observed to change significantly for different combinations of sample volume and analyte concentrations. Thus 100- μl volumes of a solution containing 0.0075 μg of Sb/ml and 15- μl volumes of a solution containing 0.05 μg of Sb/ml yielded comparable absolute detection limits within a factor of 1.4. The observations summarized in Table II suggest the combination of the tantalum filament vaporization, inductively coupled plasma excitation system with a multichannel spectrometer. This combination would thus provide the capability of performing multielement determinations (up to 20 or 30 elements) at the fractional nanogram level in microliter volumes or microgram samples in less than one minute.

An illustration of the precision obtained with the TFV-ICP system is shown in Figure 3. This figure represents the recorder tracings obtained for 15 replicate determinations of Sb at 10 times the detection limit. The relative standard deviation is 3.6%.

An analytical curve is presented in Figure 4 to demon-

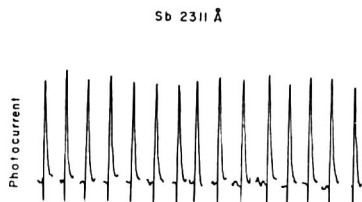


Figure 3. Reproducibility of the TFV-ICP system for 100- μ l samples of a solution containing 0.01 μ g of Sb/ml (1.0×10^{-9} g Sb)

strate the applicability of the TFV-ICP system to the analysis of samples over an extended concentration range. The curve covers the four-decade concentration range of 0.001 to 10 μ g Be/ml or from 2.5×10^{-11} to 2.5×10^{-7} gram of Be.

Discussion. A comparison of the TFV-ICP detection limits reported in Table II with the best values so far reported for the introduction of nebulized solution into the plasma shows that the TFV-ICP system is superior by 1 to 2 orders of magnitude. This appears to be the result of the increased concentration of the analyte, already desolvated and vaporized by the filament, passing through the axial channel of the plasma per unit time. The same mechanism is utilized in AAS and AFS when filament vaporization is performed, but for these techniques, the free atoms must be produced at the filament surface whereas for the plasma system it is only necessary to vaporize the analyte elements; the dissociation and excitation occur in the plasma.

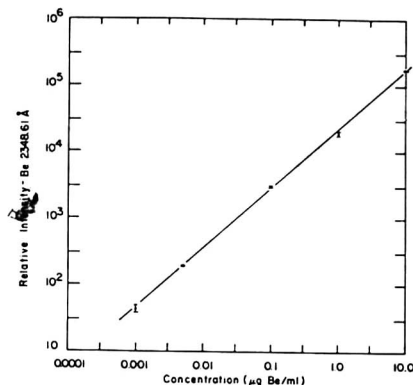


Figure 4. Typical analytical curve for Be in conductivity water covering over 4 orders of magnitude in concentration

Although the results presented here only represent studies on the behavior of a number of elements in water solutions, preliminary observations on real samples, such as blood and urine, suggest that little difficulty will be encountered in measuring ultratrace impurities in these matrices.

Received for review April 17, 1973. Accepted August 20, 1973. We wish to thank the Salsbury Laboratories, Charles City, Iowa, for providing the financial support of D. E. Nixon's graduate research assistantship.

Mode-Locked Laser Raman Spectroscopy—A New Technique for the Rejection of Interfering Background Luminescence Signals

Richard P. Van Duyne, David L. Jeanmaire, and D. F. Shriver

Department of Chemistry, Northwestern University, Evanston, Ill. 60201

A new technique for the rejection of interfering luminescence background signals employing a mode-locked argon ion laser and single photon timing detection electronics is described. Advantage is taken of the disparity between the lifetime of Raman scattering and the lifetime of luminescence emission. Only those photons emitted or scattered by the sample during the mode-locked laser pulse are passed on to the recording circuitry by the single photon timing detection system. Essentially all of the Raman signal can be recorded and a large fraction of the luminescence background is rejected. A detailed discussion of several alternative schemes for implementing this concept is given, along with a theoretical treatment of the appropriate signal-to-noise considerations. The fluorescence rejection capabilities of one of these configurations has been tested on samples consisting of a nonfluorescent Raman scatterer doped with a highly fluorescent dye impurity. The spectra obtained *via* the mode-locked technique show a substantial background suppression. Background slope is also reduced and the signal-to-noise

ratio shows an improvement consistent with our theoretical calculations based on fluorescence lifetime, laser pulse shape, laser pulse repetition rate, and average mode-locked power.

The recent development of reliable continuous wave (CW) lasers operating in the visible region of the spectrum along with advances in grating manufacture and photon detection electronics have resulted in great improvements in Raman spectrometers. The wide availability of these improved spectrometers has allowed chemists to exploit the complementary nature of infrared and Raman spectroscopy in a variety of structural, dynamic, and analytical problems (1-9). However, Raman spectroscopy

- (1) J. Loader, "Basic Laser Raman Spectroscopy," Heyden Sedtler, London 1970.
- (2) T. R. Gilson and P. J. Hendra, "Laser Raman Spectroscopy," Wiley-Interscience, New York, N.Y., 1970.
- (3) M. C. Tobin, "Laser Raman Spectroscopy," Wiley-Interscience, New York, N.Y., 1970.

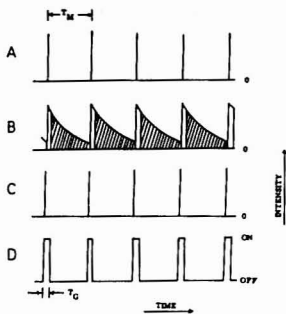


Figure 1. Schematic representation of a fluorescence rejection laser Raman experiment

A. Idealized (delta function) laser excitation pulse train, B. total emission signal from sample, C. Raman scattering signal, D. PMT gating. The cross hatched portion of the luminescence signal (B) is rejected

copy does not yet enjoy the broad applicability of infrared spectroscopy because of such experimental difficulties as sample decomposition in the laser beam and concomitant excitation of sample fluorescence. The first of these complications can be minimized by a variety of techniques such as judicious choice of the incident laser frequency, cooling of the sample *in vacuo* or under an inert gas, use of a line focus on solids to distribute the incident laser energy, and sample rotation to further distribute the energy (10).

The major remaining problem in Raman spectroscopy is elimination of fluorescent background. The detection of a weak Raman feature, which may be crucial to a correct vibrational assignment, is complicated by the high noise level associated with a large fluorescence background. A variety of fluorescence suppression tactics are available to the Raman spectroscopist including: 1) sample purification, 2) prolonged exposure of the sample to the full power of the laser beam in order to effect bleaching of the fluorescent moiety, 3) selection of an excitation wavelength producing minimum fluorescence, 4) signal averaging, and 5) temporal resolution of the Raman and fluorescence signals. Methods 1 and 2 are applicable only if the fluorescence is caused by laser excitation of an impurity; whereas methods 3, 4, and 5 are applicable to samples exhibiting intrinsic fluorescence as well. Selection of an optimum laser excitation wavelength is sometimes effective in suppressing fluorescence; however, it is not a generally applicable approach because of the breadth of many molecular electronic bands and because of the presence of a variety of absorbers in complex mixtures. Furthermore, one usually chooses the lowest energy excitation wavelength possible to minimize fluorescence and by doing so diminishes the Raman signal intensity since the scattering cross-section is inversely proportional to the fourth power of the excitation wavelength. Although signal averaging is a generally applicable method of improving the signal-to-noise ratio by averaging out the fluorescence signal shot

- (4) H. A. Szymanski, Ed., "Raman Spectroscopy," Vol. 1 and 2, Plenum Press, New York, N.Y., 1967 and 1970.
 (5) A. Anderson, "The Raman Effect," Vol. 1, Marcel Dekker, New York, N.Y., 1971.
 (6) P. J. Hendra and P. M. Strutton, *Chem. Rev.*, **69**, 325 (1969).
 (7) R. E. Hester, *Anal. Chem.*, **40**, 320R (1968); *ibid.*, **42**, 231R (1970); *ibid.*, **44**, 390R (1972).
 (8) G. A. Ozin, *Progr. Inorg. Chem.*, **14**, 173 (1971).
 (9) M. M. Suschinskii, "Raman Spectra of Molecules and Crystals," Israel Program for Scientific Translation, New York, N.Y., 1972.
 (10) W. F. Kiefer and H. J. Bernstein, *Appl. Spectrosc.*, **25**, 609 (1971).

Table I. Typical Values of Pulsed Laser Parameters

Mode	Pulse width	Rep. rate	Av. power
Mode-locked	1-1000 psec	100-130 MHz	30-40% of CW
Cavity dumped	15 ns-CW	20 MHz-DC	60-70% of CW
Q-switched	10-100 nsec	5 KHz-10 Hz	...

noise, it is not very practical in Raman applications owing to the long scan duration and long term laser power instabilities. A generally applicable method for the reduction of fluorescence background can be envisioned in which advantage is taken of the disparity between vibrational lifetimes, which are on the order of 10^{-13} to 10^{-11} sec (11), and fluorescence lifetimes, which are on the order of 10^{-9} to 10^{-7} sec for most gases, solutions, and solids of interest to chemists and biologists (12). To accomplish this, a pulsed laser excitation source is used to achieve temporal resolution between the short-lived Raman signal and the relatively long-lived fluorescence signal. An electronic time gate is then imposed on the photomultiplier tube (PMT) detection circuit and synchronized with the pulsed laser source such that short time events, primarily Raman photons, are preferentially recorded. This technique for fluorescence rejection by timing is schematically illustrated in Figure 1.

Time discrimination to reduce fluorescence background in Raman spectroscopy was apparently first mentioned by Loudon (13), although no systematic experimental verification of fluorescence suppression was carried out. Within the last year, two groups have investigated pulsed Raman techniques. Yaney (14) has described a system based on a Q-switched, frequency doubled, Nd:YAG laser; whereas Reed *et al.* (15) have explored in a preliminary way the possibilities of cavity dumping an argon ion laser. In the next section, we review the properties of various pulsed lasers and PMT time gating techniques. The reasons for our choice of a fluorescence rejection scheme based on a mode-locked laser are presented. A signal-to-noise theory appropriate to the mode-locked laser Raman spectrometer has been formulated. Mode-locked laser Raman spectra are presented which show substantial fluorescence background suppression, reduced base-line slope, and a signal-to-noise improvement consistent with the theoretical description of the technique.

INSTRUMENT DESIGN CONSIDERATIONS

The design of a practical instrumentation system for implementing the fluorescence rejection scheme depicted in Figure 1 requires the selection of a pulsed laser source and PMT gating technique that are compatible with each other and are matched to the time dependent fluorescence characteristics of the samples under investigation. Broadly speaking, CW lasers can be made to operate in three distinct pulsed modes: Q-switched, cavity dumped, and mode-locked. As summarized in Table I, these pulsed modes differ with respect to such parameters as pulse width, repetition rate, and average laser power. Pulsed nitrogen lasers, which have recently become popular, have pulse parameters similar to those of the Q-switched CW laser. The laser pulse width is perhaps the most impor-

- (11) A. Laubereau, D. von der Linde, and W. Kaiser, *Phys. Rev. Lett.*, **28**, 1162 (1972).
 (12) J. B. Birks, "Photophysics of Aromatic Molecules," Wiley, New York, N.Y., 1970.
 (13) R. Loudon, *Advan. Phys.*, **13**, 423 (1964).
 (14) P. P. Yaney, *J. Opt. Soc. Amer.*, **62**, 1297 (1972).
 (15) R. R. Reed, D. O. Landon, and J. F. Moore, Spex Industries, Meltschen, N. J., private communication, 1972.

tant parameter since it determines the time distribution of the Raman photons and the degree of temporal resolution between Raman and fluorescence photons. For most gas and liquid samples capable of emitting both Raman and fluorescence photons, the time response function in terms of the total number of photons emitted per second, $N_{\text{total}}(t)$, for a delta function excitation pulse is:

$$N_{\text{total}}(t) = C_R e^{-t/\tau_R} + C_L e^{-t/\tau_L} \quad (1)$$

where τ_R is the lifetime of the Raman scattering and τ_L is the lifetime of the interfering luminescence emission. In the solid state, other luminescence time response functions are observed which, in some cases, are characterized by a finite risetime as well as an exponential decay (16). Throughout this paper, however, we will deal only with instantaneous risetime, single exponential decay luminescence functions since they represent the most difficult case for fluorescence rejection. Since most available pulsed laser sources have finite pulse width on the Raman time scale, the observed time distribution of photons emitted from the sample $N_{\text{total}}^{\text{obs}}(t)$, will be given by the convolution of the laser pulse shape function, $G(t)$, with $N_{\text{total}}(t)$:

$$N_{\text{total}}^{\text{obs}}(t) = \int_0^t G(\lambda) C_R e^{-(t-\lambda)/\tau_R} d\lambda + \int_0^t G(\lambda) C_L e^{-(t-\lambda)/\tau_L} d\lambda \quad (2)$$

For all lasers except the mode-locked Nd:YAG (17), the limit $\tau_R \ll$ the full width-half maximum (FWHM) of $G(t)$ will apply reducing Equation 2 to:

$$N_{\text{total}}^{\text{obs}}(t) = C_R G(t) + C_L \int_0^t G(\lambda) e^{-(t-\lambda)/\tau_L} d\lambda \quad (3)$$

It is clear from Equation 3 that temporal resolution of Raman and fluorescence photons will be maximized by using a pulsed source whose $G(t)$ FWHM is as short as possible relative to τ_L .

Maximum improvement in the Raman signal-to-noise ratio will be achieved when as many Raman and as few fluorescence photons as possible are accepted in PMT time gate interval, t_g . This condition is met when t_g is small compared to the luminescence lifetime and approximately equal to the FWHM of the Raman photon time distribution. Several PMT time gating techniques have been discussed in the literature. Selection of a particular method for use in the Raman spectroscopy fluorescence rejection application is governed by the laser pulse width and repetition rate compatibility requirement. Table II summarizes the gating properties of three possible techniques. Pulsing the PMT high voltage has been used previously in a stroboscopic fluorescence lifetime apparatus (19), gated counters are presently used in conventional Raman spectroscopy, and the time-to-amplitude converter (TAC)/single channel analyzer (SCA) combination has been used for fluorescence lifetime measurements (19) as well as for the measurement of the luminescence lifetimes of GaP electroluminescent devices (20).

Our particular objective in achieving fluorescence rejection by temporal resolution is to develop an instrument capable of rejecting very short-lived fluorescence such as

Table II. Parameters for PMT Gating Techniques

Technique	Gate width	Max. repetition rate
Pulsed PMT	2 ns-CW	100 KHz
Gated counter	50 nsec-CW	1 MHz
TAC/SCA	0.5 nsec-80 μ sec	250 KHz
	0.5 nsec-1 μ sec	10 MHz*

* Reference (18).

that found in biochemically important samples. For example, the Raman spectra of small polypeptides and proteins are frequently difficult to obtain because of interfering tryptophan fluorescence which has a lifetime of only 2.8 nsec in H₂O. In addition, we find from preliminary studies of species adsorbed on surfaces (21), a substantial fluorescence background with a lifetime of approximately 4 nsec. Furthermore, it would be highly desirable to have a fluorescence rejection technique that was not limited to short-lived fluorescence rejection and at the same time retained as many of the simple operating features of conventional CW laser Raman spectroscopy as possible. These objectives lead us to choose mode-locked as the method of laser pulse generation and the TAC/SCA combination to provide compatible PMT time gating. With this approach, we achieve the maximum possible temporal resolution between Raman and fluorescence photons. Inspection of Table II indicates that the TAC/SCA gate width is compatible with mode-locked pulse generation although it appears that the repetition rate is too slow to allow every mode-locked pulse to be gated. The TAC repetition rate listed in Table II is that for START channel pulses. Thus, if the mode-locked laser provides one START pulse for each laser pulse, the TAC will indeed saturate. START channel saturation can be avoided, however, if the normal roles of START and STOP channels are inverted using the relatively low sample emission count rate to provide START pulses and the mode-locked laser to provide STOP pulses. This TAC inversion scheme for high repetition rate timing has been discussed previously in the context of nuclear physics instrumentation (18).

SIGNAL-TO-NOISE THEORY FOR MODE-LOCKED LASER RAMAN SPECTROSCOPY (MLRS)

The S/N expression for CW laser excitation and photoelectron pulse counting detection presented previously by Alfano (22) and others (3, 14) is the starting point for this discussion:

$$(S/N)_{\text{CW}} = \frac{(N_R \Delta t)^{1/2}}{[1 + 2(N_L/N_R + N_D/N_R + N_S/N_R)]^{1/2}} \quad (4)$$

where N_R = Raman signal (counts/second) for CW excitation, N_L = Luminescence background signal (counts/sec) excitation, N_S = Scattered light signal (counts/sec) excitation, N_D = Dark signal (counts/sec) excitation, and Δt = Wavelength channel dwell time (sec).

In addition the following assumptions are made: (i) $G(t)$ is the mode-locked pulse shape function. (ii) The detector time gate is rectangular in shape with an aperture of t_g seconds. (iii) The lifetime of the Raman emission is sufficiently short with respect to the FWHM of $G(t)$ that the Raman signal has a time distribution of $G(t)$. (iv) The interfering luminescence signal has an instantaneous rise-

(21) R. P. Van Duyne, D. L. Jeanmaire, and D. F. Shriver, 1973, unpublished results.

(22) R. R. Alfano and N. Ockman, *J. Opt. Soc. Amer.*, **58**, 90 (1968).

(16) B. DiBartolo, "Optical Interactions in Solids," Wiley, New York, N.Y., 1968.

(17) P. W. Smith, *Proc. IEEE*, **58**, 1342 (1970).

(18) I. J. Taylor and T. H. Becker, *Nucl. Instrum. Methods*, **99**, 387 (1972).

(19) W. R. Ware, "Transient Luminescence Measurements," in "Creation and Detection of the Excited State," A. A. Lamola, Ed., Marcel Dekker, New York, N.Y., 1971.

(20) R. Z. Bachrach, *Rev. Sci. Instrum.*, **43**, 734 (1972).

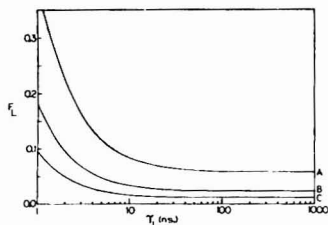


Figure 2. Dependence of the luminescence acceptance fraction, F_L , on luminescence lifetime, τ_L .

A. Gate width, $t_g = 500$ psec; B. $t_g = 200$ psec; C. $t_g = 100$ psec. Fixed parameters: Mode-locked pulse spacing, $t_M = 8.77$ nsec (17)

time and a single exponential decay function. (v) The FWHM of $G(t)$ is sufficiently narrow with respect to the mode-locked laser pulse spacing, t_M , that no overlapping of the Raman or scattered light signal occurs between adjacent pulses. (vi) Overlapping of the luminescence signal between successive pulses can occur since the luminescence lifetime can be comparable to or longer than the mode-locked pulse spacing.

Furthermore, let n_R , n_L , n_D , and n_S be the appropriate signal count rates under mode-locked conditions. The S/N for the mode-locked situation is:

$$(S/N)_{ML} = \frac{(n_R \Delta t)^{1/2}}{\left[1 + 2 \left(\frac{n_L}{n_R} + \frac{n_D}{n_R} + \frac{n_S}{n_R} \right) \right]^{1/2}} \quad (5)$$

A comparison of $(S/N)_{CW}$ and $(S/N)_{ML}$ can easily be made by relating n_R to N_R , etc. To do this, two factors need to be considered: 1) the PMT gate will accept only a certain fraction F_R , F_L , F_D , and F_S of n_R , n_L , n_D , n_S , respectively, and 2) the average mode-locked power is reduced compared to the CW power. The acceptance fractions are simply the ratio of the number of photons accepted by the gated PMT to the total number of photons in a particular signal pulse. The F 's are evaluated by integrating the temporal distribution of the appropriate signal pulse over the gate width and dividing this by the pulse integral evaluated from zero to infinity. Thus, F_R and F_S are given by:

$$F_R = \frac{\int_0^{t_g} \int_0^t G(\lambda) \exp[-(t-\lambda)/\tau_R] d\lambda dt}{\int_0^\infty \int_0^t G(\lambda) \exp[-(t-\lambda)/\tau_R] d\lambda dt} \quad (6)$$

$$F_S = \int_0^{t_g} G(t) dt / \int_0^\infty G(t) dt$$

Since the dark count time distribution is random, F_D is:

$$F_D = t_g/t_M \quad (7)$$

The expression for F_L is more complicated since pulse overlapping must be considered:

$$F_L = \frac{\lim_{k \rightarrow \infty} \sum_{i=1}^k \int_{(i-1)t_M}^{(i-1)t_M+t_g} \int_0^t G(t-\lambda) \times \exp[-(\lambda - (i-1)t_M)/\tau_L] d\lambda dt}{\int_{(k-1)t_M}^\infty \int_0^t G(t-\lambda) \exp[-(t-k-1)t_M/\tau_L] d\lambda dt} \quad (8)$$

Equation 8 is derived in the Appendix. If we multiply numerator and denominator of each of the F expressions by

the number of pulses applied to the sample in 1 second, then the F 's are also of the form:

$$F_x = \frac{n_x}{\Omega N_x} \quad x = R, L, \text{ or } S \quad (9)$$

where Ω accounts for the average power loss suffered in mode-locking the laser. Since $N_D \neq f(\text{Laser Power})$, the F_D expression is:

$$F_D = \frac{n_D}{N_D} \quad (10)$$

Solving Equations 9 and 10 for n_R , n_L , n_D , and n_S and substituting these into Equation 5 gives the final S/N expression for the mode-locked laser Raman Technique:

$$(S/N)_{ML} = \frac{[\Omega N_R \Delta t]^{1/2} F_R}{\left[F_R + 2 \left(\frac{N_L F_L}{N_R} + \frac{N_S F_S}{N_R} + \frac{N_D F_D}{N_R} \right) \right]^{1/2}} \quad (11)$$

where the F 's are defined as above. The S/N improvement factor, θ , over the CW Raman experiment is given by the ratio of Equation 11 to Equation 4.

The Delta Function Excitation Case. Equation 11 is reasonably cumbersome to evaluate for an arbitrary laser pulse shape function. However, reasonable estimates for $(S/N)_{ML}$ and θ can be obtained by assuming that the laser excitation pulse is very narrow compared to t_g . Under these circumstances, $G(t)$ is adequately represented by a delta function and F_S , F_R , and F_L can be readily evaluated to give:

$$\begin{aligned} F_S &= 1 \\ F_R &= 1 - e^{-t_g/\tau_R} \\ F_L &= \frac{1 - e^{-t_g/\tau_L}}{1 - e^{-t_M/\tau_L}} \end{aligned} \quad (12)$$

F_D is still given by Equation 7. After substitution of these results into Equation 11 and recognizing that for realistic values of t_g :

$$1 - e^{-t_g/\tau_R} \approx 1$$

we get:

$$(S/N)_{ML} = \frac{(\Omega N_R \Delta t)^{1/2}}{\left[1 + 2 \left(\frac{N_L}{N_R} \left(\frac{1 - e^{-t_g/\tau_L}}{1 - e^{-t_M/\tau_L}} \right) + \frac{N_S t_g}{N_R \Omega t_M} + \frac{N_S}{N_R} \right) \right]^{1/2}} \quad (13)$$

and

$$\theta = \frac{\left[\frac{\Omega \left[1 + 2 \left(\frac{N_L}{N_R} + \frac{N_S}{N_R} + \frac{N_D}{N_R} \right) \right]}{\left[1 + 2 \left(\frac{N_L}{N_R} \left(\frac{1 - e^{-t_g/\tau_L}}{1 - e^{-t_M/\tau_L}} \right) + \frac{N_D t_g}{N_R \Omega t_M} + \frac{N_S}{N_R} \right) \right]} \right]^{1/2}}{\quad} \quad (14)$$

In most Raman spectrometers, N_S/N_R is negligible since double or triple monochromators are usually employed. If the time discrimination technique were 100% efficient in rejecting luminescence and dark counts, the S/N improvement factor would approach a maximum value of:

$$\theta_{max} = \Omega^{1/2} \left[1 + 2 \left(\frac{N_L}{N_R} + \frac{N_D}{N_R} \right) \right]^{1/2} \quad (15)$$

The dependence of F_L on τ_L for various values of t_g is plotted in Figure 2. F_L is seen to approach a long lifetime limit of t_g/t_M . It should be noted that in the case of $t_g =$

Table III. Effect of the Ratio of Luminescence Background to Raman Intensity on the Signal-to-Noise Improvement Factors, θ ^a

N_L/N_R	N_R	$(S/N)_{CW}$	$(S/N)_{ML,max}^b$	$(S/N)_{ML,max}^c$	θ_{max}^b	θ_{max}^c
1	1000	15.77	17.32	31.6	1.098	2.004
10	1000	6.73	17.32	31.6	2.573	4.697
100	100	0.688	5.48	10.0	7.965	14.54
1000	10	0.068	1.73	3.16	15.10	45.83
N_L/N_R	$(S/N)_{ML}^b$	$(S/N)_{ML}^c$	θ^b	θ^c	θ/θ_{max}^b	θ/θ_{max}^c
1	16.21	30.31	1.027	1.922	0.935	0.959
10	13.89	25.81	2.06	3.83	0.804	0.815
100	2.14	4.08	3.11	5.93	0.390	0.408
1000	0.230	0.442	3.34	6.42	0.133	0.140

^a Fixed parameters: $t_g = 200$ psec; $t_M = 8.7719$ nsec; long lifetime limit; $\Delta t = 1.0$ sec; $N_D = 500$; $N_B = 10$. ^b Sample can withstand excitation with full CW laser power. ^c Sample can only withstand less than or equal to full mode-locked average power.

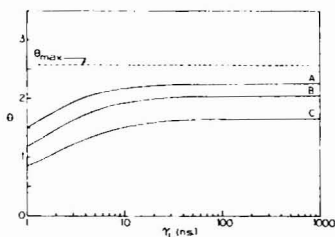


Figure 3. Signal-to-noise improvement factor, θ , as a function of luminescence lifetime, τ_L .

A. $t_g = 100$ psec. B. $t_g = 200$ psec. C. $t_g = 500$ psec. Fixed parameters: $t_M = 8.77$ nsec; $N_R = 10^3 \text{ sec}^{-1}$; $\Delta t = 1.00$ sec. $N_L/N_R = 10$; $N_D/N_R = 0.5$; $(S/N)_{CW} = 6.73$; $\theta_{max} = 2.57$

200 psec, over 90% of the luminescence background counts are rejected; even for an interference lifetime as short as 2.0 nsec. Figure 3 illustrates the typical signal-to-noise improvement factor that can be expected from the reduction of fluorescence and dark background counts by the time discrimination technique. The assumption used in plotting Figure 3 is that the sample under investigation can withstand irradiation with the full power of the CW laser without decomposition. On mode-locking the same laser, the effective power is reduced by a factor of Ω , decreasing the maximum obtainable S/N by $\Omega^{1/2}$. For many kinds of samples, especially those of biological interest, the comparison presented in Figure 3 is not fair since irradiation with the full CW power is not possible. The values of θ obtainable in the case where the maximum power that can be applied to the sample is less than or equal to the average mode-locked power are slightly less than double those shown in the figure. This effect along with the dependence of θ on N_L/N_R is illustrated in Table III. Note that for a strong Raman signal (10^3 sec^{-1}) contaminated by an equally strong background signal, 93-95% of the Raman signal shot noise limited S/N can be achieved.

Examination of the F_L expression in Equation 12 indicates that some improvement in luminescence rejection would be expected by increasing t_M . This can be accomplished in two ways: by increasing the length of the laser cavity and by acousto-optic gating of the laser pulse train so that every second or every third, or etc. mode-locked pulse would strike the sample. The effect of increasing the cavity length to the point of making the spacing between pulses twice or three times the natural pulse spacing is shown in Figure 4. The improvement in θ over a pulse spacing of t_M is small. Furthermore the stability and alignment problems of long cavity mode-locked lasers are

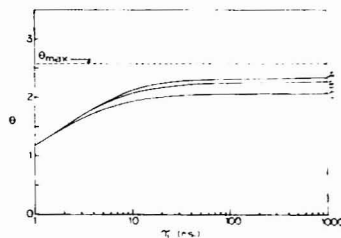


Figure 4. Signal-to-noise improvement factor, θ , as a function of luminescence lifetime, τ_L .

A. Mode-locked pulse spacing, $t_M = 3(8.77)$ nsec; B. $t_M = 2(8.77)$ nsec; C. $t_M = 8.77$ nsec. Fixed parameters: $t_g = 200$ psec; all others are the same as in Figure 3

sufficiently difficult that this appears to be an unattractive approach. Calculations of $(S/N)_{ML}$ have been made assuming a pulse spacing of $2 t_M$ achieved by acousto-optic pulse selection. The calculated $(S/N)_{ML}$ is actually less for a spacing of $2 t_M$ because the sample is irradiated with $1/2$ the average power available when the spacing is t_M . Again, if the sample cannot stand the total mode-locked average power, then some small improvement in θ is gained. We conclude that the improvement in θ is not worth the experimental difficulty associated with acousto-optic gating.

The Triangular Pulse Excitation Case. The time distribution of an actual mode-locked pulse from an Ar ion laser is shown in Figure 5 (23). This pulse shape can be well approximated by an isosceles triangle pulse of unit amplitude and FWHM t_p :

$$G(t) = \begin{cases} t/t_p & t < t_p \\ 2 - (t/t_p) & t_p \leq t \leq 2 t_p \\ 0 & t > 2 t_p \end{cases} \quad (16)$$

Laplace transform techniques were used to evaluate the convolution integrals in Equations 6 and 8. Evaluation of F_L , F_D , F_R , and F_S were carried out in a manner similar to that described for the delta function excitation case. The analytical expressions resulting from these procedures are too involved to be presented here. Suffice it to say that the shapes of the plots in Figure 2, 3, and 4 are not altered appreciably by the triangular pulse assumption but, quantitatively, the limiting value of F_L is reduced by a factor of approximately 2. The major difference between this case and the delta function case, then, is that the

(23) J. Hawkins, Coherent Radiation Laboratories, Palo Alto, Calif., private communication, 1972.

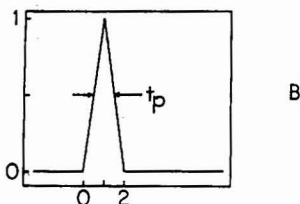
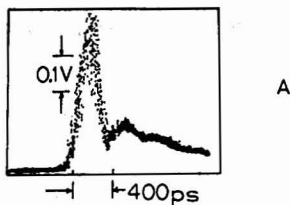


Figure 5. Mode-locked laser pulse shape

A. Actual laser pulse from CRL Model 52 argon ion laser, mode-locked with model 465. B. Triangular pulse approximation. FWHM = t_p ; base width = $2t_p$

value of F_R is a function of t_g . Consequently, the S/N cannot be monotonically improved by narrowing t_g . The optimum value of t_g is approximately t_p . This can be seen qualitatively by examining the relative areas of the Raman and luminescence photon distributions included within t_g in Figure 6. As a result, the values of θ shown in Figure 3 are expected to represent a lower limit to the actual values of θ when $t_g \geq t_p$ and an upper limit when $t_g < t_p$.

EXPERIMENTAL

Instrumental Configuration. Figure 7 illustrates a schematic diagram of the mode-locked laser Raman spectrometer used to test the temporal resolution concept for rejecting fluorescence background signals. The laser employed in these studies was a Coherent Radiation Laboratories Model 52 argon ion laser operated at 488.0 nm. Mode-locking was achieved using the CRL Model 465 accessory. The incident laser beam was passed through the diameter of 1-mm i.d. borosilicate glass sample tubes so that the total photon emission flux (Raman plus fluorescence) could be collected at right angles to the laser beam and focused on to the entrance slit of a Spex 1400-II double monochromator. To provide a realtime monitor of the mode-locked laser pulse shape so that the mode-lock drive unit could be easily tuned, approximately 10% of the laser beam was split off with a borosilicate glass beam splitter and focused on a Tropol Model 330 photodiode. The photodiode output was then observed with Tektronix 531 oscilloscope fitted with a type 1S1 sampling plug-in. Photons emergent from the monochromator exit slit were tightly focused on the center of the type 116 photocathode of an RCA 8850 PMT to minimize the photoelectron transit time spread.

The central device of the PMT time gating system is the TAC [Ortec 457]/SCA [Ortec 420A] combination operated with the normal roles of the START and STOP channels inverted to avoid START channel saturation. TAC START pulses are derived by amplifying and shaping the PMT output with a timing filter amplifier [Ortec 464], passing these output pulses on to a constant fraction of pulse height discriminator [Ortec 463] and delaying the resulting NIM standard fast output pulses with a nanosecond delay line [Ortec 425]. TAC STOP pulses are obtained from the CRL mode locker drive unit which produces a sine wave output whose frequency is equal to one-half the mode locked laser repetition rate. A NIM standard fast output pulse is generated by a zero crossing discriminator [EG and GT 140/N] each time the

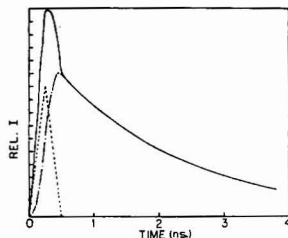


Figure 6. Relative temporal photon distributions

(---) Raman signal, (-.-.-) luminescence signal, (—) total signal. Calculated from Equation 3 using the triangular pulse approximation

sine wave passes through zero. Thus a STOP pulse train is generated that is synchronized with the laser pulse repetition rate. Since a typical pulse rate from the PMT, resulting from both Raman and fluorescence photons, is on the order of 10 KHz or less and the laser pulse frequency is 114 MHz, which corresponds to a round trip cavity transit time of 8.77 nsec, the TAC essentially has unit probability of receiving a STOP pulse after each START pulse generated by a Raman or fluorescence photon.

The TAC output pulses, whose amplitudes are proportional to the time delays between START and STOP signals, are simultaneously fed to the SCA and to the analog-to-digital converter (ADC) of a multichannel pulse height analyzer (MCPHA). The amplitude of each TAC output pulse is digitized by the ADC which then selects one of the MCPHA channels in which to store the delayed coincidence event. Because of the inverted roles of the TAC START and STOP channels, delayed coincidence events representing photons emitted a short (long) time after the laser pulse corresponding to long (short) START/STOP delays which result in large (small) amplitude TAC output pulses and after A/D conversion are stored in high (low) numbered MCPHA channels. As the acquisition and storage of delayed coincidence events proceeds, a decay curve representing the time distribution of photons emitted by the laser excited sample is recorded in the MCPHA memory. The MCPHA used in this work is a Nuclear Data Model 2400 with 1K of core memory. Although 1024 channels are available for use, all decay curves reported here were recorded in only 128 channels. The Ortec 457 TAC used in these experiments has a built-in bias amplifier which allows one to expand the full scale TAC sweep time and position the decay curve with respect to the MCPHA channels. The TAC bias controls were set so that 128 channels represent the time interval between two mode-locked laser pulses. The function of the SCA is to establish a window such that only those TAC output pulses greater than a preset minimum amplitude and less than a preset maximum amplitude are passed on to the Ortec 441 ratemeter and strip chart recorder. Thus the ratemeter records only those photons emitted in a specific time interval following each laser pulse.

Procedure for PMT Time Gate Calibration. In order to calibrate the PMT time gate for a specific time interval, which is equivalent to setting the lower level threshold and the upper level threshold of the SCA, it is necessary to record the photon time distributions of the Raman and fluorescence signals from the sample under study. In the case of samples which are intentionally doped with a fluorescent impurity, this may be done by tuning the monochromator to a Raman active vibration of the undoped scatterer and recording the photon time distribution in the MCPHA. Since $\tau_R \ll$ FWHM of $G(t)$ this decay curve represents the laser pulse shape as convoluted by the timing jitter in the TAC START and STOP channels. The addition of a fluorescent impurity allows the monitoring of the Raman plus fluorescence photon time distribution. The fluorescence photon time distribution can be measured separately by resetting the monochromator to a wavelength anticoncoident with a Raman active vibration.

The threshold levels of the SCA are then set using an auxiliary pulse generator (Data Pulse Model 101) adjusted so that its output pulse shape simulates that of the TAC output pulses. The pulse generator is then connected to the ADC of the MCPHA, in which the appropriate decay curves are stored, and its amplitude increased until it corresponds to the channel number at which it is desired to start accepting photons. The pulse generator is then connected to the SCA and its lower level threshold is adjusted

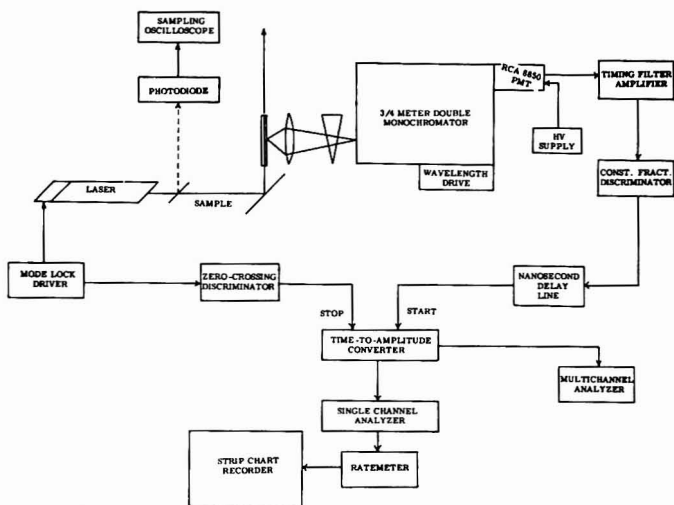


Figure 7. TAC/SCA configuration of MLLRS

until counts are just passed. The pulse generator is then reconnected to the ADC of the MCPHA and this process is repeated for the upper level of the photon acceptance window. Once the photon acceptance window has been set, the Raman spectrum of the sample may be recorded in a *totally conventional manner*.

Samples. The Raman scatterer used in these fluorescence rejection experiments was spectroquality benzene (Fisher). In particular, the 992 cm^{-1} line of benzene was studied since its Raman scattering cross section is large (24). Benzene samples were doped with the fluorescent dyes Rhodamine 6G (Allied Chemicals) or Acridine Orange (Eastman). The dyes were used without further purification. In the case of Acridine Orange which has its electronic absorption band maximum at 490 nm , only a $10^{-9}M$ solution of the dye impurity was necessary to produce a fluorescent background signal approximately three times as large as the 992 cm^{-1} neat benzene Raman signal. All liquid samples were sealed in 1-mm i.d. borosilicate glass tubes.

RESULTS

Before considering the actual mode-locked laser Raman spectra, it is useful to examine the photon time distribution curves for several samples. This information provides a critical check on the operation of the instrument, provides the necessary information for the optimal selection of the photon acceptance window, and gives a quick indication of the degree of background suppression which may be achieved. Figure 8 shows the photon time distribution curves for the 992 cm^{-1} Raman line of benzene, the fluorescence background caused by doping with Rhodamine 6G ($\tau_L = 3.9\text{ nsec}$) measured at 962 cm^{-1} with respect to the 4880-\AA laser line, and the sum of the Raman plus fluorescence signals measured at 992 cm^{-1} . The neat benzene Raman distribution curve has a FWHM of 2.5 nsec which is approximately 10 times broader than expected on the basis of the laser pulse shape demonstrated by the manufacturer in Figure 5. The breadth of this curve is traceable to substantial timing jitter in the STOP channel pulse electronics as well as an unusually wide mode-locked laser pulse (ca. 1.2 nsec) as estimated from an independent measurement on the direct laser beam using a photodiode and sampling oscilloscope. The jitter in the STOP channel was due to a frequency drift in the sine wave output (24) J. G. Skinner and W. G. Nilsen, *J. Opt. Soc. Amer.*, **58**, 113 (1968).

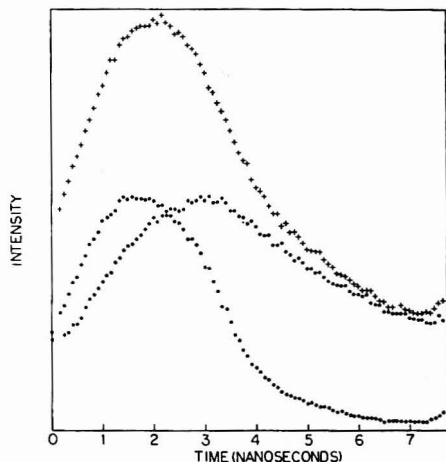


Figure 8. Photon time distributions for benzene/Rhodamine 6G system

●●● 992 cm^{-1} Raman line of neat benzene; ○○○ Rhodamine 6G fluorescence background, $\tau_L = 3.9\text{ nsec}$; ++++ sum of the Raman and fluorescence signals

from the mode-lock drive unit. With the equipment available to us at the time these experiments were performed, it was not possible to sharpen the Raman photon time distribution curve. However, foreseeable changes in the mode-locking unit and the method of STOP channel pulse generation should permit the Raman FWHM to be reduced by an order of magnitude. Under improved conditions, the experimental photon time distribution curves should look more like the theoretically calculated ones shown in Figure 6.

Figure 9 illustrates the Raman and fluorescence time distribution curves for the benzene/ $1.3 \times 10^{-9}M$ Acridine

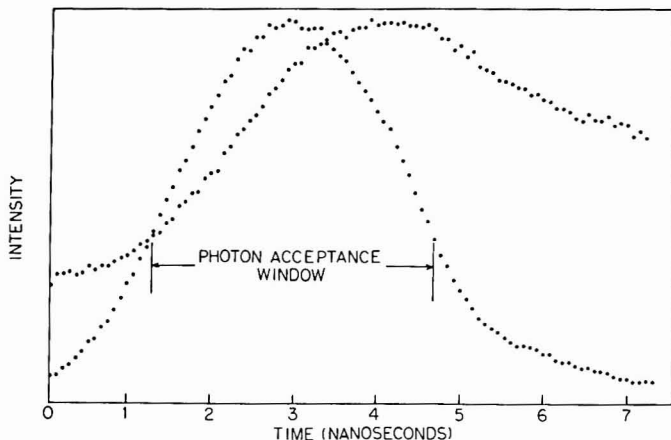


Figure 9. Photon time distributions for benzene/Acridine Orange system

OOO, 992 cm^{-1} Raman line of neat benzene; ●●●, Acridine Orange fluorescence background, $\tau_L = 4.4$ nsec, 1.3×10^{-9} M

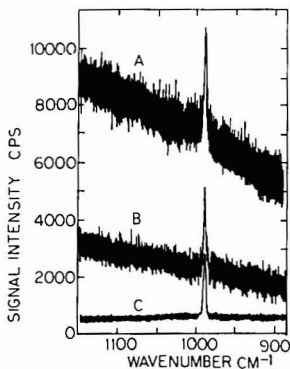


Figure 10. Mode-locked laser Raman spectra of benzene doped with Acridine Orange

A. No fluorescence rejection; B. With fluorescence rejection; C. Neat benzene under same conditions as B

Orange ($\tau_L = 4.4$ nsec) system. The photon acceptance window indicated was set up on the SCA using the auxiliary pulse generator technique described in the Experimental Section. Mode-locked laser Raman spectra were obtained both with and without the SCA time window operating. These spectra are shown in Figure 10. The upper trace was obtained with the laser mode-locked but without the SCA operating and thus represents the type of data obtainable in a conventional Raman experiment on a fluorescent sample. This spectrum is characterized by a high background level, high shot noise ($S/N = 2.47$) and a sloping base line. Introduction of the PMT time gate shown in Figure 9 produced the spectrum shown in the middle of Figure 10. This spectrum has a substantially lower ratio of background fluorescence to Raman signal, slightly improved signal-to-noise ratio ($S/N = 2.60$), and reduced base-line slope. The spectrum of neat benzene obtained under mode-locked conditions identical to those used to obtain the middle trace is shown for comparison.

DISCUSSION

The MLLRS experiments described in this paper were designed to be illustrative of the fact that substantial fluorescence background suppression can be achieved even when the lifetime of the interfering fluorescence signal is less than 10 nsec. Although we have demonstrated that MLLRS can produce spectra with a lower ratio of background fluorescence to Raman signal and reduced baseline slope, the experimentally obtained S/N improvement factor, θ_{ML}^{exp} , was quite small (1.05). This improvement factor, however, can be shown to be consistent with the theoretically expected value.

Experimental-Theoretical Comparison for TAC/SCA Configuration. The signal-to-noise improvement factor appropriate to the comparison of two spectra taken under mode-locked conditions but with different PMT time gates, such as comparison of Figure 10A and 10B is obtained by forming the ratio of Equation 11 evaluated with the experimentally used photon acceptance window, t_g , to Equation 11 evaluated with the photon acceptance window fully open to the width of one mode-locked pulse interval, $t_g = t_M$:

$$\theta_{ML}^{\text{calc}} = F_R(t_g) \times \left\{ \frac{1 + 2 \left[\frac{N_L}{N_R} + \frac{N_S}{N_R} + \frac{N_D}{\Omega N_R} \right]}{F_R(t_g) + 2 \left[\frac{N_L}{N_R} F_L(t_g) + \frac{N_S}{N_R} F_S(t_g) + \frac{N_R}{\Omega N_R} F_D(t_g) \right]} \right\}^{1/2} \quad (17)$$

Assuming that scattered light is negligible, we can evaluate Equation 17 by taking $N_L/N_R = 2.40$ from Figure 10A; the dark count rate under the conditions of Figure 10A was 300 Hz and $\Omega = 1/25$ (25) giving $N_D/\Omega N_R = 0.30$; and $F_R(t_g)$ and $F_L(t_g)$ are numerically evaluated from the photon time distribution curves in Figure 9. This is possible since the experimental photon time distributions include the effects of convolution of the Raman or fluorescence signal response functions with the laser pulse shape and the timing jitter in the detection electronics as well as flu-

(25) "Model 465 Mode-Locker," Coherent Radiation Laboratories, Palo Alto, Calif., 1972.

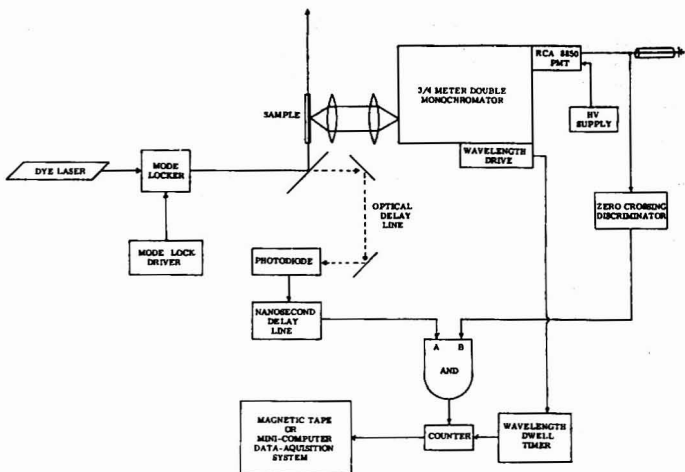


Figure 11. Schematic diagram for improved MLLRS

orescence overlapping between successive mode-locked pulses. $F_R(t_R)$ and $F_I(t_R)$ are obtained by integrating the appropriate photon time distribution curve over the photon acceptance window and dividing by the integral of the curve over the entire mode-locked interval. $F_D(t_R)$ is given by Equation 7. Evaluating these quantities gives $F_R(t_R) = 0.80$, $F_I(t_R) = 0.52$, $F_D(t_R) = 0.46$, and $\theta_{ML}^{CALCD} = 1.08$. The close agreement between θ_{ML}^{CALCD} and θ_{ML}^{EXPTL} indicates the S/N expressions that have been developed are reliable indicators for MLLRS performance.

The limiting factor in the present configuration of the MLLRS is clearly the laser pulse width and the timing jitter in the associated detection electronics. As indicated above, it should be possible to reduce the FWHM of the Raman photon time distribution curve by a factor of 10. Under these conditions and establishing a photon acceptance window of 400 psec, which is feasible with the present SCA, the values of $F_I(t_R)$ and $F_D(t_R)$ should be reduced to 0.1 and 0.05, respectively, and $F_R(t_R)$ should be increased to near 1.0. This would correspond to a projected value for $\theta_{ML}^{EXPTL} = 1.89$. This value represents attainment of 75% of the theoretical maximum signal shot noise limited θ_{ML} of 2.53.

Alternative Instrumental Configurations. Additional improvement in fluorescence rejection by the MLLRS technique, beyond that obtainable with the mode-locked argon ion laser-TAC configuration examined in this study, can only be achieved by utilizing shorter laser pulses and establishing an ultralow jitter PMT time gate that approaches the width of the laser pulse. Experiments carried out in the laser development laboratories indicate that mode-locking an argon ion laser pumped CW dye laser produces pulses with widths typically in the range of 50 psec (26) although some workers have reported occasional pulses as short as 1.5 psec (27, 28). Establishing a PMT time gate to complement a mode-locked dye laser pulse can be accomplished by performing a picosecond time scale logical AND operation on two fast timing signals. One timing signal is derived from an ultrafast rise-

time PMT which views the total emission flux, Raman plus fluorescence photons, emerging from the spectrometer. The other timing signal is obtained from a photodiode which monitors a tightly focused, optically delayed portion of the mode-locked laser beam. Only those photons which are in time coincidence with the optically delayed beam will be recorded. The picosecond AND operation can be carried out by taking advantage of the commercially available majority coincidence logic modules recently developed for use in high energy physics applications. These modules have incorporated the very fast emitter coupled logic (ECL) integrated circuits permitting their application to the study of high repetition rate (greater than 100 MHz) picosecond time scale phenomena. Furthermore, these logic devices are characterized by a coincidence curve, which is the functional relationship between the number of coincidences resulting in an output pulse and the relative time displacement of the input pulses. The coincidence curve specifies the ability of the device to distinguish simultaneity of the input pulses. For the units we are presently testing, the FWHM of the narrowest coincidence curve is typically 1.0 nsec and the slope of the coincidence curve is such that the number of output pulses drops off by a factor of greater than 100 when the input pulses are displaced from true coincidence by 15 or more psecs. At this point we effectively have a PMT time gate that is limited by the transit time spread of the PMT itself. Careful attention to minimizing the transit time variation by tightly focusing the monochromator output on the center of the PMT photocathode or by using a crossed field photomultiplier (29) will be necessary to push this approach to its time resolution limit. Figure 11 illustrates this MLLRS configuration. Our calculations indicate that we should be able to reject sufficient fluorescence with a 50 psec laser pulse and $t_R = 50$ psec to approach 95% of the signal shot noise limited S/N even for a fluorescence lifetime as short as 2.0 nsec.

CONCLUSION

The MLLRS technique has been shown to be effective in suppressing fluorescence background signals which in-

(26) A. Dienes, E. P. Ippen, and C. V. Shank, *Appl. Phys. Lett.*, **19**, 258 (1971).

(27) E. P. Ippen, C. V. Shank, and A. Dienes, *Appl. Phys. Lett.*, **21**, 348 (1972).

(28) F. O'Neill, *Opt. Commun.*, **6**, 360 (1972).

(29) R. Miller and N. Wittwer, *IEEE J. Quantum. Electron.*, **1**, 49 (1965).

terfere with the measurement of Raman spectra. Further development work is, of course, necessary before the full fluorescence rejection power of MLLRS is routinely applicable in Raman spectroscopic studies; however, the preliminary experiments reported here suggest an excellent prognosis. The unique feature of MLLRS as compared to other pulsed Raman experiments based on Q-switched (14) or cavity dumped (15) lasers is the ability to reject very short-lived, instantaneous risetime luminescence signals. In addition, the average power available from a mode-locked laser is sufficiently high that the time discrimination advantage of the pulse laser technique in improving S/N is not lost as was the case with the cavity dumping scheme reported by Reed. Furthermore, once the SCA time gate on the MLLRS instrument is set up, the operational features of recording a MLLRS spectrum are identical to those of conventional Raman spectroscopy.

Although long lifetime emissions can be rejected by MLLRS (see Figure 2), the efficiency of rejection is limited because of luminescence overlapping between the closely spaced mode-locked pulses. It is quite probable that a combination of a mode-locked laser for short lifetime fluorescence rejection and a cavity dumped laser for long lifetime rejection coupled with the TAC/SCA photomultiplier time gate or the AND gate configuration will prove to be the most convenient instrumental arrangement for handling a wide variety of samples.

APPENDIX

Derivation of Equation 8. Consider a pulse train consisting of $i = 1, 2, 3, \dots, k$ pulses of the type pictured in Figure 1. The spacing between pulses is t_M . If $t_M < 4\tau_L$, then pulse overlapping must be accounted for in an expression for F_L . F_L is the fraction of luminescence photons accepted during the time the PMT detector gate is open and includes contributions from preceding pulses as well as the pulse under consideration. If we focus attention specifically on the k th pulse and measure time $t = 0$ from the leading edge of pulse $i = 1$, then the detector time gate extends from $t = (k-1)t_M$ to $(k-1)t_M + t_R$. F_L is defined as:

$$F_L = \frac{\sum_{i=1}^{k-1} f_{L,i} + f_{L,k}}{f_{TOTAL,k}} \quad (A-1)$$

where $f_{L,k}$ is the fraction of luminescence photons in the k th pulse between $t = (k-1)t_M$ and $t = (k-1)t_M + t_R$; the Σ represents the contributions of the preceding $(k-1)$ pulses in the gate interval of the k th pulse; and $f_{TOTAL,k}$ is the total number of luminescence photons in the k th pulse.

For a delta function excitation, the time distribution of luminescence photons for the pulse train is:

$$N_L(t) = C_L [e^{-t/\tau_L} + e^{-t-\tau_M/\tau_L} + \dots e^{-t-(k-1)\tau_M/\tau_L}] \quad (A-2)$$

and for an arbitrary excitation pulse shape function, the pulse train is represented as:

$$N_L^{(i)}(t) = C_L \int_0^t G(t-\lambda) \sum_{i=1}^k \exp[-\lambda - (i-1)t_M/\tau_L] d\lambda \quad (A-3)$$

Taking the temporal distribution for the k th pulse and integrating over the gate interval, we evaluate $f_{L,k}$ as:

$$f_{L,k} = \int_{(k-1)t_M}^{(k-1)t_M+t_R} \int_0^t G(t-\lambda) \exp[-\lambda - (k-1)t_M/\tau_L] d\lambda dt \quad (A-4)$$

Similarly for the preceding pulse contributions, we have:

$$\sum_{i=1}^{k-1} f_{L,i} = \sum_{i=1}^{k-1} \int_{(i-1)t_M}^{(i-1)t_M+t_R} \int_0^t G(t-\lambda) \exp[-\lambda - (i-1)t_M/\tau_L] d\lambda dt \quad (A-5)$$

and integrating over the totality of the k th pulse to evaluate $f_{TOTAL,k}$ we get:

$$f_{TOTAL,k} = \int_{(k-1)t_M}^{\infty} \int_0^t G(t-\lambda) \exp[-\lambda - (k-1)t_M/\tau_L] d\lambda dt \quad (A-6)$$

Substituting the above results into Equation A-1 and taking the limit as the number of pulses becomes very large, we have the final expression for Equation 8.

$$F_L = \frac{\lim_{k \rightarrow \infty} \sum_{i=1}^k \int_{(i-1)t_M}^{(i-1)t_M+t_R} \int_0^t G(t-\lambda) \exp[-\lambda - (i-1)t_M/\tau_L] d\lambda dt}{\int_{(k-1)t_M}^{\infty} \int_0^t G(t-\lambda) \exp[-\lambda - (k-1)t_M/\tau_L] d\lambda dt} \quad (8)$$

ACKNOWLEDGMENT

The authors are indebted to Kenneth G. Spears for helpful discussions and technical expertise. In addition we would like to cite Coherent Radiation Laboratories for the loan of the Model 465 mode-locked and Bruce Gregg of Ortec Incorporated for arranging the loan of the zero crossing discriminator and other electronic logic modules used in the testing of the MLLRS concept.

Received for review June 12, 1973. Accepted September 13, 1973. This work has been supported in part by the National Science Foundation Grants GP 32953 and GP 28878.

Information Content of Mass Spectra as Determined by Pattern Recognition Methods

J. B. Justice and T. L. Isenhour

Department of Chemistry, University of North Carolina, Chapel Hill, N.C. 27514

Six pattern recognition methods are compared for their ability to extract information of importance to chemists from a data set of mass spectra. Predictive ability increases in the order Sum Spectra < Binary Spectra < Normalized Sum Spectra < Nonlinear Transform = Learning Machine < Nearest Neighbor. The effect on prediction of including more than one near neighbor is also examined and shown to result in poorer prediction

This study has a twofold purpose. One is to compare methods of predicting chemical properties from the mass spectra of compounds. The second is to develop an idea of the ability of mass spectra to answer questions of chemical interest. The predictive ability is an indication of the information inherent in the spectra, as related to the property predicted.

Mass spectra contain a wealth of structural information. However, extracting this information is not easy. In this study, pattern recognition methods were applied to low resolution mass spectra to determine the information content of the data as related to functional group presence and structural properties of compounds. For some properties, the information may not be present in the mass spectra, for example, *d* and *l* conformational isomers. Information about other properties may be stored in the data in such a form as to be unrecognizable. This study shows the extent to which the information is present as a linear function of the intensities in the mass spectra and illustrates how some structural properties are more easily recognized than others.

The methods used in this paper are all pattern recognition approaches to interpretation of data (1, 2). A function is developed that in some way describes a characteristic of the data. Generally the data set is divided into two or more categories and functions approximating each category are calculated. The differences in the calculated functions are then used for predicting properties of unknown patterns. The better a function can predict the proper category of unknown compounds, the more characteristic it is of the category.

The differences in the functions describing each category are more important than the functions themselves as far as predicting structural properties are concerned. A descriptor that perfectly classifies carbonyl spectra is of no use if it gives the same results for noncarbonyl compounds.

The first four discriminant functions calculated in this study are the differences of descriptive functions of each class. Three are linear and one is a nonlinear function of the intensities in the mass spectra. The linear discriminant functions describe planes separating classes in the *n*-dimensional pattern space of the spectra. Given a particular structural property, for example, the presence of a

triple bond, if the information sought were a perfect linear function of the intensity data, all spectra of compounds containing triple bonds would occur on one side of this plane while all remaining spectra would be on the opposite side of the decision plane. Therefore, the predictive ability of the decision function is an indication of the linearity of the relationship between a given structural property and the spectral intensities. Function four is a nonlinear function of the intensities and therefore the decision function generates a nonplanar surface. By not constraining the surface to a plane, a closer approximation to the true surface separating the two classes is made with concomitantly higher prediction.

METHODS

Each of the above methods was applied to 630 low resolution mass spectra taken from the American Petroleum Institute Research Project 44 tables. Calculations were done on an IBM 360/75, and Raytheon 706 and 704 computers. All programs were written in FORTRAN IV.

The approaches were evaluated by calculating a decision function using all but one spectrum and then predicting on the one "unknown" spectrum. This spectrum was then included in the function and the contribution of another spectrum removed. The removed spectrum was used for prediction and reincluded in the decision function. This process was repeated for the entire data set. In this manner, all compounds in the data were tested as unknowns.

Sum Spectra. An obvious first choice of describing a class of compounds is to calculate the average spectrum of the class. For example, one calculates the average spectrum of carbonyl compounds and the average spectrum of noncarbonyl compounds. An unknown compound is then classified by its relative distance from the means of the two classes.

$$M_1 = \frac{\sum_{i=1}^{n_1} X_{1i}}{n_1} \quad (1)$$

$$M_2 = \frac{\sum_{i=1}^{n_2} X_{2i}}{n_2} \quad (2)$$

where X_{1i} = *i*th spectrum in category 1 and X_{2i} = *i*th spectrum in category 2.

The *a priori* probabilities of the categories are included as follows:

$$M'_1 = \frac{n_1 M_1}{n_1 + n_2} \quad (3)$$

$$M'_2 = \frac{n_2 M_2}{n_1 + n_2} \quad (4)$$

where n_1 = number of compounds in class 1 and n_2 = number of compounds in class 2.

The decision vector is then:

(1) G. S. Sebestyen, "Decision-Making Processes in Pattern Recognition," The Macmillan Co., New York, N.Y., 1962.

(2) N. J. Nilsson, "Learning Machines," McGraw-Hill Book Co., New York, N.Y., 1965.

$$D = M'_1 - M'_2 \quad (5)$$

If the product of D and the unknown spectra is positive, the unknown is assigned to the category whose mean is M'_1 . If negative, it is assigned to the category of M'_2 .

Normalized Sum Spectra. An improvement on the above approach is to adjust the spectra so that each spectrum contributes equally to the average vector. Each spectrum is normalized by the sum of intensities in the spectrum.

$$X'_{ij} = \frac{X_{ij}}{\sum_{j=1}^m X_{ij}} \quad (6)$$

where m = number of mass positions and x_{ij} = intensity of j th mass position in the i th spectrum.

Binary Spectra. In order to test the information inherent in the intensities at each mass position, the data were reduced to peak/no peak spectra. Groth (3) has studied the information loss when mass spectra are reduced to peak/no peak form and found that non-identical compounds rarely produce identical binary spectra. All intensities greater than 1% were set equal to 1 while all less than 1% were set equal to 0. The means were calculated from these binary data. In the mean vectors for each class, the value in any mass position corresponds to the probability of a peak being present in a spectrum of that class. Mass positions of equal probabilities for the two classes result in a null contribution to the decision vector.

Nonlinear Transformation. This method (4) also consists of summation and calculation of means, but a nonlinear transformation is applied to the data before summation.

The transformation consists of:

$$T(I) = (e^{2I/M})^s \quad (7)$$

where I = intensity of peak and M = maximum intensity + 1.

This transformation is applied to each mass position to give a complex valued transformed mass spectrum. The transformed spectra are summed and the complex mean is calculated. The decision vector is then:

$$D = W_1 - W_2 \quad (8)$$

where W_1 = complex mean of class 1 and W_2 = complex mean of class 2.

Prediction is then accomplished by taking the product of D and an unknown spectra and noting whether the real part is positive or negative.

Nearest Neighbor Classification. The nearest neighbor approach (5, 6) is conceptually different from the four previous methods. Asserting that the best description of the data is the data themselves, a comparison is made between the unknown spectra and each of the compounds in the data set. The euclidian distance in n -dimensional space (where n is the number of mass positions) is measured using:

$$\text{DISTANCE}_j = \left[\sum_{i=1}^n (U_i - X_{ij})^2 \right]^{1/2} \quad (9)$$

where n = number of dimensions, X_j = j th spectra in the data set, and U = unknown.

The unknown is then classified according to the class of the nearest compound in the data set. Other methods of

- (3) S. L. Groth, *Anal. Chem.*, **43**, 1362 (1971).
 (4) J. B. Justice, D. N. Anderson, T. L. Isenhour, and J. C. Marshall, *Anal. Chem.*, **44**, 2087 (1972).
 (5) T. M. Cover and P. E. Hart, *IEEE Trans. Info. Theory*, **IT-13**, 21 (1967).
 (6) B. R. Kowalski and C. F. Bender, *Anal. Chem.*, **44**, 1405 (1972).

measuring distance are possible.

A modification of the nearest neighbor approach is to use the K -nearest neighbors. One vote is assigned to each of the K neighbors and a poll taken to determine the class of the unknown. Various weighting methods may be applied to the votes. In this work, the votes were weighted by dividing each vote by the distance and by the square of the distance from the unknown spectra.

$$\text{PREDICTED CLASS} = \frac{\sum_{i=1}^K \frac{V_i}{D_i}}{\sum_{i=1}^K \frac{V_i}{D_i^2}} \quad (10)$$

where $V_i = +1$ for class 1 and -1 for class 2, D_i = distance from unknown spectra, and K = number of knowns used. The result is either positive or negative, and the unknown is assigned to the positive or negative class accordingly.

Learning Machines. A learning machine (7) is a completely nonparametric approach to classification in which a classifier is developed by training on the data. The training consists of starting with an initially arbitrary vector and modifying it based on its ability to classify spectra in the data set. Negative feedback is used to alter the weights assigned to each mass position in the vector until the vector of weights needs no further modification to correctly classify all the spectra in the data set. By converging to a solution, the weight vector has learned to predict a specific characteristic of the data.

Mathematically the training is represented by:

$$W' = W - \left(\frac{2s}{X_i X_i} \right) X_i \quad (11)$$

where W' = corrected weight vector, W = previous weight vector, s = correction increment, and X_i = i th spectra in the training data set.

Error correction continues until W converges to a solution. If W converges, then the training set is linearly separable.

Prediction is accomplished by taking the product of W and the unknown spectra.

$$\text{PREDICTED CLASS} = U \cdot W \quad (12)$$

If the result is positive, the unknown is assigned to the positive training class, and if negative, to the negative class.

It is not necessary that the X_i be the original patterns. A transformation is sometimes applied (8) and training done on the transformed data.

RESULTS

The results are shown in Tables I and II and Figures 1 and 2. In Table I, the rate of correct prediction is recorded for each structural property and for average overall prediction by each method. The results for any one property are similar for all methods. Generally, the nearest neighbor approach gave more accurate results than methods based solely on the means of the classes. This is to be expected because the decision vector approach reduces the information from an entire class of vectors to a single vector. The nearest neighbor method, on the other hand, retains all the original vectors.

In the study of learning machines applied to mass spectra (3), the data set was divided into two separate data sets consisting of 387 hydrocarbons in one and 243 oxygen and nitrogen compounds in the other. This precludes di-

- (7) T. L. Isenhour and P. C. Jurs, *Anal. Chem.*, **43** (10), 20A (1971).
 (8) L. E. Wangen, N. M. Frew, T. L. Isenhour, and P. C. Jurs, *Appl. Spectrosc.*, **25**, 203 (1970).
 (9) P. C. Jurs, B. R. Kowalski, T. L. Isenhour, and C. N. Reilly, *Anal. Chem.*, **42**, 1387 (1970).

Table I. Predictive Abilities of Six Pattern Recognition Methods

Property	Sum spectra	Binary spectra	Normalized sum spectra	Nonlinear transformation ^a	Nearest neighbor	Learning machine ^b	
						CH compounds	CHON compounds
Oxygen	88.9	91.0	85.6	88.3	91.6	...	93.5
Nitrogen	91.3	88.9	92.5	90.3	94.9	...	91.4
Amine	94.6	91.9	95.4	92.9	95.6	...	92.5
Carbon-4	89.1	91.3	89.7	92.1	89.4	97.3	82.8
Carbon-5	83.2	85.2	86.7	86.4	88.4	97.9	80.0
Carbon-6	80.2	83.8	84.0	85.2	89.5	94.1	83.9
Carbon-7	82.1	84.1	83.5	88.1	89.2	93.6	90.3
Carbon-8	81.9	85.6	...	85.4	88.9	92.5	87.1
Carbon-9	88.6	89.5	88.9	90.5	91.1	89.3	94.6
Double bond-1	82.5	82.4	82.1	82.5	86.2	77.5	88.2
-2	95.2	95.1	95.2	95.2	95.7	92.5	94.6
-3	98.1	98.4	98.3	98.3	97.1	98.4	94.6
Methyl	85.4	87.1	87.9	88.7	88.9	89.3	85.0
Phenyl	97.0	97.0	96.8	96.8	96.8
C _n H _{2n}	94.1	96.8	97.6	96.8	97.0	96.8	91.4
C _n H _{2n+1}	96.0	97.3	97.8	95.6	95.4	96.8	87.1
Average	89.3	90.3	90.8	91.0	92.2	93.0	89.1

91.0

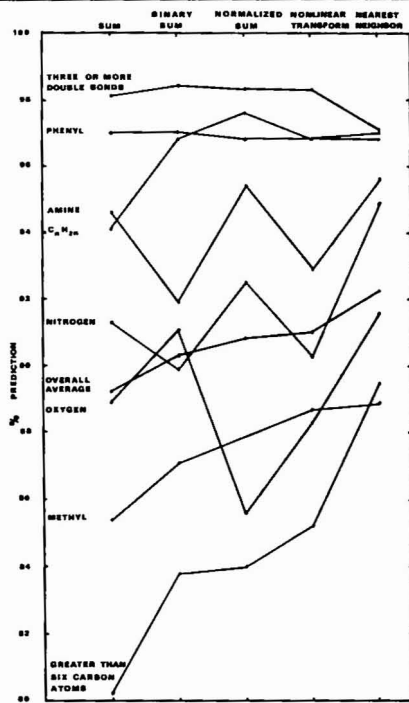
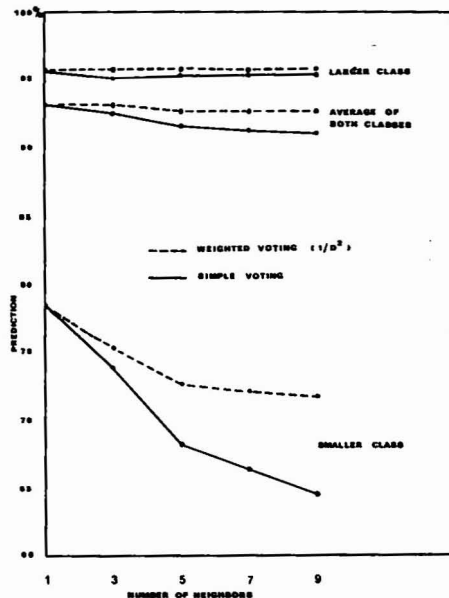
^a Ref. 4, ^b Ref. 9.

Figure 1. Per cent prediction of five pattern recognition methods for eight structural properties

Table II. Nearest Neighbor Prediction as a Function of Number of Neighbors

K	Weighted Voting (1/Distance) ²				
	1	3	5	7	9
Total	93.3	93.2	92.7	92.8	92.8
Larger class	95.8	95.9	95.6	95.8	95.8
Smaller class	77.7	75.3	72.7	72.1	71.9

Simple Voting (Unweighted)					
K	1	3	5	7	9
Total	93.3	92.7	91.6	91.4	91.2
Larger class	95.8	95.2	95.5	95.5	95.7
Smaller class	77.7	73.9	68.2	66.6	64.7


Figure 2. Per cent prediction as a function of number of neighboring spectra used

rect comparison with the results in columns 1-5 of Table I because one would expect results to be better on the more homogeneous data sets. The results do establish an upper bound for learning machine prediction based on the entire data set so that some comparisons can be made. As the overall average line in Figure 1 illustrates, the predictive ability increases in the order Sum Spectra < Peak/No Peak < Normalized Sum Spectra < CNDF = Learning Machine < Nearest Neighbor.

Calculating the means of the original spectra gave the lowest prediction rate. That the reduction to binary intensities improved prediction not only indicates that there is considerable information in binary spectra (3), but also suggests that there may be considerable noise in the original spectra as related to the identification of structural properties. The relative success of each method depends on the particular structural properties studied. Peak/no peak prediction was better than summation of the original spectra in determining the number of carbon atoms. This indicates information related to the carbon structural frame of the molecule may be obscured by functional groups whose presence adds nonlinear noise to the intensity data relevant to the carbon skeleton. Normalizing the spectra before summation resulted in improved prediction, as did applying a nonlinear transformation.

Examination of the effectiveness of the methods on individual structural properties reveals that phenyl groups, 3 or more double bonds, carbon/hydrogen ratio, nitrogen presence, and the amine functional groups were identified with greatest accuracy. Number of carbon atoms and the presence of one double bond were lowest in predictability.

Figure 2 illustrates expansion of the nearest neighbor method to include three, five, seven, and nine nearest neighbors. Overall prediction decreased as number of neighbors increased. The greatest effect occurred in the smaller of the two classes of each property and was most severe in the very small classes (approximately 50 compounds). The results are attributable to the larger class having a greater *a priori* probability of including compounds in the nearest neighbors of the unknown as the number of known neighbors used for prediction increases.

CONCLUSIONS

Six pattern recognition methods have been tested for their ability to extract information of importance to chemists from a data set of 630 low resolution mass spectra. Four of these methods involved calculation of a mean. Normalizing the spectra was shown to improve the ability of the mean to describe the data set. Little or no information was lost when the data were reduced to binary form. A nonlinear transformation applied to the data before calculation of the mean improved prediction, indicating the

classification information may be a nonlinear function of the intensities in the spectra.

The structural property information is most linearly related to the intensities in phenyl groups, 3 or more double bonds, carbon/hydrogen ratio, and nitrogen and amine presence. When prediction is improved markedly by reduction to binary data, the indication is that a close to linear relationship exists but is obscured by noise.

The nearest neighbor method resulted in generally higher predictive ability; however, this method suffers from the amount of computation necessary to determine the nearest known compound of the entire data set. Inclusion of more neighboring compounds in the prediction formula led to generally poorer prediction. Weighting the contribution of the neighboring compounds retained predictive ability somewhat, but did not improve it.

The learning machine approach was shown to be better than the methods using the means of the original data. This is encouraging because the amount of information capable of being stored by each method is the same. The learning machine is therefore more efficient in this respect. The learning machine method generally gave lower prediction rates than the nearest neighbor method. This is to be expected for the reason cited previously—*i.e.*, that the information has been reduced to a single vector.

From the overall results, some conclusions can be drawn about the ability of mass spectra to answer questions concerning the presence of functional groups and structural moieties in compounds. However, it must be borne in mind that any conclusions are ultimately determined by the data being analysed. The 630 mass spectra are only a small sample of the total recorded spectra and the total recorded spectra are but a small part of the number of chemical compounds in existence. Analysis of a larger quantity of data may modify the conclusions presented here.

For some groups and properties, the mass spectrum can determine presence or absence with almost 100% accuracy. Other properties are not so well characterized by mass spectra.

Since prediction was not perfect using any of the methods, one may infer that the information sought either doesn't exist or is stored in a manner which was not resolved by any of the six approaches. Apparently, the information is stored in a nonlinear manner which can be approximated by a linear function, to a greater or lesser degree of accuracy, depending on the information sought.

Received for review July 5, 1973. Accepted September 17, 1973. T. L. Isenhour is an Alfred P. Sloan Research Fellow, 1971-73.

Analysis of the Polychlorinated Biphenyl Problem

Application of Gas Chromatography-Mass Spectrometry with Computer Controlled Repetitive Data Acquisition from Selected Specific Ions

James W. Eichelberger, Lawrence E. Harris, and W. L. Budde¹

Environmental Protection Agency, National Environmental Research Center, Analytical Quality Control Laboratory, Cincinnati, Ohio 45268

The polychlorinated biphenyls are a difficult-to-analyze class of environmental contaminants because of the large number of possible individual isomers and their physical and chemical similarity to the chlorinated hydrocarbon pesticides. Individual mass monitoring techniques were examined in search of a procedure which is sufficiently sensitive, but which eliminates the need for elaborate separations, and does not sacrifice too much of the qualitative information content inherent in a complete mass spectrum. Several sets of candidate masses were evaluated using PCB's mixed with certain pesticides which are likely to be in a solvent extract of an environmental sample. The method was also tested with a contaminated sediment sample from an Ohio lake and appears useful for both qualitative and quantitative analyses.

The polychlorinated biphenyls (PCB's) are widely discussed environmental contaminants which have been observed in air, water, sediment, and food chain samples (1-3). Qualitative and quantitative analyses of these mixtures of mono to perchloro position isomers are complicated by the large number of possible individual isomers and by the physical and chemical similarity of this set of compounds to the chlorinated hydrocarbon pesticides, e.g., DDT, DDE, lindane, dieldrin. In an excellent review of the chromatographic and biological aspects of PCB's, Fishbein (4) points out the difficulty of analytical detection and separation of these materials. A suitable analytical method should combine high sensitivity with high qualitative information content in the response in order to obviate the need for elaborate separations and cleanup.

All reported analytical procedures for PCB's employ some type of separation of isomers and closely related compounds. Since most of these compounds are mildly polar non-ionic organic compounds, they are amenable to gas chromatography which has been employed widely. Several standard detectors respond to these compounds at environmentally significant levels, and the selective electron capture detector is capable of detecting these compounds well into the subnanogram level. However, it is now widely recognized that the qualitative information content in these detector responses is small and inadequate for analyses of mixtures of PCB's, chlorinated hy-

drocarbon pesticides, and other organic environmental pollutants.

The application of a mass spectrometer as a chromatographic detector generates the necessary qualitative information but with a substantial loss in sensitivity—perhaps a factor 10^3 – 10^5 . A conventional mass spectrometer, which focuses on the detector each sequential ion in the required mass range of about 50–500 amu, spends only a very small fraction of the total scan time focusing ions of significant information content. Perhaps for as much as 95–99% of the total scan time, the spectrometer is not focusing ions on the collector or is focusing ions which do not contain relevant information. During these periods, significant information-containing ions are continuously generated in the ion source and literally discarded with the resultant wasted sensitivity. This occurs whether the spectrometer is operated in a continuously rescanning mode (5) or not.

Substantial gains in sensitivity have been reported (6) where it was possible to rapidly switch focusing between several ions of known significance to the problem. This was accomplished with a magnetic deflection instrument by a device which quickly modified the accelerating potential; however, the technique was limited to a maximum of three ions separated by a factor of 10% in mass.

The development of the digital computer controlled quadrupole mass spectrometer (7) opened the possibility of extensive use of program controlled data acquisition with sampling of specific ions, sequences of ions, and varying dwell times on each. Data acquisition from subsets of the ions used in conventional operations should enhance sensitivity without significant loss of information content. This technique is not the same as the "mass chromatogram" concept (8) which used conventional data acquisition, with the wasted ions, but displayed the change in abundance of selected ions under program control to facilitate interpretation.

The application of subset data acquisition techniques to the problem of analyses of PCB's is attractive because of the possibility of gaining needed sensitivity without sacrificing too much of the qualitative information content inherent in a complete mass spectrum. A major problem was to define which of the many ions from the large number of isomers it was most advantageous to utilize in the method.

This paper reports the results of our study of the use of subset data acquisition techniques with a minicomputer

¹ To whom correspondence should be addressed.

(1) *Chem. Eng. News*, Dec. 13, 1971, p 32.

(2) *Science*, 175, 155 (1972).

(3) C. G. Gustafson, *Environ. Sci. Technol.*, 4, 814 (1970).

(4) L. Fishbein, *J. Chromatogr.*, 68, 345 (1972).

(5) R. A. Hites and K. Biemann, *Anal. Chem.*, 39, 965 (1967).

(6) C.-G. Hammar, B. Holmstedt, and R. Ryhage, *Anal. Biochem.*, 25, 532 (1968).

(7) W. E. Reynolds, V. A. Bacon, J. C. Bridges, T. C. Coburn, B. Halpern, J. Lederberg, E. C. Levinthal, E. Steed, and R. B. Tucker, *Anal. Chem.*, 42, 1122 (1970).

(8) R. A. Hites and K. Biemann, *Anal. Chem.*, 42, 855 (1970).

controlled quadrupole mass spectrometer. The system was equipped with a gas chromatograph inlet system and is the basis for a highly sensitive qualitative and quantitative analytical procedure for the analyses of PCB's in the environment. The technique is clearly adaptable to a variety of other analyses.

EXPERIMENTAL

Materials. The commercial polychlorinated biphenyl mixtures were obtained from the Monsanto Company, St. Louis, Mo. The mixture of seven characterized chlorinated biphenyl isomers was obtained from the Contaminants Characterization Program, Environmental Protection Agency, Southeast Environmental Research Laboratory, Athens, Ga. 30601. The characterization data will be published in a future report. The pesticides DDD, DDE, DDT, and dieldrin were provided by the Pesticide Repository of the Ferrine Primate Laboratory, Environmental Protection Agency, P.O. Box 490, Ferrine, Fla. 33157. Solvents were the best available from the Burdick & Jackson Laboratories, Muskegon, Mich. 49442. Solutions were stored in glass containers with Teflon (Du Pont) lined lids.

Instrumentation. The gas chromatograph was a Varian Model 1400 modified by removal of its conventional detector. All separations were conducted with a 6-ft coiled glass column (i.d. 0.078 in.) packed with 1.5% OV-17 plus 1.95% QF-1 on Gas-Chrom Q 100/120 mesh. Carrier gas was helium at 30 ml/min. The injector temperature was 220 °C and the column 180 °C.

The effluent was directed through an all glass jet type enrichment device and an all glass transfer line into the ion source of a Finnigan Model 1015 quadrupole mass spectrometer. Enrichment device and transfer line temperatures were maintained at 200-220 °C.

The spectrometer was scanned by applying a mass set voltage to the quadrupole rods from a 15-bit digital-to-analog converter. At a given mass set voltage, only ions of a specific mass-to-charge ratio pass through the quadrupole field to the electron multiplier detector. The system operator controls the mass set voltages through a PDP-8/E computer (4096 12-bit words) and a control program. The program uses calibration data and operator entered mass numbers, mass ranges, or subsets of mass ranges to generate appropriate 15-bit numbers to drive the digital-to-analog converter. Thus it is possible for an operator to specify a nearly inexhaustible variety of scan sequences. On a signal from the operator, the control program begins to generate repetitively the scan sequence until a given time has elapsed or the operator intervenes.

As part of the setup procedure, the operator specifies an integration time. This sets the time, between 1 and 4095 msec, during which the signal from the electron multiplier is integrated before it is converted by a 12-bit analog-to-digital converter into an ion abundance measurement. The abundance data are stored in a data buffer of the computer's core memory and subsequently on magnetic tape (Dec tape) or a disk. All integration times used in subset scans were selected to make the cycle time for a subset scan approximately the same as a conventional 40-400 amu scan, i.e., about 5 seconds. Thus, individual total ion abundance peaks appear at the same place on the spectrum index number (time) axis in both types of ion abundance chromatograms. The gain in sensitivity observed in a subset scan is the result of a time-averaging signal-to-noise ratio enhancement during the longer integration times.

In addition to the integration time, there is a 2.3-msec settling time for each mass set voltage. This provides more than adequate time for the rod voltages to stabilize before integration of the signal begins. All of the hardware and software required to accomplish these tasks are part of a standard Finnigan data system developed by System Industries, Inc., Sunnyvale, Calif. 94086. Software used was System Industries version D which is based on previously described concepts (7).

Scan parameters and quantities of materials used to produce data in Figures 2-6 are as follows:

Figure 2. Five nanograms of each of seven characterized polychlorinated biphenyl isomers was used in each experiment; 40-400 amu scan with an 11-msec integration time. PCB subset masses with a 540-msec integration time.

Figure 3. Two micrograms of Aroclor 1254 was used in each experiment; 150 ng of DDE, 150 ng of dieldrin, 400 ng of DDD, and 400 ng of DDT were added for the lower chromatogram; 40-400 amu scan with a 10-msec integration time.

Figure 4. 500 ng of Aroclor 1254 was used in each experiment;

100 ng of DDE, dieldrin, DDD, and DDT was added for the lower chromatogram. PCB subset masses with a 536-msec integration time.

Figure 5. Approximately 400 ng of Aroclor 1254 and Aroclor 1242; PCB subset masses with a 536-msec integration time.

Figure 6. Two microliters of concentrated sediment extract was used in each experiment; 40-400 amu with a 10-msec integration time; PCB subset masses with an integration time of 536 msec; 50 ng of Aroclor 1254; PCB subset masses with an integration time of 536 msec.

At the conclusion of each experiment, ion abundance data from each conventional or subset scan were summed, normalized, and plotted as a function of spectrum index number on a Houston plotter. However, PCB subset scan data for Table III were obtained in a different way. For this analysis, the variations in the absolute integer data from the analog-to-digital conversions were displayed for each subset mass and the individual peaks integrated.

Sediment Extract. The sediment collected from Grand Lake St. Mary's in Ohio was air dried, weighed, mixed with 10% distilled water, and extracted for 16 hr in a Soxhlet extractor with 200 ml of 90% hexane-acetone. The concentrated, dried solution was passed through Florisil and silica gel to remove the sulfur and other gross contaminants. This was necessary in this case because the sediment from the polluted lake contained a significant quantity of sulfur and sulfur gives a strong signal at mass 224, due to S₇, which is observed during a PCB mass subset scan. The full details of this procedure and the quantitative results of the sediment analyses will appear in a future publication from this laboratory.

RESULTS AND DISCUSSION

It was our goal to develop a method for PCB's which would have the following characteristics: a relatively high sensitivity to polychlorinated biphenyls; a relatively low sensitivity to other compounds including chlorinated hydrocarbon pesticides which are likely to be in an organic solvent extract of an environmental sample; a means of distinguishing between chlorinated biphenyl compounds with different degrees of chlorination; and simple implementation on the computer controlled quadrupole GC-mass spectrometer hardware and software widely utilized within the agency and other organizations.

The general characteristics of the mass spectra of polychlorinated biphenyls have been mentioned by several authors (4). In summary, these spectra are dominated above mass 180 by a series of chlorine isotopic distribution patterns whose centers of gravity are separated by about 36 amu. The most abundant ion of each cluster is usually at least 10% of the abundance of the base peak. The molecular ion is generally quite abundant at 70 eV even with a hot GC inlet system. The explanation for the series of chlorine isotope distribution patterns is obvious and these portions of the spectra are excellent examples of the power of mass spectrometry to characterize compounds by their fragmentation patterns.

Less obvious is the pathway for the formation of ions of mass 109 and 110. These ions are common to the spectra of most PCB's we have examined and there has been no detailed investigation of their structures or of the mechanisms of their formation. We presume their compositions as C₆H and C₆H₂, respectively. The relative abundance of each is a function of the degree of chlorination of the biphenyl with maximum abundance occurring with pentachloro- and hexachlorobiphenyl.

Another set of ions common to most PCB's occurs in the 149-153 mass range and are likely biphenyl ions completely stripped of chlorine atoms. The existence of these sets of common ions suggested their analytical use as selective monitors of the presence of PCB's in a sample. The continuously rescanning subset data acquisition technique was applied to the GC effluent from several mixtures of PCB's and chlorinated hydrocarbon pesticides using

masses 109, 110, and the 149-153 range as PCB monitors. We concluded that these masses were unsuitable for this purpose because many compounds, including pesticides, generate a low level background of ions of these masses and other masses below mass 180 and our goal of high selectivity could not be attained by using them.

Because of the large number of compounds and position isomers present in the PCB mixtures, an idealized set of mass spectra of the chlorinated biphenyls above mass 180 was prepared as a model to guide the selection of suitable ions for specific monitoring. The idealized spectra in Figure 1 assume exclusive fragmentation of all the molecular ions by sequential or simultaneous losses of chlorine atoms. The model spectra, which cover the range from mono- to hexachlorobiphenyl, were simplified further by ignoring all contributions from ^{13}C atoms, by setting the most probable ion of each cluster to the same relative abundance, and by assuming all position isomers have the same fragmentation pattern.

In reality, loss of chlorine atoms is the dominant mode of fragmentation in most of the PCB mass spectra we have examined. Biphenyls substituted by only a few chlorine atoms do tend to lose HCl which causes the clusters to shift by one mass unit and this may vary slightly depending on the particular position isomer being observed.

The probability of the occurrence of a single ^{13}C atom in a biphenyl nucleus will cause ions of about 12% of the abundance of the pure ^{12}C ion to be interspersed at alternate mass units in the clusters. However, since the probability of two ^{13}C atoms appearing in a single molecule is very small, the effect of ^{13}C on the patterns shown in Figure 1 will be negligible under ordinary operating conditions on an ordinary mass spectrometer.

Finally, actual relative abundances of the clusters will vary widely with the type of mass spectrometer, the operating parameters used, the inlet system, the condition of the equipment, and the particular compound or position isomer being observed. In practice it is possible, with the quadrupole spectrometer, to observe almost anything from a dominant molecular ion and relatively few fragment ions to about equal distribution of molecular and fragment ions to relatively little molecular ion. These instrumental variations are caused by the adjustment of rod and ion source potentials, the presence of carbon deposits on the rods or ion source, and other factors in the electronics of the separation and detection system.

It is clear from Figure 1 that continuous monitoring of the ions of mass 290 in a PCB gas chromatographic effluent will not give a unique response for a tetrachlorobiphenyl molecular ion. Mass 290 also corresponds to the ^{13}C ion from the $^{35}\text{Cl}_4$ fragment ion of a pentachlorobiphenyl molecular ion, and to the $^{35}\text{Cl}_3^{37}\text{Cl}$ fragment ion from a hexachlorobiphenyl molecular ion. Similar considerations hold for the pure ^{35}Cl ions and some isotopically mixed ions of all other PCB molecular ions. Bonelli (9) repeatedly scanned the mass range 50-410 during the GC of a PCB mixture and plotted the change in abundance of the ions of mass 290-291. Although this "mass chromatogram" showed several peaks, suggesting the presence of a tetrachlorobiphenyl compound, the complete mass spectrum corresponding to one of these was interpreted by us with the aid of Figure 1 as that of a mixture of pentachloro- and hexachlorobiphenyls.

Similar overlapping of molecular and fragment ion masses occurs with other chlorinated biphenyls, although clearly the amount of overlap depends on the mix of isomers, extent of fragmentation, type of fragmentation, i.e., loss of Cl or HCl, etc. Overlapping does not preclude the

(9) E. J. Bonelli, *Amer. Lab.*, February, 1971, p. 27.

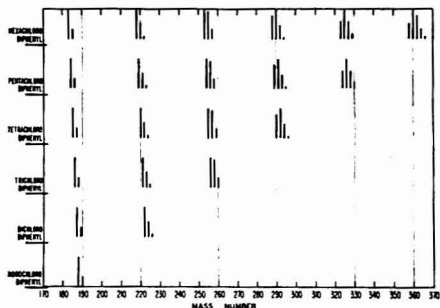


Figure 1. Idealized mass spectra of mono- to hexachlorobiphenyls above mass 180

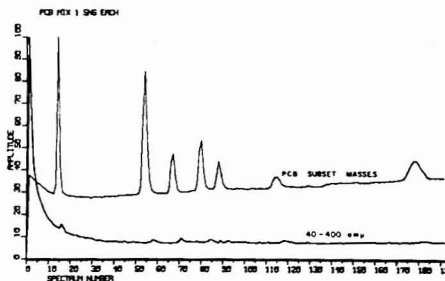


Figure 2. Ion abundance chromatograms of a mixture of 5 ng of each of seven pure PCB isomers. Lower chromatogram monitors masses 40-400; upper chromatogram monitors the PCB subset masses

use of such masses as monitors of the presence of PCB's and does, in fact, enhance sensitivity, since several different compounds contribute to the ionic abundance. However, careful selection of the ionic masses can give the desired increase in sensitivity as well as some selectivity in terms of the level of chlorination.

The ion of mass 190 in the molecular ion cluster of monochlorobiphenyl has only one-third the theoretical abundance of the mass 188 ion; however, overlap with monochloro fragment ions of more chlorinated biphenyls is minimal, being limited essentially to the ^{13}C ion of the ^{37}Cl fragment of dichlorobiphenyl. Similar considerations hold for ions of masses 224, 260, 294, 330, and 362, where overlap is restricted to a theoretically much less abundant ion assuming the same overall abundance of the molecular and fragment ions. Heptachlorobiphenyls might reasonably be monitored by the relatively more abundant mass 394 ion since very little octachlorobiphenyl is expected in any PCB mixture.

Figure 2 shows two chromatograms constructed from the ion abundance data obtained during the chromatography of a mixture of 5 ng of each of seven pure chlorinated biphenyl isomers. Table I reveals the identity and concentration of the pure isomers. The lower curve was generated from ion abundance data obtained during repetitive scans of the mass range 40-400 amu with an integration time of 11 msec on each integer mass unit. The upper curve was generated from ion abundance data obtained during repetitive scans of the PCB subset masses 190, 224, 260, 294, 330, 362, and 394 with an integration time of 540 msec on each. Total 40-400 amu and PCB subset cycle

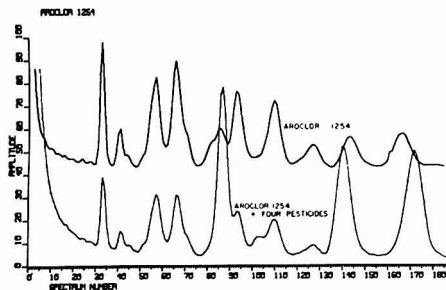


Figure 3. Ion abundance chromatograms from repetitive scans of the mass range 40-400 amu. Upper chromatogram monitors a PCB mixture, Aroclor 1254. Lower chromatogram monitors Aroclor 1254 mixed with four pesticides

Table I. Chlorinated Biphenyl Isomer Mixture

Compound	Concn, ng/ μ l	Concn, $M \times 10^6$
2-Chlorobiphenyl	5.0	2.7
4,4'-Dichlorobiphenyl	5.0	2.2
2,5,4'-Trichlorobiphenyl	5.0	1.9
2,3,2',5'-Tetrachlorobiphenyl	5.1	1.7
2,4,5,2',5'-Tetrachlorobiphenyl	5.0	1.7
2,4,5,2',5'-Pentachlorobiphenyl	5.0	1.5
2,4,5,2',4',5'-Hexachlorobiphenyl	5.05	1.4

Table II. Mass Spectra in the NIH File Which Contain PCB Subset Ions

Mass	Number of non-PCB spectra found	Non-PCB spectra in file, %
190	110	1.3
224	50	0.6
260	37	0.4
294	24	0.3
330	26	0.3
362	3	0.03
394	11	0.1

times, which include the rod voltage settling times, were approximately 5 sec. Therefore, each isomer peak appears at approximately the same place on the spectrum index number (time) axis and the two experiments may be compared on the basis that each required the same overall analysis time.

The gain in signal strength as a result of PCB subset monitoring with time averaging to enhance signal-to-noise ratio is clear from Figure 2. The absolute detection limit in either experiment will vary widely and depend on a variety of factors including those mentioned previously in the discussion of the observed fragmentation patterns of PCB isomers. At the time of this experiment with the quadrupole spectrometer, it was possible to obtain a reasonably clean (signal/noise = 25) 40-400 amu mass spectrum from about 5 ng of a pure PCB isomer.

Two approaches were used to estimate the selectivity of the PCB mass subset for polychlorinated biphenyls. Table II shows the number of non-PCB mass spectra, in a file of 8782 mass spectra, which contain the PCB subset ions in the 11-100% relative abundance range. The table was prepared by utilizing a previously described interactive computer program (10) to search a file of mass spectra. The

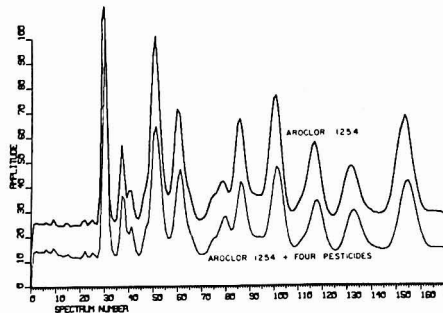


Figure 4. Ion abundance chromatograms from repetitive scans of the PCB subset masses. Upper chromatogram monitors Aroclor 1254. Lower chromatogram monitors Aroclor 1254 mixed with four pesticides

data base probably included mass spectra of most of the large volume organic compounds which may be in an organic solvent extract of an environmental sample plus many other potential pollutants. At mass 190, only 1.3% of the compounds in the file clearly interfere with the monochloro PCB monitor mass; at mass 394, 0.1% of the spectra have interferences. Since PCB's appear as mixtures of isomers which result in a series of peaks of different areas in a chromatogram (Figure 3), and since it is very unlikely that more than a few of the interfering substances would be in the same sample, we conclude that the high selectivity of the subset masses for PCB's together with the expectation of a recognizable pattern of PCB peaks limits the possibility of interfering substances being mistaken for PCB's.

The pollutants most likely to be in an organic extract of an environmental sample being analyzed for PCB's are the chemically and structurally similar persistent chlorinated hydrocarbon pesticides. These are extracted with the biphenyls and are eluted from the chromatograph with them. An ion abundance chromatogram from a commercial PCB mixture is compared in Figure 3 with a chromatogram from the same PCB mixture plus the four pesticides DDE, DDD, DDT, and dieldrin. In each experiment, the mass range 40-400 amu was repetitively scanned. Major differences in the chromatograms are clear in the regions of spectrum numbers 82-95, where *p,p'*-DDE and dieldrin elute, spectrum numbers 100-105, where *o,p*-DDD elutes, and near spectrum numbers 140 and 170, where *p,p'*-DDD and *p,p'*-DDT elute. These interferences have been the source of considerable analytical difficulties in identifying PCB mixtures by their characteristic peak patterns with conventional electron capture GC detectors. The same mixtures were chromatographed, but the PCB mass subset was repetitively scanned during elution of the components. These chromatograms are compared in Figure 4. Clearly, there is no significant interference in the PCB chromatograms by the pesticides.

It is possible to identify commercial PCB product mixtures from characteristic isomer distribution patterns observed in ion abundance chromatograms. Figure 5 shows repetitive scans of the PCB subset masses during elution of two commercial PCB mixtures. Similar identifications have been widely used in gas chromatographic analyses of PCB mixtures with the electron capture (EC) detector. However the simple EC detector is clearly far more subject to confusing interferences from a host of other electron-capturing substances than the subset scanning mass spectrometer.

(10) S. R. Heller, *Anal. Chem.*, **44**, 1951 (1972).

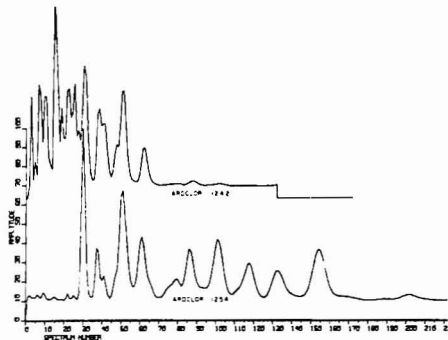


Figure 5. Ion abundance chromatograms from repetitive scans of the PCB subset masses. Upper chromatogram monitors a PCB mixture, Aroclor 1242. Lower chromatogram monitors Aroclor 1254

It would be desirable to develop a means of distinguishing between PCB compounds with different degrees of chlorination. It has been the practice to characterize PCB's found in environmental samples in terms of the commercial product mixtures and designations, *e.g.*, Aroclor 1248. While this approach has merit in pinpointing specific sources of pollution, it has several disadvantages: (a) less chlorinated biphenyl compounds are somewhat more biodegradable and environmental samples tend to become richer in the less degradable fractions; thus identification with a commercial product standard is precluded; and (b) different commercial mixtures mix in the environment and obscure identifications with standard samples. A scheme based on the relative amounts of mono-, di-, trichlorobiphenyls, etc. without regard to the specific position isomers is proposed as a meaningful way to represent PCB mixtures.

Subset mass scanning offers the possibility of a realistic method of measuring PCB's in terms of levels of chlorination. Table III shows a breakdown of the contributions to the integrated ion abundance data obtained during the chromatography of the seven pure PCB isomers with PCB subset mass scanning (Table I and Figure 2). As monochlorobiphenyl eluted, spectrum numbers 11-16, all of the integrated ion abundance was measured at mass 190. Ion abundance at other subset masses showed no significant deviation from base-line or background levels, as expected. As more chlorinated isomers emerged, interferences from fragment ions were apparent. For example, dichloro fragment ions were observed at mass 224 during the elution of tetrachlorobiphenyl isomers. However, selectivity was generally at least 80% in favor of the biphenyl actually eluting. This experiment is the basis for a method of assessing the levels of chlorination in a PCB mixture and it will be explored further in future work.

Quantitative Analysis. Quantitation of PCB's with ion abundance chromatograms from subset mass scanning is readily accomplished. For this experiment, the conventional approach was adopted and it was assumed that the PCB mixture was identified as one of the commercial mixtures. The sum of the relative ion abundance data from all the subset masses for all the PCB isomers was measured (total peak area) in three chromatograms obtained from three solutions containing 500, 300, and 100 ng, respectively, of Aroclor 1254. Each solution contained 40 ng of dimethylisophthalate which served as an internal

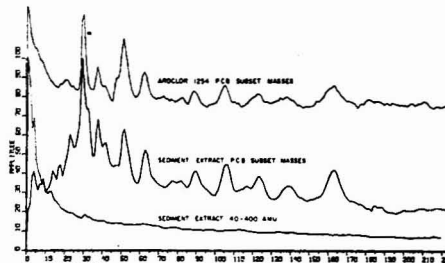


Figure 6. Ion abundance chromatograms from repetitive scans of the PCB subset masses and the mass range 40-400 amu. Lower chromatogram monitors PCB subset during sediment extract elution. Middle chromatogram monitors PCB subset during sediment extract elution. Top chromatogram monitors PCB subset during elution of a PCB mixture, Aroclor 1254

Table III. Percentage of the Integrated Ion Abundance Measured at Each Subset Mass

Compound eluting	Spectrum numbers	Subset masses					
		190	224	260	294	330	362 394
Monochloro	11-16	100	0	0	0	0	0
Dichloro	51-58	0	100	0	0	0	0
Trichloro	64-70	0	0	100	0	0	0
Tetrachloro	77-83	0	18	2	80	0	0
Tetrachloro	86-91	0	20	0	80	0	0
Pentachloro	112-119	0	0	18	0	82	0
Hexachloro	173-185	0	0	0	13	0	87

standard to normalize the PCB peak areas. A plot of total peak area against the amount of Aroclor 1254 was linear. Therefore, from this calibration, overall PCB concentrations could be calculated assuming the commercial mixture was correctly identified and the appropriate standards were used.

Application to an Environmental Sample. The PCB's like many of the persistent chlorinated hydrocarbon pesticides are water insoluble and accumulate in fatty tissue and are adsorbed on sediments beneath rivers and lakes. An extract of a sediment sample from Grand Lake St. Mary's, Ohio, was examined by GC/mass spectrometry using a conventional 40-400 amu repetitive scan. That ion abundance chromatogram is shown as the bottom trace in Figure 6. Examination of the mass spectrum at spectrum number 31 suggested the presence of a chlorinated biphenyl compound. The middle chromatogram in Figure 6 was generated by repetitive PCB subset mass scans using an identical amount of the same sample. A PCB pattern of peaks was clearly suggested. The top chromatogram was obtained by repetitive PCB subset mass scans during elution of 50 ng of Aroclor 1254.

CONCLUSION

The subset data acquisition technique with a computer controlled mass spectrometer is well suited to the analysis of PCB's in environmental samples. This technique is clearly adaptable to analyses of other environmental pollutants, *e.g.*, petroleum products, where the increased sensitivity has permitted the clear observation of molecular ions from saturated aliphatic hydrocarbons. The widespread application of computer controlled gas chromatography-mass spectrometry to problems of environmental research will no doubt result in a wide variety of other applications.

ACKNOWLEDGMENT

We wish to thank William Norris of Wright State University for the sediment sample from Grand Lake St. Mary's. Appreciation is also due Tom Bellar, of this laboratory, who extracted the sediment sample, and Ron

Webb, of the Southeast Environmental Research Laboratory, who provided the samples of characterized PCB isomers.

Received for review July 11, 1973. Accepted September 18, 1973.

Determination of the Noble Metals in Geological Materials by Neutron Activation Analysis

R. A. Nadkarni and G. H. Morrison

Department of Chemistry, Cornell University, Ithaca, N.Y. 14850

Gold, ruthenium, palladium, osmium, iridium, and platinum have been determined in geological materials using thermal neutron irradiation, selective adsorption of the noble metal group on Srafinon NMRR ion exchange resin, and high resolution gamma spectrometry. The method was used to analyze three USGS standard rocks, a meteorite, and a lunar soil sample.

The noble metals, which are strongly siderophilic and to a lesser extent chalcophilic, are important trace chemical indicators of geological processes of differentiation. A knowledge of the abundance of these elements in some meteorites is useful in estimating values for solar system atomic abundances. They provide information on the mechanisms of meteoritic and lunar evolution and permit the computation of accretion rates of cosmic material on earth and on the moon.

Because of the very low abundances of noble metals in most terrestrial materials, very few data exist on their concentrations in common igneous and sedimentary rocks, even though considerable effort has been expended to develop adequate methods for their determination. These analytical methods and techniques have recently been exhaustively reviewed (1, 2), and at the low parts-per-billion level the most widely used method is neutron activation analysis.

Instrumental neutron activation analysis has been used directly only for the determination of one or two elements—i.e., Au and Ir in favorable cases where their concentrations are high such as in meteorites, gold ores, matte, and lead assay beads (3-5). To determine all of the noble metals in a diverse variety of geological materials, radiochemical separation procedures have had to be used with neutron activation analysis. These published methods have involved fire assay, cupellation, volatilization, ion exchange, solvent extraction, and final precipitation of

individual noble metals for counting (6-19), with the disadvantages of length of time and potential losses during the radiochemical procedures.

A relatively rapid and comprehensive neutron activation method for the determination of Au, Ru, Pd, Os, Ir, and Pt in a variety of geological materials is described here, based on an ion exchange separation of these elements as a group followed by high resolution gamma spectrometry. The key aspect of the method is the use of a resin discovered in 1967 that is specific for the noble metals (20). This resin contains a guanidine group coupled to a styrene-divinylbenzene copolymer matrix. Its selectivity for noble metals is attributed to the fact that it will bind only ions with the d^8 electronic configuration forming square planar complexes. The resin has reducing properties because of the double bonds enabling it to collect species such as Pt^{4+} and Ir^{4+} which are reduced to Pt^{2+} and Ir^+ and then bound as square planar complexes.

Since publication of the original paper (20), the resin or resin-loaded paper has been used for the determination of Au (21-23) and Ir in rocks (24) by neutron activation or X-ray fluorescence spectrometry. It was also discovered that in addition to the noble metals, methylmercury and

- (1) F. E. Beamish and J. C. Van Loon, "Recent Advances in Analytical Chemistry of the Noble Metals," Pergamon Press, Oxford, 1972.
- (2) F. E. Beamish and J. C. Van Loon, *Minerals Sci. Eng.*, **4**, 3 (1972).
- (3) P. W. deLange, W. J. de Wet, J. Turkstra, and J. H. Venter, *Anal. Chem.*, **40**, 451 (1968).
- (4) J. Turkstra, P. J. Pretorius, and W. J. de Wet, *Anal. Chem.*, **42**, 835 (1970).
- (5) T. A. Linn, Jr., and C. B. Moore, *Earth Planet. Sci. Lett.*, **3**, 453 (1967).

- (6) J. H. Crockett and G. B. Skippen, *Geochim. Cosmochim. Acta*, **30**, 129 (1966).
- (7) J. H. Crockett, R. R. Keays, and S. Hsieh, *ibid.*, **31**, 1615 (1967).
- (8) J. H. Crockett, R. R. Keays, and S. Hsieh, *J. Radioanal. Chem.*, **1**, 487 (1968).
- (9) R. C. Harriss, J. H. Crockett, and M. Stanton, *Geochim. Cosmochim. Acta*, **32**, 1049 (1968).
- (10) R. Gijbels and J. Hoste, *Anal. Chim. Acta*, **41**, 419 (1968).
- (11) F. O. Simon and H. T. Millard, Jr., *Anal. Chem.*, **40**, 1150 (1968).
- (12) W. D. Ehmann, P. A. Baedecker, and D. M. McKown, *Geochim. Cosmochim. Acta*, **34**, 493 (1970).
- (13) R. R. Ruch, *Anal. Chim. Acta*, **48**, 381 (1970).
- (14) H. T. Millard and A. J. Bartel in "Activation Analysis in Geochemistry and Cosmochemistry," A. O. Brunfelt and E. Steiness, Ed., Universitetsforlaget, Oslo, 1970, p 353.
- (15) J. H. Crockett, *ibid.*, p 339.
- (16) R. R. Keays and J. M. Crockett, *Econ. Geol.*, **65**, 438 (1970).
- (17) D. E. Gillum and W. D. Ehmann, *Radiochim. Acta*, **16**, 123 (1971).
- (18) W. D. Ehmann and D. E. Gillum, *Chem. Geol.*, **9**, 1 (1972).
- (19) J. J. Rowe and F. O. Simon, *U.S. Geol. Surv. Circ.*, **599** (1968).
- (20) G. Koster and G. Schmuckler, *Anal. Chim. Acta*, **38**, 179 (1967).
- (21) T. E. Green and S. L. Law, *U.S. Bur. Mines Rep. Invest.*, **7358** (1970).
- (22) T. E. Green, S. L. Law, and W. J. Campbell, *Anal. Chem.*, **42**, 1749 (1970).
- (23) C. W. Blüunt, D. E. Leyden, T. L. Thomas, and S. M. Guill, *Anal. Chem.*, **45**, 1045 (1973).
- (24) H. A. Das, R. Janssen, and J. Zonderhuis, *Radiochem. Radioanal. Lett.*, **8**, 257 (1971).

inorganic Hg are quantitatively collected by the resin under similar conditions (25, 26).

EXPERIMENTAL

Reagents. Samples. Terrestrial rock samples analyzed included the USGS standards diabase W-1, peridotite PCC-1, and dunite DTS-1. A type C3 carbonaceous chondrite meteorite Allende was also analyzed as was lunar soil 72701 returned by Apollo 17. The samples were dried for 24 hours at 80 °C before taking aliquots for analysis.

Standards. Noble metal irradiation standards as well as the carrier solution were prepared from "Speepru" Au metal, ammonium chloroiridate $(\text{NH}_4)_2\text{IrCl}_6$, ammonium chlorosmate $(\text{NH}_4)_2\text{OsCl}_6$, ammonium chloroplatinate $(\text{NH}_4)_2\text{PtCl}_6$, ammonium chlororhodate $(\text{NH}_4)_2\text{PdCl}_6$, and ammonium chlororuthenite $(\text{NH}_4)_2\text{Ru}(\text{H}_2\text{O})\text{Cl}_6$. Appropriately diluted solutions of these were weighed out on approximately 20 mg of "Spex" high purity SiO_2 contained in quartz vials. The solutions were carefully evaporated and the vials sealed. The carrier solution contained 0.1 to 0.5 mg/ml of each of the noble metals.

Ion Exchange Resin. Srafiion NMRR resin was obtained from Ayalon Water Conditioning Co., Ltd., Haifa, Israel. It was previously marketed under the name SRXL by Ionac Chemical Co., Birmingham, N.J. The resin was soaked in 0.05N HCl for several hours before use. The resin was packed in a glass column 10 cm in length and 1.5-cm inner diameter.

Procedure. Irradiations. Geological samples weighing 0.3–0.5 gram each were sealed in high purity quartz ampoules. In the case of the lunar soil, 1.0 gram was used. The irradiation standard containing 1 to 5 μg of the individual noble metals was also sealed in a quartz ampoule. Samples and standard were irradiated in the central thimble facility of the Cornell TRIGA Mark II reactor for eight hours at a thermal neutron flux of 3.5×10^{12} n-cm⁻²-sec⁻¹. The samples were allowed to decay overnight before processing.

Radiochemical Procedure. The quartz vials were opened and the samples and standard were transferred to individual nickel crucibles. The interior of the ampoules were repeatedly washed with 8N HCl and the washings transferred to the crucibles. One milliliter of carrier solution was added to each crucible, and the solutions were carefully evaporated to dryness. Five grams of Na_2O_2 and 2 grams of NaOH were added to each crucible which was then heated to red heat. They were further heated for 10 minutes while continually swirling the contents. This fusion step ensured isotopic exchange between the added carrier and the corresponding radionuclide.

The crucibles were allowed to cool and the melts in each were dissolved in 75 ml of water in a beaker. The solutions were acidified with 8N HCl, being careful to avoid any loss by effervescence. When acidic, the solutions should be clear green in color if all of the sample has completely dissolved. The solutions were heated and oxidized by adding 2 ml of concentrated HNO_3 . The excess peroxide was destroyed by boiling. The pH of the solutions were then adjusted to 1.5–2 using dilute ammonia.

Each solution was passed through an ion exchange column at the rate of 1 ml per minute. The resin will turn from pale yellow to rose-orange color as the noble metals are adsorbed. The effluent was passed over a second resin column. The columns were then washed ten times with 10 ml each of 0.05N HCl. The resin in the two columns was transferred to a 125-ml Erlenmeyer flask and the volume adjusted to 30 ml with 0.05N HCl to provide a standard geometry for counting of samples and standard. The radiochemical procedure takes about three hours for completion.

Counting and Data Processing. The samples and standard were counted using a 30 cm³ coaxial Ge(Li) detector and 4096 channel analyzer. The system resolution was better than 2.8 KeV (FWHM) and the peak-to-Compton ratio was better than 15:1, both for the 1.332-MeV peak of ⁶⁰Co. The samples were counted at various decay periods to check isotopic half-lives. Counting times were usually on the order of one hour for the standard and 2 to 3 hours for the samples. The data from the analyzer were transferred on a magnetic tape which was then processed on a PDP-11 computer. The final computer output provided digital tables of data and calculated the peak areas corrected for background. The peaks of interest were then corrected for decay when necessary.

RESULTS AND DISCUSSION

The Srafiion NMRR resin adsorbed the noble metals and Hg at pH 0.5 to 2.5. The capacity of the resin for these elements in grams/liter is given as 150 for Au, 65 for Pt, 58 for Pd, 25 for Ir, 25 for Rh, and 75 for Hg (27). Since the only radioisotope of Rh produced by thermal neutron activation is ¹⁰⁴Rh with a half-life of 4.4 minutes, this element could not be determined using the radiochemical procedure employed in this study and will not be considered in the further discussion.

Using radioactive tracers of the noble metals and Hg in the presence of carriers of these elements, their adsorption behavior on the resin was investigated. In all cases the adsorption was 97–100% complete. Only ⁹⁷Ru and ¹⁹⁴Ir required two passes through the column to attain this level of adsorption. Another experiment was performed where two irradiated standards were passed through columns. The first was run directly, while the second was mixed with a solution prepared by dissolving 500 mg of unirradiated W-1 rock powder prior to eluting on the column. In both cases the adsorption on the resin was complete, indicating that separation is quantitative either in the presence or absence of a rock matrix.

Counting of the effluent from the standard to determine loss of the noble metals from the column revealed that the activity was 1% or less for most elements but occasionally as high as 5% for Ru and Ir. It was not possible to check the effluent from geological samples because of the presence of high activity from ²⁴Na and other isotopes formed from the major elements present in the samples.

The adsorbed noble metals can be recovered from the resin by eluting immediately after adsorption with a 5% aqueous solution of thiourea which is 0.05N in HCl. Alternatively, the resin can be slowly heated at 900–1000 °C leaving the metals in a very pure metallic form. However, in view of the quantitative adsorption of the metals on the resin, no removal step was included in the proposed procedure, and no chemical yield determinations were necessary.

Although the resin is highly selective for Hg, Au, and the platinum metals, some of the common and base metal ions can be physically retained on the column. However, washing with 0.05N HCl appears to remove this contamination as evidenced by its absence in the gamma spectra of the resin phase. Even ²⁴Na which is produced in large amounts on irradiating most geological samples was detected in only low trace amounts on the resin.

Only in the analysis of PCC-1 and DTS-1 samples was appreciable contamination of the resin spectra by ⁵¹Cr observed. Both of these rocks contain very high amount of chromium, 2730 and 4000 ppm, respectively (28). Similar adsorption of ⁵¹Cr on this resin has been observed by Das *et al.* (24). However, this in no way affected the determination of the noble metals, since the Ge(Li) detector could resolve all photopeaks of interest, without interference. Das *et al.* (24) using an NaI(Tl) detector were unable to resolve the interference of the ⁵¹Cr 320-KeV peak with the 296-, 309-, and 317-KeV peaks of ¹⁹²Ir.

Although tracer experiments indicated that Hg is quantitatively retained on the resin, analyses of geological samples using the proposed method gave consistently high results for this element. This can probably be attributed to loss or incomplete isotopic exchange in the preparation and processing of the standard. Therefore, the determination of Hg in these samples was temporarily abandoned.

(25) S. L. Law, *Science*, **174**, 285 (1971).

(26) P. J. Ke and R. J. Thibert, *Mikrochim. Acta*, **1973**, 417.

(27) Ayalon Water Conditioning Co., Ltd., Haifa, Israel, Srafiion NMRR Product Information Bulletin.

(28) F. J. Flanagan, *Geochim. Cosmochim. Acta*, **37**, 1189 (1973).

Table I. Nuclear Data (29)

Element	Isotope produced	% Abundance of target isotope	Cross-section, σ	Half-life of produced nuclide	Principal γ -ray used, MeV
Ruthenium	^{97}Ru	5.46	0.2	69.1 h	0.215
	^{103}Ru	31.5	1.4	39.5 d	0.497
Rhodium	^{104}Rh	100	11	4.3 m	0.051
Palladium	^{109}Pd	26.7	12	13.5 h	0.088
Osmium	^{191}Os	26.4	3.9	15 d	0.129
	^{193}Os	41.0	1.6	31.5 h	0.139
Iridium	^{192}Ir	38.5	750	74 d	0.317, 0.468
	^{194}Ir	61.5	110	17.4 h	0.328
Platinum	^{197}Pt	25.2	0.9	19 h	0.077
	^{199}Pt	7.19	4	30 m	...
	^{199}Au	(β -decay of ^{199}Pt)		3.15 d	0.158
Gold	^{199}Au	100	98.8	64.8 h	0.412
Mercury	$^{197\text{m}}\text{Hg}$	0.15	25	24 h	0.134
	^{197}Hg	0.15	880	65 h	0.077
	^{203}Hg	29.8	4	47 d	0.279

Table I presents the nuclear data for the elements of interest (29). In those cases where two or more isotopes of an element are produced, the shorter half-lived isotope was used where possible. Although additional gamma rays are associated with the isotopes listed, only the preferred interference-free ones have been included. Others were used for confirmation of the isotopes. A detailed discussion of the nuclear considerations and interfering reactions has been given by Gijbels (30). The (n,p) and (n, α) secondary nuclear reactions are of considerable importance in determining noble metals in other noble metals; however, in the analysis of rock samples where the concentrations of all of the noble metals are comparably low, these reactions do not pose any serious interference. In those geological samples containing uranium at levels well in excess of the noble metals, reactions such as $^{235}\text{U}(n,f)^{103}\text{Ru}$ and $^{238}\text{U}(n,f)^{109}\text{Pd}$ with a high fission yield can interfere with the determination of Ru and Pd via ^{103}Ru and ^{109}Pd , respectively. Gijbels (30) has shown using detailed calculations that for ^{109}Pd the interference is only 0.025%, whereas for ^{103}Ru it is 13%. Based on the presence of 1 ppm natural uranium, an apparent Pd content of 0.0025 ppb will be found using ^{109}Pd and a Ru content of 0.13 ppb using ^{103}Ru . Thus, the fission product contribution can be neglected in the determination of Pd. If ^{97}Ru , which is not produced by fission, is used instead of ^{103}Ru , then Ru can be determined with no interference as was the case in this study. For more detailed discussion of this problem see Gijbels (30), Crockett *et al.* (8), and Crockett (15).

Self-absorption and self-shielding problems were minimized by using standards containing less than 5 μg of each noble metal, which is about the amount present in the samples.

Platinum can be determined by counting the 19-hour nuclide ^{197}Pt or by measuring ^{199}Au , the β^- decay product of the reaction, $^{198}\text{Pt}(n,\gamma)^{199}\text{Pt}$. Since Au is present in geological samples, ^{199}Au will also be produced from the reactions $^{197}\text{Au}(n,\gamma)^{198}\text{Au}$ followed by $^{198}\text{Au}(n,\gamma)^{199}\text{Au}$. However, the production of ^{199}Au via the second path is serious only after long irradiations at high neutron fluxes. For the determination of traces of Pt in a Au matrix, these reactions present a serious problem, but in ordinary geological materials where the concentrations of both Au and Pt are about the same, this interference is not serious. Both ^{197}Pt and ^{199}Au were measured in this study, and

where necessary, appropriate correction was made for the production of ^{199}Au from ^{197}Au .

Results of the analysis of three terrestrial rocks, a meteorite, and a lunar sample using the proposed method are given in Table II. The results are based on triplicate analyses for all samples except the lunar soil, where a limited supply of the sample allowed only a single determination. The relative standard deviation for a single determination is included. Literature values based on the work of other investigators using a wide variety of methods are included in the table for comparison.

The agreement of our results with these literature values for the diabase W-1 and the Allende meteorite is excellent considering the range of values obtained by others on these samples. With regard to PCC-1, our values lie in the range of reported values except for Au and Pd, and in the case of DTS-1 only our value for Au lies outside the range. In view of the large range of values reported, there is obviously some question as to the "true" values for these samples. There may not be a "true" value for these elements because of sampling problems for noble metals in terrestrial rocks.

There are no values available for comparison of the Apollo 17 lunar soil 72701; however, the values obtained are in the same concentration range obtained by others on other lunar samples. The Pt value reported here is the

- (29) C. M. Lederer, J. M. Hollander, and I. Perlman, "Tables of Isotopes," 6th ed., John Wiley & Sons, New York, N.Y., 1967.
 (30) R. Gijbels, *Talanta*, **18**, 587 (1971).

- (31) J. C. Laul, D. R. Case, M. Wechter, F. Schmidt-Bleek, and M. E. Lipschutz, *J. Radioanal. Chem.*, **4**, 241 (1970).
 (32) J. Haffty and L. B. Riley, *Talanta*, **15**, 111 (1968).
 (33) L. P. Greenland, J. J. Rowe, and J. I. Dinnin, *U.S. Geol. Surv. Prof. Pap.*, **750B**, B-175 (1971).
 (34) P. A. Baedecker, C. L. Chou, and J. T. Wasson, "Proceedings 3rd Lunar Science Conference," Vol. 2, M.I.T. Press, Cambridge, Mass., 1972, p. 1343.
 (35) R. Gijbels, M. T. Millard, G. A. Desborough, and A. J. Bartel, in "Activation Analysis in Geochemistry and Cosmochemistry," A. O. Brunfelt and E. Steinen, Eds., Universitetsforlaget, Oslo, 1971, p. 359.
 (36) P. A. Baedecker, R. Schaudy, J. L. Elzie, J. Kimberlin, and J. T. Wasson, "Proceedings 2nd Lunar Science Conference," Vol. 2, M.I.T. Press, Cambridge, Mass., 1971, p. 1037.
 (37) R. Gijbels and A. Govaerts, International Conferences on Activation Analysis, Paris, 1972, paper M-30.
 (38) L. Grossman, *Geochim. Cosmochim. Acta*, **37**, 1119 (1973).
 (39) H. Malissa, F. Hermann, F. Kluger, and W. Kiesi, *Mikrochim. Acta*, **1972**, 434.
 (40) J. W. Morgan, T. V. Rebagay, D. L. Showalter, R. A. Nadkarni, D. E. Gillum, D. M. McKown, and W. D. Ehmann, *Nature*, **224**, 789 (1969).
 (41) M. Vobecky, J. Frana, Z. Randa, J. Benada, and J. Kuncir, *Radiochem. Radioanal. Lett.*, **6**, 237 (1971).
 (42) R. G. Wafren, M. S. Thesis, Oregon State University, Corvallis, Ore., 1971.
 (43) H. Hintenberger, K. P. Jochum, and M. Seufert, 36th Ann. Meet. Meteoritical Soc., Davos, Switzerland, 1973, p. 68.

first value for this element to be reported for any lunar sample.

The overall precision of our results is on the order of 10–40%, which is reasonable considering the fact that the method involves the determination of nanogram and sub-nanogram amounts of these elements. In addition to analytical errors, there is a strong possibility of sample inhomogeneity for these elements. In favorable cases, such as the analysis of Allende where the concentrations of the noble metals are considerably higher, the precision expressed as relative standard deviation for a single determination varied from 0.7% for platinum to 14% for ruthenium.

Thus, the proposed method for the determination of

noble metals in geological samples is capable of providing good analytical data for the platinum metals and gold. Although Ru and Os could not be determined in every terrestrial rock in this study because of their low concentrations, use of a higher neutron flux, longer irradiation time, and/or larger samples should make their determination possible using this method. The method is simple and rapid and provides data on all six elements in the same aliquot of sample.

Received for review July 9, 1973. Accepted August 23, 1973. This work was supported in part by the National Aeronautics and Space Administration under Grant NGR-33-010-166.

Instrumental Neutron Activation Analysis for Mercury in Dogs Administered Methylmercury Chloride: Use of a Low Energy Photon Detector

Melvin H. Friedman, Eugene Miller, and James T. Tanner

Bureau of Foods, Food and Drug Administration, Washington, D.C. 20204

Mercury has been determined by nondestructive neutron activation analysis in samples of brain tissue from beagles which had been fed methylmercury chloride. The mercury concentration was not uniformly distributed throughout the central nervous system and the fastest rise in concentration occurred in components of the visual system. The analytical procedure was capable of measuring mercury instrumentally and routinely in small samples of biological materials at approximately the 0.2-ppm level within a few days after irradiation with short counting times. Comparative measurements showed that mercury determination based on ^{197}Hg could be done with greater sensitivity by using a Ge(Li) low energy photon detector rather than a conventional high resolution, high efficiency coaxial Ge(Li) detector.

The Food and Drug Administration, as part of its continuing toxicological program, initiated a histopathological study of possible damage to the central nervous system of animals exposed to lethal and sublethal doses of methylmercury. Two comprehensive reports have appeared (1, 2) which pointed out the need for accurate studies of the toxicological effects of methylmercury compounds on the brain. Tissues from the central nervous system were chosen for these studies since these tissues were shown to be the ones most critically affected in methylmercury poisoning (2). Tissues from discrete parts of the central nervous system were used, rather than brain homogenates, since it was suspected that mercury might not be distributed uniformly in the brain.

The main emphasis in this report will be on the analytical technique used to determine mercury in small brain tissue samples. In addition, a summary of the major biological implications will be given. The technique employs neutron activation analysis as the analytical method. Typically, neutron activation analysis measurements have been based on ^{197}Hg or ^{203}Hg . The ^{197}Hg nuclide initially has a much greater activity than the ^{203}Hg nuclide (3) and so offers the possibility of a more sensitive measurement. However, the electromagnetic radiation (X-ray or gamma-ray) associated with the decay of ^{197}Hg is low in energy (<100 keV), and conventional measurements of low levels of mercury have been hampered by a large Compton continuum in this region and by a resolution inadequate to resolve possibly interfering X-rays from elements with adjacent atomic numbers. A Ge(Li) low energy photon detector (LEPD) was used in this work because of the smaller continuous background in the low energy region and better resolution, and so was expected to reduce these problems (4). Instrumental neutron activation analyses for mercury have been reported with a sensitivity of approximately 0.02 ppm. In these analyses, a large volume Ge(Li) detector was used. These measurements (5) involved 3-hour irradiations, 2-gram samples, and counting times of approximately 2 hours per sample. In this work, a comparison was made between a conventional large volume Ge(Li) detector and the Ge(Li) LEPD for the determination of mercury based on ^{197}Hg .

- (1) "Mercury in the Environment—A Toxicological and Epidemiological Appraisal," L. Friberg and J. Vostal, Ed., Environmental Protection Agency Report (Nov. 1971), Contract No. CPA 70-30.
- (2) G. Lofroth, "Methylmercury," Ecological Research Committee, Bulletin No. 4, Swedish Natural Science Research Council, 1970.

- (3) F. Baumgartner, "Table of Neutron Activation Constants," Verlag Karlsruher KG, Munchen, 1967, p 30.
- (4) J. Weaver, *Amer. Lab.*, March, 1973, p 36.
- (5) V. P. Guim and R. Kishore, "Proceedings of the American Nuclear Society Topical Meeting on Nuclear Methods in Environmental Research, University of Missouri, Columbia, Mo., Aug. 23–24, 1971, p 201.

EXPERIMENTAL

Apparatus. The 10-megawatt reactor [6×10^{13} neutrons/(cm² sec)] at the National Bureau of Standards, Washington, D.C., was used. An ORTEC Ge(Li) low energy photon detector was used. It has a resolution of 522 eV at 122 keV; sensitive depth, 4.83 mm; diameter of 16 mm; and a 0.13-mm beryllium window which allows low energy electromagnetic radiation to pass through with little attenuation. Signals from the detector were fed through a preamplifier, amplifier, and then into a biased amplifier and from there into a computer-based Nuclear Data 4410 analyzer. A biased amplifier was used to expand the region of interest over a few channels. Samples and standards were contained in cylindrical quartz vials, 7 × 50 mm.

Standards. Mercury standards, each consisting of 25 μ l of a dilute mercury solution adsorbed onto SiO₂ powder (99.9999% SiO₂) in a quartz vial and sealed with an oxygen-methane torch, were prepared as follows: A weighed quantity of reagent grade mercuric acetate was dissolved in acetic acid and diluted to volume with distilled water. Standards were made several times during the course of this work and contained between 12 and 15 μ g, depending on the particular standard.

Procedure. Sample Preparation. A daily dose of 3 mg/kg of methylmercury chloride in olive oil was administered orally by capsule to beagles for periods of 2, 4, 6, and 8 days. In addition, there was a control dog which was not fed any methylmercury chloride. The animals were sacrificed after a predetermined number of doses, and their brains were perfused with physiological saline solution to avoid artifacts introduced by methylmercury in the blood. Discrete areas of the central nervous system were dissected and taken for analysis. Because of the small size of the central nervous system, the sample size was typically 50–200 mg.

Samples in quartz vials were dried for 5–7 days in a vacuum desiccator to prevent possible pressure buildup during subsequent irradiation. Later experiments showed that it was unnecessary to dry the tissue because pressure buildup was negligible, and additional samples were then analyzed directly without drying. The quartz vials containing the samples were sealed with an oxygen-methane torch and scribed for identification. An empty quartz vial served as a blank.

Irradiation. The 2 mercury standards and 5 samples were packaged together in an irradiation container and irradiated for 1 hr in the high flux position of the reactor. After irradiation, the samples and standards were allowed to stand for about 3 days to permit short-lived radionuclides time to decay. The irradiation container was opened, and the vials were prepared for counting by cleaning with aqua regia (to remove any surface contamination) and then rinsing with water.

Counting. The samples and standards were analyzed with the Ge(Li) LEPD detector. Samples, standards, and blanks were counted approximately 3 cm away and with the vial's longitudinal axis parallel to the plane of the detector window. With this geometry, variations in distance between the active area of the detector and any point within the sample vial were minimized. Mercury was not detected in the blanks. A counting time of 20 min was adequate for these determinations.

Data Reduction. The spectra obtained from the low energy photon detector were read out on a magnetic tape unit compatible with the UNIVAC 1108 computer at the National Bureau of Standards. Under control of a data reduction program, spectra for each sample were read from magnetic tape and parameters describing the individual sample were read from IBM cards. The concentration of mercury or an upper limit was calculated by comparing the activity of the sample with that of the standard irradiated with it. Independent determinations of the activity of a sample or standard were obtained using the total peak area method (6) for the three most prominent Hg photo peaks (66.9, 68.8, and 77.3 keV) of the spectrum. The concentration of Hg computed from the peaks and the average were output by the computer.

RESULTS AND DISCUSSION

Validation and Sensitivity. Available NBS standard reference materials were used to validate the procedure, namely, tuna fish (SRM No 1578) and orchard leaves (SRM No. 1571). Four determinations were made on the tuna fish samples, and the results averaged 0.9 ± 0.1 ppm

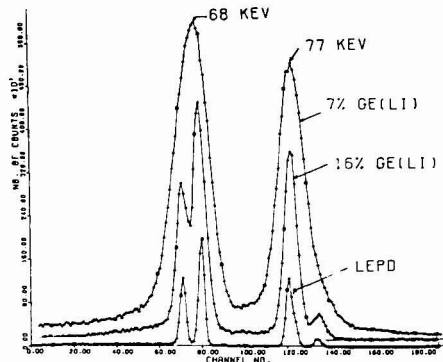


Figure 1. Comparison of a ¹⁹⁷Hg spectrum taken with a LEPD; a 16%, 2.1 keV Ge(Li) detector; and a 7%, 5 keV Ge(Li) detector. To prevent the curves from intersecting, the spectrum measured with the 7% detector was counted for the longest length of time and the spectrum measured with the LEPD was counted for the shortest length of time.

Hg, as compared with the preliminary NBS value (7) of 1.00 ± 0.04 ppm Hg. Two different determinations were made on the orchard leaves. However, a longer counting time (16 hr) and irradiation time (4 hr) were used because of the low level of mercury and the comparatively high value of the continuous background in the orchard leaf spectrum. The results obtained were 0.13 ± 0.01 and 0.15 ± 0.01 ppm Hg, as compared with the NBS certified value of 0.155 ± 0.015 ppm Hg.

The results from the orchard leaves indicate that the instrumental technique using a low energy photon detector and the ¹⁹⁷Hg nuclide can measure mercury instrumentally at approximately the 0.2-ppm level.

Evaluation of Low Energy Photon Detector. In order to determine if a LEPD had advantages over a conventional Ge(Li) detector, a spectrum of the sample was taken with each type of detector under the best conditions for that detector. A ¹⁹⁷Hg spectrum was counted: 1) with a Ge(Li) LEPD, 2) with a Ge(Li) detector of 16% efficiency [with respect to NaI(Tl)], 2.1 keV FWHM resolution at 1.33 MeV, and 3) with an older 7% Ge(Li), 5 keV FWHM detector for the purpose of comparing resolution in the 70 keV region. These results are shown in Figure 1. With the 7% detector the peaks are not resolved, while with the 16% detector the peaks are only partially resolved; this is to be compared with the resolution of the low energy photon detector where the photo peaks are completely resolved.

To determine the relative sensitivity of the 16% detector and the Ge(Li) LEPD, a mercury spectrum from a brain sample was taken with each detector. The comparison is shown in Figure 2. A counting time of 20 min was used for both detectors. To avoid having an excessive count rate with the 16% Ge(Li), it was necessary to count the sample further away with this detector than with the LEPD. The continuous background was approximately the same with both detectors. It appears from Figure 2 that for analyses based on ¹⁹⁷Hg, the LEPD can analyze for mercury instrumentally at lower levels than a conventional Ge(Li) detector. The improved sensitivity comes about because of an improved peak to adjacent Compton background ratio.

(6) P. A. Baedeker, *Anal. Chem.*, **43**, 405 (1971).

(7) P. D. LaFleur, National Bureau of Standards, Washington, D. C., personal communication, 1973.

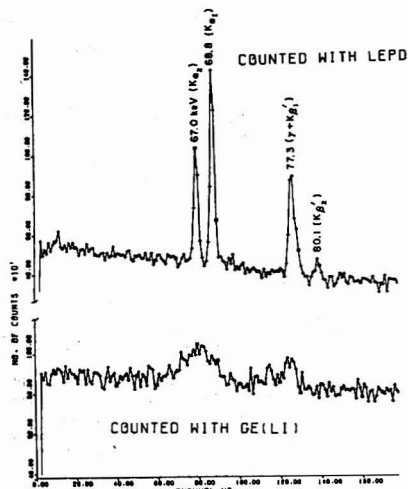


Figure 2. Comparison of a mercury spectrum from a brain tissue sample measured with a Ge(Li) detector (16% efficiency) and with a Ge(Li) LEPD

The mechanism by which the LEPD obtains a reduced Compton background in the low energy region without reducing the photopeak in this region can be understood by realizing that in going from 200 keV to 50 keV, the photoelectric cross section for germanium increases by almost two orders of magnitude (8). Thus, low energy electromagnetic radiation (~ 70 keV) will be detected with almost 100% probability after it traverses a short distance (~ 5 mm) through germanium. A thicker detector could not substantially increase the number of photoelectric events at this energy but it does increase the number of Compton events observed (9). This is shown graphically in Figure 3, where the probability for detecting a 69-keV photon (this corresponds to the strongest photo peak of ^{197}Hg) and a Compton event from a 660 keV gamma ray are plotted vs. the thickness of a Ge(Li) detector.

Interpretation of the Spectra. The two prominent low energy photo peaks and the highest energy photo peak in the LEPD spectrum (see Figure 2, first, second, and fourth peaks) correspond to the $K\alpha_2$, $K\alpha_1$, and $K\beta_2$ gold X-rays produced when ^{197}Hg undergoes electron capture. The third peak was interpreted as being an unresolved doublet which consisted of the $K\beta_1$ X-ray from gold and 77.3-keV gamma ray associated with the decay of ^{197}Hg .

There are two pieces of experimental data which indicated that the third peak (at 77 keV) was a doublet. First, close examination showed that there was a shoulder on the right side of the peak and second, the four peaks were found to have relative peak areas in the proportions of 58:100:82:83. The relative experimentally determined strengths for gold $K\alpha_2$, $K\alpha_1$, $K\beta_1$, and $K\beta_2$ peaks quoted by Wapstra *et al.* (10, 11) are 55:100:35:9. Thus, the mea-

(8) J. H. Hubbell, "Photon Cross Sections, Attenuation Coefficients, and Energy Absorption Coefficients from 10 keV to 100 GeV," National Bureau of Standards Report NSRDS-NBS 29, 1969.

(9) D. M. Walker, M. E. McLain, and G. W. Leddicotte, *IEE Trans. Nucl. Sci.*, **19**, 186 (1972).

(10) A. H. Wapstra, G. J. Nijgh, and R. van Lieshout, "Nucl. Spect. Tables," North Holland Publishing Co., Amsterdam, 1959.

(11) C. M. Lederer, J. M. Hollander, and I. Perlman, "Table of Isotopes," Sixth ed., John Wiley and Sons, New York, N.Y., 1967, p 571.

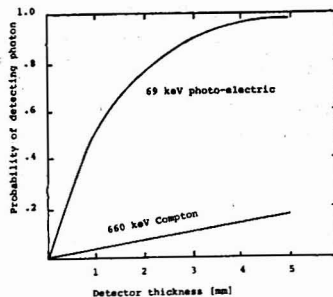


Figure 3. Probability of detecting a photon vs. detector thickness

sured relative areas of the $K\alpha_2$, $K\alpha_1$, and $K\beta_2$ peaks are in fairly good agreement with those determined by Wapstra *et al.*, but the third peak at 77 keV has more than twice the strength expected for a $K\beta_1$ X-ray. This additional strength was attributed to the 77.3-keV gamma ray

Retention of Mercury during Drying. The technique reported here, which involved drying the sample by vacuum desiccation, and the method of flameless atomic absorption spectrophotometry of Magos (12), for which no drying was necessary, were compared on several homogenized spiked and unspiked samples. The results determined were equivalent within experimental errors in all cases, indicating that losses of mercury were not a problem in this work. In addition, recent work by LaFleur (13) has also shown that methylmercury was not lost from brain tissues during freeze-drying.

Biological Implications. Table I shows the various concentrations of mercury in the central nervous system of beagles following daily administration of 3 mg/kg of methylmercury for a period of 2, 4, 6, and 8 days. Also shown are results for a control dog which received no mercury. Mercury was not distributed evenly throughout the central nervous system. The fastest rise in levels of mercury occurred in the components of the visual system (occipital and calcarine cortex). This was consistent with the observation that alkylmercury poisoning almost always results in impaired vision or blindness. Low concentrations of mercury were observed in the spinal cord.

The dose of CH_3HgCl was administered orally and the mercury in the olive oil sometimes induced vomiting at various intervals following the administration. This fact plus the biological variations between animals contributed the greatest uncertainty to the measurements. The accuracy of the analysis, apart from biological variations, was determined to be better than 10%.

Gamma and X-ray peaks associated with the decay of ^{197}Hg were not seen in the spectra of the control dog tissues. The values quoted in the first column of Table I (control dog A) are upper limits equal to 2.33 times the standard deviation of the background and correspond to the critical limit defined by Currie (14).

CONCLUSIONS

Perhaps the most significant finding with regard to methodology was that neutron activation analysis affords a specific, rapid, convenient method for mapping mercury accumulation in the central nervous system. Low concen-

(12) L. Magos, *Analyst (London)*, **96**, 847 (1971).

(13) P. D. LaFleur, *Anal. Chem.*, **45**, 1534 (1973).

(14) L. A. Currie, *Anal. Chem.*, **40**, 586 (1968).

Table I. Mercury Concentrations in Discrete Areas of the Central Nervous System of Beagles* (ppm Hg)

Structure	Control Dog A (0 doses)	Dog B (2 doses) ^b	Dog C (4 doses)	Dog D (6 doses)	Dog E (8 doses)
Motor cortex	≤0.1	2.1	5.9	9.2	16.8
Prefrontal cortex	≤0.1	1.6	5.1	7.5	16.0
Occipital cortex	≤0.2	1.6	7.4	10.9	18.4
Superior colliculus	≤0.2	1.7	5.5	8.4	15.5
Inferior colliculus	≤0.2	1.7	4.7	8.8	15.0
Caudate nucleus	≤0.2	1.8	5.4	7.3	8.4
Pons	≤0.2	2.1	3.8	6.0	7.8
Medulla	≤0.2	2.1	3.7	6.0	10.3
Vermis (of the cerebellum)	≤0.1	3.4	4.1	7.2	9.6
Cerebellum hemisphere	≤0.1	2.6	4.6	7.4	10.5
Spinal cord (cervical)	≤0.1	1.6	4.1	5.1	8.3
Spinal cord (lumbar)	≤0.1	2.0	3.9	8.7	9.0
Sciatic nerve		1.5	7.8	12.5	10.9
Optic nerve		1.9	6.1	8.3	9.4
Calcarine cortex	≤0.2	1.7	5.4	10.3	19.0

* Accuracy of measurements is discussed under "Biological Implications." ^b Dose = 3 mg MeHgCl per kg-day.

trations of mercury (below 2.0 ppm) could be quantified instrumentally in 50 mg of tissue within a few days after irradiation. The high sensitivity of the method presented an excellent tool for study of concentration as a function of time for mercury accumulation in the central nervous system at very low doses which was then correlated (15) with the ensuing overt symptoms of alkylmercury toxicity and pathological changes.

(15) E. Miller, P. Sapienza, F. L. Earl, V. L. Olivito, T. C. Michel, and E. J. Van Loon, *Fed. Proc. Fed. Amer. Soc. Exp. Biol.*, **32**, Abs. 274 (1973).

ACKNOWLEDGMENTS

We thank D. N. Lincoln, R. E. Simpson, E. J. van Loon, W. S. Forbes, and N. Tandy of the Food and Drug Administration, Washington, D.C., and the personnel of the Reactor Radiation Division, National Bureau of Standards, Washington, D.C., for their contributions to various phases of this work.

Received for review May 11, 1973. Accepted September 4, 1973.

Determination of Trace Elements in Coal, Fly Ash, Fuel Oil, and Gasoline—A Preliminary Comparison of Selected Analytical Techniques

Darryl J. von Lehmden, Robert H. Jungers, and Robert E. Lee, Jr.

Quality Assurance and Environmental Monitoring Laboratory, National Environmental Research Center, Research Triangle Park, N.C. 27711

The Environmental Protection Agency has initiated a program to monitor trace elements in fuels and related emissions to the atmosphere. As part of this program, nine laboratories using similar analytical methods were asked to determine the concentration of 28 elements in the same fuel and fly ash matrices. Among the elements investigated were mercury, beryllium, lead, cadmium, arsenic, vanadium, manganese, chromium, and fluorine. The analytical methods used included neutron activation analysis, atomic absorption, spark source mass spectrometry, optical emission spectrometry, anodic stripping voltammetry, and X-ray fluorescence. The results from the interlaboratory comparison were evaluated to assess the comparability of various methods as applied to these matrices. The wide range in reported concentrations indicates that different sample preparation and analytical

techniques can lead to erroneous results and points out the need for developing standard reference materials certified in trace elements which can be used for analytical methods evaluation and quality control. Future reports will describe the optimal analytical methods which should be used.

Accurate measurements of chemical components in ambient air and in air pollution source emissions have been underlined by the enactment of the Clean Air Act as amended in 1970 (1). Pursuant to this Act, the Administrator of the Environmental Protection Agency has promulgated national standards for several chemical compo-

(1) U. S. Congress, "Clean Air Amendments of 1970," Public Law 91-604, 91st Congress, H.R. 17255, Dec. 31, 1970.

Table I. Coal Analysis Comparison for Trace Elements by Laboratory and by Analytical Method

Laboratory code Analytical method	1	3	6	1	3	2	3	4	5	8	3
	SSMS ^a	SSMS ^a	SSMS ^a	OES ^b	OES ^b	NAA ^c	AAS				
Elements analysed, ppm (by weight)											
Hg	<2.	<2.	<0.10	NA	NA	<0.2	NA	<0.02	0.08	NA	0.051 ^d
Be	0.4	NA	0.4	<1.	<0.1	NA	NA	NA	NA	NA	NA
Cd	6.	<1.	0.7	<30.	<10.	NA	<3	<40.	NA	NA	NA
As	2.	2.	0.25	<100.	<50.	<1.	1.4	1.6	NA	<1.	NA
V	10.	NA	7.7	10.	10.	7.0	5.5	7.	NA	6.0	NA
Mn	10.	3.	1.9	10.	20.	7.6	4.8	6.7	NA	5.0	NA
Ni	<40.	4.	6.0	<10.	<20.	NA	NA	<20.	NA	NA	NA
Sb	0.6	NA	0.04	<30.	<10.	0.14	0.2	0.4	NA	NA	NA
Cr	<30.	7.	12.	<10.	<30.	3.4	5.0	4.8	NA	NA	NA
Zn	<100.	5.	6.6	<100.	<50.	NA	NA	<100.	NA	NA	NA
Cu	10.	9.	4.5	10.	10.	NA	NA	<0.4	NA	NA	NA
Pb	<4.	4.	1.8	<30.	<10.	NA	NA	NA	NA	NA	NA
Se	<15.	<8.	0.1	NA	NA	1.0	5.0	2.0	1.5	NA	NA
B	15.	5.	14.	10.	7.	NA	NA	NA	NA	NA	NA
F	<2.	4.	60.	NA							
Li	0.3	NA	2.8	<300.	10.	NA	NA	NA	NA	NA	NA
Ag	<2.	NA	<0.1	<1.	<1.	NA	NA	<2.	NA	NA	NA
Sn	3.	NA	0.19	<30.	<10.	NA	NA	NA	NA	NA	NA
Fe	2000.	2000.	1800.	2000.	3000.	2400.	2700.	3140.	NA	8000.	NA
Sr	100.	50.	46.	<30.	NA	160.	NA	120.	NA	80.	NA
Na	600.	100.	660.	300.	500.	800.	870.	840.	NA	800.	NA
K	100.	50.	200.	150.	20.	NA	2200.	280.	NA	100.	NA
Ca	10,000.	10,000.	5800.	8000.	10,000.	NA	5500.	7070.	NA	NA	NA
Si	6,000.	10,000.	10,000.	3000.	20,000.	NA	NA	NA	NA	NA	NA
Mg	2000.	700.	2000.	600.	1000.	2600.	NA	920.	NA	1000.	NA
Ba	400.	30.	110.	500.	200.	NA	220.	430.	NA	<2.0	NA

^a Analysis on sample direct. ^b DC/arc on sample direct. ^c Instrumental NAA. ^d Dissolution followed by flameless AAS. Analysis code: NAA, neutron activation analysis; SSMS, spark source mass spectrometry; OES, optical emission spectrometry; AAS, atomic absorption spectrometry; NA, no analysis.

nents including mercury and beryllium under Section 112 (National Emission Standards for Hazardous Air Pollutants) and lead and phosphorus under Section 211 (Regulation of Fuels). In setting national standards, many different source sample matrices must be analyzed to determine the impact that a variety of potential air pollution sources may have on the standard. The analyses of these sample matrices commonly require measurements of concentrations at the trace level (ppb range).

Because emissions of pollutants into the air are dependent both on the quantity of material combusted or processed and on the concentration of pollutants in the material, it becomes extremely important that measurements of trace level concentrations be precise and accurate. For example, when a large quantity is processed, concentrations measured at 0.6 ppm would result in an emission estimate three times greater than a trace value of 0.2 ppm. At the 0.6-ppm level, the source may be considered significant enough to require control, however, if the level were accurately measured at 0.2 ppm, a control standard may not be required. This illustration points out the enormous impact that trace analysis can have on federal regulations for control of emission sources.

The Environmental Protection Agency has initiated a surveillance program for determining trace elements in atmospheric source emissions, fuels, and fuel additives at the National Environmental Research Center, Research Triangle Park, N.C. In conjunction with this program, a study is presently under way to examine analytical procedures for a number of trace elements that can be applied to specific matrices. The first phase of this study, reported here, concerns the comparison of trace analytical

techniques applied to source and fuel matrices in nine laboratories, to determine the need for standardized methodology. Future reports will address the need for standard reference materials certified in trace element concentration, and the optimal analytical methodology which should be used for trace determinations in these matrices.

EXPERIMENTAL

Selection of Matrices. An analytical technique that has proved successful under research conditions using synthetic standards may give misleading results when applied to actual samples where interferences and element response may be markedly different. Each sample matrix can provide a different set of interference problems; therefore, an optimum analytical technique often requires modification of an existing technique or development of a new technique.

The following four matrices were selected for evaluation:

Coal. Coal is the most widely used fuel for heat and power generation in the world today. Projections for coal consumption in the United States indicate more coal, not less, will be needed by the year 2000 to supply electric power needs than is required today, even though nuclear power will dominate the power generation field (2). Numerous trace elements have been identified in coal (3, 4), including the 28 chemical elements under investigation in this study. Chemical characterization of the coal matrix, which consists primarily of carbon, may provide information on analytical methods that may be applied to other carbonaceous materials, including coke, carbon black, and charcoal.

- (2) J. G. Terrill, Jr., E. D. Harward, and I. P. Loggett, Jr., *J. Ind. Med. Surgery*, 36, 412 (1967).
- (3) T. Kessler, A. G. Sharkey, Jr., and R. A. Friedel, "USBM Respirable Dust Research Program TPR 42," Pittsburgh, Pa., Sept. 1971.
- (4) H. Shultz and M. D. Schliesinger, "USBM Report of Investigation 7609," Pittsburgh, Pa., 1972.

Table II. Fly Ash Analysis Comparison for Trace Elements by Laboratory and by Analytical Method

Laboratory code Analytical method	1	1	1	1	1	1	1	1	1	2	3	4	6	1	
Elements analyzed, ppm ^a	SSMS ^{b,c}	SSMS ^{b,c}	SSMS ^b	SSMS ^b	OES ^d	DRES ^e	DRES ^e	NAA/ ^f	NAA/ ^f	NAA/ ^f	AAS ^g				
Hg	<1	<0.4	<2	<0.1	<1	<1	NA	NA	NA	NA	<18	<0.3	NA	NA	0.21
Be	7	1	5	7	5	4	7	NA	3	NA	NA	NA	NA	NA	NA
Cd	<3	<6	2	2.3	<100	<100	NA	NA	NA	NA	NA	<90	NA	NA	NA
As	40	100	15	2.8	<100	<200	50	NA	NA	NA	70	54	40	40	NA
V	250	300	200	290	2000	400	200	NA	180	NA	247	382	250	300	300
Mn	300	150	300	170	500	200	500	NA	NA	NA	294	369	250	NA	NA
Ni	100	100	100	45	300	50	300	NA	NA	NA	NA	NA	NA	100	100
Sb	10	40	NA	5.6	<50	<100	NA	NA	NA	NA	<7	19	NA	NA	NA
Cr	200	100	1000	330	500	100	300	NA	80	NA	105	130	NA	150	150
Zn	200	70	1000	330	100	<200	200	NA	350	NA	NA	NA	NA	600	600
Cu	100	150	200	45	300	200	300	NA	NA	NA	NA	NA	NA	90	90
Pb	200	200	100	180	100	200	200	NA	440	NA	NA	NA	NA	NA	NA
Se	<10	15	NA	0.77	NA	NA	NA	NA	NA	NA	8.2	40	NA	NA	NA
B	500	200	300	190	300	300	500	NA	NA	NA	NA	NA	NA	NA	NA
F	30	<10	100 max	60	NA	NA	300	NA	NA	NA	NA	NA	NA	NA	NA
Li	2	60	150	190	20	100	300	NA	NA	NA	NA	NA	NA	NA	NA
Ag	<1	2	NA	0.04	<3	<2	1	NA	NA	NA	NA	NA	NA	NA	NA
Sn	6	15	NA	1.9	20	<100	NA	NA	13%	NA	17.5%	18.1%	26%	26%	17.8%
Fe	High	High	10%	5.3%	20%	10%	>5.0%	10.5%	<400	NA	520	180	<1000	NA	NA
Sr	180	200	200	69	300	200	500	NA	NA	NA	2700	2450	3500	2800	2800
Na	2000	2000	500	6600	3000	4000	3000	1400	NA	NA	2300	1.5%	2.5%	2.5%	2.0%
K	High	High	1%	1.7%	9%	2%	0.5%	NA	NA	NA	NA	3.1%	NA	NA	4.7%
Ca	High	High	4.0%	1.3%	5%	5%	3.0%	3.7%	NA	NA	NA	3.9%	NA	NA	19.5%
Si	High	High	>10%	major	20%	15%	20%	NA	3	NA	NA	NA	4000	6000	6000
Mg	10,000	10,000	5000	44,000	5000	4000	5000	4000	2200	NA	13,700	3000	4000	4000	NA
Ba	200	600	700	110	200	300	500	NA	NA	NA	200	410	400	400	NA

^a Ppm by weight, higher concentrations are specified as percent (%). ^b Analysis on sample direct. ^c Duplicate sample submitted for SSMS and OES analysis only. ^d Do not on sample direct. ^e Dissolution followed by RF spark analysis. ^f Instrumental NAA. Analysis code: NAA, neutron activation analysis; SSMS, spark source mass spectrometry; OES, optical emission spectrometry; DRES, direct reading emission spectrometry; AAS, atomic absorption spectrometry; NA, no analysis.

Table III. Residual Fuel Oil (No. 6) Analysis Comparison for Trace Elements by Laboratory and by Analytical Method

Laboratory code Analytical method	1 SSMS ^a	3 SSMS ^a	1 OES ^a	1 OES ^b	3 OES ^a	2 NAA ^c	3 NAA ^c	1 AAS ^d	3 AAS	1 XRF ^e
Elements analyzed, ppm (by weight)										
Hg	NA	0.005 ^a	NA	NA	NA	<0.006	NA	0.4 ^f	0.002 ^f	NA
Be	0.0005	0.005	<0.004	<0.01	<0.01	NA	NA	<0.5	NA	NA
Cd	0.003	0.83 ^a	0.4	1.	NA	NA	NA	<0.2	NA	NA
As	0.2	0.7	<0.4	<1.	NA	0.35	NA	NA	NA	NA
V	High	100	40.	50.	NA	113.	89.	NA	NA	100
Mn	0.4	1	0.4	0.3	NA	<1.0	0.21	0.4	NA	NA
Ni	High	90	40.	20.	50.	NA	62.	52.	NA	60
Sb	0.003	NA	<0.2	<0.5	NA	0.0062	NA	NA	NA	NA
Cr	0.8	1.	1.	4.	NA	0.92	0.7	1.0	NA	NA
Zn	0.5	NA	0.4	1.	2.	1.4	1.3	2.0	NA	NA
Cu	0.2	NA	0.4	1.	0.23	NA	NA	0.4	NA	NA
Pb	2.	2.	1.	3.	4.	NA	NA	2.2	NA	NA
Se	NA	0.02	NA	NA	0.02	0.090	0.15	NA	NA	NA
B	0.002	NA	<0.04	0.2	0.05	NA	NA	NA	NA	NA
F	0.004	NA	NA	NA	NA	NA	NA	NA	NA	NA
Li	0.02	0.03	<0.04	<3.	NA	NA	NA	NA	NA	NA
Ag	0.0006	0.1	<0.004	0.1	NA	0.019	NA	NA	NA	NA
Sn	0.01	NA	<0.1	5.	NA	NA	NA	NA	NA	NA
Fe	10.	20.	12.	10.	NA	18	11	15.6	NA	15
Sr	0.4	NA	0.4	<0.5	NA	NA	NA	0.4	NA	NA
Na	0.4	1.	<0.4	30. ^g	NA	7.7	NA	3.3	NA	NA
K	High	2.	1.	5.	1.	NA	NA	0.8	NA	NA
Ca	High	NA	8.	25. ^g	NA	<400	NA	10.0	NA	7
Si	High	30.	8.	10.	NA	NA	NA	NA	NA	NA
Mg	2.	2.	2.	3.	NA	NA	NA	2.2	NA	NA
Ba	2.	NA	2.	0.3	NA	NA	NA	NA	NA	5

^a 450 °C Ashing followed by ash analysis. ^b H₂SO₄-HNO₃ dissolution, dried and analyzed. ^c Instrument NAA. ^d Analysis on sample direct. ^e Acid dissolution followed by isotope dilution SSMS. ^f Flameless AAS. ^g High value due to contamination. Analysis code: NAA, neutron activation analysis; SSMS, spark source mass spectrometry; OES, optical emission spectrometry; AAS, atomic absorption spectrometry; XRF, X-ray fluorescence; NA, no analysis.

Fly Ash. Fly ash from coal-fired, heat-generation sources is important for two reasons. First, fly ash is a matrix similar to emissions to the atmosphere but larger in particle size. Second, there is considerable interest at the present time in determining trace element material balances on coal-fired processes, to assess the effectiveness of control techniques for removing trace elements. Essentially the same trace elements identified in coal have been identified in fly ash (3). Methods developed for characterizing the fly ash matrix, which is composed mainly of silica, alumina, and iron oxide, may be applied to similar matrices, e.g., coal bottom ash and particulate emissions to the atmosphere from combustion sources such as municipal incinerators.

Fuel Oil. A residual fuel oil, grade number 6, matrix was selected for evaluation because it is the most prevalent fuel oil used for industrial and electric power generation. Projections for fuel oil in the United States for the year 2000 show an increased need for fuel oil for electric power production (2). Numerous trace elements have been identified in residual fuel oil (5), and include vanadium, manganese, nickel, barium, and arsenic. Methods developed for characterizing the residual fuel oil matrix, which is composed primarily of high molecular weight organics, may be applied to other oil matrices such as distillate fuel oil and motor oil.

Gasoline. Gasoline was selected as a matrix for evaluation because it is the most prevalent organic fuel used in mobile emission sources for motor vehicles and aircraft. Very few data are available in the published literature on trace elements in fuels used for mobile sources. The gasoline matrix consists primarily of organics of lower molecular weight than residual fuel oil. Methods developed in the characterization of gasoline may be applied to other matrices used for mobile sources such as aviation gasoline and jet fuel.

Selection of Laboratories. All laboratories selected for participation in the evaluation had in-depth analytical experience in the determination of trace components in environmental materials, although not all had specific experience with the selected matrices. The nine participating laboratories have been coded to maintain anonymity.

(5) D. E. Bryan, V. P. Guinn, R. P. Hackleman, and H. R. Lukens, "Gulf General Atomic Inc., Report GA9889," San Diego, Calif., January 1970.

Selection of Chemical Elements. The elements selected for evaluation were mercury, beryllium, cadmium, arsenic, vanadium, manganese, nickel, antimony, chromium, zinc, copper, lead, selenium, boron, fluorine, lithium, silver, tin, iron, strontium, sodium, potassium, calcium, silicon, magnesium, barium, phosphorus, and sulfur. These elements were selected because they are associated with possible adverse health effects, vegetation damage, material soiling, corrosion, atmospheric transformations in the catalytic formation of secondary pollutants, or other effects (6).

Sample Collection and Preparation. The coal sample was obtained from the U.S. Bureau of Mines, where the sample had been prepared for an interlaboratory comparison for mercury conducted previously. The fly ash was obtained from an air pollution control device at a coal-fired electric power generation plant. The fuel oil sample was obtained directly from a midwestern refinery, and the gasoline samples were obtained from retail service station pumps in North Carolina's Research Triangle Park area.

After sample collection, the problem of ensuring complete blending so that homogeneous aliquots can be prepared can be difficult. The gasoline and fuel oil samples did not require further preparation other than mechanical agitation. The solid coal and fly ash samples, however, required grinding and sieving prior to vigorous blending. The particle sizes of coal and fly ash were determined by the United States Standard Sieve Analysis (7) and used as an indirect measure of sample homogeneity for trace elements. In preparing coal samples for analysis, the U.S. Bureau of Mines routinely crushes and sieves coal to pass through a 60-mesh or finer screen (8). Although this is not an absolute test to ensure trace element homogeneity in aliquots removed from the same bulk sample, the Bureau of Mines procedure has shown that replicate analytical results are highly consistent in samples of 60-mesh or finer (8).

All coal used in this study passed through a 48-mesh screen; 94.5% passed through a 100-mesh screen. Based on this analysis,

(6) R. E. Lee, Jr., and D. J. von Lehmden, *J. Amer. Pollut. Contr. Ass.*, in press.

(7) "1971 Annual Book of ASTM Standards," ASTM Method D-197-30, 19, 10 (1971).

(8) F. Walker, U. S. Bureau of Mines, Pittsburgh, Pa., personal communication, 1972.

Table IV. Gasoline (Premium) Analysis Comparison for Trace Elements by Laboratory and by Analytical Method^a

Laboratory code	1	1	1	4	1	1	3	2	3	7
Analytical method	SSMS ^b	OES ^b	OES ^c	NAA ^d	AAS ^b	XRF ^e	SSMP ^f	NAA ^d	NAA ^d	ASV ^g
Sample code	G-10	G-10	G-10	G-10	G-10	G-10	G-1	G-1	G-1	G-1
Elements analyzed, µg/ml										
Hg	NA	NA	NA	<0.02	0.008	NA	<0.1 ^a	<0.01	NA	NA
Be	<0.0001	<0.02	<0.01	NA	NA	NA	<0.01	NA	NA	NA
Cd	0.001	<0.1	<1.	<20.	<0.15	NA	0.023 ^a	NA	NA	0.006
As	<0.02	<0.2	<0.1	<200.	NA	NA	<0.1	<10.	NA	NA
V	<0.0001	<0.06	<0.1	<0.1	NA	NA	<0.05	<10.	0.034	NA
Mn	0.005	<0.02	<0.1	0.019	<0.1	NA	0.02	NA	NA	NA
Ni	<0.01	<0.02	<0.1	<6.	<0.2	NA	<0.2	NA	NA	NA
Sb	<0.0004	<0.1	<1.	<0.02	NA	NA	<0.5	<0.005	NA	NA
Cr	<0.001	<0.1	<0.1	<0.3	NA	NA	<0.5	<0.1	NA	NA
Zn	0.2	<0.2	0.5	<3.	1.0	NA	1.	0.36	NA	0.12
Cu	0.005	<0.006	<0.1	3.8	NA	NA	0.05	<10.	NA	2.4
Pb	High	650	2. ¹	NA	630.	560	618. ⁴	NA	NA	375.
Se	0.001	NA	NA	<0.2	NA	NA	<0.02	<0.1	NA	NA
B	<0.02	<0.1	<0.1	NA	NA	NA	0.1	NA	NA	NA
F	<0.0003	NA	NA	NA	NA	NA	NA	NA	NA	NA
Li	0.001	<0.6	<0.6	NA	NA	NA	<0.02	NA	NA	NA
Ag	<0.001	<0.02	<0.1	<0.3	NA	NA	0.02	NA	NA	0.4
Sn	<0.003	<0.1	<0.5	<7.	NA	NA	<0.1	NA	NA	NA
Fe	0.1	<0.1	0.3	<0.6	<0.3	NA	0.2	<0.1	NA	NA
Sr	<0.001	<0.1	<0.1	<8.	NA	NA	<0.1	<1.0	NA	NA
Na	<0.4	<0.2	<0.1	0.6	NA	NA	2.	<10.	NA	NA
K	0.1	<2.	<2.	<20.	NA	NA	0.2	NA	NA	NA
Ca	<0.05	<0.2	<0.2	<20.	NA	NA	1.	NA	NA	NA
Si	<1.	<2.	0.5	NA	NA	NA	5.	NA	NA	NA
Mg	0.02	<0.1	0.01	<100.	0.02	NA	0.3	NA	NA	NA
Ba	0.001	<0.2	<0.2	NA	NA	NA	<0.2	NA	NA	NA
P	0.2	<0.5	<0.5	NA	NA	NA	25	1.	NA	NA
S	NA	NA	NA	<200	NA	30	9.	NA	NA	NA

^a Comparison includes two samples (G-1 and G-10) of the same brand name collected from the pumps of two different retail service stations. ^b HCl extraction preparation. ^c Analysis of residue after combustion of sample. ^d Instrumental NAA. ^e Analysis on sample direct. ^f SSMS except Pb by thermal mass spectrometry. ^g HCl extraction preparation. ^h Isotope dilution SSMS. ⁱ Assume Pb lost during combustion preparation. Analysis code: NAA, neutron activation analysis; SSMS, spark source mass spectrometry; OES, optical emission spectrometry; AAS, atomic absorption spectrometry; XRF, X-ray fluorescence; ASV, anodic stripping voltammetry; NA, no analysis.

coal aliquots sent to participating laboratories were considered to be reasonably homogeneous. Eighty-nine per cent of the fly ash passed through a 100-mesh screen; however, 7% did not pass through a 28-mesh screen. These data suggest that some lack of homogeneity may have resulted in the fly ash aliquots. The possible effect on the trace element results will be discussed later.

Selection of Analytical Methods. The basic criteria used for selecting analytical methods were that the analysis procedure should provide multielement results, and that the cost per element should be minimal. The analytical methods selected for comparison were instrumental neutron activation analysis, spark source mass spectrometry (general scan and isotope dilution), optical emission spectrometry, atomic absorption spectrometry, X-ray fluorescence, and anodic stripping voltammetry. Each laboratory was permitted to use any sample extraction or preparation scheme it judged appropriate for the analytical technique selected. Consequently, reported results include potential inaccuracies from both sample preparation procedures and instrument analysis.

In the instrumental neutron activation analysis method, the sample is irradiated in a nuclear reactor directly, without chemical extraction or dissolution, to form radioactive isotopes of the elements present; measurement of the intensities of the various peaks in the gamma ray spectra can provide specific information on the identification and concentrations of many of the elements present. Spark source mass spectrometry entails ionization of the sample, compounded in a graphite or silver electrode, with a high intensity spark, followed by a determination of the intensities of the ions of various mass-to-charge ratios separated by a magnetic field. In emission spectrometry, the sample is excited in a spark or arc to produce line spectra of the elements present. With atomic absorption analysis, an acid extract of the sample is aspirated into a flame, to form dissociated atoms which can absorb

radiation at discrete wavelengths; the amount of energy absorbed is a measure of the concentration present in the sample. X-Ray fluorescence analysis entails irradiation of the sample directly with X-rays, to produce characteristic fluorescence spectra for many of the elements present. Anodic stripping voltammetry is an electrochemical method in which metal ions acid-extracted from the sample are plated onto an electrode by application of a negative voltage. Following plating, the electrode potential is varied linearly in an anodic direction, giving a sharp current peak proportional to concentration.

RESULTS AND DISCUSSION

Reported concentrations from the nine participating laboratories are summarized in Tables I through V. Although the trace element concentrations may vary with the source of the sample, the major components in each matrix are typical and would influence the sample preparation/analytical procedure in a similar fashion despite the source of the matrix.

Large variations were found in the reported concentrations for many elements in each of the four matrices. The concentration ranges reported are summarized in Table VI. Using only definitive concentrations, and not less-than values, the laboratory comparison for the 28 trace elements showed that at least eight trace elements in coal, fly ash, and residual fuel oil, and three trace elements in gasoline have reported concentration ranges which vary by more than one order of magnitude. These included Mn, Sb, Se, F, Li, Sn, K, and Ba in coal; As, V, Zn, Se, Li,

Table V. Gasoline (Low Lead) Analysis Comparison for Trace Elements by Laboratory and by Analytical Method

Laboratory code	3	3	2	8	7	Laboratory code	3	8	2	8	7
Analytical method	SSMS ^a	NAA ^b	NAA ^b	NAA ^b	ASV ^c	Analytical method	SSMS ^a	NAA ^b	NAA ^b	NAA ^b	ASV ^c
Elements analyzed, $\mu\text{g/ml}$						Elements analyzed, $\mu\text{g/ml}$					
Hg	<0.1 ^d	NA	<0.01	NA	NA	F	NA	NA	NA	NA	NA
Be	<0.02	NA	NA	NA	NA	Li	<0.02	NA	NA	NA	NA
Cd	0.028 ^d	NA	NA	NA	0.009	Ag	0.05	0.002	NA	NA	0.24
As	<1.	NA	<10.0	<1.	NA	Sn	<0.1	NA	NA	NA	NA
V	<0.05	0.035	<10.0	5.	NA	Fe	0.5	NA	<0.1	<75.	NA
Mn	0.05	NA	NA	<1.	NA	Sr	<0.1	NA	<1.0	<75.	NA
Ni	<0.5	NA	NA	NA	NA	Na	5.	NA	<10.0	500.	NA
Sb	<0.5	NA	<0.005	NA	NA	K	1.	NA	NA	75.	NA
Cr	<0.5	NA	<0.1	NA	NA	Ca	5.	NA	NA	NA	NA
Zn	4.	NA	0.43	NA	0.096	Si	50.	NA	NA	NA	NA
Cu	0.1	NA	<10.0	NA	0.19	Mg	0.5	NA	NA	250.	NA
Pb	18.4 ^d	NA	NA	NA	15.	Ba	<0.2	NA	NA	10.	NA
Se	<0.07	NA	<0.1	NA	NA	P	15.	NA	NA	NA	NA
B	2.	NA	NA	NA	NA	S	10.	NA	NA	NA	NA

^a SSMS except Pb by thermal mass spectrometry. ^b Instrumental NAA. ^c HCl extraction preparation. ^d Isotope dilution SSMS. Analysis code: NAA, neutron activation analysis; SSMS, spark source mass spectrometry; ASV, anodic stripping voltammetry; NA, no analysis.

Table VI. Trace Element Range Based on Reported Concentrations^a

Trace element	Coal, ppm	Fly ash, ppm ^b	Residual fuel oil, ppm	Gasoline (Premium) ^c $\mu\text{g/ml}$
Hg	0.02-2	0.1-<18	0.002-0.4	0.008-<0.02
Be	<0.1-0.4	1-7	0.0005-<0.5	<0.0001-<0.01
Cd	0.7-<30	2-<100	0.003-1	0.001-<20
As	0.25-<100	2.8-<200	0.2-<1	<0.02-<200
V	5.5-10	180-2000	40-113	<0.0001-<0.1
Mn	1.9-20	150-500	0.21-1	0.005-<0.1
Ni	4-<40	45-300	20-90	<0.01-<6
Sb	0.04-<30	5.6-<100	0.003-<0.5	<0.0004-<1
Cr	3.4-<30	80-600	0.7-4	<0.001-<0.3
Zn	5-<100	70-1000	0.4-2.0	<0.2-<3
Cu	<0.4-10	33-300	0.2-1	0.005-3.8
Pb	1.8-<30	95-440	1-4	2-650
Se	0.1-<15	0.77-40	0.02-0.15	0.001-<0.2
B	5-15	190-500	0.002-0.2	<0.02-<0.1
F	<2-60	<10-100	0.004 ^d	<0.0003 ^d
Li	0.3-<300	20-300	0.02-<3	0.001-<0.6
Ag	<0.1-<2	0.04-<3	0.0006-0.1	<0.001-<0.3
Sn	0.19-<30	1.9-<100	0.01-5	<0.003-<7
Fe	1800-8000	5.3%-26%	10-20	0.1-0.6
Sr	46-160	69-<1000	<0.4-<0.5	<0.001-<8
Na	100-870	500-6600	<0.4-30	<0.1-0.6
K	20-2200	0.5%-3.1%	0.8-5	0.1-<20
Ca	5500-1000	1.3%-5%	7-<400	<0.05-<20
Si	3000-20000	>10%-20%	8-30	0.5-<2
Mg	600-2000	2200-44000	2-3	0.01-<100
Ba	<2-500	110-700	0.3-5	0.001-<0.2
P	NA ^e	NA	NA	0.2-25
S	NA	NA	NA	30-<200

^a Based on reported concentrations in Tables I, II, III, and IV. These results are obtained from analysis of a single sample in each matrix and may not necessarily be representative of trace element content of the matrices from different sources. ^b ppm by weight, higher concentrations are specified as per cent (%). ^c Premium gasoline, sample code G-10 in Table IV. ^d Only one concentration reported. ^e NA, no analysis.

Ag, Sn, Na, and Mg in fly ash; Hg, Be, Cd, B, Ag, Sn, Na, and Ba in fuel oil; and Cu, Pb, and P in premium gasoline. Tin exhibited the greatest variation in reported concentration in three of the matrices, thereby indicating a need to more closely examine methodology for this element. The reported concentrations of Se, Li, Ba, Ag, and Na varied by more than one order-of-magnitude in two different matrices, also indicating a need for further methodology examination. The remaining elements showed an order-of-magnitude variation in only one matrix material. Of the 28 elements examined, agreement was within an order-of-magnitude for only 7 elements: Si, Ca, S, Sr, Fe, Cr, and Ni in all four matrices.

A comparison of the data derived from the various techniques and shown in Tables I through V, shows that the matrix can have a pronounced effect on the reported range of concentrations. For example, neutron activation analysis for V in coal in four laboratories gave comparable results, ranging from 5.5 to 7 ppm; for gasoline, however, the reported V values ranged from 0.035 to 5 ppm in 3 laboratories. Similar comparisons can be made for other analytical techniques examined.

Estimated precision data on the reported concentrations were submitted by most laboratories. With the exception of one laboratory (No. 3) that indicated results may be as high as 200% of the reported concentrations for some elements, all reported precision values ranged between 1 to 50%. Examination of the large variations in reported concentrations in Table VI shows that although some of the data are within this precision range, most of the data are outside this precision. No estimate of accuracies can be made on the reported concentrations since the absolute or true concentrations of elements in each matrix are not known.

As indicated previously, 89% of the fly ash passed through a 100-mesh screen. Whether the other 11%, of larger particle size, was homogeneously mixed in the samples received by the participating laboratories is not known. However, previous results reported (6) show that Fe in fly ash is concentrated in the larger particle size fractions, where it is present in per cent quantities rather than in trace quantities, thereby facilitating chemical analysis. Consequently, the variation in reported Fe values should give an indication of the homogeneity of the sample, since complete blending of the large Fe-containing particles would represent the most difficult case. Table II shows that for ten reported results from the fly ash matrix (distributed as separate aliquots), the reported

Fe concentrations ranged from 5.3 to 25%. These data, which were derived from four different analytical methods and seven laboratories, represent a per cent relative standard deviation of about 40%, suggesting that an error of approximately 40% can be attributed to inhomogeneity in the fly ash matrix. Differences greater than 40% in fly ash must be attributed to differences in sample preparation and analytical methodology.

The variations in reported concentration are due mainly to sample preparation (loss during extraction, digestion, or ashing process), interferences peculiar to the analytical method employed, or operator error. Little can be done to control discrepancies which are inherent in the analyst; however, sample preparation losses and instrumental deficiencies can be overcome. The study reported here clearly shows that total reliance on a single analytical method for trace analysis for all 28 elements examined may contribute to misleading results in a number of the elements.

CONCLUSIONS

Based on the results of a preliminary interlaboratory comparison of trace analytical methods for 28 elements in coal, fly ash, fuel oil and gasoline, procedures seem to be best (within one order of magnitude) for seven elements: Si, Ca, K, Sr, Fe, Cr, and Ni. Methods used need to be more thoroughly investigated especially for Sn, Se, Li, Ba, Ag, and Na, which varied in reported concentration by more than one order of magnitude in at least two matrices.

There is a real need to determine the accuracy of trace analytical methods in each of the matrices studied. Development of standard reference materials (SRM) certified in trace element concentrations, such as those provided by the National Bureau of Standards (NBS) can go a long way toward helping analysts evaluate their procedures and improving comparability among different methods and different laboratories. EPA in conjunction with NBS is now evaluating SRM's for coal, fly ash, gasoline and fuel oil, which will be certified for 15 trace elements. Concurrent with the certification effort, a 76-laboratory comparison study is also under way. The results of the certification effort and the laboratory study will be the subject of a subsequent report.

Received for review April 2, 1973. Accepted August 22, 1973. Presented at the 165th National Meeting, American Chemical Society, Dallas, Texas, April 1973.

Ion Electrode Based Enzymatic Analysis of Creatinine

Huvin Thompson and G. A. Rechnitz

Department of Chemistry, State University of New York, Buffalo, N.Y. 14214

A method for the selective determination of creatinine, based on the use of a commercially available membrane electrode for ammonia and the newly purified enzyme creatininase, is proposed and evaluated. The purified enzyme is shown to selectively break down creatinine in the presence of possible interferents such as urea, creatine, and arginine. The ammonia produced in the enzymatic reaction is sensed with the membrane electrode and gives rise to a potentiometric signal proportional to the creatinine concentration. Although limited by the present short supply of the purified enzyme, the proposed method is shown to yield useful analytical data over the physiological concentration range.

The recent commercial introduction of ammonia selective membrane electrodes makes possible the development of further specific enzymatic assays for a number of clinically important substances such as creatinine. Creatinine is second only to urea in being the most important nitrogenous end-product excreted by animals and yet the basic routine assay method for this substance is subject to numerous interferences (1). Based on the production of a red colored complex (Jaffé color) between creatinine and picrate in alkaline solution, this method gives erroneous results in the presence of proteins, ketone substances, and glucose. Thus methods employing preliminary separation or reaction kinetic procedures have been developed to minimize the effects of other Jaffé positive materials which are found in serum and urine (2-6). It would be advantageous, therefore, to have a more selective, or even specific, reaction on which to base new methods of analysis. This paper proposes such a method.

It has already been shown (7-16) that the combination of enzymes, to provide selective biochemical action, and ion electrodes to monitor the extent or progress of the reaction, can result in effective new analytical procedures. In the case of creatinine, the development of a novel approach required the availability of an ammonia or ammonium ion sensor not subject to alkali metal ion interference and the isolation of a suitable enzyme with high selectivity for creatinine. Both conditions have now been met.

The existence of a single enzyme capable of selectively

breaking down creatinine to ammonia and *N*-methylhydantoin was demonstrated by Szulmajster in 1958 (17). He isolated this enzyme in quite a pure form from a bacterial source. Other workers had previously failed to do so in various studies of a number of bacterial strains (18-23). In most of these cases, it is probable that a number of enzymes were present in the microorganisms since end-products varied from urea and sarcosine, to glycine, ammonia, and carbon dioxide (24). Beckman Inc. has recently introduced a similar enzyme, creatininase, which also produces ammonia and *N*-methylhydantoin stoichiometrically. Its use in a double Jaffé procedure for the determination of creatinine has been investigated (25).

The present paper investigates the application of an ammonia gas electrode in conjunction with this enzyme to the development of a specific method for routine creatinine analysis. The selectivity of the crude enzyme preparation is examined and its partial purification and subsequent application to analysis is described. Proper enzyme purification and selection of experimental conditions are vital to the success of the proposed method.

EXPERIMENTAL

Chemicals and Reagents. Creatinine (anhydrous), creatine H_2O , urea, and arginine were obtained from the Sigma Chemical Company, St. Louis, Mo. 63118. One gram per cent stock solutions of these were prepared in deionized water and stored in a refrigerator. Fresh working solutions were prepared as required by suitable dilutions of stock solutions with NaH_2PO_4/Na_2HPO_4 , $NaH_2PO_4/NaOH$, or $NaH_2PO_4/Tris$ buffer solutions. Reagent grade chemicals were used to prepare all buffer solutions.

Lyophilized creatininase was obtained from Beckman Inc. Microbics Operations, Fullerton, Calif., and reconstituted as required according to the directions supplied. Reconstituted portions were stored at $-20^\circ C$ and thawed just before use. In this frozen state the enzyme is stable for at least six months, while at room temperature, there is an 80% loss of activity in six hours. Diethylaminoethylcellulose, DE 52 (Whatman, Kent, England) was used in the chromatographic purification. The salt gradient solutions used for elution contained reagent grade sodium chloride and buffer components.

Apparatus. Potential readings of the Orion ammonia electrode (No. 95-10) were taken on a Corning Model 12 pH meter and recorded using a Beckman 10-in. recorder. Technicon AutoAnalyzer modules (Technicon Corporation, Tarrytown, N.Y.) were used in automated routine enzyme and creatinine assays based on the colorimetric procedure. A Beckman DB-G Spectrophotometer was used in all manual assays for enzyme and protein. Dialyses were carried out using hollow fiber beakers or minibeakers (Dow Chemical Company) and chromatographic fractions were collected using an LKB Automatic Fraction Collector, Type 7000.

Methods. Enzyme Assay. One unit of enzyme is defined as the amount catalyzing the hydrolysis of 1 μ mole of creatinine per

- (1) J. T. Clarke, *Clin. Chem.*, **7**, 271 (1961).
- (2) A. C. Teger-Nilsson, *Scand. J. Clin. Lab. Invest.*, **13**, 326 (1961).
- (3) R. A. Rockerbie and K. L. Rasmussen, *Clin. Chim. Acta*, **15**, 475 (1967).
- (4) R. J. Mitchell, *Clin. Chem.*, **19**, 408 (1973).
- (5) K. Larsen, *Clin. Chim. Acta*, **41**, 209 (1972).
- (6) J. Bierens de Haan, *Anal. Lett.*, **5**, 815 (1972).
- (7) S. A. Katz and G. A. Rechnitz, *Fresenius' Z. Anal. Chem.*, **196**, 248 (1965).
- (8) R. P. Buck, *Anal. Chem.*, **44**, 270R (1972).
- (9) R. L. Llenado and G. A. Rechnitz, *Anal. Chem.*, **44**, 486 (1972).
- (10) R. L. Llenado and G. A. Rechnitz, *Anal. Chem.*, **44**, 1366 (1972).
- (11) T. Neubecker and G. A. Rechnitz, *Anal. Lett.*, **5**, 653 (1972).
- (12) R. L. Llenado and G. A. Rechnitz, *Anal. Chem.*, **45**, 826 (1973).
- (13) B. Erlanger and R. Sack, *Anal. Biochem.*, **33**, 318 (1970).
- (14) G. Baum and F. Ward, *Anal. Biochem.*, **43**, 947 (1971).
- (15) G. Guillebaud, *Pure Appl. Chem.*, **25**, 727 (1971).
- (16) G. J. Papariello, A. K. Mukherji, and C. M. Shearer, *Anal. Chem.*, **45**, 790 (1973).

- (17) J. Szulmajster, *Biochim. Biophys. Acta*, **30**, 154 (1958).
- (18) D. Ackerman, *Z. Biol.*, **62**, 208 (1913).
- (19) R. Dubos and R. F. Miller, *J. Biol. Chem.*, **121**, 429 (1937).
- (20) H. A. Krebs and L. V. Eggleston, *Enzymologia*, **1**, 320 (1939).
- (21) S. Akamatsu and R. Miyashita, *Enzymologia*, **15**, 122 (1951).
- (22) J. Roche, G. Lacombe, and H. Girard, *Biochem. Biophys. Acta*, **6**, 210 (1950).
- (23) J. Szulmajster and R. C. Gardiner, *Biochem. Biophys. Acta*, **39**, 167 (1960).
- (24) A. Brunel, G. Brunel-Capelle, and A. Graziana-Sautier, *C. R. Acad. Sci., Ser. D*, **273**, 1799 (1971).
- (25) J. R. Riese and R. S. Davis, Beckman Microbics Operations, La Habra, Calif., private communication, Sept. 1972.

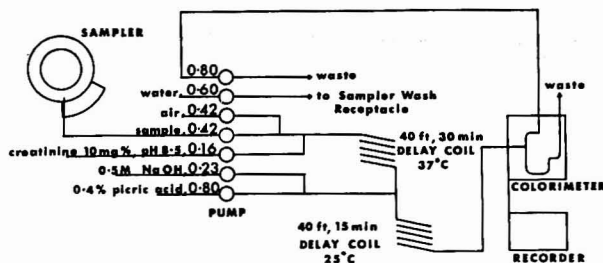


Figure 1. Schematic of continuous flow apparatus for routine enzyme assay

minute at 37 °C and pH 8.5. The following procedure was used for the manual measurement of enzyme activity: 100 μ l of enzyme solution was incubated with an equal volume of 8 μ M creatinine solution, pH 8.5, for the desired time (usually 30 minutes) at 37 °C in a water bath. Enzymatic action was arrested and color development initiated by the addition of 2 ml of alkaline picrate solution (0.2% picric acid, 0.175M NaOH freshly prepared daily). After a further 15-minute incubation at room temperature, the absorbance of the solution was measured at 540 nm against alkaline picrate solution in 5-mm cells. This reading was compared to a blank in which deionized water replaced the enzyme solution.

An automated procedure using the AutoAnalyzer set up, detailed in Figure 1, was used to assay all fractions obtained from the chromatographic column for enzyme activity. This was primarily used to determine the point at which enzyme was being eluted from the column and was sensitive to 0.005 unit ml^{-1} . Since no detailed quantitative information was sought, it was possible to run the assay at 40 samples per hour with a 1:2 sample to wash ratio. This allowed individual peaks to be distinguished while at the same time conserving enzyme fractions. Jaffé color development was measured at 505 nm using a 15-mm flow cell in the filter colorimeter.

Protein Assay. An estimate of the protein content of each fraction was made by taking absorbance readings at 280 nm and 260 nm vs. water in 1-mm quartz cells. The protein content was then calculated using Warburg and Christian's expression (26),

$$C_p = \frac{2.303}{\beta_{280}} \times \frac{\text{per cent protein}}{100} \times \frac{1}{d} \times A_{280}$$

relating concentration of protein, C_p , to molar absorptivity β_{280} , cell path length d , absorbance A_{280} and per cent protein in the protein-nucleic acid mixtures. The value of the expression

$$\frac{2.303}{\beta_{280}} \times \frac{\text{per cent protein}}{100}$$

is related to the ratio of absorbances at 280 nm and 260 nm, A_{280}/A_{260} and is found from tables (26).

Electrode Creatinine Assay. For studies with the crude enzyme, 5-ml samples of 1 to 100 mg % creatinine solutions, pH 8.5, were incubated with 0.25 ml of enzyme solution (approximately 1 unit) for the desired time, at the chosen temperature and in tightly capped vials. The mixtures were then quenched with 50 μ l of 3.8M NaOH which adjusts the pH to approximately 12. At this pH, the ammonia-ammonium ion equilibrium is held almost 100% in favor of the ammonia form and thus the ammonia concentration measured using the electrode is that formed during incubation.

When purified enzyme fractions are used, equal volumes (100 μ l) of enzyme and creatinine solutions are mixed and incubated in sealed vials for 1 hour at 37 °C. Before measuring, the mixtures are quenched with 10 μ l of 1M NaOH. Because of the small volume involved, care should be taken during measurement to ensure that no air bubbles are trapped next to the membrane of the electrode as these may cause errors or sluggish response.

Dialysis and Ion Exchange Chromatography. Hollow fiber dialysis devices proved the most rapid and efficient means of reducing the initial salt concentration of the enzyme preparation to tolerable levels (approximately 10^{-4} M). The minibaker device used had a capacity of 7 ml. The enzyme solution was placed in the

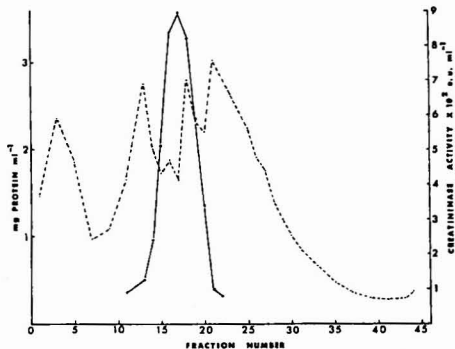


Figure 2. Protein and enzyme activity profile obtained by chromatographic fractionation

Solid line refers to enzyme activity while broken line refers to protein concentration

outer chamber and stirred vigorously by means of a magnetic stirrer while deionized water was passed through the fibers at a rate of 10 ml min^{-1} . The process, carried out in a cold room at 4 °C, was continued for at least 90 minutes. During dialysis, the inlets to the outer chamber were kept sealed to prevent dilution of the enzyme preparation by osmosis.

A typical chromatographic separation of proteins, graphically represented in Figure 2, was carried out using a DEAE cellulose column 1.3 cm in diameter and 4.5 cm long. This was conditioned to the appropriate pH, 6.8 or 8.5, with 25mM buffer. It was found to have a capacity of about 150 mg of protein when loaded with the dialyzed enzyme solution in a 1-hour period. The column was eluted with a salt gradient produced by 50 ml of 25mM buffer and 50 ml of 0.4M NaCl in buffer, 2.5-ml fractions being collected at a rate of 0.5 ml min^{-1} . The entire operation was performed in a cold room at 4 °C.

RESULTS AND DISCUSSION

Studies with Crude Enzyme. In preliminary experiments, the presence of relatively large concentrations of ammonium ions (10^{-2} M) in the crude enzyme preparation was noticed, requiring dialysis of the preparation before further study. The results of these studies using the dialyzed product and different combinations of incubation time and temperature for the range of creatinine concentrations 1-100 mg % are shown in Table I. It can be seen that down to 1 mg % (8.85×10^{-6} M) creatinine, all calibrations are useful but for the short incubation time at 25 °C, the plot becomes curved between 40 and 100 mg %. This indicates that there was incomplete conversion of all creatinine present to ammonia. The slopes of the calibrations carried out with incubation at 25 °C for 60 minutes and at 35 °C for 20 minutes are 47.9 and 49.0 mV per dec-

(28) O. Warburg and W. Christian, *Biochem. Z.*, 310, 384 (1941).

Table I. Creatinine Assay at Different Incubation Times and Temperatures

Creatinine concn, mg %	mV reading		
	25 °C		
	60 Min.	20 Min.	20 Min.
1	21.7	21.5	24.0
10	-21.9	-23.2	-23.5
20	-37.1	-35.6	-38.0
40	-53.4	-49.5	-57.1
60	-62.3	-55.6	-64.8
100	-74.1	-61.9	-74.4

Table II. Reproducibility of the Method

Creatinine concn, mg %	mV readings		
	No. 1	No. 2	No. 3
1	23.0	22.4	24.1
5	-9.8	-10.2	-10.1
10	-22.0	-21.9	-22.0
20	-36.5	-36.3	-36.5
100	-70.0	-70.0	-69.7

ade change in creatinine concentration, respectively. While these do not agree with the theoretically predicted slope of 59.2 mV per decade, the discrepancy might be explained by a slight departure from stoichiometry of the enzyme reaction as was reported by Szulmajster (17). In addition the slight deviation from linearity observed below 10 mg % also serves to reduce the overall slope as calculated by the least squares method.

The reproducibility of the method over the same wide range is shown by the results in Table II. Three replicate samples of each concentration were incubated under identical conditions of time and temperature, 40 minutes at 25 °C. The subsequent potential readings show excellent agreement over the complete range.

A similar set of experiments carried out in the presence of various amounts of three different possible interfering substances which are usually found in serum and urine gave the results shown in Table III. This shows that various other enzymes must be present in the crude preparation since excess ammonia was formed in the case of each interferent tested. Even in the absence of creatinine, ammonia was produced from urea, arginine, and creatine. This, of course, is no problem when colorimetric monitoring of the enzyme reaction is performed (25) but when ammonia production is followed, as in the present study, some method of masking these other effects or of purifying the crude enzyme must be found. The fact that the final step in the production of ammonia from arginine is known to involve urea and urease and the same final step is thought to occur in the bacterial breakdown of creatine (24) prompted the thought that masking the urease enzymes present may eliminate these interferences. Unfortunately, effective urease inhibitors such as silver ions (27) also were found to inhibit creatinase. It was, therefore, necessary to purify the enzyme.

Enzyme Purification Studies. Although the enzyme obtained from Beckman comes from a different source than that studied by Szulmajster, we attempted to modify Szulmajster's purification method for our purposes. Of the two recommended operations—i.e., ammonium sulfate fractionation and ion-exchange chromatography—the former proved ineffective in the present situation. Only small amounts of the protein were precipitated outside (27) J. F. Ambrose, G. B. Kistakowsky, and A. G. Kridl, *J. Amer. Chem. Soc.*, **73**, 1232 (1951).

Table III. Study of the Effects of Urea, Arginine, and Creatine Impurities

Creatinine concn, mg %	mV readings		
	Blank	50 mg % creatine	20 mg % arginine
1	-1.4	-30.4	-22.3
5	-20.5	-36.1	-31.5
20	-36.1	-45.7	-41.2
100	-88.8	-89.5	-89.5

Table IV. Study of Urea Interference When Purified Enzyme Is Used

Creatinine concn, mg %	mV reading	
	Blank	With 200 mg % urea
1	+51.2	+49.3
5	+35.5	+33.5
10	+22.2	+23.0
40	-16.0	-10.5
100	-36.3	-34.1

the recommended 40 to 60% saturation range and even these still contained enzymatic activity.

Chromatographic fractionation, however, proved somewhat more successful, though minor modifications had to be made in Szulmajster's procedure. To increase column capacity, albeit at some slight reduction in flow rate, microgranular DEAE was used as opposed to the fibrous variety. In addition, the column was preconditioned with 25mM buffer instead of distilled water. The fractions collected from the application of a 0-0.3M NaCl gradient, however, showed only one major enzyme peak occurring over the concentration range 0.09-0.12M NaCl and corresponding roughly to the initial stages of the second major protein peak (Figure 2). The specific activity of the most active fractions of this peak was only a slight improvement on the starting specific activity of approximately 30 eu g⁻¹. In later experiments, when the salt gradient was increased to 0-0.5M NaCl and the pH reduced to 6.8, a very minor peak of activity, about one fifth the size of the major peak, occurred around the 0.4M NaCl point. This corresponded to an area of low protein and, thus, the specific activity was in the region of 80 eu g⁻¹. Total activity of this peak was very low and these fractions were not of use in the studies with the purified enzyme detailed below.

While all fractions with creatinase activity displayed no urease activity when tested, the total activity recovered from each column was never greater than 25-30% of that initially bound to the cellulose. At the same time, protein recovery was at least 80%. Such losses indicate that further studies in the purification are necessary.

Studies with Purified Enzyme. Preliminary experiments in which portions of the purified enzyme fractions were incubated for two to sixteen hours with 50 mg % solutions of creatinine, creatine, urea, and arginine showed that only creatinine solutions released any species to which the ammonia electrode was sensitive. It is thus likely that at least the contaminating urease has been removed from the enzyme preparation. Figure 3 shows the trace obtained when a set of ammonia standards and the enzyme substrate mixtures, incubated for two hours at 35 °C were measured with the electrode in a flowing system. The peak displayed by the creatinine/enzyme mixture corresponds well to almost complete conversion of the 50 mg % creatinine to ammonia while ammonia levels in the

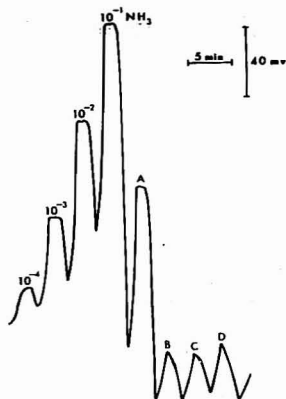


Figure 3. Electrode response to ammonia standards compared to ammonia formed by purified enzyme incubation with various substances

A, 50 mg % creatinine + enzyme; B, 50 mg % creatine + enzyme; C, 50 mg % arginine + enzyme; D, 50 mg % urea + enzyme

creatinine, arginine, and urea incubation mixtures are less than $10^{-5}M$, sufficiently low for even 1 mg % creatinine determinations ($8.85 \times 10^{-5}M$) to be possible.

Table IV shows the results of two parallel runs on a series of creatinine solutions. One series contained only creatinine in buffer while the other had, in addition, 200 mg % of urea. All mixtures were incubated 14 hours at 25 °C before quenching and good agreement is shown between the two series.

If slightly more concentrated enzyme solutions are used, approximately 0.15 eu ml^{-1} , incubation for 30 minutes at 37 °C is sufficient to hydrolyze all creatinine in the 1–100 mg % range. Such enzyme solutions were obtained by reducing the total volume of eluent used in the chromatographic fractionation to 40 ml and collecting 1.5-ml fractions. Using such fractions the calibration plot shown in Figure 4 was obtained.

CONCLUSION

The application of an ammonia gas electrode in conjunction with the enzyme creatininase provides a good

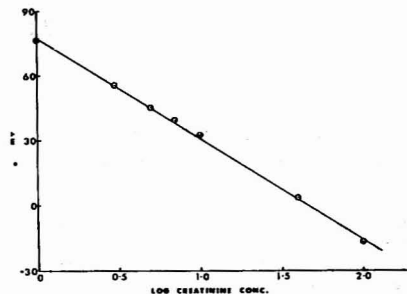


Figure 4. Calibration line for creatinine in 1–100 mg % range

basis for the development of a new method for the determination of creatinine in solution. The purification of the enzyme to a point where arginine, creatine, and urea interferences were eliminated has been demonstrated, and the purified product used to construct a calibration curve in the 1–100 mg % range. While this already covers the complete normal range of creatinine levels found in both serum and urine, it could easily be extended to 500 or 1000 mg %, given a more active enzyme preparation. This possibility of direct measurement over such a wide range is an improvement over the colorimetric procedure which is linear only over a very restricted concentration range. In addition, if purer, more concentrated enzyme preparations were available, the time required for the determinations could be reduced to a few minutes since no lengthy color development periods are required. As a result, the proposed method offers attractive advantages over presently used methods and awaits only the wider availability of purified creatininase enzyme as a condition for routine use.

ACKNOWLEDGMENT

We gratefully acknowledge the loan of AutoAnalyzer components by the Technicon Corporation. Thanks are also due to Sam Otiemo, Oliver Dolly, and colleagues for their assistance with, and helpful discussion of, the enzyme purification procedure.

Received for review June 15, 1973. Accepted September 6, 1973. Work supported by the National Institutes of Health.

Serum Protein Monitoring and Analysis with Ion-Selective Electrodes

P. W. Alexander¹ and G. A. Rechnitz

Department of Chemistry, State University of New York, Buffalo, N. Y. 14214

The highly sensitive response of the silver sulfide membrane electrode to silver ions and sulfur containing functional groups is utilized, in a novel manner, to provide direct potentiometric measurement of individual proteins and protein mixtures in serum. A procedure is developed to minimize protein poisoning of the electrode and to permit its long term use for protein measurements in isotonic saline solution. The results of studies on native and denatured proteins, deproteination of serum samples, and denaturation kinetics are reported and discussed in relation to possible applications in diagnostic medicine.

Clinical applications of ion selective membrane electrodes are becoming increasingly significant as evidenced by the large number of recent publications (1). The main areas of interest so far have been in enzyme analysis (2-4), alkali and alkaline earth metal ion analysis (5), and amino acid analysis (6). However, no methods have yet been published on the direct potentiometric determination of serum proteins using ion selective electrodes. Indirect titrimetric methods have recently been reported for the determination of thiols and disulfide groups in proteins by potentiometric titrations using solid membrane electrodes (7-9), by a silver metal electrode (10), and by coulometric titration (11), while amperometric and spectrophotometric methods have been reviewed in detail (12, 13). An earlier potentiometric method for thiols using a silver "thiol" electrode (14-16) proved to be unsuitable for measurements in protein solutions because of protein poisoning (17).

We therefore investigated the possibility of directly monitoring changes in protein concentration or structure under various reaction conditions and of measuring the rates of such reactions by potentiometry. This paper reports the results of studies using a silver sulfide membrane electrode for the direct determination of changes in protein concentration in blood serum. The method is based on the measurement of the free silver ion activity

after silver mercaptide formation with sulfur groups in proteins. Applications are shown to be possible in areas of interest to clinical analysis including changes in total protein levels and albumin/globulin ratios in serum, the kinetics of protein denaturation, and the analysis of serum filtrates.

EXPERIMENTAL

Apparatus. A Radiometer pH meter Model No. 26 was used for all pH and mV measurements which were carried out in an Orion microdish. The indicator electrode was a silver sulfide membrane electrode, fabricated by a procedure previously reported (18), and used with a double junction reference electrode (Orion Model 90-02-00). The indicator electrode showed Nernstian response to standard silver ion solutions in the concentration range of 10^{-2} - $10^{-6}M$.

Reagents. Silver nitrate of analytical reagent grade was used for preparation of a stock 0.01M silver ion and was standardized by potentiometric titration with 0.01M sodium chloride. The silver-blank solutions, to which protein solutions were subsequently added, were prepared as follows where silver ion was added last in order to prevent precipitation of silver chloride: Blank A. Silver nitrate ($6 \times 10^{-6}M$) in isotonic saline (0.9%) and borax buffer (0.015M boric acid and 0.00375M sodium borate) at pH 8.4; Blank B. Silver nitrate ($6 \times 10^{-6}M$) in a solution of sodium hydroxide (1M) and isotonic saline (0.9%).

Proteins were obtained from the following sources: bovine serum albumin, Cohn Fraction V, from Sigma Chemical Co.; human serum albumin from Nutritional Biochemicals Corporation; human α -globulin, Cohn Fraction III, and human γ -globulin, Cohn Fraction II, purity >99% by electrophoresis from Calbiochem. A standard reference solution of human albumin was obtained from Miles Laboratories, Inc., lot No. 17/A8931 containing 10.3 gram % protein concentration by Kjeldahl and 10.9% by the biuret method, and chloride (8.4 mg/ml). Whole human serum was either Technicon reference serum, lot No. B2C061, containing 6.6 gram % total protein and 4.2 gram % albumin, or Calbiochem Control-340 Mixpack, lot No. 13042, containing 6.4 gram % total protein by the biuret method.

Electrode Conditioning. The silver ion response of the indicator electrode was found to be dependent on conditions of prior exposure to protein solutions. Immediately after polishing the electrode surface, the potential was very slow to reach a steady value for silver ion in protein solutions. However, by conditioning the electrode in a solution of Blank A containing 10 mg/ml albumin with efficient stirring for 48 hr, the response was improved significantly, as shown in the Result Section.

Procedures. For each protein, stock solutions (ca. 50 mg/ml) were freshly prepared before use by dissolving the appropriate protein in isotonic saline solution with gentle stirring. The solutions were standardized by the biuret method (19) using the standard 10 gram % human serum albumin as reference.

For the study of native protein solutions, all potentiometric measurements were made in isotonic saline solutions buffered at pH 8.4. To 1.0 ml of Blank A was added 1-100 μ l of the appropriate protein solution, keeping the total volume constant at 1.50 ml by addition of isotonic saline. This gave a final total Ag^+ concentration of $4 \times 10^{-6}M$ in 0.01M borax buffer and isotonic saline. Potential readings were taken exactly 100 sec after the electrodes were immersed in the solution contained in the Orion microdish with continuous magnetic stirring using a small glass-encased metal bar of size approximately 100 mm \times 1 mm.

Alkaline denaturation was carried out in the following way:

¹ On leave from Chemistry Department, University of New South Wales, Australia.

- (1) R. P. Buck, *Anal. Chem.*, **44** (5), 270R (1972).
- (2) R. A. Lenardo and G. A. Rechnitz, *Anal. Chem.*, **45**, 826 (1973).
- (3) *Ibid.*, **44**, 1366 (1972).
- (4) *Ibid.*, p 468.
- (5) "Ion Selective Electrodes," R. A. Durst, Ed., NBS Special Publication No. 314, U.S. Government Printing Office, Washington, D.C., 1969.
- (6) M. Matsui and H. Freiser, *Anal. Lett.*, **3**, 161 (1970).
- (7) L. C. Gruen and B. S. Harrap, *Anal. Biochem.*, **42**, 377 (1971).
- (8) B. S. Harrap and L. C. Gruen, *ibid.*, p 398.
- (9) W. Selig, *Mikrochim. Acta*, **1973**, p 453.
- (10) T. Y. Toribara and L. Koval, *Talanta*, **17**, 1003 (1970).
- (11) J. H. Ladenson and W. C. Purdy, *Anal. Chim. Acta*, **64**, 259 (1973).
- (12) S. J. Leach, *Anal. Methods Protein Chem.*, **4**, 3 (1966).
- (13) R. Benesch and R. E. Benesch, *Methods Biochem. Anal.*, **10**, 43 (1962).
- (14) R. Cecil and J. R. McPhee, *Biochem. J.*, **59**, 234 (1955).
- (15) R. Cecil, *ibid.*, **58**, III (1954).
- (16) D. Freedman and A. H. Corwin, *J. Biol. Chem.*, **181**, 601 (1949).
- (17) R. Cecil and J. R. McPhee, *Advan. Protein Chem.*, **14**, 255 (1959).

- (18) G. A. Rechnitz and J. Czaban, *Anal. Chem.*, **45**, 471 (1973).
- (19) E. Layne, *Methods Enzymol.*, **3**, 447-53 (1956).

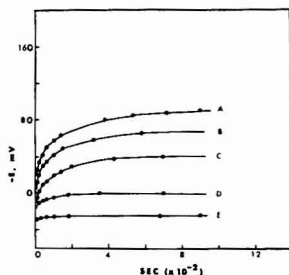


Figure 1. Electrode response times in protein solutions

Solutions of bovine serum albumin in Blank A for concentration: (A) 2.0, (B) 1.4, (C) 0.6, (D) 0.4, (E) 0.2 mg protein/ml

to 0.3 ml of a solution of NaOH (1.0M) and isotonic saline (0.9%) in a 3-ml centrifuge tube was added 1-100 μ l of the appropriate protein solution, again maintaining constant total volume at 1.50 ml by addition of isotonic saline. The solutions were allowed to stand at room temperature for 2 hr and then refrigerated overnight for a total of 24 hr. A 1.0-ml quantity of Blank A was then added, giving a final pH 11.8. The solutions were finally transferred to the microdish and the potential was measured 100 sec after immersion of the electrodes.

The kinetics of the alkaline denaturation process were monitored immediately after the addition of protein solution (1-100 μ l) to Blank B (1.0 ml), keeping total volume constant at 1.10 ml by addition of isotonic saline. Potentials were plotted as a function of time from the point of addition of the protein to the alkaline blank.

Analysis of serum filtrates was carried out in the following way: to 1.0 ml of Blank B in a 3-ml centrifuge tube serum was added in the range 10-100 μ l, followed by isotonic saline to maintain constant volume at 1.10 ml. After standing for 45 min, 1.0 ml of a solution 20% in sulfosalicylic acid and 0.9% in saline was added and the solution was well stirred. The resulting precipitate was centrifuged and the potential of the clear supernatant was measured 100 sec after immersion of the electrodes in the test solution. Potentials were plotted as a function of total protein in the original test solution.

It should be noted that in no instance was any special precaution taken to maintain air-free conditions. This point is discussed in more detail in the Result Section. All measurements were made in the temperature range $25 \pm 1^\circ\text{C}$.

RESULTS

The simple method described for membrane conditioning has allowed the use of the silver electrode in a number of applications of direct potentiometry to the analysis of protein solutions under various reaction conditions, potentially of interest in both fundamental and clinical studies. However, reproducible potential measurements in protein solutions were obtained only by adhering to the definite procedure discussed below.

Electrode Response Times. After conditioning the electrode, the response to changes in pAg on altering the total protein concentration became very much faster. Typical response times are shown in Figure 1 indicating an exponential approach to a steady potential at a given native protein concentration.

The procedure for measurement of silver ion potentials consisted of: first, measurement of the potential at exactly 100 sec after immersion of the electrode in the test solution and, second, measurement for Blank A after each test reading, prior to analysis of the next test solution. The second step was found to be necessary to reproduce the potential readings, otherwise the potentials for consecutive readings of a series of samples were dependent on the potential taken just prior to the solution being tested.

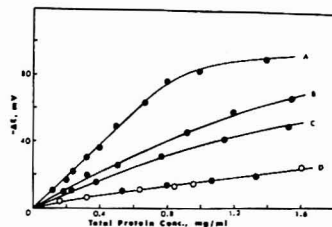


Figure 2. Calibration of native proteins in Blank A at pH 8.4

(A) Bovine albumin, (B) Human serum, (C) Human albumin, (D) Human globulins: α -globulin (O), γ -globulin (●)

Table I. Reproducibility of Ag-Potentials in BSA Solutions*

[BSA] = 4.0 mg/ml			[BSA] = 1.0 mg/ml		
$-E_{Ag}$	E_{blank}	$-\Delta E$	$-E_{Ag}$	E_{blank}	$-\Delta E$
48	61	109	26	58	84
48	60	108	25	58	83
50	60	110	19	58	77
49	59	108	21	58	79
50	54	104			

* $[Ag^+]_{Total} = 4 \times 10^{-6}M$, [Borax Buffer] = 0.01M, [NaCl] = 0.9%.

Table II. Effect of Silver Ion Concentration on Ag-Potential in Solutions of BSA*

$[Ag^+]_{Total}$	E_{Ag}
$0.1 \times 10^{-6}M$	-10
0.4	-51
0.6	-50
1.0	-27

* [BSA]_{Total} = 2 mg/ml, [NaCl] = 0.9%, [Borax Buffer] = 0.01M.

This effect is typical of protein poisoning of electrode membranes and has been observed previously (5) for a calcium ion liquid membrane electrode.

Even after membrane conditioning, a very slow drift in blank potentials occurred over a period of 12 weeks, during which time the electrode was in continuous use with protein solutions without having been repolished. However, the potential differences between Blank A and test protein solutions remained constant and were reproducible. Typical data for reproducibility are given in Table I.

The effect of varying total silver ion concentration in buffered isotonic saline solutions of proteins was also investigated over the small range possible. At concentrations greater than $1 \times 10^{-6}M$, silver chloride precipitate was visible. At concentrations less than $1 \times 10^{-6}M$, it is well known (5) that the electrode response is no longer Nernstian. In the range $1 \times 10^{-6}M$ to $1 \times 10^{-5}M$ silver ion, no visible precipitation occurred if Ag^+ was added last to the buffered saline solution. When bovine serum albumin (BSA) was at a concentration of 2 mg/ml in the buffered silver ion solution, the largest change in potential was observed with the silver ion concentration in the range $4 \times 10^{-6}M$ to $6 \times 10^{-6}M$, as shown in Table II.

Native Protein Calibration. The extent of silver ion binding by proteins was investigated using a solution of silver ion at $4 \times 10^{-6}M$ in buffered saline at pH 8.4. Figure 2 shows potentials as a function of total protein concentration for various protein solutions, indicating appreciable changes in potential with increasing protein con-

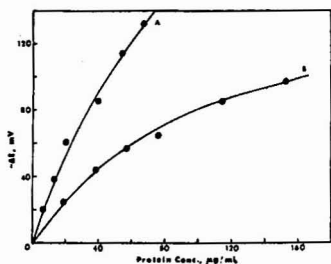


Figure 3. Calibration of proteins after alkaline denaturation for 24 hr

(A) Human albumin, (B) Human γ -globulin

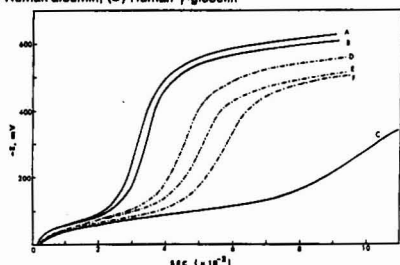


Figure 4. Rate of alkaline denaturation of human proteins

Concentrations of proteins in $\mu\text{g/ml}$ in solutions of Blank B. (A) Total 6.0, Alb/Glob 5.0, (B) Albumin 5.0, (C) γ -globulin 1.0, (D) Total 6.0, Alb/Glob 0.2, (E) γ -Globulin 5.0, (F) Albumin 1.0

centration even in the presence of a large excess of chloride. For BSA, the potential change was approximately linear over a 10-fold change in protein concentration, but thereafter became independent of further changes in BSA concentration. Similar results were observed with the other proteins given in Figure 2 but the slopes were considerably lower, indicating a lesser extent of silver ion-binding than by BSA.

Human serum gave an effect similar to the individual proteins, the potential change being approximately as expected from the sum of the changes for each major protein constituent of the serum. The effect therefore was additive and must be attributed to total serum protein binding of silver ion and not to changes in $[\text{Cl}^-]$ since constant chloride concentration was maintained in the test solution as the serum volume was altered.

Alkaline Denaturation of Proteins. The potential changes observed for the native proteins were quite small, particularly for the globulins. To obtain larger potential changes and, hence, a more sensitive method for determining variations in protein concentration, a possible approach was to denature the proteins, since it is well known (17, 20) that denaturation exposes active groups capable of strong binding of metal ions. Alkaline denaturation was chosen for investigation of this effect on pAg values.

Denaturation of HSA with alkaline saline for 24 hr followed by addition of the buffered Blank A gave very large changes in potential. The potential change was close to linear over a wide concentration of HSA from 1–100 $\mu\text{g/ml}$, as shown in Figure 3. A similar effect was observed for γ -globulin, but again the potential change was less marked than for albumin.

(20) C. Tanford, *Advan. Protein Chem.*, **23**, 122 (1968).

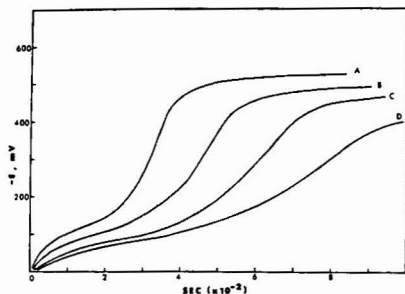


Figure 5. Rate of alkaline denaturation of total protein in human serum

Volumes of serum diluted to 1.10 ml in Blank B. (A) 50, (B) 30, (C) 20, (D) 10 μl

It was therefore possible to determine proteins in the range 1–100 $\mu\text{g/ml}$ corresponding to potential changes up to 130 mV, provided that time was allowed for the denaturation process to approach completion.

Kinetics of Protein Denaturation. Since large changes in potentials occurred on denaturation for 24 hr, the possibility arose that the kinetics of the reaction over a much shorter time interval could also be monitored. In alkaline saline, results given in Figure 4 showed that a sharp transition in protein conformation occurred at the higher protein concentration range after relatively short reaction times. Figure 4 compares the rate profiles of solutions of HSA and γ -globulin, each showing a sharp transition at half-times depending on both the total protein concentration and albumin/globulin (A/G) ratio. In addition, Figure 4 shows a fast initial transition of relatively small potential change, preceding the sharp second transition of large potential change, and this was then followed by a slow continuous negative drift in potential over a 24-hr period.

The effect of alkaline denaturation of normal human serum was found to be similar to that of HSA, as shown in Figure 5. The half-time of the second transition was again dependent on the total serum protein concentration after dilution in the test solution, and an almost linear calibration curve was obtained for the range 10–50 μl of serum diluted to a final volume of 1.10 ml in the alkaline saline, as shown in Figure 6. The analogous calibration curve for HSA was compared to serum in Figure 6 in which potentials measured at 400 sec were plotted against protein concentration. The change in half-time with concentration indicated at least a second-order reaction with respect to protein; nevertheless, analysis for protein was possible within the limits given in Figure 6.

However, since the denaturation reaction was at least second order in protein, it would be expected that mixtures of proteins, e.g. in serum, would be denatured at rates quite different from the individual proteins. This is proved by the results given in Figure 4 and is further illustrated by Figure 6 where it is shown that there is not an exact correlation between the potentials for a given total protein content of serum and for the concentration of a single protein, HSA. It is therefore clear that the half-time of denaturation is closely related to both the A/G ratio and the total protein content of a mixture.

Serum Deproteinization. After alkaline denaturation of serum in silver ion solution followed by acidification with sulfosalicylic acid, protein precipitation occurred. After centrifuging, sufficient soluble products were found to be

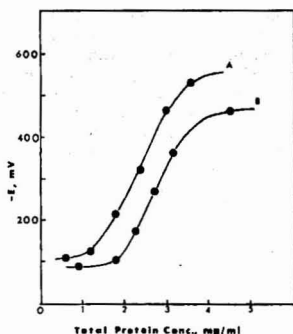


Figure 6. Calibration of proteins measured 400 sec after initiation of alkaline denaturation

(A) Human serum, (B) Human albumin

present in the supernatant to be monitored using the silver electrode. The potential of the supernatant was measured immediately after centrifuging and plotted as a function of total serum protein content of the serum volume originally sampled, as shown in Figure 7. The silver potential change was found to be linear with increasing volumes of serum sampled in the range 10–100 μ l, i.e., dependent on the total serum protein concentration initially denatured.

The potentials, however, were found to change after excessive exposure of the test solution to air. Figure 7 shows the potentials taken $\frac{1}{2}$ hr after the initial readings. This effect would be expected (17) for thiols which are easily air oxidized in the presence of metal ions. This tendency was not observed in alkaline denatured protein solutions since there was a continuous negative change in potential even when measuring the solutions exposed to air. The increased stability toward oxidation in alkaline solution can possibly be attributed (20) to cross-linking between sulfhydryl groups of nonprecipitable species and disulfide groups in the protein.

DISCUSSION

The silver sulfide electrode is known to possess unique properties regarding Nernstian response over a very wide concentration range of free silver ion (5) and satisfactory function at high pH (21). These properties have permitted the development of direct potentiometric methods of analysis of interest in both fundamental and clinical aspects of protein chemistry.

The applications of protein analytical methods in medical diagnosis are of course, well known (22, 23) and include analysis for total protein, specific methods for albumin and globulin, and A/G ratios as well as chromatographic and immunochemical methods of separation. The electrode method reported here represents a single technique for measuring a number of different protein values: changes in total protein concentration, A/G ratio, and serum filtrate thiol content. The proposed procedures are easily carried out and are reproducible providing that the slow response of the electrode is taken into account.

One point of interest arising from these results is the identity of the species responsible for the potential changes. In native protein solutions, the reaction of Ag^+

- (21) G. A. Rechnitz and T. M. Hsue, *Anal. Chem.*, **40**, 1054 (1968).
 (22) R. J. Henry, "Clinical Chemistry: Principles and Technics," Hoeber Medical Division, Harper and Row, New York, N.Y., 1968.
 (23) F. W. Sunderman and F. W. Sunderman, Jr., "The Serum Proteins and Dysproteinemias," J. B. Lippincott Co., Philadelphia, Pa., 1964.

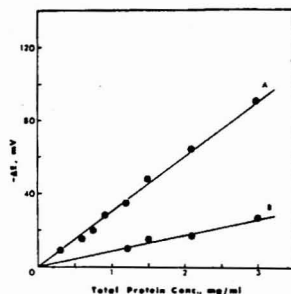


Figure 7. Calibration of protein degradation products in serum centrifugates after deproteinization of denatured serum

(A) Immediately after centrifuging, (B) 30 min after exposure to air

with protein-thiol groups to give silver mercaptides would be expected to change pAg values and hence the potential, although some doubt still exists on the stoichiometry of this reaction (7, 9). This was confirmed by the nonlinear shape of the calibration curves in Figure 2, which reached a limiting value due to effectively complete silver mercaptide formation in the presence of excess protein. It is emphasized that potential changes were observable even in the presence of excess chloride which markedly decreased the free silver ion concentration available for mercaptide formation.

In alkaline denatured protein solutions, disulfide cross-links are known (17, 20) to be ruptured, producing thiol groups in excess of the silver ion concentration. Thiols affect the potential of silver sulfide membrane electrodes whether added silver ion is present or not (7, 9) and, hence, the calibration curve in Figure 2 was linear over a much wider range of denatured protein concentrations than in the case of native proteins. The main problem in solutions of high thiol concentration is the very slow response of the electrode when it is re-immersed in the blank solution, taking up to 20 min to return to the base potential before the next test solution can be measured.

Figures 2 and 3 also show that total protein analysis is possible in a biological fluid such as blood serum with little pretreatment either in the native or denatured state. The method, like most other protein analytical methods (9), suffers from the fact that the response to individual native or denatured proteins varies. However, the electrode method is more sensitive than the biuret method and is less liable to interference from turbidity or ammonium salts.

Of even greater interest is the capability of the electrode to monitor the kinetics of protein denaturation at high pH, and to analyze serum filtrates. It has been established in Figures 4 and 5 that sharp transitions in protein conformation occurred in alkaline silver ion solutions. Rate data at extremely high pH have not been reported previously using the common techniques for monitoring denaturation reactions such as optical rotatory dispersion, intrinsic viscosity, and difference spectroscopy (20, 24). Alkaline denaturation is not well understood (20), but because of the specificity of the silver electrode for thiol groups, it seems certain that the transition observed in Figures 4 and 5 can be attributed at least partially to random-coil formation on rupture of the disulfide cross-links of the serum proteins. The method therefore appears promising for use in fundamental studies on protein conformation.

- (24) W. Kauzmann, *Advan. Protein Chem.*, **14**, 1 (1959).

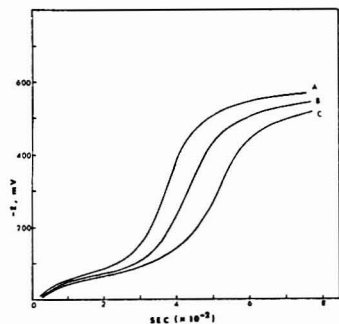


Figure 8. Comparison of rate of alkaline denaturation of protein mixtures approximating to normal and abnormal serum samples

Albumin/ γ -Globulin ratios in mg/ml after dilution by a factor of 12.5. Normal: (A) 3.6/2.2; Abnormals: (B) 2.2/2.5, (C) 1.6/3.0

Furthermore, in Figure 4 it has been shown that the rates of these reactions depend first on protein structure and second, on the total protein composition of a mixture. Serum albumin thus reacts at a faster rate than γ -globulin at the same concentration. Keeping the total concentration constant in a mixture of these two proteins, but changing A/G ratio from 5.0 to 0.2, gave quite different half-times. Therefore, for conditions where albumin is in excess, the half-time of the reaction approaches the value for albumin itself. In abnormal serum samples, in which globulin is in excess (hyperglobulinemia), the half-time would be expected to approach the value for globulin. Measurement of the half-times of normal controls as compared to unknowns can therefore be used to distinguish this condition, in conjunction with the total protein analysis.

As an example, synthetic solutions were prepared containing A/G ratios published for abnormal and normal cases (5). Figure 8 shows that the rates of denaturation of the samples were quite different. As expected from Figures 4-6, the rate of denaturation of the normal sample was considerably faster than the abnormal and measurement of potentials at 400 sec gave remarkably large potential differences.

However, hyperglobulinemia is certainly not diagnostic of any one disease (22, 23) and is characteristic, for exam-

ple, of most inflammatory conditions. Better specificity of diagnosis might be expected (25) if the above determinations were used in conjunction with analysis of protein degradation products after deproteination of the denatured serum, as shown in Figure 7. Analogous determinations have previously been carried out by polarography using the Brdicka serological filtrate test, recently reviewed by Homolka (25). In conjunction with this test, Müller and Davis (26) proposed the calculation of the so-called protein index, viz. the ratio of serum filtrate sulfur components to total serum denatured protein sulfur levels determined by polarography. Such data are of particular interest in cancer studies and, although not specific for cancer, gave some correlation with malignant conditions (25).

It is now clear that similar studies can be carried out using ion electrode potentiometry, with the well known advantages of simplicity of potentiometry over polarography. It is emphasized that the most important property of the electrode kinetic method is the extremely sensitive change in potential with small changes in serum volume as shown in Figures 5 and 6. The potential difference between 20- and 30- μ l samples in Figure 5 measured at 500 sec was approximately 200 mV, equivalent to a change in free Ag^+ concentration of a factor of over 1000 for a change in total protein concentration of a factor of only 1.5. This high sensitivity is ideally suited to clinical analysis for differentiating between normal and abnormal protein levels in serum.

On the other hand, it is clear from these kinetic studies that if the denaturation is allowed to proceed too long, as shown in Figure 8, then the potential differences between abnormal and normals become very small relative to the overall change. This is possibly the reason for the relatively small differences between normal and abnormal samples observed by Brdicka (27) using polarography of alkaline denatured serum. The electrode methods described herein therefore offer interesting possibilities in clinical analysis, particularly with regard to determination of the protein index in cancer studies.

Received for review June 20, 1973. Accepted September 10, 1973. Financial support by the National Institutes of Health is gratefully acknowledged.

(25) J. Homolka, *Methods Biochem. Anal.*, **19**, 435 (1971).

(26) O. H. Müller and J. S. Davis, Jr., *J. Biol. Chem.*, **159**, 667 (1945).

(27) R. Brdicka, *Nature (London)*, **139**, 330 (1937).

Glass Electrode Responses Interpreted by the Solid State Homogeneous- and Heterogeneous-Site Membrane Potential Theory

Richard P. Buck, John H. Boles, Robin D. Porter, and Jeffrey A. Margolis

The William Rand Kenan, Jr., Laboratories of Chemistry, University of North Carolina, Chapel Hill, N.C. 27514

A new theory of glass membrane electrode response based on a solid state model is illustrated by application to lithium and sodium responses of five commercially available low-error pH glass electrodes. Mobility, ion exchange, and overall selectivity parameters have been calculated at several interference activities and temperatures from 6 to 55 °C. Beckman sodium selective electrode responses were measured for hydrogen, lithium, and potassium ions and characteristic parameters calculated. For the latter electrodes, conditions giving slow response, non-Nernstian slopes, and long-term drift were explored. The pH glass results suggest that the cation mobilities exceed those of protons while the reverse is found for the sodium-selective glass. The overriding effect of ion exchange selectivity follows from the theoretical fit of the experimental data.

A new solid-state theory of glass electrode responses (1) reduces, for homogeneous-site glasses, to the expression,

$$\phi'' - \phi' = \phi^0 + \frac{RT}{F} \ln \left\{ [a_H' + K_{H/M} (K_1 a_H' a_M')^{1/2}] [1 + K_1 a_M' / a_H']^{1/2} \right\} \quad (1)$$

where the test solution is the prime side and the inner, constant reference solution is the double prime side. The two parameters are K_1 , the ion exchange constant for metal ions replacing protons on silica sites, and $K_{H/M}$, a mobility and defect generation ratio term.

$$K_{H/M} = \frac{u_i^M k_{i1}^M \gamma_{iM}}{u_i^H k_{i1}^H \gamma_{iH}} \quad (2)$$

In the Eisenman model (2-4), the final pH response at constant interference activity a_M' is related to K^{POT} , which in our theory is

$$K^{POT} = K_{H/M} K_1 \quad (3)$$

$K_{H/M}$ being formally identical to the mobility ratio in Eisenman's (4) model. The cross terms in Equation 1 give an effect similar, but not identical, to the Eisenman, Rudin, and Casby "n-type" non-ideality (2). The two theories give responses which are not congruent. However, there is a best n value curve which passes through the solid state curve at the intersection $pH = K^{POT} a_M'$ and is given by

$$n = \frac{59.14}{17.7} \ln \left\{ (1 + K_{H/M}^{1/2}) (1 + 1/K_{H/M}^{1/2}) \right\} \quad (4)$$

Note that in the original text (1), both Equations 1 and 4 occur as Equations 31 and 43 and 44, and contain typographical errors. Similarly, for cation selective glasses containing heterogeneous sites, typically AlO^- , the potential response was derived as

$$\phi'' - \phi' = \phi^0 + \frac{RT}{F} \ln \left\{ [a_{Na}' + K_{Na/M} (a_{Na}' a_M')^{1/2}] \times [1 + K_{Na/M} (a_M' / a_{Na}')^{1/2}] \right\} \quad (5a)$$

$$= \phi^0 + \frac{RT}{F} \ln \left\{ K_{Na/M} (a_{Na}' a_M')^{1/2} + \frac{RT}{F} \times \right.$$

$$\left. \ln \left\{ [a_M' + K_{M/Na} (a_{Na}' a_M')^{1/2}] [1 + K_{M/Na} (a_{Na}' / a_M')^{1/2}] \right\} \right\} \quad (5b)$$

$$K_{Na/M}^{(1)} = 1/K_{M/Na}^{(1)} = \left[\frac{k_{21}^M \gamma_{2M}^M K_2}{k_{21}^H \gamma_{2H}^H} \right]^{1/2} \quad (6a)$$

$$K_{Na/M}^{(2)} = 1/K_{M/Na}^{(2)} = \frac{u_i^M}{u_i^{Na}} K_{Na/M}^{(1)} \quad (6b)$$

for a sodium selective example under conditions where a_M is the interfering ion. In this case, the best n-type non-ideal curve is found from

$$n = \frac{59.14}{17.7} \ln \left\{ \left(1 + \sqrt{\frac{u_i^M}{u_i^{Na}}} \right) \left(1 + \sqrt{\frac{u_i^{Na}}{u_i^M}} \right) \right\} \quad (7)$$

Equations 5a, b have forms very similar to Equation 1. However, the former Equation 1 was derived from the assumption of few mobile defect interstitial cations, while Equation 5 follows from the assumption that cations belonging to hetero-sites are completely dissociated and mobile.

Response data for monovalent ion interferences of pH and sodium-ion sensitive electrodes over a wide activity range are infrequently reported in the literature and in manufacturer's data sheets. The sodium errors of several pH glasses (in pH units) are collected in Bates (5), Mattock and Taylor (6), and Simon and Wegmann (7). Mixture responses for sodium and other cation-selective compositions are presented in a review (3) and in a book edited by Eisenman (4), and in papers by Savage and Isard (8), Eckfeldt and Proctor (9), Townsing, Posner, and Quirk (10), Stefanac and Simon (11), and Nicolsky and

(1) R. P. Buck, *Anal. Chem.*, **45**, 654 (1973).

(2) G. Eisenman, D. O. Rudin, and J. V. Casby, *Science*, **126**, 831 (1957).

(3) G. Eisenman, "Advances in Analytical Chemistry and Instrumentation," C. N. Reilley, Ed., Interscience, New York, N.Y., 1964, Vol. 4, pp 213-369.

(4) G. Eisenman, "Glass Electrodes for Hydrogen and Other Cations," G. Eisenman, Ed., Marcel Dekker, New York, N.Y. 1967, Chap. 5, pp 133-173.

(5) R. G. Bates, "Determination of pH—Theory and Practice," Wiley and Sons, New York, N.Y., 1964, p 316.

(6) G. Mattock and G. Ross Taylor, "pH Measurement and Titration," The Macmillan Co., New York, N.Y., 1961, p 107.

(7) W. Simon and D. Wegmann, *Helv. Chim. Acta*, **41**, 2308 (1958).

(8) J. A. Savage and J. O. Isard, *Phys. Chem. Glasses*, **7** (2), 60 (1966).

(9) E. L. Eckfeldt and W. E. Proctor, Jr., *Anal. Chem.*, **43**, 332 (1971).

(10) P. C. Townsing, A. M. Posner, and J. P. Quirk, *Anal. Chim. Acta*, **38**, 464 (1967).

(11) Z. Stefanac and W. Simon, *Anal. Lett.*, **1** (2), 1 (1967).

Shultz (12). The Beckman No. 39278 sodium selective electrode was studied originally by Budd (13). We do not agree with his result that the electrode is insensitive to lithium activities. In addition, we do find the pH sensitivity agrees with the manufacturer's early Bulletin No. 1155B, but not with later information, Beckman Bulletin 7145 (1968) or work by Stock (14). Other comments on the reliability of this electrode in application studies are given by Shatkey and Lerman (15), Gardner and Nancollas (16), and Huston and Butler (17).

The author has previously noted the lack of systematic error response data on commercial glass electrodes (18). Perhaps it is understandable, on the basis of variability of raw material compositions and the possibility of improved or changed formulations; manufacturers prefer to state only maximum error over a prescribed test solution composition range. Furthermore, it is probable that selectivity coefficients vary with the age of an electrode. This point has been verified for cation-selective glasses (19). As we shall demonstrate in the following, no single concentration-independent selectivity coefficient of the Nicolsky or Eisenman ($n = 1$) types will fit the response over a wide concentration range. Although we prefer Equation 1 above, it or another two-parameter function such as the Eisenman-Rudin-Casby equation (2) is necessary for a reliable data fit. These factors may have discouraged earlier researchers from reporting the responses of glass electrodes in quantitative form.

In this study of monovalent cation errors of glass electrodes, we have focused attention on Beckman commercially available products based on lithia-silica compositions. These are the low sodium error E-2 glass, moderate sodium error General Purpose glass, and the optimized sodium-selective glass. The method of mixtures has been used to obtain parameters describing pH, pNa, pLi and pK responses over a temperature range 6-55 °C. We have also investigated lithium and sodium responses of Corning, Radiometer, and Leeds and Northrup pH glasses, but in less detail.

EXPERIMENTAL

Apparatus. All responses were measured with the expanded scale on a Beckman Model 76 Century SS pH Meter and a Beckman 10-in. recorder (No. 100502). The electrodes studied in detail were Beckman Type E-2 (No. 39004), General Purpose (No. 41263) and Sodium Ion electrode (No. 39278). Comparative measurements using fewer points and narrower temperature range were performed on the Leeds and Northrup pH electrode No. 117235, Radiometer pH electrode Type G202B and the Corning pH electrode No. 476020. A Fisher calomel electrode was used as reference. Because of the significant sodium and lithium errors at pH values 11 and above, a hydrogen electrode was used to measure and monitor the pH of salt solutions above pH 8. The preparation and design was similar to that suggested by Ives and Janz (20). A large coiled wire of platinum was used instead of the square sheet. The electrode was quick to respond (5 seconds) and was not easily contaminated. A Leeds and Northrup Black Dot electrode was used for pH monitoring during the sodium-selective electrode study. A water jacket cell connected to a Beckman Thermocirculator kept solutions held in Teflon beakers at constant temperature.

Reagents. All chemicals were analytical reagent grade. Beckman standard buffers of pH 4.01, 6.86, and 9.18 at 25 °C were used for standardizing the pH meter and calibrating pH electrodes. Secondary standards, stirred saturated solutions of barium, calcium, and magnesium hydroxides were used for pH 13.35, 12.45, and 10.4, respectively. All water used was doubly deionized and distilled. Sodium content was below $10^{-6}M$, when analyzed by flame emission.

Procedure for pH Glass Measurements. The hydrogen electrode response was checked against standard buffers to establish potential *vs.* pH at each temperature. If the agreement was not within ± 1 mV of the usual value, or the response was sluggish or unsteady, the surface was cleaned and replatinized. Stock solutions of interfering ions, sodium, potassium, and lithium chlorides, were made at concentrations of 0.1, 0.3, 1.0, and 3.0M. Each series of response measurements used one of those solutions at varying pH established by a titration method as follows: the pH was increased by incremental addition of 10^{-2} and 1M potassium hydroxide solutions to the stirred stock solutions. Potassium hydroxide was selected because this cation has little interference effect on these pH glass electrodes. In every case, the potassium error at 1M KCl in saturated barium hydroxide was less than 5 mV. Each potassium hydroxide solution contained the same concentration of interfering ion as the solution to which it was added; thus, the interference concentration was maintained constant although the ionic strength was not simultaneously maintained. This method, using dilute KOH permitted many measurements at intermediate pH values. However, at high pH, an uncertainty in the activity coefficients of Li⁺ and Na⁺ in the mixtures was created. Even when pure NaOH or LiOH was used as titrant to maintain constant ionic strength, there was still an uncertainty in the single ion activities at high pH. Approximate activity coefficients were obtained from Robinson and Stokes (21). Measurements were started at approximately neutral pH, since the response of the electrodes was determined to be Nernstian below this pH for all concentrations of interfering ions in this experiment.

Solutions were continuously stirred and readings taken 2 minutes after each pH change. The electrodes gave a steady response (± 1.0 mV) after 1 minute during each run. After a series of measurements with one concentration of interfering ion, electrodes were soaked at least 15 hours in pH 4 buffer. The potential responses of the two types of Beckman pH glass electrodes were measured at 10, 25, 40, and 55 °C in 1.0M lithium chloride and 1.0M sodium chloride with variable pH.

Procedure for Sodium Electrode Measurements. Sodium sensitive electrodes were characterized at 6, 14, 25, and 41 °C using 10^{-4} to 1M NaCl in saturated buffers at pH 10.4, 12.45, and 13.35. After correction to activities, least square 25 °C slopes were determined to be 58.6, 58.6, and 58.4. It is important that the electrodes be stored in buffer-free 0.1M NaCl. The slopes are significantly degraded from 10^{-2} to $10^{-4}M$ when the electrodes are stored in either pH 12.45 or 13.35 buffer. The best slopes obtained, while low, are within manufacturer's specifications. The titration method was used to determine the hydrogen ion interference. Stock solutions 0.7M NaOH, 0.03M sodium phthalate, and 0.7M NaCl, 0.3M HCl were serially diluted to provide nearly constant ionic strength, constant sodium activity basic solutions, and corresponding titrants. Sodium responses were measured from basic to acidic in stirred solutions. After each acid increment was added, the solution was stirred for 1 minute and readings were recorded continuously over a 3-minute period. Presence of phthalate permitted slight buffering in the neutral to weak acid region so that many points could be readily measured. At higher acidities, pH 1-3, the electrode potential was very unstable, and potentials had to be observed quickly with some loss of accuracy.

Exposure to high interference levels of H⁺, K⁺, and Li⁺, caused long drift times in returning to basic reference solutions for further experiment. Potassium interferences were measured in KCl-NaCl mixtures saturated with MgO, while lithium responses were determined in Ca(OH)₂-saturated LiCl, NaCl mixtures. Constant ionic strength could not be maintained in these experiments. Interferences believed to be caused by Ca(OH)⁺ and Ba(OH)⁺ were observed and these effects were comparable in magnitude to the potassium error. Consequently, MgO at pH 10.4 was used in the measurements of potassium responses.

(12) B. P. Nicolsky and M. M. Shultz, *Vestn. Leningrad. Univ.*, No. 4, 73-186 (1983).

(13) A. L. Budd, *J. Electroanal. Chem.*, 5, 35 (1963).

(14) J. T. Stock, *J. Chem. Educ.*, 47, 593 (1970).

(15) A. Shatkey and A. Lerman, *Anal. Chem.*, 41, 514 (1969).

(16) G. L. Gardner and G. H. Nancollas, *Anal. Chem.*, 41, 202 (1969).

(17) R. Huston and J. N. Butler, *Anal. Chem.*, 41, 1695 (1969).

(18) R. P. Buck, "Physical Methods of Chemistry," B. Rossiter and A. Weissberger, Ed., Wiley and Sons, New York, N.Y., 1971, Chap. 2, Vol. 1, Part 2A, p 89.

(19) E. W. Moore and J. W. Ross, *Science*, 148, 71, (1965).

(20) D. J. G. Ives and G. J. Janz, "Reference Electrodes, Theory and Practice," Academic Press, New York, N.Y., 1961.

(21) R. A. Robinson and R. H. Stokes, "Electrolyte Solutions," Butterworths London, 1955, Appendix 8.10.

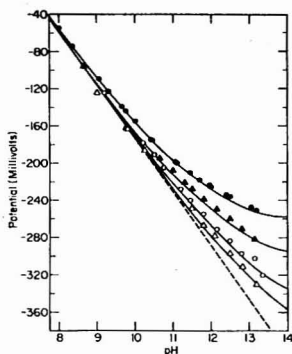


Figure 1. Response of the Beckman General Purpose Electrode (No. 41263) to pH with sodium as an interfering ion, $\phi^0 = 416$ mV, 25 °C

●, 3.0M; ▲, 1.0M; ○, 0.3M; △, 0.1M

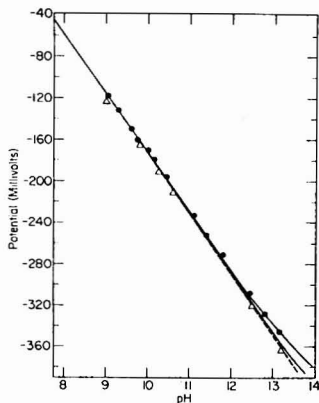


Figure 2. Response of the Beckman Type E-2 Electrode (No. 39004) to pH with sodium as an interfering ion, $\phi^0 = 414$ mV, 25 °C

●, 3.0M; △, 0.1M

RESULTS AND DISCUSSION

pH Electrodes. Figure 1 shows the response of the Beckman No. 41263 General Purpose electrode to pH with sodium as an interfering ion. The dotted line on the following graphs is the estimated or measured pure response without interference. The solid curves are theoretical calculations using Equation 1 with parameters listed in Tables I and II. Figure 2 shows the response of the Beckman No. 39004 E-2 electrode to pH with sodium as an interfering ion. The results bear out the manufacturer's claim in Beckman Bulletin No. 678-D that this electrode shows little sodium error throughout the pH range.

Figures 3 and 4 show the electrode responses, respectively, for pH with lithium as an interference. In both cases, the electrodes are more sensitive to lithium than to sodium. In Figures 1, 3, and 4, a characteristic feature of the solid state theory is apparent, *viz.*, the interference response is prolonged into the low pH regions. The simpler theories, for example of the Nicolsky form, would predict only a few millivolts error at pH 11 for 1M NaCl

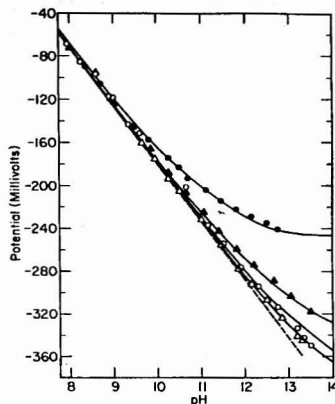


Figure 3. Response of the Beckman General Purpose Electrode (No. 41263) to pH with lithium as an interfering ion $\phi^0 = 413$ mV, 25 °C

●, 3.0M; ▲, 1.0M; ○, 0.3M; △, 0.1M

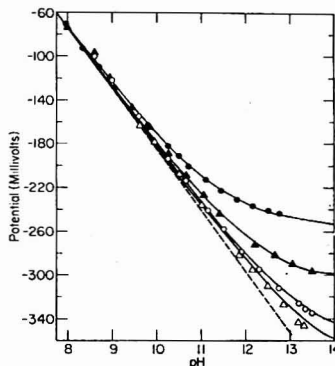


Figure 4. Response of the Beckman Type E-2 Electrode (No. 39004) to pH with lithium as an interfering ion, $\phi^0 = 407$ mV, 25 °C

●, 3.0M; ▲, 1.0M; ○, 0.3M; △, 0.1M

with $K^{POT} = 1.5 \times 10^{-12}$ using the General Purpose electrode. From the raw data used for the theoretical data fits in those figures, the fundamental parameters $K_{H/M}$ and K_1 of our theory can be computed and combined in Table I. The parameters were systematically varied to obtain a fit, but the results were not least square optimized, and the values are not better than a factor of two.

Electrode responses *vs.* pH and 1.0M sodium and lithium ions and different temperatures from 10 to 55 °C are illustrated in Figures 5-7. The solid curves are theoretical fits using the constants in Table II. The variations in ϕ^0 are believed to be partly junction potential differences and asymmetry effects which may, in fact, reflect slow rates of response. The mobility parameter $K_{H/M}$ has very little concentration dependence. However, there is some temperature dependence corresponding to a slightly smaller activation energy for sodium and lithium compared with hydrogen transport. At 50 °C, the mobility ratio $u(\text{Li}^+)/u(\text{H}^+)$ has been measured at 56.5 by Baucke

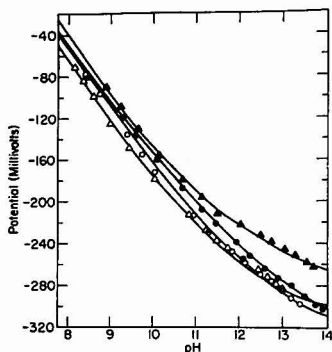


Figure 5. Response of the Beckman General Purpose Electrode (No. 41263) to pH at four temperatures with 1.0M sodium as interfering ion

Symbol	Temp, °C	φ^0 mV
●	10	401
○	25	420
△	40	432
▲	55	480

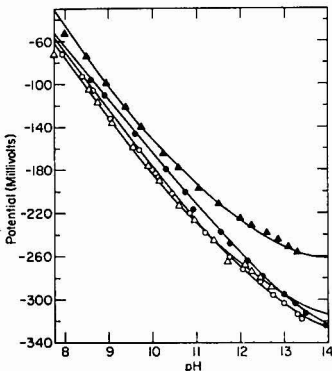


Figure 6. Response of the Beckman General Purpose Electrode (No. 41263) to pH at four temperatures with 1.0M lithium as interfering ion

Symbol	Temp, °C	φ^0 mV
●	10	395
○	25	403
△	40	422
▲	55	475

(22) for a Jaener pH glass. The constant K_1 is a pseudo thermodynamic exchange constant since it involves solution activities and surface concentrations, and should be both concentration and temperature dependent. Increasing solution salt activity or raising the temperature at constant salt activity favors increased exchange of the metal ions and increased error response.

Computed results for three commercially available pH electrodes are summarized in Table III. The data for the highest pH responses were weighted most heavily so that the final K^{POT} values are considered accurate. The subdivision of this value into $K_{H/M}$ and K_1 depends, as above, on small error responses at lower pH values, and is less

(22). F. G. K. Baucke, *Z. Naturforsch.*, **28**, 1778 (1971).

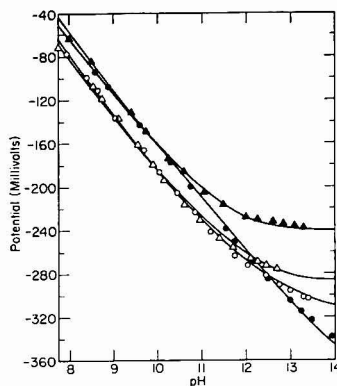


Figure 7. Response of the Beckman Type E-2 Electrode (No. 39004) to pH at four temperatures with 1.0M lithium as interfering ion

Symbol	Temp, °C	φ^0 mV
●	10	395
○	25	392
△	40	419
▲	55	463

Table I. Li^+ and Na^+ Response Parameters for Beckman Instrument Glasses at 25 °C

General Purpose Glass	pH	$K_{H/M}$	K_1	$K_{H/M}^{POT}$
Electrode (No. 41263)				
3.0M Sodium	20	7.5×10^{-14}	1.5×10^{-12}	
1.0M Sodium	20	7.5×10^{-14}	1.5×10^{-12}	
0.3M Sodium	20	$5. \times 10^{-14}$	1.0×10^{-12}	
0.1M Sodium	20	$1. \times 10^{-14}$	$2. \times 10^{-12}$	
3.0M Lithium	20	$1. \times 10^{-13}$	$2. \times 10^{-12}$	
1.0M Lithium	20	$1. \times 10^{-14}$	$2. \times 10^{-12}$	
0.3M Lithium	18	6.5×10^{-15}	1.2×10^{-12}	
0.1M Lithium	20	$8. \times 10^{-15}$	1.6×10^{-13}	
E-2 Glass pH Electrode (No. 39004)				
3.0M Sodium	10	$1. \times 10^{-16}$	$1. \times 10^{-15}$	
0.1M Sodium	10	$1. \times 10^{-16}$	$1. \times 10^{-15}$	
3.0M Lithium	19	$1. \times 10^{-12}$	$2. \times 10^{-12}$	
1.0M Lithium	15	$1. \times 10^{-13}$	1.5×10^{-12}	
0.3M Lithium	18	2.5×10^{-14}	4.5×10^{-13}	
0.1M Lithium	18	2.5×10^{-14}	4.5×10^{-13}	

accurate. It is clear by comparing K^{POT} values that the error responses due to lithium at 25 °C increase at constant lithium in the sequence:

Radiometer \approx L and N < Beckman Gen. Purp. < Corning < Beckman E-2 while the corresponding sodium error sequence is: Beckman E-2 \approx Corning < Radiometer <

L and N < Beckman Gen Purp. The Leeds and Northrup Black Dot electrode error in lithium is remarkably insensitive to temperature, while the sodium error of the Corning electrode is nearly constant. All are excellent glasses in terms of their freedom from sodium error in the practical range of pH, less than 12.

Na Selective Electrodes. The constant sodium, variable pH responses of the Beckman Sodium-selective electrode are illustrated for three concentrations at four temperatures in Figures 8-11. These data are complicated by slow responses of the electrode at high acidities. The data fit for the theoretical equation is very good in some cases, but only fair in others. The fit can be done much more

Table II. Temperature Dependence of Response Parameters for Beckman Instrument Glasses

General Purpose Glass pH Electrode (No. 41263) $\Delta H^\circ = 20$ Kcal		Temp, °C	$K_{H/Na}$	K_1	$K_{H/Na}^{POT}$
1.0M Sodium		10	10	$1. \times 10^{-14}$	$1. \times 10^{-13}$
		25	15	2.5×10^{-14}	$4. \times 10^{-13}$
		40	17.5	$1. \times 10^{-13}$	1.8×10^{-12}
		55	25	2.5×10^{-13}	6.3×10^{-12}
1.0M Lithium		10	5	$1. \times 10^{-14}$	$5. \times 10^{-14}$
		25	10	2.5×10^{-14}	2.5×10^{-13}
		40	30	$3. \times 10^{-14}$	$9. \times 10^{-12}$
		55	40	$1. \times 10^{-12}$	$4. \times 10^{-12}$
E-2 Glass pH Electrode (No. 39004) $\Delta H^\circ = 17$ Kcal					
1.0M Lithium		10	4	$1. \times 10^{-15}$	$4. \times 10^{-15}$
		25	17.5	$5. \times 10^{-14}$	$9. \times 10^{-13}$
		40	12.5	$3. \times 10^{-13}$	7.5×10^{-12}
		55	15	$1. \times 10^{-12}$	1.5×10^{-11}

Table III. Li⁺ and Na⁺ Response Parameters of pH Glass Electrodes

Electrode	Parameter	15 °C value	25 °C value	35 °C value
Leeds and Northrup Black Dot No. 117235	$K_{H/Li}^{POT}$	1.1×10^{-13}	$1. \times 10^{-13}$	5.4×10^{-13}
	$K_1(H/Li)$	$3. \times 10^{-14}$	$1. \times 10^{-14}$	$8. \times 10^{-14}$
	$K_{H/Li}$	3.8	10	6.8
	$K_{H/Na}^{POT}$	$5. \times 10^{-14}$	4.5×10^{-14}	2.6×10^{-14}
	$K_1(H/Na)$	$5. \times 10^{-14}$	$1. \times 10^{-14}$	$2. \times 10^{-14}$
	$K_{H/Na}$	10	4.5	13
	$K_{H/Na}^{POT}$	5.6×10^{-14}	4.7×10^{-13}	2.2×10^{-12}
Corning No. 476020	$K_1(H/Li)$	$2. \times 10^{-14}$	$1. \times 10^{-13}$	$3. \times 10^{-13}$
	$K_{H/Li}$	2.8	4.7	7.3
	$K_{H/Na}^{POT}$	1.1×10^{-13}	$2. \times 10^{-13}$	$3. \times 10^{-13}$
	$K_1(H/Na)$	$8. \times 10^{-14}$	$1. \times 10^{-13}$	$1. \times 10^{-13}$
	$K_{H/Na}$	1.4	2.	3.
	$K_{H/Na}^{POT}$	5.6×10^{-14}	$1. \times 10^{-13}$	1.5×10^{-13}
	$K_1(H/Li)$	$2. \times 10^{-14}$	$1. \times 10^{-14}$	2.8×10^{-13}
Radiometer Type G202B	$K_{H/Li}$	2.8	10	5.3
	$K_{H/Na}^{POT}$	$3. \times 10^{-14}$	4.5×10^{-13}	$2. \times 10^{-13}$
	$K_1(H/Na)$	$7. \times 10^{-14}$	$5. \times 10^{-13}$	$8. \times 10^{-14}$
	$K_{H/Na}$	4.5	9.	2.5

Table IV. H⁺ Response Parameters of Sodium Selective Glass Electrode, Beckman No. 39278

Temperature, °C	Sodium concn, M	a_{Na^+}/a_{H^+}	$K_{H/Na}^{(1)}$	$K_{H/Na}^{(2)}$	$K_{H/Na}^{POT} \times 10^4$
6	0.7	0.1	1.5×10^{-3}	$2. \times 10^{-3}$	2.9
	0.07	0.1	1.5×10^{-3}	1.5×10^{-3}	2.3
	0.007	0.3	1.5×10^{-3}	2.3×10^{-3}	3.4
14	0.7	0.6	1.5×10^{-3}	$8. \times 10^{-3}$	1.2
	0.07	0.7	3.5×10^{-3}	$3. \times 10^{-3}$	1.
	0.007	2.3	$9. \times 10^{-3}$	1.5×10^{-3}	1.4
25	0.7	2.5	1.2×10^{-1}	2.3×10^{-1}	2.8
	0.07	1.4	$7. \times 10^{-2}$	2.7×10^{-2}	1.9
	0.007	0.6	$1. \times 10^{-2}$	2.7×10^{-2}	2.8
41	0.7	1.2	7.7×10^{-2}	4.1×10^{-2}	3.2
	0.07	1.2	$8. \times 10^{-2}$	4.3×10^{-2}	3.4
	0.007	1.1	$8. \times 10^{-2}$	5.1×10^{-2}	4.

precisely by adjusting the ϕ^0 values for each level of sodium or each temperature. However, except for residual junction potentials, there is no justification unless slow attainment of equilibrium results in apparent shifts in ϕ^0 to more positive values at high sodium and hydrogen activities. Prolonged exposure to high acidities destroys the rapid response of these electrodes. Our best derived parameters are given in Table IV.

The $K_{H/Na}^{POT}$ value, typically 2.5×10^{-4} at 25 °C is the reciprocal of the normal $K_{Na/H}^{POT} = 4. \times 10^3$ corresponding to hydrogen interference of the sodium electrode. The electrode is clearly more responsive to H⁺ than to Na⁺, and in our opinion 4×10^3 is a better value than

36 reported by the manufacturer. We have confirmed the order of magnitude by measurements on two other electrodes from which we obtained values of 1 and 2×10^3 .

Potassium interference has been reported as $K_{Na/K}^{POT} = 5 \times 10^{-3}$ in Beckman Bulletin 7145-A. We have confirmed this value using comparison of responses of 0.01M NaCl and 0.01M KCl buffered with saturated calcium or barium hydroxides. However, the slope of response vs. log $a(K^+)$ in these buffers is substantially sub-Nernstian (~ 40 mV/decade from 1M to 10^{-2} M) and the selectivity coefficient depends on the ratio $a(K^+)/a(Na^+)$. When MgO is used as a buffer, the potassium response is Nernstian and uniformly more negative. Using the mixture

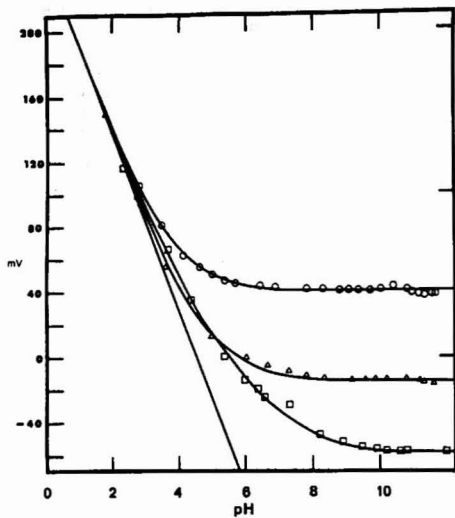


Figure 8. Response of the Beckman Sodium Ion Electrode (No. 39278) to pH at 6 °C
 O, 0.7M sodium; Δ , 0.07M sodium; \square , 0.007M sodium; $\varphi^0 = 245$ mV

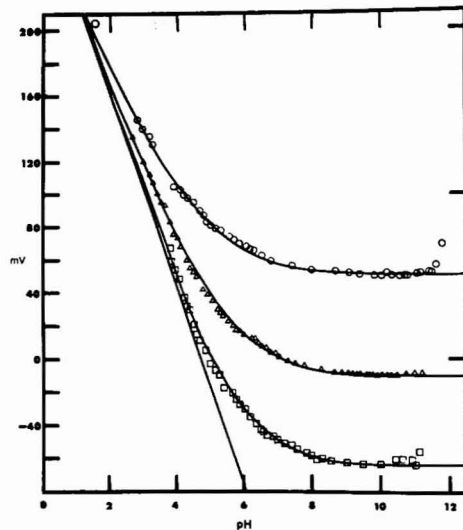


Figure 10. Response of the Beckman Sodium Ion Electrode (No. 39278) to pH at 25 °C
 O, 0.7M sodium; Δ , 0.07M sodium; \square , 0.007M sodium; $\varphi^0 = 281$ mV

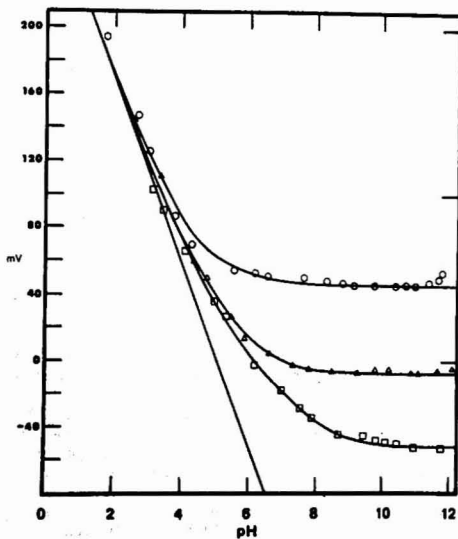


Figure 9. Response of the Beckman Sodium Ion Electrode (No. 39278) to pH at 14 °C
 O, 0.7M sodium; Δ , 0.07M sodium; \square , 0.007M sodium; $\varphi^0 = 280$ mV

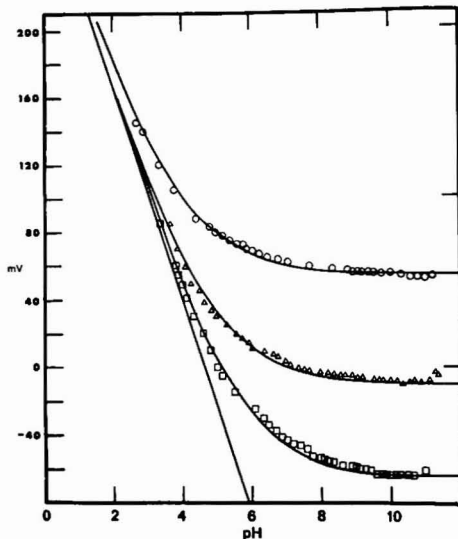


Figure 11. Response of the Beckman Sodium Ion Electrode (No. 39278) to pH at 41 °C
 O, 0.7M sodium; Δ , 0.07M sodium; \square , 0.007M sodium; $\varphi^0 = 299$ mV

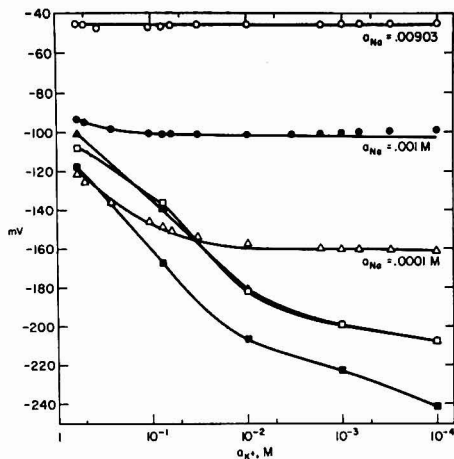


Figure 12. Mixed potassium-sodium responses of the Beckman Sodium Ion Electrode (No. 39278) at 25 °C in saturated MgO. □, potassium chloride in saturated Ca(OH)₂, pH 12.45; ▲, potassium chloride in saturated Ba(OH)₂, pH 13.35; ■, potassium chloride in saturated MgO, pH 10.4

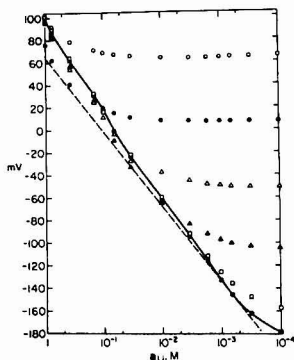


Figure 13. Mixed lithium-sodium responses of the Beckman Sodium Ion Electrode. (No. 39278) at 25 °C in saturated Ca(OH)₂. ○, 1M sodium; ●, 0.1M sodium; ▲, 0.01M sodium; △, 0.001M sodium; □, 0.0001M sodium; ■, pure lithium chloride response

method of variable KCl at three levels of NaCl in MgO saturated buffer, a constant value $K_{Na/K}^{POT} = 7 \times 10^{-4}$ was found. These results suggest, as shown in Figure 12, specific interference response by components of the buffers. Sodium and potassium were found negligible by atomic emission.

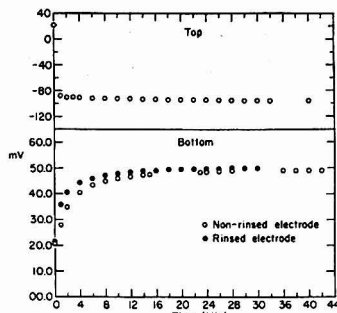


Figure 14. Time responses of the Beckman Sodium Ion Electrode (No. 39278) at 25 °C in saturated Ca(OH)₂. Upper: transfer from 0.1M NaCl to 0.1M KCl. Lower: transfer from 0.1M NaCl to 0.1M LiCl

Lithium response was determined from LiCl and LiCl-NaCl mixtures in saturated calcium hydroxide at pH 12.45. The response to lithium was sufficiently intense that buffer interference was not a factor. However, the response was very slow. In Figure 13 are results showing, by the solid line, 3-minute lithium responses, and by the dashed line, the envelope of mixture values. Both are super-Nernstian. One expects, then, a variable $K_{Na/Li}^{POT}$. Calculations at $10^{-2}M Li^+$ give 0.3 and at $1M Li^+$, a value 4.; thus, $0.3 < K_{Na/Li}^{POT} < 4$, at 25 °C.

A qualitative appreciation of the uncertainty of measurement of the selectivity parameters can be gained by noting the slow response of the electrode on transfer to lithium compared with potassium solutions. In Figure 14 is the time-response plot for 40 minutes. The top portion shows time-response on moving the electrode from 0.1M NaCl to 0.1M KCl, while the lower part gives the effects on transferring to 0.1M LiCl. All solutions were buffered with calcium hydroxide. In neither case is the 3-minute response precisely the steady state value. But, in addition to this transient effect, there is a further long-time drift even when the electrode is exposed exclusively to unbuffered sodium chloride solutions. We have noted above that the response from 10^{-4} to $1M$ is nearly Nernstian. Measurement over 16 days of continuous soaking in 0.1M NaCl, except when determining the slope, showed that the latter was unchanged, but ϕ^0 shifted progressively more negatively: -5 mV after 2 days, -9 mV after 5 days, and -13 mV after 16 days.

ACKNOWLEDGMENT

The authors thank Joseph Edwards for help during the early stages of this work.

Received for review June 1, 1973. Accepted September 24, 1973. The authors recognize support by the Materials Research Center (University of North Carolina) under Contract DAHC-15-C-0223 with the Advanced Research Projects Agency and National Science Foundation Grant GP 20524.

Determination of Antimony Using Forced-Flow Liquid Chromatography with a Coulometric Detector

Larry R. Taylor¹ and Dennis C. Johnson²

Department of Chemistry, Iowa State University, Ames, Iowa 50010

The highly irreversible electrochemical oxidation of Sb(III) at a platinum electrode in dilute HCl is electrocatalyzed by I^- or I_2 specifically adsorbed at the electrode surface. This phenomenon was applied for the determination of antimony in several standard alloys and in human hair by a highly sensitive and selective method using forced-flow liquid chromatography with a platinum coulometric detector. Because the electrolytic efficiency of the detector was 100%, the quantity of Sb(III) in the samples was calculated directly from the integral of the current-time peak for Sb(III) using Faraday's law. Use of a calibration curve was unnecessary.

Johnson and Laroche recently described a simple design for a tubular electrode (1). When packed with chips of platinum, the electrode can be operated with 100% electrolytic efficiency for a large range of fluid flow rates. The electrode was successfully applied as a detector for forced-flow liquid chromatography and the determination of Cu and Fe in several standard NBS alloys. As a result of the 100% efficiency, the time integral, Q , of the electrical current for the elution and electrolysis of an electroactive species is related to the number of gram-equivalents by the Faraday equation

$$Q = F(\text{g-equiv}) \quad (1)$$

where F is the Faraday constant (96,480 coulombs/g-equiv). The goal of extensive research in our laboratory has been the development of a coulometric procedure suitable for the determination of Sb(III) in the effluent stream of the liquid chromatograph. Coulometric procedures for the determination of antimony using solid electrodes have previously been based on the oxidation of Sb(III) to Sb(V) by Br_2 (2), I_2 (3, 4), and $Cr_2O_7^{2-}$ (5) electrogenerated at constant current. The general irreversibility of the Sb(III)-Sb(V) couple has prevented development of controlled-potential techniques based on their direct electrooxidation or reduction. Controlled-potential deposition of Sb^0 at noble metal electrodes is accompanied by simultaneous evolution of H_2 and is not useful for coulometry or amperometry.

Taylor, Davenport, and Johnson (6) investigated the catalytic enhancement by Sb(III) of the anodic wave for Br^- at a rotating platinum disk electrode in acidic solutions of Br^- . The enhancement current is proportional to the analytical concentration of Sb(III), provided the concentration of Sb(III) is less than that of Br^- . A coulometric

electrode was tested for its applicability to the determination of Sb(III) by this scheme. Samples of Sb(III) in 1.00mM NaBr-1.0M H_2SO_4 were injected into a stream of 1.00mM NaBr-1.0M H_2SO_4 . A current peak for oxidation of the Sb(III) was observed on the base line for oxidation of Br^- . The relative error for the determination of peak area was <3%, provided the quantity of Sb(III) was >1.5 μg . A large number of chemical species interfere in the determination. More recently, Davenport and Johnson (7) discovered that the highly irreversible electrooxidation of Sb(III) at a platinum electrode in dilute HCl is electrocatalyzed by I^- specifically adsorbed at the electrode surface. The choice of supporting electrolyte is important; the anodic process is not electrocatalyzed in H_2SO_4 or $HClO_4$. In 1-2M HCl, the predominant antimony species is $SbCl_4^-$ and a mechanism was proposed according to which adsorbed I^- functions as an electron-transfer bridge. The limiting current for the anodic process at a rotating disk electrode was determined to be controlled by convective-diffusional processes of mass transport over a large range of rotational velocity and concentration. Hubbard, Osteryoung, and Anson (8) found that the adsorption of I^- at platinum electrodes is irreversible and desorption does not occur even when the electrode surface is washed in an I^- -free solution.

We report here the application of liquid chromatography and the electrocatalyzed oxidation of Sb(III) in a platinum coulometric detector for the determination of Sb in several standard alloys and in human hair.

EXPERIMENTAL

Apparatus. The tubular electrode was constructed by Pine Instrument Co. of Grove City, Pa., and was packed with platinum chips as described in Ref. (1). The reference electrode was a Beckman Model 39270 Calomel Electrode filled with a saturated solution of NaCl. Electrode potentials were measured with respect to the reference using a Model 260 Digital Voltmeter from Data Technology Corp. The counter electrode was a coil of 20-gauge platinum wire wound around the tip of the reference electrode.

The three-electrode potentiostat was constructed with operational amplifiers and is described in Ref. (9). Current-potential (I - E) curves were recorded on a Model 815 X-Y Recorder from Bolt, Beranek, and Newman, Inc. Current-time (I - t) curves were recorded with a Model XL 860 Stripchart Recorder from Leeds & Northrup or a Model SRG from Sargent Welch Co. The I - t peaks obtained for analysis of samples were integrated by a Keuffel and Esser Compensating Planimeter. The I - t peaks obtained for the characterization of the coulometric detector were integrated electronically by an analog integrator constructed from a Zeltex ZA-801-M2 operational amplifier. The integrator was calibrated by integration of the electrical current passing through a standard 10-K resistor connected to a 0.250-V signal for a known time period.

The liquid chromatograph was constructed from a design by Seymour, Sickafoose, and Fritz (10). The chromatograph is de-

¹ Present address, Standard Oil of Ohio, Research, Cleveland, Ohio 44128.

² Person to whom correspondence should be addressed.

- (1) D. C. Johnson and J. H. Laroche, *Talanta*, **20**, 959 (1973).
- (2) R. A. Brown and E. H. Swift, *J. Amer. Chem. Soc.*, **71**, 2717 (1949).
- (3) J. J. Lingane and A. J. Bard, *Anal. Chim. Acta*, **16**, 271 (1957).
- (4) W. M. Wise and J. P. Williams, *Anal. Chem.*, **36**, 1863 (1964).
- (5) A. J. Kostromin and A. H. Akhmetov, *Zh. Anal. Khim.*, **24**, 503 (1969).
- (6) L. R. Taylor, R. J. Davenport, and D. C. Johnson, *Talanta*, **20**, 947 (1973).

- (7) R. J. Davenport and D. C. Johnson, *Anal. Chem.*, **45**, 1755 (1973).
- (8) A. T. Hubbard, R. A. Osteryoung, and F. C. Anson, *Anal. Chem.*, **38**, 692 (1966).
- (9) L. R. Taylor, Ph.D. Thesis, Iowa State University, Ames, Iowa 1973.
- (10) M. D. Seymour, J. P. Sickafoose, and J. S. Fritz, *Anal. Chem.*, **43**, 1734 (1963).

scribed in Ref. (1). Two different sample loops were used. The volume of each was standardized according to the procedure described in Ref. (1). The values were determined to be 0.5065 and 2.017 ml.

Eluents were contained in polyethylene or glass bottles. It was determined that extended contact of the acids with polyethylene (>6 months) resulted in contamination of the acids. Results reported here were obtained with uncontaminated solutions in new bottles. Eluent flow was maintained by pressurizing the bottles with compressed He. A mixing chamber, Model 2MC constructed by Pine Instrument Co., was used for injecting a solution of NaI into the effluent stream prior to its passage through the detector. This injection was part of the pretreatment procedure for the electrode.

Reagents. A 1.0mM stock solution of Sb(III) was prepared by dissolving Analytical Reagent Sb_2O_3 from Baker Chemical Co. in 30 ml of concentrated HCl. The solution was diluted with a mixture of HCl and H_2O and the final acid concentration was 2M HCl. A second solution of 2.0mM Sb(III) was prepared by dissolving Sb_2O_3 in hot, concentrated H_2SO_4 . The acidity after dilution was 1M H_2SO_4 . The stock solutions of Sb(III) were standardized using constant-current coulometry with electrogeneration of Br_2 . The procedure is described in Ref. (6). Dilutions of the standard solution of Sb(III) were made using a Gilmont micrometer buret and calibrated volumetric flasks.

Two standard alloys from National Bureau of Standards were analyzed. Their certificate values were as follows: NBS-53 contained 78.87% Pb, 10.91% Sn, 10.09% Sb, and <0.1% of Bi, Cu, Fe, and As; NBS-124b contained 83.69% Cu, 5.40% Zn, 4.93% Sn, 4.64% Pb, 0.76% Ni, 0.26% Fe, 0.20% Sb, and <0.1% of S, P, Si, and Al. Four alloys were prepared by John D. Verhoeven of the Department of Metallurgy at Iowa State University and the Ames Laboratory of the Atomic Energy Commission. Their compositions were as follows: ISU-1 contained 96.00% Pb and 4.00% Sb; ISU-2 contained 56.00% Sn, 40.00% Pb, and 4.00% Sb; ISU-3 contained 96.00% Sn and 4.00% Sb; TP-100 C contained 95.98% Sn and 4.02% Sb. Lead and tin-based alloys were dissolved according to the procedure described in Ref. (6, 11, 12). The copper-based alloy was dissolved in 8 ml of 1:1 HNO_3-H_2O without heating. Thirty milliliters of 1M $HClO_4$ were added and N_2 was bubbled through the solution to remove oxides of nitrogen. The solution was diluted to 100.0 ml with 1M $HClO_4$.

Samples of human hair (0.3-1.0 gram) were dissolved in 1:1 $HClO_4-HNO_3$ according to the procedure described in Ref. (13) (Procedure A) or in 10 ml of hot 1:1 $H_2SO_4-HNO_3$ (Procedure B). Excess HNO_3 was removed after dissolution by boiling. Ten milliliters of H_2O were added and the solution was boiled for 5 min. Fifteen milliliters of 1% $NaHSO_3$ was added to reduce any Sb(V) to Sb(III) and the excess HSO_3^- was destroyed by gentle boiling until the volume was decreased by 50%.

Interference studies were performed for various cations using solutions of their soluble chloride or sulfate salts when available from commercial sources. Stock solutions were made 0.01M in cation (Pb^{2+} was 0.001M) and 2M in HCl. The solution of Se(IV) was prepared by dissolving the metal in hot, concentrated HNO_3 ; As_2O_3 was dissolved in 8% NaOH; Fe was dissolved in 5:1 HCl- HNO_3 .

All solutions were prepared with triply distilled water prepared using a deionization following the first distillation. The second distillation was from alkaline permanganate solution.

Electrochemical Procedure. At the beginning of each experimental day, 2M HCl was passed through the detector and the potential of the detector, E , was set successively at 1.2, -0.6, and 0.0 V for 3 min. The potential was then switched to 0.30 V and the flow of acid stopped. A 10-20 ml portion of 0.01M NaI was passed through the detector and the flow of acid was resumed.

The range of detector potentials for oxidation of Sb(III) was determined as follows: 0.506-ml aliquots of a solution of 1.00×10^{-5} M Sb(III) in 2M HCl were injected into a stream of 2M HCl passing through the detector at a constant flow rate. The potential of the detector was increased by 50 mV in the range 0.600-0.900 V after each successive injection. The charging current was allowed to decay to zero after each change of potential before another sample was injected. The $I-t$ peaks resulting from each injection of Sb(III) were integrated electronically and the values of

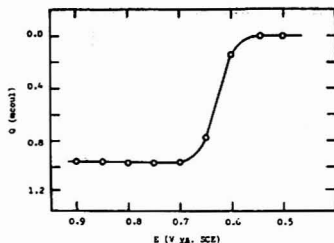


Figure 1. $Q-E$ plot for electrocatalyzed oxidation of Sb(III) in coulometric electrode

1M HCl, $v_f = 1.0$ ml/min; 0.62 μ g Sb(III) in each aliquot

Q plotted vs. the corresponding value of E . This plot has the same shape as an $I-E$ curve. The $I-E$ curve was not obtained by linear scan voltammetry because the charging current background was much larger than the faradaic current.

Separation Procedure. The separation was developed using Amberlite IRA-400 cation-exchange resin from Rohm and Haas Co. based on results reported by Jander and Hartmann (14) and by Strelow (15). In 1M $HClO_4$, Sb(III) exists as SbO^+ and is quantitatively retained on cation-exchange resins (14). In 2M HCl, Sb(III) exists as $SbCl_4^-$ and the adsorbed species is eluted from the cation-exchange column. Most heavy metals which are not alkali or alkaline earths exist as anionic chloro complexes in strong HCl (16) and 4M HCl was used to remove all metals from the resin column.

Several grams of the resin were washed with acetone and air dried. The resin was ground with a mortar and pestle and then sieved. The 100-140 mesh fraction was back-washed in a buret to remove the fines not eliminated by sieving. The remaining resin was used to pack a glass column with the interior dimensions 2 mm \times 8 cm. Small plugs of glass wool at each end of the column prevented loss of the resin during chromatographic operations.

The resin was pretreated before each sample injection by passing 1M $HClO_4$ having a flow rate of 0.4-0.5 ml/min. The eluent was switched to 2M HCl 1.0 min after the sample was injected to elute Sb(III). The eluent was changed to 4M HCl approximately 3.5 min after sample injection to remove other heavy metals.

RESULTS AND DISCUSSION

Characterization of the Electrode. The time integral of the electrical current was obtained as a function of electrode potential for a series of injections of 0.5065 ml of 1.00×10^{-5} M Sb(III). A plot of Q vs. E is shown in Figure 1. The plot has a limiting plateau for $0.70 \text{ V} < E \leq 0.90 \text{ V}$ which is consistent with $I-E$ curves shown in Ref. (7). A potential of 0.800 V was chosen for use in all succeeding studies.

The electrolytic efficiency of the packed tubular electrode was studied as a function of flow rate, v_f , and was determined to be 100% for $v_f \leq 4.1$ ml/min. The precision for application of the injection valve and coulometric detector was determined for electrolysis of Sb(III) in 15 injections of 0.5065-ml aliquots of 2M HCl containing 0.618 μ g Sb(III) into a stream of 2M HCl. The average relative deviation of the results was 4.5 ppt. This precision is better than normally associated with amperometric techniques.

Interference Study. The interference of various cations and acids was determined by mixing aliquots of Sb(III) in 2M HCl with solutions of the interfering species in 2M HCl. The values of Q resulting for injections of 0.5065-ml

(11) L. A. Wooten and C. L. Luke, *Ind. Eng. Chem.*, **13**, 771 (1941).

(12) A. J. Vogel, "Quantitative Inorganic Analysis," 3rd ed., Wiley, New York, 1961, p. 369.

(13) H. Dietl, "Quantitative Analysis," Oakland Street Science Press, Ames, Iowa, 1970, pp 315-16.

(14) V. G. Jander and H. J. Hartmann, *Z. Anorg. Allg. Chem.*, **339**, 256 (1965).

(15) F. W. E. Strelow, *Anal. Chem.*, **32**, 1185 (1960).

(16) K. A. Kraus and F. Nelson, *Proceedings of the First United Nations International Conference on the Peaceful Uses of Atomic Energy*, **7**, 113 (1956).

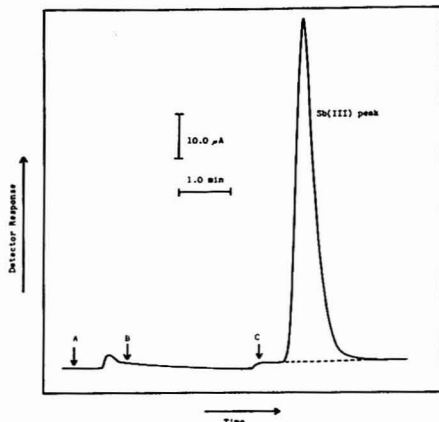


Figure 2. *I-t* curves for elution of Sb(III)

$v_f = 0.4-0.5$ ml/min, $0.618 \mu\text{g}$ Sb(III), $E = 0.800$ V; — *I-t* curve, --- base line used for integration; A, sample injection; B, change of eluent to 2M HCl; C, change of eluent to 4M HCl

Table I. Interference Study^a

Interfering species	Sb found, %		
	$10^{-2}M$	$10^{-1}M$	$10^{-1}M$
Al(III)	101	101	100
Ti(III)	102	173	1270
Ti(IV)	100	100	102
V(V)	100	98	98
Cr(III)	100	99	101
Mn(II)	100	100	100
Fe(III)	94	81	12
Co(II)	99	99	99
Ni(II)	100	100	99
Cu(II)	99	99	99
Zn(II)	100	99	99
As(III)	100	100	108
Se(IV)	101	101	100
Mo(VI)	100	100	99
Cd(II)	101	101	100
Sn(IV)	100	100	100
Ce(IV)	93	54	-236 ^b
Hg(II)	99	96	88
Pb(II)	100	99	—
Bi(III)	97	89	72
U(VI)	100	100	99
	$10^{-2}M$	$10^{-1}M$	$10^{-1}M$
HClO ₄	100	100	90
HNO ₃	100	99	98
H ₂ SO ₄	99	100	99
H ₃ PO ₄	99	98	98

^a Sample volume = 0.5065 ml. Sb(III) present = $0.618 \mu\text{g}$ ($1.00 \times 10^{-2}M$). ^b Negative sign denotes that net current was cathodic.

aliquots of the mixture were determined and compared with the theoretical result. The quantity of Sb(III) in each injected sample was $0.618 \mu\text{g}$. The results of this study are given in Table I for various concentrations of the interfering species in the sample.

A large positive interference resulted from Ti(III) because it is oxidized at $E = 0.800$ V. The negative interference for Ce(IV) resulted because it is reduced to Ce(III) at $E = 0.800$ V. It is not expected that Ce(IV) and Ti(III) will be frequently found in samples to be analyzed for

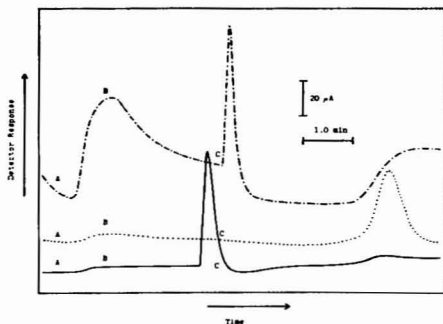


Figure 3. *I-t* curves for elution of Fe(III), Bi(III), and Hg(II)

$v_f = 0.4-0.5$ ml/min; --- $2.84 \mu\text{g}$ Fe(III) $E = 0.000$ V; - · - · - $10.6 \mu\text{g}$ Bi(III), $E = -0.200$ V; — $10.1 \mu\text{g}$ Hg(II), $E = 0.000$ V; A, sample injection; B, change of eluent to 2M HCl; C, change of eluent to 4M HCl

Sb(III). Appreciable negative interference was also observed for Fe(III), Hg(II), and Bi(III), even though these species are not electroactive at the potential used. It is our supposition that the interference resulted because these species are adsorbed at the electrode surface, thereby decreasing the number of active sites available for electrocatalysis. No explanation is known for the interference by HClO₄. All interfering species were determined to be easily removed from the detector by eluting with 4M HCl.

Ion-Exchange Separation. The separation procedure described in an earlier section was tested to determine the effectiveness for separating Sb(III) from the interfering species Hg(II), Bi(III), and Fe(III). The *I-t* curve for elution of Sb(III) by this procedure is shown in Figure 2. Point A in Figure 2 corresponds to sample injection and point B to the change of the eluent selector to 2M HCl. Point C corresponds to the change of the eluent selector to 4M HCl. Eluted SbCl₄⁻ reached the detector approximately 3.1 min after changing of the eluent selector. The *I-t* curves for elution of the interfering species are shown in Figure 3. Single elution peaks were obtained for Fe(III) and Hg(II) at $E = 0.000$ V. The curve for Bi(III) was recorded at $E = -0.200$ V. At that potential, electrochemical reduction of hydrogen ions occurs at a platinum electrode in strongly acidic media. The acidity of the effluent increased significantly due to desorption of protons from the cation exchanger following injection of the Bi(III) sample. This resulted in a wave beginning approximately 0.5 min after sample injection. Bismuth(III) was eluted in a sharp peak approximately 2.3 min after the eluent selector was switched to 2M HCl. The change of the eluent selector to 4M HCl (point C) resulted in an increasing cathodic current approximately 2.3 min later when the eluent front reached the detector. A slight overlap existed for the elution peaks of Sb(III) and Bi(III). Chromatograms were obtained for mixtures of Sb(III) and Bi(III). Results for Sb(III) were in error >2% only when the ratio Bi(III):Sb(III) was >7:1.

Calibration Study. A study was performed to determine the range of quantities of Sb(III) over which Equation 1 is applicable. The results are shown plotted in Figure 4 for 2.5 ng-6.3 μg Sb(III). The upper limit was due to ohmic shift of the electrode potential off the region of the limiting current plateau for Sb(III) during peak elution.

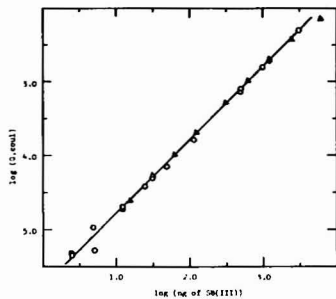


Figure 4. Calibration plot for Sb(III)

$v_f = 0.4\text{--}0.5$ ml/min, $E = 0.800$ V; Δ , electrocatalysis by adsorbed I_2 , \circ , electrocatalysis by adsorbed I^- , — theoretical, calculated using Equation 1

The agreement between the experimental results and theory is excellent.

Pretreatment of Detector. Both I^- and I_2 are adsorbed at a platinum electrode by irreversible processes (8, 17). It was discovered that adsorbed I_2 also electrocatalyzes the electrochemical oxidation of Sb(III) in dilute HCl. Results of the application of adsorbed I_2 for coulometric determination of Sb(III) are included in Figure 4. Adsorbed I^- and I_2 are not desorbed even if the electrode surface is rinsed with pure water (8, 17). A single pretreatment of the detector at the start of each experimental day, as described in an earlier section, was sufficient to produce a detector with 100% efficiency for any desired period of continuous operation.

Base-Line Signal. The composition and electrical charge of the double layer at the detector-solution interface is dependent on the ionic composition and concentration of the solution. Hence, background current peaks are to be expected following sample injection and changes of eluents during separation. In Figure 2, a charging current peak is shown beginning approximately 0.5 min after sample injection (point A). Changing the eluent from 1M HClO₄ to 2M HCl (point B) results in a charging current peak observed approximately 2.4 min later. Similar peaks are observed when the sample contains no Sb(III). The eluent front for 2M HCl required a longer time to reach the detector than the front for the sample because the volume of the stream between the eluent selector valve and the detector was greater than the volume between the sample injection valve and detector [see Figure 1 in Ref. (1)]. The internal volume of the flow meter alone is estimated to be approximately 0.4 ml. The charging current peak resulting from the change of eluent to 4M HCl (point C) also is observed beginning 2.4 min after the change.

The charging current peaks interfere with accurate integration of the current peak for detection of small amounts of Sb(III). The chromatogram for 12.3 ng Sb(III) is shown in Figure 5. The constructed base line used for peak integration is shown. The area determined for the Sb(III) peak agreed well with theory as shown by Figure 4. High frequency noise shown in Figure 4 resulted when small bubbles of He on the surface of the detector electrode dislodged under the force of convection. The bubbles formed because of degassing of the eluent due to the drop in pressure at the ion-exchange column.

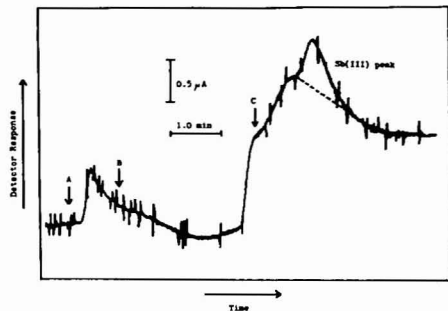


Figure 5. $I-t$ curve for 12.3 ng Sb(III)

$v_f = 0.4\text{--}0.5$ ml/min, $E = 0.800$ V; — $I-t$ curve, --- base line used for integration; A, sample injection; B, change of eluent to 2M HCl; C, change of eluent to 4M HCl

Table II. Determination of Sb in Standard Alloys*

Sample	Sb, %	No. of detets	Sb found, %	Av rel dev, ppb	Rel. error, ppb
NBS-124b	0.20	4	0.20	1.8	0.0
NBS-53	10.09	4	10.09	2.1	0.0
NBS-53	10.09	4	10.2	0.6	+1.1
ISU-1	4.00	3	3.98	1.3	-0.6
ISU-1	4.00	5	3.95	1.6	-1.3
ISU-2	4.00	3	3.99	1.5	-0.3
ISU-3	4.00	3	3.98	1.3	-0.5
TP-100C	4.02	5	4.01	0.7	-0.3

* $v_f = 0.4$ ml/min; $E = 0.800$ V; sample volume = 0.5065 ml.

Table III. Determination of Sb in Hair*

Subject	Age, yr	No. of detets	Sb found, ppm
L.R.T.	25	5	1.3
M.S.T.	22	2	0.6
J.H.L.	25	1	0.9
J.K.L.	3	1	0.0

* $v_f = 0.5$ ml/min; $E = 0.800$ V; sample volume = 2.017 ml.

The detection limit (approximately 50% uncertainty in peak area) was found experimentally to be approximately 1 ng of Sb(III). Studies are presently in progress to lead to a better understanding of the charging peaks and possible methods of decreasing their effect on the determination.

Analysis of Samples. The results of the determinations of Sb in the standard alloys are given in Table II. The values determined are in excellent agreement with certificate values. The relative error exceeded 1% only in two instances.

Hair samples from four persons with varying involvement in the research were analyzed for Sb. M.S.T. was the wife of L.R.T. and made occasional visits to the laboratory where antimony compounds were used. J.H.L. shared the same laboratory with L.R.T. L.K.L. was the three-year-old daughter of J.H.L. The analytical results are given in Table III, and they correlate very well with the relative exposure of the persons to this research.

(17) D. C. Johnson, *J. Electrochem. Soc.*, **119**, 331 (1972).

The results reported here are evidence of the applicability of controlled-potential electrolysis in a coulometric electrode in conjunction with forced-flow liquid chromatography for quantitative determination of Sb(III) over a large range of concentrations. The separation scheme described can be used to concentrate Sb(III) on the ion-exchange column from sample volumes considerably larger

than used in this work. It is concluded the procedure is suitable for determinations of Sb(III) at the sub-ppb level.

Received for review June 6, 1973. Accepted August 16, 1973. The authors thank Pine Instrument Company for a Research Assistantship for L.R. Taylor during the summer of 1972.

Characterization of Heavy Residual Fuel Oils and Asphalts by Infrared Spectrophotometry Using Statistical Discriminant Function Analysis

F. K. Kawahara, J. F. Santner, and E. C. Jullian

U.S. Environmental Protection Agency, National Environmental Research Center, Analytical Quality Control Laboratory, Cincinnati, Ohio 45268

Spilled asphaltic materials and heavy residual fuel oils, because of their high molecular weights, complexity, and physical nature, cannot be readily identified to a source since these materials are not usually amenable to analysis by gas chromatography with flame ionization detector. The limiting difficulty is the inability to vaporize and to separate the high molecular weight components in the GC column. Infrared spectrophotometry is a useful technique for characterization of these materials. A combination of infrared spectrophotometry, data treatment, data transformation, and discriminant function analysis through computer assistance has resulted in effecting a more precise and accurate method of distinguishing between these two heavy petroleum products. An established statistical technique has been successfully applied to a recently developed infrared procedure for heavier petroleum products to provide a useful and powerful technique for classification of samples.

Among the many efforts for upgrading the environment are the control of stack emissions, the wise use of pesticides, reduction of pollutants in automotive exhausts, efficient management of solid wastes, and the improvement of water quality. One of the serious and continuing water problems is the discharge of oils into surface waters. Thus, analytical procedures for the identification of discharged petroleum products and the successful application of these techniques are significant contributions to law enforcement and environmental improvement.

Asphaltic materials and heavy residual fuel oils, because of their high molecular weights, complexity, and physical nature, cannot be readily identified to a source since these materials are not usually amenable to analysis by gas chromatography with flame ionization detector. The limiting difficulty is the inability to vaporize and to separate the high molecular weight components in the GC column. However, one feasible approach leading to identification is the analysis of the passively labeled fluorinated phenolic ethers and thioether derivatives of the weak acids present in discharged heavier petroleum products (1,

2) by the use of electron capture detector gas chromatography.

Infrared spectrophotometry is a useful technique presented for the characterization of these heavier residual fuel oils. Initial screening tests will eliminate aromatic lube oils and No. 2 fuel oils. Differences in density, solubility in hexane, and much weaker infrared absorptivities distinguish these lighter products from the heavier products. Also, No. 1 and No. 2 fuel oils have distinctive infrared absorptivities at other wavenumbers.

An application of this technique is described by Kawahara and Ballinger (3). Numerous unidentified oil samples collected from the surface waters of several locations in the United States were analyzed by infrared spectrophotometry using peaks at six wavenumbers. For rapid field evaluation, the graphic method with the use of two key ratios, $810\text{ cm}^{-1}/1375\text{ cm}^{-1}$ and $810\text{ cm}^{-1}/720\text{ cm}^{-1}$, was useful for the initial classification of unknown oil spill samples among asphalts, No. 6 fuel oils, No. 5 fuel oils, and a lube oil.

A demonstration of the effectiveness of the infrared method of ratios for heavier residual fuel oils was illustrated in the recent publication (1) where two different spills in the same general area resulted in samples being collected at two possible sources. The two different spills were characterized as being entirely unlike while a source sample was coupled to each spill and shown to be alike, respectively. In addition, each of the six ratios of infrared absorbances of commercial asphalts, No. 6 fuel oils, No. 5 fuel oils, and cutter stocks were distinctly characteristic for each product. The ratios of absorbance generated in that study are shown in Table I and are illustrative of the data used in this paper.

To further improve the characterization potential using infrared spectrophotometry and to eliminate the small indeterminate region previously observed, linear discriminant function analysis using 42 variables was applied to data points obtained previously (3).

(2) F. K. Kawahara, Division of Water, Air and Waste Chemistry, 161st National Meeting, American Chemical Society, Los Angeles, Calif., March 28-April 2, 1971, Abstract No. 3.

(3) F. K. Kawahara and D. G. Ballinger, *Ind. Eng. Chem., Prod. Res. Develop.*, **9**, 553 (1970).

(1) F. K. Kawahara, *J. Chromatogr. Sci.*, **10**, 629 (1972).

LINEAR DISCRIMINANT FUNCTION

A linear discriminant function is a function that is linear in the variables and discriminates or classifies data into one of the groups under consideration. (4). Two groups or products are considered in this paper—namely, heavy residual fuel oils and asphalts.

A separate linear discriminant function is obtained for each product. The forms of these two functions are:

$$z_a = b_0 + b_1x_1 + b_2x_2 + b_3x_3 + b_4x_4 + b_5x_5 + \dots + b_{36}x_{36} \quad (1)$$

$$z_o = b'_0 + b'_1x_1 + b'_2x_2 + b'_3x_3 + b'_4x_4 + b'_5x_5 + \dots + b'_{36}x_{36} \quad (2)$$

where z_a and z_o designate the asphalt and heavy residual fuel oil functions, respectively. The x_i 's are the variables used in the problem. The coefficients or parameters (primed and unprimed b 's) are determined by maximizing the ratio of the "between" group variance (heavy residual fuel oils and asphalts) to the "within" group variance (heavy residual fuel oils or asphalts). To evaluate both discriminant functions, the variable values of an unknown sample are used. The unknown would then be assigned to that product whose discriminant value, z_a or z_o , was a maximum or the larger. In addition to classifying a sample, the probability of correct classification into either group can be calculated. An example of both procedures with a specific example is given in a later section.

The linear discriminant function procedures as used in this paper will classify any sample as either a heavy residual fuel oil or an asphalt (5, 6). In the present form, it is a dichotomous classification procedure; however, the extension to any number of groups may be considered and is limited only by computer capability.

EXPERIMENTAL

For analyses of infrared spectra, samples were prepared by techniques described earlier (3). The thickness of the liquid cell or film was adjusted so that the transmittance readings varied from 80 to 95% of the full scale at 2925 cm^{-1} .

PREPARATION OF DATA FOR DISCRIMINANT ANALYSIS AND SUMMARY OF RESULTS

The data preparation prior to performing discriminant analysis is described below. The data for this problem in discriminant analysis consist of data elements of two groups (asphalts and heavy residual fuel oils), and of 69 and 77 observations, respectively. Each observation of data consists of measurements from seven peaks from which net absorbances are calculated. Peak and base-line distances for each peak were measured in centimeters to the nearest 0.01 cm. In order that the effects of variation in cell path length be minimized, 42 ratios of these absorbances were selected for calculation. Cells of fixed path length are now used where samples are sufficiently liquid. A schematic layout of absorbance ratios from data previously obtained (3) is shown in Table II.

In Table II, three replicates (R_{2111} , R_{2112} , and R_{2113}) are shown for Group II, heavy residual fuel oils, the first ratio of absorbances, 720 cm^{-1} /810 cm^{-1} ; and sample

(4) M. G. Kendall and A. Stuart, "The Advanced Theory of Statistics," Volume III, Hafner Publishing Company, New York, N.Y., 1946, Chapter 44.

(5) E. C. Julian, "Application of Discriminant Function Analysis to Infrared Data," Newsletter, No. 14, p. 8, July (1972), J. B. Anderson, Ed., published by the Analytical Quality Control Laboratory, NERC, Environmental Protection Agency, 1014 Broadway, Cincinnati, Ohio 45202.

(6) J. F. Santner, "Status of Research Report," memorandum to W. J. Benoit, National Environmental Protection Agency, Cincinnati, Environmental Protection Agency, July 10, 1972.

Table I. Ratios of Infrared Absorbances of Enforcement Samples

Ratio of infrared absorbance	Sample 1	Sample 2	Sample 3	Sample 4	Sample 5
720 cm^{-1} 1375 cm^{-1}	0.08	0.11	0.08	0.12	0.06
3050 cm^{-1} 2925 cm^{-1}	0.16	0.07	0.16	0.09	0.14
1600 cm^{-1} 1375 cm^{-1}	0.63	0.24	0.73	0.31	0.60
1600 cm^{-1} 720 cm^{-1}	8.20	2.24	9.66	2.46	9.41
810 cm^{-1} 1375 cm^{-1}	0.77	0.25	0.90	0.31	0.74
810 cm^{-1} 720 cm^{-1}	9.96	2.29	11.89	2.53	11.60

number one. The notations for the three replicates, R_{2111} , R_{2112} , and R_{2113} are derived from the general notation, R_{ijkl} which stands for the original ratio of infrared absorbances.

The term $i = 1$ (asphalt), 2 (No. 6 fuel oil); $j = 1, 2, \dots, 42$ (ratio identification); $k = 1, 2, \dots, 18$ or 20 (sample number identification); and $l = 1, 2, 3, 4$, or 5 (non-uniform replicate identification).

Two changes in the data handling marked the difference between the previous analysis (3) and the analysis in this paper. In the previous paper, averages, not replicates, were used in the analysis. For example, $\bar{R}_{2111} = (R_{2111} + R_{2112} + R_{2113})/3$ was used instead of the three replicates. In this paper, the three replicates R_{2111} , R_{2112} , and R_{2113} were used as such.

The second change involved the standardization of the data of Table II before performing discriminant analysis. Data were standardized by subtracting from each table entry the corresponding sample column mean \bar{R}_j which equals the sum of all ratios of absorbances in one column of Table II, including all samples and replicates within both groups, divided by n , ($n = 146$), the total number of replicates. This difference is divided by the sample column standard deviation, s_j over both groups. The term $s_j = \sqrt{\sum(R_j - \bar{R}_j)^2/(n - 1)}$ where R_j = value of a single ratio, \bar{R}_j = mean value of ratios of absorbances of the corresponding column, and n = number of replicates.

The total number of asphalt and oil samples and their respective replicates are indicated in Table II. The equation for the standardization of the ratio variable is

$$x_{ijkl} = (R_{ijkl} - \bar{R}_j)/s_j$$

where \bar{R} and s_j values are given in Table III.

Discriminant analysis on the standardized data was performed with a computer program described by Dixon (7).

The output of the program (7), in part, consists of:

- (1) At each step:
 - (a) Variables included and F to remove.
 - (b) Variables not included and F to enter.
- (2) After the last step:
 - (a) Classification functions (discriminant functions).
- (3) For each case (observation):
 - (a) The posterior probability of the case coming from each group.

(7) W. J. Dixon, "BMD, Biomedical Computer Programs," University of California Press, Berkeley, Calif., 1971, p. 214A-214L.

Table II. Schematic Layout of the Absorbance Ratio Data

	No. of samples per group	No. of replicates per sample	Ratio of absorbances			
			$R_{i,1,k,l}$	$R_{i,2,k,l}$...	$R_{i,42,k,l}$
			720 cm ⁻¹	870 cm ⁻¹	...	1600 cm ⁻¹
Group I Asphalts <i>i</i> = 1	<i>k</i> = 1	<i>l</i> = 1,2,3,4
		<i>l</i> = 1	$R_{1,1,1,1}$	$R_{1,2,1,1}$...	$R_{1,42,1,1}$
		<i>l</i> = 2	$R_{1,1,1,2}$	$R_{1,2,1,2}$...	$R_{1,42,1,2}$
		<i>l</i> = 3	$R_{1,1,1,3}$	$R_{1,2,1,3}$...	$R_{1,42,1,3}$
Subtotal for Asphalts		69				
Group II Heavy residual fuel oils <i>i</i> = 2	<i>k</i> = 1	<i>l</i> = 1	$R_{2,1,1,1}$	$R_{2,2,1,1}$...	$R_{2,42,1,1}$
		<i>l</i> = 2	$R_{2,1,1,2}$	$R_{2,2,1,2}$...	$R_{2,42,1,2}$
		<i>l</i> = 3	$R_{2,1,1,3}$	$R_{2,2,1,3}$...	$R_{2,42,1,3}$
	
Subtotal for heavy residual fuel oils		77				
Total, two groups	38	146				
$R_{i,j,k}$			<i>i</i> = 1, (Asphalts), <i>i</i> = 2, (Heavy residual fuel oils)			
			<i>j</i> = 1, 2, ..., 42 (Ratio identification)			
			<i>k</i> = 1, 2, ..., 18 or 20 (Sample number identification)			
			<i>l</i> = 1, 2, 3 or 4 or 5 (Non-uniform replicate identification)			

Table III. Ratios, Sample Means, and Standard Deviations Used in the Standardization

Variable indices	Ratios, cm ⁻¹ /cm ⁻¹	Sample means over both groups \bar{R}_j	Sample std dev over both groups s_j	<i>J</i> -Number	Variable indices	Ratios, cm ⁻¹ /cm ⁻¹	Sample means over both groups \bar{R}_j	Sample std dev over both groups s_j	<i>J</i> -Number
1	720/ 810	0.9011	0.4417	1	22	810/ 720	1.5605	1.0913	18
2	720/ 870	0.9282	0.4402	2	23	870/ 720	1.4492	0.9325	19
3	720/1027	2.0848	1.1422	...	24	1027/ 720	0.6627	0.3977	20
4	720/1375	0.1673	0.0483	...	25	1375/ 720	6.5536	2.1227	21
5	720/1460	0.0668	0.0202	...	26	1460/ 720	16.4365	5.1924	22
6	720/1600	0.4790	0.1913	3	27	1600/ 720	2.5047	1.2217	23
7	810/ 870	1.0709	0.2267	4	28	870/ 810	0.9746	0.2014	24
8	810/1027	2.4697	0.8863	5	29	1027/ 810	0.4752	0.2326	25
9	810/1375	0.2400	0.1411	6	30	1375/ 810	5.5035	2.5259	...
10	810/1460	0.0920	0.0468	7	31	1460/ 810	13.3866	5.4041	26
11	810/1600	0.5965	0.1914	8	32	1600/ 810	1.8530	0.5763	27
12	870/1027	2.3682	0.8840	9	33	1027/ 870	0.5035	0.2760	28
13	870/1375	0.2293	0.1274	...	34	1375/ 870	5.8899	3.1589	29
14	870/1460	0.0881	0.0427	10	35	1460/ 870	14.2983	6.9191	...
15	870/1600	0.5633	0.1608	11	36	1600/ 870	1.9241	0.5508	30
16	1027/1375	0.1023	0.0515	12	37	1375/1027	12.7261	6.6201	31
17	1027/1460	0.0399	0.0186	13	38	1460/1027	31.3061	15.3465	32
18	1027/1600	0.2636	0.0985	14	39	1600/1027	4.3411	1.7111	33
19	1375/1460	0.4013	0.0479	15	40	1460/1375	2.5261	0.2961	34
20	1375/1600	2.9257	1.0648	16	41	1600/1375	0.3867	0.1351	35
21	1460/1600	7.2261	2.3874	17	42	1600/1460	0.1514	0.0435	36

This program performed a multiple discriminant analysis in a stepwise manner. At each step, one variable was entered into the set of discriminating variables. The variable having the largest *F* was selected for inclusion. A minimum *F* value for inclusion (*F* to enter) of 0.01, a reasonable criterion, was placed in the input to the program.

Execution of the stepwise discriminant analysis resulted in the inclusion of 36 of the 42 variables. The 42 variable indices and the 36 selected *j*-numbers are shown in Table III. The analysis provided the *b*'s for Equations 1 and 2, respectively, as shown in Table IV.

The foregoing data transformations and evaluations of the discriminant functions are illustrated by the following example: let the length from base to peak for wavenumber 720 cm⁻¹ be 0.70 cm. Let the length from peak to bottom of the spectrum at *A* = ∞ be 6.80 cm. Using a copy of the original infrared spectrum, Figure 1, the values at the other wavenumbers are, for 810 cm⁻¹ = 1.75 and 6.00; for 870 cm⁻¹ = 1.80 and 6.80; for 1027 cm⁻¹ = 1.10 and 8.35; for 1375 cm⁻¹ = 2.95 and 4.60; for 1460 cm⁻¹ = 6.20 and 2.30; and for 1600 cm⁻¹ = 2.35 and 6.95, all in centimeters.

Table IV. Coefficients for Both Discriminant Functions When Using Standardized Variables in Equations 1 and 2

(1)	Asphalts	(2)	Heavy residual fuel oils	(1)	Asphalts	(2)	Heavy residual fuel oils
b_0	-7.60987	b_0'	-6.24480	b_{19}	-43.55099	b_{19}'	39.02415
b_1	-25.58461	b_1'	22.90611	b_{20}	4.07508	b_{20}'	-3.64347
b_2	26.62715	b_2'	-23.81479	b_{21}	-29.84641	b_{21}'	26.78763
b_3	-11.64139	b_3'	10.41510	b_{22}	11.77883	b_{22}'	-10.59161
b_4	-36.14394	b_4'	32.34564	b_{23}	-7.65198	b_{23}'	6.85141
b_5	-1.98233	b_5'	1.75529	b_{24}	39.78601	b_{24}'	-35.56705
b_6	-4.09560	b_6'	3.87530	b_{25}	-9.39279	b_{25}'	8.42572
b_7	-68.58247	b_7'	61.14029	b_{26}	46.71219	b_{26}'	-41.73645
b_8	62.78983	b_8'	-56.07736	b_{27}	-74.16132	b_{27}'	66.26096
b_9	5.81115	b_9'	-5.20976	b_{28}	-9.84835	b_{28}'	8.81127
b_{10}	62.29706	b_{10}'	-55.72067	b_{29}	-47.45398	b_{29}'	42.41000
b_{11}	-67.18605	b_{11}'	60.05365	b_{30}	72.33095	b_{30}'	-64.69716
b_{12}	-33.92418	b_{12}'	30.28230	b_{31}	9.34523	b_{31}'	-8.37640
b_{13}	22.86368	b_{13}'	-20.40642	b_{32}	-2.56282	b_{32}'	2.32982
b_{14}	24.45306	b_{14}'	-21.88516	b_{33}	-7.29110	b_{33}'	6.53285
b_{15}	8.81806	b_{15}'	-7.90065	b_{34}	3.05424	b_{34}'	-3.03080
b_{16}	25.18460	b_{16}'	-22.33339	b_{35}	11.34435	b_{35}'	-10.42913
b_{17}	-24.20792	b_{17}'	21.43787	b_{36}	-1.50103	b_{36}'	1.60187
b_{18}	63.63580	b_{18}'	-57.02377				

The absorbances were calculated from the above seven pairs of values and were: at 720 cm^{-1} = 0.0426; at 810 cm^{-1} = 0.1112; at 870 cm^{-1} = 0.1020; at 1027 cm^{-1} = 0.0537; at 1375 cm^{-1} = 0.2152; at 1460 cm^{-1} = 0.5677; and at 1600 cm^{-1} = 0.1265.

At this point computer assistance was necessary because of the large numbers of calculations required in obtaining the 42 possible absorbance ratios, their standardization, and the deletion of the standardized ratios excluded by the stepwise discriminant analysis.

Table V shows the wavenumber ratios in the order generated, the 42 absorbance ratios, the 42 standardized absorbance ratios, and the 36 j -numbers utilized by the stepwise discriminant analysis (from the list of included variates). The 36 standardized ratios are substituted in Equations 1 and 2 where the coefficients for these equations are found in Table IV. The manner of calculation and the results are shown in Table VI. Since the z_0 function calculates to be a greater value than the z_1 function, -3.157 vs. -11.079, the unknown is classified as a heavy residual fuel oil. For each observation, ratios of absorbances are formed and then standardized, and both discrimi-

Table V. Example of the Calculation of Absorbance Ratios, Standardization of Absorbance Ratios, and the Selection of the 36 Included Ratios

Wavenumbers, $\text{cm}^{-1}/\text{cm}^{-1}$	Absorbance ratios	Standardized absorbance ratios	J -Number
720/ 810	0.3816	-1.1762	1
720/ 870	0.4172	-1.1609	2
720/1027	0.7917	-1.1321	..
720/1375	0.1977	0.6295	..
720/1460	0.0750	0.4024	..
720/1600	0.3364	-0.7456	3
810/ 870	1.0933	0.0987	4
810/1027	2.0747	-0.4457	5
810/1375	0.5182	1.9718	6
810/1460	0.1964	2.2322	7
810/1600	0.8815	1.4894	8
870/1027	1.8977	-0.5323	9
870/1375	0.4740	1.9214	..
870/1460	0.1797	2.1457	10
870/1600	0.8063	1.5113	11
1027/1375	0.2498	2.8633	12
1027/1460	0.0947	2.9506	13
1027/1600	0.4249	1.6365	14
1375/1460	0.3791	-0.4655	15
1375/1600	1.7011	-1.1501	16
1460/1600	4.4877	-1.1470	17
810/ 720	2.6204	0.9712	18
870/ 720	2.3968	1.0163	19
1027/ 720	1.2630	1.5093	20
1375/ 720	5.0571	-0.7050	21
1460/ 720	13.3411	-0.5961	22
1600/ 720	2.9728	0.3831	23
870/ 810	0.9147	-0.2975	24
1027/ 810	0.4820	0.0290	25
1375/ 810	1.9299	-1.4148	..
1460/ 810	5.0912	-1.5350	26
1600/ 810	1.1345	-1.2467	27
1027/ 870	0.5270	0.0852	28
1375/ 870	2.1099	-1.1966	29
1460/ 870	5.5661	-1.2620	..
1600/ 870	1.2403	-1.2416	30
1375/1027	4.0039	-1.3175	31
1460/1027	10.5627	-1.3517	32
1600/1027	2.3537	-1.1615	33
1460/1375	2.6381	0.3783	34
1600/1375	0.5878	1.4887	35
1600/1460	0.2228	1.6418	36

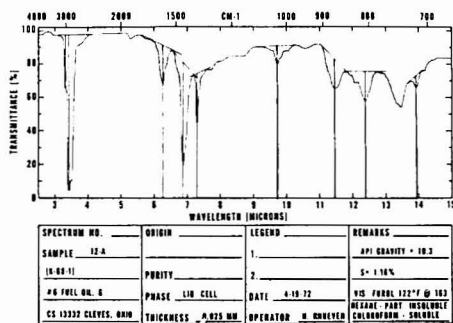


Figure 1. Infrared spectrum of a heavy residual fuel oil, No. 6, having the following properties: Sulfur, 1.16%; API gravity, 10.3; viscosity furl at 122 °F, 163. Source, Mid-Continent, summer production

Table VI. Example for the Calculation of Discriminant Functions

Term	Equation 1		Equation 2	
	b_j 's	x_i 's	b_j 's	x_i 's
Constant	-7.60987	+	-6.24480	+
1	(-25.58461)	(-1.1762)	(+22.90611)	(-1.1762)
2	(+26.62715)	(-1.1609)	(-23.81479)	(-1.1609)
3	(-11.64139)	(-0.7456)	(+10.41510)	(-0.7456)
4	(-36.14394)	(+0.0987)	(+32.34564)	(+0.0987)
5	(-1.98233)	(-0.4457)	(+1.75529)	(-0.4457)
6	(-4.09560)	(+1.9718)	(+3.87530)	(+1.9718)
7	(-68.58247)	(+2.2322)	(+61.14029)	(+2.2322)
8	(+62.78983)	(+1.4894)	(-56.07736)	(+1.4894)
9	(+5.81115)	(-0.5323)	(-5.20976)	(-0.5323)
10	(+62.29706)	(+2.1457)	(-55.72067)	(+2.1457)
11	(-67.18605)	(+1.5113)	(+60.05365)	(+1.5113)
12	(-33.92418)	(+2.8633)	(+30.28230)	(+2.8633)
13	(+22.85368)	(+2.9506)	(-20.40642)	(+2.9506)
14	(+24.45306)	(+1.6365)	(-21.88516)	(+1.6365)
15	(+8.81806)	(-0.4655)	(-7.90065)	(-0.4655)
16	(+25.18460)	(-1.1501)	(-22.33339)	(-1.1501)
17	(-24.20792)	(-1.1470)	(+21.43787)	(-1.1470)
18	(+63.63580)	(+0.9712)	(-57.02377)	(+0.9712)
19	(-43.55099)	(+1.0163)	(+39.02415)	(+1.0163)
20	(+4.07508)	(+1.5003)	(-3.64347)	(+1.5093)
21	(-29.84641)	(-0.7050)	(+26.78763)	(-0.7050)
22	(+11.77883)	(-0.5961)	(-10.59161)	(-0.5961)
23	(-7.65198)	(+0.3831)	(+6.85141)	(+0.3831)
24	(+39.78601)	(-0.2975)	(-35.56705)	(-0.2975)
25	(-9.39279)	(+0.0290)	(-8.42572)	(+0.0290)
26	(+46.71219)	(-1.5350)	(-41.73645)	(-1.5350)
27	(-74.16132)	(-1.2467)	(+66.26096)	(-1.2467)
28	(-9.84835)	(+0.0852)	(-8.81127)	(-0.0852)
29	(-47.45398)	(-1.1966)	(+42.41000)	(-1.1966)
30	(+72.33095)	(-1.2416)	(-64.69716)	(-1.2416)
31	(+9.34523)	(-1.3175)	(-8.37640)	(-1.3175)
32	(-2.56282)	(-1.3517)	(+2.32982)	(-1.3517)
33	(-7.29110)	(-1.1615)	(+6.53285)	(-1.1615)
34	(+3.54245)	(+0.3783)	(-3.03080)	(+0.3783)
35	(+11.34435)	(+1.4887)	(-10.42193)	(+1.4887)
36	(-1.50103)	(+1.6418)	(+1.60187)	(+1.6418)
	$z_a = -11.079056$		$z_o = -3.156959$	

Table VII. Parameters of Standardized Data

Variable, cm ⁻¹ /cm ⁻¹	Means		Standard deviations		Variable cm ⁻¹ /cm ⁻¹	Means		Standard deviations			
	Asphalts	Heavy residual fuel oils	Over both groups	Heavy residual fuel oils		Asphalts	Heavy residual fuel oils	Over both groups	Asphalts	Heavy residual fuel oils	
720/810	0.756	-0.678	0.000	0.723	0.675	810/720	-0.633	0.567	0.000	0.223	1.083
720/870	0.462	-0.414	0.000	0.714	1.041	870/720	-0.533	0.477	0.000	0.282	1.161
720/1027	0.354	-0.317	0.000	0.996	0.897	1027/720	-0.302	0.270	0.000	0.977	0.947
720/1375	0.439	-0.393	0.000	0.853	0.962	1375/720	-0.460	0.413	0.000	0.616	1.097
720/1460	0.579	-0.519	0.000	0.909	0.769	1460/720	-0.573	0.514	0.000	0.626	0.995
720/1600	0.354	-0.317	0.000	0.771	1.077	1600/720	-0.445	0.399	0.000	0.423	1.186
810/870	-0.634	0.568	0.000	0.719	0.869	870/810	0.672	-0.602	0.000	0.916	0.617
810/1027	-0.548	0.491	0.000	0.877	0.838	1027/810	0.509	-0.456	0.000	1.183	0.458
810/1375	-0.564	0.505	0.000	0.363	1.115	1375/810	0.476	-0.426	0.000	0.666	1.059
810/1460	-0.552	0.494	0.000	0.416	1.109	1460/810	0.495	-0.444	0.000	0.683	1.034
810/1600	-0.763	0.683	0.000	0.464	0.845	1600/810	0.773	-0.693	0.000	0.721	0.644
870/1027	-0.127	0.114	0.000	1.232	0.722	1027/870	0.242	-0.216	0.000	1.278	0.589
870/1375	-0.401	0.359	0.000	0.494	1.189	1375/870	0.110	-0.098	0.000	0.633	1.236
870/1460	-0.347	0.311	0.000	0.557	1.193	1460/870	0.081	-0.073	0.000	0.605	1.253
870/1600	-0.440	0.394	0.000	0.569	1.134	1600/870	0.321	-0.287	0.000	0.720	1.126
1027/1375	-0.162	0.136	0.000	0.927	1.048	1375/1027	0.089	-0.080	0.000	0.948	1.044
1027/1460	-0.057	0.051	0.000	1.028	0.978	1460/1027	0.030	-0.027	0.000	0.935	1.060
1027/1600	0.035	-0.031	0.000	1.282	0.659	1600/1027	0.146	-0.131	0.000	1.234	0.714
1375/1460	0.338	-0.302	0.000	0.924	0.974	1460/1375	-0.357	0.320	0.000	0.836	1.031
1375/1600	0.023	-0.021	0.000	0.668	1.228	1600/1375	-0.209	0.187	0.000	0.633	1.214
1460/1600	-0.068	0.061	0.000	0.623	1.246	1600/1460	-0.074	0.066	0.000	0.754	1.179

Table VIII. Results of Discriminant Function Analysis—146 Samples

Asphalts			Heavy residual fuel oils			Asphalts			Heavy residual fuel oils		
A	B	C	A	B	C	A	B	C	A	B	C
1	a	1.000	1	o	1.000	40	a	1.000	40	o	1.000
2	a	1.000	2	o	1.000	41	a	1.000	41	o	1.000
3	a	1.000	3	o	1.000	42	a	1.000	42	o	1.000
4	a	1.000	4	o	1.000	43	a	1.000	43	o	1.000
5	a	1.000	5	o	1.000	44	a	1.000	44	o	1.000
6	a	1.000	6	o	1.000	45	a	1.000	45	o	1.000
7	a	1.000	7	o	1.000	46	a	1.000	46	o	1.000
8	a	1.000	8	o	1.000	47	a	1.000	47	o	1.000
9	a	1.000	9	o	1.000	48	a	1.000	48	o	1.000
10	a	1.000	10	o	1.000	49	a	1.000	49	o	1.000
11	a	1.000	11	o	1.000	50	a	1.000	50	o	1.000
12	a	1.000	12	o	1.000	51	a	1.000	51	o	1.000
13	a	1.000	13	o	1.000	52	a	1.000	52	o	1.000
14	a	1.000	14	o	1.000	53	a	1.000	53	o	1.000
15	a	1.000	15	o	1.000	54	a	1.000	54	o	1.000
16	a	1.000	16	o	1.000	55	a	1.000	55	o	1.000
17	a	1.000	17	o	1.000	56	a	1.000	56	o	1.000
18	a	1.000	18	o	1.000	57	a	1.000	57	o	1.000
19	a	1.000	19	o	1.000	58	a	1.000	58	o	1.000
20	a	1.000	20	o	0.999	59	a	1.000	59	o	1.000
21	a	1.000	21	o	1.000	60	a	1.000	60	o	1.000
22	a	1.000	22	o	1.000	61	a	1.000	61	o	1.000
23	a	1.000	23	o	1.000	62	a	1.000	62	o	1.000
24	a	1.000	24	o	1.000	63	a	1.000	63	o	1.000
25	a	1.000	25	o	1.000	64	a	1.000	64	o	1.000
26	a	1.000	26	o	1.000	65	a	1.000	65	o	1.000
27	a	1.000	27	o	1.000	66	a	1.000	66	o	1.000
28	a	1.000	28	o	1.000	67	a	1.000	67	o	1.000
29	a	1.000	29	o	1.000	68	a	1.000	68	o	1.000
30	a	1.000	30	o	1.000	69	a	1.000	69	o	1.000
31	a	0.999	31	o	1.000				70	o	1.000
32	a	1.000	32	o	1.000				71	o	1.000
33	a	1.000	33	o	1.000				72	o	1.000
34	a	0.895	34	o	1.000				73	o	1.000
35	a	1.000	35	o	1.000				74	o	1.000
36	a	1.000	36	o	1.000				75	o	1.000
37	a	1.000	37	o	1.000				76	o	1.000
38	a	1.000	38	o	1.000				77	o	1.000
39	a	1.000	39	o	1.000						

* Column heading definitions: A, observation number; B, classified as a = asphalt, o = heavy residual fuel oil; C, probability for correct classification.

Table IX. Average Probability of Correctly Classifying 146 Samples

Groups	Average probability of correct classification
Asphalts	0.999
Heavy residual fuel oils	0.999
Average over both groups	0.999

nant functions are evaluated. The higher algebraic value, whether of z_o or of z_a , will determine the classification of the given replicate.

Since the data have been standardized, all variables have approximately the same mean and standard deviation, Table VII.

Therefore, the magnitude of the coefficients, b_j 's and b_j' 's, for the variables contained in Table IV can be considered as a measure of discriminatory power for each ratio or variable. The five most important variables in decreasing order of importance are $1600\text{ cm}^{-1}/810\text{ cm}^{-1}$,

Table X. Classification of Observations

Probability of correct classification	Numbers of observations			Per cent	Cumulative per cent for both groups	
	By group		Both groups, total		From top	From bottom
	Asphalts	Heavy residual fuel oils				
1.000	67	76	143	97.9	97.9	100.0
0.999 to less than 1.000	1	1	2	1.4	99.3	2.1
0.900 to less than 0.999	0	0	0	0.0	99.3	0.7
0.800 to less than 0.900	1	0	1	0.7	100.0	0.7
Total	69	77	146	100.0		

Table XI. Characterization of Unknown Samples Using Linear Discriminant Function Analysis

Wavenumber ratios, $\text{cm}^{-1}/\text{cm}^{-1}$	J-Value	Sample 1		Sample 2	
		Absorbance ratios	Standardized absorbance ratios	Absorbance ratios	Standardized absorbance ratios
720/810	1	1.2645	0.8227	1.1895	0.6531
720/870	2	0.9325	0.0096	0.7995	-0.2925
720/1600	3	0.3503	-0.6726	0.3311	-0.7732
810/870	4	0.7374	-1.4707	0.6721	-1.7588
810/1027	5	2.0568	-0.4659	2.3750	-0.1069
810/1375	6	0.1506	-0.6339	0.1478	-0.6543
810/1460	7	0.0591	-0.7057	0.0643	-0.5933
810/1600	8	0.2771	-1.6692	0.2784	-1.6625
870/1027	9	2.7891	0.4762	3.5338	1.3186
870/1460	10	0.0801	-0.1881	0.0957	0.1775
870/1600	11	0.3757	-1.1664	0.4142	-0.9273
1027/1375	12	0.0732	-0.5644	0.0622	-0.7784
1027/1460	13	0.0287	-0.6043	0.0271	-0.6925
1027/1600	14	0.1347	-1.3085	0.1172	-1.4862
1375/1460	15	0.3921	-0.1940	0.4352	0.7078
1375/1600	16	1.8394	-1.0202	1.8839	-0.9784
1460/1600	17	4.6917	-1.0616	4.3286	-1.2137
810/720	18	0.7908	-0.7053	0.8407	-0.6596
870/720	19	1.0724	-0.4041	1.2508	-0.2128
1027/720	20	0.3845	-0.6995	0.3540	-0.7763
1375/720	21	5.2503	-0.6140	5.6895	-0.4070
1460/720	22	13.3918	-0.5864	13.0727	-0.6478
1600/720	23	2.8543	0.2861	3.0201	0.4218
870/810	24	1.3561	1.8942	1.4879	2.5487
1027/810	25	0.4862	0.0471	0.4210	-0.2330
1460/810	26	16.9335	0.6563	15.5505	0.4004
1600/810	27	3.6092	3.0472	3.5925	3.0182
1027/870	28	0.3585	-0.5272	0.2830	-0.8019
1375/870	29	4.8957	-0.3147	4.5487	-0.4246
1600/870	30	2.6616	1.3389	2.4145	0.8903
1375/1027	31	13.6547	0.1403	16.0740	0.5057
1460/1027	32	34.8285	0.2295	36.9327	0.3666
1600/1027	33	7.4234	1.8013	8.5323	2.4494
1460/1375	34	2.5507	0.0850	2.2977	-0.7714
1600/1375	35	0.5436	1.1617	0.5308	1.0667
1600/1460	36	0.2131	1.4192	0.2310	1.8300

1600 cm^{-1} /870 cm^{-1} , 810 cm^{-1} /1460 cm^{-1} , 870 cm^{-1} /1600 cm^{-1} , and 810 cm^{-1} /720 cm^{-1} . The five least important variables in decreasing order are 1027 cm^{-1} /720 cm^{-1} , 1460 cm^{-1} /1375 cm^{-1} , 1460 cm^{-1} /1027 cm^{-1} , 810 cm^{-1} /1027 cm^{-1} , and 1600 cm^{-1} /1460 cm^{-1} . The *j*-numbers are ranked in descending order of the absolute magnitude of the coefficients. These *j*-numbers are: 27, 30, 07, 11, 18, 08, 10, 29, 26, 19, 24, 04, 12, 21, 02, 01, 16, 14, 17, 13, 22, 03, 35, 28, 25, 31, 15, 23, 33, 09, 06, 20, 34, 32, 05, 36. The wavenumber ratios corresponding to these *j*-values are found in Table V.

The evaluation by both discriminant functions of the 146 observations and resulting probability for correct classification are shown in Table VIII.

Sample one, replicate one in the asphalt group has a probability of 1.000 of being an asphalt and probability of 1.000 - 1.000 = 0.000 of being an oil and was assigned to the asphalt group. By discriminant analysis, all of the replicates were correctly classified as an asphalt or a heavy residual fuel oil. Table IX gives the average probability of correct classification for each group taken separately and both groups collectively.

From the last line of that table, it can be seen that the odds of correct classification are 0.999 to 0.001 or about 999 to 1.

Some interpretation of the frequency distribution of the probabilities shown in Table X follows: 97.9% of the 146 observations had a probability of correct classification equal to 1.000. From the last column, 2.1% had a proba-

bility of less than 1.000, or, in the next to last column, 99.3% had a probability of 0.999 or greater.

Several asphalts and No. 6 residual fuel oils that were not included in the original 146 replicates were tested using this procedure. The ratios of absorbances were standardized and the discriminant functions evaluated. Results revealed that asphalts and No. 6 residual fuel oils not taken from the original 146 observations, but representative of the two groups, can be correctly classified with a high degree of certainty.

Table XI shows the data on tested materials associated with a spill believed to be asphalt that was obtained on the Ohio River near Pittsburgh, Pa. For sample 1, from the spill itself, the two function values are: $z_a = -4.68050$, $z_o = -8.92630$, and the probabilities for correct classification are: Group *a* = 0.985, Group *o* = 0.015. For sample 2, a suspected source asphalt, the two function values are: $z_a = -5.22735$, $z_o = -8.40503$, and the probabilities for correct classification are: Group *a* = 0.960, Group *o* = 0.040. The two samples were correctly classified with a high degree of probability. From the results of this study, the potential for detailed identification of environmental samples is recognized.

CONCLUSION

The objectives mentioned in this paper have been realized in that the observations on 18 asphalt samples and on 20 heavy residual fuel oil samples, for the first time, have been correctly classified. Discriminant function analysis is

a technique for utilizing more of the information which has been generated in the laboratory. Thus, a combination of infrared measurements, data treatment and transformation, and discriminant function analysis through computer assistance has resulted in effecting a more precise and accurate method of distinguishing between these heavy petroleum materials. An established statistical technique has hereby been applied successfully to a recently developed infrared procedure for heavier petroleum products to provide a useful and powerful technique for classification and may result in a promising application to further identification.

ACKNOWLEDGMENT

It is a special pleasure to acknowledge the support and interest given by D. G. Ballinger, Director of the Analytical Quality Control Laboratory, throughout the investigation. Much credit is due R. C. Kroner, Chief, Physical and Chemical Methods, for his interest and help in this study. The assistance given by Hilda Knueven is greatly appreciated.

Received for review January 4, 1973. Accepted August 16, 1973. Mention of the products and manufacturers is for identification purposes only and does not imply endorsement by the Environmental Protection Agency.

Molecular Interactions of Asphalt: An Infrared Study of the Hydrogen-Bonding Basicity of Asphalt

R. V. Barbour and J. C. Petersen

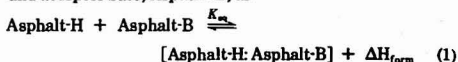
Laramie Energy Research Center, Bureau of Mines, U.S. Department of the Interior, Laramie, Wyo. 82070

The hydrogen-bonding basicity of asphalts, oxidized asphalts, and asphalt fractions has been investigated by infrared techniques using phenol as the hydrogen-bonding acid. Evidence has been obtained that asphalts exhibit strong hydrogen-bonding basicity. Infrared frequency shift data give enthalpies of formation in the range 6–8 kcal/mole for the asphalt-phenol hydrogen bond in CCl_4 solution. The phenol interaction data suggest a hydrogen-bonding base concentration of at least 2 mmoles per gram of asphalt. Air oxidation of asphalts at elevated temperatures increased the measured hydrogen-bonding basicity of the asphalt and suggests the formation of new hydrogen-bonding bases. Sulfur-containing molecules are suggested as important to the hydrogen-bonding basicity of asphalts, and the oxidation of the sulfur in these molecules could account for some of the increased basicity on air oxidation. Data from the methylation of an asphalt and its fractions with diazomethane suggest the occurrence of molecular aggregation *via* hydrogen bonding.

Intermolecular association forces have long been acknowledged as fundamental to the overall physical properties of materials (1–3). Previous reports (4) have suggested that intermolecular forces in asphalt, such as dipole, dispersion, electron donor-acceptor, and hydrogen-bonding forces, are important to the macroproperties of asphalt; and several studies (4–6) have appeared concerning the possible chemical origin of these attractive forces. These reported studies, and our continued interest in the molecular interactions of asphalt, prompted this in-

vestigation of hydrogen-bonding in asphalt and, in particular, the existence and nature of hydrogen-bonding bases in asphalt.

The formation of intermolecular hydrogen bonds in asphalt requires the specific interaction of two molecular functions—a proton donor, or hydrogen-bonding acid, and a proton acceptor, or hydrogen-bonding base (7). This interaction to form the hydrogen-bonded complex can be depicted in the general case of the donor acid, Asphalt-H, and acceptor base, Asphalt-B, as



This interaction is a rapid, reversible equilibrium and is characterized by an equilibrium constant, K_{eq} , and a formation enthalpy or hydrogen bond strength, ΔH_{form} .

In asphalt the natural occurrence of such hydrogen-bonding acids as carboxylic acids, phenols, amides, and pyrroles is generally accepted (8, 9). Previous work has shown that several of these molecular types form hydrogen bonds in asphalt (6). Petersen (5) has tentatively identified a cyclic amide compound type in asphalt and has demonstrated the ability of these amides to associate strongly with carboxylic acids. Another study (6) has pointed to the involvement of OH and NH functionality in asphalt as hydrogen-bonding acids.

The hydrogen-bonding bases in asphalt have received much less study. Yen (10) has found that large π -aromatic systems in asphaltene are capable of electron donor-electron acceptor activity, and he suggests that π -aromatic systems may participate as electron-donor bases. Petersen (5, 11) has shown that carboxylic acids and cyclic amides act as hydrogen-bonding bases in asphalts by self-association to form dimer structures.

- (1) D. J. Williams, "Polymer Science and Engineering," Prentice-Hall, Inc., Englewood Cliffs, N.J., 1971, pp 19–22.
- (2) F. Rodriguez, "Principles of Polymer Systems," McGraw-Hill Book Co., New York, N.Y., 1970, pp 11–14.
- (3) M. C. Shen, J. D. Strong, and F. J. Matusik, *J. Macromol. Sci., Part B*, **1**, 15, (1967).
- (4) C. Mack, "Bituminous Materials: Asphalts, Tars, and Pitches, Vol. 1," A. J. Holberg, Ed., Interscience Publishers, New York, N.Y., 1964, pp 31–6.
- (5) J. C. Petersen, R. V. Barbour, S. M. Dorrence, F. A. Barbour, and R. V. Heim, *Anal. Chem.*, **43**, 1491 (1971).
- (6) J. C. Petersen, *Fuel*, **46**, 285 (1967).

- (7) G. C. Pimental and A. L. McClellan, "The Hydrogen Bond," W. H. Freeman and Co., San Francisco, Calif., 1960.
- (8) R. N. Traxler, "Asphalt, Its Composition, Properties, and Uses," Reinhold Publishing Corp., New York, N.Y., 1961, pp 7–32.
- (9) E. J. Barth, "Asphalt," Gordon and Breach Science Publishers, Inc., New York, N.Y., 1962, pp 109–81.
- (10) T. F. Yen, *Amer. Chem. Soc., Div. Fuel Chem., Prepr.*, **15**, (1) 93 (1971).
- (11) J. C. Petersen, *J. Phys. Chem.*, **75**, 1129 (1971).

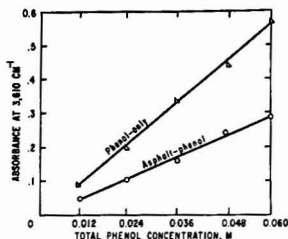


Figure 1. Absorbance of free phenolic OH (3610 cm^{-1}) vs. total phenol concentration for phenol-only and asphalt-phenol mixtures (asphalt concentration, 0.05 gram/ml)

In this study, we report the spectroscopic observation and measurement of the intermolecular association of the hydrogen-bonding acid, phenol, with asphalts, with oxidized asphalts, and with asphalt fractions. Experimental evidence is presented that asphalts possess considerable hydrogen-bonding basicity, that this basicity increases upon oxidation, and that the hydrogen-bonding bases naturally present are capable of forming energetically strong hydrogen bonds. Additionally, we present evidence for molecular aggregation in asphalts attributable to hydrogen bonding.

EXPERIMENTAL

Materials. Five asphalts were used in this study, four of which were used as supplied by the Federal Highway Administration (FHWA) from the California Road Test series (12) and the fifth a Wilmington (Calif.) asphalt previously described (13-16). The oxidized asphalt samples were prepared by air oxidation in an inverse gas-liquid chromatographic column (17) at 130°C for 24 hours. Phenol was Eastman reagent grade and was distilled just prior to use. Carbon tetrachloride (CCl_4) was Baker and Adamson reagent grade distilled from phosphorus pentoxide prior to use and stored over 4A molecular sieve. Chromatographic-grade basic alumina, 100-200 mesh, Activity 1, from Bio-Rad Laboratories was used for the chromatography without further activation. Diazald, for the preparation of diazomethane, was obtained from Aldrich Chemical Company. Tetrahydrofuran was used as received from Eastman Chemical Company.

Infrared Spectra. Infrared spectra were recorded on a Perkin-Elmer Model 521 infrared spectrophotometer. All spectra were obtained using a 0.5-mm pathlength sample cell and a matching reference cell (NaCl windows). The sample cell was maintained at a constant temperature of $30 \pm 0.5^\circ\text{C}$ using a Barnes Engineering Co. thermoelectric temperature chamber with KBr windows. The sample cell was allowed to thermally equilibrate 20 minutes in the temperature chamber prior to recording each spectrum. Machine spectral response was monitored and maintained constant throughout each series of spectra by regular recalibration with a 0.060M phenol solution.

Determination of Phenol Interaction Value. Solutions of phenol in CCl_4 were prepared in 100-ml volumetric flasks at concentrations of 0.024, 0.050, 0.072, 0.096, and 0.120M. A 100.0 mg/ml solution of the desired asphalt sample in CCl_4 was prepared in a 10-ml volumetric flask. Spectral samples of the phenol-only solutions were prepared by making a 1:1 quantitative dilution of each phenol solution with CCl_4 in a 5-ml septum-capped vial, using a hypodermic syringe. Spectra of the phenol-only solutions in the region of $4000\text{--}3000\text{ cm}^{-1}$ at the concentrations of 0.012, 0.025, 0.036, 0.048, and 0.060M were recorded. In a similar manner, using septum-capped vials, five asphalt-phenol solutions were prepared by mixing quantitatively 1 ml of the asphalt solution

with 1 ml of each of the standard phenol solutions. Spectra, in the region of $4000\text{--}3000\text{ cm}^{-1}$ were recorded for each of these asphalt-phenol mixtures. Absorbance of the free phenolic OH band at 3610 cm^{-1} was read directly from the spectrum using the baseline method. Interfering phenolic absorbance at 3610 cm^{-1} due to the phenols naturally present in the asphalt as measured by a separate spectrum of asphalt-only (50.0 mg/ml solution), was subtracted from the recorded free phenolic band of the asphalt-phenol mixture.

A plot (Figure 1) was made of free phenol absorbance vs. total added phenol for the phenol-only solutions and the asphalt-phenol mixtures. The difference in area under the two lines after extrapolation to the origin, expressed as a percentage of the total area under the phenol-only line, was the phenol interaction value (PIV) for the asphalt sample. PIV's were calculated as follows:

$$\text{PIV} = \frac{A-B}{A} \times 100 \quad (2)$$

where A = area under phenol-only line and B = area under asphalt-phenol line. PIV's were found to be reproducible to ± 1 PIV unit upon repetitive determinations.

Fractionation of Wilmington Asphalt. The asphalt, 50 grams, was deasphalted by digestion overnight with 2.5 l. of n -pentane. The mixture was vacuum-filtered to collect the asphaltenes which were then exhaustively extracted in a Soxhlet extractor with n -pentane and dried under vacuum to give 6.5 grams (13%) asphaltenes. The Soxhlet extract was combined with the initial filtrate and the resulting maltenes were recovered by rotary evaporation of this combined solution. Thirty grams of maltenes was dissolved in 100 ml of n -hexane and charged to a column ($1.25\text{ m} \times 35\text{ mm}$) of 900 grams of basic alumina wet packed in n -hexane. Successive elutions with 3 l. of n -hexane, 3 l. of benzene, and 3 l. of 4:1 benzene/methanol yielded 7.9 grams (26%) saturates, 10.6 grams (35%) aromatics, and 8.8 grams (29%) polar aromatics, respectively. Solvent was removed from each of these fractions by exhaustive rotary evaporation under vacuum.

Methylation. Approximately 0.025 mole of diazomethane (explosive and extremely toxic) was generated as previously described (18) using the precursor N -methyl- N -nitroso- p -toluenesulfonamide (Diazald). A high-boiling alcohol, 2-(2-ethoxyethoxy)ethanol, was used in place of ethanol in the diazomethane generator to avoid contamination of the methylated asphalt with traces of alcohol. The diazomethane-ethyl ether solution was distilled from the generation flask into a stirred, cooled (0°C) solution of 2.5 grams of asphalt in 100 ml of anhydrous tetrahydrofuran. After addition of the diazomethane, the asphalt solution was stirred for 2 hours at 0°C and allowed to stand at room temperature for 16 hours. Unreacted diazomethane was removed by bubbling dry nitrogen gas through the solution for 2 hours. Solvent was removed from the asphalt sample by rotary evaporation under vacuum while heating the sample flask with boiling water.

RESULTS AND DISCUSSION

The use of phenol as a test hydrogen-bonding acid in both spectroscopic (19-23) and calorimetric (24-27) investigations of hydrogen-bonding bases is well documented. In the present study, our choice of phenol as the test hydrogen-bonding acid was based on three factors: the ability to reliably observe and measure spectroscopically the free and the bonded phenolic OH group in the infrared in mixed asphalt-phenol solutions; the ability to work with high (up to 0.06M) test-acid concentrations without seri-

- (12) F. N. Hveem, E. Zube, and J. Skog, *Amer. Soc. Test. Mater., Spec. Tech. Publ.*, **227**, 3 (1959).
 (13) R. V. Heim, *Anal. Chem.*, **41**, 1342 (1969).
 (14) R. V. Heim and J. C. Petersen, *Anal. Chem.*, **40**, 1100 (1968).
 (15) T. C. Davis, J. C. Petersen, and W. E. Haines, *Anal. Chem.*, **38**, 241 (1966).
 (16) J. W. Ramsey, F. R. McDonald, and J. C. Petersen, *Ind. Eng. Chem., Prod. Res. Develop.*, **6**, 231 (1967).
 (17) T. C. Davis and J. C. Petersen, *Anal. Chem.*, **38**, 1938 (1966).

- (18) T. H. J. DeBoer and N. J. Backer, *Rec. Trav. Chim. Pays-Bas*, **73**, 229 (1954).
 (19) J. H. Nelson, L. C. Nathan, and R. O. Ragsdale, *J. Amer. Chem. Soc.*, **90**, 5754 (1968).
 (20) T. Gramslad, *Spectrochim. Acta*, **19**, 497 (1963).
 (21) B. B. Wayland and R. S. Drago, *J. Amer. Chem. Soc.*, **86**, 5240 (1964).
 (22) Z. Yoshida and E. Osawa, *J. Amer. Chem. Soc.*, **87**, 1467 (1965).
 (23) D. P. Eyrman and R. S. Drago, *J. Amer. Chem. Soc.*, **88**, 1617 (1966).
 (24) T. D. Epley and R. S. Drago, *J. Amer. Chem. Soc.*, **89**, 5770 (1967).
 (25) D. Neerincx, *Ann. Chim.*, **4**, 43 (1969).
 (26) E. M. Arnett, T. S. R. Murty, P. von R. Schleyer, and L. Joris, *J. Amer. Chem. Soc.*, **89**, 5955 (1967).
 (27) S. S. Barton, J. P. Krall, T. R. Owens, and L. J. Skinner, *J. Chem. Soc.*, **3**, 339 (1972).

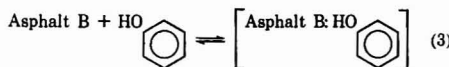
Table I. Phenol Interaction Values for Unoxidized and Oxidized Whole Asphalts

Asphalt	PIV	
	Unoxidized	Oxidized*
A	25	31
H	24	28
J	13	23
D	22	32
Wilmington asphalt	25	33

* Air oxidized as 15- μ film, 24 hr at 130 °C.

ous complication from test-acid self-association; and the mutual compatibility of phenol and asphalt in CCl_4 solution.

The hydrogen-bonding interaction of direct interest was the association of phenol with asphalt. This interaction can be represented in a simplistic manner as



The determination of a conventional equilibrium constant for the interaction was not possible for lack of a reliable molar concentration term representing the concentration of asphalt bases. Although it was possible to calculate an equilibrium constant based on the osmometric determination of the average molecular weight for the asphalt, the use of average molecular weight as a measure of the molar concentration of hydrogen-bonding base functionality is clearly misleading. The complex chemical composition of asphalt prohibits such use except as a first approximation.

An infrared technique was therefore devised to measure the relative hydrogen-bonding basicity of asphalt with respect to phenol. The spectra of a series of asphalt-phenol solutions were obtained holding the asphalt concentration constant while varying the concentration of phenol. The spectra of a corresponding series of phenol-only solutions were also obtained. A plot was then made for each series of spectra, plotting absorbance of the free phenolic OH band at 3610 cm^{-1} vs. total phenol concentration. A representative plot is shown in Figure 1. The difference in area under the lines in the plot was used as a direct measure of the percentage of the added phenol which was involved in a hydrogen-bonding interaction with the asphalt. This percentage of phenol bonded was termed the "phenol interaction value," or PIV.

In all samples studied, confirming evidence that the loss of free phenolic OH absorbance resulted from hydrogen bonding between the phenol and a hydrogen-bonding base in the asphalt rather than some unsuspected phenol-consuming reaction was the corresponding appearance in the asphalt-phenol spectra of a broad band centered between $3100\text{--}3350 \text{ cm}^{-1}$ which is characteristic of hydrogen-bonded phenol (28). In addition, an increase in temperature of the asphalt-phenol solution in the sample cell caused dissociation of the hydrogen-bonded complex as evidenced by the decrease in bonded OH and increase in free OH absorbances.

Phenol Interaction of Asphalts and Oxidized Asphalts. Five asphalts were selected for investigation. Four were asphalts from the California Zaca-Wigmore Road Test series (12), and the fifth was a Wilmington asphalt chosen because of the extensive studies previously reported (13-16) on this particular asphalt. Phenol interac-

tion values, reported in Table I, were determined for each of these asphalts, unoxidized and oxidized. With all of the unoxidized asphalts except asphalt J, 22 to 26% of the added phenol entered into a hydrogen-bonding interaction with the asphalt; with asphalt J, only a 13% interaction was observed. Oxidation with air at 130 °C produced a considerable increase in hydrogen-bonding basicity in every asphalt tested. This increase, ranging from 4 to 10 PIV units for the five asphalts, supports the previous observation (6) that naturally occurring hydrogen-bonding acids (OH and NH) in asphalt are more highly associated in oxidized asphalts than in unoxidized asphalts. The proposed explanation that oxidation of asphalts leads to the formation of new hydrogen-bonding bases appears to be valid and suggests that a part of the physical hardening observed in asphalts upon oxidative aging is related to an increase in intermolecular association due to hydrogen bonding.

With all the asphalts examined, plots of free phenol concentration vs. total phenol concentration, at a fixed asphalt concentration, resulted in a straight line with no noticeable curvature even at high phenol concentrations. Calculations based on the equilibrium reaction of Equation 1 indicate that, within the range of phenol concentrations considered in these experiments, straight-line plots would be obtained only under restricted conditions of equilibrium constant and base concentration values. If the equilibrium constant is small (<1.0), a straight-line plot will result down to base concentrations as low as $0.01M$. If, however, the equilibrium constant is large (in the range 10-100), base concentrations higher than $0.01M$ must be present to give the observed straight line. Equilibrium constants of 10-100 have been reported (29-31) for phenol hydrogen bonding in CCl_4 with a variety of model organic bases. Assuming the hydrogen-bonding bases in asphalt display similar equilibrium constants with phenol as do the model bases, calculations indicate that the basic hydrogen-bonding functionality in asphalt must be at the concentration of 2 mmoles/gram of asphalt, or greater.

Phenol Interaction of Asphalt Fractions and Methylated Asphalt Fractions. The Wilmington asphalt sample was deasphalted with *n*-pentane, and the resulting maltenes were separated into three fractions using an absorption chromatographic separation method. The mass balance in the separation and the elemental nitrogen and sulfur analyses of the samples are shown in Table II. An 8% weight loss was incurred during the chromatography due to irreversible adsorption of asphaltic material on the alumina.

Infrared examination and elemental nitrogen and sulfur analyses of the asphaltenes and of the three fractions from the maltenes indicated sharp differences in their composition. The saturate fraction was low in nitrogen, 0.05%, but contained appreciable sulfur; infrared spectra showed no phenolic (3610 cm^{-1}), carboxylic acid (3540 cm^{-1}), pyrolic (3480 cm^{-1}), or carbonyl (1700 cm^{-1}) absorption. The aromatic fraction showed only low concentrations of pyrolic and carbonyl-type functionality in addition to the usual hydrocarbon and aromatic bands. The polar aromatic fraction indicated higher concentrations of phenolic, pyrolic, and carbonyl functionality and contained moderate nitrogen and sulfur. The asphaltenes contained very high nitrogen and sulfur and indicated the highest functionality of any of the samples per unit weight, as measured in the infrared.

(28) L. J. Bellamy, "The Infrared Spectra of Complex Molecules," 2nd ed., John Wiley and Sons, Inc., New York, N.Y., 1959, pp 95-106.

(29) T. D. Epley and R. S. Drago, *J. Amer. Chem. Soc.*, **89**, 5770 (1967).

(30) H. Dunken and H. Fritzsche, *Z. Chem.*, **2**, 345 (1962).

(31) E. Osawa and Z. Yoshida, *J. Amer. Chem. Soc.*, **88**, 4019 (1966).

Table II. Mass Balance, Elemental Analysis, and Phenol Interaction Values for Wilmington Asphalt and Its Component Fractions

Asphalt sample	Wt % of total asphalt	N, %	S, %	PIV	
				Original sample	Methylated sample
Wilmington asphalt	100	1.08	2.08	25	26
Asphaltenes	13	2.37	2.85	24	35
Maltenes	87	0.84	2.23	29	31
Saturates	23	0.05	1.34	7	8
Aromatics	31	1.01	2.86	32	36
Polar aromatics	25	1.70	2.47	31	46

Phenol interaction values were obtained on the asphalt, on the maltenes and asphaltenes, and on the three maltene chromatographic fractions; these values are reported in Table II. If the phenol interaction values were related in a straightforward manner to the functional group content of an asphalt they should increase in the order saturates < aromatics < polar aromatics < asphaltenes, with the whole asphalt and maltenes appearing between extremes. The saturate fraction did, in fact, prove to be the weakest hydrogen-bonding base, showing the lowest PIV. However, the second weakest hydrogen-bonding base proved to be the asphaltenes. The polar aromatic fraction showed a higher basicity than the saturates or asphaltenes; but the aromatic fraction, despite its low apparent polarity and functionality, gave the highest basicity. The comparatively low PIV's for the polar aromatics and particularly for the asphaltenes relative to their known functionality and probable polarity suggest that many of the reactive basic sites in these fractions are unavailable to the phenol for interaction. Molecular aggregation in these highly functional and polar components is a plausible explanation for this anomaly. Asphalt is known to contain acids which may be strongly hydrogen-bonded to many of the basic sites on other asphalt molecules. This hydrogen bonding would result in molecular aggregation of varying degrees within the asphalt and this molecular aggregation may in turn render some unbonded basic sites unavailable to phenol simply because they are buried within the molecular aggregate or micelle.

Further evidence for molecular aggregation *via* hydrogen bonding was obtained by methylation of the asphalt fractions with diazomethane. The methylation was conducted to convert acidic hydrogen functions into their corresponding methyl derivatives, thereby preventing the hydrogen-bonding interactions of these acids. Intermolecular association within the asphalt would therefore be disrupted releasing basic sites for interaction with the added phenol. Tetrahydrofuran was used as the reaction solvent because it has been shown (5) to reduce molecular aggregation in asphalts and would be expected to assist in the dissociation of molecular complexes and thus expose hydrogen-bonding acids for methylation.

Phenol interaction values for the methylated samples are reported in Table II. All of the samples showed increased hydrogen-bonding basicity upon methylation. The relative increase in PIV was small for the whole asphalt and the maltene, saturate, and aromatic fractions. The asphaltene and polar aromatic fractions, however, showed large increases in PIV after methylation—11 units (46%) for the asphaltenes and 15 units (48%) for the polar aromatics. This large increase in PIV on methylation of the asphaltenes and polar aromatics is particularly significant in view of the unexpectedly low PIV observed in the unmethylated samples of these two components.

This large increase in PIV for these two fractions is most easily explained in terms of molecular aggregation

within these components and implies aggregation within the whole asphalt itself. The methylation reaction blocks many of the naturally occurring acids in the asphalt, thus liberating basic sites for interaction with the phenol. It is not possible to distinguish whether the basic sites are liberated from a previously hydrogen-bonded condition or a physically hindered state; both mechanisms may be involved. The data do suggest that the most polar fractions (asphaltene and polar aromatic) are highly self-associated in CCl₄ (low PIV's) and have greater potential for hydrogen-bonding interactions than are manifest by measurement of the PIV's in CCl₄ solution.

An attempt was made to characterize the acidic functions responsible for the molecular aggregation. The methyl ester of carboxylic acids was identified spectroscopically (carbonyl absorption at 1735 cm⁻¹) in the methylated samples of asphalt, asphaltenes, and maltenes. No carboxylic esters could be detected in the chromatographic fractions of the maltenes, suggesting that carboxylic acids account in part for material lost upon chromatography. Carboxylic acids are known to be strongly adsorbed on alumina. Diazomethane is a very reactive reagent, and it is unlikely that reaction of it with asphalt would be limited solely to formation of carboxylic methyl esters. Indeed, the large increase in PIV observed in the polar aromatics upon methylation in spite of the lack of carboxylic ester formation, suggests that hydrogen-bonding functionality, other than carboxylic acids, is methylated and removed from interaction with bases or molecular aggregates. The specific nature of this functionality is unknown, but it is suggested that this material contributes strongly to the overall hydrogen bonding in asphalt.

Enthalpies of Interaction. Drago (29, 32, 33) and others (34) have recently presented evidence that the hydrogen-bond strength, or enthalpy of formation, ΔH_{form} , of the association of phenol with a variety of organic hydrogen-bonding bases is linearly related to the infrared frequency shift observed between the free phenolic OH and bonded OH absorption bands. Drago proposed, based on numerous spectrometric and calorimetric measurements, the formula $\Delta H_{form} = 0.011 \Delta \nu_{OH} + 2.79$ as a correlation between the phenolic OH frequency shift, $\Delta \nu_{OH}$, and the enthalpy of formation of the corresponding hydrogen bond.

Examination of the infrared spectra of asphalt-phenol mixtures in CCl₄ indicated the applicability of this bond-strength measuring technique to the asphalt-phenol system. The OH frequency shift of asphalt-phenol mixtures is readily observable; the free phenolic OH band appears as a sharp spike at 3610 cm⁻¹, and the bonded OH band appears as a broad band with a maximum in the range

(32) R. S. Drago, *Chem. Brit.* 3, 518 (1967).

(33) K. F. Purcell and R. S. Drago, *J. Amer. Chem. Soc.*, 89, 2874 (1967).

(34) G. Sellier and B. Wojtkowick, *J. Chim. Phys. Physicochim. Biol.* 65, 936 (1968).

Table III. Enthalpy of Formation of Asphalt-Phenol Hydrogen Bonds

Asphalt sample	OH frequency shift ν_{OH} , cm^{-1}	ΔH_{form} , kcal/mole
Wilmington asphalt	330, 410*	6.4, 7.3
Asphaltenes	250, 350, 460	5.5, 6.6, 7.9
Maltenes	340, 450	6.5, 7.7
Saturates	340	6.5
Aromatics	290, 430	6.0, 7.5
Polar aromatics	290, 430	6.0, 7.5

* Two bands were discernible.

3100–3350 cm^{-1} . Frequency shift data obtained on the Wilmington asphalt, maltene, asphaltene, and three maltene chromatographic fractions were used to calculate the enthalpy of formation values given in Table III. The range of bond energies was found to be from 6–8 kcal/mole in all cases examined.

The apparent lack of low energy hydrogen bonds does not exclude the existence of weak hydrogen-bonding bases in asphalt but is more likely a reflection of the experimental conditions; i.e., dilute solutions of asphalt and phenol preclude the observation of very weak hydrogen bonds because of the unfavorable equilibria involved. The results do indicate, however, that bases capable of forming very strong hydrogen bonds are present in all the asphaltic samples investigated.

This poses the question of the possible chemical nature of the hydrogen-bonding bases in asphalt and raises the particularly intriguing question of the nature of the bases in the saturate and aromatic fractions that are capable of such high energy interactions. Reported (27, 31, 35–38) values of the hydrogen-bond strength of phenol-base interactions range from 0.5 kcal/mole for interactions of phenol with π -aromatic type bases up to 9 kcal/mole for interaction with molecular species containing the heteroatoms nitrogen and sulfur. The presence of high energy hydrogen bonds, however, points to the involvement of the nitrogen- and sulfur-containing molecular species in the interaction. The strong interaction observed for the polar aromatic and asphaltene fractions is easily rationalized because both are high in nitrogen and sulfur and, additionally, would be expected to contain the most polar molecules. The strong interaction observed for the saturate fraction, and to a lesser extent the aromatic fraction, despite their low polarity and low nitrogen content, suggests that hydrogen-bonding bases are present in these fractions that exhibit the properties of a weak interaction with alumina but strong hydrogen-bonding base character. The high sulfur content in all samples invites speculation that sulfur compounds play an important role as

hydrogen-bonding bases in asphalt. Reports (23, 39) have indicated that certain sulfur-containing alicyclic compounds such as thiacyclopentane exhibit strong hydrogen-bonding basicities. The ease of air oxidation of these sulfur heterocycles, together with the known strong hydrogen-bonding basicities of the product oxysulfur compounds (40), particularly sulfoxide compounds, suggests the presence of these sulfur-containing molecules in asphalt and points to the oxidation of these compounds as an explanation, in part, for the increased basicity observed in asphalts on air oxidation.

CONCLUSIONS

Data obtained from the infrared study of the hydrogen-bonding interaction of phenol with asphalts and asphalt fractions showed that asphalts contain molecular systems exhibiting strong hydrogen-bonding basicity. Based on infrared frequency shift data, the bond enthalpies for the interaction have been estimated to be in the range of 6 to 8 kcal/mole. The absolute concentration of hydrogen-bonding bases in asphalts cannot be determined with certainty by this technique. However, based on the assumption of an equilibrium constant for the overall association reaction of 10 or greater, the hydrogen-bonding bases are in concentrations of 2 mmole/gram of asphalt, or greater.

Air oxidation of asphalts at elevated temperatures caused an increase in the measured hydrogen-bonding basicity of the asphalt. The formation of new hydrogen-bonding bases by oxidation is suggested, although the chemical nature of these new bases is not presently known.

Increases in measured basicity upon methylation suggest that considerable hydrogen bonding occurs within the asphalt between naturally occurring hydrogen-bonding acids and bases. The increase is interpreted as resulting from two possible causes: blocking of acidic functions in the asphalt by methylation, thereby releasing the previously associated basic sites for interaction with phenol; and disruption of hydrogen-bonded molecular aggregates in the asphalt, therefore allowing unbonded basic sites physically buried within the aggregates to be exposed for interaction with phenol. Both effects may contribute to the overall increased basicity observed.

Sulfur-containing molecular species are proposed as important hydrogen-bonding bases in asphalt. Oxidation of sulfur compounds may account, in part, for the increase in hydrogen-bonding basicity of asphalt on air oxidation.

Received for review May 16, 1973. Accepted September 12, 1973. Mention of specific brand names or models of equipment is made for information only and does not imply endorsement by the Bureau of Mines.

- (35) E. Osawa, T. Kato, and Z. Yoshida, *J. Org. Chem.*, **32**, 2803 (1967).
 (36) R. Oda, Z. Yoshida, and E. Osawa, *Proc. Int. Symp. Mol. Struct. Spectrosc.*, Tokyo, D118 (1962).
 (37) Z. Yoshida and E. Osawa, *Nippon Kagaku Zasshi*, **87**, 509 (1966).
 (38) K. B. Whetsel, *Appl. Spectrosc. Rev.*, **2**, 51 (1968).

- (39) R. J. Niedzelski, R. S. Drago, and R. L. Middaugh, *J. Amer. Chem. Soc.*, **86**, 1694 (1964).
 (40) C. H. Henrickson, K. M. Nykevck, and D. P. Eymann, *Inorg. Chem.*, **7**, 1026 (1968).

Determination of Total Mercury in Air by Charcoal Adsorption and Ultraviolet Spectrophotometry

Frank P. Scaringelli, John C. Puzak, Berne I. Bennett, and Robert L. Denny

Quality Control Branch, Quality Assurance and Environmental Monitoring Laboratory, National Environmental Research Center, Environmental Protection Agency, Research Triangle Park, N.C. 27711

This paper describes a simple inexpensive method for determining concentrations of total mercury in the atmosphere. Mercury and its compounds are effectively collected by passing ambient air through activated charcoal contained in Vycor tubes. The charcoal tubes are prepared by heating under nitrogen to activate the charcoal and to remove impurities. Immediately after cleaning, the tubes are sealed with ball joints until ready for sample collection to prevent contamination. After sampling, the tubes are resealed for transport to the laboratory where they become an integral part of the analytical gas train. The mercury and its compounds are vaporized by heating under a stream of nitrogen and carried to a thermal reactor, which converts the compounds to the elemental state. Elemental mercury then amalgamates on silver, allowing potential interferences to pass through the absorption cell. The silver amalgam is heated to 300 °C to give the absorption peaks in the ultraviolet at 253.7 nm that are sharp and reproducible. The method was tested with simulated and real atmospheres under field conditions. Precision and accuracy of the method was greater than 95% within the range of 0.15 to 1.5 $\mu\text{g}/\text{m}^3$. Outside this range, the error would be greater; however, the dynamic range may be shifted upward or downward by changing sampling rates, samples times, or cell path and by combination of these variables.

During the past few years, a considerable amount of attention has been directed toward the potential hazards of mercury and its compounds in our environment (1, 2). There are several articles dealing specifically with the presence of mercury in air (3, 4). Mercury is found in the elemental state, as a vapor or adsorbed on particulate matter, or in other states. Other mercury compounds that may also be present at certain locales include methylmercury, dimethylmercury, diethylmercury, phenylmercuric chloride, phenylmercuric acetate, mercurous chloride, mercuric chloride, mercuric sulfide, mercuric oxides, and other halides of mercury. These mercury compounds may be photochemically decomposed in the presence of sunlight releasing elemental mercury (1). As a result of increased awareness of mercury in our environment and because of its hazardous nature, emission standards for mer-

cury have been proposed and promulgated by the Environmental Protection Agency to ensure that ambient air concentrations do not exceed 1 $\mu\text{g}/\text{m}^3$ of Hg (4, 5).

Methods developed to measure mercury in various substances have been reviewed recently (6). Heretofore, two manual methods, iodine monochloride (7) and potassium permanganate (8), were most commonly used to collect mercury and its compounds in ambient air. These methods were evaluated under field conditions in the vicinity of a chlor-alkali plant and were found unsatisfactory for determining mercury at ambient air levels. Contamination resulting from use of wet chemical reagents and the many required pieces of glassware presented a serious problem. The resulting data were imprecise and unreliable at the concentrations usually encountered.

Attention was directed to developing a new method that would determine not only elemental mercury but its compounds as well. The method had to be accurate at 1 $\mu\text{g}/\text{m}^3$ and suitable for network operations. Moffitt and Kupel reported that activated charcoal impregnated with iodine would satisfactorily collect airborne mercury at industrial hygiene levels (9). Kupel also suggested that impregnated carbon may not be necessary (10). Flameless or cold vapor atomic absorption in the ultraviolet (UV) is a sensitive method for detecting elemental mercury. This detection principle was suggested and applied by Polvektov *et al.* (11) and Hatch and Ott (12).

Using the two principles of adsorption on carbon and detection by UV absorption, a reliable method was developed for determining total mercury in ambient air having maximum precision and accuracy at 1 $\mu\text{g}/\text{m}^3$.

EXPERIMENTAL

The apparatus for the analytical system was designed and assembled in accordance with the instructions detailed in the procedure.

Apparatus. The sampling train, Figure 1, consists of a 25-cm section of 0.9-cm i.d. Vycor sampling tube with an 18/9 ball on one end and an 18/9 socket on the other, a 2.5-cm (1-inch) filter of glass fiber having a pore size of 0.3 μ with a plastic holder, flow controlling device, a flow measuring device, and a vacuum pump. Sealed borosilicate glass ball and socket joints are clamped to the sampling tube during storage to prevent contamination. Sampling tubes are packed with 2.4 to 5.5-cm⁻¹ (6 to 14 mesh) coconut charcoal to a depth of 15.5 cm. Tightly packed quartz wool of 1.5 cm is used to keep the charcoal in place. Plastic filter holders that will house filters of glass fibers are commercially available. Filters are washed with a 5% solution of HNO₃ and dried before

- (1) E. L. Kothny, "The Three-Phase Equilibrium of Mercury in Nature," presented at the 162nd National American Chemical Society Meeting, Washington, D.C. (Sept. 12-17); address: E. L. Kothny, Air and Industrial Hygiene Laboratory, State of California Department of Public Health, 2151 Berkeley Way, Berkeley, Calif. 94704.
- (2) F. M. D'Itri, "The Environmental Mercury Problem," Chemical Rubber Company Press, Cleveland, Ohio, 44129, 1972.
- (3) O. R. Sisti, "Preliminary Air Pollution Survey of Mercury and Its Compounds," EPA Publication APTD 69-40, Research Triangle Park, N.C., October 1969.
- (4) "Background Information—Proposed National Emission Standards for Hazardous Air Pollutants: Asbestos, Beryllium, Mercury," EPA Publication APTD-0753, Research Triangle Park, N.C., December 1971.

- (5) *Fed. Regis.*, 38, No. 66, 8820-8850, April 6, 1973.
- (6) R. A. Baker and M. D. Luh, "Mercury Analyses and Toxicity—A Review, Part 1," *Industrial Waste*, IW 31, (May-June), 1972.
- (7) A. L. Linch, R. F. Stalzer, and D. T. Loefferts, *Amer. Ind. Hyg. Ass. J.*, 29, 79 (1968).
- (8) L. V. Hoff, Industrial Chemical Division, Allied Chemical Corp., private communication, 1971.
- (9) A. E. Moffitt, Jr. and R. E. Kupel, *Amer. Ind. Hyg. Ass. J.*, 32, 614 (1971).
- (10) R. E. Kupel, Bureau of Occupational Health, 1014 Broadway, Cincinnati, Ohio 45202, private communication.
- (11) N. S. Polvektov, R. A. Vitkun, and Y. V. Zelyukova, *Zh. Anal. Khim.*, 19, 937 (1964).
- (12) W. R. Hatch and W. L. Ott, *Anal. Chem.*, 40, 2085 (1968).

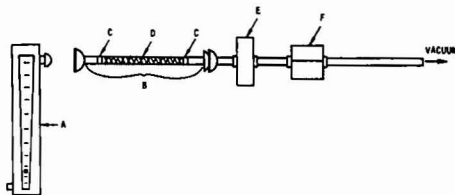


Figure 1. Sampling train

(A) Flow measuring device (0–1 l./min); (B) Carbon sampling tube (25 cm); (C) Quartz plug (1.5 cm); (D) Charcoal (15.5 cm); (E) Glass fiber filter and holder; and (F) Flow control device (needle valve or orifice 0–1 l./min)

use. Membrane filters are unsuitable because moisture adsorption on the filter results in variable flow rates. A needle valve or critical orifice controls flow between 0.2 and 0.6 l./min. Calibrated flowmeters should have an accuracy of 2 to 3% at these flow rates. The vacuum pump should be capable of maintaining a pressure differential across the flow controller of at least 0.6 atmosphere with the system completely assembled.

The analytical train, Figure 2, consists of a cylinder of dry nitrogen, two-stage regulator, two flow controllers, calibration ports, sampling tube, a micro oven pyrolyzer, three-way valve, amalgamator, a flow-through absorption cell, flowmeter, and an UV detector with recorder and integrator. The dry nitrogen in a cylinder, equipped with CGA 580 pressure regulator, is further purified with scrubbers consisting of activated charcoal and Molecular Sieve 5A. Needle valves control the flow between 0 and 2.5 l./min. The injection ports are glass tees capped with a serum bottle septum which keeps the system gastight and allows for syringe calibration.

Pyrolyzers are prepared from Vycor tubes with the same dimensions as the sampling tube but with a 10/30 inner tapered joint on the downstream end. The tube is packed tightly with quartz wool to a depth of 14.0 cm terminating with a 2.5-cm plug of silver wool on the downstream end to protect the amalgamator. Heating wire made of Nichrome, size 20, is coiled about the tube and then wrapped with asbestos. The leads from the heating wire are connected to a powerstat, which controls temperature at 850

°C. A three-way valve of borosilicate glass with tapered joints allows rapid shifting of the gas stream without changing the setting on the flow regulators.

The amalgamator is a Vycor tube, 25 cm by 9 mm, with 10/30 standard tapered joints. The tube is tightly packed with 10 grams of silver micro-wool to a length of about 14 cm and coiled with Nichrome heating wire which is connected to a powerstat for temperature regulation.

The detector consisted of a flow-through 10-cm absorption cell with two 2.5-cm diameter windows that are transparent to ultraviolet radiation at 253.7 nm and a spectrophotometer to measure the absorption of mercury vapor at this wavelength. A flowmeter downstream of the absorption cell monitors the flow in the range of 0 to 2 l./min. To prevent condensation of moisture within the flowmeter during the heating cycle, we installed a three-way stopcock, which diverts the moisture to exhaust.

A potentiometric recorder with a ball and disc integrator is used to record peak heights and areas. The integrator is not absolutely essential, but increases the repeatability of the method by accurately measuring the area under the curve. The area under the curve is less dependent on flow rate than peak heights. The entire glass system, except the amalgamator, is wrapped with heating tape and maintained at 65 °C to reduce adsorption of mercury and vapor on the walls.

Pretreatment of sample collected on filters requires a tube furnace, a combustion tube of zirconium oxide, and a ceramic boat, Figure 3. The combustion tube is fitted with a ball joint by means of a small section of Tygon tubing to provide a butt-to-butt connection. A cylinder of zero air with a two-stage regulator provides the carrier gas. A flowmeter connects at the open end of the sampling tube.

Reagents. All chemicals were ACS analytical grade unless otherwise specified. Reagents for sample collection were activated coconut charcoal, 2.5 to 5.5-cm (6 to 14) mesh, for packing absorption tubes and coarse quartz wool. Elemental mercury, dimethylmercury (Eastman), and mercuric chloride were used as calibrating reagents. The nitrogen carrier gas was a prepurified grade, and silver wool was special micro grade.

Prepare sampling tubes by plugging one end of the Vycor absorption tube with 1.5 cm of quartz wool about 2.5 cm from the ball joint and packing with activated charcoal tightly to a depth of 14 cm using a vibrator, and plugging with 1.5 cm of quartz wool on the other end. Place 2 ml of distilled H₂O on charcoal. By means of a furnace, heat the tube under a stream of nitrogen at a temperature of 500 °C for 10 minutes or, if the downstream side is

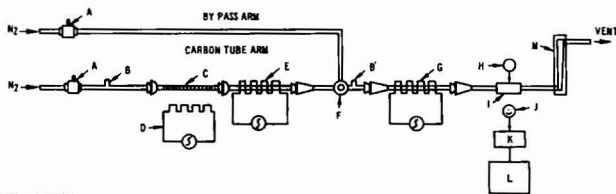


Figure 2. Mercury analytical train

(A) Flow control device (0–2 l./min); (B) Septum injection port; (B') Septum injection port; (C) Sampling tube; (D) Moving sample tube furnace (500 °C); (E) Pyrolyzer and heater (850 °C); (F) 3-Way stopcock; (G) Silver amalgamator and heater; (H) Light source (253.7 nm); (I) 10-cm flow through cell; (J) Photo detector; (K) Amplifier; (L) Recorder; and (M) Flow measuring device

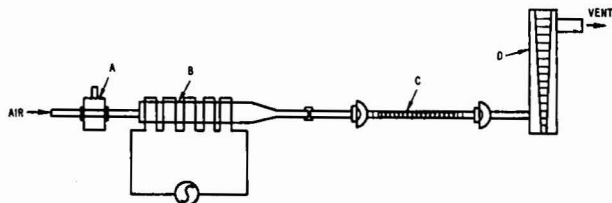


Figure 3. Filter analysis train

(A) Flow control device; (B) Combustion tube and furnace; (C) Carbon sampling tube; and (D) Flow measuring device

connected to the absorption cell, until no absorption appears at 253.7 nm. After cleaning, immediately cap the ends with the sealed borosilicate glass ball joints.

Sampling Procedure. Samples are collected using a sampling train shown in Figure 1. A box should be provided to protect the collection assembly from the weather and perhaps from vandalism during field sampling. The sample tube should remain capped until ready to start sampling. Remove the cap, start the pump, and record the time. Place a calibrated flowmeter temporarily on the inlet and record the flow rate. For 24-hour samples, collect at a sampling rate of 0.2 l./min. At the end of 24 hours, recheck the flow and record the exact time and flow rate. Remove the tube and filter. Seal the tube with caps and put the filter into a clean glass jar and transport both to the laboratory for analysis.

Analytical Procedure. The essential steps in the analytical process are to vaporize the mercury from the carbon tube under nitrogen; to convert its compounds to the elemental state by the pyrolyzer; to collect the mercury on silver; to release the mercury; and to measure the response at 253.7 nm. The silver amalgamator serves to separate the mercury from the impurities, to concentrate the mercury, and to release the mercury rapidly producing a sharp peak on the recorder. Important parameters during the amalgamation cycle are the nitrogen flow rate and temperatures of the sampling tube, pyrolyzer, and silver amalgamator. During the measurement cycle, the important parameters are the flow rate of nitrogen and the temperature of the amalgamator. These parameters were optimized to increase the signal size, reduce peak spread, and eliminate variability. Other parameters were also optimized by changing one variable at a time while keeping all others constant.

After the analytical system has been checked for correct zero response and has been calibrated, check the critical flow rates and temperature. Place 2 ml of distilled water on the carbon and position the tube in the analytical train. Turn the three-way stopcock to the position that allows nitrogen to flow through the carbon tube at a rate of 0.9 l./min. Set the amalgamator powerstat to the position corresponding to 40 °C. Heat the carbon tube with microfurnace at 500 °C for 7 minutes. Impurities and water vapor will usually drive the recorder off scale. After 5 minutes, the recorder should return to zero. It may prove desirable to keep this signal from reaching the recorder as it will be off scale in most cases. Remove the microfurnace from the sample tube and set the three-way stopcock so that N₂ flow is through the bypass arm. Adjust flow to 1.6 l./min, if necessary. Set the amalgamator powerstat to the 300 °C position and heat for 1 minute. A peak will appear on the recorder which is proportional to the total amount of elemental mercury in the sample. Calculate the amount of mercury from the calibration curve. Remove the carbon sampling tube and seal with ball joint caps. The tube may now be used for sampling without further treatment. Repeat this procedure for the other samples. After every 10 determinations, check the system response with a standard in the range of the samples which have just been observed.

The particulate mercury on the filter of glass fiber is analyzed by placing the filter in a ceramic boat and introducing them into the furnace tube shown in Figure 3. The flow rate of air through the tube should be 150 ml/min. The air stream is passed for 10 minutes through a carbon sampling tube, and the collected mercury is determined by the analytical procedure. The amount of mercury found on the filter is then added to the value obtained from the corresponding sampling tube.

Calibration and Standards. Direct injection of air saturated with mercury vapor provides a convenient means for checking and calibrating the analytical system. Two ports, B and B', Figure 2, are provided in the analytical gas train for these purposes. Place triply-distilled mercury into a round bottom flask that has a port with a septum through which a 3.8 cm (1½-inch), 22-gauge needle may be inserted. Place the flask into a constant temperature bath, 5 °C below room temperature, and allow 1 hour for equilibration; then withdraw an exact volume and inject into the analytical train either at port B or B'. The actual quantity of mercury taken for calibration is calculated from the vapor pressure of mercury. The system is then operated as described in the procedure above using a clean sampling tube. Initially the syringe and needle may have to be equilibrated with mercury by moving the plunger up and down rapidly a dozen times while in contact with the mercury atmosphere. After the injection is made into the calibration port, a volume of air is returned to the flask equal to the quantity for the next injection. The flask is again allowed to equilibrate. Injections into port B through an empty sampling tube are used to check losses in the pyrolyzer. Injections into port

B' are used to find the response of a known amount of mercury from the amalgamator. The system response to injections into port B or port B' should agree to within 5%.

The analytical system is calibrated by injecting standards through port B. With a clean carbon sampling tube connected only to port B and a nitrogen flow rate through the tube at 0.2 l./min, inject a known volume of saturated mercury vapor into the gas stream using the technique described above. Repeat this procedure using clean tubes and different volumes of calibrating gas to span the range of mercury concentrations. Analyze these tubes as described in the analytical procedure and record peak areas. Draw a curve best fitting the points obtained when the response is plotted vs. concentrations and use this curve to calculate the amount of mercury in the sample.

Alternatively, the system may be calibrated with a permeation tube containing elemental mercury. By collecting the mercury from a permeation tube for varying times, mercury samples may be prepared to calibrate the analytical system. Samples containing zero concentrations are obtained by adding 2 ml of water to a clean tube and analyzing in the usual manner.

Calibration with Pyrolyzer. Weigh 189.5 mg of HgCl₂ and transfer quantitatively to a 500-ml flask and bring to volume with 0.3N HCl. Dilute twice with 0.3N HCl by pipetting 5 to 100 ml. The second dilution (contains 0.700 µg/ml of Hg) and is the working standard. With a 1-ml syringe, transfer 0.2- to 1-ml aliquots to a carbon sampling tube and treat as a regular air sample.

Test Atmospheres. O'Keefe and Ortman suggested Teflon (FEP) permeation tubes as primary standards for generating low concentrations of pollutants (13). Using permeation tubes of silicone rubber containing elemental mercury or of Teflon containing dimethylmercury, test atmospheres were generated with the dilution system described by Scaringelli *et al.* (14, 15) and also cited in the Federal Register (16). The silicone rubber tubes have not yet been accurately calibrated gravimetrically, but do permeate elemental mercury at a constant rate at a constant temperature (17).

RESULTS AND DISCUSSION

The responses obtained by changing flow rates during the measurement cycle are shown in Figure 4. All parameters were selected to give optimum signals with the exception of the flow rate during the measurement cycle. This flow rate of 1.6 l./min was selected to give maximum reproducibility rather than optimum response. Temperature of the amalgamator should be kept well below 80 °C. At this temperature, mercury migrates through the silver resulting in losses of mercury. In all cases, variation of the recommended parameters of ±10% produced less than a 2% change in the peak area.

Calibration. The analytical system was first calibrated by injecting known volumes of air saturated with mercury into a stream of dry nitrogen. The mercury in the gas was collected on activated carbon and analyzed in accordance with the recommended procedure. A typical curve is shown, Figure 5, which depicts the arbitrary units (proportional to area under the peak) plotted vs. the quantity of mercury added. The response was linear between 70 to 500 ng of mercury per sample. From 500 to 750 ng and from 70 to 5 ng, the response deviated from linearity and was best expressed by the parabolic equation, $Area = 7.6 + 1.2 Hg - 3.7 \times 10^{-4} Hg^2$, where Hg is the amount of mercury in nanograms. The range of the method can be extended upward or downward by changing sampling rates, sampling times, and cell length.

Permeation tubes of silicone rubber containing elemental mercury could not be accurately calibrated by periodic weighings because of the extreme hygroscopicity of the silicone rubber. The quantity of moisture that the silicone

- (13) A. E. O'Keefe and G. C. Ortman, *Anal. Chem.*, **38**, 760 (1966).
- (14) F. P. Scaringelli, S. A. Frey, and B. E. Seltzman, *Amer. Ind. Hyg. Ass.*, **28**, 260 (1967).
- (15) F. P. Scaringelli, A. E. O'Keefe, E. Rosenberg, and J. Bell, *Anal. Chem.*, **42**, 871 (1970).
- (16) *Fed. Regis.*, **36**, No. 84, 8191 (1971).
- (17) F. P. Scaringelli, J. Puzak, B. Bennett, and R. Denny, unpublished data, EPA, Research Triangle Park, N.C. 27711.

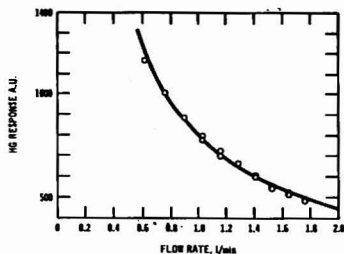


Figure 4. Analytical system response vs. flow

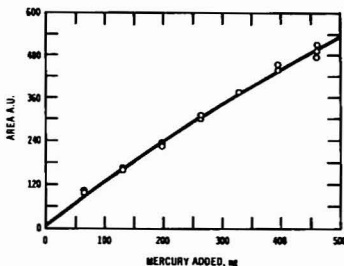


Figure 5. Calibration from saturated mercury vapor

rubber absorbed by going from a dry to a humid atmosphere was sufficiently large as to invalidate the weighing procedure. However, chemical analyses and continuous monitoring instruments indicate that these tubes have been permeating mercury at a constant rate at a constant temperature for more than a year. Hence these tubes must be calibrated indirectly.

In Figure 6, we show the area under the curve obtained from the analysis of samples collected from the permeation tube with increasing sampling times. The curve obtained is similar in shape to the curve obtained with the mercury vapor calibration. By substituting values for the area from the mercury vapor calibration, the permeation rate was calculated. The results, shown in Table I, indicate a constant permeation of 16.9 ± 0.49 ng per minute.

Permeation tubes of Teflon containing dimethylmercury could be calibrated by periodic weighings. The rate of permeation at 25°C was 320 ng/min. Constancy of the permeation rate was also confirmed by sampling continuously with a mercury monitor. However, a pyrolyzer containing quartz wool was necessary to convert the dimethylmercury to a detectable form. The results of analyses of samples of dimethylmercury in air are shown in Figure 7. The quantity of mercury found was determined by mercury vapor calibration and plotted vs. the amount of mercury added, calculated from the dimethylmercury permeation rate. The results indicate a linear relationship with a collection and conversion efficiency of 93 to 108%. Hence, quartz wool at 850°C effectively converts dimethylmercury to the elemental state, and activated charcoal effectively collects dimethylmercury.

For inorganic mercury, solutions of nanogram quantities of mercuric chloride were prepared and injected with a syringe directly into the carbon tube and analyzed. The results of the analysis are shown in Figure 7. Again, a 1 to 1 relationship exists between the quantity found by vapor calibration and the quantity added as mercuric chloride.

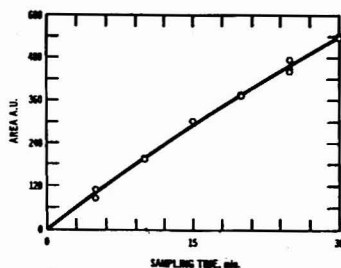


Figure 6. Response to Hg permeation tube at 25°C

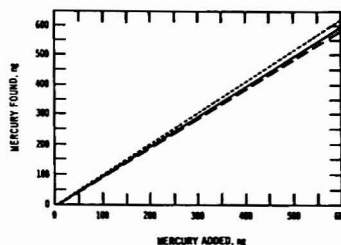


Figure 7. Comparison of calibration methods. Slopes values are 1.03, 1.00, and 0.98, for dimethylmercury, mercury, and mercuric chloride, respectively

---, $(\text{CH}_3)_2\text{Hg}$; —, Hg; - · -, HgCl_2

Table I. Permeation Rate of Elemental Mercury Tubes

Collection time, min	Amount collected, μg	Rate, $\mu\text{g}/\text{min}$
30	0.514	0.0171
25	0.420	0.0168
20	0.335	0.0167
15	0.262	0.0175
10	0.162	0.0162

Hence, the mercuric chloride is quantitatively converted and detected.

Test Atmosphere. Initially the permeation system was set to deliver concentrations of $180 \mu\text{g}/\text{m}^3$ of elemental mercury and short-term samples were taken over a period of several months. Subsequently, temperature of the permeation tube was reduced to 15°C to simulate concentrations of 0.02 to $3 \mu\text{g}/\text{m}^3$. Test atmospheres of dimethylmercury were generated between 25 to $100 \mu\text{g}/\text{m}^3$. Additional dilution air could not be introduced because of the geometry of the system. Operation of the permeation system at subambient temperature and gravimetric calibration at that temperature would require an excessively long time. However, it was demonstrated that small quantities of dimethylmercury that would be encountered in ambient air could be collected on and recovered from the charcoal by taking short-term samples.

Precision. In addition to the precision and accuracy values indicated in previous experiments, studies were also conducted with the permeation system closely simulating atmospheric concentrations. Typical data obtained at $1 \mu\text{g}/\text{m}^3$ only are shown in Table II. The relative standard deviation was 2.6% or less, and the accuracy was better than 95%. The accuracy figure includes the vari-

Table II. Precision and Accuracy of Simulated Samples

Day	Added	Concentrations, $\mu\text{g}/\text{m}^3$			Relative standard deviation, %	Error, %
		Tube 1	Tube 2	Tube 3		
1	1.176	1.140	1.089	1.118	2.3	-4.9
2	1.169	1.144	1.100	1.090	2.6	-4.9
3	1.190	1.202	1.189	1.247	2.5	+1.9
4	1.291	1.288	1.267	1.274	0.8	-1.1
5	1.291	1.233	1.231	1.283	2.4	-3.3

Table III. Collection Efficiency of Charcoal Tubes

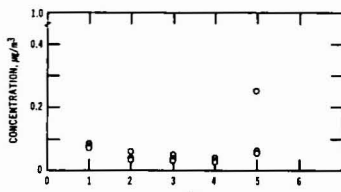
Sampling rates, l./min	Front tube, $\mu\text{g Hg}$	Back tube, $\mu\text{g Hg}$	Collection efficiency, %
0.200	0.407	0.003	99
	0.441	0.002	
	0.435	0.006	
0.450	0.440	0.003	99
	0.439	0.003	
	0.446	0.005	
0.740	0.430	0.014	97
	0.429	0.015	
	0.427	0.008	
1.05	0.442	0.006	97
	0.427	0.014	
	0.427	0.014	

Table IV. Interference Study

Interferent, μg	Hg added, μg	Hg found, μg	Recovery, %
Acetone	0	0.418	99
	618	0.394	97
	1237	0.398	96
	1855	0.411	95
Benzene	0	0.408	103
	0	0.318	96
	256	0.299	101
	512	0.302	103
Ethanol	768	0.319	90
	0	0.307	101
	0	0.355	99
	316	0.344	99
Nitrogen dioxide	475	0.365	96
	633	0.346	94
	0	0.355	101
	0	0.360	102
Sulfur dioxide	1440	0.362	106
	600	0.349	101
	90	0.418	103
	0	0.421	100
Sulfur dioxide	0	0.346	101
	960	0.336	104
	1560	0.356	100
	2880	0.348	108
	2880	0.334	100
	0	0.343	102

Table V. Stability of Mercury on Charcoal

Time, days	Mercury, μg		
	Set 1; Added: 0.460	Set 2; Added: 0.380	Set 3; Added: 0.460
0	0.445	0.375	0.461
2	0.463	0.388	...
21	0.447	0.386	0.458
28	0.470	0.394	0.471
120	0.467


Figure 8. Field study concentration levels

ability resulting from the permeation rate and the dilution system.

Collection efficiency at various sampling rates was determined by sampling from the permeation system under simulated conditions with two tubes in tandem. The results, shown in Table III, indicate that for sampling rates below 0.4 l./min and below 1 l./min, the collection efficiency is 99 and 97%, respectively.

Collection efficiencies for particulate matter were determined by using an aerosol generator. Particles of mercuric chloride were generated by sublimation and condensation in an air stream. The results indicated a collection efficiency of 80% for particulates having a diameter of 0.3 to 0.8 μ by the carbon tube alone. A collection efficiency of 99.9% for particles of 0.3 μ was found when the glass fiber filter was included in the analyses. Particle sizes were determined with an aerosol photometer which fractionated the particles and gave a number count.

Interference Study. Mayz *et al.* reported interference from a number of compounds which have adsorption at the mercury line (18). Several of the compounds named were studied as potential interferences. Varying quantities of the interferent were adsorbed on clean carbon tubes. These tubes were then connected in parallel with control tubes to the ports of the permeation system. Simulated samples were taken and analyzed. The results of the interference studies, shown in Table IV, indicate no substantial interference.

Stability. Table V gives a portion of the results from several stability studies. Sample Sets 1 and 2 were prepared from the permeation system and Set 3 was prepared by injections of mercury vapor. During storage, Set 3 was transported to and from a field study, 1600 km away. The results indicate no substantial losses from carbon for periods up to 120 days.

Field Study. Samples were collected in triplicate for 24 hours approximately 1.6 km downwind of a chlor-alkali plant. After collection, the samples were returned to the laboratory 1600 km away and analyzed. The results are shown in Figure 8. All results obtained at this site were below 1 $\mu\text{g}/\text{m}^3$. The quantity of mercury collected was within the range of 10 to 25 ng per sample. These quantities were near the limits of detection of the analytical

(18) E. Mayz, M. Corn, and G. Barry, *Amer. Ind. Hyg. Ass. J.*, **32**(6), 373 (1971).

system, which was designed primarily for 24-hour sampling at a flow rate of 0.2 l./min and concentrations between 0.05 and 1.5 $\mu\text{g}/\text{m}^3$ without attenuation of response; nevertheless, the precision was good except for one outlier on the fifth day. During this sampling period, meteorological instruments indicated that winds from the plant seldom fumigated the sampling—hence, the low concentration of mercury encountered. Continuous monitors for elemental mercury and short-term samples confirmed that mercury levels were highly dependent on wind direction.

CONCLUSION

Based on the results of this study, it may be concluded that: The method is highly specific for total mercury and relatively free from contamination from extrinsic mercury. The method is sufficiently sensitive to measure ambient

levels of mercury in air. The method has precision and accuracy of 95% or greater. Activated carbon provides a simple, inexpensive technique for the manual collection of mercury from air.

ACKNOWLEDGMENT

The authors wish to express their thanks to G. C. Ortman for preparing and supplying permeation tubes of elemental and dimethylmercury and to Richard Patterson for his assistance in the construction of the analytical train during the early stages of this study.

Received for review March 23, 1973. Accepted September 21, 1973. Presented at the 165th National Meeting of the American Chemical Society, Dallas, Texas, April 8–13, 1973.

NOTES

Informing Power of a Chromatographic Method and Its Use as a Quality Criterion

D. L. Massart and R. Smits

Pharmaceutical Institute, Vrije Universiteit Brussel, 67, Paardenstraat, B-1640 Sint Genesius Rode, Belgium

One of the tasks of analytical chemists is to optimize analytical procedures. It occurred to us that operational research, which has been used in many other branches of science, should render services in this respect. More particularly, the application possibilities in the field of chromatography were investigated.

One can distinguish basically two different topological structures in chromatography. Kaiser (1) has called them tree and chain structures. The first describes dichotomic schemes in which the group of ions originally present is divided into smaller and smaller parts by means of clear-cut separations until complete separation is obtained. The obvious optimization criterion here is time. Methods using the theory of graphs (2) and dynamic programming (3) were proposed by Massart and coworkers for the selection of the fastest separation scheme.

The second topological structure is represented by, for example, separations of the rare-earth group on one cation exchange column, or of methyl esters of fatty acids by gas-liquid chromatography. Several optimization criteria are now possible according to whether one is carrying out a qualitative or a quantitative analysis. In qualitative analysis, one is essentially interested in knowing how many different substances or groups of substances can be distinguished in a chromatogram. One of the authors (4) of the present article proposed the use of the information content, as defined by Shannon. It appears that the in-

formation content of thin layer chromatographic separations can be calculated and used to compare the merits of different solvents for the separation of the same group of compounds. An analogous application to gas-liquid chromatography has also been reported (5).

In quantitative chromatography, the usual quality criterion is the resolution, R , defined as

$$R = \Delta z / 4\sigma \quad (1)$$

(see Figure 1). This can be calculated only for two (usually neighboring) peaks, but does not allow an over-all picture of the quality of a multipeak separation. The question then arises which quantity or which criterion can replace the resolution for this kind of application. The quantity in question should take into account the precision for the measurement of each peak. Also, a procedure will be considered better when it enables one to analyze more peaks in a given time. One can therefore state that the optimization criterion (CR) must be represented as follows:

$$CR = f(\text{number of peaks per unit of time } (n), \text{ mean precision in the determination of one peak}) \quad (2)$$

Instead of minimizing the precision itself, one can also maximize the reciprocal precision. The latter represents the number of steps, S , that can be distinguished on a concentration scale. For example if the precision is 1%, then $S = 100$.

Kaiser (6) has introduced in analytical chemistry the

(1) H. Kaiser, in "Methodicum Chemicum, Volume 1," F. Korte, Ed., G. Thieme, Stuttgart, 1973, Chap. 1.

(2) D. L. Massart, C. Janssens, L. Kaufmann, and R. Smits, *Anal. Chem.*, **44**, 2390 (1972).

(3) D. L. Massart, R. Smits, and L. Kaufmann, *Fresenius' Z. Anal. Chem.*, **264**, 273 (1973).

(4) D. L. Massart, *J. Chromatogr.*, **79**, 157 (1973).

(5) J. H. W. Bruins Slot and A. Dijkstra, *Chem. Weekblad*, **68** (50), 13 (1972).

(6) H. Kaiser *Anal. Chem.*, **42** (2), 24A (1970).

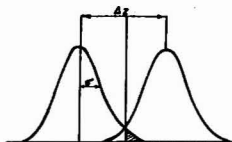


Figure 1. Symbols used for elution chromatographic curves

quantity P_{inf} , the informing power of an analytical heterochromatic (spectroscopical) method. Equations 3 and 4 (7c and 7d of the cited article)

$$P_{inf} = \sum_{i=1}^n [\log_2 S_i] \quad (3)$$

$$P_{inf} = n \log_2 S \quad (4)$$

correspond with Equation 2 of this article

For Equation 3, this becomes apparent when writing it as

$$n \left(\frac{\sum_{i=1}^n \log_2 S_i}{n} \right)$$

Equation 4 is valid in the special case that S is the same for all peaks. Therefore one can propose the use of P_{inf} as an optimization criterion in quantitative chromatography. The informing power is expressed in bit.

One sees that one arrives at making an analogy between spectroscopical and chromatographic methods. This must not be considered strange since both groups of methods yield a number of signals containing information on the qualitative and quantitative composition of complex mixtures and since there is a formal resemblance in the way these signals are presented: both methods yield a spectrum. It is therefore not surprising that if an informing power of a spectroscopic method can be calculated, this should also be the case for a chromatographic technique.

The redefinition of the quality criterion for chromatographic separations as an informing power is useful in that it shows that such a criterion permits one to penetrate to the essence of what is the purpose of chromatography (and, in fact, all analytical methods), namely the obtaining of information. It is therefore more fundamental than, for example, a resolution. There is no need to discuss further the implications of using the informing power concept for an analytical method, such as chromatography. This has been done in a very lucid way by Kaiser (6). One should, however, be aware of the fact that the word resolution, which plays a central role both in Kaiser's and in this article, has different meanings in spectroscopy and in chromatography. (In spectroscopy, "resolution" is defined as $\nu/\delta\nu$, which is a local quantity but contains also—via ν —the position within the spectrum. However, in chromatography, "resolution" $\Delta z/4\sigma$ is nothing more than the local "peak separation" not involving the position of the peak within the whole of the chromatogram.) It is unfortunate that a harmonization seems impossible because the different meanings have become universally accepted in their respective domains. In this article, resolution is always used in the sense of chromatography (see also Equation 1).

This brings us back to resolution in chromatography. It is interesting to investigate how resolution and informing power are related. As said before, the resolution is one of the parameters most employed to describe the efficiency

of a chromatographic system. In general, one assumes that it is desirable that the resolution be equal to unity. Grushka (7) for example, states that the system is inefficient when the resolution is less than unity and wasteful when it is greater. In practice, there is no doubt that this is an excellent criterion, although as already said, its application possibilities are limited. One can also ask the question whether it is well founded from a more theoretical point of view.

If one keeps constant the number of plates of the column and increases the resolution, the number of peaks per unit of time of an actual separation or the peak capacity, as defined by Giddings (8) and Grushka (7) decrease. This means that one obtains better results for a smaller number of components per unit of time or, to put it another way, that to obtain more quantitative information in a certain amount of time, one loses qualitative information. The question which has to be asked, is what is the best compromise between both.

For a two-peak separation it is commonly accepted that this compromise occurs at a value of $R = 1$. For multi-component separations P_{inf} has to be maximized.

In the special case that there is a constant R between neighboring peaks, one can investigate which R corresponds with the maximum value of P_{inf} .

On the condition that the method of measurement is sufficiently precise, the over-all precision in quantitative chromatography is determined by the extent to which overlap between neighboring peaks occurs. As a first working hypothesis, one can state that there is no sense in determining peak areas with a precision larger than the fractional overlap Ω between neighboring peaks, or even 2Ω since every peak except the first and the last have two neighbors. Therefore:

$$S = \frac{1}{2\Omega} \quad (5)$$

In chromatographic practice, this corresponds with a procedure in which the peaks are first collected in fractions, after which one determines the main component of each peak by a specific method. In modern chromatography, one usually follows other procedures, particularly in gas chromatography and high-pressure liquid chromatography. These methods will be discussed later.

The peak capacity as a function of the resolution and the number of plates is obtained from an equation given by Vink (9):

$$n = \frac{\log \left(1 + \frac{1}{b} \sum_{i=1}^n \Delta\gamma_i \right)}{\log \left(1 + \frac{1}{\sqrt{N} - \frac{1}{2}} \right)} \quad (6)$$

where n = peak capacity, $\Delta\gamma_i$ = difference in partition coefficient between peaks i and $i + 1$, b = ratio between the volumes of mobile and stationary phases, N = number of plates, and R = resolution.

The use of this equation implies two assumptions—namely, that the area under the peak is the same for all n peaks and that N remains constant over the whole γ -range considered. The last assumption is, of course, not true. The resulting error can be minimized by redefining N as the harmonic average of N for the peaks considered.

(7) E. Grushka, *Anal. Chem.*, **42**, 1142 (1970).

(8) J. C. Giddings, *Anal. Chem.*, **39**, 1027 (1967).

(9) H. Vink, *J. Chromatogr.*, **89**, 237 (1972).

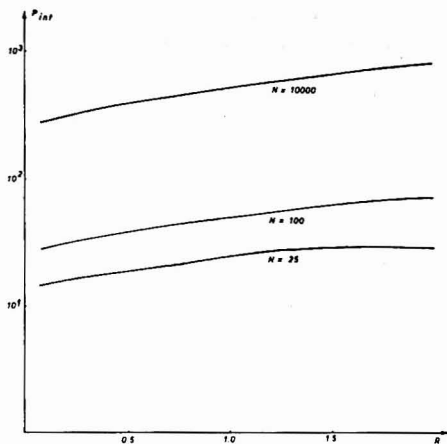


Figure 2. $\log P_{inf} = f(R)$ for different number of plates N

Equations for fractional recovery or overlap were given for example by Glueckauf (10) and Said (11). The area under the Gauss-curve is given by:

$$\int_{-\infty}^{+\infty} e^{-x^2/2\sigma} dx = \sqrt{2\pi} \quad (7)$$

If one considers two peaks, separated by a distance Δz (see Figure 1), the shaded area is equal to:

$$\Omega = 1 - \frac{1}{\sqrt{2\pi}} \int_{-\Delta z/2\sigma}^{\Delta z/2\sigma} e^{-x^2/2\sigma} dx = 1 - A(\Delta z/2\sigma) \quad (8)$$

where $\Delta z/2$ is the distance from the maximum of one peak to the cut, between both peaks.

By definition $R = \Delta z/4\sigma$ so that

$$\Omega = 1 - A(2R) \quad (9)$$

and taking into account Equation 5:

$$S = \frac{1}{2[1 - A(2R)]} \quad (10)$$

In this approximate model, S is the same for all peaks. Then Equation 4 can be used and together with Equations 6 and 10, this yields:

$$P_{inf} = 3.32 \frac{\log\left(1 + \frac{1}{b} \sum_{i=1}^n \Delta\gamma_i\right)}{\log\left(1 + \frac{1}{\sqrt{N}} \frac{1}{4R - \frac{1}{2}}\right)} \log \frac{1}{2[1 - A(2R)]} \quad (11)$$

Since the time during which the separation is carried out is constant, this is in fact a P_{inf} /unit of time.

Figure 2 represents $\log P_{inf} = f(R)$ for values of b and $\sum_{i=1}^n \Delta\gamma_i$ which are realistic for cation exchange chromatography on resins of the Dowex 50 WX series, namely $b = 1$ and $\sum_{i=1}^n \Delta\gamma_i = 99$. The choice of these numerical values has an influence on the absolute values of P_{inf} but not on the shape of the $\log P_{inf} = f(R)$ curve. The values of $1 - A(2R)$ were taken from Reference (11).

(10) E. Glueckauf, *Trans. Faraday Soc.*, 51, 34 (1955).

(11) A. S. Said, *J. Gas Chromatogr.*, 60 (1964).

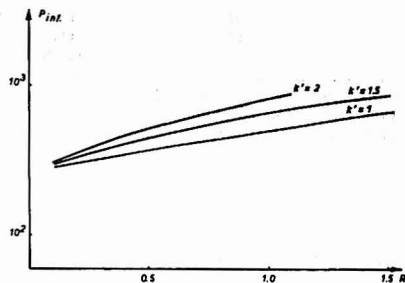


Figure 3. $\log P_{inf} = f(R)$ for resolutions multiplied by $k' = 1, 1.5$, and 2

In modern chromatography one often monitors continuously the effluent and obtains the concentration of the individual components from the area under the peaks. Overlapping peaks are resolved by calculations usually with a computer. In this case the working hypothesis, which led to Equation 5 does not hold any longer since the precision is now better than 2Ω . One can suppose that computer calculations artificially increase the resolution with a constant factor $k' (k' > 1)$. The results of such calculations are represented in Figure 3, for $b = 1$, $\sum_{i=1}^n \Delta\gamma_i = 99$, $\sqrt{N} = 100$ and for resolutions multiplied by $k' = 2, 1.5$, and 1. As was the case for the first working hypothesis (Figure 2), the informing power increases continuously with increasing R . At first sight, this would lead to the conclusion that $R = 1$ is not an optimal choice. However, one must take into account that, in practice, the obtainable precision is limited. If one assumes that this limit is situated around 1%, then S cannot increase beyond about 100. Taking $S = 100$ as a limit, one must use Equation 11 for $S < 100$ and Equation 12 for $S > 100$.

$$P_{inf} = 3.32 \frac{\log\left(1 + \frac{1}{b} \sum_{i=1}^n \Delta\gamma_i\right)}{\log\left(1 + \frac{1}{\sqrt{N}} \frac{1}{4R - \frac{1}{2}}\right)} \log 100 \quad (12)$$

Equation 12 represents a continuously decreasing function of R , so that, for the whole range of S -values, one now obtains a maximum of P_{inf} at the resolution where $S = 100$.

For $b = 1$, $\sum_{i=1}^n \Delta\gamma_i = 99$, $\sqrt{N} = 100$, and $k' = 1$, this maximum is situated near $R = 1.3$, for $k' = 1.5$ near $R = 0.8$, and for $k' = 2$ near 0.7.

One can conclude that the informing power concept allows a critical investigation of the $R = 1$ criterion in chromatography. This investigation shows that the maximum value of P_{inf} per unit of time occurs at a resolution around $R = 1$, depending on the assumption one makes.

Of course, the model used here is a very simple and unrealistic one. Chromatographic separations of perfectly Gaussian peaks with the same area and with constant resolution between neighboring peaks do not exist. For practical work therefore, Equations 11 and 12 cannot be used. However Equation 3 can be employed to characterize actual separations, thereby making it possible to assign a figure of merit to these separations and to compare them. At this moment, no other such criterion exists.

For theoretical work, the model used here serves to introduce P_{inf} and to relate this quantity approximately to R . Much more realistic models are difficult to construct

for this purpose because *R* is limited in use to the description of two-peak separations, so that assumptions such as the constancy of *R* in a multi-peak separation are necessary. To establish further the value of P_{int} as a criterion, a more systematic investigation analogous for example to the work of Grushka on chromatographic peak capacity and the factors influencing it, would be necessary.

ACKNOWLEDGMENT

The authors thank H. Kaiser and G. Deiningner for valuable advice.

Received for review January 30, 1973. Accepted June 25, 1973. Work was supported by the "Fonds voor kollektief en fundamenteel onderzoek."

Thin Layer Chromatographic-Spectrophotofluorometric Analysis of Amphetamine and Amphetamine Analogs after Reaction with 4-Chloro-7-Nitrobenzo-2,1,3-Oxadiazole

François Van Hoof and Aubin Heyndrickx

Department of Toxicology, State University of Ghent, Ghent, Belgium

Amphetamine and many other sympathomimetic drugs are actually of great importance as drugs of abuse, appetite depressors, and stimulants used by men in sports.

Several methods have been developed to identify these compounds by spectrophotometry, thin layer chromatography, and gas chromatography. Most existing thin layer chromatographic detection methods suffer from a lack of sensitivity because for most compounds, several micrograms are needed for visualization.

Nanogram amounts of sympathomimetic drugs can be detected by gas chromatography only if derivative formation is combined with electron capture detectors.

An excellent review of existing methods for analysis of amphetamine analogs has recently been published (1). Miles and Schenk made use of the natural fluorescence of phenylethylamines to assay these compounds in pharmaceutical preparations (2). Few attempts have been made to form fluorescent derivatives of amphetamine and related substances (3-5).

In our work, 4-chloro-7-nitrobenzo-2,1,3-oxadiazole (NBD-Cl) is used to form fluorescent derivatives. The reaction between amphetamine and NBD-Cl is shown in Figure 1.

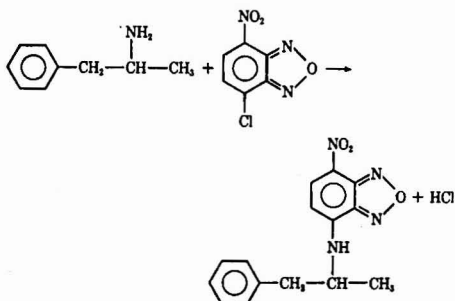


Figure 1. Reaction scheme for coupling of amphetamine and NBD-Cl

- (1) K. K. Kaisha, *J. Pharm. Sci.*, **61**, 655 (1972).
- (2) C. I. Miles and G. H. Schenk, *Anal. Chem.*, **45**, 130 (1973).
- (3) J. T. Stewart and D. M. Lotti, *J. Pharm. Sci.*, **60**, 461 (1971).

NBD-Cl was first used by Ghosh and Whitehouse as a labeling agent for amino acids (6). NBD-Cl was applied in former studies for identification of phenylethylamines (7-9) and for quantitative determination of carbamate insecticides (10, 11) and dithiocarbamate fungicides (12).

EXPERIMENTAL

Reagents. Pure NBD-Cl was obtained from Serva, Heidelberg, Germany. Stock solutions, 1%, were prepared in methyl isobutyl ketone and methyl *n*-amyl ketone.

The products investigated are: amphetamine phosphate (1-phenyl-2-aminopropane phosphate); pervitine hydrochloride (1-phenyl-2-methylaminopropane hydrochloride); ethylamphetamine hydrochloride (1-phenyl-2-ethylaminopropane hydrochloride); ritaline hydrochloride (2-phenyl- α -2-piperidine acetic acid methyl ester hydrochloride); lidépran hydrochloride (α -phenyl-2-piperidine methanacetate hydrochloride); preludeine hydrochloride (3-methyl-2-phenylmorpholine hydrochloride); sympatol (*p*-hydroxy- α -(methylamino)methyl benzylalcohol tartrate); effortil (α -(ethylamino)methyl-*m*-hydroxybenzylalcohol hydrochloride); chlorphentermine hydrochloride (4-chloro- α , α -dimethylphenethylamine hydrochloride); vasculat (α -(butylamino)methyl-*p*-hydroxybenzylalcohol sulfate); β -phenylethylamine hydrochloride (1-amino-2-phenyl-ethane hydrochloride); ephedrine hydrochloride (α -1-(methylamino)ethyl benzylalcohol hydrochloride); heptaminol hydrochloride (6-amino-2-methyl-2-heptaminol hydrochloride); methoxyphenamine hydrochloride (α -(1-amino ethyl)-2,5 dimethoxy benzylalcohol hydrochloride).

Stock solution of all compounds were prepared in distilled water at a concentration of 10 mg base/ml. All solvents used for chromatography were analytical reagent grade quality.

A 1M H_3BO_3 -NaCl- Na_2CO_3 buffer was prepared by adding 370 ml of a 1M Na_2CO_3 solution to 630 ml of a 1M H_3BO_3 -NaCl solution. pH of the buffer solution is 9. Chlorotrimethylsilane was obtained from Merck, Darmstadt, Germany. Test tubes used for

- (4) W. Rusiecki and J. Brezzenzski, *Diss. Pharm. Pharmacol.*, **19**, 315 (1967).
- (5) N. Seiler and M. Weichmann, *Hoppe-Seyler's Z. Physiol. Chem.*, **337**, 229 (1964).
- (6) P. B. Ghosh and M. W. Whitehouse, *Biochem. J.*, **108**, 155 (1968).
- (7) J. Monforte, R. J. Barth, and I. Sunshine, *Clin. Chem.*, **18**, 11, 1329 (1972).
- (8) J. Reisch, H. J. Kommerl, H. Alfes, and H. Mollman, *Fresenius' Z. Anal. Chem.*, **245**, 56 (1969).
- (9) D. Clasing, H. Alfes, H. Mollman, and J. Reisch, *Z. Klin. Chem. Klin. Biochem.*, **7**, 648 (1969).
- (10) J. F. Lawrence and R. W. Frei, *Anal. Chem.*, **44**, 2046 (1972).
- (11) R. W. Frei and J. F. Lawrence, *J. Ass. Offic. Anal. Chem.*, **55**, 1259-64 (1972).
- (12) F. Van Hoof and A. Heyndrickx, *Med. Fak. Landbouwwet.*, in press (1973).

Table I. R_F Values of Sympathomimetic Drugs in Different Solvent Systems*

Compound	A	B	C	D	Color
Amphetamine	0.70	0.53	0.65	0.52	Yellow
Pervitine	0.65	0.47	0.42	0.34	Orange
Methoxyphenamine	0.76	0.41	0.54	0.62	Yellow
Ethylamphetamine	0.73	0.48	0.42	0.62	Pink
Ritaline	0.72	0.48	0.29	0.54	Pink
Lidopran	0.10	0.34	0.15	0.29	Pink
Preludine	0.73	0.42	0.23	0.45	Orange
Sympatol	0.00	0.13	0.05	0.06	Orange
Effortil	0.00	0.23	0.07	0.12	Orange
Chlorphentermine	0.78	0.69	0.29	0.17	Red
Vasculat	0.00	0.37	0.13	0.05	Orange
β -Phenylethylamine	0.76	0.72	0.30	0.50	Yellow
Ephedrine	0.20	0.42	0.07	0.19	Orange
Heptaminol	0.00	0.16	0.15	0.10	Yellow

* A, 1,2-dichloroethane; B, ethyl acetate-cyclohexane (3:2); C, ethyl acetate-cyclohexane (2:3); and D, chloroform-tetrahydrofuran (98:2).

evaporation of ether layers were put overnight in a 5% chlorotri-methylsilane solution in toluene. They were rinsed afterward with methanol and dried at 70°C.

Reaction Procedure. A 10- μ l sample of each stock solution is evaporated in a test tube at 80°C on a warm-water bath under a smooth stream of nitrogen. Then 0.2 ml of a 0.1M NaHCO₃ solution is added. The mixture is mechanically stirred.

Next, 0.2 ml of a 1% solution of NBD-Cl in MIBK is applied on top of the bicarbonate solution. The test tube is stoppered and heated at 80°C during 30 minutes on a warm-water bath. After cooling, a 10- μ l aliquot of the upper phase was used for chromatography.

Chromatography. Thin layer plates (20 cm \times 20 cm) coated with a 0.25-mm thick layer of Silica gel GF 254 (Merck, Darmstadt, Germany) were used throughout the study. Solvent systems employed were: 1,2-dichloroethane (A); ethyl acetate-cyclohexane (3:2) (B); ethyl acetate-cyclohexane (2:3) (C); chloroform-tetrahydrofuran (98:2) (D). Spots were visualized under a Camag TL 900 Universal UV lamp at 350 nm.

Instrumental Analysis. All fluorescence measurements were made *in situ* with an Aminco Bowman spectrophotofluorometer equipped with a thin film scanner. Slit width was kept constant at 0.5 mm. Fluorescence spectra were recorded on an MFE 1620-855 x-y recorder.

For quantitative work, a Hitachi 159 1-mV recorder was used. An attenuator was placed between photometer exit (50 mV full scale) and the Hitachi 159 recorder entrance (1 mV). For quantitative determinations with NBD-amphetamine, the excitation monochromator was set at 482 nm and the emission monochromator at 523 nm, scan program 2 was used for the thin film scanner; the recorder chart speed was 10 mm/min.

Peak heights were plotted against quantities of amphetamine applied on thin layer plates in order to obtain calibration curves.

Extraction of Urine Samples. Three 5-ml urine samples were fortified with 5 μ g of amphetamine giving an amphetamine concentration of 1 ppm. A few drops of 2N NaOH were added to obtain an alkaline medium. Extraction was done by mechanically shaking the two 20-ml portions of diethyl ether. The combined ether layers were washed twice with 5 ml of 0.005N NaOH. The ether phase was dried over anhydrous Na₂SO₄.

Complete evaporation of the ether layer was done in a glass, silanized test tube, containing 0.1 ml of 0.1N HCl, on a warm-water bath at 35°C under a smooth stream of nitrogen. To the residue, 0.2 ml of 0.1M NaHCO₃ was added and the reaction was carried out as described above.

Extraction of Blood Samples. To three 1.0-ml blood samples fortified with 100 ng of amphetamine, 5 ml of a 1M H₂BO₃-NaCl-Na₂CO₃ buffer was added. Extraction was done by shaking twice with 10 ml of ether for 10 minutes. Blood and ether layers were separated by centrifuging for 10 minutes at 2500 rpm. The ether layers were taken from the blood with a Pasteur pipet. The combined ether layers were dried over anhydrous Na₂SO₄ and evaporated in a silanized glass test tube, containing 0.1 ml of 0.1N HCl, at 35°C under a gentle stream of nitrogen. The evaporation residue was treated as described under the following Reaction Procedure, but 100 μ l of the MIBK phase was applied on a thin layer plate.

Table II. Maxima in Fluorescence Spectra of NBD-Derivatives

Compound	Maximum in fluorescence spectrum (in nm)
Amphetamine	523
Pervitine	537
Methoxyphenamine	535
Ethylamphetamine	530
Ritaline	535
Lidopran	535
Preludine	535
Sympatol	525
Effortil	545
Chlorphentermine	535
Vasculat	525
β -Phenylethylamine	540
Ephedrine	525
Heptaminol	512

RESULTS AND DISCUSSION

Reaction Procedure. The reaction underlying the determination is the coupling of primary or secondary alkylamine functions with NBD-Cl. The reaction was carried out in a two-phase (0.1M NaHCO₃-MIBK) system as the coupling proceeds better in organic solvents, and salts had to be converted into free bases which are better soluble in MIBK.

The reaction was complete after heating at 80°C for 30 minutes. Longer reaction times (up to 60 minutes) and higher reaction temperatures (up to 100°C) did not yield more intense fluorescence for amphetamine. For reaction at 100°C, a 1% solution of NBD-Cl in methyl *n*-amyl ketone was used instead of 1% NBD-Cl in MIBK to prevent losses of organic solvent by evaporation.

Chromatography. R_F values and colors of all compounds are summarized in Table I. R_F values for amphetamine in different solvent systems were: 0.70 (A), 0.53 (B), 0.65 (C), and 0.52 (D). Systems B and C offer a better separation than A and D. These solvents should be preferred if only qualitative work has to be done. Some substances with high R_F values in systems B and C can be covered by an excess of NBD-Cl, which in all systems concentrates at elevated R_F values.

For quantitative work, system A was preferred as spots were kept very narrow during chromatography. These spots gave very narrow peaks from which quantitative data could be derived by measuring peak heights, avoiding planimetry. Nevertheless system D yields compact spots for most compounds and can be used for quantitative work as well. Primary amines gave a yellow color in daylight; secondary amines gave orange or pink spots. All compounds, except chlorphentermine, could be visualized under a Camag TL 900 Universal UV lamp at 350 nm down to 1 ng/spot.

Fluorescence Phenomena. All fluorescent derivatives have a maximum in their fluorescence spectrum between 510 and 545 nm (Table II). Excitation spectrum maxima were observed at 482 nm for all compounds, except lidopran (484 nm). The similarity in fluorescence spectra makes it impossible to identify an unknown sympathomimetic drug through its NBD derivative in MIBK solution. Moreover, we found that a 1% NBD-Cl solution in MIBK yields an intense fluorescence when excited at 482 nm. The maximum in the NBD-Cl fluorescence spectrum was found at 518 nm.

Quantitative Analysis. The precision of the method was controlled by applying 10, 20, 30, 50, and 100-ng

Table III. Precision Study of Amphetamine

Quantity amphetamine applied, ng	Av rel std dev, %
10	9.5
20	4.5
30	7.4
50	6.3
100	5.0

amounts of amphetamine on thin layer plates and measuring fluorescence intensities after chromatography in 1,2-dichloroethane.

Standard deviations obtained from at least six measurements at each concentration are summarized in Table III. With each quantitative analysis, 10-ng, 50-ng, and 100-ng amphetamine standards underwent the reaction procedure and were applied to the thin layer plate to obtain correct calibration curves.

Linear relationships between peak height and applied quantity were obtained up to 500 ng of amphetamine/spot. No interferences from coextractives of urine or blood samples were found.

Using the extraction procedure described, 83 ± 6% am-

phetamine was recovered from urine samples. Recovery from blood was 70 ± 3%.

In order to obtain satisfactory recoveries, addition of 0.1 ml of 0.1N HCl before evaporation was necessary to prevent loss of amphetamine by volatilization. Coating of glass test tubes with chlorotrimethylsilane improved recoveries, preventing adherence of amphetamine to the glass surface.

CONCLUSIONS

The method presented allows a fast identification of most important amphetamine analogs. Only substances lacking primary or secondary alkylamine functions (diethyl propionate) cannot be detected. No interferences from nicotine or other coextractives are encountered. The method is more sensitive than existing TLC detection methods and allows quantitative determination of therapeutic amphetamine levels on 1-ml blood samples.

ACKNOWLEDGMENT

The skillful technical assistance of J. Pollet was greatly appreciated.

Received for review May 31, 1973. Accepted September 21, 1973.

Rapid, Sensitive Gas-Liquid Chromatographic Screening Procedure for Cocaine

J. W. Blake, R. S. Ray, J. S. Noonan, and P. W. Murdick

Equine Research Center, Ohio State University, Columbus, Ohio 43210

Cocaine is an alkaloid which is isolated from the leaves of the plant *Erythroxylon coca*. The drug may also be prepared semi-synthetically from the acid, ecgonine. Based upon the observations of Nieman, Koller, and Freud, circa 1884, the use of cocaine as an anesthetic spread rapidly through the medical community. The drug served as a local anesthetic until supplanted to a great extent by Einhorn's introduction of procaine in 1905. The addictive nature of cocaine was recognized early (1). Cocaine causes feelings of elation in the user. Chronic abuse of the drug may cause mental impairment, loss of appetite, and a tendency to withdraw from society.

The pure drug is extensively metabolized in the body. The major metabolite of cocaine is benzoylecgonine (2).

Presently used screening tests are for the most part chromatographic techniques. Thin layer chromatography and gas-liquid chromatography are in common use (3, 4).

The technique of analysis to be described uses an O-acylated derivative of the drug and employs an electron capture detector to greatly increase the sensitivity of the gas-liquid chromatographic method.

- (1) "Drill's Pharmacology in Medicine," 4th ed.; J. R. DiPalma, Ed. McGraw-Hill, New York, N.Y., 1971, p 190.
- (2) F. Fish and W. C. C. Wilson, *J. Pharm. Pharmacol.*, 21, 135S (1969).
- (3) E. G. C. Clarke, "Isolation and Identification of Drugs," The Pharmaceutical Press, London, 1969, p 267.
- (4) Perkin-Elmer Corporation, "Clinical Chemistry Application Study 41," p 6, July 1971.

EXPERIMENTAL

Apparatus. The gas chromatograph used was a Beckman GC-5 equipped with a Beckman electron capture detector. The column was a four-foot, 4-mm i.d. glass column packed with 3% OV-1 on 80/100 mesh Chromasorb GHP provided by Supelco, Inc. Extracts, reduction, derivatization, and washes were performed in Kimble glass culture tubes, 125 mm in length, employing screw-on polypropylene caps. Extractions and washes were made by inverting the capped tubes on a "Rotorack" sold by Fisher Scientific Company. "Dispo" micropipets of 50- μ l capacity, purchased from Scientific Products Company, were used to transfer the reducing and derivatizing reagents. The centrifuge used was an International Model HN.

Reagents. The sodium tetraborate decahydrate powder was procured from the J. T. Baker Co. Pesticide quality cyclohexane and heptafluorobutyric anhydride were purchased from Matheson, Coleman, and Bell. Pentafluoropropionic anhydride, which provided a better derivative yield, was a product of Pierce Chemical Company. Lithium aluminum hydride was purchased from K and K Laboratories, Inc. The diethyl ether was B and A reagent grade (Allied Chemical). A diethyl ether solution saturated with lithium aluminum hydride provided a reducing reagent.

Procedure. To 5.0 ml of aqueous solution containing cocaine was added 1 ml of a saturated sodium tetraborate solution and 2.0 ml of cyclohexane. To determine method sensitivity with urine, cocaine was added to horse urine prior to extraction. The drug was extracted into the cyclohexane phase by rotating on the "Rotorack" at moderate speed for four minutes. Following centrifugation, the cyclohexane phase was transferred to a clean culture tube.

To the cyclohexane phase in the culture tube were then added 50 μ l of the LiAlH₄-ether solution. Reduction was allowed to pro-

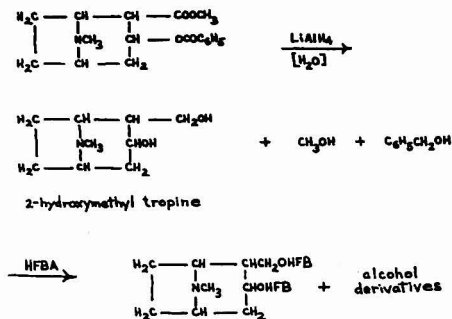


Figure 1. Reduction and acylation of cocaine to produce an electron capturing derivative

ceed for three minutes. Then 50 μl of distilled water were added to the cyclohexane, and the mixture was shaken. Next 50 μl of heptafluorobutyric anhydride (or alternatively pentafluoropropionic anhydride) were added to the cyclohexane phase and allowed to react 3-5 minutes at room temperature. The 2.0 ml of cyclohexane containing the reduced, derivatized moiety were washed in about 6 ml of the saturated tetraborate solution by rotating the cyclohexane and tetraborate on the "Rotorack." The cyclohexane phase was transferred to a clean tube from which an aliquot of derivatized drug could be taken for gas chromatographic-electron capture analysis.

The derivatized drug was chromatographed isothermally at an oven temperature of 150 $^{\circ}\text{C}$. Employing on-column injection, the inlet temperature was 210 $^{\circ}\text{C}$. Detector temperature was 300 $^{\circ}\text{C}$. The elution time of the drug derivative was 2 minutes and 36 seconds at a helium carrier gas flow of 60 cm^3/min .

RESULTS AND DISCUSSION

The method as presented is a screening procedure, because cocaine as such is not detected, but rather a reduced, derivatized product is detected (See Figure 1). Presently used confirmation tests are necessary. The acylated derivative of cocaine, as well as acylated amphetamine and methamphetamine, can be determined under the conditions described above. Relative elution times for 2-hydroxymethyl tropine, amphetamine, and methamphetamine derivatized with heptafluorobutyric and pentafluoropropionic anhydrides are shown in Table I. The gas chromatographic conditions were as noted under Procedure. The HFBA derivative of benzyl alcohol, the reduction product of the benzoyl radical, can be seen on the chromatogram at $R_T = 0.40$ with respect to amphetamine-HFB.

The derivative of cocaine noted in Figure 1, 2-hydroxymethyl tropine-HFB, has been verified by mass spectro-

Table I. Elution Data for Electron Capturing Drug Derivatives^a

	R_t
Amphetamine-PFP	0.83
Amphetamine-HFB	1.00
Methamphetamine-PFP	1.44
Methamphetamine-HFB	1.60
2-Hydroxymethyltropine-PFP	1.40
2-Hydroxymethyltropine-HFB	1.92

^a GLC conditions noted under procedure.

metric analysis (5). Also verified by mass spectrometry was the HFBA derivative of benzyl alcohol.

Cocaine was added to horse urine at concentrations of 39 $\mu\text{g}/\text{ml}$, 3.9 $\mu\text{g}/\text{ml}$, 390 ng/ml , and 39 ng/ml . Using the procedure cited, which involves a 2.5-fold concentration factor in extraction, and employing the pentafluoropropionic anhydride derivative, the sample containing 39 ng/ml cocaine in urine gave an average S/N ratio of 14:1 for 1.0 μl injected. Therefore, sensitivities of 20-30 ng of drug/milliliter of sample could be achieved without concentration through evaporation procedures.

As described, the procedure using the Beckman instrument provides a rapid, sensitive, and relatively specific screening procedure for cocaine, as well as amphetamine and methylamphetamine.

ACKNOWLEDGMENT

The authors wish to thank George Maylin of the New York State Veterinary College, Cornell University, Ithaca, N.Y., for the mass spectrometric analyses of the drug derivatization products.

Received for review February 14, 1973. Accepted August 15, 1973. The work was conducted under a grant from The Ohio State Racing Commission, Columbus, Ohio 43215.

(5) G. Maylin, New York State Veterinary College, Cornell University, Ithaca, N.Y., personal communication, 1972.

CORRECTION

Annual Subject Index

Through an error on our part, two page numbers were transposed in the annual subject index of *Analytical Chemistry*, December 1973. The material on page 2469 should be in the "S" section where page 2477 is located. The subject matter on page 2477 belongs in the "G" section, where page 2469 is located.

Dual-Load Porous-Layer Open Tubular Gas Chromatography Columns

J. G. Nikelly

Department of Chemistry, Philadelphia College of Pharmacy and Science, Philadelphia, Pa. 19104

The advantages of dual-load gas chromatography columns were described recently (1). Dual-load columns, containing in the front half about double the concentration of liquid phase as in the back half, show increased performance compared to equivalent single-load columns. A typical increase in column performance, measured as the number of effective plates per unit retention time, is 30%. However, when the capacity factors are relatively high ($k' > 20$), the dual-load advantage is compensated by peak broadening that results as the peaks pass from the high- to the low-load—i.e., the front of a peak moves faster than the tail (2).

Consequently, as open tubular columns normally have capacity factors considerably lower than those of packed columns, they appeared to be interesting for studying the dual-load effect. Furthermore, the fact that dual-load columns permit larger injected sample volumes, was particularly promising for application to open tubular columns which are generally limited to relatively smaller sample injection volumes.

This paper, therefore, describes the application of the dual-load principle on open tubular columns, specifically on porous layer open tubular (PLOT) columns which were chosen for this study over standard, wall-coated columns, not only because of their performance advantages, (3-5), but more importantly, because they can be conveniently made in the laboratory with different loads of liquid phase (3, 4, 6).

EXPERIMENTAL

Apparatus. The same column-coating apparatus was used as described earlier (4, 6).

The columns were made from Type 304 stainless steel tubing, 0.03-in. i.d. and 0.062-in. o.d., available from Superior Tube Company, Norristown, Pa. 19404.

All separations were made on a Gow-Mac gas chromatograph, Model 69-700 (Gow-Mac Instrument Company, Madison, N.J. 07940). The $\frac{1}{8}$ -in. fittings were modified to take $\frac{1}{16}$ -in. columns by using, at the inlet, a $\frac{1}{8}$ - to $\frac{1}{16}$ -in. adapter (made locally) and, at the outlet, a Teflon reducing ferrule (RF 200/100, Alltech Associates, Arlington Heights, Ill. 60004), which allowed the column to extend 4 cm into the detector housing. Recordings were obtained by a 1-mV strip chart recorder, Model 1027 (McKee-Pedersen Instruments, Danville, Calif. 94526). The chart speed was 0.5-in. per min except in the case of very short retention times, such as for a nonretained component, methane, in which case the chart speed was 2-in. per min.

Flow rates were measured with flow meters (Brooks Instrument Company, Hatfield, Pa. 19440) which were calibrated with a soap bubble meter at the column outlet. For all columns, the carrier gas (He) flow rate was usually adjusted to 7 cm³ per min.

Reagents. The coating mixtures were prepared using, as solid support, Chromosorb R6470-1, a finely divided diatomaceous silica available from Johns-Manville, Manville, N.J. 08835. The sup-

port was used as received—i.e., without pretreatment such as sizing or drying.

Procedure. Columns. Column lengths varied from 15 to 45 ft as this range is suitable for the coating procedure (dynamic method) and, at the same time, it is sufficient for producing the required number of theoretical plates, up to 10,000, which is adequate for most separations. A suitable length of 0.03-in. i.d. tubing was coiled, connected to the filling tube, and flushed with a few milliliters of CHCl₃ using air (or nitrogen) pressure. The coating suspension was prepared by mixing and shaking in a small capped vial 2 ml of 2 to 9% chloroform solution of liquid phase (Carbowax 1540) and 0.2 gram of the solid support. About 1 ml of coating mixture was then added to the filling tube and forced through the capillary tubing under 10 to 20 psig air pressure, which was allowed to continue flowing for a few minutes after the excess coating mixture emerged from the column. The column lengths were then used singly or in combinations, as shown in Table I. The combinations (dual-loads) were made by connecting single-load sections with "zero-dead volume" Swagelok unions (G.C. 100-6, Crawford Fitting Company, Solon, Ohio 44139).

As shown in Table I, all the dual-load columns used in this work have a liquid phase concentration ratio (front to back section) of 2.0, as this ratio was previously found to be near optimum (1). As distinct from the concentration ratio, the load ratio of the dual-load columns varied between 0.6 and 1.3. This is the ratio of the total amount of liquid phase, not merely the concentration; in the case of packed columns (1), it has no significant effect on column performance, provided it is not too far from unity—i.e., with about half of the total liquid load in the front and half in the back section.

Columns A through E, Table I, have a higher liquid load, an average of 2.4 mg per ft, while columns F through K have a lower load, an average of 1.1 mg per ft. Two load levels were used to determine the effect of total load on dual-load columns; furthermore, this range of loads is typical for PLOT columns.

For each level of total load, three reference, single-load columns were used, each reference column being equivalent to the corresponding dual-load column. Equivalency was based on column length or on total liquid load. Naturally, both the concentration ratio and the load ratio of the single-load columns is unity.

Analytical Samples. The main test sample, consisting of four normal alcohols shown in Table II, was chosen to provide the appropriate range of capacity factors, $k' \approx 0.4$ to 8, and, at the same time, it was suitable for the liquid phase chosen for this work. The capacity factors listed in Table II represent average values for separations carried out at 60 to 70 °C column temperatures. Column temperatures were selected for each column combination on the basis of retention time normalization, about 6 minutes for the last peak.

The volume of injected sample was approximately 0.05 μ l except in the experiments on trace analysis where a different sample was used, 0.02% 3-methyl-1-butanol, in which case the injected volume was 0.6 μ l. Sample injections were made (without a stream splitter) using a 1- μ l syringe, Cat. No. 14011, Precision Sampling Corporation, Baton Rouge, La. 70815, or a regular 5- μ l syringe.

Column Evaluation. The dual-load columns were evaluated by comparing them with various single-load reference columns also listed in Table I. Several reference columns were used of different length and liquid phase loading to make the comparison as reliable as possible. The criteria of comparison were plate heights (HETP) and column performance (7) defined as

$$\frac{N_{\text{eff}}}{t} \quad (1)$$

(7) B. L. Karger, "Modern Practice of Liquid Chromatography," J. J. Kirkland, Ed., Wiley-Interscience, New York, N.Y., 1971, pp 17 and 36.

- (1) J. G. Nikelly, *Anal. Chem.*, **45**, 1284 (1973).
- (2) D. C. Locke and C. E. Meloan, *Anal. Chem.*, **36**, 2234 (1964).
- (3) J. G. Nikelly, *Anal. Chem.*, **45**, 2280 (1973).
- (4) Max Blumer, *Anal. Chem.*, **45**, 980 (1973).
- (5) Perkin-Elmer Corporation, Norwalk, Conn., *Chromatogr. Newslett.*, **1**, 27 (1972).
- (6) J. G. Nikelly, *Anal. Chem.*, **44**, 623 (1972).

Table I. Dual- and Single-Load (Reference) PLOT Columns

Column	Length, ft × load/length, mg/ft			Ratio	
	Front section	Back section	Overall	Load	Concn
A (dual)	10 × 4.0	15 × 2.0	25 × 2.8	1.3	2.0
B (dual)	10 × 4.0	25 × 2.0	35 × 2.6	0.8	2.0
C (single)	25 × 2.0	1.0	1.0
D (single)	35 × 2.0	1.0	1.0
E (single)	35 × 2.6	1.0	1.0
F (dual)	10 × 2.0	15 × 0.9	25 × 1.3	1.5	2.2
G (dual)	10 × 2.0	25 × 0.9	35 × 1.2	0.9	2.2
H (dual)	10 × 2.0	35 × 0.9	45 × 1.1	0.6	2.2
I (single)	25 × 0.9	1.0	1.0
J (single)	35 × 0.9	1.0	1.0
K (single)	35 × 1.2	1.0	1.0

Table II. Composition of Test Sample

Compound	Concn, %	Approx. capacity factor, <i>k'</i>
2-Methyl-2-propanol	7	0.4
2-Methyl-1-propanol	10	2
3-Methyl-1-butanol	14	5
1-Pentanol	69	8

Table III. Column Comparison, 2.4 mg/ft Average Load

Column	HETP		Performance	
	<i>k</i> ≈ 2	<i>k</i> ≈ 5	<i>k</i> ≈ 2	<i>k</i> ≈ 5
A (dual)	1.8	3.0	16.6	7.3
B (dual)	2.1	3.2	15.6	8.6
C (single)	1.7	2.7	17.2	7.5
D (single)	2.0	3.2	15.3	8.9
E (single)	2.2	3.4	14.2	10.3

where

$$N_{eff} = N \left[\frac{k'}{k' + 1} \right]^2 \quad (2)$$

and *N* = number of theoretical plates, *k'* = partition ratio or capacity factor, and *t* = retention time in seconds.

RESULTS AND DISCUSSION

The results are listed in Tables III, IV, and V from which several observations are made and discussed on the basis of total liquid load and *k'* (choice of sample component and column temperature).

Effect of Total Load. It is interesting, if not surprising, to note that notwithstanding the relatively low loads of open tubular columns, the dual-load effect is not observed unless the amount of liquid phase is less than 2 mg per ft. As shown in Table III, dual-load columns A and B are no better than single-load columns C, D, and E. This was confirmed by testing several other columns with loads up to 8 mg per ft which are not listed in Table I since the results were negative.

At lower liquid loads—i.e., in the 1 to 2 mg per ft range—the dual load effect is significant. Dual-load columns F, G, and H, Table IV, show a very significant improvement over the reference columns I, J, and K. The improvement is due to both a reduction in plate height and an increase in effective plates per second.

Since the dual-load effect was found only in the case of low liquid loads, it was important to ascertain that such columns have sufficient capacity for separating "difficult" pairs, such as MeOH/EtOH, of low capacity factor. This is demonstrated in Figure 1 which shows that the MeOH/EtOH pair has more than adequate resolution.

Table IV. Column Comparison, 1.1 mg/ft Average Load

Column	HETP			Performance		
	<i>k</i> ≈ 0.4	<i>k</i> ≈ 2	<i>k</i> ≈ 5	<i>k</i> ≈ 0.4	<i>k</i> ≈ 2	<i>k</i> ≈ 5
F (dual)	1.7	1.6	2.1	9.7	20.2	10.8
G (dual)	2.3	1.5	2.4	6.5	20.7	10.4
H (dual)	1.9	1.6	2.0	23.6*	19.0	17.3*
I (single)	2.5	1.8	2.7	4.3	17.0	8.6
J (single)	2.2	1.9	2.7	6.9	16.8	8.1
K (single)	3.0	2.3	3.5	8.1	14.2	8.3
Av % change	-15	-22	-27	+27	+27	+28

* Omitted in the calculation of av % change.

Table V. Column Comparison in Trace Analysis

	Low load ^a	High load ^b
Single-load, HETP, mm	4.4	3.8
Dual-load, HETP, mm	3.0	3.1
Effect of dual load on HETP	-32%	-18%

^a 1.1 mg per ft average load. ^b 2.4 mg per ft average load.

Choice of Sample Component (Effect of *k'*). Although the analytical sample consisted of four components ranging from early (*k'* ≈ 1) to intermediate (*k'* ≈ 8) peaks, only the first three components were used for column com-

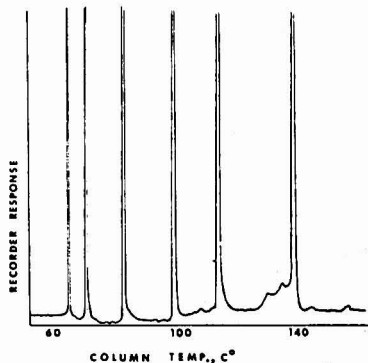


Figure 1. Resolution of alcohols on a dual low liquid loading PLOT column

Column, (10 ft × 2.0 mg/ft) + (35 ft × 0.9 mg/ft), 03-in. i.d., 1540 Carbowax. Flow rate, 7 ml/min. Temp. programmed from 60 to 140 °C. Sample, 0.05 μl normal alcohols, MeOH through hexanol

parison (Table IV), as these components are more representative of typical separations and are suitable for showing the dual-load effect and its dependence on k' .

As shown in Table IV, last row, the dual-load effect (decrease in plate height) is less for the lower k' values—e.g., 15% decrease for $k' = 0.4$ vs. 27% decrease for $k' = 5$. This may be explained by the increased overloading effect expected for early peaks. According to Harris (8), the sample injection volume in microliters for a component should not exceed

$$\frac{V}{2\sqrt{N}} \quad (3)$$

where V is the retention volume in milliliters and N is the plate number; for $k' < 1$, overloading is dominant over the dual-load effect.

On the other hand, the increase in column performance is about the same for k' values between 0.4 and 5. Apparently, the increased improvement expected for the lower k' values is compensated, but not dominated, by the overloading effect mentioned above.

Of course, at higher k' values, the improvement in column performance would decrease to zero, as in the case of packed columns (1).

Column Temperature. One means of increasing the validity of column comparison is the use of constant retention time—i.e., time-normalization. As columns varied in load and length, time-normalization was maintained by judicious choice of column temperature, which was found

(8) W. E. Harris, *J. Chromatogr. Sci.*, 11, 184 (1973).

to be between 60 and 70 °C. Columns were thus compared at approximately fixed k' values.

When retention and, consequently, k' is reduced by using a higher column temperature, as in the case of column H, Table IV, where k was reduced from 5 to 0.4, column performance (but not HETP) is improved significantly. Thus, if either a more volatile sample or a higher column temperature were used in this study, column performance might be further increased.

Trace Analysis. When large volumes of sample were injected as in the case of trace analysis, dual-load columns were particularly useful as shown in Table V. This lists the average plate numbers obtained when injecting 0.6- μ l of the analytical sample (Table II) on four different 35-foot columns of two different liquid loads. At the low liquid load, HETP is improved by 32%. Even at the high liquid load (where it may be recalled that there was no dual-load effect for 0.1- μ l sample injection volume, Table III), there is an 18% decrease in HETP.

CONCLUSION

If the amount of liquid phase per unit length is a conveniently variable parameter, as in cases where open tubular columns are made by combining two or more lengths, and particularly where the columns are coated in the laboratory (locally), it may be advantageous to use a higher liquid load in the front length.

Received for review July 31, 1973. Accepted October 1, 1973.

Cryostat for Optical Spectroscopy

J. Szóke and I. Szilágyi¹

Physical Optics Department, Central Research Institute for Physics, Budapest, Hungary

In modern spectroscopic studies, the spectrum under investigation must be measured at different temperatures. While thermodynamic constants can be more accurately determined at elevated temperatures, for the analysis of spectroscopic fine structure, low-temperature measurements are preferable, because the resolution improves as the temperature decreases; that is, the component bands produce higher and smaller peaks, while the integrated intensity remains constant. However, the increase in the resolution is not continuous, and, especially in electronic spectroscopy, the different types of transition (combinations of electron jump with vibrations, rotations, excitons, phonons, magnons, etc.) often vary selectively with temperature. The temperature range of phase transitions is particularly rich in information. A spectrum therefore needs to be examined over a wide range of low-temperature values, e.g., at intervals of 5 or 10 °C going from room temperature down to liquid nitrogen temperature.

These requirements fix the specifications which must be met by any cryostat used for temperature regulation of samples studied spectroscopically: The sample chamber (in the cryostat) must be transparent in the spectral region of interest. The windows of the cryostat must be kept

at room temperature to protect them from condensation of water vapor. The sample temperature must be constant during the measurement, particularly in the illuminated region.

All but the last requirement are easy to achieve. The difficulty of keeping the sample at a constant temperature is due to the fact that the examined area of the sample is exposed to a substantial quantity of light from the radiation field. This is particularly true in the infrared region, where almost all the absorbed energy is converted into heat. The temperature of the illuminated volume (or surface area, in the case of reflection) cannot be locally controlled, so the sample temperature can be cryostated only if the sample is a good conductive material. Usually this is not the case.

In heat-conducting cryostats the liquid coolant(s) is in direct contact with the sample, and the heat generated in the sample by radiation from the various sources (mainly the light source) is dissipated by conduction through this medium. The sample temperature is in this case determined by the rates of heat uptake and heat conduction.

In the gas-flow-type cryostat cold (usually thermoregulated) gas streams around the sample. The heat absorbed by the sample is taken up by the molecules of the gas, and thus sample temperature is determined by the temperature and flow rate of the gas stream.

¹ Present address, Chinoin Pharmaceutical and Chemical Factory, Budapest, Hungary

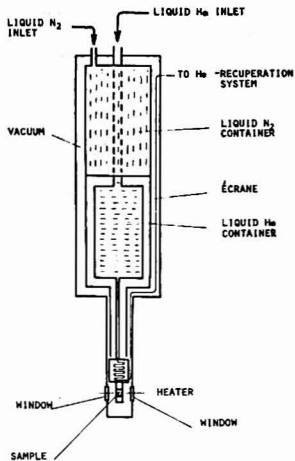


Figure 1. Outline of the thermoconductive helium cryostat (It was used only with N_2 filling)

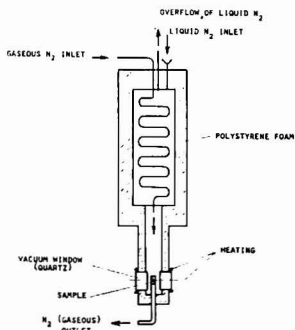


Figure 2. Outline of the gas-flow-type N_2 cryostat

EXPERIMENTAL

The fluorescence spectrum of solid ammonium uranyl-trisacetate was measured. The microcrystalline sample was prepared by the method of Dieke (1) and was packed in a vertical target with moderate pressing. The sample was illuminated by focusing the exit slit of the exciting monochromator. The emitted light was dispersed by a high resolution plane-grating monochromator (1200 lines/mm; 100×100 mm ruled area; $f = 100$ cm) in Czerny-Turner arrangement. The instrument was developed in this laboratory.

The two types of cryostat utilized are depicted schematically in Figures 1 and 2; the points at which the sample temperature was measured are shown in Figure 3.

The temperature was measured by using a T-type (copper-constantan) thermocouple to a precision of $\pm 1^\circ C$ between room and liquid N_2 temperature.

The temperature was controlled by a precision proportional regulatory system (2).

In the conduction type cryostat, the coolant is transferred through a heating block to the sample holder. The heating current is determined by the difference between the setting and the actual thermo sample signal level. The flow rate of the coolants can be changed by a mechanical valve.

(1) W. Lenz, *Z. Anal. Chem.*, **52**, 90 (1913).

(2) J. Balla, K. Tompa, and F. Tóth, *Cryogenics*, **8**, 47 (1968).

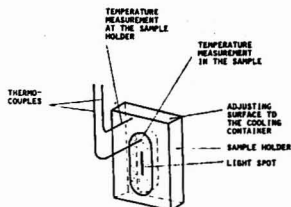


Figure 3. Thermoconductive sample holder

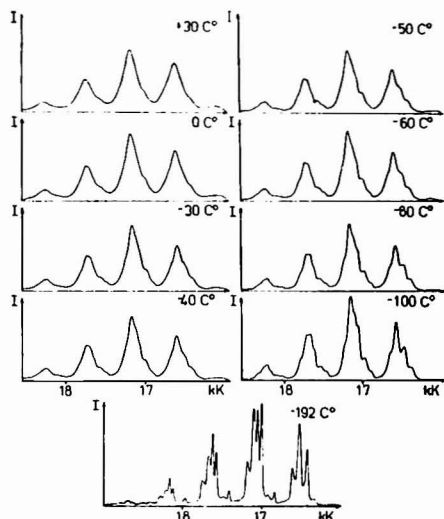


Figure 4. Fluorescence spectra of ammonium uranyl-trisacetate at different temperatures measured in a gas-flow-type cryostat

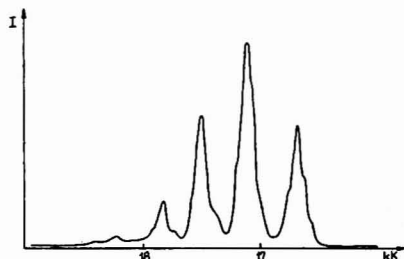


Figure 5. Luminescence spectrum of ammonium uranyl-trisacetate in a thermoconductive cryostat after 8-hr cooling with liquid nitrogen

The temperature can be quickly set $10^\circ C/min$ at the sample holder and it can be controlled easily; while at the powdered sample, it changes slowly and it is uncontrollable. Therefore, we did not use temperature controller. The temperature of the sample and the sample holder was measured as can be seen in Figure 4.

In the gas-flow type cryostat, the pressure is atmospheric, and the temperature can be measured equivalently in the sample at the sample holder or in the chamber and it was controllable in all cases with a precision to $\pm 1^\circ\text{C}$. The spectra measured at the same temperature were reproducible within $\pm 2\%$ in intensity.

RESULTS AND DISCUSSION

Figure 4 shows spectra taken while using the gas-flow cryostat. The increasingly good resolution is due to the cold effect (The spectroscopic interpretation will be published later).

In Figure 5, the best result obtained with the heat-conducting cryostat can be seen. In this case, the copper transfer block and non-illuminated parts of the sample were kept at the experimental temperature of -190°C . The measured spectrum thus corresponds to a spectrum at about -50°C .

The figures demonstrate clearly that the gas-flow technique is the more effective. With this technique, the tem-

perature can be set in less than 10 seconds per $^\circ\text{C}$. The conductive cryostat does not work satisfactorily if the contact between heat transfer block and sample is imperfect or if the sample material is of poor thermal conductivity. Generally neither of these conditions is fulfilled.

It can be concluded that the spectroscopic data obtained at temperatures cryostated with heat-conducting devices are of questionable reliability. Reports in the literature of small temperature effects may be therefore attributable rather to poor construction of the cryostat than to temperature insensitivity of the material.

ACKNOWLEDGMENT

The authors wish to thank J. Balla and I. Peter for helpful discussions and Mrs. B. Szabó and B. Bencze for the useful technical assistance.

Received for review February 1, 1973. Accepted August 17, 1973.

Multiclass Linear Classifier for Spectral Interpretation (Pattern Recognition)

C. F. Bender

Lawrence Livermore Laboratory, University of California, Livermore, Calif. 94550

B. R. Kowalski

Department of Chemistry, University of Washington, Seattle, Wash. 98195

Linear classifiers were originally designed to construct decision hyperplanes for binary (yes/no) decisions (1). A linear classifier was the first pattern recognition technique applied to the interpretation of spectroscopic data (2). With this technique, a number of binary decisions were used to predict structural information directly from low-resolution mass spectra. Although the problem is multiclass in nature, a complicated use of the linear classifier gave very encouraging results. Difficulties arise in trying to define multiclass linear machines (1); hence, a considerable effort has been spent on improving the linear, binary classifier (3).

Recently we used a multiclass technique, the K-Nearest Neighbor Rule (4), for the interpretation of NMR spectra. For this particular application, the multiclass technique outperformed the technique using linear classifiers as outlined above. The K-Nearest Neighbor Rule is expensive to use and not suited to small laboratory computers. This problem has been partially solved by reducing the number of variables (5, 6), but the K-Nearest Neighbor Rule is still best suited to computers with a large amount of fast storage.

The purpose of this note is to present an efficient multiclass linear classifier which can be easily applied, yet retains the power and simplicity of the binary classifier. This is accomplished by compromising linear separability for interclass separability.

DEFINITIONS AND METHOD

A pattern space, X , is a collection of patterns, X_p

$$X = (X_1, X_2, X_3, \dots, X_p) = \begin{pmatrix} X_{11} & X_{12} & X_{13} & \dots & X_{1p} \\ X_{21} & X_{22} & X_{23} & \dots & X_{2p} \\ X_{31} & X_{32} & X_{33} & \dots & X_{3p} \\ X_{41} & X_{42} & X_{43} & \dots & X_{4p} \\ \vdots & \vdots & \vdots & \ddots & \vdots \\ X_{m1} & X_{m2} & X_{m3} & \dots & X_{mp} \end{pmatrix} \quad (1)$$

where X_{ip} is the i th variable of the p th pattern. In spectral analysis, each spectrum is a pattern and the variables are related to the spectral intensities and positions of the peaks. A class is a collection of patterns in which all members have a common feature. Pattern recognition methods are used to extract this feature from the variables.

Binary decisions are made using a linear classifier by noting the value of the dot product of a weight vector, W , and a pattern X_p ,

$$S_p = X_p^+ W \quad (2)$$

Here $+$ denotes matrix transpose. If S_p is greater than some number, S_0 , the decision is yes, and if S_p is less

- (1) N. J. Nilsson, "Learning Machines," McGraw-Hill, New York, N.Y., 1965.
- (2) P. C. Jurs, B. R. Kowalski, and T. L. Isenhour, *Anal. Chem.*, **41**, 21 (1969).
- (3) L. E. Wangen, N. W. Frew, and T. L. Isenhour, *Anal. Chem.*, **43**, 845 (1971).
- (4) B. R. Kowalski and C. F. Bender, *Anal. Chem.*, **44**, 1405 (1972).
- (5) C. F. Bender and B. R. Kowalski, *Anal. Chem.*, **45**, 590 (1973).
- (6) C. F. Bender and H. D. Shepherd, and B. R. Kowalski, *Anal. Chem.*, **45**, 617 (1973).

than or equal to S_0 , the "machine" response is no. Often the dimensionality of W is increased by one and a row of 1's is added to the pattern space, thereby allowing S_0 to be set to zero. Of the many possible methods for determining the weight vector (7) only two have appeared in the chemical literature, negative feed-back (2) and least-squares (8). Except for one recent study (9), only limited success has been attained in extending the binary classifier to handle the multiclass case. The difficulty usually arises in requiring each class to be linearly separable from all other classes. Figure 1 shows an example in which this is possible (linear classifiers in two dimensions generate lines); line I separates region A from regions B and C, line II separates region B from region C, while line III separates region C from regions A and B. Figure 2 shows a case in which the regions are not linearly separable using the above definition; region B cannot be separated from regions A and C by using one straight line.

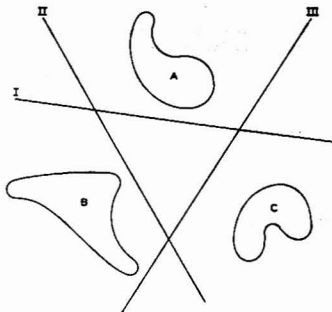


Figure 1. Linearly separable regions (A, B, C) in two dimensions.

The technique presented in this paper does not require the notion of linear separability but does require inter-class separability. Binary decisions are used to separate each class from each of the other classes. If there are n classes, then $n(n-1)/2$ weight vectors are calculated. Enumeration of the number of positive votes for the proper class yields $n-1$ and less for all others. This can be easily seen in the first example (Figure 1), by using line I as the A-C separator, line II as the A-B separator, and line III as the B-C separator. Notice that now the regions in the second example (Figure 2) can also be correctly classified using line I as the A-B separator, line II as the A-C separator, and line III as the B-C separator. Clearly, a pattern in class A would be classified "A" by separator I, "A" by separator II, and "B" by separator III. Hence, the overall classification would be correctly determined by majority vote as class A ($3-1=2$).

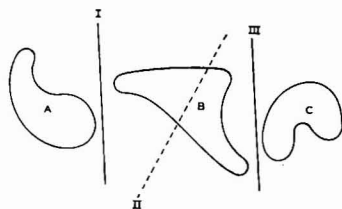


Figure 2. Regions (A, B, C) which are not linearly separable

where

$$A = \left(\sum_i w_i \right)^{-1} \quad (7)$$

$$B = \left(\sum_i v_i \right)^{-1} \quad (8)$$

The linear separation problem is further complicated when attempts are made to interpret chemical information because the classes cannot be totally separated. In fact, the pattern space of hydrocarbons having increasing carbon number has a remarkable resemblance to the second example. Nonseparability does not create a great difficulty for the present method since a majority rule can be invoked. There is one drawback, however; such techniques can lead to "null" classifications (*i.e.*, ties).

The merits of such a representation have been discussed elsewhere (6).

Three preprocessing techniques were applied to the moments data. By using more than one representation of the spectra, the effectiveness of the multiclass technique can be evaluated in greater depth. The first preprocessing technique was autoscaling (10); here each variable is scaled to have unit variance and the average value of the variable is shifted to zero. By multiplying each autoscaled variable by a "class-separating" weight (10), the second set of preprocessed data was generated. In this case the variances of more important (in a class separating sense) variables are increased, while less important variances are decreased. Finally, a recently developed (5) linear transformation of the variables was used. The variables defined by this technique are optimum for separating classes and have proved to be most effective for the interpretation of mass spectral data.

EXPERIMENTAL

The data used were the same as those in the optimum variable study (5) and consisted of low resolution mass spectra for hydrocarbons containing six, seven, and eight carbon atoms. The "unmeasurable" common property to be extracted was the carbon number. For each class, 40 spectra were used in the training set and 10 for evaluation. There were a total of 120 spectra in the training set and 30 spectra in the evaluation set.

As in similar studies, moments were used to represent each spectrum. For each nonzero intensity, the mass to charge ratio (v_i) and the square root of the intensity (w_i) were employed to calculate the ten moments used.

$$X_1 = A \sum_i w_i v_i \quad (3)$$

$$X_k = A \sum_i w_i (v_i - x_1)^k, k = 2, \dots, 5 \quad (4)$$

$$X_6 = B \sum_i w_i v_i \quad (5)$$

$$X_{k+5} = B \sum_i v_i (w_i - X_6)^k, k = 2, \dots, 5 \quad (6)$$

RESULTS AND DISCUSSION

Table I presents the results of applying three classification techniques to the three sets of preprocessed mass spectral data described in the last section. The first classification method was the linear classifier (1) where the weight vector was found by a least squares procedure (a) and also by the feedback procedure (b). The first number represents the classification performance (per cent correct) obtained for the training set and the second number is the evaluation set performance. Patterns in the evaluation set were not used to train the classifiers and are considered as true unknowns. The poor performance for the linear classifier is due to the nonlinear separability of the data used in this study. Also, since the least squares

(10) B. R. Kowalski and C. F. Bender, *J. Amer. Chem. Soc.*, **84**, 5632 (1972).

(7) G. Nagy, *Proc. IEEE*, **5**, 836 (1968).

(8) B. R. Kowalski, P. C. Jura, T. L. Isenhour, and C. N. Reilley, *Anal. Chem.*, **41**, 895 (1969).

(9) N. M. Fraw, L. E. Wangen, and T. L. Isenhour, *Pattern Recognition*, **3**, 281 (1971).

Table I. Per Cent Correct Classifications (Training Set/Evaluation Set)

Classification method	Preprocessing technique		
	Autoscale	Weighted autoscale	Optimum linear transformation
I. Linear classifier			
a) Least-squares	83/83	83/83	83/83
b) Negative feedback	56/83	77/70	74/87
II. 3-Nearest Neighbor	80/60	89/80	92/97
III. Multiclass classifier			
a) Least-squares	91/87	91/87	91/87
b) Negative feedback	94/90	93/90	78/90

method is invariant to all linear transformations, the results are the same for the three preprocessed sets of mass spectral data.

The second classification method used in this study was the K-Nearest Neighbor Classification Rule (4) with K

equal to three. This method is a multiclass method that does not depend upon linear separability. Hence, classification performance is improved in the last two sets of preprocessed data. The attributes and limitations of this method can be found in the chemical literature (4).

The results of the multiclass classifier (III) introduced in this paper are also found in Table I. Here again, the least squares procedure (a) and the error correction feedback procedure (b) were used to calculate the necessary weight vectors. The multiclass procedure performed very well. The overall performance indicates that the least squares procedure for calculating the weight vector is best. Again, note that least squares solutions are unique and are invariant to all linear transformations of the data. These attributes recommend the least squares multiclass procedure for applications which involve more than two classes. The method is at least as effective as other linear classifiers and comparable in accuracy to the more expensive K-Nearest Neighbor Rule.

Received for review February 26, 1973. Accepted August 27, 1973. Work performed under the auspices of the U. S. Atomic Energy Commission.

Identification of Heroin and Its Diluents by Chemical Ionization Mass Spectroscopy

Jew-Ming Chao, Richard Saferstein, and John Manura

New Jersey State Police, Forensic Science Bureau, West Trenton, N.J. 08625

Forensic laboratories currently use a variety of techniques to identify illicit seizures of heroin (diacetylmorphine). These methods include color and microcrystal tests, absorption spectrophotometry, thin-layer and gas chromatography (1), as well as electron impact (EI) mass spectroscopy (2). However, no one of the above techniques in itself combines the speed, accuracy, and sensitivity that is necessary for an identification of heroin and its organic diluents. The possible presence of numerous organic components in an illicit heroin mixture, will almost always preclude the examination of the powder directly in the EI mass spectrometer and therefore necessitates interfacing the mass spectrometer to a gas chromatograph.

Increasingly, forensic laboratories are being required to identify all the components of an illicit drug mixture. This analysis may provide investigating authorities with valuable intelligence information regarding the illicit material's synthesis and origin.

The application of chemical ionization (CI) mass spectroscopy to drug identification has recently been reported (3-7). This technique has now been utilized as a rapid

and sensitive means of identifying heroin and its common diluents. The procedure requires no sample preparation or prior chromatographic treatment, and its sensitivity permits a direct and rapid identification of microgram quantities of illicit heroin preparations.

EXPERIMENTAL

Apparatus. A Du Pont 21-490 single focusing mass spectrophotometer equipped with a dual EI/CI source was used. The instrument has a resolution of 600 with 10% valley, a 90° magnetic sector, and is equipped with differential pumping. The reagent gas was isobutane (99.9% pure). The source was operated at a pressure of 0.5-1 Torr and at a temperature of 200 ± 10 °C. The ionizing voltage was set at 300 eV in the CI mode.

Procedure. Approximately a microgram of the illicit powder was added to a capillary tube. The tube was introduced by the direct probe of the mass spectrometer and the probe temperature was raised to 200 °C. Scans were taken at a rate of 10 sec/decade after 1 and 2 minutes.

RESULTS AND DISCUSSION

The application of CI mass spectroscopy to forensic identification lies in the ability of the operator to control the complexity of the spectra that are generated through the choice of the CI reagent gas. The ionization process can occur through a charge or proton transfer processes, depending on the nature of the reagent gas. The former results in spectra resembling that of conventional EI spectroscopy, the latter produces spectra that are generally less complex. As the present study has as its objective the identification of heroin in the presence of its diluents, isobutane was the reagent gas of choice. This gas has previously been demonstrated as having yielded the least

(1) E. G. C. Clarke, "Isolation and Identification of Drugs," Pharmaceutical Press, London, 1969.

(2) G. R. Nakamura, T. T. Noguchi, D. Jackson, and D. Banks, *Anal. Chem.*, **44**, 408 (1972).

(3) G. W. A. Milne, H. M. Fales, and T. Axenrod, *Anal. Chem.*, **43**, 1815 (1971).

(4) H. M. Fales, G. W. A. Milne, and T. Axenrod, *Anal. Chem.*, **42**, 1432 (1970).

(5) D. F. Hunt and J. F. Ryan, *Anal. Chem.*, **44**, 1306 (1972).

(6) R. L. Foltz, M. W. Couch, M. Geer, K. N. Scott, and C. M. Williams, *Biochem. Med.*, **6**, 294 (1972).

(7) R. Saferstein and J. Chao, *J. Ass. Offic. Anal. Chem.*, **58**, 1234 (1973).

Table I. Isobutane CI Mass Spectra of Heroin and Common Diluents^{a,b}

Compound	Mol wt	Peaks			
		1	2	3	4
Heroin	369	310	370 (83%)	268 (14%)	
Acetylcodeine	341	282	342 (15%)		
Quinine	324	325	326 (25%)	136 (20%)	307 (10%)
Caffeine	194	195			
Procaine	236	237	100 (16%)	99 (10%)	
Methapyrilene	261	262			
Mannitol	182	183	165 (20%)	147 (10%)	129 (10%)
Sorbitol	182	183	165 (20%)	147 (10%)	129 (10%)
Glucose	180	163	145 (85%)	127 (25%)	
Fructose	180	163	145 (85%)	127 (25%)	
Galactose	180	163	145 (85%)	127 (25%)	
Mannose	180	163	145 (85%)	127 (25%)	
Sucrose	342	163	145 (85%)	127 (25%)	
Lactose	342	163	145 (85%)	127 (25%)	

^a All peaks are listed in descending order of intensity with their abundances in parentheses. ^b Only those peaks with abundance of 10% or greater are shown.

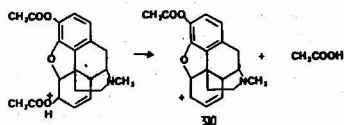


Figure 1. Mechanism for the fragmentation of heroin

complex CI spectra (8). The simplicity of an isobutane CI spectra suggests its application to the characterization of multicomponent mixtures as those most frequently encountered in illicit drug determinations. The isobutane CI spectra of drugs generally display only one to three ions with abundances greater than 10% (3, 7). The majority of these drugs show an (M + 1) peak as the predominant ion; the presence of other ions can generally be accounted for by mechanisms common to carbonium ion chemistry.

The isobutane CI spectra of heroin and its common diluents are listed in Table I. The CI spectrum of heroin has its base peak at *m/e* 310. This ion is attributed to the protonation of the acetyl group on the C-6 carbon and its subsequent loss as acetic acid (Figure 1). Loss of the acetic acid from C-3 is unlikely as it would result in a highly unstable aryl ion.

Heroin usually contains *O*⁶-monoacetylmorphine and acetylcodeine (9). The former is a degradation product and the latter is a by-product of the heroin synthesis. Acetylcodeine has its major peak at *m/e* 282; this peak also represents the loss of acetic acid from the (M + 1) ion. Its presence in a heroin preparation is illustrated in Figure 2.

Though a standard *O*⁶-monoacetylmorphine was not available for analysis, it is assumed that its predominant ion would be the MH-CH₃COOH ion at *m/e* 268, a (M + 1) ion would also be present at *m/e* 328; its presence in illicit heroin preparations is shown in Figure 3. The spectra of the heroin diluents that were examined are characterized by their simple fragmentation patterns. Caffeine and methapyrilene have only (M + 1) ions at *m/e* 195 and 262, respectively. Quinine and procaine, while exhibiting other ions, show strong (M + 1) ions as their base peaks at *m/e* 325 and 237, respectively.

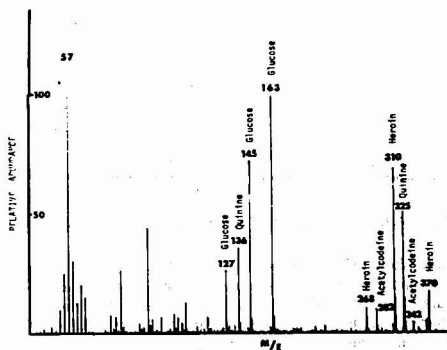


Figure 2. CI mass spectrum of heroin, acetylcodeine, quinine, and glucose

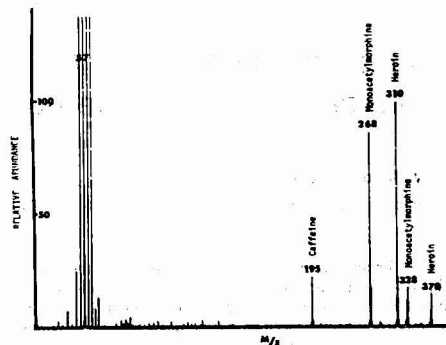


Figure 3. CI mass spectrum of heroin, caffeine, and monoacetylmorphine

(8) M. S. B. Munson, *Anal. Chem.*, **43**, (13), 28A (1971).

(9) J. M. Moore, *Micrograms*, **5**, 38 (1972).

Mannitol and sugars are popular diluents for illicit heroin. The isomeric hexahydric alcohols of mannitol and sorbitol cannot be distinguished by CI mass spectroscopy.

Table II. CI Mass Spectra of Salts and Corresponding Free Bases^a

Compound	Mol wt	Peaks			
		1	2	3	4
Heroin free base	369	310	370 (33%)	268 (14%)	
Heroin hydrochloride	423	310	370 (38%)	268 (14%)	
Quinine free base	324	325	326 (25%)	136 (20%)	307 (10%)
Quinine hydrochloride	386	325	326 (25%)	136 (20%)	307 (10%)
Quinine sulfate	782	325	326 (25%)	136 (20%)	307 (10%)
Quinine gluconate	520	325	326 (25%)	136 (20%)	307 (10%)

^a All peaks are listed in descending order of intensity with their abundance in parentheses. ^b Only those peaks with abundance of 10% or greater are shown.

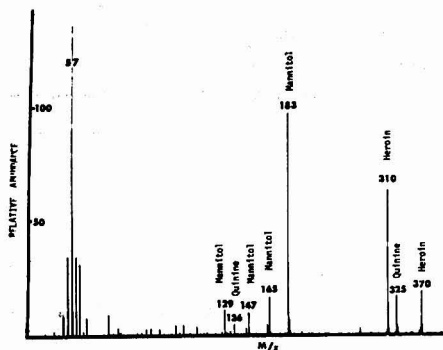


Figure 4. CI mass spectrum of heroin, quinine, and mannitol

Both show (M + 1) ions at 183; the 165, 147, and 129 ions correspond to the loss of one, two, and three water molecules from the (M + 1) ion, respectively. The monosaccharides, glucose, fructose, galactose, and mannose all have the same CI spectra. The base peak is that of (M + 1)-H₂O at m/e 163. The 145 and 127 ions are (M + 1)-

2H₂O and (M + 1)-3H₂O, respectively. The disaccharides examined, sucrose and lactose, all exhibit CI spectra similar to those of the monosaccharides; this is attributed to their decomposition in the CI source prior to ionization.

Identical CI spectra are produced by a compound in both the salt and free-base form (Table II). This observation therefore precludes the necessity of any sample preparation prior to the insertion of the illicit powder in the direct probe of the mass spectrometer. Similar observations have previously been made regarding the EI spectra of barbiturates in both the salt and free-acid forms (10).

The CI spectra of illicit heroin preparations are shown in Figures 2-4. Though a definitive forensic identification of the components of a heroin mixture cannot be made by isobutane CI spectroscopy alone, its utilization for screening or for confirmation of other testing procedures is quite apparent. Additionally, the spectrum will yield a "fingerprint" pattern of the powder, that could be useful in characterizing the production and source of the illicit material. The technique is both rapid and sensitive. Microgram quantities of powder can be analyzed in three minutes.

Received for review June 18, 1973. Accepted August 13, 1973.

(10) J. D. McChesney, D. K. Beal, and R. M. Fox, *J. Pharm. Sci.*, **61**, 310 (1972).

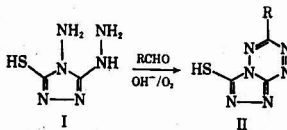
Spectrometric Assay of Aldehydes as 6-Mercapto-3-substituted-s-triazolo(4,3-b)-s-tetrazines

N. W. Jacobsen and R. G. Dickinson

Department of Chemistry, University of Queensland, St. Lucia, 4067, Queensland, Australia

The formation of magenta and violet colored 6-mercapto-3-substituted-s-triazolo(4,3-b)-s-tetrazine derivatives (II) from 4-amino-3-hydrazino-5-mercapto-1,2,4-triazole (I) has been described as the basis of a sensitive and specific qualitative test for aliphatic and aromatic aldehydes (1). The intense colors which were produced in these tests by the absorption of light by the anion of the 6-mercapto-s-triazolo(4,3-b)-s-tetrazine system were recognized as being the basis of a new and useful quantitative test for aldehydes.

(1) R. G. Dickinson and N. W. Jacobsen, *Chem. Commun.*, 1970, 1719.



Encouraged by the interest shown by a number of chemical industries needing to measure and control the level of small quantities of formaldehyde in their processes, we sought to exemplify a quantitative method by

Table I. Measured Absorbances for Known Concentrations of Formaldehyde

Formaldehyde concn, ppm	Absorbance at 549 nm			
0.5	0.16	0.16	0.16	0.165
1.0	0.325	0.325	0.32	0.325
2.0	0.62	0.65	0.63	0.635
3.0	0.95	0.95	0.96	0.95
4.0	1.24	1.26	1.25	1.24
5.0	1.56	1.59	1.58	1.58

adaptation of the qualitative procedure to suit the assay of this aldehyde in concentrations down to one half part per million by weight.

EXPERIMENTAL

Calibration for the Analytical Procedure. Standard solutions of formaldehyde in the range 0.5–5.0 ppm were prepared from a stock solution of formalin assayed independently by the peroxide oxidation method (2).

The special reagent 4-amino-3-hydrazino-5-mercapto-1,2,4-triazole (3) (0.1 gram) was dissolved in *N*-sodium hydroxide (10 ml) in a 25-ml standard flask (stock solutions of the reagent were not used because of their limited shelf-life). The formaldehyde test solution (10 ml) was then added and the mixture aerated (100 ml/min) for 30 minutes at 20 °C by means of a small Pasteur pipet connected to a steady source of clean compressed air. At the end of this period of aeration, the colored solution was immediately made up to 25 ml with distilled water, and the absorbance at the λ_{max} value of 549 nm measured in 1-cm cells using as reference a blank solution prepared in the same manner.

RESULTS

Table I shows the measured absorbances for known concentrations of formaldehyde. The linear relationship (Beer's law) that was obtained between the two parameters was represented by the equation:

$$\text{Concn (ppm)} = 3.16 \times \text{Absorbance} \pm 3\% \quad (1)$$

Formaldehyde solutions of concentrations 5–20 ppm were also measured within the accuracy limits of 3% by appropriate dilution (after aeration with the reagent) of the test solution and reference with 0.4*N* sodium hydroxide to allow the absorbances to be measured in the most sensitive range of the spectrophotometer.

Formaldehyde solutions of concentration greater than 20 ppm were reliably measured by suitable dilution before assay.

The major source of error in the analytical procedure was in the delivery of a constant volume of air to the reaction mixture. This error may be reduced by selection of a longer period of aeration (Figure 1) when errors in both time of aeration and rate of delivery of air become less significant. For example, the calibration relationship for an aeration time of 60 minutes was determined as:

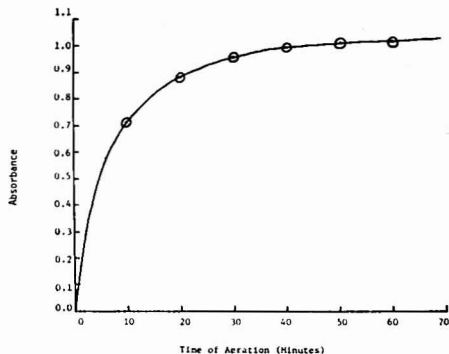


Figure 1. Graph showing relationship between the time of aeration at 100 ml/min of a 3-ppm formaldehyde solution and the absorbance at 549 nm as measured in a 1-cm cell

Table II. Wavelength for Maximum Absorption

Aldehyde	λ_{max} (nm) for 6-mercapto-3-substituted-s-triazolo-(4,3-b)-s-tetrazine
Formaldehyde	549
Acetaldehyde	537
Propionaldehyde	536
Butyraldehyde	532
Benzaldehyde	540

$$\text{Concn (ppm)} = 2.94 \times \text{Absorbance} \pm 2\% \quad (2)$$

Application to Industrial Samples. In use on industrial samples known to contain varying quantities of formaldehyde in substrates ranging from paper pulp to gelatinous adhesives and frothy detergents, the method gave reproducible results. In practice, samples were filtered where deemed advisable, and aqueous extracts made of paper pulp specimens.

SCOPE

After preparation of the appropriate calibration equation, this analytical procedure could clearly be used for the assay of other aldehydes. Table II lists the wavelength at which maximum absorption occurs for the 6-mercapto-3-substituted-s-triazolo(4,3-b)-s-tetrazines prepared from the given aldehydes. The absorption maxima, however, are too close to allow the application of the analysis to mixtures of aldehydes.

Received for review August 7, 1972. Resubmitted September 24, 1973. Accepted September 24, 1973. The authors thank the Reserve Bank of Australia for support of this work through a Rural Credits Development Fund Research Grant.

(2) U.S. Pharmacopoeia, 17th revision, Mack Printing Co., Easton, Pa., 1965, p 260.

(3) R. G. Dickinson and N. W. Jacobsen, "Organic Preparations and Procedures International," in press.

Liquid-Liquid Extraction of Zinc with Aliquat 336-S-I from Aqueous Iodide Solutions

Curtis W. McDonald¹ and Thornton Rhodes

Department of Chemistry, Southern University, Baton Rouge, La. 70813

Cadmium has been firmly established as a highly toxic metal (1). Extensive research is currently under way to develop new and better analytical methods for the detection and determination of this toxic material. There has also been considerable interest recently in developing pollution abatement processes to remove cadmium from industrial waste before it is allowed to enter the environment. In nature, this toxic metal is always found in trace quantities in zinc minerals and ores. Any industrial process for the removal of cadmium must take into account the presence of zinc which will usually be in large excess with respect to cadmium.

Liquid-liquid extractions using high-molecular-weight amines show great promise for processes for the rapid removal of toxic metal ions from aqueous solutions. The high-molecular-weight quaternary amine, Aliquat 336-S, has been recommended for the removal of mercuric and cadmium ions from industrial waste water (2-4). Aliquat 336-S is especially attractive in that it extracts mercuric and cadmium ions from both acidic and alkaline solutions.

In this communication, we have investigated the extraction behavior of zinc from aqueous iodide solutions with Aliquat 336-S. We compared our results with similar investigations with mercury and cadmium to ascertain any periodic trends in the zinc family. In addition, a method was developed for separating cadmium from zinc which shows promise for industrial applications.

EXPERIMENTAL

Apparatus. A NaI(Tl) well type gamma scintillation counter, 1.75 x 2.0 inches, was used for gamma counting. A Sargent heavy duty electrolytic analyzer was used for the electrogravimetric analyses. A Sargent NX digital pH meter was used to make the pH measurements.

Reagents. Aliquat 336-S (impure tricaprylammonium chloride) is a quaternary amine chloride available from General Mills, Inc., Kankakee, Ill. A 30% Aliquat 336-S-Cl stock solution was prepared by dilution with reagent grade xylene. The amine chloride was converted to the iodide by the method described by McDonald and Moore (4).

Cadmium-109 and zinc-65 tracers were obtained from New England Nuclear Corporation, Boston 18, Mass.

All other chemicals were reagent grade.

Extraction Procedure. Five milliliters of the indicated aqueous phase containing approximately 1×10^5 gamma counts per minute of zinc-65 were extracted at room temperature with an equal volume of Aliquat 336-S-I-xylene in 50-ml heavy-duty glass centrifuge tubes for five minutes. High speed motor stirrers, equipped with glass paddles, were used to carry out the extractions. After extraction, the tubes were centrifuged in a clinical centrifuge for two minutes. Each phase was then analyzed for zinc-65 by counting 1-ml aliquots in culture tubes with a well-type gamma scintillation counter.

¹ To whom correspondence should be addressed. Present address, Department of Chemistry, Texas Southern University, Houston, Texas 77004.

- (1) "Our Chemical Environment," J. Giddings and M. Monroe, Ed., Cantfield Press, San Francisco, Calif., 1972, p 158.
- (2) F. L. Moore, *Environ. Sci. Technol.*, **4**, 525 (1972).
- (3) F. L. Moore, *Separ. Sci.*, **7**, 505 (1972).
- (4) C. W. McDonald and F. L. Moore, *Anal. Chem.*, **45**, 983 (1973).

RESULTS

Aliquat 336-S-I and its salt with the iodo complex of zinc are essentially insoluble in aqueous solutions but show very high solubility in most common organic solvents.

The pertinent variables of the zinc-Aliquat 336-S-I extraction system were investigated by use of the evaluation procedure previously described. Each solution studied contained 1 mg/ml zinc as zinc iodide unless otherwise specified.

A minimum of approximately 4% Aliquat 336-S-I-xylene is required for quantitative removal of the zinc in an equal volume of a solution which is 1 mg/ml zinc 1M in HI. There was no measurable extraction observed when attempts were made to extract zinc from aqueous iodide with pure xylene or xylene which had been treated with 1M HI. A 5% Aliquat 336-S-I-xylene solution was used in the later investigations.

The extraction of zinc with 5% Aliquat 336-S-I-xylene as a function of HI concentration (Table I) shows that a relatively high HI concentration (approximately 0.8M) is required to remove the zinc essentially quantitatively from aqueous iodide solutions.

The effect of pH on the extractability of zinc is closely related to the effect of HI concentration. A solution at pH 1.0, containing approximately $10^{-2}M$ iodide added with the carrier and as HI in adjusting the pH, is 64% extracted with Aliquat 336-S-I-xylene. At a pH of 2.0, the per cent extracted is reduced to 27. If, on the other hand, the aqueous solution is made 1.0M in iodide with KI, the per cent extracted is increased to 98.3 for the pH 1.0 solution and 97.5 for the pH 2.0 solution. At a pH ≥ 4 , precipitation was observed in the solution containing excess iodide.

Equilibrium is achieved fairly rapidly; a mixing period of about two minutes proved to be adequate for essentially quantitative extraction. Five-minute extraction periods were used in the evaluation procedure.

Several aqueous reagents (Table II) were evaluated to determine their ability to strip zinc from 5% Aliquat 336-S-I-xylene solutions. The organic phase, initially containing a mg/ml zinc as the iodo zinc complex salt of Aliquat 336-S-I was stripped by extracting for five minutes with equal volume portions of the various strippants. All the strippants investigated stripped the zinc substantially with the majority removing more than 99% of the element from the organic phase. Those strippants removing more than 99% of the zinc include 0.5M Na₂S, Na₂SO₃ ($\geq 0.3M$), NaOH ($\geq 0.05M$), NH₃ ($\geq 0.05M$), EDTA ($\geq 0.2\%$), and EDTA ($\geq 0.05M$).

SEPARATION OF ZINC FROM CADMIUM

Since cadmium always occurs in trace quantities with zinc in nature and neither cadmium or zinc can be extracted selectively with Aliquat 336-S-I-xylene solutions when the two elements occur together in aqueous solution, a rapid, simple, quantitative method for separating the two is of utmost importance. Further studies of the Aliquat 336-S-I-xylene system led to a method of separating

Table I. Extraction of Zinc as a Function of HI Concentration^a

HI concentration, M	Zinc extracted, %
0.01	17.0
0.02	28.9
0.10	60.0
0.20	78.8
0.40	92.4
0.60	96.8
0.82	>99.5
1.64	>99.5

^a Initial aqueous solution contained 1 mg/ml zinc; solvent, 5% Aliquat 336-S-I-xylene.

these elements based on the selective stripping of zinc from the organic phase with an aqueous solution of Na_2SO_3 .

In a typical experiment, two solutions were used. Each solution contained 0.5 mg/ml cadmium carrier, 0.5 mg/ml zinc carrier and was 1.0M in HI. The first solution contained zinc-65 tracer (5×10^5 gamma counts per minute) and no radioactive cadmium, whereas the second solution contained cadmium-109 tracer and no radioactive zinc. Ten milliliters of each solution were extracted for 5 minutes with equal volumes of 5% Aliquat 336-S-I-xylene. Both cadmium and zinc extracted quantitatively. The two organic phases from these extractions were stripped for 5 minutes with equal volumes of 1M Na_2SO_3 and each phase was measured for its gamma activity. The organic phase of the solution originating from the solution containing the zinc-65 had no gamma activity and the aqueous phase had the predicted gamma activity. In the second solution, there was no measurable activity in the aqueous phase and the predicted number of counts in the organic phase was evident. The cadmium was stripped from the organic phase with concentrated ammonia (4). The carrier cadmium and zinc were determined from the two aqueous solutions by electrogravimetry (5). Better than 99% separation was achieved.

DISCUSSION

The proposed mechanism for the extraction of zinc from aqueous iodide solutions with Aliquat 336-S-I is the same as that proposed for mercury (3) and cadmium (4). This investigation with zinc completes studies of the elements in the IIB family. Definite periodic trends have emerged.

The least difficulty is encountered in extracting mercury, in that this element can be quantitatively removed from aqueous solutions that are highly acidic to solutions at a pH of 12.5. Cadmium can be extracted from acidic solutions, but for solutions with a pH >7 excess iodide is required for quantitative extraction. Zinc can be quantitatively extracted only from fairly acidic solutions, even in the presence of excess iodide.

Zinc requires a longer mixing time for quantitative separation than does mercury or cadmium. Very large aqueous

Table II. Stripping of Zinc from Aliquat 336-S-I-Xylene Solutions

Strippant	Zinc stripped, %	
Na_2S , M	0.1	63.0
	0.5	94.7
	1.0	>99.0
Na_2SO_3 , M	0.1	75.1
	0.5	>99.5
	1.0	>99.5
NaOH, M	0.025	88.6
	0.05	>99.5
	0.50	>99.5
NH_3 , M	0.025	90.2
	0.05	>99.5
	0.50	>99.5
EDA, %	0.1	96.1
	0.2	>99.5
	2.5	>99.5
EDTA, M	0.05	>99.5
	0.10	>99.5

ous phase to organic phase ratios can be used for extracting mercury and cadmium, whereas small ratios are required for zinc.

The reverse trend was observed for the stripping studies. Zinc is easily stripped from the organic phase with a wide variety of aqueous solutions; a smaller number can strip cadmium and only alkaline cysteine, of all the solutions tested, stripped mercury.

The results indicate that the complex salt formed by the interaction of the tetraiodomercurate(II) anion with Aliquat 336-S-I was more stable than the salts formed with the iodo complexes of cadmium and zinc. The order of stability of the complex salts is $\text{Hg} > \text{Cd} > \text{Zn}$. It is noteworthy to point out that the stability of the salts is in the same order as that of the iodo complexes—i.e., $\text{HgI}_4^{2-} > \text{CdI}_4^{2-} > \text{ZnI}_4^{2-}$.

The method of separating cadmium from zinc is rapid, simple, quantitative, and uses very inexpensive chemicals. It therefore shows some promise for large scale industrial use. It can also be used by the analytical chemist to make this separation on the laboratory scale.

The Aliquat 336-S-I-zinc extraction system is also of particular value to the analytical chemist since it offers a rapid, simple method for concentrating zinc from aqueous solutions containing only trace quantities of the element. The organic phase containing zinc can be used directly in atomic absorption determinations in which the analyst can benefit from both the solvent concentration and enhanced sensitivity of zinc.

ACKNOWLEDGMENT

The authors wish to thank their colleagues J. H. Jefferson and Celestine Tillman for helpful discussions and technical assistance.

Received for review June 25, 1973. Accepted August 20, 1973. Work supported by the United States Atomic Energy Commission, Contract Number AT-(40-1)-1452.

(5) "Handbook of Analytical Chemistry," L. Meites, Ed., McGraw-Hill, New York, N.Y., 1963, pp 5-174 and 5-181.

Rapid Determination of the Nitrogen Content of Cellulose Nitrate and Other Nitrate Esters by Means of a Modified Devarda Method

J. G. M. M. Smeenk¹

Technological Laboratory, the Netherlands Organization for Applied Scientific Research TNO, Rijswijk (Z.H.), The Netherlands

The nitrogen content of cellulose nitrate (CN) is commonly determined by the Lunge, the Schlösing, or the Devarda method. However, these methods are slow and very sensitive to environmental conditions (atmospheric pressure, temperature, solubility, and vapor pressure factors).

In practice this means that exact and reproducible results can only be produced by a specialized, skilled analyst. At the Technological Laboratory of the Netherlands Organization for Applied Scientific Research, a rapid method of determining the nitrogen content of cellulose nitrate was needed. This method should be at least as accurate as the Schlösing method, and less dependent on the specialization and skill of the analyst. These requirements were met by a modified Devarda method. In its classical way of operation (1-3) the Devarda method is rather time-consuming. Some time ago Potrafka *et al.* described an apparatus in which Devarda analyses of inorganic nitrate could be completed in a few minutes (4). For the analysis of organic nitrates, this time gain is almost totally offset by the slow conversion of the nitrate ester into an inorganic nitrate in alkaline medium, which must necessarily precede the Devarda reaction. For CN, this hydrolysis can take as much as 1.5 hr. In addition, this conversion is not always quantitative, as is the case with pentaerythritol tetranitrate (PETN).

Vinsson *et al.* (5) showed that certain stable esters hydrolyze very rapidly in a medium containing dimethylsulfoxide (DMSO), water, and alkali. Combination of this rapid hydrolysis technique with the apparatus described by Potrafka made possible a rapid and accurate determination of the nitrogen content of CN. In addition, the method is also practicable for the analysis of other nitrate esters such as glyceryl trinitrate (GN) and PETN.

EXPERIMENTAL

Apparatus. The apparatus is similar to the apparatus described by Potrafka. Over the titration vessel, a suction pipe has been installed to remove vapors of DMSO.

Reagents. The reagents used, except CN, GN, and PETN, were of analytical reagent quality and were used without further purification. All solutions were made using deionized water if not otherwise specified. Hydrogen peroxide was used as a 20% solution and sodium hydroxide as a 30% solution.

The indicator solution was prepared by mixing 1 part of Methyl Red solution (0.1%) and 9 parts of Bromocresol Green (0.1%).

Procedure. Samples containing GN or PETN are dried under vacuum at 30 °C for 2 hr and stored in a vacuum desiccator. After quickly weighing approximately 100 mg of CN or 80 mg of PETN in the reaction vessel, the sample is "wetted" with a few drops of ethanol. It is important that the sample does not contain coarse particles as this will result in low recoveries.

¹ Present address, Laboratorium Drinkwaterleiding Amsterdam, 73, Leidse Vaartweg, Heemstede, The Netherlands.

- (1) P. Howard, *Chem. Ind. (London)*, 1963, 1031.
- (2) M. M. Koshier *et al.*, *Ann. Chim. Anal. Appl. Ind.*, 18, 45 (1913).
- (3) Y. Lacroix *et al.*, *Mém. Poudres*, 39, 459-68 (1957).
- (4) K. A. Potrafka *et al.*, *Anal. Chim. Acta*, 31, 128-38 (1964).
- (5) J. A. Vinsson *et al.*, *Talanta*, 13, 1673-77 (1966).

Samples of approximately 80 mg of GN are dissolved in 3 ml of methylene chloride.

Five millimeters of DMSO are now added to the sample, which dissolves rapidly. Very carefully, 1 ml of 20% hydrogen peroxide is added; then the solution starts to generate heat. After adding 5 drops of 30% sodium hydroxide, the hydrolysis proceeds rapidly.

As a result of the reaction with DMSO, the hydrogen peroxide is readily consumed, and therefore at regular intervals a few drops of hydrogen peroxide are carefully added to the solution. In this way, approximately 2 ml of 20% hydrogen peroxide are added.

Thus a clear solution is obtained from which ethanol and methylene chloride (if present) have evaporated. As heat is generated, the solution starts boiling and, as a consequence, the last traces of hydrogen peroxide are removed.

The solution is cooled to room temperature and approximately 1 ml of 30% sodium hydroxide is added.

Five drops of silicon oil and 1 gram of Devarda alloy are added and the reaction vessel is inserted in the apparatus. The apparatus is now ready for the titration of the distilling ammonia.

In the same way, a blank is carried out.

The normality of the titrant (approximately 0.05N H₂SO₄) can be determined by repeating this procedure with pure, dried, potassium nitrate.

RESULTS AND DISCUSSION

Cellulose Nitrate. The quality of this procedure was checked by means of three samples of CN, whose nitrogen content was also determined by the Schlösing method (6), modified by Schulze and Tiemann (7) and by the Dumas method. PETN was used as a test compound. The results of the nitrogen determinations in the CN samples and the PETN sample by the Schlösing method and the Dumas method are presented in Table III. The results of the Devarda analyses are listed in Table I.

In general, the conversion of the nitrate ester into inorganic nitrate is a critical step in the analysis. It may be the cause of too low a nitrogen content. For instance, during an acid hydrolysis, evolution of nitric oxide is possible and, during an alkaline hydrolysis, reduction of the nitrate ester to nitric oxide, nitrogen, and ammonia should be prevented.

According to Howard (1) this reduction can be prevented by adding hydrogen peroxide during alkaline hydrolysis. It is clear from Table I that the results of the Devarda analysis are somewhat lower than the results of the Schlösing method. This is not specific for the application of DMSO in the hydrolysis medium.

The classical Devarda method, in which aqueous alkali and hydrogen peroxide are used, shows results which do not significantly differ from the results, found with the application of DMSO, if the same CN samples are analyzed. This may be seen from Table II.

The occurrence of a similar systematic error was confirmed by the results of the analysis of PETN. For this compound, the modified Devarda method gave a nitrogen content of 17.60%, whereas the Dumas analysis of this

- (6) M. Schlösing, *Justus Liebig's Ann. Chem.*, 40 (3), 479 (1853).
- (7) M. Tiemann, *Ber. Deut. Chem. Ges.*, 6, 1034 (1873).

Table I. Results of Nitrogen Determinations in 3 Cellulose Nitrate Samples by the Modified Devarda Method, Using DMSO in the Conversion Reaction

Nitrate ester	CN Sample A, CN Sample B, CN Sample C,		Modified Devarda method (corrected for hydrolysis error), % N
	% N	% N	
	13.50	12.84	11.93
	13.45	12.84	11.92
	13.43	12.79	11.95
	13.47	12.79	11.90
	13.45	12.76	11.88
	13.39	12.79	11.90
	13.43	12.80	11.90
	13.39	12.81	11.94
	13.43	12.81	11.94
	13.39		
Mean	13.43	12.80	11.92
Absolute std dev	0.04	0.03	0.02
Schlösing method	13.53	12.95	12.02

Table II. Results of Nitrogen Determination in 3 CN Samples by the Devarda Method, without DMSO in the Conversion Reaction

Nitrate ester	CN Sample A, CN Sample B, CN Sample C,		Modified Devarda method
	% N	% N	
	13.46	12.81	11.95
	13.44	12.78	11.97
	13.42	12.81	11.91
	13.48	12.82	11.91
	13.42	12.81	11.89
	13.46	12.84	
	13.41		
	13.42		
	13.45		
	13.45		
	13.46		
	13.45		
Mean	13.44	12.81	11.93
Absolute std dev	0.04
Modified Devarda method	13.43	12.80	11.92

^a Value not calculated.

compound gave 17.70%. This indicates that the application of hydrogen peroxide, which according to Howard should prevent loss of nitrogen-containing compounds, does not totally exclude these losses. This error did not originate from imperfect performance of the apparatus as could be proved by comparing the normalities of the titrant found by acidimetry and analyzing pure samples of potassium nitrate.

So it seemed necessary to use a correction factor, indicating the ratio between the Dumas and Devarda value of PETN. Table III shows the Devarda results which are corrected in this way. As may be seen, the agreement between the Schlösing method, the modified Devarda method, and the Dumas method is satisfactory.

Glyceryl Trinitrate and Pentaerythrite Tetranitrate. The results of these analyses are presented in Table IV. As in practice GN often occurs in combination with 2-nitrodiphenylamine and sometimes with diphenylamine, we also checked the influence of these compounds on the GN analysis. From Table IV, it is evident that 2-nitrodiphenylamine interferes to some extent with the GN determinations. As mentioned earlier, the conversion of the nitrate esters into sodium nitrate is accompanied by a small

Table III. Results of Nitrogen Determinations in Samples CN and PETN by the Dumas Method, the Schlösing Method, and the Modified Devarda Method

Nitrate ester	Schlösing method, % N	Dumas method, % N	Modified Devarda method (corrected for hydrolysis error), % N
	CN Sample A	13.53 ^a	13.53 ^a
CN Sample B	12.95 ^a	12.87 ^b	12.87 ^c
CN Sample C	12.02 ^a	12.03 ^d	11.99 ^e
PETN	...	17.70 ^a	17.70 ^f

^a Mean value of two determinations. ^b Mean value of five determinations. ^c Value not determined. ^d Mean value of four determinations. ^e Mean value of ten determinations. ^f Mean value of nine determinations.

Table IV. Results of the Analysis of GN and PETN Samples by the Modified Devarda Method

Nitrate ester	Sample, mg	Recovery	
		Uncorrected, mg	Corrected, mg
Glyceryl trinitrate	45.9	45.4	45.7
	45.9	45.3	45.6
	100.2	99.5	100.1
	69.0	68.3	68.6
Glyceryl trinitrate (+12.7 mg diphenylamine)	48.3	47.7	48.0
Glyceryl trinitrate (+3.6 mg 2-nitrodiphenylamine)	63.0	61.7	62.0
Glyceryl trinitrate (+9.7 mg 2-nitrodiphenylamine)	60.2	59.1	59.5
PETN	110.1	109.7	110.3
	80.1	79.5	80.0
	78.0	77.3	77.7
	81.2	80.6	81.1

systematic error, as was evident from the results of the analysis of PETN.

This error is ca. 0.4% (relative). By using pure PETN as a standard, it is possible to apply a correction factor for this systematic error in the GN determination in the same way as for CN.

CONCLUSIONS

The procedure described is accurate (mean absolute standard deviation $\pm 0.03\%$). The exactness of the nitrogen determinations in CN is a little difficult to judge, because one has to make a comparison with the results of another method of nitrogen determination.

From Table III, it is clear that the Dumas results can be used as a reference as appears from the results obtained with this method for PETN.

As may be seen from Table III, the agreement between the corrected results of the modified Devarda method and the Dumas method is satisfactory. The application of DMSO in the hydrolysis medium combines well with the Devarda method and is especially convenient for nitrate esters such as PETN and CN which hydrolyze slowly in aqueous alkaline medium. The conversion of the samples into inorganic nitrate is completed in ca. 10–15 minutes. The following Devarda reaction and the titration of the distilling ammonia take ca. 15–20 minutes.

If more than one sample has to be analyzed, the hydrolysis step can easily be performed for a series of samples.

The combination of a rapid hydrolysis of the nitrate ester with the Devarda reaction and a simple titration of the distilling ammonia has resulted in a rapid method, which is less sensitive to environmental influence and "operator experience" than the gas-volumetric techniques such as the Lunge method and the Schlösing method.

It is pointed out that the application of an automatic titration of the distilling ammonia could further reduce the possibility of human errors.

ACKNOWLEDGMENT

The technical assistance of W. R. Urban is gratefully acknowledged. Thanks are also due to the department of analytical chemistry of the Technical University Twente for performing the Dumas analyses.

Received for review April 6, 1973. Accepted September 4, 1973.

Consecutive Titration of Calcium and Magnesium in Ethanol-Water Mixture

Bo Wallén

Department of Analytical Chemistry, University of Uppsala, S-751 21 Uppsala 1, Sweden

Recently Rorabacher *et al.* (1) suggested that the result of an analytical procedure normally carried out in water might be improved if performed in a mixed solvent. This suggestion was based on the results of a determination of the stability constants of some metal ions with polyamines and polyaminopolycarboxylic acids in water-methanol mixtures. The values of the stability constants generally increased with the methanol content of the medium. End-point determinations in complexometric titrations may hence be improved in mixed solvents [See also (2) and (3)]. It was also observed that the changes in the stabilities of the complexes varied from one metal ion to another, a fact that might be used to increase the selectivity of a titration.

Some years ago a method based on these effects was developed in this laboratory for the simultaneous determination of calcium and magnesium. It will now be briefly presented as an example of what can be achieved by changing the medium. With a mercury indicator electrode, two potential breaks are obtained when a mixture of calcium and magnesium is titrated with ethylene glycol bis-(β -aminoethyl ether)-*N,N*-tetraacetic acid (EGTA) at pH 10 in an aqueous medium containing 70-80% (v/v) ethanol or methanol. In water, only the break corresponding to the titration of calcium is observed. The magnesium end-point break is obtained, however, at the expense of the quality of the calcium end-point break. To avoid this negative effect, calcium is titrated as usual in water at pH 8.5-9.0. When the end-point break for the calcium titration has been obtained, the titration is interrupted and alcohol added to make the solution 70-80% (v/v) with respect to this component. The pH is raised at the same time to about 10 and the titration continued until the magnesium end-point break is obtained.

EXPERIMENTAL

Apparatus. A fiber-tip, mercury(I) sulfate reference electrode and an amalgamated silver wire indicator electrode (4) were used.

- (1) D. B. Rorabacher, B. J. Blencoe, and D. W. Parker, *Anal. Chem.*, **44**, 2359 (1972).
- (2) G. Schwarzenbach and H. Ackermann, *Helv. Chim. Acta*, **31**, 1029 (1948).
- (3) T. A. Kiss, F. F. Gabl, T. M. Surányi, and I. J. Zsigrai, *Anal. Chim. Acta*, **43**, 340 (1968).
- (4) C. N. Reilley, R. W. Schmid, and D. W. Lamson, *Anal. Chem.*, **30**, 953 (1958).

The titration curves were recorded with a Metrohm Potentiograph E 336. A Metrohm pH meter E 396 equipped with a Metrohm 109 UX glass electrode and a mercury(I) sulfate reference electrode were used in the adjustment of pH. The instrument was calibrated against NBS standard buffers.

Solutions. Standard solutions (0.01M) of calcium and magnesium were prepared by dissolving weighed amounts of primary standard calcium carbonate and magnesium metal in nitric acid and sulfuric acid, respectively. The calcium carbonate (Merck) was dried for 24 hours at 150 °C before use. The magnesium metal (Johnson, Matthey & Co., Ltd.) contained not more than 0.01% by weight of total metallic impurities. The metal was washed successively in 5M hydrochloric acid, water, ethanol, and acetone and was allowed to dry at room temperature. A 0.01M solution of EGTA (Eastman) was prepared by dissolving the acid in the appropriate amount of sodium hydroxide. The solution was standardized against calcium at pH 9.0. A solution (0.002M) of EGTA-mercurate(II) was prepared by mixing equivalent amounts of mercury(II)acetate (Mallinckrodt p.a.) and EGTA (Eastman).

Ammonium nitrate (1M) and concentrated ammonia solution were used for buffering.

End Point. The end point was determined either from the inflection point of the curve or in the case of asymmetrical titration curves from the point of steepest potential break. The uncertainty in the end-point volume was estimated to ± 0.01 cm³ or less.

Procedure. Add 2 cm³ of 1M ammonium nitrate to the sample, which contains 0.005-0.1 mmole of each of calcium and magnesium, and introduce concentrated ammonia dropwise until the pH is 8.8-9.0. Add a few drops of 0.002M mercury(II)-EGTA and titrate with 0.01M EGTA using the amalgamated silver wire-mercury(II) sulfate electrode combination. Stop the titration shortly after the first end-point break, which corresponds to the amount of calcium present, and make the solution 80% (v/v) in ethanol. Add a few drops of concentrated ammonia solution, so that the pH meter reading is 10. Continue the titration until a potential break is obtained. The EGTA consumed between the first and second potential break corresponds to the amount of magnesium present.

RESULTS AND DISCUSSION

A representative selection of results is shown in Table I. The errors in the calcium titrations are probably due to the uncertainty in the location of the end point, since the theoretically calculated titration errors (5, 6) are less than 0.1% assuming $\Delta pM = 0.1$. The differences, which appear to be systematic in nature, correspond to an overtitration

- (5) L. G. Sillén in "Treatise on Analytical Chemistry," I. M. Kolthoff and P. J. Elving, Ed., Part 1, Vol. 1. The Interscience Encyclopedia, Inc., New York, N.Y., 1959.
- (6) A. Johansson and E. Wanninen, *Sv. Kem. Tidskr.*, **77**, 492 (1965).

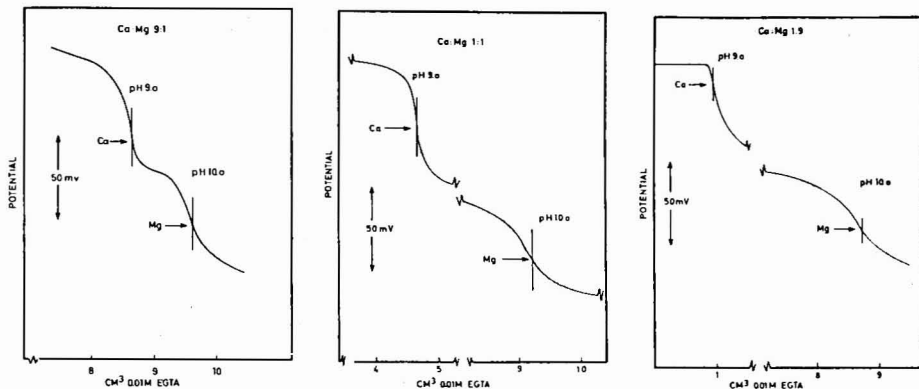


Figure 1. Titration of mixtures of calcium and magnesium with 0.0100M EGTA

Table I. Recovery of Calcium and Magnesium from Standard Solutions

Calcium, mg			Magnesium, mg			Ca:Mg mole ratio
Taken	Found	Difference, %	Taken	Found	Difference, %	
0.201	0.202	+0.5	1.235	1.229	-0.5	1:10
0.402	0.405	+0.7	2.223	2.216	-0.3	1:9
0.402	0.403	+0.2	1.235	1.220	-1.2	1:5
1.207	1.212	+0.4	1.235	1.230	-0.4	6:10
2.013	2.017	+0.2	0.123	0.120	-2.2	10:1
3.622	3.630	+0.2	0.247	0.244	-1.2	9:1
2.013	2.015	+0.1	0.247	0.243	-1.5	5:1
2.013	2.020	+0.3	1.235	1.225	-0.8	1:1
2.013	2.015	+0.1	0.741	0.725	-2.2	10:6

by 0.01 cm³. A similar error is present in the magnesium determinations.

Titration Curves. Titration curves for different ratios of calcium and magnesium in the sample are reproduced in Figure 1. They show that the potential of the indicator electrode changes sharply at the equivalence point corresponding to the titration of calcium, whereas the end-point break of magnesium is less sharp.

Attempts have been made to use a Gran function to determine the equivalence point of magnesium. Gran functions have proved useful, when one is dealing with less sharp end-point breaks (7-10). The data obtained in the titrations of aqueous solutions of calcium with EGTA in ammonia buffer at pH 9.0 did not, however, give straight lines when the values of the appropriate Gran function (10) were plotted *vs.* the volume of added EGTA after the equivalence point. Further investigations of the be-

havior of the mercury electrode [J-type (4)] in different buffers, which presently are performed in this laboratory, seem to confirm that this electrode does not follow Nernst's equation at higher pH and especially not in ammonia buffer. Potential-pH titrations according to Reilly and Schmid (11) of calcium and magnesium with EGTA have been made in different ethanol-water mixtures. Our preliminary experiments have shown that the potentials in the pH-independent regions are shifted toward higher potentials with increasing concentrations of ethanol. Furthermore the change of the magnesium level is consistently greater than that of calcium. This seems to be in agreement with the results reported by Rorabacher *et al.* (1) and also explains why the stepwise titration of calcium and magnesium is possible.

ACKNOWLEDGMENT

I wish to thank F. Nydahl for suggesting this problem and Å. Olin for helpful discussions.

Received for review June 25, 1973. Accepted August 28, 1973.

- (7) G. Gran, *Analyst (London)*, **77**, 661 (1952).
 (8) F. Ingman and E. Stihl, *Talanta*, **13**, 1431 (1966).
 (9) D. Dyrssen, D. Jagner, and F. Wengelin, "Calculation of Ionic Equilibria and Titration Procedures," Almquist & Wiksell, Stockholm, Sweden, 1968; Wiley, New York, N.Y., 1968, p 204.
 (10) A. Johansson, *Talanta*, **20**, 89 (1973).

- (11) C. N. Reilly and R. W. Schmid, *Anal. Chem.*, **30**, 947 (1958).

Solvent Extraction Studies of Chromium(III) with Tri-*n*-octylamine

B. E. McClellan,¹ M. K. Meredith,² Ray Parmelee, and J. P. Beck³

Department of Chemistry, Murray State University, Murray, Ky. 42071

Chromium(III) has been reported to be non-extractable as an ion association complex with high molecular weight amines (1). This is probably due to the slowness with which the coordinated water molecules are replaced by negative ions. Stability constant data show that chromium(III) should form an anionic complex with thiocyanate which might be extractable as an ion association complex with high molecular weight amines (2). This study examines the extraction characteristics of such a system and attempts to separate other transition metal ions from chromium(III).

EXPERIMENTAL

Apparatus. A Tracerlab Model P-20D scintillation detector connected to a Model SC-71 scaler was used to count the gamma-emitting isotopes in both the organic and the aqueous phases. An Eberbach water bath shaker was used for agitation of the samples.

Reagents. Chromium(III) Solution. A 30 gram/l. solution of chromium nitrate was prepared from Matheson Coleman and Bell reagent grade material. Enough chromium-51 (Nuclear Science and Engineering Corporation) in the plus three oxidation state was added to give approximately 10,000 counts per minute per milliliter of the aqueous solution.

Potassium Thiocyanate. A saturated solution of the reagent grade material (Matheson Coleman and Bell) was prepared in deionized water.

Tri-*n*-octylamine. A 5% solution of the liquid (Eastman Organic Chemicals) was prepared in reagent grade carbon tetrachloride.

Procedure. Five milliliters of an aqueous phase consisting of chromium(III) at a concentration of $4 \times 10^{-4}M$ (20 ppm), plus enough chromium-51 to give a count of approximately 10,000 cpm/ml, and thiocyanate at a concentration of 4.75M was allowed to stand at 25 °C and 35 °C in a constant temperature water bath for periods ranging from 5 minutes to 2 hours. Following the standing period, the aqueous phase was made 0.1M in hydrochloric acid and extracted with 0.25M tri-*n*-octylamine in carbon tetrachloride by agitation in a 125-ml separatory funnel for 2 minutes on a mechanical shaker. The phases were allowed to separate, and were counted for gamma activity to obtain the per cent extraction of the chromium(III).

In order to study the effect of the thiocyanate concentration on the extractability of chromium(III), a chromium(III) solution of $4 \times 10^{-4}M$, spiked with chromium-51, was allowed to stand at 40 °C for 2 hours in a water bath in the presence of various concentrations of thiocyanate ranging from 0 to 9.5M. Following the standing period, an aliquot of the aqueous phase was made 0.1M in HCl and extracted with 0.25M tri-*n*-octylamine in CCl₄ by shaking for 2 minutes. The phases were allowed to separate and were counted.

A study of the effect of the tri-*n*-octylamine concentration on the per cent extraction of chromium(III) was made. The chromium(III) concentration, plus chromium-51 was again $4 \times 10^{-4}M$ and the thiocyanate concentration was 4.75M. The aqueous solutions were allowed to stand at 50 °C for 2 hours prior to making 0.1M in HCl and extracting with tri-*n*-octylamine in CCl₄ in concentrations from 0.001 to 1.0M. The phases were allowed to separate and were counted.

¹ Author to whom inquiries should be addressed.

² Present address, Seagram's Distillery, Louisville, Ky. 40201.

³ Present address, Dow-Corning, Elizabethtown Plant, Elizabethtown, Ky. 42701.

(1) B. E. McClellan and V. M. Benson, *Anal. Chem.*, **36**, 1985 (1964).

(2) Henry Freiser and Quintus Fernando, "Ionic Equilibria in Analytical Chemistry," John Wiley and Sons, New York, N.Y., 1963, p 311.

The effect of acidity on the extraction of chromium(III) with tri-*n*-octylamine was studied using conditions similar to the previous experiments. The hydrochloric acid concentration was varied from 0.01 to 2.0M.

A study of the effect of the chromium(III) concentration on the per cent extraction of the ion with the tri-*n*-octylamine system was made. The optimum extraction conditions described above were used and the chromium(III) concentration was varied from 0.01 to 20 ppm.

Studies of the extraction characteristics of other transition metal ions such as Co(II), Zn(II), Fe(III), Mn(II), Cd(II), and Hg(II) were also made. The metal ion concentration, plus radioactive tracer, was in the range of $10^{-4}M$. The thiocyanate, tri-*n*-octylamine, and hydrogen ion concentrations were varied in order to determine the optimum conditions. The mole ratios of amine to metal were also determined for each ion.

Extractions were performed at 25 °C to determine the effectiveness of the method for the separation of Co(II), Zn(II), Fe(III), and Hg(II) from chromium(III). The [CNS⁻] was 1M, the [TOA] was 0.1M, the [H⁺] was 0.1M, and the metal ion concentrations were all $1 \times 10^{-4}M$. The shaking time was 2 minutes. Gamma-emitting isotopes were used as tracers to determine the distribution of all ions.

RESULTS AND DISCUSSION

A graph of per cent extraction of chromium(III) as the thiocyanate complex with tri-*n*-octylamine in carbon tetrachloride vs. time at 25 °C and 35 °C is shown in Figure 1. This plot reflects the slowness with which coordinated water molecules are replaced with thiocyanate anions to form the negative species such as $Cr(H_2O)_2(CNS)_4^-$. Heating greatly facilitates the removal of the coordinated water. Only about 42% extraction of chromium(III) occurred after 60-hour standing at 25 °C as compared to the much more rapid and complete formation of the extractable species at 35 °C. The complex, probably $Cr(H_2O)_2(CNS)_4^-$, was found to be immediately extractable as the ion association complex with tri-*n*-octylamine following its slow formation.

A plot of per cent extraction of chromium(III) vs. thiocyanate concentration is shown in Figure 2. At these particular conditions, about 90% extraction occurs above 5M thiocyanate. The high concentration of thiocyanate required reflects the moderate stability of anion complexes such as $Cr(H_2O)_2(CNS)_4^-$ ($\log k_1 k_2 k_3 k_4 = 1.7$) (2).

The equation for the distribution ratio of ion association complexes with high molecular weight amines takes the form $D = K^* [R_3N]_n$, if all other variables such as thiocyanate and acidity are held constant (1). Therefore, $\log D = n \log [R_3N] + \log K^*$ and a plot of $\log D$ vs. $\log [R_3N]$ should yield a straight line with a slope of n where n is the number of amines per chromium in the complex. Figure 3 shows such a plot where the slope of the straight line is unity. This indicates a complex with the probable formula $R_3N^+ HCr(H_2O)_2(CNS)_4^-$ as the extracted species.

A plot of per cent extraction of chromium(III) vs. hydrochloric acid concentration (Figure 4) shows an unexpectedly high dependence on the [HCl] of the aqueous phase. A maximum of 97% extraction of chromium(III) occurred at an [HCl] of 0.07M from a thiocyanate medium of 4.75M using 0.25M amine solution in CCl₄. The chro-

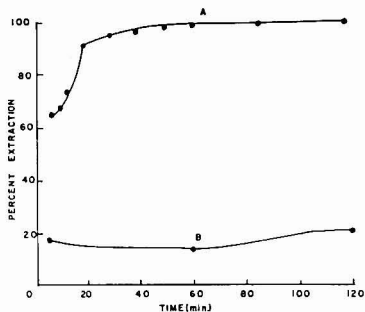


Figure 1. Extraction of chromium(III) as the thiocyanate complex with tri-*n*-octylamine

A. 35 °C, B. 25 °C $[Cr^{3+}] = 4 \times 10^{-4}$, $[CNS^-] = 4.75$, $[Amine] = 0.25$

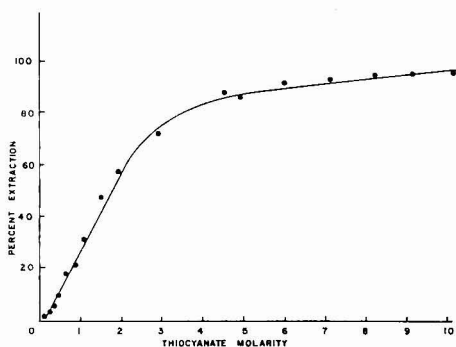


Figure 2. Extraction of chromium(III) with tri-*n*-octylamine at various concentrations of thiocyanate

$[Cr^{3+}] = 4 \times 10^{-4}$, $[H^+] = 0.1$, $[Amine] = 0.25$

mium(III) solution was allowed to stand in a constant temperature water bath at 50 °C for 1 hour prior to the 2-minute extraction period. If the solution is allowed to stand at room temperature following the 1-hour heating period, for any appreciable length of time prior to extraction, a decomposition of the thiocyanate complex occurs. The solution, however, may remain at room temperature for up to 1 hour without any appreciable decomposition. After standing for 60 hours, the per cent extraction decreased from 94% to 67%. It is essential that the hydrochloric acid be added just prior to extraction with tri-*n*-octylamine solution, as a precipitate (probably sulfur) results on heating thiocyanate in the presence of hydrochloric acid. The acid, however, is necessary to form the amine hydrochloride from the free base. For this reason, a reflux method such as that suggested by Morrison and Freiser for the extraction of chromium(III) with acetylacetone is ineffective (3).

The per cent extraction of chromium(III) with tri-*n*-octylamine was independent of the chromium(III) concentration in the range studied. In the chromium(III) concentration range of 0.01 to 20 ppm ($4 \times 10^{-4}M$), the per cent extraction values varied from 95.8 to 96.1%. This is in agreement with previous findings as the per cent extraction normally does not vary with the metal ion concentra-

(3) George Morrison and Henry Freiser, "Solvent Extraction in Analytical Chemistry," John Wiley and Sons, New York, N.Y., 1957, p 201.

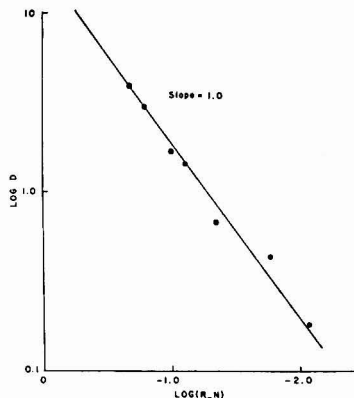


Figure 3. Plot of $\log D$ vs. $\log [R_3N]$ for the extraction of chromium(III) with tri-*n*-octylamine

$[Cr^{3+}] = 4 \times 10^{-4}$, $[CNS^-] = 4.75$, $[H^+] = 0.1$

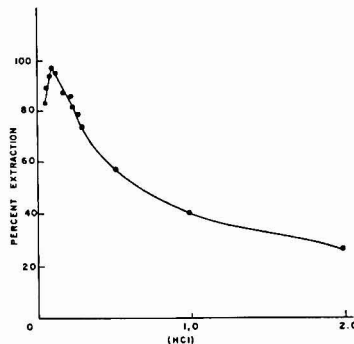


Figure 4. Extraction of chromium(III) as the thiocyanate complex with tri-*n*-octylamine at various concentrations of HCl

$[Cr^{3+}] = 4 \times 10^{-4}$, $[CNS^-] = 4.75$, $[Amine] = 0.25$

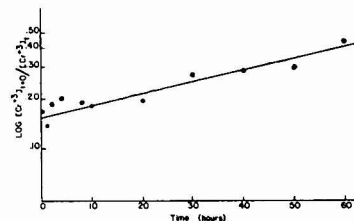


Figure 5. Plot of $\log [Cr(III)]_{t=0} / [Cr(III)]_t$ vs. time

$[Cr^{3+}] = 4 \times 10^{-4}$, $[CNS^-] = 4.75$, $[Amine] = 0.25$, $[H^+] = 0.07$, $t = 25$ °C

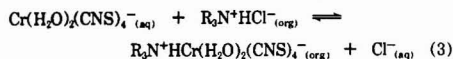
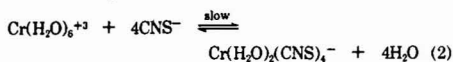
tion as long as the ligand/metal ion ratio is high enough to supply at least a stoichiometric amount of ligand.

A plot of $\log [Cr^{3+}]_{t=0} / [Cr^{3+}]_t$ vs. time is shown in Figure 5. The initial chromium(III) concentration was $4 \times$

Table I. Optimum Conditions for the Extraction of Selected Transition Metals

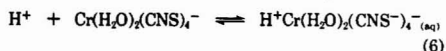
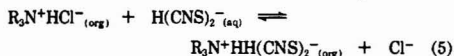
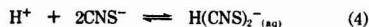
Metal ion	[M ⁺]	[CNS ⁻]	[TOA]	[H ⁺]	Max. % E	Mole ratio
Cr(III)	4 × 10 ⁻⁴	4.75M	0.25M	0.07M	97.0%	1:1
Co(II)	1 × 10 ⁻⁴	0.90M	0.10M	0.15M	99.8%	2:1
Zn(II)	1 × 10 ⁻⁴	0.90M	0.10M	0.30M	99.9%	2:1
Fe(III)	1 × 10 ⁻⁴	1.50M	0.05M	0.075M	98.5%	1:1,2:1,3:1
Mn(II)	5 × 10 ⁻⁴	6.00M	0.30M	0.30M	70.0%	...
Cd(II)	1 × 10 ⁻⁴	3.00M	0.10M	0.075M	74.6%	1:1
Hg(II)	1 × 10 ⁻⁴	0.10M	0.25M	0.075M	99.0%	2:1

10⁻⁴M, the thiocyanate concentration 4.75M, the trioctylamine concentration 0.25M, the [H⁺] 0.07M, and the temperature was 25 °C. The straight line plot obtained indicates a first-order reaction in chromium(III). A mechanism similar to that proposed by various authors (1, 4, 5) is postulated for the ion association system as follows:



Step 2 is the slow process, with step 3 and the distribution of the extractable complex from aqueous to organic phase being rapid. This is evidenced by the fact that the extraction of chromium(III) complex is very rapid once it has formed in the preliminary heating and standing process.

Some possible competing reactions are:



Good *et al.* (6) proposed a competing reaction analogous to step 6 for the extraction of iron(III) from a chloride system with high molecular weight amines.

The green color of chromium(III) darkens to a deep violet when heated with excess thiocyanate. If the pH is held constant, Beer's law is obeyed between 0.01 and 0.20 mg/ml of chromium at a wavelength of 568 nm. The method, however, has little to recommend it as the molar absorptivity is low (180).

Chromium(VI) as CrO₄²⁻ or Cr₂O₇²⁻ was found to be immediately extractable with tri-*n*-octylamine without the addition of thiocyanate as the chromium is already in the anionic form. Although no detailed study of this system has been made at this time, the extracted species would be expected to be [R₃N⁺H]₂CrO₄²⁻ or [R₃N⁺H]₂Cr₂O₇²⁻. Fasolo *et al.* have reported a similar extraction of chromium(VI) with tribenzylamine (7).

Separation of many transition metals from chromium(III) is possible using this extraction system by virtue of the rapid formation of the anionic thiocyanate complexes of most metals as compared to the relatively slow formation of the Cr(H₂O)₂(CNS)₄⁻ complex. Table I shows the conditions determined for extraction of selected transition metal ions with TOA. Since Co(II), Zn(II), Fe(III), and Hg(II) all show quantitative extraction at much lower CNS⁻ concentration than does chromium(III), this alone allows the separation of these ions from chromium(III). Also, these ions extract very rapidly at room temperature as opposed to the very slow formation of the extractable complex of chromium(III). Mn(II) and Cd(II) cannot be completely extracted with TOA. Therefore, considering the fact that the other transition metals studied were extractable from lower thiocyanate concentrations than that required for chromium(III) and that the chromium(III)-thiocyanate complex is quite slow in forming, it is easy to separate these other transition metals from chromium(III).

Several extractions were performed using mixtures of 1 × 10⁻⁴M Cr(III), Co(II), Zn(II), Fe(III), and Hg(II) under the conditions described in the experimental section. Very little (<5%) chromium(III) extracts while quantitative (98-100%) extraction of Co(II), Zn(II), Fe(III), and Hg(II) was achieved in all cases. Approximately 30% of the Mn(II) and Cd(II) is left in the aqueous phase along with the chromium(III); therefore, the separation of these ions from chromium(III) is not feasible by the method.

Received for review April 4, 1973. Accepted August 16, 1973. The authors are indebted to the Department of Chemistry, Murray State University, and to the Committee on Institutional Studies and Research for financial support of this project.

(4) M. L. Good and S. E. Bryan, *J. Inorg. Nucl. Chem.*, **20**, 140 (1961).
 (5) J. Y. Ellenburg, G. W. Leddicotte, and F. L. Moore, *Anal. Chem.*, **26**, 1045 (1954).
 (6) M. L. Good, S. E. Bryan, F. F. Holland, and G. J. Maus, Jr., *J. Inorg. Nucl. Chem.*, **25**, 1187 (1963).

(7) G. B. Fasolo, R. Malvano, and A. Massaglia, *Anal. Chim. Acta*, **29**, 569 (1963).

Selective Separation and Concentration of Silver via Precipitation Chromatography

William P. Zeronsa,¹ Gregory Dabkowski, and Sidney Siggia

Department of Chemistry, University of Massachusetts, Amherst, Mass. 01002

The particular reaction of certain metal ions with monosubstituted acetylenic compounds is well known (1).



The unique character of this reaction has served as a basis for the qualitative and quantitative determination of the acetylenic functionality. Little use has been made of this specific reactivity for the analysis or separation of the silver ion. This work demonstrates the application of terminal acetylenics to the selective analytical separation and concentration of silver.

Nieuwland (2) divides the metalloacetylenic derivatives on the basis of whether the triple bond persists and hydrogen atoms are released or whether metal compounds add to the acetylenic compound with no loss of hydrogen, i.e.,



This work is concerned with those metallo-derivatives which form easily and are reversible in aqueous systems. This limits our interest to silver(I), copper(I), and mercury(I and II), because none of the others proceed to completion or react at all.

Analytical separation (3-5) of copper and silver from other metals, using acetylenes, encountered stoichiometric difficulties and varying degrees of hazard. The selectivity of acetylides for copper and silver has been employed in flotation processes (6) as well as in precipitation from ammoniacal solution in batch processes (7). Also, many standard techniques have been described (8-10) for quantitative analysis of acetylenes.

This led our work to the field of precipitation chromatography, employing a solid support and an organic precipitating agent immobilized on the support. The solution of silver ion to be analyzed is treated with a 2% w/v sodium acetate solution to attain a basic pH. The solution is then passed through a 6-cm \times 1-cm i.d. column of 20% 1-pentadecyne coated on 100-110 Anakrom AB at a flow rate of 3 ml/min. Final elution was accomplished with 50 or 100 ml of 1:1 nitric acid-water eluent after the column is washed with 50 ml of deionized water.

¹ Present address, Charles Pfizer Inc., Groton, Conn.

- (1) J. A. Nieuwland and R. R. Vogt, "The Chemistry of Acetylenes," Reinhold Publishing Corp., New York, N.Y., 1945, Chap. 2.
- (2) *Ibid.*, p 41.
- (3) J. Scheiber, *Fresenius' Z. Anal. Chem.*, **48**, 529 (1909).
- (4) V. F. Brameld, M. T. Clark, and A. P. Seyfang, *Chem. Ind. (London)*, **66**, 346 (1947).
- (5) F. Pollitzer, *Angew. Chem.*, **36**, 262 (1923).
- (6) J. T. Terry, U. S. Patent 1544197 (1925); *Chem. Abstr.*, **19**, 26 31 (1925).
- (7) G. S. Masaidova, A. S. Yulkinina, L. S. Gal'braikh, and Z. A. Rogovin, *Vysokomol. Soedin.*, **8**, 865 (1966).
- (8) S. Siggia, "Quantitative Organic Analysis Via Functional Groups," 3rd ed., John Wiley and Sons, New York, N.Y., 1967, Chap. 9.
- (9) M. Micoque and J. A. Gautier, *Bull. Soc. Chim.*, **1958**, 467.
- (10) S. Prevost, W. Chodkiewicz, P. Cadlot, and A. Willemart, *Bull. Soc. Chim.*, **1960**, 1742.

EXPERIMENTAL

Apparatus. Analysis was accomplished by using the Perkin-Elmer Models 403 and 290 atomic absorption spectrophotometers. In the upper ranges, the Volhard titration method was used.

Reagents. All water used to make up the reagents was passed through a Culligan deionizer after being distilled.

Sodium Acetate Solution: 2% w/v Sodium Acetate in Water. Reagent grade sodium acetate, obtained from the J. T. Baker Chemical Company, was purified by recrystallization from hot methanol and water. A 2% weight/volume solution was prepared and passed through the acetylenic column to further purify it of silver. Evaporation under reduced pressure recovered the sodium acetate free of silver in a reasonable period of time.

Eluent: 1:1 HNO₃:H₂O. Concentrated nitric acid was obtained from the Fisher Scientific Company and diluted 1:1 by volume with distilled deionized water.

Standard Silver Solutions. A 1000-ppm stock solution of silver was obtained from the Barnes Engineering Company. Standards ranging from 0.05 to 10.0 ppm were obtained by taking aliquots of the stock and diluting with 1:1 HNO₃:H₂O. The standards were used to calibrate the atomic absorption spectrophotometer and were made fresh prior to the analysis step.

The trial silver sample solutions were also made from the stock silver solution and the 2% sodium acetate solution was used to make the proper dilutions.

1-Pentadecyne was obtained from Farchan Research Laboratories and used directly.

100-110 Anakrom AB was obtained from Analabs, Inc.

Procedure. Liquid phases were coated by slurring weighed amounts of the acetylenics with weighed solid supports using anhydrous ethyl ether as solvent. The ether was then evaporated by employing a rotary evaporator connected to a water aspirator. Final solvent removal was accomplished by spreading the support on aluminum foil and air drying. Percentage loading was verified by thermogravimetric analysis.

Columns were prepared by first slurring the prepared support with deionized distilled water and then pouring the mixture into a buret. A glass wool plug was used to retain the support in the column, and to prevent agitation of the upper layers of the support by the eluent.

The column was conditioned by passing 5 ml of 2-ppm silver solution in the sodium acetate solution through the column and eluting with 1:1 HNO₃:H₂O. This was repeated three times to take up any nonreversible sites available. The column was then rinsed with the 2% sodium acetate solution in preparation for the following sample run. The low-ppm samples were concentrated at a flow rate of 3 ml/min. The column was washed with 50 or 100 ml of 1:1 HNO₃:H₂O after rinsing with 50 ml of deionized water. Column life is extended by immediately rinsing the excess acid from the column with distilled water followed with about 25 ml of the 2% sodium acetate solution.

Standard Perkin-Elmer atomic absorption techniques were followed in the final analysis. Where applicable, the Volhard titration method was used (11).

RESULTS AND DISCUSSION

A series of acetylenic compounds and supports were evaluated for column use. From Table I, it can be seen that the field was narrowed to four acetylenes coated on 100-110 Anakrom AB. Of these four, the most efficient was 1-pentadecyne. The capacity of the pentadecyne column was determined by a batch experiment to be 0.83 mg Ag⁺/gram dry resin.

- (11) I. M. Kolthoff and E. B. Sandell, "Textbook of Quantitative Inorganic Analysis," 3rd ed., Macmillan, New York, N.Y., 1965, p 545.

Table I. Comparison of Stationary Phases and Supports on Anakrom AB

Stationary phases	State at 25 °C	Column performance
1. 1-Hexyne	Liquid	Washed off
2. 1,7-Octadecyne	Liquid	Washed off
3. 1-Dodecyne	Liquid	Retained
4. 3-Phenyl-3-hydroxy-1-butyne	Solid	Washed off
5. 1-Phenyl-2-propyn-1-ol	Liquid	Washed off
6. 1-Pentadecyne	Liquid	Retained
7. 1-Octadecyne	Liquid, solid	Retained
8. Dipropargyl-1,4-benzenedicarboxylate	Solid	Retained

Supports	Comment	Code
Celite	a, c	a. Activity for silver
Aluminum oxide	a, f	b. Difficult to pack when loaded
CTFE 2300	b, e	c. Good packing and high loading
Anakrom AB (100-110)	c	d. Poor flow properties
Anakrom AB (300)	c, d	e. Hydrophobic when coated
Anakrom ABS (100-110)	b, e	f. Low affinity for acetylenic phase

Table II. Recovery of Silver upon Injections

Soln concn, ppm	Soln vol, ml	Total Ag* injected, µg	Amt Ag recovered, µg	Recovery, %	Av recovery and rel std dev
0.197	50	9.85	9.95	101.0	
0.197	50	9.85	9.95	101.0	100.3 ± 1.6
0.197	50	9.85	9.75	89.9	
0.394	50	19.70	19.75	100.2	
0.394	50	19.70	19.75	100.2	99.8 ± 0.9
0.394	50	19.70	19.50	98.9	
0.591	50	29.55	29.15	98.7	
0.591	50	29.55	29.75	101.7	99.3 ± 2.3
0.591	50	29.55	29.15	98.7	

Table III. Recoveries of Silver Solutions

Original volume, l	Flow rate, ml/min	Original concn, ppm	Final concn, ppm	Final elution vol, ml	Recovery, %	Av recovery and rel std dev	Concn factor
1	3	20.0	200	100	100		10
1	5	20.0	198	100	99		10
1	10	20.0	199	100	99.5		10
1	22	20.0	198	100	99		10
1	30	20.0	198	100	99		10
1	35	20.0	198	100	99		10
1	45	20.0	198	100	99		10
1	45	20.0	194	100	97		10
1	100	45.0	445	100	99		10
10	45	2.00	190	100	95		100
10	45	2.00	192	100	96		100
10	48	2.00	194	100	98		100
1	45	0.200	198	100	99		100
5	3	0.0005	0.043	50	86		100
5	3	0.0005	0.046	50	93	88 ± 6	100
5	3	0.0005	0.042	50	85		100
5	3	0.001	0.084	50	84		100
5	3	0.001	0.081	50	81	81 ± 3	100
5	3	0.001	0.079	50	79		100
5	3	0.002	0.156	50	78		100
5	3	0.002	0.150	50	75	78 ± 3.5	100
5	3	0.002	0.161	50	81		100
5	3	0.003	0.237	50	79		100
5	3	0.003	0.217	50	72	76 ± 6	100
5	3	0.003	0.227	50	76		100

A series of eluents were evaluated for elution efficiency. Both 0.10M EDTA and 0.10M ammonium hydroxide failed to elute any silver. Up to 8M sulfuric acid eluted up to 50% of the silver in 50 ml. Varying concentrations of nitric acid were tested for silver removal. From these data as shown in Figure 1, a 1:1 mixture of nitric acid to water was chosen.

An elution profile for silver using 1:1 HNO₃:H₂O is shown in Figure 2. Table II demonstrates silver recoveries for the 1-pentadecyne column upon injection of 50 ml of standard silver solutions containing ~2% w/v sodium acetate.

Recoveries of silver ion from solutions containing as low as 0.5 ppb were accomplished. For solutions whose origi-

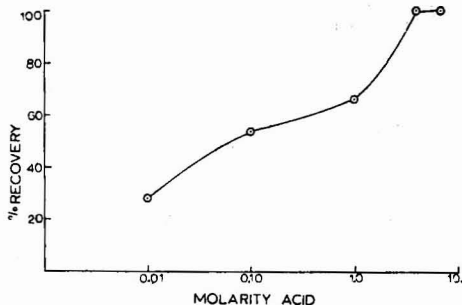


Figure 1. Efficiency of silver elution vs. nitric acid concentration

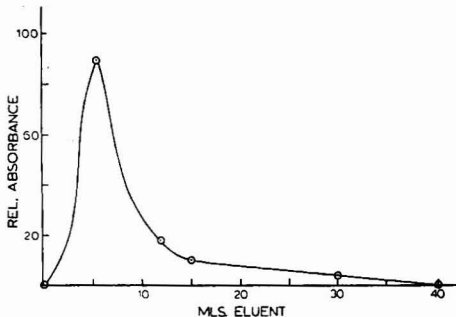


Figure 2. Elution curve for silver with 8M nitric acid

nal concentrations were 0.2 ppm and below, final analysis was performed by atomic absorption. Above that level, final analysis was performed using the Volhard titration (Table III).

To demonstrate the selectivity of the column for silver, 1 liter of a solution containing 60 ppm copper, 10 ppm nickel, 20 ppm zinc, 0.25 ppm lead, 20 ppm calcium, 0.22 ppm manganese, 0.06 ppm iron, 20 ppm cadmium, and 20 ppm Ag was passed through it at a flow rate of 3 ml/min. Recoveries for silver averaged $97.0 \pm 1.1\%$. Copper(I) and mercury(I) and (II) were the only interferences. No other ions were retained by the column. The ease of oxidation of Cu(I) left only mercury(I) and (II) as interferences. Mercury works its interference in two ways. Mercury(I) will react with the acetylene to the extent that if 250 ml of solution at a concentration of 500 ppm of mercury(I) is passed through the column, 14% is retained. At the same concentration, mercury(II) is retained to the extent of 4%. Mercury(II) under acidic conditions can hydrate the acetylene to the corresponding ketone (12). However, selective reduction or analysis by atomic absorption provides a means of selectively nullifying the interference.

CONCLUSIONS

A commercially available, long chain terminal acetylene coated on a solid support has the ability to selectively concentrate and/or separate silver from a variety of cations over a wide range of concentrations. Its advantages

(12) M. Kutscherov, *Chem. Ber.*, **14**, 1532 (1881).

lie in its ease of preparation and minimum amount of sample handling and treatment. Cationic interferences are minimal and can be excluded with relative ease. Furthermore, a study of the acetylides formed using differential scanning calorimetry demonstrated no safety hazard requiring unusual precautions for the laboratory use of acetylenics as column materials.

Considering the recovery of silver, adsorption effects account for silver losses (13, 14). Radiometric methods using ^{110}Ag have been used to follow concentration steps and account for silver losses (15). To obtain reproducible results, one must be mindful of adsorption effects which are buffer, container, concentration, time, temperature, and technique dependent.

The overall performance of the acetylenic column is comparable with other existing silver concentration techniques (16). With regard to its selectivity, its performance is unchallenged.

Received for review April 30, 1973. Accepted October 5, 1973. This work was supported under Grant PRF 5399AC by the Donors of the Petroleum Research Fund administered by the American Chemical Society.

(13) F. K. West, P. W. West, and F. A. Iddings, *Anal. Chem.*, **38**, 1566 (1966).

(14) R. Woodruff, B. R. Culver, D. Schrader, and A. B. Super, *Anal. Chem.*, **45**, 231 (1973).

(15) T. Chao, M. Fishman, and J. Ball, *Anal. Chim. Acta*, **47**, 169 (1969).

(16) *Ibid.*, p. 190.

Determination of Total Cyanide in the Presence of Palladium

George W. Latimer, Jr., L. Ruth Payne, and Marguerite Smith

PPG Industries, P. O. Box 4026, Corpus Christi, Texas 78408

The problem of determining cyanide in the presence of metal ions which form acid-stable, cyano complexes has been dealt with in a number of ways. If the sample is a solid and free from other nitrogen-containing materials, carbon and nitrogen values have been used (1-3), although not always successfully (3). Fusion with potassium

(1) F. Feigl and G. B. Heisig, *J. Amer. Chem. Soc.*, **73**, 5630-5 (1951).

(2) W. L. Magnuson, E. Griswald, and J. Kleinberg, *Inorg. Chem.*, **3**, 89-93 (1964).

(3) C. J. L. Lock and G. Wilkinson, *J. Chem. Soc.*, **1962**, 2281-5.

in a nickel bomb has proved satisfactory for cyano-rhenium complexes (3), but is tedious and cannot be applied directly to aqueous systems. Many acid-stable complexes are analyzed by distilling the cyanide from acidified mercuric magnesium chloride solution or after refluxing the compound with cuprous chloride (4); however, even with such vigorous conditions, recoveries of cyanide from systems containing palladium, mercury, and cobalt range between 4-90% (4).

(4) C. T. Ely, *J. Water Pollut. Contr. Fed.*, **40**, 848-56 (1968).

Table I. Effect of Conditions on Recovery of Cyanide from Pd Solutions^a

Run	Conditions	Cyanide recovered, %
1	Schulek titration of sample only, <i>i.e.</i> , without distillation	None
2	Mercaptoacetic acid omitted; 20 ml H ₃ PO ₄ present during distillation	10
3	Mercaptoacetic acid present; H ₂ SO ₄ substituted for H ₃ PO ₄	90
4	Distillation with mercaptoacetic acid and 20 ml H ₃ PO ₄ present	99.5 ± 0.6 ^b

^a Systems contained weighed amounts (approximately 0.1 g each) of Pd and KCN. ^b Confidence limits (95%) for 5 determinations.

Although this paper describes a procedure for the determination of cyanide in palladium-containing solutions and in palladium cyanide, the method should be applicable to many acid-stable complexes.

EXPERIMENTAL

Apparatus. The distillation unit was either commercial Kjeldahl equipment or a simple ground-glass setup equipped with a separatory funnel for adding reagents to the reaction flask. The delivery tubes, containing wads of glass wool saturated with NaOH solution to ensure intimate contact of the first vapors with base, led directly to 500-ml volumetric flasks which served as the HCN absorbers.

Reagents and Solutions. Palladium cyanide was either purchased commercially or prepared by reaction between palladium chloride and mercuric cyanide (3). The palladium standard was prepared by dissolving the metal in aqua regia, adding H₂SO₄, and evaporating to fumes of SO₃. Standard solutions of palladium and cyanide were prepared by adjusting the pH of a solution containing 0.1 gram of Pd to 10 with ammonia and then adding a weighed amount (about 0.13 gram) of cyanide. The scrubbers used to recover the cyanide contained 10 ml of a 2% ZnCl₂ solution (prepared by dissolving the requisite amount of ZnCl₂ in 100 ml of water and adding sodium hydroxide until all the precipitate which formed redissolved) and about 85 ml of water.

Procedure. Samples were placed in distillation flasks containing 100 ml of water. Solid palladium cyanide samples (~0.1 gram) were dissolved by adding sufficient ammonia to give a pH of 10 and heating gently. The solution was transferred to the distillation equipment and 20 ml of H₂PO₄ and 10 ml of 2% w/v mercaptoacetic acid were added. After thorough mixing, the solution was distilled to the point that the residue began to char. The ZnCl₂-NaOH scrubber was acidified with 35 ml of 20% phosphoric acid, cyanide oxidized to BrCN by adding Br₂ water until the solution retained a deep yellow color, the unreacted Br₂ removed with phenol, and the BrCN determined iodometrically. (The details of the cyanide completion, known as the Schulek titration, can be found in reference 5.)

(5) I. M. Kolthoff and R. Belcher, "Volumetric Analysis III," Interscience, New York, N.Y., 1947, p. 303.

Table II. Analysis of Pd(CN)₂

Sample description	Wt % Pd(CN) ₂ calculated from determination of				Mole ratio, Pd/CN
	Pd	CN	C	N	
Commercial Pd(CN)₂					
Lot 1	91.2 ^a	90.9	93.4 ^d	93.7 ^d	0.501
Lot 2	93.2 ^b	94.6 ^c	0.493
Pd(CN)₂ prepared in this Laboratory					
	91.2 ^a	92.1 ^c	93.4 ^d	93.7 ^d	0.495

^a Determined by fusing the sample with pyrosulfate, boiling an aliquot with NaCl, and precipitating the nioximate. ^b Determined on residues left after distilling the cyanide. The range for the two determinations was 0.8%. ^c The range for two determinations was 0.8%. ^d These samples also show 0.61 wt % hydrogen, equivalent to 11.0% water.

RESULTS AND DISCUSSION

The effects of various experimental conditions on the results of analysis of standards are shown in Table I, the analysis of various palladium cyanide materials in Table II. For comparison, Table II shows palladium cyanide purities calculated from carbon and nitrogen values. According to suppliers, commercial Pd(CN)₂ products are analyzed by igniting the material and weighing the residue.

Palladium cyanide complexes are exceedingly stable; palladium sulfide does not precipitate when diamminodicyano palladium(II) is treated with ammonium sulfide (1). However, PdS can be precipitated from the corresponding cyanocomplex in acid solution. Since addition of thiourea to acid Pd-CN solutions and of mercaptoacetic acid to either acid or basic solutions turned the colorless solutions yellow and since cyanide could only be distilled in their presence (*cf.* Table I), the Pd-thiourea (6) and the Pd-mercaptoacetic acid (7) complexes must be more stable than the cyanide complex. Mercaptoacetic acid was selected for use over thiourea because it appears to form a complex stable over a wider pH range and to minimize H₂S production from the hydrolysis of the excess complexing agent.

The iodometric titration of the evolved cyanide was selected because sulfide—if present—does not interfere.

The remainder of the Pd(CN)₂ samples appear to be water. The data suggest that these samples were, in actuality, monohydrates.

Received for review June 28, 1973. Accepted August 20, 1973.

(6) I. L. Bagbanly and B. Z. Rzaeva, *Azerb. Khim. Zh.*, 1967, 117-20; *Chem. Abstr.*, 67, 9075g (1968).

(7) A. T. Piliipenko and N. N. Nasiei, *Ukr. Khim. Zh.*, 33, 730-4 (1967); *Chem. Abstr.*, 67, 96555s (1967).

Sampling Variance in Analysis for Trace Components in Solids

Preparation of Reference Samples

W. E. Harris and Byron Kratochvil

Department of Chemistry, University of Alberta, Edmonton, Alberta, Canada

Sampling errors may be classified as determinate or indeterminate. We consider here a statistical approach to the question of variance of sampling of particulate matter, as distinct from the variance of analysis, with special emphasis on problems in trace analysis. In addition, the related topic of preparation of reference samples for trace measurements is considered.

Sampling Variance in Solids. When traces of material in solids are to be determined, minimization of sampling errors can in some cases impose extreme demands on the size and preparation of samples. In real situations, solid samples are often complex mixtures of several components with varying particle size, each particle containing the constituent of interest at a different concentration. The magnitude of sampling variance, or error, is then a function of particle size, heterogeneity of the material sampled, relative density of the compounds, and the desired precision of analysis. One question faced by an analyst is predicting the minimum amount of sample to be taken if the sampling error is to be less than a predetermined value. Although rigorous statistical evaluation of indeterminate (*i*) error (fluctuations arising as a result of the application of a random sampling procedure and denoted by the appropriate sampling error) in the sampling of complex mixtures is impractical, with several simplifying assumptions some guiding conclusions can be drawn.

Consider a simplified system in which the material to be sampled consists of a mixture of small spherical particles of the same size and of uniform density, but of two types—one, A, containing some quantity of the component of interest, the other, B, none of it. Also assume that each type of particle is uniform in composition, and that the distribution of the two types is random. For such a system, the properties of a binomial distribution (2, 3) permit the standard deviation (square root of the variance) of A in a sample to be calculated from the relation

$$\sigma_n = \sqrt{np(1-p)} \quad (1)$$

where n is the number of particles, p the fraction of the desired component A, and $(1-p)$ the fraction of diluent B. The relative standard deviation (in per cent) for component A is

$$\sigma_s = 100 \sqrt{(1-p)/np} \quad (2)$$

We will call the relative standard deviation the sampling error; fractions or multiples of σ_s also could be chosen as circumstances warrant. Figure 1 indicates the relative standard deviation, or sampling error, for values of p

ranging from 0.0001 to 0.999, (*i.e.*, 0.01 to 99.9%), for particles containing either 100 or 0% of the component A. When the constituent being analyzed for is present as only a small fraction of the total, the number of units or particles required in the sample becomes enormous if the sampling error is to be kept small.

In practice, the factor of interest is most often the weight of sample to be taken for analysis. Figure 2 gives the approximate relation between the mesh size of spherical particles of varying density and the number of particles per gram of material. For example, if 10^6 particles are needed to hold the sampling error to a predetermined level, material of density equal to 3 should be ground to pass a 200-mesh sieve. For high-precision analysis of traces in heterogeneous materials, it is a formidable task to grind the material sufficiently fine that samples of reasonably small weight can be taken.

In Figure 1, the component of interest is assumed to be present only as pure (100%) discrete particles. Often this is not the case, and single particles may contain both component A and inert material. Consider now a situation where two kinds of uniform particles are present as before, but have compositions less diverse than 0 and 100% in the component of interest. Benedetti-Pichler (4) developed the following formula for the number of units required in this case to obtain a random sample:

$$n = p(1-p) \left(\frac{d_1 d_2}{d^2} \right)^2 \left(\frac{(P_1 - P_2)100}{P_{av} \sigma_s} \right)^2 \quad (3)$$

where d_1 and d_2 are the densities of the two types of units making up the sample; d is the overall sample density; P_1 and P_2 are the percentages of A in the richer and leaner of the two types of particles; P_{av} is the percentage of A in the overall sample; and σ_s is the per cent relative standard deviation (Equation 2).

With the simplifying assumption that $d_1 = d_2 = 1$, Figure 3 shows the relation between the number of units required to keep sampling error within predetermined limits and the percentage of the component of interest in a sample that contains two kinds of particles with a relative difference in composition of from 100 to 10%. The per cent relative difference in composition, $100(P_1 - P_2)/P_1$, is used to label the curves so that any range of absolute values on the horizontal axis can be chosen.

Figure 3 indicates that sampling error decreases sharply as the relative difference in percentage of the sought-for substance in the two kinds of particles becomes smaller. On the other hand, when the relative difference in composition is 100% (topmost curve in Figure 3), it is difficult to provide a sufficient number of particles per sample as the concentration P_{av} of the constituent of interest decreases.

- (1) I. M. Kolthoff, E. B. Sandell, E. J. Meehan, and S. Bruckenstein, "Quantitative Chemical Analysis," 4th ed, Macmillan, New York, N.Y., 1969, p 385.
- (2) M. R. Spiegel, "Statistics," McGraw-Hill, New York, N.Y., 1961, p 122.
- (3) W. J. Dixon and F. J. Massey, "Introduction to Statistical Analysis," 3rd ed, McGraw-Hill, New York, N.Y., 1969, p 413.

- (4) A. A. Benedetti-Pichler in "Physical Methods of Chemical Analysis," W. M. Berl, Ed., Vol. 3, Academic Press, New York, N.Y., 1956, p 183.

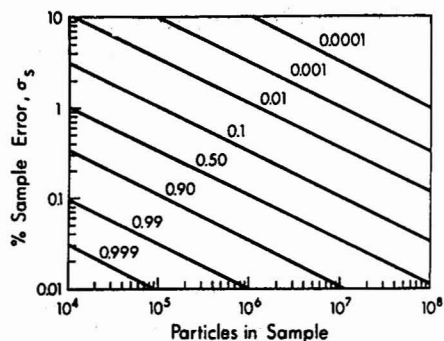


Figure 1. Relation between the sampling error σ_s in percentage and the total number of particles n for samples in which ρ ranges from 0.0001 to 0.999

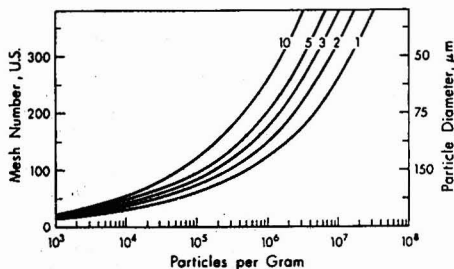


Figure 2. Approximate relation between the number of spherical particles per gram of sample and mesh size (U.S. Sieve Series, ASTM E-11-61) or particle diameter, for densities from 1 to 10

In practice, samples consisting of particles whose compositions diverge strongly on a relative basis (left side of Figure 3) should be avoided unless they contain more than about 10^6 particles if the error is to be kept to an acceptable level. Often a larger sampling variance may have to be accepted because the sampling operation becomes too difficult. In regions near the left edge of Figure 3, the amount of sample required becomes excessive, even with extensive particle size reduction through grinding. It is thus apparent that in the analysis of, for example, airborne particulate matter for a specific trace element, small particles are essential if gross sampling errors are to be avoided (unless either large samples or a large number of samples are analyzed).

The effect of the difference in density of the two types of particles can be deduced directly from Equation 3. The effect of the more complicated factor of variable particle size has been treated by Benedetti-Pichler; in essence, there is little advantage to fine grinding only a fraction, even a substantial fraction, of a sample.

Preparation of Reference Samples for Trace Components. An extension of the basic problem of sampling error is the preparation of reference samples of materials in which the component of interest is present at trace levels. Here an attempt to reduce sampling error by simply increasing sample size may be unacceptable because of the procedures used. The alternative of reducing the material

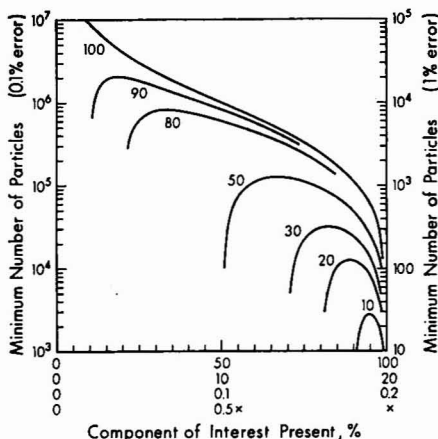


Figure 3. Relation between the minimum number of units in a sample required for sampling errors (relative standard deviations in percentage) of 0.1 and 1% (y-axis) and the overall composition of a sample (x-axis), for mixtures having two types of particles with a relative difference in composition ranging from 100 to 10%

to small particle size would require an unreasonable amount of grinding. The finer a material is ground, the more trouble it is to sieve, the more likely changes in composition will occur, and the more likely problems with caking and static charges during mixing will arise. Therefore, the largest particle size consistent with acceptable sampling error is the most desirable.

A third technique is to prepare samples from two uniform materials, each containing the component of interest. For example, if a series of samples for chloride analysis are to be prepared, there is great advantage in using mixtures of NaCl and KCl instead of mixtures of NaCl with an inert diluent such as Na_2SO_4 . When a sample contains only NaCl (60.66% chloride) or only KCl (47.55% chloride), sampling error is zero and is not a function of particle size. Maximum sampling error occurs with an approximately 40:60 NaCl-KCl mixture; if in this case a sampling error of 0.5 ppt is acceptable, about 60,000 particles must be taken for analysis. For a 1-gram sample, this corresponds to grinding the mixture to pass a 50-mesh sieve. When the mixture composition varies either side of 40% NaCl, a larger particle size can be tolerated. Thus techniques for reduction to modest size are required throughout. If Na_2SO_4 is used as diluent, sampling error exceeds 1 ppt for 50-mesh material when the Na_2SO_4 level is greater than 5% of the total composition of the sample. Extending this approach to the preparation of reference materials for traces by mixing a small amount of pure substance with a large quantity of diluent presents a virtually impossible sampling problem. With 0.1% or less sampling error and a reasonable sample size, the lowest percentage that can be prepared in this way without grinding to finer than 400 mesh is about 10%.

Circumvention of this problem may be illustrated by the following example. A series of reference samples containing from 0.1 to 0.2% copper were required for atomic absorption analysis. First, a quantity of small (200 mesh) pure-nickel beads of uniform diameter were prepared by a

hydrometallurgical technique. A thin layer of copper was deposited on the surface of the beads, followed by a layer of nickel. Two batches, one containing approximately 0.1% and the other 0.2% copper, were each prepared and analyzed carefully by two independent methods. The two materials then were mixed in varying proportions to give a series of 10 to 20 samples. From Figure 3, the relative sampling error for these samples should be no greater than 0.1% if 10^8 particles are taken (the most unfavorable mixture has about 1 part of 0.1% to 2 parts of 0.2%). For 200-mesh materials, a sampling error below 0.1% is easily achieved with samples of 0.2 gram (Figure 2). If these samples were prepared from pure copper and a diluent such as pure nickel, 10^{10} particles (about 20 kg) would be required for each sample analyzed.

In summary, the sampling of heterogeneous solids may be a major source of error if the sought-for component is

present in small quantity in discrete particles. Poor precision in trace analysis may be the result of variation in sample composition. In the preparation of reference materials for trace components, the use of inert material plus pure component is not recommended. Other approaches to their preparation, particularly use of homogeneous material or of two materials close together in percentage of the sought-for component, should be used.

ACKNOWLEDGMENT

The assistance and cooperation of D. R. Weir and Sherritt-Gordon Mines, Ltd., Fort Saskatchewan, Alberta, in the preparation of the copper-in-nickel reference materials is gratefully acknowledged.

Received for review July 31, 1973. Accepted October 4, 1973.

New Method for Calibration of Permeation Wafer and Diffusion Devices

Russell N. Dietz, Edgar A. Cote, and James D. Smith

Department of Applied Science, Brookhaven National Laboratory, Associated Universities, Inc., Upton, N. Y. 11973

Standard reference materials for calibrated sources of gaseous pollutants at ppm and ppb levels are needed to provide improved calibration of current air monitoring instruments. Permeation Teflon (Du Pont) tubes containing liquified gases were developed as such sources and have recently been standardized for $\text{SO}_2(1a)$. Permeation tubes for condensable gases, originally suggested by O'Keefe and Ortman (2) and evaluated for SO_2 by Scaringelli, Frey, and Saltzman (3), have been calibrated by their weight loss with time (4, 5) and more recently by volumetric displacement (6, 7) and by pressure differential measurements with a capacitance manometer (8). However, the rates are inconveniently high for ambient air applications (1500 ng/min per cm of length), the tubes last only a few months, and the permeation rates for NO_2 decline with time because of interaction with moisture. Permeation bottles capped with Teflon disks reduce the rates by about an order of magnitude, but calibration by conventional weight loss measurements is extraordinarily long—about 1 month. Utilization of a recording electrobalance (9) reduces the calibration time, but the total weight of the permeation device is limited.

Noncondensable pollutant gases such as nitric oxide, methane, and carbon monoxide can permeate through Teflon, but permeation tubes have not been made since the gases cannot be liquified at ordinary temperatures. Other suitable NO source materials are being investigated including encapsulated gas bubbles, molecular complexing in conjunction with the permeation tube principle, certification of $\text{NO}-\text{N}_2$ mixtures in cylinders, and quantitative catalytic conversion of NO_2 from permeation tubes to $\text{NO}(1c)$. Monitoring instruments for the determination of CH_4 and CO in the environment (10) are presently calibrated by preparing mixtures in cylinders at about 10 ppm (11); however, there is no way to check the accuracy of these preparations or to determine the loss of calibration with time. McKinley (8) measured permeation rates of noncondensable gases through polymeric membranes (e.g., FEP Teflon tubing) by a pressure differential technique, although many of the experimental details were not given.

This paper describes a new pressure differential method for the calibration of permeation wafer and diffusion devices for both noncondensable and condensable gases. Permeation rates less than 5 ng/min can be accurately determined in hours instead of weeks.

EXPERIMENTAL

The permeation wafer device consisted of a Teflon disk held by compression in a Swagelok tee such that the leg containing the disk was connected to the pollutant gas source and the other connections provided the diluent gas input and output flow ports (cf. Figure 1). For calibration, the diluent side was connected to a

- (1) J. R. McNesby and R. Byerly, Jr., "Measures for Air Quality. Annual Report-FY 1971," *Nat. Bur. Stand. (U.S.) Tech. Note*, 711, January 1972; a. The Sulfur Dioxide Permeation Tube, p 68; b. The Nitrogen Dioxide Permeation Tube, p 70; c. Molecular Complexes of Gaseous Pollutants, pp 29-32.
- (2) A. E. O'Keefe and G. C. Ortman, *Anal. Chem.*, 38, 760 (1966).
- (3) F. P. Scaringelli, S. A. Frey, and B. E. Saltzman, *Amer. Ind. Hyg. Ass.*, 28, 260 (1967).
- (4) F. P. Scaringelli, A. E. O'Keefe, E. Rosenberg, and J. P. Bell, *Anal. Chem.*, 42, 871 (1970).
- (5) F. P. Scaringelli, E. Rosenberg, and K. A. Rehme, *Environ. Sci. Technol.*, 4, 924 (1970).
- (6) B. E. Saltzman, C. R. Feldmann, and A. E. O'Keefe, *Environ. Sci. Technol.*, 3, 1275 (1969).
- (7) B. E. Saltzman, W. R. Burg, and G. Ramaswamy, *Environ. Sci. Technol.*, 5, 1121 (1971).
- (8) J. J. McKinley, "A Calibration System for Trace Analyzers," 16th National Symposium, Instrument Society of America, Pittsburgh, Pa., May 1970.
- (9) L. J. Purdue and R. J. Thompson, *Anal. Chem.*, 44, 1034 (1972).

- (10) R. K. Stevens, T. A. Clark, C. E. Decker, and L. F. Ballard, "Field Performance Characteristics of Advanced Monitors for Oxides of Nitrogen, SO_2 , CO , CH_4 , and Non-Methane HC," 68th APCA Meeting, Miami, Fla., June 1972.
- (11) E. E. Hughes and J. K. Taylor, "Standard Reference Materials For Air Pollution and Gas Analysis," 164th National Meeting AEC, New York, N.Y., *Amer. Chem. Soc., Div. Water, Air, Waste Chem., Gen. Pap.*, 12(2), 238 (1972).

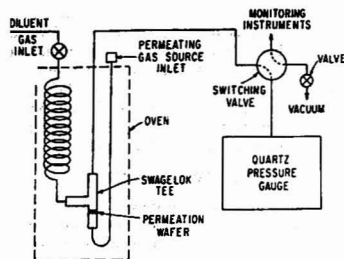


Figure 1. Permeation calibration and dilution apparatus



Figure 2. Permeation wafer device

quartz Bourdon pressure gauge (Texas Instrument, Model 141) having a resolution of 0.01 mm Hg. Temperature was measured at three important locations—the permeation device chamber, the quartz pressure gauge, and the interconnecting line—using mercury thermometers with a resolution of 0.1 °C and, later, digital thermistor thermometers (Digitec, 25 to 45 °C) and digital semiconductor thermometers (Electronic Research Co., -60 to 150 °C) with a resolution of 0.01 °C. The Teflon disk as well as about 50% of the internal volume was temperature controlled with a power proportioning controller to about 0.01 °C. With an accurately measured total internal volume of about 10 cm³, as little as 0.3 μl (~0.0000006 gram) of permeated gas could be detected. Using the correction equations for compressibility (non-ideality) and back-diffusion developed by Saltzman for NO₂ permeation (7), the pressure and temperature measurements were converted, with the aid of a programmable computer-calculator, to the mass of permeated gas. For each measurement, the program printed the weight of permeated gas, the time from the start of the run, and, for the case of NO₂, the compressibility and reverse diffusion corrections employed; then the least mean square permeation rate, its standard deviation, and the intercept were computed.

The permeation wafer device (cf. Figure 2) was so constructed that it could be used with noncondensable gases such as nitric oxide, by attachment to a supply of about the size of a lecture bottle. Any gas could be used in the apparatus provided it was compatible with stainless steel, Teflon, and quartz. As long as dry diluent gases were used in the device, the problem of mois-

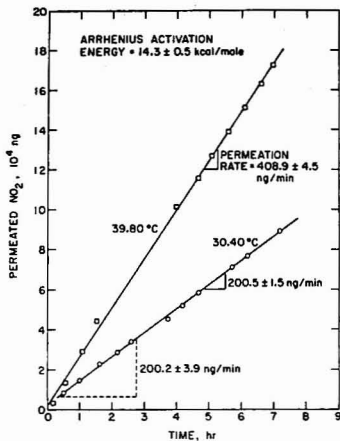


Figure 3. Permeation of NO₂ through a TFE Teflon wafer

ture diffusion and blistering was eliminated since the Teflon wafer was assembled and evacuated in place *before* admission of the permeating gas. With a specially fabricated 4-way stainless steel ball valve (Whitey No. 43YF52-316) between the permeation wafer device and the quartz pressure gauge, either calibrations could be performed or part per billion concentration mixtures could be withdrawn.

The diffusion restrictors used essentially the same apparatus but, in place of the Teflon disk, either a stainless steel capillary tube or a rod within a stainless steel tube provided the diffusion resistance.

Permeation tubes were also calibrated by the same technique, but a glass chamber of about 50 cm³ volume was used to contain the tube. However, the tubes are exposed to the atmosphere during preparation, transportation, and storage and thus can be affected by moisture.

RESULTS

The initial version of the device was assembled using a tetrafluoroethylene (TFE) Teflon wafer 0.0813 cm thick with a surface area available for permeation of about 0.15 cm². Temperature was measured with mercury thermometers with divisions only every 0.1 °C, and NO₂ was chosen as the permeating gas. As shown in Figure 3, data obtained at 30.4 and 39.8 °C gave permeation rates of 200.5 and 408.9 ng/min, respectively. The calculated activated energy of 14.3 kcal/g-mol agreed very well with that of 14.6, reported by Saltzman (7).

The glass chamber apparatus for permeation tubes was used to determine the rate for an SO₂ permeation tube at temperatures of 30.0, 50.5, and 60.0 °C (cf. Figure 4), giving an activation energy of 12.6 kcal/g-mol. The permeation rate determined at 30 °C (1510 ng/min) compared very favorably with the certified (Analytical Instrument Development Inc.) rate of 1510 ng/min, determined by weight-loss measurements. The positive intercept for the 50.5 °C data indicates that sufficient time was not allowed to achieve steady-state conditions.

A preliminary evaluation of the diffusion of methane through a capillary stainless steel tube, which had been rolled to further reduce the inside diameter, gave diffusion rates at several pressures as shown in Figure 5. For this tube, the rates were high; for example, at a pressure differential of 20 psi, the methane diffused at 0.0247 cm³/min which, with a diluent air flow of 1000 cm³/min, would give 24.7 ppm CH₄. The rates were correspondingly

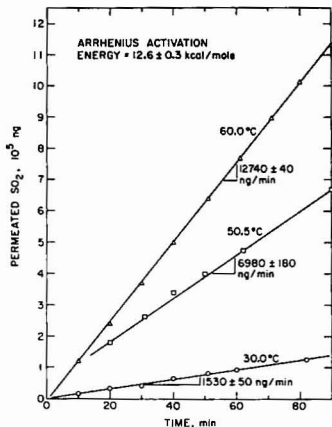


Figure 4. Permeation of SO_2 through a Teflon tube

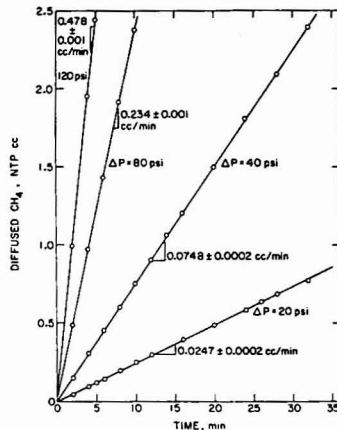


Figure 5. Diffusion of CH_4 through a capillary tube

Table I. Comparison of Calibration Methods at Minimum Time to Determine Permeation Rate with 2% Precision

Determining method	Permeation rate, ng/minute	Minimum time	
		Hours	Days
Weighing ^a (microbalance)	2000	100	4
	200	1000	40
	20	10,000	400
Volumetric ^b	2000	2 1/2	...
	200	25	1
	20	250	10
Weighing ^c (electrobalance)	2	2500	100
	200	10	0.4
	20	100	4
This method	2	1000	40
	200	1	...
	20	10	0.4
	2	100	4

^a Assuming 2% precision for a weight change of 0.012 gram. ^b Based on the technique of Saltzman *et al.* (7). ^c Based on the Purdue and Thompson method (9).

higher at higher pressure. Repetition of this type of restrictor seemed very good; a determination one day later at 20 psi gave $0.0244 \pm 0.0001 \text{ cm}^3/\text{min}$ —a reproducibility of about 1%.

Lower methane diffusion rates were achieved with a Swagelok restrictor, as shown in Figure 6. At 100 psi, a flow of $0.00663 \pm 0.00006 \text{ cm}^3/\text{min}$ was obtained, corresponding to 6.6 ppm at $1000 \text{ cm}^3/\text{min}$ total flow. A description of the Swagelok orifice design, which was developed for the Brookhaven ^{90}Sr ozone generator, is given elsewhere (12). Both types of diffusion restrictors appear capable of use as readily-calibrated, standard reference sources.

DISCUSSION

The 30.4°C NO_2 run with the permeation wafer device (Figure 3) shows that a $200 \text{ ng}/\text{min}$ permeation rate can be determined with 2% precision from 5 measurements

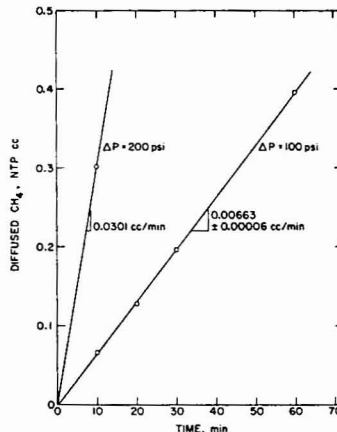


Figure 6. Diffusion of CH_4 through a Swagelok restrictor

taken over 2.5 hours. With the use of digital thermometers (0.01°C resolution) in place of the mercury thermometers (0.1°C resolution), at least a 3-fold improvement in the precision should be attained. Table I gives the comparative times to obtain several permeation rates by various techniques. For the conventional weighing method, it was assumed that a minimum weight change of 0.012 gram would be necessary to achieve a 2% precision in the permeation rate. For the electromicrobalance technique, it appeared that a $20 \text{ ng}/\text{min}$ rate could be calibrated within 2% in four days. And Saltzman indicated that about 30 minutes was required for 2% precision at a rate of $10,000 \text{ ng}/\text{min}$.

To obtain calibrated concentrations of NO_2 in air near ambient values, about 5 ppb, requires low permeation rates even at moderate flow rates. The concentration of a permeated gas in a diluent gas stream is given by

(12) M. Steinberg and R. N. Dietz, " ^{90}Sr Ozone Generator for Sub-ppm Concentration Range," Brookhaven National Laboratory, BNL 14199, November 1969.

$$\text{Concn. ppb} = \frac{RV_m}{FW_m} \quad (1)$$

where R = permeation rate, ng/min; F = diluent gas flow rate, cm^3/min ; V_m = molar volume at 0 °C and 1 atm, 22414 cm^3/mol ; and W_m = molecular weight. For NO_2 ($W_m = 46$), Equation 1 can be approximated by

$$\text{Concn. of } \text{NO}_2 \text{ ppb} \approx 500 R/F \quad (2)$$

Thus 5 ppb of NO_2 can be achieved with a permeation rate of 20 ng/min at a flow rate of 2000 cm^3/min . At 20 ng/min, Table I shows that the conventional weighing technique would require more than one year to perform the calibration, the Saltzman volumetric apparatus would take 10 days (250 hours), and the electromicrobalance technique about 100 hours; however, the present method would require only 10 hours. In certain applications where lower concentrations or lower diluent gas flow rates are desirable, permeation rates as low as 2 ng/min may be required; the method discussed here is the only practical approach to the absolute calibration of such a low permeation rate. The volumetric technique of Saltzman may be

limited further by competitive reaction with the glass walls and the manometric fluid at low permeation rates, and the electromicrobalance method is limited to condensable gases with exposure to the environment still a problem.

CONCLUSIONS

Preliminary results with the permeation wafer and diffusion devices indicated that the new calibration technique will more quickly provide accurate calibration of elution rates of condensable and noncondensable gases from the devices for use as standard reference materials. Various methods of fabricating the devices as well as automatic data collection procedures are currently being evaluated and will be described in a future article.

Received for review August 3, 1973. Accepted September 28, 1973. Presented in part at the 166th National Meeting American Chemical Society, Chicago, Ill., August 1973. This work was performed under the auspices of the United States Atomic Energy Commission in contract with the Environmental Protection Agency.

CORRESPONDENCE

Self-Reversal in a Copper Pulsed Hollow Cathode Lamp

Sir: During time-resolved studies of atomic line emission profiles from a copper hollow cathode lamp, we have observed extreme self-reversal under pulsed conditions that are similar though not identical, to the intermittent mode used by Cordos and Malmstadt (1), and the pulsed mode used by Dawson and Ellis (2). Of particular interest is the fact that extreme self-reversal was present in spite of a linear relationship between wavelength integrated line intensity and lamp pulse current. A linear or slightly curved relationship of this type has led some investigators to believe that only slight self-absorption might be present.

The instrumentation will be explained in detail in a more comprehensive paper to be published later. The purpose of this paper is to present timely results. A Westinghouse copper lamp No. 23042 was pulsed for 5 msec at a rate of 10 Hz with currents up to 300 mA. The total line intensity (wavelength integrated) for the Cu(I) 324.7-nm line vs. lamp pulse current is shown in Figure 1. Measurements were made using an oscilloscope and the scatter of the data points is due primarily to shot noise. The relationship is linear within the expected uncertainty of the data points and passes through the origin.

A computer controlled analog-to-digital converter with a time jitter of 17 μsec was then used to collect intensity data at time intervals spaced at 0.5 msec during the 5-msec pulse, starting with the first 21 μsec of the pulse. A piezoelectrically scanned Fabry-Perot interferometer with a scanning aperture limited finesse of 23 was used to obtain wavelength resolution. The data resulting from many pulses were time averaged and sorted by the computer and plotted on an X-Y recorder.

Figure 2 shows the time and wavelength resolved Cu(I) 324.7-nm line for pulses of 100 mA, and 200 mA. Each of the five curves in Figure 2 represents a point in time (with a jitter of 17 μsec). The first four or five of a set of ten points in time, spaced at intervals of 0.5 msec, are shown; the later points are not presented because they are essentially the same as the last point shown. The left hand profile represents the line profile from 4–21 μsec following the start of the pulse. There are two lines due to hyperfine splitting (3) of the 324.7-nm line. The lines are 0.0040 nm apart. Although during the first 21 μsec , the two lines show no self reversal, the 200-mA lines are broader than the 100-mA lines. Similar line profiles for 150-mA pulses during the first 21- μsec interval show a peak intensity that is about twice as high as those for the 100-mA or 200-mA pulses, and a line width at half height that lies between the 100-mA and 200-mA line widths. Apparently, therefore, self-absorption causes the broadening and reduced peak intensity of the 200-mA pulse during the first 21- μsec interval.

By the next point in time, 504–521 μsec , the two lines appear to be 4 lines, because of self-reversal. Self-reversal remains strong for succeeding points out to the end of the pulse.

Two of these pulse levels, 150 mA and 200 mA, were studied during the first 210 μsec of the 5-msec pulse. Points were as closely spaced as possible, 21 μsec . The results are shown in Figure 3 for the 200-mA pulse. Intensity scales for these profiles are the same as for those of Figure 2. The profiles taken during the first 210 μsec show that the reversal starts early in the pulse and reaches a steady state (no change in intensity or profile with time) after

(1) E. Cordos and H. V. Malmstadt, *Anal. Chem.*, **45**, 27 (1973).

(2) J. B. Dawson and D. J. Ellis, *Spectrochim. Acta*, **23A**, 565 (1967).

(3) P. Brix and W. Humbach, *Z. Phys.*, **128**, 506 (1950).

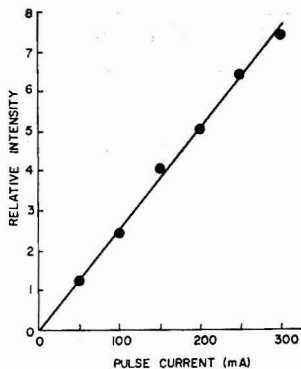


Figure 1. Relative integrated Cu intensity vs. pulse current for the commercial hollow cathode lamp

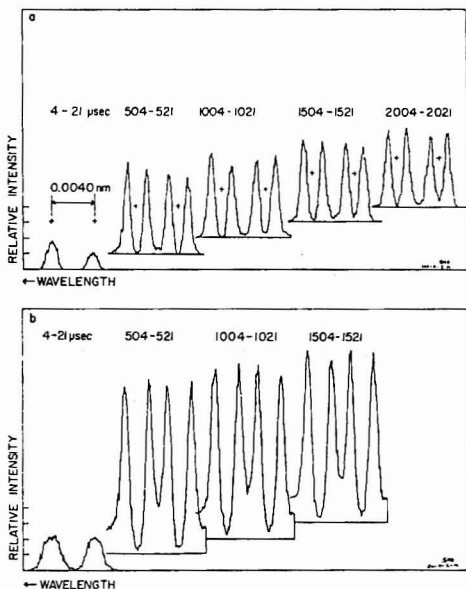


Figure 2. Time-resolved line profiles of the Cu(I) 324.7-nm emission doublet. Line profiles are 0.5 msec apart starting at the beginning of a 5-msec pulse. (a) Pulse current = 100 mA, (b) pulse current = 200 mA

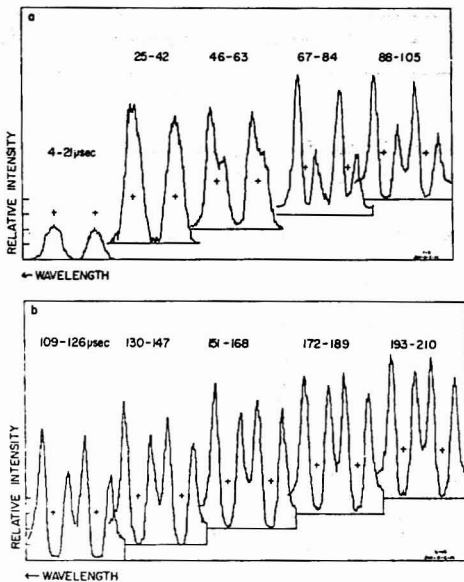


Figure 3. Time-resolved line profiles of the Cu(I) 324.7-nm emission doublet. Line profiles taken sequentially 21 μ sec apart from the beginning of a 5-msec pulse. Pulse current = 200 mA. (a) Time periods 1 through 5, (b) time periods 6 through 10

about 100 μ sec for the 150-mA pulse and after 200 μ sec for the 200-mA pulse. The asymmetry of the self-reversed lines is more pronounced earlier in the life of a pulse than later on.

Thus, while the wavelength integrated intensity for a pulse increases linearly with pulse current, there remains strong self-reversal in the Cu doublet line, even for long pulses at low pulse rates. This indicates that great care must be taken in the interpretation of data for pulsed systems in which there are large concentration and energy gradients, and where one parameter, such as lamp current, may change not only the sampling rate but also other variables such as the shape or size of the various discharge regions.

G. J. DeJong
E. H. Piepmeier

Department of Chemistry
Oregon State University
Corvallis, Ore. 97330

Received for review July 23, 1973. Accepted October 23, 1973. This work was supported in part by National Science Foundation Grant No. GP-28069.

AIDS FOR ANALYTICAL CHEMISTS

Relay Circuit for Integrating a Gas-Liquid Chromatography Temperature Programmer with an Automatic Sample Injector

H. A. McLeod, Ronald Bolohan, and Maarten Van Dyk

Food Research Laboratories, Health Protection Branch, Department of National Health and Welfare, Ottawa, Ontario

GLC temperature programmers integrated with automatic sample injection systems are not readily available to the analytical laboratory and are expensive when purchased on a custom basis. During the development of an automated GLC system in our laboratory, a need arose to synchronize the triggering of the automatic injection unit with the restarting of the temperature program cycle. This was accomplished by devising a simple relay circuit, integrated with the oven cool-down cycle. The system has proved reliable in operation, and its concept can be adapted to various models of equipment.

The temperature program circuits of different gas chromatographs have the same cool-down sequence in many respects. Voltage under the control of a logic circuit is supplied to a motor or solenoid to operate an oven-venting mechanism and turn on lights indicating the program status. A re-cycle is initiated by closing a start switch(es), momentarily. Depending upon the model of temperature programmer, a voltage can be selected that will trigger a relay or series of relays, whose contacts are appropriately wired across the contacts of the manually operated start switches.

Figure 1 outlines the relay and other component circuitry installed in our GLC. Component description is given in Table I. All parts are standard electronic components that are available from an electronic supply house. The values used here may not be satisfactory for some models, but will be for others. Choice will be based on the value of voltages available to trigger the re-cycling circuitry.

Table I. Component Specifications for Circuit in Figure 1

Component	Number required	Circuit No.	Description
Relay	2	K1 & K3	110-volt ac double pole, double throw, 5-ampere rating.
Relay	1	K2	110-volt dc double pole, double throw, 5-ampere rating.
Capacitor	1	C1	100 MFD, minimum 150 VDC.
Switch	1	S1	Toggle, single pole, double throw, 5-ampere rating.
Rectifier	1	10D8	Diode, 1 ampere, PIV 800 V.

The sequence of operation (Figure 1) in the automatic mode for our machine is as follows:

The oven is equilibrated to the initial temperature, the various program parameters are set, and continuous operation is initiated by closing the start switches of the automatic injector and temperature programmer. When the oven vent opening motor is energized at the beginning of the cool-down cycle, the same voltage energizes relays K1 and K2, but 110 VAC does not reach K3 because the con-

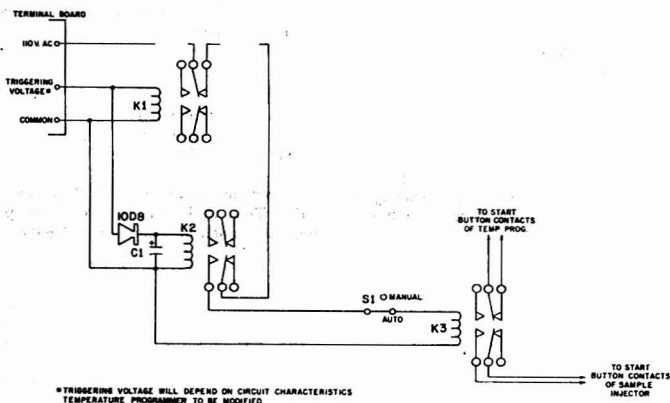


Figure 1. Relay circuit for repetitive temperature programming and sample injection

tacts, at K1 open. As the vent fully opens, the power to the motor is interrupted by a cam-switch arrangement at the motor. However, K1 and K2 remain energized as they are supplied by the voltage leading to the cam-switch circuitry. When the door is closed, this voltage is also removed and K1 is de-energized. The 110 VAC contacts close at K1 and remain closed at K2 because of the charge on C1; thus, K3 is energized. The pair of contacts at K3, paralleling the manually operated start switches, are closed for a time period determined by C1 (approximately 1 second), and a new cycle is initiated.

Switch S1 in the circuit allows selection of the automatic repetitive temperature programming, or, when in the manual position, disconnects K3 so that programming is restricted to one cycle only.

ACKNOWLEDGMENT

The authors thank Mrs. Janet Chapman for preparing the circuit drawing.

Received for review January 12, 1973. Accepted July 27, 1973.

Simple Method for Continuous Monitoring of Electrode Rotation Rate

Ira B. Goldberg, Richard S. Carpenter II, and W. F. Goepfinger

Science Center, Rockwell International, Thousand Oaks, Calif. 91360

Rotating electrodes are a valuable tool for the study of electrode processes (1, 2). A rotating ring-disk electrode assembly, similar to those discussed in the literature (3), was set up in this laboratory. In these cases, rotation rates were calibrated separately from the actual experiment. The experiments were done using a motor-tachometer-generator, which feeds into a speed control unit that regulates the voltage to the motor. A ten-turn potentiometer is used to regulate the rotation rate. After several calibration runs on various days, we have found that for a given potentiometer setting on the speed controller, the rotation rate may vary by as much as 5%, even though the rotation rate is constant to within 0.2% over a period of an hour or more. This suggests the need to monitor the rotation rate continuously or at least to calibrate the rotation rate prior to each experiment. Another alternative would be to use a precise frequency generator and power amplifier to control the rotation rate.

Little attention has been given to the continuous measurement of rotation rate. Sonner *et al.* (4) use a photoelectric pick off on a reflective surface on the shaft of the electrode to measure the rotation rate. The time interval is monitored by a frequency counter. Hintermann and Suter (5) mounted a disk with holes on the shaft of the electrode. A light was placed under the disk and a phototransistor was placed over the disk so that a number of light pulses proportional to the rotation rate were detected and counted with a frequency counter. Other mechanical devices were also devised to give an electrical impulse per revolution (6). The goals which were kept in mind for the electrode assembly used in this laboratory were that the rotation rate could be monitored on an inexpensive frequency counter or timer, the electrochemical system could be easily interfaced with a computer for interactive control, the electrodes could be easily interchanged, and the entire assembly should be compact enough to be easily transported.

- (1) R. N. Adams, "Electrochemistry at Solid Electrodes," Marcel Dekker, New York, N.Y., 1969.
- (2) W. J. Albery and M. L. Hitchman, "Ring-Disk Electrodes," Clarendon Press, Oxford, England, 1971.
- (3) V. J. Puglisi and A. J. Bard, *J. Electrochem. Soc.*, **119**, 829 (1972).
- (4) R. H. Sonner, B. Miller, and R. E. Visco, *Anal. Chem.*, **41**, 1498 (1969).
- (5) H. E. Hintermann and E. Suter, *Rev. Sci. Instrum.*, **36**, 1610 (1964).
- (6) J. Wojtowicz and B. E. Conway, *J. Electroanal. Chem.*, **13**, 333 (1967).

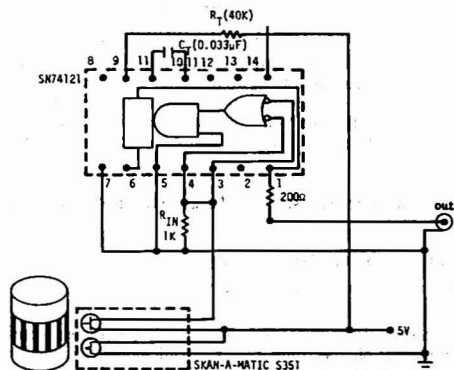


Figure 1. Schematic diagram of synchronous pulse generator for the measurement of rotation speeds

EXPERIMENTAL

A Fine Instrument Co. (Grove City, Pa.) rotating ring-disk electrode was connected to an Electrocraft (Hopkins, Minn.) speed controlled Model 550 motor, using a stainless steel collet. Ten nonreflective strips were painted on a 5-mm strip of reflective tape which was equal in length to the circumference of the collet. The tape was carefully placed around the collet so that the light of a Skan-a-matic Corp. (Elbridge, N.Y.) Model S-351 miniature reflective scanner illuminated the tape. Ten light pulses are obtained at the phototransistor for each revolution of the rotating electrode. The small scanner actually permits the use of more than ten stripes to be painted on the reflective tape if desired. Although the transistor of the scanner is rated at up to 30 V, it was convenient to use a 5-V input. The low voltage side of the phototransistor was connected to a resistor R_{IN} (Figure 1) and to the negative edge trigger input of a Motorola SN74121 monostable multivibrator. R_{IN} is adjusted so that the voltage maximum and minimum at this point are about 2 to 0.8 V to enable the multivibrator to trigger. Since these voltages vary among these components, R_{IN} must be determined empirically. In our case, 1 K Ω was sufficient for the device to trigger even when the photodetector was used in room light with no particular shielding. The pulse duration was set for 90% of the minimum pulse rate (about 1 msec) by adjusting R_T and C_T given by the tables in the manufacturer's literature. The monostable multivibrator provides a

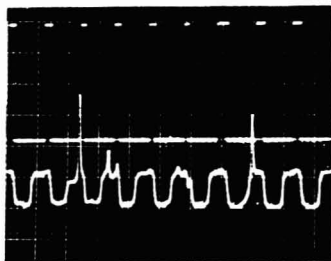


Figure 2. Measurements taken with sensor 1.4 cm from rotating band.

Upper curve: Output of monostable multivibrator (1 V/div); the lower dashed line is the 1-msec output. Lower curve: Input to monostable (0.5 V/div)—base line is +0.5 V. Time base, 1 msec/cm; rotation rate, 5400 rpm

normal output in which a 5-V output is triggered from a base line of about 1 V and an inverted output in which a 1-V output is triggered from a 5-V base line. We have arbitrarily chosen to use the inverting input to measure the frequency.

RESULTS AND DISCUSSION

Figure 2 shows the resulting waveform from the sensor when the sensor is 1.4 cm from the rotating striped band, and also the output from the multivibrator. An inverted pulse is delivered from the monostable multivibrator which is triggered on the declining portion of the signal

from the phototransistor. In normal use, much better waveforms are obtained when the sensor is about 3 mm from the band; however, this photograph shows more dramatically how the waveform is improved by the multivibrator.

The spikes from the phototransistor shown in Figure 2 do not trigger the multivibrator. Good output waveforms were obtained at rotation rates from less than 0.1 to 5000 rpm. The latter speed is faster than would normally be used in electrochemical studies. At slow speeds where only a few pulses per second are observed, an event timer can be used to measure the rotation rate. At the slower rotation rates, the output of the phototransistor was not sharp enough to trigger the frequency counter. If an event timer is to be used, then one stripe could be painted on the reflective tape and smaller values of C_T and R_T (Figure 1) can be used to obtain a sharper pulse. This would also be desirable for computer interfacing.

If a sine wave generator and power amplifier are used to power a synchronous motor, highly stable rotation rates can be obtained. However, we have found that the system described here conveniently provides a high degree of accuracy for the value of the rotation rate. The speed controller alone provided a constant rotation rate, but it was not highly reproducible. Another advantage of this system is that the uniform pulse shape is easily interfaced with a computer so that the rotation rate could be stored with electrochemical variables if desired.

Received for review June 25, 1973. Accepted August 15, 1973.

Device for the Accurate Electronic Measurement of Microliter Sample Volumes

L. R. Layman and G. M. Hietfle

Department of Chemistry, Indiana University, Bloomington, Ind. 47401

In several analytical techniques, such as a nonflame atomic absorption spectrometry, small (microliter) volumes of sample solution must be accurately measured and evaporated before a determination can be made. The measurement and transfer of these small volumes by micropipet or syringe often contributes an important fraction of the total error in the determination (1). In this report, a method is described that minimizes these difficulties by indirectly measuring the mass of liquid after it is placed in the apparatus. This measurement is based on a determination of the time required to evaporate the liquid using a constant rate of heat input. To determine this time, a suitable support for the liquid (a wire filament in this case) is heated by a constant current, with changes in the support temperature monitored as a drop of sample is placed on the support and evaporates.

The simple apparatus necessary for this measurement is shown in Figure 1 and consists of a 0.010-inch diameter tungsten or platinum wire filament (or other heated evaporator) enclosed in a glass tube and surrounded by a controlled atmosphere, a constant current supply (OA1 and the booster amplifier), an operational amplifier derivative circuit (OA2 and OA3), and either a digital timer or strip chart recorder.

In the procedure, the filament is heated by a 1- to 2-ampere constant current to a temperature below the boil-

ing point of the solvent. A microliter sample placed on the warm filament then produces a rapid drop in filament temperature which is reflected in a corresponding decrease in filament resistance. This reduction in resistance is registered as a drop in voltage and converted to a negative voltage peak by the operational amplifier derivative circuit, as shown in Figure 2.

As the liquid evaporates, the filament remains at this lower temperature, allowing the voltage derivative to return to zero. When the last of the liquid has evaporated, the filament quickly returns to its original temperature, causing the filament voltage to rise and producing a positive peak in the derivative circuit. The time between the negative and positive derivative peaks is measured either from a strip chart recorder output, or directly on an electronic timer. The volume of the sample is then directly proportional to the measured time. Of course, for this proportionality to hold, the gas composition and flow rate, the current, and the nature of the solvent must be held constant.

In this method, the greatest precision was obtained using an automatically triggered electronic timer. This timing system, shown in Figure 1, consists of two comparators and an electronic clock. The comparator reference voltages are set such that the first comparator triggers on a negative voltage level, while the second responds to a positive voltage. The derivative circuit output is therefore converted to fast-rising square pulses which are used to start and stop the clock.

(1) C. F. Emanuel, *Anal. Chem.*, **45**, 1568 (1973).

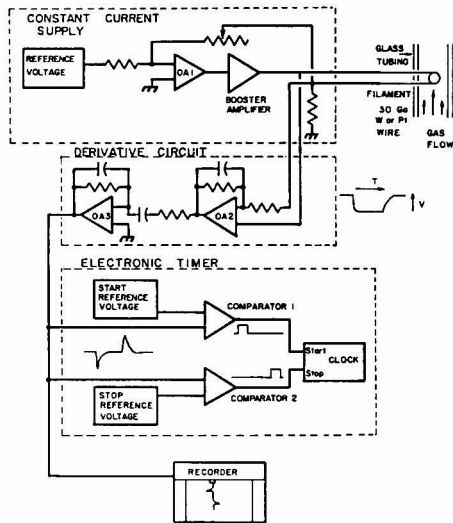


Figure 1. Schematic of drop volume measuring system showing constant current supply, heated filament, derivative circuit, and time measurement devices. Voltage waveforms are shown at several points in the circuit

If a strip chart recorder is used for timing, the distance between the leading edge of the negative peak (the moment the sample is applied) and the top of the positive peak (the moment evaporation is complete) is the value directly proportional to sample volume. The measurement points are shown in Figure 2.

This method has been shown to be very accurate and linear over a wide range of volumes and under a variety of conditions. Both tungsten and platinum wire filaments have been successfully used in still and flowing air or argon atmospheres. The precision obtained with 15 trials at 1- μ l volume was 1.83% relative standard deviation, most of which could be ascribed to syringe errors. The precision of the syringe was ascertained by weighing 20 samples of 2 μ l each on a microbalance. After correction for evaporation, the relative standard deviation was 1.93%, of which the balance contributed approximately 0.1%. Therefore, the error in the apparatus presented herein is significantly less than that of the syringe. As seen in Figure 3, the linearity of the system was also well within the syringe error over the entire measured range of 0.5 to 5.0 μ l. With the present filament size, samples larger than 5.0 μ l could not be measured because they would not adhere to the filament; volumes smaller than 0.5 μ l could not be accurately tested because of limitations in the reproducibility of the 5- μ l syringe.

This technique for the measurement of microliter samples should be applicable to a number of other evaporative systems now employed in chemical analysis, such as the rod, boat, and filament type of atomizers becoming popular in atomic absorption spectrometry. In addition, it could be applied to gas chromatography inlet systems, if modification to allow very fast evaporation were made.

This measurement device is presently being used in conjunction with a microwave-excited atomic emission source, which is operated under complete computer con-

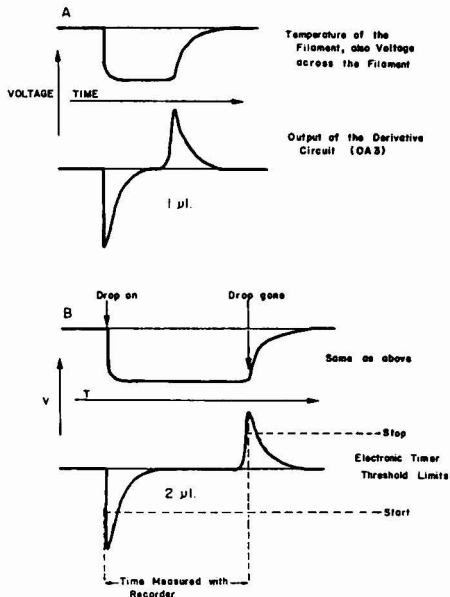


Figure 2. Waveforms generated at the atomizing filament and by the derivative circuit. Timing points are shown in B. (A) 1- μ l sample size, (B) 2- μ l sample size

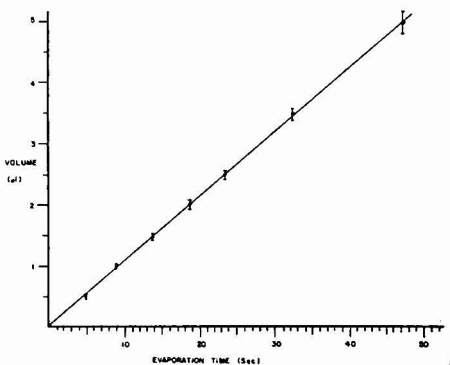


Figure 3. Relationship between evaporation time and sample volume. Line shown is a least squares fit to the points. Hash marks above and below each point represent the $\pm 95\%$ confidence limits for that point

rol. The real time clock in the computer provides the necessary timing so that the volume of each sample is automatically and accurately determined. Thus, the entire system is automated for maximum convenience and precision in analysis of samples of, for example, clinical importance.

Received for review August 13, 1973. Accepted September 19, 1973. The authors gratefully acknowledge support of this work by Public Health Services Grant GM 17904-02.

Analysis of Background Copper Concentration in Sea Water by Electron Spin Resonance

Y. P. Virmani¹ and E. J. Zeller

Radiation Physics Laboratory, Space Technology Center, University of Kansas, Lawrence, Kansas 66044

A technique has been tested which makes possible the rapid analysis of the copper concentration in sea water in ranges as low as 0.1 ppb. The system makes use of Electron Spin Resonance (ESR) combined with concentration enhancement by chelation and solvent extraction. Copper can be observed by ESR in the aqueous phase.

Fujiwara and Hayashi (1) studied Cu^{2+} ions at various concentrations in distilled water and observed a single line spectrum with a line width of ~ 150 gauss below $0.05M$ concentration. They did not attempt measurements below 64 ppm.

Copper has also been extensively studied by the ESR technique after complexing with various chelates in a wide variety of solvents (2-5). These studies were designed primarily to investigate the relaxation behavior and hyperfine coupling and to locate the site of bonding of Cu^{2+} with chelates. Since the objective of these studies was not to detect Cu^{2+} in trace amounts, all of them were conducted at high copper concentrations.

In our experiments, a concentration of 0.1% 8-hydroxyquinoline was tested in various organic solvents such as ethyl propionate, 3-propanone, ethyl acetate, butyl ether, methyl isobutyl ketone, and cyclohexene. Ethyl propionate was the most satisfactory solvent for the sea water extractions.

Reagent grade cupric chloride was utilized for making spiked samples of sea water. Analar grade 8-hydroxyquinoline was used for extraction of copper in various organic solvents. To avoid any adsorption of trace elements on the surface of the container, polyethylene and quartz vessels were utilized (6).

ESR analyses were carried out on a Varian V-4502 spectrometer system equipped with audio and 100 kHz modulation units and operated in the low power bridge configuration. Quartz tubes were utilized for the measurements which were made on the organic phase after solvent extraction. In these experiments, the organic solvent contained a chelating agent which selectively removed Cu^{2+} from the aqueous phase (7-9).

Ethyl propionate has a solubility of $2 \text{ cm}^3/100 \text{ cm}^3$ of sea water. Three cubic centimeters of 0.1% 8-hydroxyquinoline in ethyl propionate per 100 cm^3 of sea water was used for extraction. Sea water and ethyl propionate containing 8-hydroxyquinoline were shaken for 2 minutes in polyethylene bottles and then poured into a polypropylene separatory funnel. The two layers were separated after 2

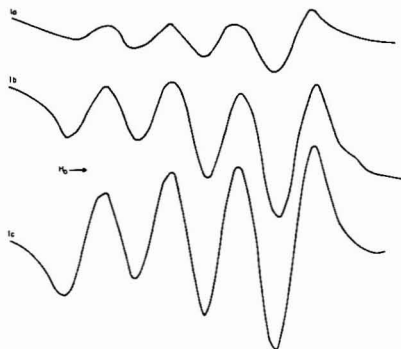


Figure 1. ESR spectrum of ethyl propionate containing 0.1% 8-hydroxyquinoline after extraction of Cu^{2+}

(a) Unspiked sea water, (b) spiked sea water with 4 ppb Cu^{2+} , (c) spiked sea water with 8 ppb Cu^{2+}

minutes. The organic phase, which was about 1 cm^3 , was introduced into the ESR tube for analysis. Figure 1 is an example of the types of spectra obtained from unspiked and spiked sea water. Signal to noise ratio was very good even in the sample of unspiked sea as shown in Figure 1a. Samples spiked with 4 and 8 ppb Cu^{2+} showed a very strong signal (Figures 1b and 1c).

Figure 1 shows a four-line spectrum. Tikhomirova and Zamaraev (3), Gersmann and Swalen (4), and Maki and McGarvey (5) have studied complexes of Cu^{2+} with various chelates and have recorded a wide variety of spectra depending upon the type of bonding of Cu^{2+} with the chelate and also on various other factors such as the concentration of the chelate as compared to the copper and the nature of the chelate. Tikhomirova and Zamaraev obtained a four-line spectrum of copper ethylene diamine (where the ratio of the Cu^{2+} ion to the chelate is less than 0.5) which appears similar to that we obtained for the copper-8-hydroxyquinoline complex. The four-line spectrum arises because of the interaction of unpaired electrons in d of the Cu^{2+} ion with nuclear spin of $\frac{3}{2}$. The hyperfine coupling constant is 88 gauss and line width is about 40 gauss.

We have recorded the ESR spectra of Cu^{2+} spiked with 2 ppb to 10 ppb Cu^{2+} and the results are shown in Figure 2. The concentration of Cu^{2+} in ppb is plotted vs. the ESR signal intensity on a linear scale. The resultant is also linear within the range of concentration studied. This data were analyzed by an IBM System 370, Model 155 using a BMODSR Polynomial Regression Program supplied by the Health Science Computing Facility at UCLA. The line plotted on the graph in Figure 2 is the best fit line obtained from the computer analysis. The standard deviation is ± 3.0 which corresponds to a 99% confidence

¹ Present address, Planning and Development, State Highway Commission, 2300 Van Buren, Topeka, Kansas 66611.

- (1) S. Fujiwara and H. Hayashi, *J. Chem. Phys.*, **43**, 23 (1965).
- (2) A. K. Wiersma and J. J. Windle, *J. Phys. Chem.*, **68**, 2316 (1964).
- (3) N. N. Tikhomirova and K. I. Zamaraev, *Zh. Strukt. Khim.*, **4**, 224 (1963).
- (4) H. R. Gersmann and J. D. Swalen, *J. Chem. Phys.*, **36**, 3221 (1962).
- (5) A. H. Maki and B. R. McGarvey, *J. Chem. Phys.*, **31**, 29, 35 (1958).
- (6) R. Thiers, "Trace Analysis," S. Wiley and Sons, New York, N.Y., 1957.
- (7) J. Culp, R. Windham, and R. Whealy, *Anal. Chem.*, **43**, 1321 (1971).
- (8) S. Sachev and P. West, *Anal. Chim. Acta*, **44**, 301 (1969).
- (9) J. Jones and R. Eddy, *Anal. Chim. Acta*, **43**, 165 (1968).

level. The maximum error between the observed signal intensity and the best fit line corresponds to an error in the Cu^{2+} concentration of ± 0.2 ppb.

Also of interest is the fact that the Y axis intercept at $X = 0$ indicates that the copper concentration in the unspiked sea water sample was 2.6 ppb. This value is in good agreement with the average value of 3.0 ppb reported by Goldberg (10). Tests made using an ion selective electrode yielded a value of 1.6 ppb for this sea water sample (11).

The error contribution from the ESR apparatus itself is $\pm 3\%$. The most significant error in the analytical method is related to the extraction system which was used in these experiments. The samples were shaken by hand and the separations were performed on a per sample basis. Although care was taken, there is little doubt that irregularities in these operations contribute substantially to the total error in the measurement. Adsorption of Cu^{2+} on the walls of the extraction vessels may also have varied from one extraction run to the next and the evaluation of this

- (10) E. D. Goldberg, "Chemical Oceanography," Academic Press, New York, N.Y., 1965, p 183.
 (11) Chemical Waste Detection, Quarterly Technical Report, Texas Instruments, Houston, Texas, 1972.

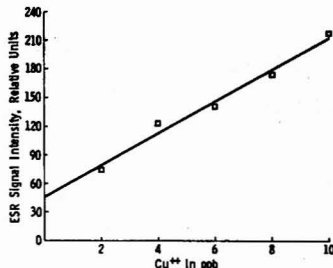


Figure 2. Plot of Cu^{2+} in ppb vs. ESR signal intensity. Actual signal intensity in sea water spiked with copper.

factor is extremely difficult. A continuous countercurrent extraction system could be constructed and would eliminate most of the variations in the extraction process. Such a system could be designed to permit continuous monitoring of copper concentration in sea water.

Received for review April 9, 1973. Accepted July 20, 1973.

Device to Seal Ends of Gas Chromatography Columns with a Filter Disk

Francis W. Karasek

Department of Chemistry, University of Waterloo, Waterloo, Ontario, Canada

When preparing packed GC columns, it is common practice to insert a plug of glass wool into one end to retain the packing during the filling process and hold it in place during use. Following filling, the packing at the sample injection end is retained by inserting a similar plug of glass wool at that point. The performance of these glass wool plugs as retainers is highly variable, depending upon the skill and technique of the experimenter preparing them. Some particularly undesirable results can arise at the detector end from a poorly prepared glass wool plug. Not only can unnecessary dead space result, but column packing particles can be carried through the glass wool by carrier flow to contaminate the detector.

When using metal columns, an effective retainer can be provided by sealing a thin stainless steel filter disk in the detector end of the column. A hand-operated device to accomplish the task is shown in Figure 1. The GC column is inserted in the left end of the unit through the Jacobs chuck jaws and tightened in place with the end placed just short of the reamer passage located at the right end. A T-drill reamer is inserted through the reamer passage, and a cavity between $\frac{3}{32}$ and $\frac{1}{16}$ inch deep is made in the tubing end. For $\frac{1}{8}$ -in. o.d. stainless steel tubing, a $\frac{1}{16}$ -in. drill with the cutting end flattened to almost a right angle will produce a "U"-shaped cavity after reaming. A hand drill can be used instead of the T-drill reamer, but then a vise is needed to hold the unit. Once the column end has been reamed, a filter disk is inserted and the T-drill reamer with its guide is removed. Then the swaging tool shown in the lower center of Figure 1 is inserted to swage over the tube end and to permanently seal in the filter.

The swaging tool head is machined from tool steel and then hardened. It is silver-soldered to the end of a threaded bolt which screws through a guide for insertion in the body of the device. The swaging pressure is applied by a few turns of the tool, once contact is made with the tube end.

By using the punch unit shown in Figure 2, filter disks are punched from stainless steel cloth of the desired mesh size to retain the smallest particles anticipated in the packing. The plunger and die of the punch are made of hardened tool steel and dimensioned to accurately cut a filter disk about 0.003 inch smaller than the drill of the reamer. Careful preparation of the filter disk with such a punch or similar unit is important, so that when inserted

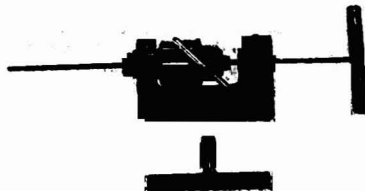


Figure 1. A view of the device used to seal GC column ends with a filter disk. A short section of $\frac{1}{8}$ -in. SS tubing is inserted to illustrate relative positions of the T-drill reamer (right) and tubing end being prepared. The swaging tool subsequently inserted after the reamer is shown (lower center).

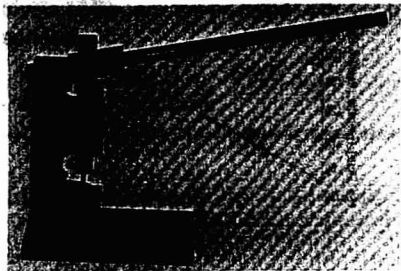


Figure 2. Punch unit used to prepare filter disks. The plunger and die will accurately cut a disk to fit tightly in the end of a prepared column

the disk not only will be retained tightly in the tube end during the swaging operation, but also will make a good seal when swaged.

For on-column injection, only the detector end of the column is sealed. When a gas-sampling valve is used, or the injection end terminates in a Swagelock type of fitting, both ends can be sealed with this procedure. A highly magnified view of the end of a $\frac{1}{8}$ -in. o.d. column with a $10\text{-}\mu\text{m}$ mesh filter disk sealed in place is shown in Figure



Figure 3. Highly magnified view of a GC column end with the filter disk permanently swaged in place

3. It is apparent that the filter permanently seals the column end and reduces dead space at this point to a minimum.

The device is shown as designed for use with $\frac{1}{8}$ -in. o.d. columns. To use for columns of other sizes, the removable units of the T-drill reamer, swaging insert, and punch dies are replaced with those of appropriate sizes. The entire unit can be made from a few purchased parts (drill, Jacobs chuck) and the services of a small university-type machine shop. Detailed drawings are available from the author. During the past year, many GC columns have been prepared in our laboratories using this device. It has been found very effective and quite simple to operate.

Received for review July 19, 1973. Accepted September 21, 1973.

Teflon Apparatus for Vapor Phase Destruction of Silicate Materials

J. W. Mitchell and D. L. Nash

Bell Laboratories, Murray Hill, N.J. 07974

Silicon, fused silica, and glass frequently require sample treatment or dissolution prior to the determination of trace elements below 1 ppm. Because of great vulnerability to contamination from impurities in reagents and contaminants from vessels, conventional methods for the dissolution of samples by acid digestion are not acceptable for the determination of trace components of ultrapure materials. Thus, new approaches have been sought to ensure noncontaminating techniques for dissolving samples, concentrating trace impurities, and removing matrix elements.

In the case of certain samples, gas-phase reactions that either produce decomposition of the matrix or selectively evolve gaseous products of trace elements are highly effective for preventing contamination. These approaches are therefore preferred whenever applicable (1-7). They are particularly valuable in the case of silicon matrices, which can be volatilized very efficiently to leave residues of non-volatile impurities. Pohl, for example, has used a special quartz apparatus to dissolve solid pieces of silicon in vapors of bromine (8, 9). Zil'bershtein and coworkers determined nonvolatile fluorides in samples of silicon by emission spectrometry following their decomposition in a gaseous mixture of HF-HNO₃ (10). In their most recent report, these investigators have used successfully a graphite-polytetrafluoroethylene (Fluoroplast) vessel for treating silicon with acid vapors; however, the unit as designed, would be extremely expensive to fabricate (11). Our purpose in this paper is to describe an apparatus which we have constructed economically and found very satisfactory

for the vapor phase decomposition by HF of ultrapure silicon dioxide, fused silica, and sodium-lime silicate glasses.

EXPERIMENTAL

Apparatus. An inexpensive preliminary apparatus was constructed by appropriately connecting a 32-oz FEP bottle fitted with a TFE chimney, a 1-liter FEP beaker, and a TFE top. Although this unit was found to be adequate for many purposes, the more elaborate apparatus now to be described, is recommended if analyses of samples will be required over a long period.

In Figure 1 are shown all parts of the apparatus that were machined from virgin Teflon (TFE) stock. Detailed dimensions of these items are shown in Figure 2. The reagent reservoir (D) makes a pressure seal with a groove machined on the bottom of vapor chamber (C). The doughnut-shaped sample-rack (B) then

- (1) A. Mizulke, in "Trace Analysis, Physical Methods," G. H. Morrison, Ed., Wiley, New York, N.Y., 1965.
- (2) J. Inzdy, *Period. Polytech., Chem. Eng.*, **14**, 149 (1970).
- (3) P. Jannasch and R. Seisak, *J. Chem. Soc.*, **114**, 480 (1918).
- (4) P. Jannasch and O. Laubi, *J. Prakt. Chem.*, **97**, 150 (1918).
- (5) K. G. Isave and L. G. Zhuraviev, *Anal. Abstr.*, **7**, 3183 (1950).
- (6) J. Dolezal, P. Povondra, and Z. Suleck, "Decomposition Techniques in Inorganic Analysis," HIME, London, 1968.
- (7) V. R. Wiederkehr and G. W. Goward, *Anal. Chem.*, **31**, 2102 (1959).
- (8) F. A. Pohl, *Chem. Eng. Tech.*, **30**, 347 (1958).
- (9) F. A. Pohl, K. Koker, and W. Bonsels, *Fresenius' Z. Anal. Chem.*, **174**, 6 (1960).
- (10) K. I. Zil'bershtein, M. M. Pirytko, O. N. Nikitina, Yu. F. Federov, and A. V. Nenarokov, *Zavodsk. Lab.*, **29**, 1266 (1963).
- (11) K. I. Zil'bershtein and O. N. Nikitina, in "Analysis of High-Purity Materials," I. P. Alimarin, Ed., Israel Program for Scientific Translations, Jerusalem, 1968, pp 82-85.

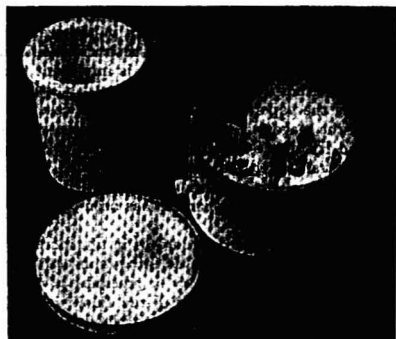
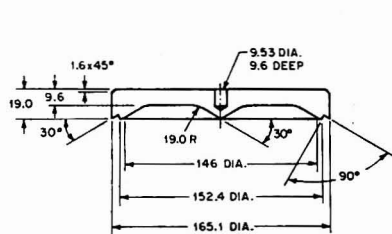
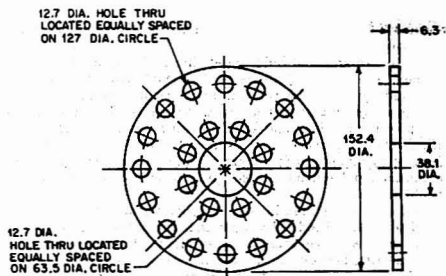


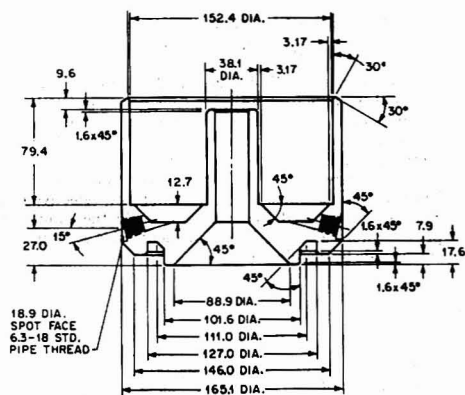
Figure 1. Teflon parts of vapor chamber



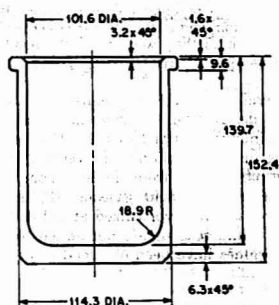
CHAMBER CAP (A)



SAMPLE RACK (B)



VAPOR CHAMBER (C)



REAGENT RESERVOIR (D)

Figure 2. Detailed drawings of Teflon apparatus

fits snugly onto the chimney of the vapor chamber, and is positioned by depressing the plate until it rests on the mantle at the bottom of the chamber. Up to six Teflon beakers (39-mm diameter \times 48 mm) can be placed on the rack for containing samples. After the chamber cap, machined to fit the top rim of the vapor chamber, is positioned, the assembled unit is supported and sealed tightly by enclosing it in an aluminum framework. A picture of the assembled apparatus is shown in Figure 3.

The vapor chamber and reagent reservoir are jacketed with custom-fitted silicon-rubber heating blankets. The blanket on the latter, purchased from Labindustries, has a thermostatic regulator for controlling temperature to $\pm 5^\circ\text{C}$. The former, purchased from Watlow Electric Company is regulated via an appropriate Variac. The heaters supply a maximum of 6 watts/in.² of power for heating chamber (C) and reservoir (D). Dial or Variac settings were correlated with temperature by heating H_2SO_4 in the chamber and measuring the temperature with a thermometer.

Procedure for Destruction of Silicates. After the apparatus is leached at 80°C for 5 days with 1:1 HNO_3 , the unit is assembled in a laminar-flow clean hood and placed in the aluminum housing. Three hundred ml of HF, either reagent grade, isopiestically distilled, or Ultrax (J. T. Baker Chemical Reagent), are carefully poured into the reagent reservoir via a polyethylene funnel inserted into the chimney of the vapor chamber. The samples are



Figure 3. Assembled vapor chamber

weighed into 50-ml Teflon beakers and then placed on the perforated sample rack.

One to two grams of bulk, fused silica, silicon, silicon dioxide, or glass, and up to 10 grams of these materials in granular or powdered form can be treated. Fracture of bulk samples into smaller pieces by placing between thin sheets of Teflon, enclosing in a polyethylene bag, and striking with a hammer increases the efficiency of decomposition. This must be followed by appropriate cleaning to remove surface contaminants. To obviate gross contamination, pulverizing samples prior to exposure to HF vapors should be avoided.

After capping and sealing the chamber, the apparatus is transferred to a fume hood. The vapor chamber is then heated to 160 °C and allowed to equilibrate for 30 minutes before the regulator of the heating blanket on the reagent reservoir is turned to a setting that maintains the temperature at ~110 °C. By operating in this manner no HF or water vapors condense in the sample chamber. Excess HF vapors and volatile decomposition products leave the vapor chamber via a Teflon (FEP) tube, attached to an adapter (see Figure 3) and connected to a polyethylene, water-reservoir (a beaker or bottle of H₂O).

A set of 6 × 3-gram samples of granular silicon dioxide require 10 hours of continuous exposure while bulk 1-gram samples require up to 24 hours of treatment.

The operation is terminated by removing the exit tube from the water reservoir, and turning off the power to the reagent reservoir. After 30 minutes, the power to the vapor chamber is shut off.

DISCUSSION

Several advantages are realized by using this apparatus for the destruction of silicate matrices. The closed system is continuously purged by a positive pressure of HF vapor during operation, thereby preventing the entrance of airborne particulates from the atmosphere. By using vapors from hydrofluoric acid, gaseous HF, and/or the azeotropic mixture, which is volatilized at 111.4 °C, trace impurities in the liquid reagent are not added to the sample. Thus, blank values have been observed to be considerably lower

than those occurring during the dissolution of silicates in liquid HF, where trace contaminants in the reagent are concentrated into the sample during repetitive boiling and fuming with fresh portions of HF. It is important to note that reagent grade HF can be used since purification occurs during the vaporization process. In this case, violent boiling in the reagent reservoir must be eliminated to prevent liquid HF in the form of small droplets of fine spray from being transferred into the vapor chamber. For maximum efficiency of decomposition, fresh portions of reagent should be used after the apparatus has been operated continuously for 48 hours.

At this laboratory, trace impurities in ultrapure silicate materials have been concentrated into graphite and determined by emission spectrometry or precipitated with carriers and measured by Coprex X-ray fluorescence (12). Results by X-ray fluorescence showed blanks with average mean deviations (4 individual measurements) of ±0.7 to ±3.0% for Cu, Ni, Co, Mn, and Cr. The precision for Fe was ±12%. Comparison of these blank values with data for 100 ng of each cation indicated less than 20 ng of the cations in the blank. Blank levels increased by a factor of 10 or more when high-purity liquid HF was used. These data and information on the quantitative recovery of trace elements from silicon dioxide will be given in future reports (13).

ACKNOWLEDGMENT

The authors wish to thank S. S. DeBala who contributed greatly to the design and construction of the apparatus. Helpful discussions with J. E. Kessler were also appreciated.

Received for review July 13, 1973. Accepted October 30, 1973.

- (12) J. E. Kessler, Bell Laboratories, Murray Hill, N.J., unpublished work, 1973.
 (13) J. W. Mitchell, D. L. Nash, and J. E. Kessler, Bell Laboratories, Murray Hill, N.J., unpublished work, 1973.

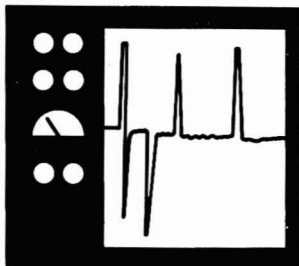
CORRECTION

Potentiometric Determination of Cyanide with an Ion Selective Electrode

In this paper, by W. J. Blaedel, D. B. Easty, L. Anderson, and T. R. Farrell [*Anal. Chem.*, 43, 890 (1971)], an incorrect citation was made to the work of B. György, L. André, L. Stehli, and E. Pungor, titled, "Direct Potentiometric Determination of Cyanide in Biological Systems," which appeared in *Anal. Chim. Acta*, 46, 318 (1969). These authors showed that the cyanide ion selective electrode could be used to measure directly the cyanide in plant hydrolyzates and liquors without prior separation of the cyanide by distillation.

Pesticides Identification

at the Residue Level



ADVANCES IN CHEMISTRY
SERIES No. 104

Ten papers from a symposium by the Division of Pesticide Chemistry of the American Chemical Society chaired by Francis J. Birros.

Pesticides—key to abundance or the beginning of the end? Whether their use leads to more abundant production or to a "silent spring" could well depend on the development and use of analytical techniques. Residues of pesticides and their derivatives have been reported throughout the world and blamed for endangering countless forms of life. Which is actually at fault—the pesticides or the analytical techniques? Some of the topics examined are

- gas-liquid chromatographic detectors
- infrared and ultraviolet spectrophotometry
- thin-layer and paper chromatography
- mass spectrometry
- neutron activation analysis
- biological assay methods

Here is a guide for future research and development in the battle against one type of environmental pollution.

182 pages with index.
Cloth bound (1971) \$8.50
Postpaid in U.S. and Canada; plus 40 cents elsewhere.
Set of L.C. cards with library orders upon request.

Order from:
Special Issues Sales
American Chemical Society
1155 16th St., N.W.
Washington, D.C. 20036

LABORATORY SUPPLY CENTER

CABLE ADDRESS: SACTEX

PROMPT SHIPMENT

POLAROGRAPHIC ELECTROMETRIC REAGENTS

Quaternary ammonium compounds.
Highly purified salts and solutions.



**SOUTHWESTERN ANALYTICAL
CHEMICALS** BOX 485 — AUSTIN, TEX
AREA 512 444-3626

—literature on request

Optical Purity Analysis By NMR

KIRALSHIFT® REAGENTS

Kiralshift E-7 Eu(hfbc), 1g/\$16
Kiralshift E-3 Eu(tfac), 1g/\$18
Kiralshift P-7 Pr(hfbc), 1g/\$18
Kiralshift P-3 Pr(tfac), 1g/\$18

Also Available As Standard Solutions
Write For Details

Regis Chemical Company
8210 Austin • Morton Grove, IL 60053

Do You Need....

DEUTERIUM OXIDE?

99.8 mol%/100.0 mol%
For new low prices call: (415) 234-4130

BIO-RAD Laboratories

32nd and Griffin Ave., Richmond, California

POLLUTION STUDIES

- AIR, WATER & INDUSTRIAL ENVIRONMENTS
- CONTAMINATION IN FOOD & PACKAGING

Write for Brochure

**GOLLOB
ANALYTICAL
SERVICE CORP.**

46 Industrial Road,
Berkeley Heights, N. J.
07922
201-484-3331

4-Aminohippuric Acid & Sodium Salt • Ammonium Reineckate • Anthrone
DL-Aspartic Acid • Bromocresol Purple • tert-Butyl Chloride
α-Chloralose • Dichloroacetic Acid • 2,6-Dichloroindophenol, Sodium
Dulcitol • Esculin • Ethyl Levulinate • Hydroxylamine Sulfate
Malonamide • Malonic Acid • Methyl Glutaric Anhydride • Orcinol
Phenoxyacetic Acid • Phenylphosphate Disodium Salt • Phenylthiourea
Rhodanine • Sodium Dithionite • Sodium Malonate • Sodium Pyruvate
Tetrahydrofurfuryl Acetate • 2,2,2-Trichloroethanol • o-Vanillin

Write for our NEW Products List of over 3,000 chemicals

Tel.: 516-273-0900

TWX: 510-227-6230

EASTERN CHEMICAL

BOX 2500 K

Division of GUARDIAN CHEMICAL CORP.

HAUPPAUGE, N. Y. 11787

Rates Available

on Request

ANALYTICAL CHEMISTRY

Donna C. Bifano
Production Assistant

142 East Ave.
Norwalk, Conn. 06851
203-853-4488

CONSIDERING MÖSSBAUER?

CALL COLLECT OR WRITE:
AUSTIN SCIENCE ASSOCIATES, INC.
5982 West Bee Caves Rd., Austin, Texas 78746
TELEPHONE: 512 327-1257

Water-Soluble NMR Standard

(CH₃)₃SIC₂H₅CO₂Na
3-(Trimethylsilyl)propionic acid,
sodium salt

Cat. No. 1295A 1 g. \$8.50 5 g. \$30.00

SILAR LABORATORIES, INC.
P.O. Box 86, Watervliet, N.Y. 12189

GC/MS—Finnegan Model 3100D GC/MS System with System 250 Computer Control and Graphic Output System—Accessory items include solid sample inlet, inlet pumping system, variable leak sample inlet, three channel light beam oscilloscope recorder, strip chart recorder, mass marker, spare parts, libraries, and all detailed catalogues and instructions. System purchased new March, 1973, and total utilization less than 100 hours. Total investment in excess of \$100,000.00. Price open to negotiation. Please respond to: Altor Corp., 414 Pendleton Way, Oakland, Ca. 94621

INDEX TO ADVERTISERS IN THIS ISSUE

*Alltech Associates, Inc. 213A	*Crawford Fitting Company 153A	*Helma International, Inc. 250A
Peterson & Wentzel, Inc.	Falls Advertising Company	Miller Advertising Agency Inc.
Alex Scientific, Inc. 104A	CVC Products Inc. 152A	*Hewlett-Packard, Avondale Division. 85A
Smith Reynolds		Richardson, Thomas & Bushman, Inc.
American Elsevier Publishing Company, Inc. 156A	*Dohrmann, Div. of Envirotech. 250A	*Hewlett-Packard, San Diego Div. 110A-111A
	Fred Schott and Associates	Phillips Ramsey Advertising
*American Instrument Company, Division of Travenol Laboratories Inc. 230A	*E. I. du Pont de Nemours & Co., Inc. 106A, 136A, 183A	*Houston Instrument, Div. of Bausch & Lomb. 102A
Industrial Advertising Associates	N. W. Ayer & Son, Inc.	Ray Cooley and Associates, Inc.
*Analabs, Inc., Div. of New England Nuclear. 161A	*Eastman Kodak Company. 227A	
Grover and Erickson, Inc.	Rumrill-Hoyt, Inc.	Inax Instruments Ltd. 138A
Autolab Div., Spectra-Physics. 126A-127A	Eberbach Corporation. 218A	*Instrumentation Laboratory Inc. 181A
Lincoln Associates, Inc.	Drury, Lucy Inc.	Aries Advertising Inc.
	Edax International, Inc. 213A	*ISCO. 212A
	Amith Advertising Associates	Graham Printing & Advertising
J. T. Baker Chemical Company. 216A-217A	Elkay Laboratory Products. 90A	
deMartin Marona & Associates	Don Hodes Advertising Inc.	Jarrell-Ash Division, Fisher Scientific Co. 192A
Bausch & Lomb, Analytical Systems Division. 129A	Elscint, Inc. 184A	JASCO, INC. 177A
Wolf Associates, Inc.	GT Advertising Associates	S. M. Sachs & Associates, Inc.
*Beckman Instrument Inc. 254A	EM Laboratories, Inc. 252A, 253A	*Johns-Manville, Celite Division. 151A
Lescarboursa Advertising Inc.	Kenyon Hoag Associates	Frye-Sills, Inc.
*Beckman Instruments, SID. 86A, 122A-123A, 209A	Engelhard Industries, Div. of Engelhard Minerals and Chemicals Corporation. 109A	Joint Committee on Powder Diffraction Standards. 178A
N. W. Ayer/Jorgensen/MacDonald, Inc.	Keys, Martin & Company	
*Bel-Art Products. 178A	Environmental Sciences Assoc. 92A	
Gallard Advertising Agency, Inc.	Val Laughner Associates, Inc.	
Bethlehem Apparatus Co., Inc. 226A	Etec Corporation. 175A	
Beaumont, Heller & Sperling, Inc.	Allen & Dorward, Inc.	Keithley Instruments, Inc. 233A
*Bio-Rad Laboratories. 152A		Chagrin Valley Marketing Associates
Fred Schott & Associates	Finnigan Corporation. 149A, 182A	Kontes Glass Company. 185A
Brinkmann Instruments, Inc. OBC	Bachrach Advertising	Aitkin-Kynett Co., Inc.
Blatt Advertising, Inc.	*Fisher Scientific Company. 155A	Kontes/Martin. 202A
*Bruker Scientific Inc. 147A	Tech-Ad Associates	Aitkin-Kynett Co., Inc.
Schwietzer Advertising	*Floridin Company. 232A	
Buchler Instruments Div. of D. G. Dearle Analytic. 224A	Marsteller Inc.	*Labindustries. 225A
Jud Jaffe Advertising		Fred Schott and Associates
*Cahn Instruments. 124A	*GCA/McPherson Instrument. 121A, 180A	*Laboratory Data Control. 187A
Mealer & Emerson, Inc.	Culver Advertising, Inc.	A. B. W. Toft and Company
Camag Inc. 174A	*GCA/Precision Scientific. 1FC	*Leeco Corporation. 176A
Donald E. Heinz and Associates	Tri-State Advertising	Juhl Advertising Agency, Inc.
Canberra Industries. 203A	General Electric, Aircraft Equipment Division. 214A	*Leeds & Northrup Company. 112A-113A
Amplitudes, Inc.	Robert S. Cragin, Inc.	Schaefer Advertising Inc.
The Carborundum Co., Tem-Press Research Div. 229A	*Gifford Instrument Laboratories. 118A	*The London Company. 215A
	The Bayless-Kerr Company	Technical Marketing Associates of Cleveland
*Carle Instruments, Inc. 167A	*Gilon Medical Electronics Inc. 207A	LSI Spectrometrics. 186A
Cochrane Chase & Co., Inc.	Gow-Mac Instrument. 159A	Industrial Advertising Associates
Chemical Research Services, Inc. 195A	Kenyon Hoag Associates	3M Company. 194A
Ross Llewellyn, Inc.		D'Arcy-MacManus & Masius Advertising
Coates & Welter Instruments Corporation. 234A	*Hach Chemical Company. 148A	*Mallinckrodt Chemical Works. 1BC
Moran, Lanig & Ducan	Wesley Day and Company, Inc.	Batz, Hodgson, Neuwachner, Inc.
*Columbia Scientific Industries. 116A	*Hamamatsu Corporation. 107A	McKee-Pederson Instruments. 257A
Evans & Associates	Unlimited Sales Assistance	William G. Alexander Associates
Conostan Division, Continental Oil Company. 141A	*Hamilton Company. 171A	Micromeritics Instruments Corporation. 207A, 236A
	Mealer and Emerson, Inc.	Ad Graphics
Corning Glass Works. 93A-100A	W. A. Hammond Drierite Company. 213A	MKS Instruments. 264A
Rumrill-Hoyt, Inc.	Harrick Scientific Corporation. 207A	Chambers Wiswell & Moore, Inc.
	*The Harshaw Chemical Company. 253A	*Mettler Instrument Corporation. 117A, 219A, 255A, 257A, 259A
	Industry Advertising Co.	Harris D. McKinney Inc.
	*Heath/Schlumberger Instruments. 237A-239A	
	Advance Advertising Service	

*See ad in ACS Laboratory Guide

**Company so marked has advertisement in the foreign regional edition only.

INDEX TO ADVERTISERS IN THIS ISSUE

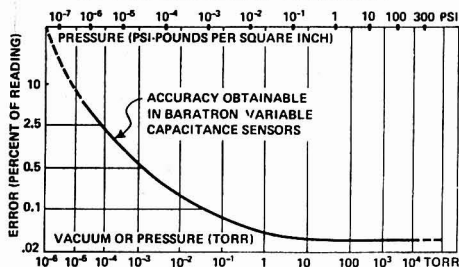
<p>*MFE Corporation 228A The Brightman Company, Inc.</p> <p>Moletron Corporation 150A McCaule Associates</p> <p>Nalgene Labware Div., Nalge Co., Div. of Sybron Corporation 134A Wolf Associates, Inc.</p> <p>Nicolet Instrument Corporation 142A, 173A Hagen Advertising Inc.</p> <p>*Orion Research Inc. 89A Visual Research & Design</p> <p>Ortec Incorporated 145A Thomas R. Sundheim Inc.</p> <p>Parr Instrument Company 250A F. Willard Hills Advertising Service</p> <p>*The Perkin-Elmer Corporation 130A-131A, 133A, 135A, 137A, 139A, 193A Gaynor & Ducaz Advertising</p> <p>*Pharmacia Fine Chemicals Inc. 246A Cummins, MacFail & Nutry, Inc.</p> <p>Philips Electronic Instruments 231A J & M Condon Inc.</p> <p>Pierce Chemical Company 256A Advertising Design</p> <p>Physical Electronics Industries, Inc. 197A Visual-Media Inc.</p> <p>Plenum Publishing 204A Franklin Spier Inc.</p> <p>*Precision Sampling Corporation 190A William U. Stracener</p> <p>Prentice-Hall, Inc., College Division 226A Wateman, Getz, Niedelman Advertising</p> <p>*Princeton Applied Research Corporation 164A The Message Center, Inc.</p> <p>Princeton Gamma-Tech 199A The Sanford Solarz Company</p> <p>*Rigaku Denki Co., Ltd. 211A Asia Advertising Agency, Inc.</p> <p>*Sargent-Welch Scientific 169A Polytech Advertising</p> <p>**Sartorius Membranfilter GMBH... FI Linder Presse Union GMBH</p> <p>Savant Cells 250A Co-Art Associates, Inc.</p> <p>Scientific Industries, Inc. 257A Mandabach & Simms, Inc.</p> <p>Scientific Products 91A Mitchel Suttner McPhilliamy Inc.</p> <p>Scientific Research Instruments 221A Advertising Etc.</p>	<p>*SGA Scientific Inc. 108A Lakewood Advertising Agency</p> <p>Shradler Analytical & Consulting Laboratories Inc. 180A</p> <p>Spex Industries Inc. 247A Commercial ART Service</p> <p>Spectrum Scientific Corporation 256A Louridas Studios</p> <p>Springer-Verlag New York, Inc. 242A</p> <p>*SSR Instruments Company 179A Averill Advertising Inc.</p> <p>Systems Industries 201A</p> <p>*Teche Inc. 245A Brunswick Advertising</p> <p>*Texas Instruments Inc., Digital Systems Div. 115A Albert Frank-Guenther Law</p> <p>*Thermolyne Corporation 191A, 193A, 195A E. R. Hollingsworth & Associates</p> <p>Thermo-Systems, Inc. 250A Gordon Kosholt & Company</p> <p>*Arthur H. Thomas Company 132A Harris D. McKinney, Inc.</p> <p>*Tokyo Kasei Kogyo Co., Ltd. 254A Intercommunications, Inc.</p> <p>*Tracor Analytical Instruments 162A Aim Advertising Agency</p> <p>*Tracor Northern 163A Shurway Advertising Inc.</p> <p>Uthe Technology International 249A Lincoln Associates, Inc.</p> <p>*Varian 114A, 244A-245A Ahern Advertising Agency</p> <p>Varian MAT 258A</p> <p>Verifo Corporation 191A Cerrito Graphic Arts Advtg. Agency</p> <p>John Wiley & Sons 222A 605 Advertising Group</p> <p>*Wilks Scientific Corporation 146A Five Company</p> <p style="text-align: center;">▼ ▼ ▼</p> <p>LABORATORY SUPPLY CENTER 261A Austin Science Associates, Inc. Bio-Rad Laboratories Eastern Chemical Div. of Guardian Chemical Corporation Gollob Analytical Service Corporation Regis Chemical Company SILAR Laboratories, Inc. Southwestern Analytical Chemicals Ultrachem Corporation</p>	<p style="text-align: center;"><i>Advertising Management for the American Chemical Society Publications</i></p> <p style="text-align: center;">CENTCOM, LTD. Thomas N. J. Koerwer, President; Clay S. Holdem, Vice President; Benjamin W. Jones, Vice President; Robert L. Voepel, Vice President; C. Douglas Wallach, Vice President; 142 East Avenue, Norwalk, Connecticut 06851 (Area Code 203) 853-4488</p> <p style="text-align: center;">ADVERTISING SALES MANAGER Thomas N. J. Koerwer</p> <p style="text-align: center;">SALES REPRESENTATIVES</p> <p>Chicago . . . Eugene Eldridge, CENTCOM, LTD., 540 Frontage Rd., Northfield, Ill. 60093. 312-441-6383.</p> <p>Cleveland . . . Michael Hayes, CENTCOM, LTD., 20340 Center Ridge Rd., Rocky River, Ohio 44116. 216-331-2324.</p> <p>Houston . . . Michael Hayes, CENTCOM, LTD., 216-331-2324</p> <p>Denver . . . Clay S. Holdem, CENTCOM LTD., 213-776-0552.</p> <p>Los Angeles 90045 . . . Clay S. Holdem, CENTCOM, LTD., Airport Arcade Bldg., 8820 S. Sepulveda Blvd., Suite 215, 213-776-0552</p> <p>Norwalk 06851 . . . Don Davis, CENTCOM, LTD., 142 East Avenue, 203-853-4488.</p> <p>Philadelphia . . . Robert E. Moran, Eastern Regional Sales Manager, CENTCOM LTD., 535 Pennsylvania Avenue, Fort Washington, Pa., 19034. 215-643-2586.</p> <p>San Francisco . . . Clay S. Holdem, CENTCOM, LTD., 213-776-0552</p> <p>Great Britain and Western Europe . . . Brayton Nichols, Technomedia Ltd., Wood Cottage, Beenhams Heath, Shurlock Row, Reading RG10 0QE, Berkshire, England.</p> <p>Japan . . . Haruo Moribayashi, International Media Representatives, Ltd., 1 Shiba-Kotohiracho, Minato-Ku, Tokyo, Telephone 502-0656.</p> <p style="text-align: center;">PRODUCTION DEPARTMENT <i>Production Director</i> Joseph P. Stenza</p> <p style="text-align: center;"><i>Advertising Production Assistant</i> Donna C. Bifano</p>
---	--	---

*See ad in ACS Laboratory Guide

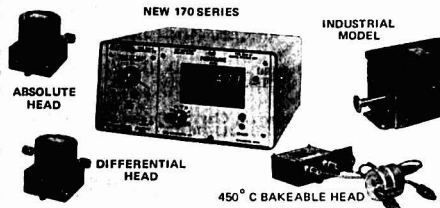
**Company so marked has advertisement in the foreign regional edition only.

MEASURE VACUUM & PRESSURE

TO THIS DEGREE OF ACCURACY



WITH THE MKS BARATRON[®] CAPACITANCE MANOMETER SYSTEMS



MKS BARATRON Capacitance Manometer Systems use a thin, radially-tensioned metal diaphragm and capacitive sensing to achieve 10^{-7} torr sensitivity in a simple, rugged, and highly accurate vacuum or pressure measuring system. Ranges from 10^{-6} to 15,000 torr (10^{-7} to 300 psi).

Because of the diaphragm technique used, measurement is unaffected by gas composition, changes of composition or presence of vapors. Vacuum models can be baked out to 450°C and operated hot to avoid condensation. These gauges eliminate glass and mercury handling problems, and will handle many industrial gases and corrosives including UF_6 and fluorine.

Many models to choose from, including ultra high accuracy laboratory models and new rugged, economical industrial models for low pressure process work. Digital, analog, or meter readouts remote to 1,000 feet. Direct pressure unit readings.

TYPICAL APPLICATIONS INCLUDE

- Replacement of liquid manometers and McLeod gauges.
- Replacement of Thermocouple, Pirani and Alphatron gauges.
- Industrial: pressure control; leak testing; gas flow; vacuum metallurgy; pollution control; chemical and UF_6 process, and food process.
- Calibration standard and vacuum standard.
- Sputtering and vacuum furnace.
- Analysis: mass spectrometer, surface area, and adsorption.
- High Purity - 450°C bakeout.
- Gas backfilling or mixing.
- Wind tunnel and space chambers.
- Corrosive gases, dirty gases, radioactive and conductive gases.



Representatives throughout the world

MKS INSTRUMENTS, INC.
PRECISION PRESSURE-VACUUM MEASUREMENT

25 Adams St. Burlington, Mass. 01803 Tel: 617-272-9255 Telex: 94-9375

CIRCLE 167 ON READER SERVICE CARD

264 A • ANALYTICAL CHEMISTRY, VOL. 46, NO. 2, FEBRUARY 1974

Future Articles

Electron Capture Derivative for Determination of Nicotine in Sub-Picomole Quantities

Lakshmanan Neelakantan and H. B. Kostenbauder

Quantitative Analysis of a Multicomponent Drug Product Using Liquid Chromatography

J. S. Mayell, C. F. Hiskey, and Leon Lachman

Direct X-Ray Spectrometric Determination of Bromine in Water

Yoetz Deutsch

Determination of Lead Using Charged Particle Activation Analysis

David C. Riddle and Emile A. Schweikert

Potentiometric Titration of Monofunctional Bases in Ion-Exchanger-Aqueous Solution Medium—An Investigation of Multiple Equilibria

Frederick F. Cantwell and Donald J. Pietrzyk

Computer Controlled Television Scan System for Direct Encoding of Chemical Structure Models

W. S. Woodward and T. L. Isehour

Influence of Flame Gas Thermal Conductivity on Atom Formation in Flame Spectrometry

N. C. Clampitt and G. M. Hietlje

Potentiometric Measurement of Copper in Seawater with Ion Selective Electrodes

Raymond Jasinski, Issac Trachtenberg, and Dmetro Andrychuk

Combined Sampling-Analysis Method for the Determination of Trace Elements in Atmospheric Particulates

J. L. Seeley and R. K. Skogerboe

Spectrochemical Method for the Determination of 36 Elements in Industrial Effluent

V. M. LeRoy and A. J. Lincoln

Amperometric Titrations Employing Differential Pulse Polarography

David J. Meyers and Janet Osteryoung

High Pressure Chromatography on XAD-2, A Porous Polystyrene-Divinylbenzene Support—Separation of Organic Bases

Chi-Hong Chu and Donald J. Pietrzyk

Constant-Rate Titrations in Studies of Chemical Kinetics—A General Technique for the Elucidation of Reaction Mechanisms and the Evaluation of Rate Constants. The Titration of Nitromethane with Sodium Hydroxide

Bruce H. Campbell, Louis Meites, and Peter W. Carr

Determination of Hydrogen Sulfide in Air—An Assessment of Impregnated Paper Tape Methods

D. F. S. Natusch, J. R. Sewell, and R. L. Tanner

Theoretical Treatment of Pulsed Voltammetric Stripping at the Thin Film Mercury Electrode

Robert A. Osteryoung and Joseph H. Christie

Computer-Assisted Assignment of Retention Indices in Gas Chromatography—Mass Spectrometry and Its Application to Mixtures of Biological Origin

H. Nau and K. Biemann